Université d'Ottawa · University of Ottawa

Free Vibration and Buckling Analysis of Thin Rectangular Plates with Classical Boundary Conditions Under Unilateral In-Plane Loads

Thesis submitted to the School of Graduate Studies
as partial fulfilment of the requirements for the
Degree of Master of Applied Science.

David J. Michelussi

Department of Mechanical Engineering
UNIVERSITY OF OTTAWA
August, 1996

0-612-20937-7

Abstract

Interest in the free vibration of thin rectangular plates has emerged due to the rapid growth in computer technology. Delicate electronic components mounted on circuit boards may be placed in environments under dynamic loadings. The designer may need to control the natural frequency or mode shape of a specific board if a known excitation is causing reliability problems in the hardware. Fortunately, constant in-plane loads can be applied to the plate, affecting its stiffness, and hence dynamic characteristics. This method of control is convenient since the circuit board does not need to be redesigned.

The method of superposition is used to obtain analytical-type solutions for the free vibration of thin rectangular plates under constant in-plane loads in this thesis. A total of nine plate configurations are examined, each of which possess at least one free edge. Eight building blocks are derived and used to solve the plates under consideration. Each building block solution is of the Lévy-type and is analytically exact. Since plate buckling is a limiting case of plate vibration, the solutions obtained can also be used to solve plate buckling problems. Results are calculated for nine plate aspect ratios. Buckling loads, frequencies, and mode shapes are shown. Excellent agreement is found in comparisons with other solution methods.

Acknowledgements

I would first like to express my deep appreciation to Dr. H. T. Saliba for his guidance and council during my time at Lakehead University. His patience and encouragement made this thesis possible. I would also like to thank Dr. D. J. Gorman for his efforts and suggestions while I was completing my course work at the University of Ottawa. Both of these Professors are a credit to their respective schools.

I would like to thank Ms. Solange Amyot for constantly helping me with paperwork, especially when I was off-campus.

I am also indept to my supervisor at Babcock and Wilcox, Mr. R. Garg, who gave me the time I needed to finish my work as a graduate student.

Finally, I would like to thank my parents, in-laws, friends, and especially my wife, Karin, who believed in me and encouraged me right to the end. A special note should be made to Peter Wojciechowski, who allowed me the use of his computer while in Thunder Bay.

Table of Contents

List of Figures

List of Tables

List of Symbols

a	lateral plate dimension in the x-direction (in)
b	lateral plate dimension in the y-direction (in)
D	$= E\, h^3 / \{12\,(1 - \nu^2)\}$, flexural rigidity of plate (in lb)
E	Young's modulus of elasticity of plate material (psi)
f	natural frequency of plate (Hz)
h	plate thickness (in)
I	$= b\, h^3 / 12$, moment of inertia of slender plate or beam (in^4)
k	number of terms in a series solution
N_x	$= P_x / b$, distributed in-plane load (lb / in)
P_x	total in-plane load (lb)
P_ξ	$= - N_x\, b^2 / D$, dimensionless in-plane load
$W(x,y)$	plate displacement (in)
$W(\xi,\eta)$	dimensionless plate displacement
x	plate spatial coordinate
y	plate spatial coordinate
λ^2	$= \omega\, a^2\, (\rho / D)^{1/2}$, plate eigenvalue or dimensionless frequency
ρ	area density of plate material (lb / in^2)
ω	$= 2\,\pi\, f$, circular natural frequency of plate (rad. / s)
ϕ	$= b / a$, plate aspect ratio
ν	Poisson's ratio of plate material
ξ	$= x / a$, dimensionless plate spacial coordinate
η	$= y / b$, dimensionless plate spacial coordinate

1 Introduction

1.1 Problem Definition

In recent times, the thin rectangular plate has been used as a base for mapping electronic circuitry. The microchip, a basic component on many circuit boards, has been evolving at an exponential rate, allowing its integration into modern vehicles and machines to be both economical and powerful. However, these complex control devices can be damaged by excessive vibration. Large displacements can occur when the board is exposed to a harmonic load which varies at one of its natural frequencies. This is called resonance and can be avoided by adjusting the board's mass and stiffness. Thus, the board's free vibration frequencies affect component reliability. A component can be placed along a nodal line to resist against damage from a specific mode of vibration. Methods of predicting natural frequencies and mode shapes can be used by the engineer to optimize the design for component reliability. The dynamic behaviour of a circuit board is dependent upon its size, composition, and edge conditions. Any one of these can be appropriately modified to obtain a satisfactory design.

The dynamic response of a thin rectangular plate can also be regulated by modifying its stiffness using static in-plane loads. This allows the engineer to optimize the design without imposing drastic physical changes. Compressive in-plane loads will decrease overall plate stiffness and hence lower the free vibration frequencies. The converse is true for tensile in-plane loads. These configurations can be physically obtained by using proprietary-type clamping devices to mount the circuit board. Despite the large number of technical papers written on plate vibration [1], the number of available solutions for plates with free edges under in-plane loads is limited.

1.2 Literature Review

The vibration analysis of plates under in-plane loads did not receive much attention until the late 1960's. The majority of the publications reviewed utilize approximating techniques in their solutions. The boundary element, finite element, and finite difference methods can only approach exact values since the continuous plate under investigation must be partitioned. The Ritz method provides good results if the initially assumed shape functions for plate displacement satisfy both the governing equation of motion and the prescribed boundary conditions. However, inferior results are often obtained for plates with free edges. Analytic-type solutions are currently gaining popularity due to their clear approach and extremely convergent results. Traditionally, studies have been directed towards plates with pinned and fixed edges, with very little regard given to the free edge. The plate vibration and buckling papers surveyed are now discussed.

1.2.1 Finite Element and Finite Difference Methods

Anderson, Irons, and Zienkiewicz [2] used the finite element method with non-conforming triangular plate bending elements to study the dynamic response and stability of a thin simply supported square plate subject to unilateral in-plane loads. Element properties are derived by performing numerical integration, allowing element thickness to change within the plate. Buckling loads are evaluated for several uniform plate divisions, and good agreement is shown when compared with the analytically exact value. However, a very fine mesh is required to reduce error to less than 1%, and the eigenvalue solutions of full matrices are very expensive in terms of computing time and storage. The first four natural frequencies of the plate are also calculated for various in-plane loads, which are expressed as percentages of the buckling load. Anderson states, "The effect of any in-plane compressive stress on a plate is to reduce its bending stiffness. Similarly an in-plane tensile stress effectively increases the stiffness. Thus, in the first case, the natural frequency of the plate is lowered and in the second raised."

Chan and Foo [3] used the finite strip method to evaluate the natural frequencies of square simply supported and clamped plates under uni-axial compression. This variation of the finite element method assumes the plate to be made up of a finite number of thin plate strips. The lateral displacement, along the strip length, is represented by continuous characteristic beam vibration functions which satisfy the boundary conditions of the subdivided plate edges. Polynomials are used to represent displacement across the strip. Calculated numerical results compare well with the finite element and analytic values presented. Classical finite element methods usually demand considerable computational resources due to the large matrices developed in discretizing the plate. In the finite strip method, the subdivision of the plate occurs along two parallel plate edges only. This significantly reduces the bandwidth of the matrices, making the method more attractive in terms of numerical efficiency.

Virk [4] investigates the first three modes of free flexural vibration for the simply supported square plate under different bi-axial stresses. The finite element displacement method is used by modifying the element stiffness matrices to account for the effects of the in-plane static loads. Rectangular plane stress elements are used to obtain the static stress distribution, and rectangular plate bending elements are used for the flexural vibrations. Small deflection theory is used and the thin plate is considered to be composed of linearly elastic, isotropic and homogeneous material. The rectangular elements are expected to yield better results than triangular elements since they are of slightly higher order. The results presented suggest that in-plane compression and tension decrease and increase, respectively, the plate stiffness and natural frequencies. Unfortunately, no comparisons are made with existing data.

Tabarrok, Fenton, and Elsaie [5] used a refined triangular plate bending element with eighteen degrees of freedom. These eighteen elemental quantities identify nodal displacements and their first and second derivatives. Assembling the elemental matrices gives global equations of the form

$$\left([K] - [K_b] - \omega^2[M]\right)[q] = 0,$$

where $[K]$ is the stiffness matrix of the whole plate, $[K_b]$ is its buckling stiffness matrix, $[M]$ is its consistent mass matrix, and $[q]$ is the vector of displacement parameters in the global coordinate system. Static buckling loads are calculated by setting the frequency parameter ω to zero. The first three modes of vibration are determined for square plates under in-plane loads, which are allowed to increase from zero to the buckling load. Specifically, the fully pinned, fully clamped, and pinned-clamped-pinned-clamped plates are investigated. Tabarrok states, "Selection of a suitable shape function to specify the displacement of the interior of an element for finite element computation is a difficult task. Even for the simple triangular element, complete displacement compatibility along inter-element boundaries can be satisfied only if the displacement function is at least a quintic polynomial. A refined plate bending element with a quintic polynomial displacement function is superior in time, cost, and accuracy for solving plate buckling problems." This is shown by comparison to Anderson [2]. The results presented are in good agreement with those obtained by other researchers.

Singh and Dey [6] used a variational finite difference approach to analyze the free vibration of rectangular plates subjected to normal in-plane loads. The total energy of the system is expressed in terms of discrete displacements at grid points. Derivative terms in the energy equation are replaced by their finite difference equivalents. Central difference operators of constant order of truncation error are used where necessary. A typical eigenvalue problem is obtained by applying energy minimization principles. For the simply supported square plate with compressive loads on all edges, satisfactory convergence is observed with an 8×8 mesh division, and good agreement is found with the finite element, finite strip, and analytical results presented. Results for the fully clamped plate, loaded along two opposite edges, compare well with the finite strip method. Comparing frequency values for the unloaded pinned-clamped-pinned-clamped plate with those found by Gorman [16] using the superposition technique suggest that higher modes require a finer plate division. The method proves to be economical when compared to the finite element method with regard to computer time and storage.

1.2.2 Rayleigh and Ritz Methods

Dickinson [7] used a Ritz method to analyze simply supported plates subject to both direct shear and in-plane forces. The presence of the twist term in the governing partial differential equation does not seem to complicate energy methods of solution. The constant thickness plate is made of isotropic, homogeneous and elastic material and small displacement theory is considered. An expression for circular frequency is obtained by equating maximum strain energy to maximum kinetic energy,

$$V_{max}(W(x,y)) = \omega^2 \, T_{max}(W(x,y)) \, ,$$

giving

$$\omega^2 = \frac{V_{max}(W(x,y))}{T_{max}(W(x,y))} \, ,$$

where T_{max} is the kinetic energy and V_{max} is the strain energy. The deflection function W(x,y) is chosen such that the geometric boundary conditions of the plate are satisfied. This method leads to an eigenvalue problem which must be solved by use of a computer. Convergence of the solution is shown to be good for plates of aspect ratio 1/1, 1/2, and 1/3. Mode shapes are not presented in the paper.

Dickinson [8] extended his work to include plates made of orthotropic material. The approach used in his previous paper is modified to analyze a square clamped orthotropic plate subject to hydrostatic in-plane forces. Dickinson states that orthotropy in the plate simply changes the constants in the governing partial differential equation without adding any extra terms.

Bassily and Dickinson [9] examined thin rectangular plates subject to in-plane stresses having any combination of fixed, free, or pinned edges by use of the Ritz method. The plate is assumed to be made of flat, isotropic, homogenous material of constant thickness, and small deflection theory is considered. The in-plane loads are membrane stress fields assumed to be constant with time, and the variations they undergo as the plate is bent are negligible and disregarded. The shape functions are series composed of multiplications of beam functions. The beam functions satisfy the plate boundary conditions exactly in the case of clamped and simply supported edges, and approximately for a free edge. Free vibration results for unloaded plates with clamped and pinned edges are compared to results generated by other authors. This is also done for plate buckling. Although good agreement was seen in the results presented, very little work was shown on plates possessing free edges.

Bassily and Dickinson [10] continued their research on the in-plane loading and consequent out-of-plane buckling and vibrational characteristics of plates. It was shown that convergence to a correct solution could not always be assured when using ordinary beam vibration functions to represent the plate deflection form in the Ritz method. A new set of functions, "degenerated beam functions", was postulated, and gave more accurate results for plates with free edges. The simple polynomials used in earlier studies did not realistically represent the middle surface stresses of such plates. Several numerical examples are presented, illustrating the applicability of the approach and giving an indication of the order of errors that may result. Bassily states that assumptions used to simplify the in-plane stress distribution within a loaded plate can lead to a considerable loss of accuracy in predicting buckling and lateral vibration behaviour.

A simple formula for approximate natural frequencies of isotropic plates, originally developed by Warburton using characteristic beam functions in Rayleigh's method, was modified by Dickinson [11] to include specially orthotropic plates and direct in-plane loads. The formula also gives solutions for buckling problems. The plate must be of uniform thickness and at least rectangularly orthotropic material. Small deflection theory was used. Constant in-plane forces per unit length, N_x and N_y (tensile forces positive), act in the middle surface of the plate. Maximum kinetic and strain energies are equated according to Rayleigh's method, ultimately giving an expression for plate frequency. For an isotropic plate under a single unilateral in-plane load, the formula becomes

$$\lambda^2 = \frac{\pi^2}{\phi}\left[\phi^4 G_\xi^4 + 2\phi^2\left[\nu H_\xi H_\eta + (1-\nu)J_\xi J_\eta\right] + G_\eta^4 + \frac{P_\xi \phi^2}{\pi^2} J_\xi\right]^{1/2} \qquad (1.1)$$

where coefficients G_ξ, G_η, H_ξ, H_η, J_ξ, and J_η change for different plate configurations and are listed in a table. For plate buckling,

$$P_\xi = -\frac{\pi^2}{\phi^2 J_\xi}\left[\phi^4 G_\xi^4 + 2\phi^2\left[\nu H_\xi H_\eta + (1-\nu) J_\xi J_\eta\right] + G_\eta^4\right] \tag{1.2}$$

is used to find the critical load. Any combination of pinned, clamped, and free edge conditions can be examined using the above equations along with the coefficient values given in the paper. The approach is powerful since natural frequencies and buckling loads can be calculated by hand without explicitly knowing plate vibration or buckling theory. However, unacceptable error in calculated values may occur since the solution is approximate.

1.2.3 Analytical Methods

Soni and Amba Rao [12] derived closed-form solutions for the free vibration of orthotropic plates under in-plane forces. Four sets of boundary conditions were considered: pinned-clamped-pinned-clamped (SCSC), pinned-clamped-pinned-pinned (SCSS), pinned-clamped-pinned-free (SCSF), and pinned-pinned-pinned-free (SSSF). The governing equation of motion, based on classical thin plate theory, was solved for using a displacement function taken as the product of two functions; one satisfying the boundary conditions at the simply supported edges and the other a general function. This is commonly referred to as a Lévy-type solution in the technical literature. Since buckling is a limiting case of free vibration, critical buckling loads are also examined. All derived solutions are analytically exact.

Yu and Gorman [13] investigated the free vibration of fully clamped isotropic plates under in-plane loads. Four building block Lévy-type solutions are superimposed to obtain an analytic-type solution for the fully clamped plate. A building block is a plate which possess a harmonic edge condition which can be adjusted to control its amplitude. Yu uses a harmonic edge moment in each building block to enforce zero slope along the clamped edges. Eigenvalues are presented for plates of aspect ratio 1.0 and 1.5 under various loadings. Results are extremely convergent.

Cleghorn and Yu [14] used the same building blocks presented in [13] to analyze the buckling of plates possessing clamped and pinned edges.

1.3 Method of Solution

Very few papers deal with the free vibration analysis of laterally loaded thin plates possessing free edges. This thesis presents analytic-type solutions for the free vibration and buckling of unilateral in-plane stressed thin rectangular plates (Figure 1.1) which possess at least one free edge. Lateral loads are applied along edges located at $\xi = 0$ and $\xi = 1$, which will be either pinned or clamped. Loaded free edges are not discussed due to the additional case solutions which would need to be considered. The plate is made of isotropic material and classical thin plate theory is utilized. The approach used involves superimposing Lévy-type building block solutions. Eight derived building block solutions are appropriately assembled to analyze nine different plate configurations. Buckling loads, natural frequencies, and mode shapes are presented for plates of aspect ratio 1/3, 2/5, 1/2, 2/3, 1/1, 3/2, 2/1, 5/2, and 3/1. Finite element results are obtained by use of ANSYS version 5.2 and presented for comparison purposes.

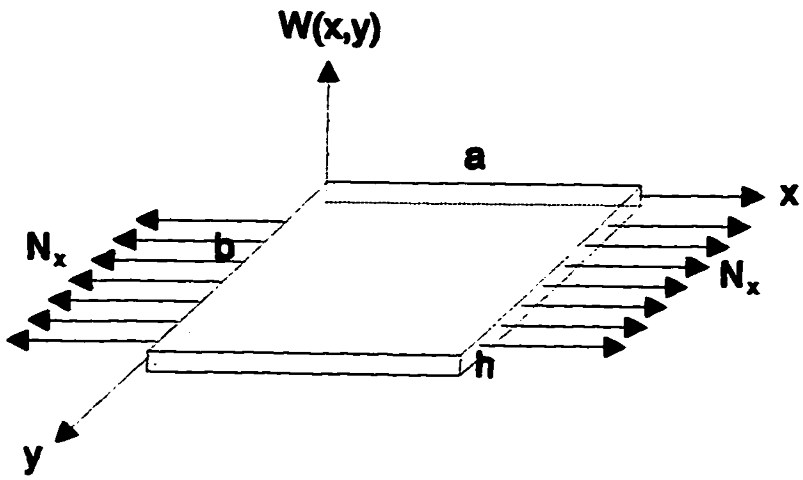

Figure 1.1 A thin rectangular plate subject to unilateral in-plane forces.

2 Fundamental Equations and Theory

A dimensionless coordinate system is utilized in the solutions. The advantage of doing this becomes evident in the generation of data, where families of plates are analyzed instead of a single plate, permitting an efficient presentation of the results.

2.1 Governing Partial Differential Equation

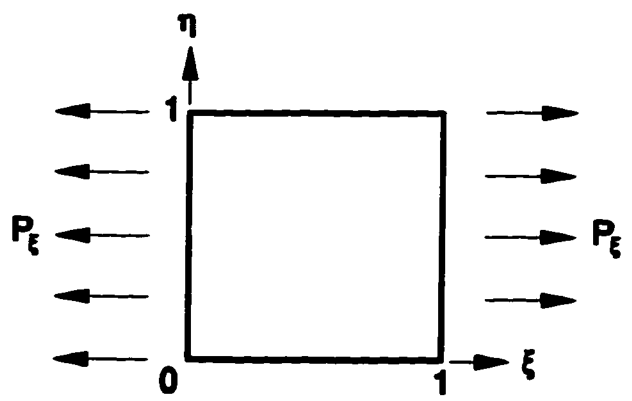

Figure 2.1 A thin rectangular plate in dimensionless coordinates.

The thin rectangular plates analyzed here are assumed to be composed of homogeneous, isotropic material. Small deflection theory was used by Timoshenko [15] in the derivation of the governing differential equation, which assumes:

1. The plate thickness is small in comparison to its lateral dimensions and the distance between nodal lines.
2. The maximum displacement is small in comparison to plate thickness.
3. The effects of transverse shear and rotary inertia can be neglected.

These assumptions satisfy many practical situations. The unilateral in-plane load is constant and evenly distributed along edges $\xi = 0$ and $\xi = 1$, as shown in Figure 2.1. The dimensionless free vibration equation is

$$\frac{\partial^4 W(\xi,\eta)}{\partial\eta^4}+2\phi^2\frac{\partial^4 W(\xi,\eta)}{\partial\eta^2\partial\xi^2}+\phi^4\frac{\partial^4 W(\xi,\eta)}{\partial\xi^4}+P_\xi\phi^2\frac{\partial^2 W(\xi,\eta)}{\partial\xi^2}-\lambda^4\phi^4 W(\xi,\eta) = 0, \quad (2.1)$$

where symbols are as defined in the list of symbols. The dimensionless in-plane load parameter P_ξ is positive in compression and negative in tension. Hence, P_ξ shown in Figure 2.1 is negative. An analytical solution is desired for $W(\xi,\eta)$ which will exactly satisfy both equation (2.1) and the specified boundary conditions for each plate.

2.2 Boundary Conditions

Boundary conditions are defined by combinations of prescribed edge displacement, slope, bending moment, and shear force. Expressions for these have been derived by Timoshenko [15] and translated into dimensionless coordinates by Gorman [16], and are reviewed here for convenience. Note that all quantities are expressed in terms of the plate displacement $W(\xi,\eta)$. The mathematical formulation for the slope is

$$S_\xi = \frac{\partial W(\xi,\eta)}{\partial\xi} \quad (2.2)$$

for lines parallel to the ξ-axis, and

$$S_\eta = \frac{\partial W(\xi,\eta)}{\partial\eta} \quad (2.3)$$

for lines parallel to the η-axis. The distributed bending moment is

$$M_\xi = -\frac{D}{a}\left(\frac{\partial^2 W(\xi,\eta)}{\partial\xi^2} + \frac{\nu}{\phi^2}\frac{\partial^2 W(\xi,\eta)}{\partial\eta^2}\right) \quad (2.4)$$

about edges perpendicular to the ξ-axis, and

$$M_\eta = -\frac{D}{b\phi}\left(\frac{\partial^2 W(\xi,\eta)}{\partial\eta^2} + \nu\phi^2\frac{\partial^2 W(\xi,\eta)}{\partial\xi^2}\right) \tag{2.5}$$

about edges perpendicular to the η-axis. The distributed shear force is

$$V_\xi = -\frac{D}{a^2}\left(\frac{\partial^3 W(\xi,\eta)}{\partial\xi^3} + \frac{(2-\nu)}{\phi^2}\frac{\partial^3 W(\xi,\eta)}{\partial\xi\,\partial\eta^2} + \frac{P_\xi}{\phi^2}\frac{\partial W(\xi,\eta)}{\partial\xi}\right) \tag{2.6}$$

for edges perpendicular to the ξ-axis, and

$$V_\eta = -\frac{D}{b^2\phi}\left(\frac{\partial^3 W(\xi,\eta)}{\partial\eta^3} + (2-\nu)\phi^2\frac{\partial^3 W(\xi,\eta)}{\partial\eta\,\partial\xi^2}\right) \tag{2.7}$$

for edges perpendicular to the η-axis. When used, these equations are usually equated to zero, and constants outside of the large parentheses can be omitted.

2.2.1 Pinned Edge

A pin forbids displacement yet permits rotation. These characteristics indicate that a state of zero displacement and zero bending moment must exist along a simply supported or pinned edge. Once the zero displacement condition is enforced, all partial derivatives of the displacement in the direction of the constant edge will become zero. Knowing this, contributions from equations (2.4) and (2.5) for bending moment may be simplified. The pinned edge is defined by

$$W(\xi,\eta) = \frac{\partial^2 W(\xi,\eta)}{\partial\xi^2} = 0 \tag{2.8}$$

for edges perpendicular to the ξ-axis, and

$$W(\xi,\eta) = \frac{\partial^2 W(\xi,\eta)}{\partial\eta^2} = 0 \tag{2.9}$$

for edges perpendicular to the η-axis.

2.2.2 Clamped Edge

A clamp or fixed support restrains the plate from both displacing and rotating. These characteristics indicate that a state of zero displacement and zero slope must exist along the edge. Contributions for slope are given by equations (2.2) and (2.3). The clamped edge is defined by

$$W(\xi,\eta) = \frac{\partial W(\xi,\eta)}{\partial \xi} = 0 \tag{2.10}$$

for edges perpendicular to the ξ-axis, and

$$W(\xi,\eta) = \frac{\partial W(\xi,\eta)}{\partial \eta} = 0 \tag{2.11}$$

for edges perpendicular to the η-axis.

2.2.3 Free Edge

As the name suggests, a free edge is not restrained and may both displace and rotate. These characteristics indicate that a state of zero bending moment and zero shear force must exist along the edge. Contributions for bending moment and shear force are given by equations (2.4), (2.5), (2.6), and (2.7). The free edge is defined by

$$\frac{\partial^2 W(\xi,\eta)}{\partial \xi^2} + \frac{\nu}{\phi^2}\frac{\partial^2 W(\xi,\eta)}{\partial \eta^2} = \frac{\partial^3 W(\xi,\eta)}{\partial \xi^3} + \frac{(2-\nu)}{\phi^2}\frac{\partial^3 W(\xi,\eta)}{\partial \xi\,\partial \eta^2} + \frac{P_\xi}{\phi^2}\frac{\partial W(\xi,\eta)}{\partial \xi} = 0 \tag{2.12}$$

for edges perpendicular to the ξ-axis, and

$$\frac{\partial^2 W(\xi,\eta)}{\partial \eta^2} + \nu\phi^2\frac{\partial^2 W(\xi,\eta)}{\partial \xi^2} = \frac{\partial^3 W(\xi,\eta)}{\partial \eta^3} + (2-\nu)\phi^2\frac{\partial^3 W(\xi,\eta)}{\partial \eta\,\partial \xi^2} = 0 \tag{2.13}$$

for edges perpendicular to the η-axis.

2.2.4 Slip Shear Conditions

A fourth condition of interest, slip shear, exists in all symmetrical modes of plate vibration. Slip shear is identified by zero slope and zero shear force, and is rarely encountered on the edge of an actual plate. However, its definition is invaluable when investigating plate vibration by the method of superposition. Contributions for slope are given by equations (2.2) and (2.3). Contributions from equations (2.6) and (2.7) for shear force are simplified by realizing that the first order partial derivative terms represent slope, and consequently must vanish. Slip shear conditions are defined by

$$\frac{\partial W(\xi,\eta)}{\partial \xi} = \frac{\partial^3 W(\xi,\eta)}{\partial \xi^3} = 0 \tag{2.14}$$

for edges perpendicular to the ξ-axis, and

$$\frac{\partial W(\xi,\eta)}{\partial \eta} = \frac{\partial^3 W(\xi,\eta)}{\partial \eta^3} = 0 \tag{2.15}$$

for edges perpendicular to the η-axis.

2.3 Lévy-Type Solution

Of the four classical boundary conditions described above, only the pinned and slip shear edges properly accommodate the trigonometric functions in a Lévy-type solution. The Lévy-type solution is a series solution involving Fourier sine or cosine series of one coordinate, where the associated coefficients are functions of the other coordinate. The trigonometric term is appropriately chosen so that the prescribed boundary conditions at two opposing extremities are automatically satisfied. It is very important that, upon substitution into the governing equation and boundary conditions, derivatives of the trigonometric terms form linear multiples of themselves, permitting the separation of variables to occur. A plate will adopt a specific form of solution based upon the type of edge conditions present:

$$W(\xi,\eta) = \sum_{m=1,2,3}^{\infty} Y_m(\eta) \sin(m\pi\xi) \tag{2.16}$$

for simply supported conditions along both $\xi = 0$ and $\xi = 1$,

$$W(\xi,\eta) = \sum_{m=0,1,2}^{\infty} Y_m(\eta)\cos(m\pi\xi) \tag{2.17}$$

for slip shear conditions along both $\xi = 0$ and $\xi = 1$,

$$W(\xi,\eta) = \sum_{m=1,3,5}^{\infty} Y_m(\eta)\sin(m\pi\xi/2) \tag{2.18}$$

for simply supported conditions along $\xi = 0$ and slip shear conditions along $\xi = 1$,

$$W(\xi,\eta) = \sum_{m=1,3,5}^{\infty} Y_m(\eta)\cos(m\pi\xi/2) \tag{2.19}$$

for slip shear conditions along $\xi = 0$ and simply supported conditions along $\xi = 1$,

$$W(\xi,\eta) = \sum_{n=1,2,3}^{\infty} Y_n(\xi)\sin(n\pi\eta) \tag{2.20}$$

for simply supported conditions along both $\eta = 0$ and $\eta = 1$,

$$W(\xi,\eta) = \sum_{n=0,1,2}^{\infty} Y_n(\xi)\cos(n\pi\eta) \tag{2.21}$$

for slip shear conditions along both $\eta = 0$ and $\eta = 1$,

$$W(\xi,\eta) = \sum_{n=1,3,5}^{\infty} Y_n(\xi)\sin(n\pi\eta/2) \tag{2.22}$$

for simply supported conditions along $\eta = 0$ and slip shear conditions along $\eta = 1$, and

$$W(\xi,\eta) = \sum_{n=1,3,5}^{\infty} Y_n(\xi)\cos(n\pi\eta/2) \tag{2.23}$$

for slip shear conditions along $\eta = 0$ and simply supported conditions along $\eta = 1$.

2.4 Method of Superposition

A simple Lévy-type solution cannot be derived for plates not meeting the minimum requirement of two opposite edges having pinned or slip shear conditions. Instead, two or more appropriate plate problems (or building blocks), whose Lévy-type solutions can be obtained, are superimposed. Each building block possesses a harmonically varying boundary condition, either slope or bending moment. By properly adjusting these in the superimposed solution, the prescribed boundary conditions of the original plate are satisfied to any desired degree of accuracy.

The terminology used to describe the boundary conditions of the plates considered in this paper is now introduced. It follows a system adopted by Leissa [1] where the boundary conditions of each side are listed in a standard order, namely $\xi = 0$, $\eta = 0$, $\xi = 1$, and $\eta = 1$. This is equivalent to labelling the left side of the plate first and proceeding in a counter-clockwise manner conforming to the axis orientation used in this paper. Each side is assigned a single letter which, according to Table 2.1, identifies the type of edge present.

Table 2.1 Plate edge labelling guide.

Label	Edge type	Boundary conditions
C	Clamped	W = 0 and S = 0.
F	Free	M = 0 and V = 0.
R	Slip shear	S = 0 and V = 0.
S	Simply supported	W = 0 and M = 0.
V	Zero shear force	V = 0 and S is a Fourier series.
W	Zero displacement	W = 0 and M is a Fourier series.

Pinned and slip shear edge conditions support a Lévy-type solution, as explained in section 2.3. Hence, the method of superposition is usually employed in the presence of either a clamped or free edge.

3 Derived Analytic Solutions

The fundamental equations and theory can now be utilized to derive analytic solutions for the plate problems under investigation. A straightforward Lévy-type solution is used for the SSSF plate. All other plate solutions are obtained by superimposing two or more building blocks to satisfy the boundary conditions of clamped or free edges. The CCCF plate solution is obtained by superimposing four building blocks: the SSSV, SSWR, SWSR, and WSSR plates. Combinations of these four building blocks are used to solve the CSCF, SCCF, SSCF, and SCSF plates. The CFCF plate solution is obtained by superimposing four different building blocks: the SRSV, SRWR, SVSR, and WRSR plates. Combinations of these four building blocks are used to solve the SFCF and SFSF plates. The specific building blocks used in each plate solution are shown in Figure 3.1. Although the Lévy-type solutions of the SCSF and SFSF plates can be obtained directly, it is more efficient to solve the problems by superimposing existing building blocks.

Note that a clamped edge is modelled by first enforcing zero vertical edge displacement in all building blocks and then adjusting a harmonic bending moment about that edge to properly achieve the zero slope condition. This is accomplished by superimposing a zero displacement edge (W) on a number of pinned edges (S).

Similarly, a free edge is modelled by first enforcing zero vertical edge reaction in all building blocks and then adjusting a harmonic slope about that edge to properly achieve the zero bending moment condition. This is accomplished by superimposing a zero shear force edge (V) on a number of slip shear edges (R).

Application of the Lévy-type solution to plate problems is first introduced by analyzing the SSSF plate. By doing this, the basis for determining building block solutions is established. Once the building block solutions are available, analytic solutions for the remaining problems can be found by using the method of superposition.

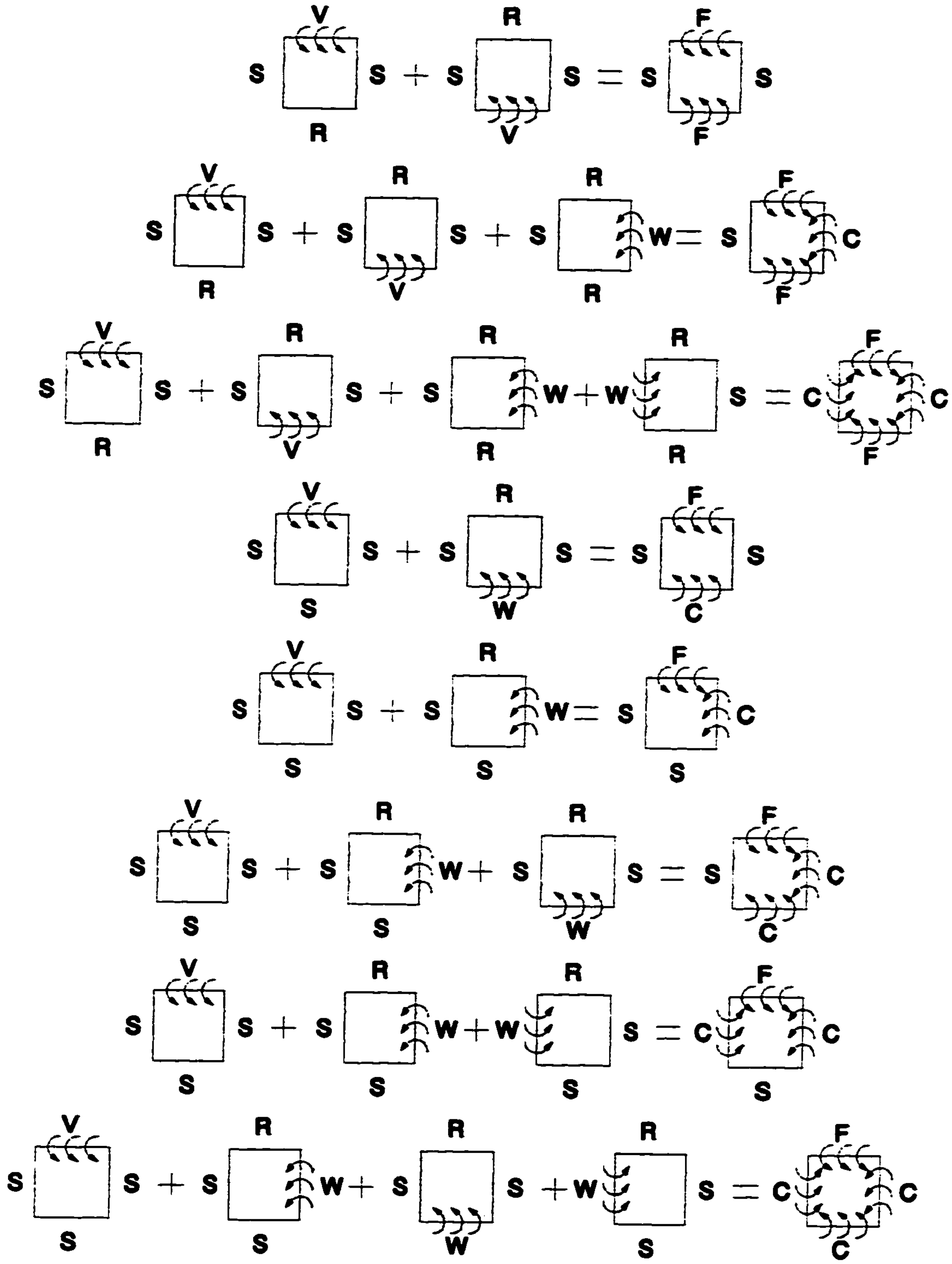

Figure 3.1 The building blocks superimposed to solve the plate problems.

3.1 The SSSF Plate

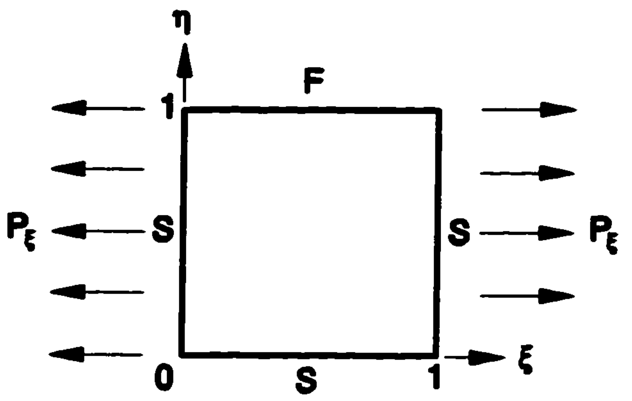

Figure 3.2 The SSSF thin rectangular plate under unilateral in-plane load.

Consider the plate presented in Figure 3.2. A direct Lévy-type solution is feasible since the edges at $\xi = 0$ and $\xi = 1$ are both pinned. The explicit solution is derived by substituting the Lévy-type solution, equation (2.16), into the governing equation of motion, equation (2.1), giving

$$\sum_{m=1,2,3}^{\infty}\left[Y_m''''(\eta)-2(\phi m\pi)^2 Y_m''(\eta)+\left((\phi m\pi)^4-(\phi\lambda)^4-P_\xi(\phi m\pi)^2\right)Y_m(\eta)\right]\sin(m\pi\xi)=0\,. \qquad (3.1)$$

Equation (3.1) is a product of two independent functions which equal zero, and $\sin(m\pi\xi)$ cannot equal zero for all values of ξ. Therefore, the function of η within the square brackets must equal zero for any value of m. Separating the variables produces an ordinary homogeneous differential equation of the form

$$Y_m''''(\eta) - 2\phi^2\delta_m Y_m''(\eta) + \phi^4\Delta_m Y_m(\eta) = 0 \qquad (3.2)$$

where

$$\delta_m = (m\pi)^2$$

and

$$\Delta_m = (m\pi)^4 - \lambda^4 - P_\xi (m\pi/\phi)^2 \, .$$

The four characteristic roots of equation (3.2) are defined by

$$r = \pm\phi\sqrt{\delta_m \pm \sqrt{\delta_m^2 - \Delta_m}} \, . \tag{3.3}$$

Real, imaginary, and complex roots can be obtained from equation (3.3) depending upon the values of the δ_m and Δ_m parameters. Consequently, three different harmonic general solutions exist for $Y_m(\eta)$ which satisfy the governing equation of motion.

The four arbitrary constants within a general solution for $Y_m(\eta)$ are determined by enforcing four boundary conditions. The simply supported edge at $\eta = 0$ and the free edge at $\eta = 1$ provide the expressions needed. Since there are three general solutions to be examined, expressing the boundary relations in terms of $Y_m(\eta)$ would be convenient. This is accomplished by separating the variables in the boundary condition equations. The Lévy-type solution, equation (2.16), is first substituted into equations (2.9) and (2.13). The resulting equations are then respectively evaluated at $\eta = 0$ and $\eta = 1$, giving

$$\sum_{m=1,2,3}^{\infty} Y_m(0)\,\sin(m\pi\xi) = 0 \, ,$$

$$\sum_{m=1,2,3}^{\infty} Y_m''(0)\,\sin(m\pi\xi) = 0 \, ,$$

$$\sum_{m=1,2,3}^{\infty} \left[Y_m''(1) - \nu(m\pi\phi)^2 Y_m(1)\right] \sin(m\pi\xi) = 0 \, ,$$

and

$$\sum_{m=1,2,3}^{\infty} \left[Y_m'''(1) - (2-\nu)(m\pi\phi)^2 Y_m'(1)\right] \sin(m\pi\xi) = 0 \, .$$

Since $\sin(m\pi\xi)$ cannot equal zero for all values of ξ in the above equations, the evaluated functions of $Y_m(\eta)$ must equal zero for any value of m. This procedure is similar to that performed in the derivation of equation (3.2). The boundary conditions are now

$$Y_m(0) = 0\,, \tag{3.4}$$

$$Y_m''(0) = 0\,, \tag{3.5}$$

$$Y_m''(1) - \nu(m\pi\phi)^2 Y_m(1) = 0\,, \tag{3.6}$$

and

$$Y_m'''(1) - (2-\nu)(m\pi\phi)^2 Y_m'(1) = 0\,. \tag{3.7}$$

Equations (3.2) to (3.7) are exploited in the following sections to specifically obtain solutions for $Y_m(\eta)$. The reader should take note that the original partial differential equation problem has been significantly reduced to an ordinary differential equation problem.

3.1.1 Case 1 Solution

Four distinct complex roots result when $\delta_m^2 < \Delta_m$ in equation (3.3). These roots are defined by $\pm\,\beta_m \pm \gamma_m i$, which yield a general solution of the form

$$\begin{aligned} Y_m(\eta) &= A_m \sinh(\beta_m\eta)\sin(\gamma_m\eta) + B_m \sinh(\beta_m\eta)\cos(\gamma_m\eta) \\ &\quad + C_m \cosh(\beta_m\eta)\sin(\gamma_m\eta) + D_m \cosh(\beta_m\eta)\cos(\gamma_m\eta) \end{aligned} \tag{3.8}$$

where

$$\beta_m = \phi\sqrt{\frac{\sqrt{\Delta_m} + \delta_m}{2}}$$

and

$$\gamma_m = \phi\sqrt{\frac{\sqrt{\Delta_m} - \delta_m}{2}}\,.$$

The first and last terms of the solution are even while the two middle terms are odd.

Constants A_m, B_m, C_m, and D_m are determined by enforcing equations (3.4) to (3.7). Substituting the present solution, equation (3.8), into equations (3.4) and (3.5), yields

$$D_m = 0$$

and

$$D_m(\beta_m^2 - \gamma_m^2) + 2A_m\beta_m\gamma_m = 0 .$$

Thus, constants A_m and D_m, which are associated with the even terms in equation (3.8), are zero. One may intuitively conclude that only odd terms will satisfy the constraints set by simple support boundary conditions for an edge at $\eta = 0$ or $\xi = 0$. This pattern is reflected in the Lévy-type plate solutions of section 2.3.

Next, the simplified solution is substituted into equations (3.6) and (3.7). The resulting equations are rearranged, giving

$$B_m\left[\left(\beta_m^2 - \gamma_m^2 - \nu\,(m\pi\phi)^2\right)\sinh(\beta_m)\cos(\gamma_m) - 2\beta_m\gamma_m\cosh(\beta_m)\sin(\gamma_m)\right]$$
$$+ C_m\left[\left(\beta_m^2 - \gamma_m^2 - \nu\,(m\pi\phi)^2\right)\cosh(\beta_m)\sin(\gamma_m) + 2\beta_m\gamma_m\sinh(\beta_m)\cos(\gamma_m)\right] = 0$$

and

$$B_m\Big[\left(\beta_m^2 - 3\gamma_m^2 - (2-\nu)(m\pi\phi)^2\right)\beta_m\cosh(\beta_m)\cos(\gamma_m)$$
$$+\left(\gamma_m^2 - 3\beta_m^2 + (2-\nu)(m\pi\phi)^2\right)\gamma_m\sinh(\beta_m)\sin(\gamma_m)\Big]$$
$$+ C_m\Big[\left(\beta_m^2 - 3\gamma_m^2 - (2-\nu)(m\pi\phi)^2\right)\beta_m\sinh(\beta_m)\sin(\gamma_m)$$
$$-\left(\gamma_m^2 - 3\beta_m^2 + (2-\nu)(m\pi\phi)^2\right)\gamma_m\cosh(\beta_m)\cos(\gamma_m)\Big] = 0 .$$

The above linear algebraic equations form a homogeneous system when written in matrix form. Non-trivial solutions for B_m and C_m are obtained by setting the determinant of the system's coefficient matrix equal to zero, yielding

$$\left[(\beta_m^2 - \gamma_m^2 - \nu\,(m\pi\phi)^2)\sinh(\beta_m)\cos(\gamma_m) - 2\beta_m\gamma_m\cosh(\beta_m)\sin(\gamma_m)\right] \times$$
$$[\,\beta_m(\beta_m^2 - 3\gamma_m^2 - (2-\nu)(m\pi\phi)^2)\sinh(\beta_m)\sin(\gamma_m) -$$
$$\gamma_m(\gamma_m^2 - 3\beta_m^2 + (2-\nu)(m\pi\phi)^2)\sinh(\beta_m)\sin(\gamma_m)\,] +$$
$$\left[(\beta_m^2 - \gamma_m^2 - \nu\,(m\pi\phi)^2)\cosh(\beta_m)\sin(\gamma_m) + 2\beta_m\gamma_m\sinh(\beta_m)\cos(\gamma_m)\right] \times$$
$$[\,\beta_m(\beta_m^2 - 3\gamma_m^2 - (2-\nu)(m\pi\phi)^2)\cosh(\beta_m)\cos(\gamma_m) +$$
$$\gamma_m(\gamma_m^2 - 3\beta_m^2 + (2-\nu)(m\pi\phi)^2)\sinh(\beta_m)\sin(\gamma_m)\,] = 0 . \qquad (3.9)$$

Equation (3.9) is used to determine eigenvalues for the free vibration of the thin

SSSF plate when $\delta_m^2 < \Delta_m$. Once an eigenvalue is calculated, the associated mode shape can be obtained by substituting

$$B_m = (\beta_m^2 - \gamma_m^2 - \nu(m\pi\phi)^2)\cosh(\beta_m)\sin(\gamma_m) + 2\beta_m\gamma_m\sinh(\beta_m)\cos(\gamma_m) \quad (3.10)$$

and

$$C_m = -(\beta_m^2 - \gamma_m^2 - \nu(m\pi\phi)^2)\sinh(\beta_m)\cos(\gamma_m) + 2\beta_m\gamma_m\cosh(\beta_m)\sin(\gamma_m) \quad (3.11)$$

into the explicit solution for the plate which is given by equations (3.8) and (2.16). Equations (3.10) and (3.11) represent the eigenvector values associated with an eigenvalue. Note that A_m and D_m are zero. The remaining case solutions are obtained by following the same procedure described above.

3.1.2 Case 2 Solution

Two imaginary and two real roots result when $\delta_m^2 > \Delta_m$ and $\Delta_m < 0$ in equation (3.3). These roots are defined by $\pm\,\beta_m$ and $\pm\,\gamma_m i$, which yield a general solution of the form

$$Y_m(\eta) = A_m\sinh(\beta_m\eta) + B_m\cosh(\beta_m\eta) + C_m\sin(\gamma_m\eta) + D_m\cos(\gamma_m\eta) \quad (3.12)$$

where

$$\beta_m = \phi\sqrt{\sqrt{\delta_m^2 - \Delta_m} + \delta_m}$$

and

$$\gamma_m = \phi\sqrt{\sqrt{\delta_m^2 - \Delta_m} - \delta_m}\,.$$

The first and third terms of the solution are odd while the second and fourth terms are even.

The procedure used to determine constants A_m, B_m, C_m, and D_m in section 3.1.1 is repeated here. Equations (3.4) and (3.5), which represent the pinned edge boundary conditions at $\eta = 0$, are enforced by eliminating the even terms in equation (3.12). Therefore B_m and D_m equal zero. The remaining odd terms are substituted into equations (3.6) and (3.7) to enforce the free edge at $\eta = 1$. The resulting homogeneous algebraic equations are rearranged, yielding

$$A_m\left[\beta_m^2-\nu\,(m\pi\phi)^2\right]\sinh(\beta_m)\ -\ C_m\left[\gamma_m^2+\nu\,(m\pi\phi)^2\right]\sin(\gamma_m)\ =0$$

and

$$A_m\left[\beta_m^2-(2-\nu)\,(m\pi\phi)^2\right]\beta_m\cosh(\beta_m)-C_m\left[\gamma_m^2+(2-\nu)\,(m\pi\phi)^2\right]\gamma_m\cos(\gamma_m)=0\,.$$

This system of linear equations, which has no unique solution for A_m and C_m, is put into matrix form. The determinant of the coefficient matrix is set to zero, giving

$$\beta_m\cosh(\beta_m)\sin(\gamma_m)\left[\beta_m^2-(2-\nu)\,(m\pi\phi)^2\right]\left[\gamma_m^2+\nu\,(m\pi\phi)^2\right]$$

$$-\ \gamma_m\cos(\gamma_m)\sinh(\beta_m)\left[\gamma_m^2+(2-\nu)\,(m\pi\phi)^2\right]\left[\beta_m^2-\nu\,(m\pi\phi)^2\right]\ =0\,. \qquad (3.13)$$

Equation (3.13) is used to determine eigenvalues when $\delta_m^2 > \Delta_m$ and $\Delta_m < 0$. Once an eigenvalue is calculated, the associated mode shape can be obtained by substituting

$$A_m\ =\left(\gamma_m^2+\nu\,(m\pi\phi)^2\right)\sin(\gamma_m) \qquad (3.14)$$

and

$$C_m\ =\left(\beta_m^2-\nu\,(m\pi\phi)^2\right)\sinh(\beta_m) \qquad (3.15)$$

into the explicit solution for the plate which is given by equations (3.12) and (2.16).

3.1.3 Case 3 Solution

Four distinct real roots result when $\delta_m^2 > \Delta_m$ and $\Delta_m > 0$ in equation (3.3). These roots are defined by $\pm\,\beta_m$ and $\pm\,\gamma_m$, which yield a general solution of the form

$$Y_m(\eta)\ =A_m\sinh(\beta_m\eta)\ +\ B_m\cosh(\beta_m\eta)\ +\ C_m\sinh(\gamma_m\eta)\ +\ D_m\cosh(\gamma_m\eta) \qquad (3.16)$$

where

$$\beta_m\ =\phi\sqrt{\delta_m+\sqrt{\delta_m^2-\Delta_m}}$$

and

$$\gamma_m\ =\phi\sqrt{\delta_m-\sqrt{\delta_m^2-\Delta_m}}\,.$$

The first and third terms of the solution are odd while the second and fourth terms are even.

Constants B_m and D_m become zero in order to satisfy the pinned edge boundary conditions at $\eta = 0$. The odd terms in equation (3.16) are substituted into equations (3.6) and (3.7) to enforce the free edge boundary conditions at $\eta = 1$. The resulting homogeneous algebraic equations are rearranged, yielding

$$A_m\left[\beta_m^2 - \nu\,(m\pi\phi)^2\right]\sinh(\beta_m) + C_m\left[\gamma_m^2 - \nu\,(m\pi\phi)^2\right]\sinh(\gamma_m) = 0$$

and

$$A_m\left[\beta_m^2 - (2-\nu)(m\pi\phi)^2\right]\beta_m\cosh(\beta_m) + C_m\left[\gamma_m^2 - (2-\nu)(m\pi\phi)^2\right]\gamma_m\cosh(\gamma_m) = 0.$$

This system of linear homogeneous equations of A_m and C_m is put into matrix form. The determinant of the coefficient matrix is set to zero, giving

$$\begin{aligned}&\beta_m\cosh(\beta_m)\sinh(\gamma_m)\left[\beta_m^2 - (2-\nu)(m\pi\phi)^2\right]\left[\gamma_m^2 - \nu\,(m\pi\phi)^2\right]\\ &- \gamma_m\cosh(\gamma_m)\sinh(\beta_m)\left[\gamma_m^2 - (2-\nu)(m\pi\phi)^2\right]\left[\beta_m^2 - \nu\,(m\pi\phi)^2\right] = 0. \end{aligned} \tag{3.17}$$

Equation (3.17) is used to determine eigenvalues when $\delta_m^2 > \Delta_m$ and $\Delta_m > 0$. Once an eigenvalue is calculated, the associated mode shape can be obtained by substituting

$$A_m = \left(\gamma_m^2 - \nu\,(m\pi\phi)^2\right)\sinh(\gamma_m) \tag{3.18}$$

and

$$C_m = -\left(\beta_m^2 - \nu\,(m\pi\phi)^2\right)\sinh(\beta_m) \tag{3.19}$$

into the explicit solution for the plate which is given by equations (3.16) and (2.16).

Exact eigenvalues for plates of specific composition, aspect ratio, and in-plane load are numerically calculated by considering the left sides of equations (3.9), (3.13), and (3.17) to be functions of λ^2. Eigenvalue (λ^2) versus determinant value ($f(\lambda^2)$) data is generated so that possible root locations can be determined. The bisection method is then used to obtain accurate roots.

3.2 The SSSV Building Block

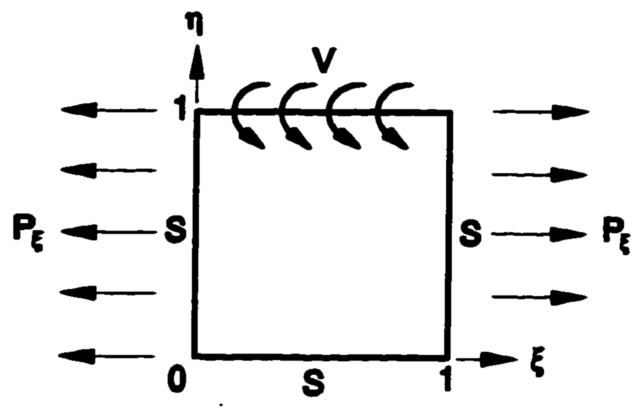

Figure 3.3 The SSSV building block under unilateral in-plane load.

The pinned edge boundary conditions at $\xi = 0$ and $\xi = 1$ of the SSSV building block, shown in Figure 3.3, are automatically satisfied by Lévy-type solution (2.16). This is the same Lévy-type solution used in section 3.1 for the SSSF plate. Hence, derivations of the case solutions here will be similar to those presented in the previous section. Separating the ξ and η variables in equation (2.1) (the governing partial differential equation of motion) produces equation (3.2) (an ordinary differential equation of $Y_m(\eta)$) whose characteristic roots are defined by equation (3.3). Real, imaginary, and complex roots can be obtained from equation (3.3). Consequently, three different harmonic general solutions exist for $Y_m(\eta)$. The case solutions are equations (3.8), (3.12), and (3.16) in sections 3.1.1, 3.1.2, and 3.1.3 respectively.

The undetermined coefficients A_m, B_m, C_m, and D_m in the above noted case solutions are found by enforcing four boundary condition equations. These derive from the simply supported edge at $\eta = 0$ and the zero shear force edge at $\eta = 1$. The separation of variables gives boundary conditions in terms of $Y_m(\eta)$. First, Lévy-type solution (2.16) is substituted into equation (2.9) and evaluated at $\eta = 0$, giving

$$\sum_{m=1,2,3}^{\infty} Y_m(0)\,\sin(m\pi\xi) = 0$$

and

$$\sum_{m=1,2,3}^{\infty} Y_m''(0)\,\sin(m\pi\xi) = 0\ .$$

Since $\sin(m\pi\xi)$ cannot equal zero for all values of ξ in the above equations, the evaluated functions of $Y_m(\eta)$ must equal zero for any value of m. The above equations become

$$Y_m(0) = 0 \tag{3.20}$$

and

$$Y_m''(0) = 0\ , \tag{3.21}$$

which are used to enforce the simply supported edge at $\eta = 0$. Since the edge at $\eta = 0$ is pinned in both the SSSF and SSSV plates, we expect coefficients preceding even terms to become zero, as seen in section 3.1.

The zero shear force edge at $\eta = 1$ is examined next. Lévy-type solution (2.16) is substituted into the harmonic slope function,

$$\frac{\partial W(\xi,\eta)}{\partial \eta} = \sum_{m=1,2,3}^{\infty} E_m \sin(m\pi\xi)\ ,$$

and the zero shear force equation,

$$\frac{\partial^3 W(\xi,\eta)}{\partial \eta^3} + (2-\nu)\phi^2 \frac{\partial^3 W(\xi,\eta)}{\partial \eta\, \partial \xi^2} = 0\ .$$

Note that the harmonic slope function is a Fourier sine series; the same type of series as the Lévy-type solution. The resulting equations are evaluated at $\eta = 1$ and rearranged, giving

$$\sum_{m=1,2,3}^{\infty} Y_m'(1)\sin(m\pi\xi) = \sum_{m=1,2,3}^{\infty} E_m \sin(m\pi\xi)$$

and

$$\sum_{m=1,2,3}^{\infty} Y_m'''(1)\sin(m\pi\xi) - \sum_{m=1,2,3}^{\infty} Y_m'(1)(2-\nu)(m\pi\phi)^2\sin(m\pi\xi) = 0 \,.$$

The preceding two equations are true if and only if the coefficients in the Fourier sine series are equivalent. This allows us to simplify the equations to

$$Y_m'(1) = E_m \tag{3.22}$$

and

$$Y_m'''(1) = E_m(2-\nu)(m\pi\phi)^2 \,. \tag{3.23}$$

Equations (3.2), (3.3), and (3.20) to (3.23) are exploited in the following sections to specifically obtain solutions for $Y_m(\eta)$. The only difference between the SSSF and SSSV plates is the edge type at $\eta = 1$. Hence, the following case solution derivations are identical to those presented in section 3.1 with boundary equations (3.6) and (3.7) being replaced by (3.22) and (3.23).

3.2.1 Case 1 Solution

Four distinct complex roots result when $\delta_m^2 < \Delta_m$ in equation (3.3). The roots are defined by $\pm\beta_m \pm \gamma_m i$, giving general solution (3.8) of section 3.1.1. The first and last terms of the solution are eliminated upon enforcing boundary equations (3.20) and (3.21) for the pinned edge at $\eta = 0$. The simplified solution is substituted into equations (3.22) and (3.23). The resulting equations are rearranged, giving

$$B_m(\beta_m\cosh(\beta_m)\cos(\gamma_m) - \gamma_m\sinh(\beta_m)\sin(\gamma_m))$$
$$+ C_m(\beta_m\sinh(\beta_m)\sin(\gamma_m) + \gamma_m\cosh(\beta_m)\cos(\gamma_m)) = E_m$$

and

$$B_m\left(\beta_m(\beta_m^2-3\gamma_m^2)\cosh(\beta_m)\cos(\gamma_m) - \gamma_m(3\beta_m^2-\gamma_m^2)\sinh(\beta_m)\sin(\gamma_m)\right) +$$
$$C_m\left(\beta_m(\beta_m^2-3\gamma_m^2)\sinh(\beta_m)\sin(\gamma_m) + \gamma_m(3\beta_m^2-\gamma_m^2)\cosh(\beta_m)\cos(\gamma_m)\right) = (2-\nu)(m\pi\phi)^2E_m$$

respectively. This system of equations is arranged in matrix form so that Cramer's Rule can be used to easily solve for constants B_m and C_m. The constants are

$$B_m = E_m\left[\frac{\beta_m(\beta_m^2-3\gamma_m^2)\sinh(\beta_m)\sin(\gamma_m)+\gamma_m(3\beta_m^2-\gamma_m^2)\cosh(\beta_m)\cos(\gamma_m)}{2\beta_m\gamma_m(\beta_m^2+\gamma_m^2)(\sinh^2(\beta_m)+\cos^2(\gamma_m))}\right]$$

$$- E_m\left[\frac{(2-\nu)(m\pi\phi)^2(\beta_m\sinh(\beta_m)\sin(\gamma_m)+\gamma_m\cosh(\beta_m)\cos(\gamma_m))}{2\beta_m\gamma_m(\beta_m^2+\gamma_m^2)(\sinh^2(\beta_m)+\cos^2(\gamma_m))}\right] \qquad (3.24)$$

and

$$C_m = E_m\left[\frac{(2-\nu)(m\pi\phi)^2(\beta_m\cosh(\beta_m)\cos(\gamma_m)-\gamma_m\sinh(\beta_m)\sin(\gamma_m))}{2\beta_m\gamma_m(\beta_m^2+\gamma_m^2)(\sinh^2(\beta_m)+\cos^2(\gamma_m))}\right]$$

$$- E_m\left[\frac{\beta_m(\beta_m^2-3\gamma_m^2)\cosh(\beta_m)\cos(\gamma_m)-\gamma_m(3\beta_m^2-\gamma_m^2)\sinh(\beta_m)\sin(\gamma_m)}{2\beta_m\gamma_m(\beta_m^2+\gamma_m^2)(\sinh^2(\beta_m)+\cos^2(\gamma_m))}\right]. \qquad (3.25)$$

All four constants in equation (3.8) are now known in terms of E_m. Remember that A_m and D_m are zero. Slope parameter E_m controls the building block's amplitude in each case solution.

3.2.2 Case 2 Solution

Two imaginary and two real roots result when $\delta_m^2 > \Delta_m$ and $\Delta_m < 0$ in equation (3.3). The roots are defined by $\pm\,\beta_m$ and $\pm\,\gamma_m i$, giving general solution (3.12) of section 3.1.2. The second and fourth terms of the solution are eliminated upon enforcing boundary equations (3.20) and (3.21) for the pinned edge at $\eta = 0$. The remaining odd terms in equation (3.12) are substituted into equations (3.22) and (3.23) to enforce the slip shear edge at $\eta = 1$. The resulting algebraic equations are rearranged, yielding

$$A_m\beta_m\cosh(\beta_m) + C_m\gamma_m\cos(\gamma_m) = E_m$$

and

$$A_m\beta_m^3\cosh(\beta_m) - C_m\gamma_m^3\cos(\gamma_m) = (2-\nu)(m\pi\phi)^2E_m$$

respectively. Solving for A_m and C_m gives

$$A_m = E_m \left[\frac{\gamma_m^2 + (2-\nu)(m\pi\phi)^2}{\beta_m(\beta_m^2+\gamma_m^2)\cosh(\beta_m)} \right] \tag{3.26}$$

and

$$C_m = E_m \left[\frac{\beta_m^2 - (2-\nu)(m\pi\phi)^2}{\gamma_m(\beta_m^2+\gamma_m^2)\cos(\gamma_m)} \right]. \tag{3.27}$$

Remember that B_m and D_m are zero.

3.2.3 Case 3 Solution

Four distinct real roots result when $\delta_m^2 > \Delta_m$ and $\Delta_m > 0$ in equation (3.3). The roots are defined by $\pm\beta_m$ and $\pm\gamma_m$, giving general solution (3.16) of section 3.1.3. The second and fourth terms of the solution are eliminated upon enforcing boundary equations (3.20) and (3.21) for the pinned edge at $\eta = 0$. The remaining odd terms in equation (3.16) are substituted into equations (3.22) and (3.23) to enforce the slip shear edge at $\eta = 1$. The resulting algebraic equations are rearranged, yielding

$$A_m\beta_m\cosh(\beta_m) + C_m\gamma_m\cosh(\gamma_m) = E_m$$

and

$$A_m\beta_m^3\cosh(\beta_m) + C_m\gamma_m^3\cosh(\gamma_m) = (2-\nu)(m\pi\phi)^2E_m$$

respectively. This leads to

$$A_m = E_m \left[\frac{(2-\nu)(m\pi\phi)^2 - \gamma_m^2}{\beta_m(\beta_m^2-\gamma_m^2)\cosh(\beta_m)} \right] \tag{3.28}$$

and

$$C_m = E_m \left[\frac{\beta_m^2 - (2-\nu)(m\pi\phi)^2}{\gamma_m(\beta_m^2-\gamma_m^2)\cosh(\gamma_m)} \right]. \tag{3.29}$$

Remember that B_m and D_m are zero.

3.3 The SSWR Building Block

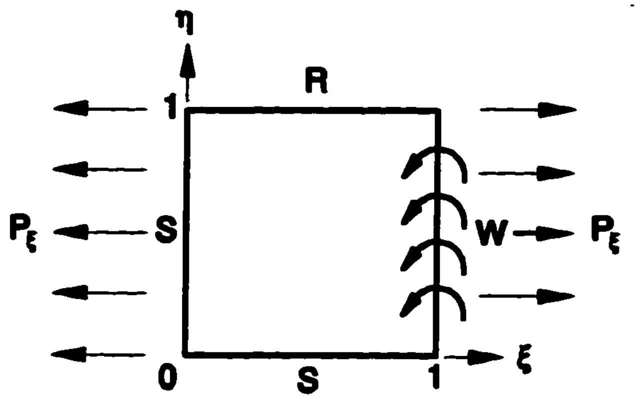

Figure 3.4 The SSWR building block under unilateral in-plane load.

Consider the plate presented in Figure 3.4. Lévy-type solution (2.22) satisfies the boundary conditions of the pinned edge at $\eta = 0$ and the slip shear edge at $\eta = 1$. Substituting equation (2.22) into the governing equation of motion, equation (2.1), gives an explicit solution of the form

$$\sum_{n=1,3,5}^{\infty}\left[\phi^4 Y_n''''(\xi) - 2\phi^2\left(\left(\frac{n\pi}{2}\right)^2 - \frac{P_\xi}{2}\right)Y_n''(\xi) + \left(\left(\frac{n\pi}{2}\right)^4 - \lambda^4\phi^4\right)Y_n(\xi)\right]\sin\left(\frac{n\pi\eta}{2}\right) = 0\,. \tag{3.30}$$

The function of ξ within the square brackets must equal zero, for any value of n, for equation (3.30) to be valid. Dividing through by ϕ^4 and separating variables produces an ordinary homogeneous differential equation of the form

$$Y_n''''(\xi) - \frac{2\delta_n}{\phi^2}Y_n''(\xi) + \frac{\Delta_n}{\phi^4}Y_n(\xi) = 0 \tag{3.31}$$

where

$$\delta_n = \left(\frac{n\pi}{2}\right)^2 - \frac{P_\xi}{2}$$

and

$$\Delta_n = \left(\frac{n\pi}{2}\right)^4 - \lambda^4\phi^4 .$$

The characteristic roots of equation (3.31) are defined by

$$r = \pm\frac{1}{\phi}\sqrt{\delta_n \pm \sqrt{\delta_n^2 - \Delta_n}} . \tag{3.32}$$

Real, imaginary, and complex roots can be obtained from equation (3.32) depending upon the values of δ_n and Δ_n.

General solutions for $Y_n(\xi)$ are easily obtained by the method of undetermined coefficients. Each general solution will contain four terms of the form

$$C\, e^{r\xi}$$

(where C is a coefficient and r a characteristic root) since equation (3.31) is a fourth order differential equation. The coefficients are defined by enforcing four boundary conditions. The simply supported edge at $\xi = 0$ and the zero displacement edge at $\xi = 1$ provide the expressions needed. The boundary relations, originally functions of $W(\xi,\eta)$, can be expressed in terms of $Y_n(\xi)$ through the separation of variables.

The Lévy-type solution, equation (2.22), is first substituted into equation (2.8) and evaluated at $\xi = 0$, giving

$$\sum_{n=1,3,5}^{\infty} Y_n(0)\, \sin\left(\frac{n\pi\eta}{2}\right) = 0$$

and

$$\sum_{n=1,3,5}^{\infty} Y_n''(0)\, \sin\left(\frac{n\pi\eta}{2}\right) = 0 .$$

The evaluated functions of $Y_n(\xi)$ must equal zero for any value of n. Therefore,

$$Y_n(0) = 0 \tag{3.33}$$

and

$$Y_n''(0) = 0 \tag{3.34}$$

are the reduced boundary conditions of the simply supported edge at $\xi = 0$. Section 3.1.1 showed that only odd trigonometric terms satisfy pinned edge boundary conditions at

$\xi = 0$. Since equations (3.33) and (3.34) are equivalent to equations (3.4) and (3.5) respectively, the even terms in the following case solutions will vanish.

The boundary conditions for the zero displacement edge at $\xi = 1$ are defined by

$$W(\xi,\eta) = 0$$

and

$$-\frac{D}{a}\left(\frac{\partial^2 W(\xi,\eta)}{\partial \xi^2} + \frac{\nu}{\phi^2}\frac{\partial^2 W(\xi,\eta)}{\partial \eta^2}\right) = \sum_{n=1,3,5}^{\infty} E_n \sin\left(\frac{n\pi\eta}{2}\right).$$

The trigonometric term used for the harmonic moment function is identical to that found in the Lévy-type solution. The left hand side of the moment condition is equation (2.4) and is simplified in two stages. First, the -D/a constant is absorbed into the currently undetermined Fourier coefficient E_n. Then, the zero displacement condition is used to eliminate the $\partial^2 W(\xi,\eta)/\partial\eta^2$ term. Note that it is logical to conclude that $\partial^2 W(1,\eta)/\partial\eta^2$ and $\partial W(1,\eta)/\partial\eta$ will equal zero if $W(1,\eta)$ is equal to zero. This is similar to stating that the slope and concavity of a horizontal line are zero. Separating the variables begins by substituting Lévy-type solution (2.22) into the reduced equations. Evaluating the resulting equations at $\xi = 1$ and rearranging gives

$$\sum_{n=1,3,5}^{\infty} Y_n(1) \sin\left(\frac{n\pi\eta}{2}\right) = 0$$

and

$$\sum_{n=1,3,5}^{\infty} Y_n''(1) \sin\left(\frac{n\pi\eta}{2}\right) = \sum_{n=1,3,5}^{\infty} E_n \sin\left(\frac{n\pi\eta}{2}\right).$$

The preceding two equations are further simplified to

$$Y_n(1) = 0 \qquad (3.35)$$

and

$$Y_n''(1) = E_n\,. \qquad (3.36)$$

Equations (3.31) to (3.36) are implemented in the following sections to specifically obtain solutions for $Y_n(\xi)$.

3.3.1 Case 1 Solution

The similarities between equations (3.32) and (3.3) should cause one to speculate that the first three case solutions of the current plate will correspond to those derived in section 3.1. Four distinct complex roots are obtained when $\delta_n^2 < \Delta_n$ in equation (3.32). These roots are defined by $\pm\,\beta_n \pm \gamma_n i$, which give a general solution of the form

$$Y_n(\xi) = A_n \sinh(\beta_n\xi)\sin(\gamma_n\xi) + B_n \sinh(\beta_n\xi)\cos(\gamma_n\xi)$$

$$+ C_n \cosh(\beta_n\xi)\sin(\gamma_n\xi) + D_n \cosh(\beta_n\xi)\cos(\gamma_n\xi) \tag{3.37}$$

where

$$\beta_n = \frac{1}{\phi}\sqrt{\frac{\sqrt{\Delta_n} + \delta_n}{2}}$$

and

$$\gamma_n = \frac{1}{\phi}\sqrt{\frac{\sqrt{\Delta_n} - \delta_n}{2}} \, .$$

The first and last terms of the solution are even while the two middle terms are odd.

Constants A_n, B_n, C_n, and D_n are determined by enforcing equations (3.33) to (3.36). Substituting solution (3.37) into conditions (3.33) and (3.34) yields

$$D_n = 0$$

and

$$D_n(\beta_n^2 - \gamma_n^2) + 2A_n\beta_n\gamma_n = 0 \, .$$

Thus, constants A_n and D_n, which are associated with the even terms in equation (3.37), are zero. In the remaining case solutions, the even terms will simply be removed to enforce the pinned edge. Next, the simplified solution is substituted into equations (3.35) and (3.36). The resulting homogeneous algebraic equations are

$$B_n \sinh(\beta_n)\cos(\gamma_n) + C_n \cosh(\beta_n)\sin(\gamma_n) = 0$$

and

$$B_n\left[(\beta_n^2-\gamma_n^2)\sinh(\beta_n)\cos(\gamma_n)-2\beta_n\gamma_n\cosh(\beta_n)\sin(\gamma_n)\right]$$
$$+\ C_n\left[(\beta_n^2-\gamma_n^2)\cosh(\beta_n)\sin(\gamma_n)+2\beta_n\gamma_n\sinh(\beta_n)\cos(\gamma_n)\right]=E_n\ .$$

Solving for B_n and C_n gives

$$B_n = E_n\left[\frac{\cosh(\beta_n)\sin(\gamma_n)}{2\beta_n\gamma_n(\cos^2(\gamma_n)-\cosh^2(\beta_n))}\right] \tag{3.38}$$

and

$$C_n = -E_n\left[\frac{\sinh(\beta_n)\cos(\gamma_n)}{2\beta_n\gamma_n(\cos^2(\gamma_n)-\cosh^2(\beta_n))}\right]. \tag{3.39}$$

Note that the bending moment parameter E_n controls the building block's amplitude in all case solutions.

3.3.2 Case 2 Solution

Two imaginary and two real roots are obtained when $\delta_n^2 > \Delta_n$ and $\Delta_n < 0$ in equation (3.32). These roots are defined by $\pm\,\beta_n$ and $\pm\,\gamma_n i$, which give a general solution of

$$Y_n(\xi) = A_n\sinh(\beta_n\xi) + B_n\cosh(\beta_n\xi) + C_n\sin(\gamma_n\xi) + D_n\cos(\gamma_n\xi) \tag{3.40}$$

where

$$\beta_n = \frac{1}{\phi}\sqrt{\sqrt{\delta_n^2-\Delta_n}+\delta_n}$$

and

$$\gamma_n = \frac{1}{\phi}\sqrt{\sqrt{\delta_n^2-\Delta_n}-\delta_n}\ .$$

The first and third terms of the solution are odd while the second and fourth terms are even.

The procedure used to determine constants A_n, B_n, C_n, and D_n in section 3.3.1 is repeated here. Setting B_n and D_n equal to zero eliminates the even terms and satisfies the pinned edge boundary conditions at $\xi = 0$. The remaining odd terms in equation (3.40) are substituted into equations (3.35) and (3.36) to enforce the zero displacement edge at $\xi = 1$. The resulting algebraic equations are

$$A_n \sinh(\beta_n) + C_n \sin(\gamma_n) = 0$$

and

$$A_n \beta_n^2 \sinh(\beta_n) - C_n \gamma_n^2 \sin(\gamma_n) = E_n \ .$$

This leads to

$$A_n = \frac{E_n}{(\beta_n^2 + \gamma_n^2)\sinh(\beta_n)} \tag{3.41}$$

and

$$C_n = -\frac{E_n}{(\beta_n^2 + \gamma_n^2)\sin(\gamma_n)} \ . \tag{3.42}$$

3.3.3 Case 3 Solution

Four distinct real roots result when $\delta_n^2 > \Delta_n$ and $\Delta_n > 0$ and $\delta_n > 0$ in equation (3.32). These roots are defined by $\pm\,\beta_n$ and $\pm\,\gamma_n$, which give a general solution of

$$Y_n(\xi) = A_n \sinh(\beta_n \xi) + B_n \cosh(\beta_n \xi) + C_n \sinh(\gamma_n \xi) + D_n \cosh(\gamma_n \xi) \tag{3.43}$$

where

$$\beta_n = \frac{1}{\phi}\sqrt{\delta_n + \sqrt{\delta_n^2 - \Delta_n}}$$

and

$$\gamma_n = \frac{1}{\phi}\sqrt{\delta_n - \sqrt{\delta_n^2 - \Delta_n}} \ .$$

The first and third terms of the solution are odd while the second and fourth terms are even.

Constants B_n and D_n must equal zero in order to satisfy the pinned edge boundary conditions at $\xi = 0$. The remaining odd terms in equation (3.43) are substituted into equations (3.35) and (3.36) to enforce the zero displacement edge at $\xi = 1$. The resulting algebraic equations are

$$A_n \sinh(\beta_n) + C_n \sinh(\gamma_n) = 0$$

and

$$A_n \beta_n^2 \sinh(\beta_n) + C_n \gamma_n^2 \sinh(\gamma_n) = E_n \ .$$

Solving these equations for A_n and C_n leads to

$$A_n = \frac{E_n}{(\beta_n^2 - \gamma_n^2)\sinh(\beta_n)} \tag{3.44}$$

and

$$C_n = -\frac{E_n}{(\beta_n^2 - \gamma_n^2)\sinh(\gamma_n)} \ . \tag{3.45}$$

3.3.4 Case 4 Solution

As expected, the first three general solutions of the SSWR plate (equations (3.37), (3.40), and (3.43)) are comparable to those of the SSSF plate (equations (3.8), (3.12), and (3.16)). The following differences exist between the two sets of general solutions: coordinate η is replaced by ξ, index m is replaced by n, and plate aspect ratio ϕ is replaced by $1/\phi$. In the new fourth case, four distinct imaginary roots are obtained when $\delta_n^2 > \Delta_n$ and $\Delta_n > 0$ and $\delta_n < 0$ in equation (3.32). These roots are defined by $\pm\, \beta_n i$ and $\pm\, \gamma_n i$, giving a general solution of the form

$$Y_n(\xi) = A_n \sin(\beta_n \xi) + B_n \cos(\beta_n \xi) + C_n \sin(\gamma_n \xi) + D_n \cos(\gamma_n \xi) \tag{3.46}$$

where

$$\beta_n = \frac{1}{\phi}\sqrt{-\delta_n - \sqrt{\delta_n^2 - \Delta_n}}$$

and

$$\gamma_n = \frac{1}{\phi}\sqrt{-\delta_n + \sqrt{\delta_n^2 - \Delta_n}}\ .$$

The first and third terms of the solution are odd while the second and fourth terms are even.

Constants B_n and D_n must equal zero in order to satisfy the pinned edge boundary conditions at $\xi = 0$. The remaining odd terms in equation (3.46) are substituted into equations (3.35) and (3.36) to enforce the zero displacement edge at $\xi = 1$. The resulting algebraic equations are

$$A_n \sin(\beta_n) + C_n \sin(\gamma_n) = 0$$

and

$$-A_n \beta_n^2 \sin(\beta_n) - C_n \gamma_n^2 \sin(\gamma_n) = E_n\ .$$

Expressing this system of equations in matrix form and using Cramer's Rule to solve for constants A_n and C_n gives

$$A_n = \frac{E_n}{(\gamma_n^2 - \beta_n^2)\sin(\beta_n)} \tag{3.47}$$

and

$$C_n = -\frac{E_n}{(\gamma_n^2 - \beta_n^2)\sin(\gamma_n)}\ . \tag{3.48}$$

3.4 The SWSR Building Block

Lévy-type solution (2.16) automatically satisfies the pinned edge boundary conditions at $\xi = 0$ and $\xi = 1$ of the building block shown in Figure 3.5. This is the same Lévy-type solution used in sections 3.1 and 3.2. The ξ and η variables in equation (2.1) are separated to produce equation (3.2), a fourth order ordinary homogeneous differential equation in η. The real, imaginary, and complex characteristic roots calculated from equation (3.3) lead to three unique general solutions for $Y_m(\eta)$. These general or case solutions are defined by equations (3.8), (3.12), and (3.16).

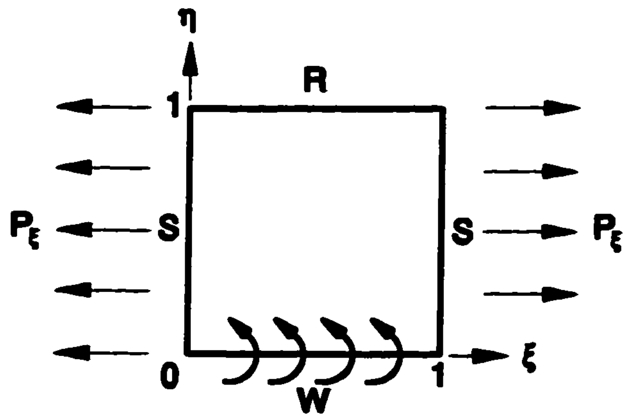

Figure 3.5 The SWSR building block under unilateral in-plane load.

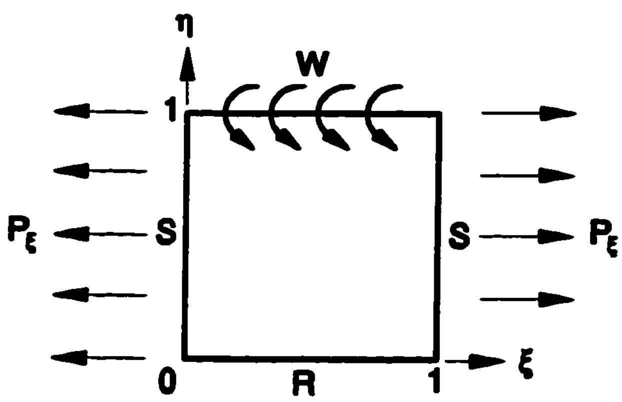

Figure 3.6 The SRSW building block under unilateral in-plane load.

The constants in the case solutions are determined by enforcing the boundary conditions at $\eta = 0$ and $\eta = 1$. Recall that the pinned edge boundary conditions at $\eta = 0$ in the SSSF and SSSV plates were enforced by simply eliminating the even terms. This phenomenon also extends to a slip shear edge at $\eta = 0$ where the odd terms are nullified instead, as shown in section 2.3. This simplification is utilized in the current problem upon exchanging the edge conditions at $\eta = 0$ with those at $\eta = 1$. The η-axis of the final solution is later transformed appropriately. In essence, a solution for the SWSR plate is found by examining the SRSW plate of Figure 3.6, whose constants are easily obtainable.

The four boundary conditions required to solve for $Y_m(\eta)$ in equation (3.2) are provided by the slip shear edge at $\eta = 0$ and the zero displacement edge at $\eta = 1$ of the SRSW plate. The boundary conditions, originally functions of $W(\xi,\eta)$, are expressed in terms of $Y_m(\eta)$ so that they can be directly applied to the general solutions. This is done through the separation of variables. First, Lévy-type solution (2.16) is substituted into equation (2.15) and evaluated at $\eta = 0$, giving

$$\sum_{m=1,2,3}^{\infty} Y_m'(0)\ \sin(m\pi\xi) = 0$$

and

$$\sum_{m=1,2,3}^{\infty} Y_m'''(0)\ \sin(m\pi\xi) = 0\ .$$

Since $\sin(m\pi\xi)$ cannot equal zero for all values of ξ in the above equations, the evaluated functions of $Y_m(\eta)$ must equal zero for any value of m. The above equations become

$$Y_m'(0) = 0 \tag{3.49}$$

and

$$Y_m'''(0) = 0\ , \tag{3.50}$$

which are used to enforce the slip shear edge at $\eta = 0$. The zero displacement edge at $\eta = 1$ is examined next. Lévy-type solution (2.16) is substituted into the zero displacement equation

$$W(\xi,\eta) = 0$$

and the harmonic bending moment equation

$$-\frac{D}{b\phi}\left(\frac{\partial^2 W(\xi,\eta)}{\partial\eta^2} + \nu\phi^2\frac{\partial^2 W(\xi,\eta)}{\partial\xi^2}\right) = \sum_{m=1,2,3}^{\infty} E_m \sin(m\pi\xi)\ .$$

The trigonometric term used for the harmonic moment function is identical to that found in the Lévy-type solution. The left hand side of the moment condition is equation (2.4) and is simplified in two stages. First, the $-D/b\phi$ constant is absorbed into the currently undetermined Fourier coefficient E_m. Then, the zero displacement condition is used to eliminate the $\partial^2W(\xi,\eta)/\partial\xi^2$ term. Note that it is logical to conclude that $\partial^2W(\xi,\eta)/\partial\xi^2$ and $\partial W(\xi,\eta)/\partial\xi$ will equal zero if $W(\xi,\eta)$ is equal to zero along $\eta = 1$. This is similar to stating that the slope and concavity of a horizontal line are zero. Lévy-type solution (2.16) is substituted into the reduced equations. Evaluating the resulting equations at $\eta = 1$ and rearranging gives

$$\sum_{m=1,2,3}^{\infty} Y_m(1)\sin(m\pi\xi) = 0$$

and

$$\sum_{m=1,2,3}^{\infty} Y_m''(1)\sin(m\pi\xi) = \sum_{m=1,2,3}^{\infty} E_m\sin(m\pi\xi) .$$

The preceding two equations are further simplified to

$$Y_m(1) = 0 \tag{3.51}$$

and

$$Y_m''(1) = E_m . \tag{3.52}$$

Equations (3.2), (3.3), and (3.49) to (3.52) are exploited in the following sections to specifically obtain solutions for $Y_m(\eta)$ of the SRSW plate. The η-axis of the final SRSW plate solutions are transformed to obtain the SWSR plate solutions.

3.4.1 Case 1 Solution

Four distinct complex roots result when $\delta_m^2 < \Delta_m$ in equation (3.3). The roots are defined by $\pm\ \beta_m \pm \gamma_m i$, giving general solution (3.8) of section 3.1.1.

The constants are determined by enforcing equations (3.49) to (3.52). Substituting solution (3.8) into equations (3.49) and (3.50) yields

$$B_m\beta_m + C_m\gamma_m = 0$$

and

$$B_m\beta_m\left(\beta_m^2 - 3\gamma_m^2\right) - C_m\gamma_m\left(\gamma_m^2 - 3\beta_m^2\right) = 0 \ .$$

Thus, constants B_m and C_m, which are associated with the odd terms in equation (3.8), are zero. One may intuitively conclude that only even terms will satisfy the constraints set by equations (3.49) and (3.50). In the remaining case solutions, the odd terms will simply be removed to enforce the slip shear edge at η = 0. Next, the simplified solution is substituted into equations (3.51) and (3.52). The resulting algebraic equations are

$$A_m \sinh(\beta_m)\sin(\gamma_m) + D_m \cosh(\beta_m)\cos(\gamma_m) = 0$$

and

$$A_m\left[(\beta_m^2 - \gamma_m^2)\sinh(\beta_m)\sin(\gamma_m) + 2\beta_m\gamma_m\cosh(\beta_m)\cos(\gamma_m)\right]$$
$$+ D_m\left[(\beta_m^2 - \gamma_m^2)\cosh(\beta_m)\cos(\gamma_m) - 2\beta_m\gamma_m\sinh(\beta_m)\sin(\gamma_m)\right] = E_m$$

respectively. This system of equations is put into matrix form so that Cramer's Rule can be used to solve for constants A_m and D_m. The constants are

$$A_m = \frac{E_m \cosh(\beta_m)\cos(\gamma_m)}{2\beta_m\gamma_m\left(\sinh^2(\beta_m) + \cos^2(\gamma_m)\right)} \tag{3.53}$$

and

$$D_m = -\frac{E_m \sinh(\beta_m)\sin(\gamma_m)}{2\beta_m\gamma_m\left(\sinh^2(\beta_m) + \cos^2(\gamma_m)\right)} \ . \tag{3.54}$$

Bending moment parameter E_m controls the building block's amplitude. Remember that replacing coordinate η with 1 - η in the SRSW solutions gives the SWSR solutions.

3.4.2 Case 2 Solution

Two imaginary and two real roots result when $\delta_m^2 > \Delta_m$ and $\Delta_m < 0$ in equation (3.3). The roots are defined by $\pm\,\beta_m$ and $\pm\,\gamma_m i$, giving general solution (3.12) of section 3.1.2.

The procedure used to determine coefficients A_m, B_m, C_m, and D_m in section 3.4.1 is repeated here. Setting A_m and C_m equal to zero eliminates the odd terms in equation (3.12) and satisfies the slip shear boundary conditions at η = 0. The remaining even terms are substituted into equations (3.51) and (3.52). Enforcing the zero displacement edge at η = 1 gives algebraic equations of the form

$$B_m \cosh(\beta_m) + D_m \cos(\gamma_m) = 0$$

and

$$B_m \beta_m^2 \cosh(\beta_m) - D_m \gamma_m^2 \cos(\gamma_m) = E_m \, .$$

These equations provide

$$B_m = \frac{E_m}{\left(\beta_m^2 + \gamma_m^2\right)\cosh(\beta_m)} \tag{3.55}$$

and

$$D_m = -\frac{E_m}{\left(\beta_m^2 + \gamma_m^2\right)\cos(\gamma_m)} \, . \tag{3.56}$$

3.4.3 Case 3 Solution

Four distinct real roots result when $\delta_m^2 > \Delta_m$ and $\Delta_m > 0$ in equation (3.3). The roots are defined by $\pm\,\beta_m$ and $\pm\,\gamma_m$, giving general solution (3.16) of section 3.1.3.

Constants A_m and D_m must equal zero in order to satisfy the slip shear boundary conditions at η = 0. The remaining even terms in equation (3.16) are substituted into equations (3.51) and (3.52) to enforce the zero displacement edge at η = 1. The resulting algebraic equations are

$$B_m \cosh(\beta_m) + D_m \cosh(\gamma_m) = 0$$

and

$$B_m \beta_m^2 \cosh(\beta_m) + D_m \gamma_m^2 \cosh(\gamma_m) = E_m \, ,$$

leading to

$$B_m = \frac{E_m}{\left(\beta_m^2 - \gamma_m^2\right)\cosh(\beta_m)} \tag{3.57}$$

and

$$D_m = -\frac{E_m}{\left(\beta_m^2 - \gamma_m^2\right)\cosh(\gamma_m)} \ . \tag{3.58}$$

3.5 The WSSR Building Block

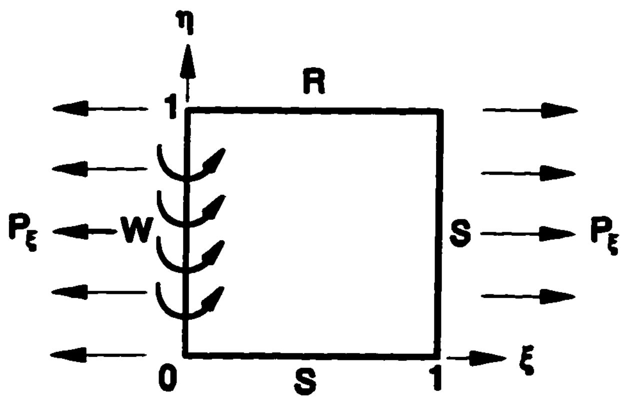

Figure 3.7 The WSSR building block under unilateral in-plane load.

Consider the WSSR building block shown in Figure 3.7. Note that the SSWR plate, shown in Figure 3.4, is similar to the present plate except for the boundary conditions along the edges $\xi = 0$ and $\xi = 1$, which are reversed. Solutions for this plate can be derived from those presented in section 3.3 by simply replacing coordinate ξ with $1 - \xi$. The Lévy-type solution will look like

$$W(\xi,\eta) = \sum_{q=1,3,5}^{\infty} Y_q(1-\xi)\ \sin(q\pi\eta/2) \ .$$

This is equation (2.22) with the ξ coordinate replaced by $1 - \xi$. The following is a brief summary of the individual case solutions.

3.5.1 Case 1 Solution

The first case solution of the WSSR plate arises when $\delta_q^2 < \Delta_q$. It is defined by equation (3.37), where index n is replaced by q and coordinate ξ is replaced by $1 - \xi$. The constants A_q and D_q are zero, and B_q and C_q are defined by equations (3.38) and (3.39) respectively, where index n is replaced by q.

3.5.2 Case 2 Solution

The second case solution of the WSSR plate is obtained when $\delta_q^2 > \Delta_q$ and $\Delta_q < 0$. It is defined by equation (3.40), where index n is replaced by q and coordinate ξ is replaced by $1 - \xi$. The constants B_q and D_q are zero, and A_q and C_q are defined by equations (3.41) and (3.42) respectively, where index n is replaced by q.

3.5.3 Case 3 Solution

The third case solution of the WSSR plate is contemplated when $\delta_q^2 > \Delta_q$ and $\Delta_q > 0$ and $\delta_q > 0$. It is defined by equation (3.43), where index n is replaced by q and coordinate ξ is replaced by $1 - \xi$. The constants B_q and D_q are zero, and A_q and C_q are defined by equations (3.44) and (3.45) respectively, where index n is replaced by q.

3.5.4 Case 4 Solution

The fourth case solution of the WSSR plate is valid when $\delta_q^2 > \Delta_q$ and $\Delta_q > 0$ and $\delta_q < 0$. It is defined by equation (3.46), where index n is replaced by q and coordinate ξ is replaced by $1 - \xi$. The constants B_q and D_q are zero, and A_q and C_q are defined by equations (3.47) and (3.48) respectively, where index n is replaced by q.

3.6 The SRSV Building Block

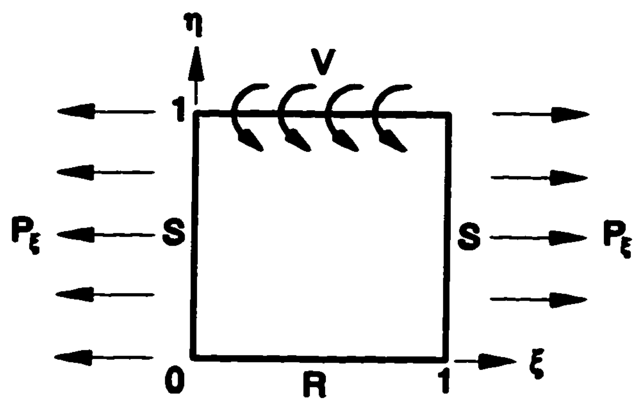

Figure 3.8 The SRSV building block under unilateral in-plane load.

Lévy-type solution (2.16) automatically satisfies the pinned edge boundary conditions at $\xi = 0$ and $\xi = 1$ of the SRSV building block shown in Figure 3.8. This is the same Lévy-type solution used in sections 3.1, 3.2, and 3.4. The ξ and η variables in equation (2.1) are separated to produce equation (3.2), a fourth order ordinary homogeneous differential equation in η. The real, imaginary, and complex characteristic roots of equation (3.3) lead to three unique general solutions for $Y_m(\eta)$. These general or case solutions are defined by equations (3.8), (3.12), and (3.16).

The undetermined coefficients in the case solutions are defined by enforcing the boundary conditions at $\eta = 0$ and $\eta = 1$. The boundary conditions, initially functions of $W(\xi,\eta)$, are expressed in terms of $Y_m(\eta)$ so that they can be directly applied to the general solutions. This is accomplished through the separation of variables. The boundary conditions for a slip shear edge at $\eta = 0$ have already been examined in section 3.4 for the SRSW plate, producing equations (3.49) and (3.50). Enforcing these equations eliminated odd terms in the case solutions. Therefore, only even terms will appear in the following case solutions to satisfy the slip shear boundary conditions at $\eta = 0$. The zero shear force edge at $\eta = 1$ was previously encountered in section 3.2 for the SSSV building block. Since Lévy-type solution (2.16) was used for both the present and aforementioned building block, equations (3.22) and (3.23) can be applied directly to the following case solutions to enforce the zero shear force edge boundary conditions. The above noted equations are exploited in the following sections to obtain solutions for $Y_m(\eta)$ of the SRSV building block.

3.6.1 Case 1 Solution

Four distinct complex roots result when $\delta_m{}^2 < \Delta_m$ in equation (3.3). The roots are defined by $\pm\,\beta_m \pm \gamma_m i$, giving general solution (3.8) of section 3.1.1.

The constants are determined by enforcing equations (3.49), (3.50), (3.22), and (3.23). Setting B_m and C_m equal to zero eliminates the odd terms in equation (3.8), which satisfies the slip shear boundary conditions at $\eta = 0$. The remaining even terms are substituted into equations (3.22) and (3.23). The resulting algebraic equations, evaluated at $\eta = 1$, are

$$\begin{aligned} &A_m(\beta_m\cosh(\beta_m)\sin(\gamma_m) + \gamma_m\sinh(\beta_m)\cos(\gamma_m)) \\ &+ D_m(\beta_m\sinh(\beta_m)\cos(\gamma_m) - \gamma_m\cosh(\beta_m)\sin(\gamma_m)) = E_m \end{aligned}$$

and

$$\begin{aligned} &A_m\left(\beta_m(\beta_m^2-3\gamma_m^2)\cosh(\beta_m)\sin(\gamma_m) + \gamma_m(3\beta_m^2-\gamma_m^2)\sinh(\beta_m)\cos(\gamma_m)\right) + \\ &D_m\left(\beta_m(\beta_m^2-3\gamma_m^2)\sinh(\beta_m)\cos(\gamma_m) - \gamma_m(3\beta_m^2-\gamma_m^2)\cosh(\beta_m)\sin(\gamma_m)\right) = (2-\nu)(m\pi\phi)^2E_m\ . \end{aligned}$$

Expressed in matrix form, and solved for A_m and D_m in terms of E_m, the above equations lead to

$$\begin{aligned} A_m = &\ E_m\left[\frac{\beta_m(\beta_m^2-3\gamma_m^2)\sinh(\beta_m)\cos(\gamma_m)-\gamma_m(3\beta_m^2-\gamma_m^2)\cosh(\beta_m)\sin(\gamma_m)}{-2\beta_m\gamma_m(\beta_m^2+\gamma_m^2)(\sinh^2(\beta_m)+\sin^2(\gamma_m))}\right] \\ &- E_m\left[\frac{(2-\nu)(m\pi\phi)^2(\beta_m\sinh(\beta_m)\cos(\gamma_m)-\gamma_m\cosh(\beta_m)\sin(\gamma_m))}{-2\beta_m\gamma_m(\beta_m^2+\gamma_m^2)(\sinh^2(\beta_m)+\sin^2(\gamma_m))}\right] \end{aligned} \tag{3.59}$$

and

$$D_m = E_m\left[\frac{(2-\nu)(m\pi\phi)^2(\beta_m\cosh(\beta_m)\sin(\gamma_m)+\gamma_m\sinh(\beta_m)\cos(\gamma_m))}{-2\beta_m\gamma_m(\beta_m^2+\gamma_m^2)(\sinh^2(\beta_m)+\sin^2(\gamma_m))}\right]$$

$$-\ E_m\left[\frac{\beta_m(\beta_m^2-3\gamma_m^2)\cosh(\beta_m)\sin(\gamma_m)+\gamma_m(3\beta_m^2-\gamma_m^2)\sinh(\beta_m)\cos(\gamma_m)}{-2\beta_m\gamma_m(\beta_m^2+\gamma_m^2)(\sinh^2(\beta_m)+\sin^2(\gamma_m))}\right]. \quad (3.60)$$

Slope parameter E_m controls the building block's amplitude.

3.6.2 Case 2 Solution

Two imaginary and two real roots result when $\delta_m^2 > \Delta_m$ and $\Delta_m < 0$ in equation (3.3). The roots are defined by $\pm\,\beta_m$ and $\pm\,\gamma_m i$, giving general solution (3.12) of section 3.1.2.

The procedure used to determine coefficients A_m, B_m, C_m, and D_m in section 3.6.1 is repeated here. Setting A_m and C_m equal to zero satisfies the slip shear boundary conditions at $\eta = 0$. The remaining even terms are substituted into equations (3.22) and (3.23). The resulting algebraic equations, evaluated at $\eta = 1$, are

$$B_m\beta_m\sinh(\beta_m) - D_m\gamma_m\sin(\gamma_m) = E_m$$

and

$$B_m\beta_m^3\sinh(\beta_m) + D_m\gamma_m^3\sin(\gamma_m) = (2-\nu)(m\pi\phi)^2E_m .$$

Solving for B_m and D_m gives

$$B_m = E_m\left[\frac{\gamma_m^2 + (2-\nu)(m\pi\phi)^2}{\beta_m(\beta_m^2+\gamma_m^2)\sinh(\beta_m)}\right] \quad (3.61)$$

and

$$D_m = -E_m\left[\frac{\beta_m^2 - (2-\nu)(m\pi\phi)^2}{\gamma_m(\beta_m^2+\gamma_m^2)\sin(\gamma_m)}\right]. \quad (3.62)$$

3.6.3 Case 3 Solution

Four distinct real roots result when $\delta_m{}^2 > \Delta_m$ and $\Delta_m > 0$ in equation (3.3). The roots are defined by $\pm\,\beta_m$ and $\pm\,\gamma_m$, giving general solution (3.16) of section 3.1.3.

Constants A_m and C_m must equal zero in order to satisfy the slip shear boundary conditions at $\eta = 0$. The even terms in equation (3.16) are then substituted into equations (3.22) and (3.23) to enforce the zero shear force edge. The resulting algebraic equations, evaluated at $\eta = 1$, are

$$B_m\,\beta_m \sinh(\beta_m) + D_m\,\gamma_m \sinh(\gamma_m) = E_m$$

and

$$B_m\,\beta_m^3 \sinh(\beta_m) + D_m\,\gamma_m^3 \sinh(\gamma_m) = (2-\nu)(m\pi\phi)^2 E_m$$

Solving for constants B_m and D_m gives

$$B_m = E_m\left[\frac{(2-\nu)(m\pi\phi)^2 - \gamma_m^2}{\beta_m(\beta_m^2-\gamma_m^2)\sinh(\beta_m)}\right] \tag{3.63}$$

and

$$D_m = E_m\left[\frac{\beta_m^2 - (2-\nu)(m\pi\phi)^2}{\gamma_m(\beta_m^2-\gamma_m^2)\sinh(\gamma_m)}\right]. \tag{3.64}$$

3.7 The SRWR Building Block

Consider the SRWR building block presented in Figure 3.9. Lévy-type solution (2.21) satisfies the slip shear boundary conditions at $\eta = 0$ and $\eta = 1$. Substituting equation (2.21) into the governing differential equation of motion, equation (2.1), gives

$$\sum_{n=0,1,2}^{\infty}\left[\phi^4 Y_n''''(\xi) - 2\phi^2\left((n\pi)^2 - \frac{P_\xi}{2}\right)Y_n''(\xi) + \left((n\pi)^4 - \lambda^4\phi^4\right)Y_n(\xi)\right]\cos(n\pi\eta) = 0. \tag{3.65}$$

The function of ξ within the square brackets must equal zero for any value of n.

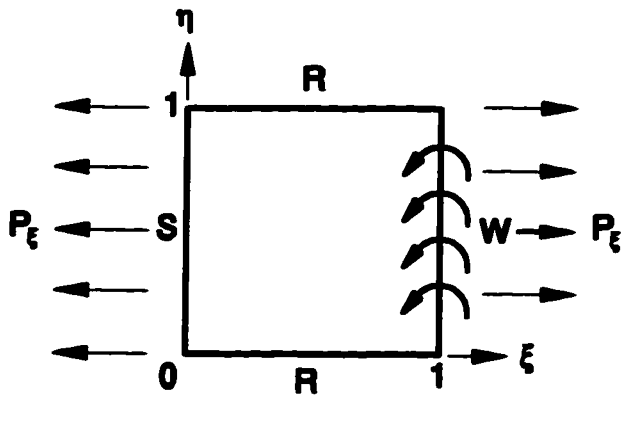

Figure 3.9 The SRWR building block under unilateral in-plane load.

Separating variables and dividing through by ϕ^4 produces

$$Y_n''''(\xi) - \frac{2\delta_n}{\phi^2} Y_n''(\xi) + \frac{\Delta_n}{\phi^4} Y_n(\xi) = 0 \, , \tag{3.66}$$

where

$$\delta_n = (n\pi)^2 - \frac{P_\xi}{2}$$

and

$$\Delta_n = (n\pi)^4 - \lambda^4 \phi^4 \, .$$

Equation (3.66) is an ordinary homogeneous differential equation. General solutions for $Y_n(\xi)$ are easily obtained by the method of undetermined coefficients. Each general solution will contain four terms of the form

$$C \, e^{r\xi} \, ,$$

where C is an undetermined coefficient and r is a characteristic root. The four characteristic roots are defined by

$$r = \pm \frac{1}{\phi} \sqrt{\delta_n \pm \sqrt{\delta_n^2 - \Delta_n}} \, . \tag{3.67}$$

Real, imaginary, and complex roots can be obtained from equation (3.67), depending upon the values of δ_n and Δ_n. Note that characteristic equation (3.67) is the same as the characteristic equation (3.32) in section 3.3. Since general solutions derive from the characteristic roots, equations (3.37), (3.40), (3.43), and (3.46) are appropriate case solutions for the present analysis.

Coefficients are determined by enforcing boundary conditions at $\xi = 0$ and $\xi = 1$. The boundary conditions, initially functions of $W(\xi,\eta)$, are expressed in terms of $Y_n(\xi)$. This is accomplished through the separation of variables and allows the direct application of boundary conditions to the general solutions. The boundary conditions for a pinned edge at $\xi = 0$ were examined in section 3.3 for the SSWR plate, producing equations (3.33) and (3.34). Enforcing these equations eliminated even terms. Therefore, only odd terms are considered here. The boundary conditions for the zero displacement edge at $\xi = 1$ are defined by

$$W(\xi,\eta) = 0$$

and

$$-\frac{D}{a}\left(\frac{\partial^2 W(\xi,\eta)}{\partial \xi^2} + \frac{\nu}{\phi^2}\frac{\partial^2 W(\xi,\eta)}{\partial \eta^2}\right) = \sum_{n=0,1,2}^{\infty} E_n \cos(n\pi\eta) \ .$$

The trigonometric term used for the harmonic moment function is identical to that found in the Lévy-type solution. The left hand side of the moment condition is equation (2.4) and is simplified in two stages. First, the -D/a constant is absorbed into the Fourier coefficient E_n. The zero displacement condition is then used to eliminate the $\partial^2 W(\xi,\eta)/\partial\eta^2$ term. Note that $\partial^2 W(1,\eta)/\partial\eta^2$ and $\partial W(1,\eta)/\partial\eta$ will equal zero if $W(1,\eta)$ equals zero. This is equivalent to stating that the slope and concavity of a horizontal line are zero. Separating the variables begins by substituting Lévy-type solution (2.21) into the reduced equations. Evaluating the resulting equations at $\xi = 1$ and rearranging gives

$$\sum_{n=0,1,2}^{\infty} Y_n(1) \cos(n\pi\eta) = 0$$

and

$$\sum_{n=0,1,2}^{\infty} Y_n''(1) \cos(n\pi\eta) = \sum_{n=0,1,2}^{\infty} E_n \cos(n\pi\eta) \ .$$

The preceding two equations are further simplified to

$$Y_n(1) = 0 \tag{3.68}$$

and

$$Y_n''(1) = E_n \,. \tag{3.69}$$

Equations (3.68) and (3.69) are identical to equations (3.35) and (3.36). In actuality, all equations used to derive solutions for $Y_n(\xi)$ are identical for the SSWR and SRWR plates. Only constants δ_n and Δ_n, used to calculate β_n and γ_n in the general solutions, are slightly different due to the Lévy-type solutions used for the different building blocks. Therefore, solutions derived in section 3.3 are suitable for the SRWR building block. The following sections briefly summarize the individual solutions.

3.7.1 Case 1 Solution

Equation (3.37) is appropriate when $\delta_n^2 < \Delta_n$. Constants δ_n and Δ_n are defined in section 3.7. Constants A_n and D_n are zero, while B_n and C_n are defined by equations (3.38) and (3.39) respectively.

3.7.2 Case 2 Solution

Equation (3.40) is the solution when $\delta_n^2 > \Delta_n$ and $\Delta_n < 0$. Constants δ_n and Δ_n are defined in section 3.7. Constants B_n and D_n are zero, while A_n and C_n are defined by equations (3.41) and (3.42) respectively.

3.7.3 Case 3 Solution

When $\delta_n^2 > \Delta_n$ and $\Delta_n > 0$ and $\delta_n > 0$, the solution is given by equation (3.43). Constants δ_n and Δ_n are defined in section 3.7. Constants B_n and D_n are zero, while A_n and C_n are defined by equations (3.44) and (3.45) respectively.

3.7.4 Case 4 Solution

Equation (3.46) is used when $\delta_n^2 > \Delta_n$ and $\Delta_n > 0$ and $\delta_n < 0$. Constants δ_n and Δ_n are defined in section 3.7. Constants B_n and D_n are zero, while A_n and C_n are defined by equations (3.47) and (3.48) respectively.

3.8 The SVSR Building Block

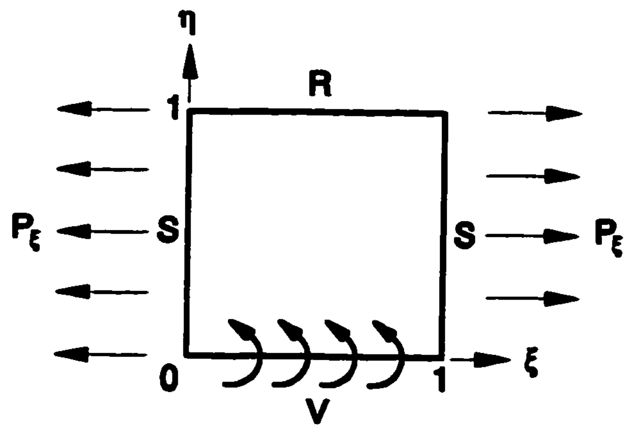

Figure 3.10 The SVSR building block under unilateral in-plane load.

Consider the SVSR building block shown in Figure 3.10. A quick inspection of the SRSV plate of Figure 3.8 reveals that solutions for the SVSR plate can be derived from those presented in section 3.6 by simply replacing coordinate η by 1 - η. The Lévy-type solution becomes

$$W(\xi,\eta) = \sum_{p=1,2,3}^{\infty} Y_p(1-\eta)\,\sin(p\pi\xi)\ .$$

This is equation (2.16) with the η coordinate replaced by 1 - η. The following is a brief summary of the individual case solutions.

3.8.1 Case 1 Solution

The first case solution arises when $\delta_p^2 < \Delta_p$. It is defined by equation (3.8) of section 3.1.1, where coordinate η is replaced by $1 - \eta$. Constants B_p and C_p are zero, while A_p and D_p are defined by equations (3.59) and (3.60) respectively, as shown in section 3.6.1.

3.8.2 Case 2 Solution

The second case solution is considered when $\delta_p^2 > \Delta_p$ and $\Delta_p < 0$. It is defined by equation (3.12) of section 3.1.2, where coordinate η is replaced by $1 - \eta$. Constants A_p and C_p are zero, while B_p and D_p are defined by equations (3.61) and (3.62) respectively, as shown in section 3.6.2.

3.8.3 Case 3 Solution

The third case solution is valid when $\delta_p^2 > \Delta_p$ and $\Delta_p > 0$ and $\delta_p > 0$. It is defined by equation (3.16), where coordinate η is replaced by $1 - \eta$. Constants A_p and C_p are zero, while B_p and D_p are defined by equations (3.63) and (3.64) respectively, as shown in section 3.6.3.

3.9 The WRSR Building Block

The WRSR building block is shown in Figure 3.11. A close look at the SRWR plate, shown in Figure 3.9, reveals that solutions for the WRSR plate can be derived from those presented in section 3.7 simply by replacing coordinate ξ by $1 - \xi$. The Lévy-type solution would be

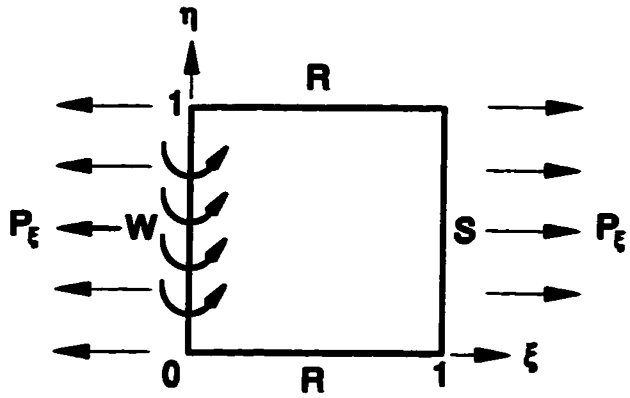

Figure 3.11 The WRSR building block under unilateral in-plane load.

$$W(\xi,\eta) = \sum_{q=0,1,2}^{\infty} Y_q(1-\xi)\cos(q\pi\eta) .$$

This is equation (2.21) with the coordinate ξ replaced by $1 - \xi$. The individual case solutions are as follows.

3.9.1 Case 1 Solution

When $\delta_q^2 < \Delta_q$, the solution is given by equation (3.37) of section 3.3.1, where coordinate ξ is replaced by $1 - \xi$. Constants A_q and D_q are zero, while B_q and C_q are defined by equations (3.38) and (3.39) respectively.

3.9.2 Case 2 Solution

The second case solution is considered when $\delta_q^2 > \Delta_q$ and $\Delta_q < 0$. It is given by equation (3.40) of section 3.3.2, where coordinate ξ is replaced by $1 - \xi$. Constants B_q and D_q are zero, while A_q and C_q are defined by equations (3.41) and (3.42) respectively.

3.9.3 Case 3 Solution

The third case solution arises when $\delta_q^2 > \Delta_q$ and $\Delta_q > 0$ and $\delta_q > 0$. It is expressed by equation (3.43), where coordinate ξ is replaced by $1 - \xi$. Constants B_q and D_q are zero, while A_q and C_q are defined by equations (3.44) and (3.45) respectively.

3.9.4 Case 4 Solution

The fourth case solution is encountered when $\delta_q^2 > \Delta_q$ and $\Delta_q > 0$ and $\delta_q < 0$. It is defined by equation (3.46), where coordinate ξ is replaced by $1 - \xi$. Constants B_q and D_q are zero, while A_q and C_q are defined by equations (3.47) and (3.48) respectively.

3.10 The SFSF Plate

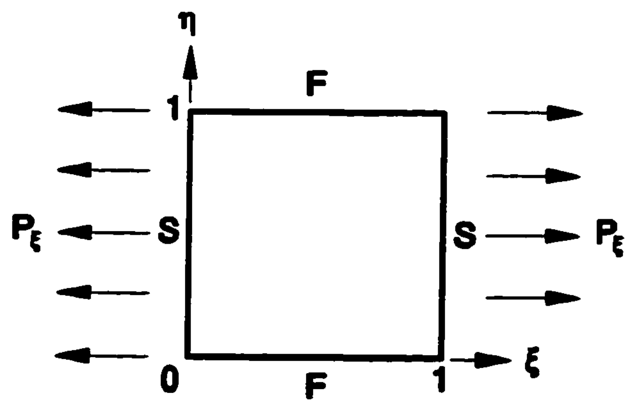

Figure 3.12 The SFSF plate under unilateral in-plane load.

Lévy-type solution (2.16) could be used to directly obtain an analytical solution for the SFSF plate shown in Figure 3.12. General solutions (3.8), (3.12), and (3.16) of section 3.1 would be suitable for this approach. However, enforcing boundary conditions (2.13) for the free edges at $\eta = 1$ and $\eta = 0$ would be a tedious task due to the mixed higher order derivative terms present. An alternative method of solution involves superimposing the SRSV (section 3.6) and SVSR (section 3.8) building blocks, as shown in Figure 3.1. This approach is economical since the noted building block solutions are already available.

Table 3.1 Boundary conditions summary of the SFSF plate and its building blocks.

	Boundary conditions at specified edge			
Plate	$\xi = 0$	$\eta = 0$	$\xi = 1$	$\eta = 1$
SRSV	$W = 0,\ M_\xi = 0$	$S_\eta = 0,\ V_\eta = 0$	$W = 0,\ M_\xi = 0$	$S_\eta \propto E_m,\ V_\eta = 0$
SVSR	$W = 0,\ M_\xi = 0$	$S_\eta \propto E_p,\ V_\eta = 0$	$W = 0,\ M_\xi = 0$	$S_\eta = 0,\ V_\eta = 0$
SFSF	$W = 0,\ M_\xi = 0$	$M_\eta = 0,\ V_\eta = 0$	$W = 0,\ M_\xi = 0$	$M_\eta = 0,\ V_\eta = 0$

The definition of superimpose is to lay something over another thing. Hence, the SFSF plate solution becomes the sum of its building block solutions,

$$W(\xi,\eta) = W_{SRSV}(\xi,\eta) + W_{SVSR}(\xi,\eta)$$

or

$$W(\xi,\eta) = \sum_{m=1,2,3}^{\infty} Y_m(\eta)\sin(m\pi\xi) + \sum_{p=1,2,3}^{\infty} Y_p(1-\eta)\sin(p\pi\xi)\ . \tag{3.70}$$

Each building block possesses an edge with a sinusoidally driven slope which controls its amplitude. Boundary conditions for the SRSV and SVSR building blocks and the SFSF plate are summarized in Table 3.1. A final solution is attained once the building block amplitudes are determined so that the bending moments at $\eta = 1$ and $\eta = 0$ vanish. Note that the remaining boundary conditions of the SFSF plate are already enforced in each individual building block. Expressions for $Y_m(\eta)$ (of the SVSR plate) and $Y_p(1\text{-}\eta)$ (of the SRSV plate) are summarized in Table 3.2. Note that all coefficients not equal to zero are linearly proportional to E (the plate amplitude factor).

Superimposed solution (3.70) is substituted into bending moment equation (2.5), simplified, and evaluated at $\eta = 1$ and $\eta = 0$, giving

Table 3.2 Solutions summary for the SFSF building blocks.

Building block	Case solution		Solution coefficients (X)	
	Case	Equation	X = 0	X ≠ 0
SRSV Section 3.6 $Y_m(\eta)$	1	(3.8)	B_m, C_m	A_m (3.59), D_m (3.60)
	2	(3.12)	A_m, C_m	B_m (3.61), D_m (3.62)
	3	(3.16)	A_m, C_m	B_m (3.63), D_m (3.64)
SVSR Section 3.8 $Y_p(1-\eta)$	1	(3.8)*	B_p, C_p	A_p (3.59), D_p (3.60)
	2	(3.12)*	A_p, C_p	B_p (3.61), D_p (3.62)
	3	(3.16)*	A_p, C_p	B_p (3.63), D_p (3.64)

* Replace coordinate η with $1-\eta$.

$$\sum_{m=1,2,3}^{\infty}\left[Y_m''(1) - \nu(m\pi\phi)^2 Y_m(1)\right]\sin(m\pi\xi) +$$

$$\sum_{p=1,2,3}^{\infty}\left[Y_p''(0) - \nu(p\pi\phi)^2 Y_p(0)\right]\sin(p\pi\xi) = 0 \tag{3.71}$$

and

$$\sum_{m=1,2,3}^{\infty}\left[Y_m''(0) - \nu(m\pi\phi)^2 Y_m(0)\right]\sin(m\pi\xi) +$$

$$\sum_{p=1,2,3}^{\infty}\left[Y_p''(1) - \nu(p\pi\phi)^2 Y_p(1)\right]\sin(p\pi\xi) = 0\ . \tag{3.72}$$

Since indices m and p consist of the same sequence of numbers, the individual summation signs in each of the above equations can be combined. Note that $\sin(m\pi\xi)$ cannot equal zero for all values of ξ. Utilizing these concepts gives

$$\sum_{m,p=1,2,3}^{\infty}\left[Y_m''(1) - \nu(m\pi\phi)^2 Y_m(1) + Y_p''(0) - \nu(p\pi\phi)^2 Y_p(0)\right] = 0 \tag{3.73}$$

and

$$\sum_{m,p=1,2,3}^{\infty}\left[Y_m''(0) - \nu(m\pi\phi)^2 Y_m(0) + Y_p''(1) - \nu(p\pi\phi)^2 Y_p(1)\right] = 0 \qquad (3.74)$$

respectively. The above equations are further simplified by isolating the E factors (or building block amplitudes) from the remaining terms. Equation (3.73) becomes

$$\sum_{m,p=1,2,3}^{\infty}\left[\, a_m E_m + c_p E_p \,\right] = 0 \qquad (3.75)$$

and equation (3.74) becomes

$$\sum_{m,p=1,2,3}^{\infty}\left[\, l_m E_m + k_p E_p \,\right] = 0\,. \qquad (3.76)$$

$$\begin{array}{c c}
 & \begin{array}{ccc ccc} & \text{SRSV} & & & \text{SVSR} & \end{array} \\
\begin{array}{c} \\ (3.75) \\ \\ \\ (3.76) \\ \\ \end{array} &
\begin{bmatrix}
a_1 & 0 & 0 & c_1 & 0 & 0 \\
0 & a_2 & 0 & 0 & c_2 & 0 \\
0 & 0 & a_3 & 0 & 0 & c_3 \\
l_1 & 0 & 0 & k_1 & 0 & 0 \\
0 & l_2 & 0 & 0 & k_2 & 0 \\
0 & 0 & l_3 & 0 & 0 & k_3
\end{bmatrix}
\begin{Bmatrix} E_{m-1} \\ E_{m-2} \\ E_{m-3} \\ E_{p-1} \\ E_{p-2} \\ E_{p-3} \end{Bmatrix}
=
\begin{Bmatrix} 0 \\ 0 \\ 0 \\ 0 \\ 0 \\ 0 \end{Bmatrix}
\end{array}$$

Figure 3.13 A three term expansion of the algebraic equations for the SFSF plate.

Equations (3.75) and (3.76) are expanded by k terms, producing 2k linear homogeneous equations with 2k unknown plate amplitudes E. Figure 3.13 portrays the system of equations, in matrix form, resulting from a three term expansion. The elements within the coefficient matrix correspond to building block contributions for each boundary condition equation in the expansion. These coefficients are defined in appendix A.

Eigenvalues are found by requiring that the determinant of the coefficient matrix equals zero. Approximate eigenvalues are acquired by examining eigenvalue versus determinant value graphs, which are plotted from generated data. Exact eigenvalues are calculated by refining these approximate roots using a numerical bisection method. Once an eigenvalue is determined, the associated eigenvector, whose elements are the amplitudes of the superimposed building blocks, is calculated. The mode shape is created by back-substituting these amplitudes into the original building block solutions. The above procedure is common for all superimposed solutions.

3.11 The SFCF Plate

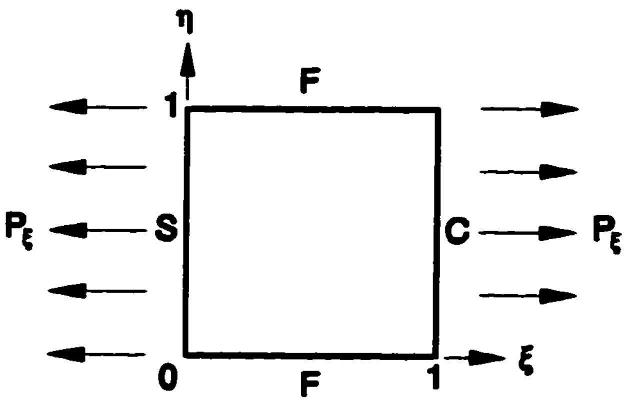

Figure 3.14 The SFCF plate under unilateral in-plane load.

Table 3.3 Boundary conditions summary of the SFCF plate and its building blocks.

	Boundary conditions at specified edge			
Plate	$\xi = 0$	$\eta = 0$	$\xi = 1$	$\eta = 1$
SRSV	$W = 0,\ M_\xi = 0$	$S_\eta = 0,\ V_\eta = 0$	$W = 0,\ M_\xi = 0$	$S_\eta \propto E_m,\ V_\eta = 0$
SRWR	$W = 0,\ M_\xi = 0$	$S_\eta = 0,\ V_\eta = 0$	$W = 0,\ M_\xi \propto E_n$	$S_\eta = 0,\ V_\eta = 0$
SVSR	$W = 0,\ M_\xi = 0$	$S_\eta \propto E_p,\ V_\eta = 0$	$W = 0,\ M_\xi = 0$	$S_\eta = 0,\ V_\eta = 0$
SFCF	$W = 0,\ M_\xi = 0$	$M_\eta = 0,\ V_\eta = 0$	$W = 0,\ S_\xi = 0$	$M_\eta = 0,\ V_\eta = 0$

An analytical-type solution for the SFCF plate is obtained by superimposing the SRSV (section 3.6), SVSR (section 3.8), and SRWR (section 3.7) building blocks, as shown in Figure 3.1. The procedure used here to determine amplitude factors for each of the building blocks is similar to that demonstrated in section 3.10 for the SFSF plate. In fact, the first two building blocks were also used for the SFSF plate. The additional SRWR plate is used to enforce the clamped edge at $\xi = 1$. This becomes apparent by examining the summarized boundary conditions in Table 3.3 and comparing them to those listed in Table 3.1 for the SFSF plate.

The SFCF solution becomes

$$W(\xi,\eta) = W_{SRSV}(\xi,\eta) + W_{SRWR}(\xi,\eta) + W_{SVSR}(\xi,\eta)$$

or

$$W(\xi,\eta) = \sum_{m=1,2,3}^{\infty} Y_m(\eta)\sin(m\pi\xi) + \sum_{n=0,1,2}^{\infty} Y_n(\xi)\cos(n\pi\eta)$$

$$+ \sum_{p=1,2,3}^{\infty} Y_p(1-\eta)\sin(p\pi\xi) \ . \tag{3.77}$$

Expressions for $Y_m(\eta)$ (of the SRSV plate), $Y_n(\xi)$ (of the SRWR plate), and $Y_p(1\text{-}\eta)$ (of the SVSR plate) are summarized in Table 3.4. All coefficients in the building block solutions are linearly proportional to their respective plate amplitude (E) factors. Only three of the eight boundary conditions required for the SFCF plate have yet to be satisfied in the superimposed solution given by equation (3.77). Each building block's E factor is properly adjusted to enforce one of the three remaining conditions. In reviewing Table 3.3, the following solution properties are revealed: E_m (of the SRSV plate) must zero the bending moment at $\eta = 1$, E_p (of the SVSR plate) must zero the bending moment at $\eta = 0$, and E_n (of the SRWR plate) must zero the slope at $\xi = 1$.

The zero bending moment conditions are enforced by substituting equation (3.77) into equation (2.5), simplifying, and evaluating at $\eta = 1$ and $\eta = 0$ respectively, giving

$$\sum_{m=1,2,3}^{\infty}\left[Y_m''(1) - \nu(m\pi\phi)^2 Y_m(1)\right]\sin(m\pi\xi) + \sum_{n=0,1,2}^{\infty}\left[-(n\pi)^2 Y_n(\xi) + \nu\phi^2 Y_n''(\xi)\right]\cos(n\pi) +$$

$$\sum_{p=1,2,3}^{\infty}\left[Y_p''(0) - \nu(p\pi\phi)^2 Y_p(0)\right]\sin(p\pi\xi) = 0 \tag{3.78}$$

Table 3.4 Solutions summary for the SFCF building blocks.

Building block	Case solution		Solution coefficients (X)	
	Case	Equation	X = 0	X ≠ 0
SRSV Section 3.6 $Y_m(\eta)$	1	(3.8)	B_m, C_m	A_m (3.59), D_m (3.60)
	2	(3.12)	A_m, C_m	B_m (3.61), D_m (3.62)
	3	(3.16)	A_m, C_m	B_m (3.63), D_m (3.64)
SVSR Section 3.8 $Y_p(1-\eta)$	1	(3.8)*	B_p, C_p	A_p (3.59), D_p (3.60)
	2	(3.12)*	A_p, C_p	B_p (3.61), D_p (3.62)
	3	(3.16)*	A_p, C_p	B_p (3.63), D_p (3.64)
SRWR Section 3.7 $Y_n(\xi)$	1	(3.37)	A_n, D_n	B_n (3.38), C_n (3.39)
	2	(3.40)	B_n, D_n	A_n (3.41), C_n (3.42)
	3	(3.43)	B_n, D_n	A_n (3.44), C_n (3.45)
	4	(3.46)	B_n, D_n	A_n (3.47), C_n (3.48)

* Replace coordinate η with $1-\eta$.

and

$$\sum_{m=1,2,3}^{\infty}\left[Y_m''(0)-\nu(m\pi\phi)^2Y_m(0)\right]\sin(m\pi\xi)+\sum_{n=0,1,2}^{\infty}\left[-(n\pi)^2Y_n(\xi)+\nu\phi^2Y_n''(\xi)\right]+$$

$$\sum_{p=1,2,3}^{\infty}\left[Y_p''(1)-\nu(p\pi\phi)^2Y_p(1)\right]\sin(p\pi\xi)=0\,. \qquad (3.79)$$

It is important to properly express equations (3.78) and (3.79) so that the influence of building block amplitude factors in the superimposed solution can be determined. This is accomplished by eliminating the ξ variable. Note that the m and p indices consist of the same sequence of numbers. Hence, they can be associated with a single summation sign. The $Y_n(\xi)$ and $Y_n''(\xi)$ terms under the second summation are expanded into $\sin(m\pi\xi)$ series. With some simplification, equations (3.78) and (3.79) become

$$\sum_{m,p=1,2,3}^{\infty} \sum_{n=0,1,2}^{\infty} \Bigg\{ Y_m''(1) - \nu(m\pi\phi)^2 Y_m(1) - 2(n\pi)^2(-1)^n \int_0^1 Y_n(\xi)\sin(m\pi\xi)\,d\xi$$

$$+ 2\nu\phi^2(-1)^n \int_0^1 Y_n''(\xi)\sin(m\pi\xi)\,d\xi + Y_p''(0) - \nu(p\pi\phi)^2 Y_p(0) \Bigg\} \sin(m\pi\xi) = 0 \quad (3.80)$$

and

$$\sum_{m,p=1,2,3}^{\infty} \sum_{n=0,1,2}^{\infty} \Bigg\{ Y_m''(0) - \nu(m\pi\phi)^2 Y_m(0) - 2(n\pi)^2 \int_0^1 Y_n(\xi)\sin(m\pi\xi)\,d\xi$$

$$+ 2\nu\phi^2 \int_0^1 Y_n''(\xi)\sin(m\pi\xi)\,d\xi + Y_p''(1) - \nu(p\pi\phi)^2 Y_p(1) \Bigg\} \sin(m\pi\xi) = 0 \quad (3.81)$$

respectively. Sin($m\pi\xi$) cannot equal zero for all values of ξ. Hence, parathesized quantities must equal zero for each value of m or p. These quantities are expressed in terms of E factors (or building block amplitudes). Equation (3.80) becomes

$$\sum_{m,p=1,2,3}^{\infty} \sum_{n=0,1,2}^{\infty} [\, a_m E_m + b_{mn} E_n + c_p E_p \,] = 0 \quad (3.82)$$

while equation (3.81) becomes

$$\sum_{m,p=1,2,3}^{\infty} \sum_{n=0,1,2}^{\infty} [\, i_m E_m + j_{mn} E_n + k_p E_p \,] = 0 \,. \quad (3.83)$$

With the bending moment conditions fulfilled, attention is focused on satisfying the zero slope condition at $\xi = 1$. This is done by substituting superimposed solution (3.77) into slope equation (2.2). The resulting expression is equated to zero, simplified, and evaluated at $\xi = 1$, giving

$$\sum_{m=1,2,3}^{\infty} (m\pi) Y_m(\eta)\cos(m\pi) + \sum_{n=0,1,2}^{\infty} Y_n'(1)\cos(n\pi\eta) +$$

$$\sum_{p=1,2,3}^{\infty} (p\pi) Y_p(1-\eta)\cos(p\pi) = 0 \,. \quad (3.84)$$

The dependency of the above equation to coordinate η is suspended by expanding $Y_m(\eta)$ and $Y_p(\eta)$ into $\cos(n\pi\eta)$ series. Conducting this procedure yields

$$\sum_{m,p=1,2,3}^{\infty} \left\{ m\pi(-1)^m \int_0^1 Y_m(\eta)\,d\eta + Y_n'(1) + p\pi(-1)^p \int_0^1 Y_p(1-\eta)\,d\eta \right\} = 0$$

for n = 0 and

$$\sum_{m,p=1,2,3}^{\infty} \sum_{n=1,2}^{\infty} \left\{ 2m\pi(-1)^m \int_0^1 Y_m(\eta)\cos(n\pi\eta)\,d\eta + Y_n'(1) \right.$$

$$\left. + 2p\pi(-1)^p \int_0^1 Y_p(1-\eta)\cos(n\pi\eta)\,d\eta \right\} \cos(n\pi\eta) = 0 \qquad (3.85)$$

for $n \neq 0$. The coefficients of this Fourier series must equal zero for each value of n. Equation (3.85) is expressed as

$$\sum_{m,p=1,2,3}^{\infty} \sum_{n=0,1,2}^{\infty} \left[e_{mn}E_m + f_nE_n + g_{pn}E_p \right] = 0 \,. \qquad (3.86)$$

$$
\begin{array}{cc}
 & \qquad \text{SRSV} \qquad\qquad \text{SRWR} \qquad\qquad \text{SVSR} \\
\begin{array}{c} \\ (3.82) \\ \\ \\ (3.86) \\ \\ \\ (3.83) \\ \\ \end{array} &
\left[\begin{array}{ccccccccc}
a_1 & 0 & 0 & b_{10} & b_{11} & b_{12} & c_1 & 0 & 0 \\
0 & a_2 & 0 & b_{20} & b_{21} & b_{22} & 0 & c_2 & 0 \\
0 & 0 & a_3 & b_{30} & b_{31} & b_{32} & 0 & 0 & c_3 \\
e_{10} & e_{20} & e_{30} & f_0 & 0 & 0 & g_{10} & g_{20} & g_{30} \\
e_{11} & e_{21} & e_{31} & 0 & f_1 & 0 & g_{11} & g_{21} & g_{31} \\
e_{12} & e_{22} & e_{32} & 0 & 0 & f_2 & g_{12} & g_{22} & g_{32} \\
i_1 & 0 & 0 & j_{10} & j_{11} & j_{12} & k_1 & 0 & 0 \\
0 & i_2 & 0 & j_{20} & j_{21} & j_{22} & 0 & k_2 & 0 \\
0 & 0 & i_3 & j_{30} & j_{31} & j_{32} & 0 & 0 & k_3
\end{array}\right]
\end{array}
\begin{Bmatrix} E_{m=1} \\ E_{m=2} \\ E_{m=3} \\ E_{n=0} \\ E_{n=1} \\ E_{n=2} \\ E_{p=1} \\ E_{p=2} \\ E_{p=3} \end{Bmatrix}
=
\begin{Bmatrix} 0 \\ 0 \\ 0 \\ 0 \\ 0 \\ 0 \\ 0 \\ 0 \\ 0 \end{Bmatrix}
$$

Figure 3.15 A three term expansion of the algebraic equations for the SFCF plate.

Equations (3.82), (3.83), and (3.86) are expanded by k terms, producing 3k linear homogeneous equations with 3k unknown E factors. Figure 3.15 portrays the system of equations, in matrix form, resulting from a three term expansion. Coefficients leading each E factor are building block contributions and are defined in appendix A. Eigenvalues and mode shapes are obtained by following the same procedure presented in section 3.10 for the SFSF plate.

3.12 The CFCF Plate

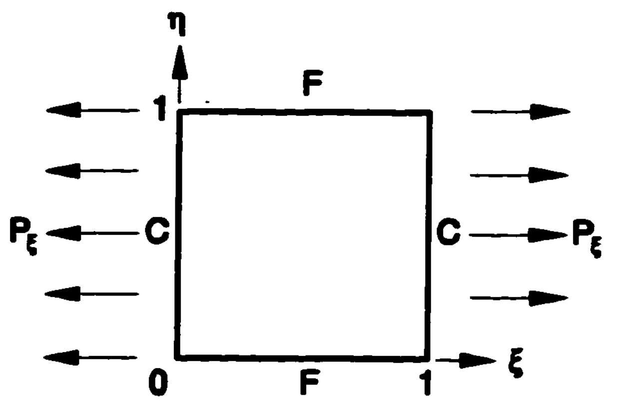

Figure 3.16 The CFCF thin rectangular plate under unilateral in-plane load.

Table 3.5 Boundary conditions summary of the CFCF plate and its building blocks.

	Boundary conditions at specified edge			
Plate	$\xi = 0$	$\eta = 0$	$\xi = 1$	$\eta = 1$
SRSV	$W = 0,\ M_\xi = 0$	$S_\eta = 0,\ V_\eta = 0$	$W = 0,\ M_\xi = 0$	$S_\eta \propto E_m,\ V_\eta = 0$
SRWR	$W = 0,\ M_\xi = 0$	$S_\eta = 0,\ V_\eta = 0$	$W = 0,\ M_\xi \propto E_n$	$S_\eta = 0,\ V_\eta = 0$
SVSR	$W = 0,\ M_\xi = 0$	$S_\eta \propto E_p,\ V_\eta = 0$	$W = 0,\ M_\xi = 0$	$S_\eta = 0,\ V_\eta = 0$
WRSR	$W = 0,\ M_\xi \propto E_q$	$S_\eta = 0,\ V_\eta = 0$	$W = 0,\ M_\xi = 0$	$S_\eta = 0,\ V_\eta = 0$
CFCF	$W = 0,\ S_\xi = 0$	$M_\eta = 0,\ V_\eta = 0$	$W = 0,\ S_\xi = 0$	$M_\eta = 0,\ V_\eta = 0$

Table 3.6 Solutions summary for the CFCF building blocks.

Building block	Case solution		Solution coefficients (X)	
	Case	Equation	X = 0	X ≠ 0
SRSV Section 3.6 $Y_m(\eta)$	1	(3.8)	B_m, C_m	A_m (3.59), D_m (3.60)
	2	(3.12)	A_m, C_m	B_m (3.61), D_m (3.62)
	3	(3.16)	A_m, C_m	B_m (3.63), D_m (3.64)
SRWR Section 3.7 $Y_n(\xi)$	1	(3.37)	A_n, D_n	B_n (3.38), C_n (3.39)
	2	(3.40)	B_n, D_n	A_n (3.41), C_n (3.42)
	3	(3.43)	B_n, D_n	A_n (3.44), C_n (3.45)
	4	(3.46)	B_n, D_n	A_n (3.47), C_n (3.48)
SVSR Section 3.8 $Y_p(1-\eta)$	1	(3.8)*	B_p, C_p	A_p (3.59), D_p (3.60)
	2	(3.12)*	A_p, C_p	B_p (3.61), D_p (3.62)
	3	(3.16)*	A_p, C_p	B_p (3.63), D_p (3.64)
WRSR Section 3.9 $Y_q(1-\xi)$	1	(3.37)**	A_n, D_n	B_n (3.38), C_n (3.39)
	2	(3.40)**	B_n, D_n	A_n (3.41), C_n (3.42)
	3	(3.43)**	B_n, D_n	A_n (3.44), C_n (3.45)
	4	(3.46)**	B_n, D_n	A_n (3.47), C_n (3.48)

* Replace coordinate η with $1-\eta$.
** Replace coordinate ξ with $1-\xi$.

Consider the plate presented in Figure 3.16, where none of the edges are either simply supported or slip shear. Obviously, the method of superposition must be utilized. Recall that clamped edges are duplicated by superimposing a zero displacement edge with any number of pinned edges. Similarly, free edges are reproduced by superimposing a zero shear force edge with any number of slip shear edges. Applying this knowledge to the CFCF plate yields a superimposed solution consisting of the SRSV, SRWR, SVSR, and WRSR building blocks, as shown in Figure 3.1. The building block solutions are derived in sections 3.6 through 3.9 inclusively. The CFCF plate solution becomes

$$W(\xi,\eta) = W_{SRSV}(\xi,\eta) + W_{SRWR}(\xi,\eta) + W_{SVSR}(\xi,\eta) + W_{WRSR}(\xi,\eta)$$

or

$$W(\xi,\eta) = \sum_{m=1,2,3}^{\infty} Y_m(\eta)\sin(m\pi\xi) + \sum_{n=0,1,2}^{\infty} Y_n(\xi)\cos(n\pi\eta)$$

$$+ \sum_{p=1,2,3}^{\infty} Y_p(1-\eta)\sin(p\pi\xi) + \sum_{q=0,1,2}^{\infty} Y_q(1-\xi)\cos(q\pi\eta)\,. \tag{3.87}$$

Table 3.6 summarizes the building block solutions. Each building block possesses a distinct harmonic boundary condition which regulates its amplitude. The final solution is achieved once the harmonic rotations and moments are adequately adjusted to enforce the four remaining boundary conditions. According to Table 3.5, these include the zero bending moments for the free edges at $\eta = 1$ and $\eta = 0$, and the zero slopes for the clamped edges at $\xi = 1$ and $\xi = 0$.

Bending moments defined by equation (2.5) along the free edges are equated to zero. Equation (3.87) for $W(\xi,\eta)$ is substituted into the expression. Evaluation at $\eta = 1$ and $\eta = 0$ gives

$$\sum_{m=1,2,3}^{\infty}\left[Y_m''(1) - \nu(m\pi\phi)^2 Y_m(1)\right]\sin(m\pi\xi) +$$

$$\sum_{n=0,1,2}^{\infty}\left[-(n\pi)^2 Y_n(\xi) + \nu\phi^2 Y_n''(\xi)\right]\cos(n\pi) +$$

$$\sum_{p=1,2,3}^{\infty}\left[Y_p''(0) - \nu(p\pi\phi)^2 Y_p(0)\right]\sin(p\pi\xi) +$$

$$\sum_{q=0,1,2}^{\infty}\left[-(q\pi)^2 Y_q(1-\xi) + \nu\phi^2 Y_q''(1-\xi)\right]\cos(q\pi) = 0 \tag{3.88}$$

and

$$\sum_{m=1,2,3}^{\infty}\left[Y_m''(0) - \nu(m\pi\phi)^2 Y_m(0)\right]\sin(m\pi\xi) +$$

$$\sum_{n=0,1,2}^{\infty}\left[-(n\pi)^2 Y_n(\xi) + \nu\phi^2 Y_n''(\xi)\right] +$$

$$\sum_{p=1,2,3}^{\infty}\left[Y_p''(1) - \nu(p\pi\phi)^2 Y_p(1)\right]\sin(p\pi\xi) +$$

$$\sum_{q=0,1,2}^{\infty}\left[-(q\pi)^2 Y_q(1-\xi) + \nu\phi^2 Y_q''(1-\xi)\right] = 0 \tag{3.89}$$

respectively. Indices m and p are assigned to a single summation sign since they consist of the same sequence of numbers. The same is done with indices n and q. The $Y_n(\xi)$, $Y_n''(\xi)$, $Y_q(1-\xi)$, and $Y_q''(1-\xi)$ terms in equations (3.88) and (3.89) are expanded into Fourier $\sin(m\pi\xi)$ series, giving

$$\sum_{m,p=1,2,3}^{\infty}\ \sum_{n,q=0,1,2}^{\infty}\left\{Y_m''(1) - \nu(m\pi\phi)^2 Y_m(1) - 2(n\pi)^2(-1)^n\int_0^1 Y_n(\xi)\sin(m\pi\xi)\,d\xi\right.$$

$$+ 2\nu\phi^2(-1)^n\int_0^1 Y_n''(\xi)\sin(m\pi\xi)\,d\xi + Y_p''(0) - \nu(p\pi\phi)^2 Y_p(0) \tag{3.90}$$

$$\left.- 2(q\pi)^2(-1)^q\int_0^1 Y_q(1-\xi)\sin(m\pi\xi)\,d\xi + 2\nu\phi^2(-1)^q\int_0^1 Y_q''(1-\xi)\sin(m\pi\xi)\,d\xi\right\}\sin(m\pi\xi) = 0$$

and

$$\sum_{m,p=1,2,3}^{\infty}\ \sum_{n,q=0,1,2}^{\infty}\left\{Y_m''(0) - \nu(m\pi\phi)^2 Y_m(0) - 2(n\pi)^2\int_0^1 Y_n(\xi)\sin(m\pi\xi)\,d\xi\right.$$

$$+ 2\nu\phi^2\int_0^1 Y_n''(\xi)\sin(m\pi\xi)\,d\xi + Y_p''(1) - \nu(p\pi\phi)^2 Y_p(1) \tag{3.91}$$

$$- 2(q\pi)^2 \int_0^1 Y_q(1-\xi)\sin(m\pi\xi)\,d\xi + 2\nu\phi^2 \int_0^1 Y_q''(1-\xi)\sin(m\pi\xi)\,d\xi \Bigg\} \sin(m\pi\xi) = 0$$

respectively. Note that the $\sin(m\pi\xi)$ functions cannot equal zero for all values of ξ. Equations (3.90) and (3.91) are restated in terms of E factors as

$$\sum_{m,p=1,2,3}^{\infty} \sum_{n,q=0,1,2}^{\infty} [\, a_m E_m + b_{mn} E_n + c_p E_p + d_{mq} E_q \,] = 0 \qquad (3.92)$$

and

$$\sum_{m,p=1,2,3}^{\infty} \sum_{n,q=0,1,2}^{\infty} [\, i_m E_m + j_{mn} E_n + k_p E_p + l_{mq} E_q \,] = 0 \qquad (3.93)$$

respectively. The coefficient leading each E factor (or plate amplitude) is defined in appendix A and can be described as a building block contribution in the superimposed solution.

Slope along the clamped edges are defined by equation (2.2) and are set equal to zero. Once again, the superimposed solution, given by equation (3.87), is used for $W(\xi,\eta)$ in the expression. Evaluation results in

$$\sum_{m=1,2,3}^{\infty} (m\pi) Y_m(\eta)\cos(m\pi) + \sum_{n=0,1,2}^{\infty} Y_n'(1)\cos(n\pi\eta) +$$

$$\sum_{p=1,2,3}^{\infty} (p\pi) Y_p(1-\eta)\cos(p\pi) - \sum_{q=0,1,2}^{\infty} Y_q'(0)\cos(q\pi\eta) = 0 \qquad (3.94)$$

for $\xi = 1$ and

$$\sum_{m=1,2,3}^{\infty} (m\pi) Y_m(\eta) + \sum_{n=0,1,2}^{\infty} Y_n'(0)\cos(n\pi\eta) +$$

$$\sum_{p=1,2,3}^{\infty} (p\pi) Y_p(1-\eta) - \sum_{q=0,1,2}^{\infty} Y_q'(1)\cos(q\pi\eta) = 0 \qquad (3.95)$$

for $\xi = 0$. The first and third terms in both of the above equations are expanded into

Fourier $\cos(n\pi\eta)$ series. Equations (3.94) becomes

$$\sum_{m,p=1,2,3}^{\infty}\left\{m\pi(-1)^m\int_0^1 Y_m(\eta)\,d\eta + Y_n'(1) + p\pi(-1)^p\int_0^1 Y_p(1-\eta)\,d\eta - Y_q'(0)\right\} = 0$$

for n = 0 and

$$\sum_{m,p=1,2,3}^{\infty}\ \sum_{n,q=1,2}^{\infty}\left\{2m\pi(-1)^m\int_0^1 Y_m(\eta)\cos(n\pi\eta)\,d\eta + Y_n'(1)\right.$$

$$\left. + 2p\pi(-1)^p\int_0^1 Y_p(1-\eta)\cos(n\pi\eta)\,d\eta - Y_q'(0)\right\}\cos(n\pi\eta) = 0 \tag{3.96}$$

for n ≠ 0 while equation (3.95) becomes

$$\sum_{m,p=1,2,3}^{\infty}\left\{m\pi\int_0^1 Y_m(\eta)\,d\eta + Y_n'(0) + p\pi\int_0^1 Y_p(1-\eta)\,d\eta - Y_q'(1)\right\} = 0$$

for n = 0 and

$$\sum_{m,p=1,2,3}^{\infty}\ \sum_{n,q=1,2}^{\infty}\left\{2m\pi\int_0^1 Y_m(\eta)\cos(n\pi\eta)\,d\eta + Y_n'(0)\right.$$

$$\left. + 2p\pi\int_0^1 Y_p(1-\eta)\cos(n\pi\eta)\,d\eta - Y_q'(1)\right\}\cos(n\pi\eta) = 0 \tag{3.97}$$

for n ≠ 0. The final forms of equations (3.96) and (3.97) are

$$\sum_{m,p=1,2,3}^{\infty}\ \sum_{n,q=0,1,2}^{\infty}\left[\,e_{mn}E_m + f_nE_n + g_{pn}E_p + h_qE_q\,\right] = 0 \tag{3.98}$$

and

$$\sum_{m,p=1,2,3}^{\infty}\ \sum_{n,q=0,1,2}^{\infty}\left[\,s_{mn}E_m + t_nE_n + u_{pn}E_p + v_qE_q\,\right] = 0 \tag{3.99}$$

respectively. Once again, the building block contributions are listed in appendix A.

Figure 3.17 is a matrix representation of the linear equations resulting from a three term expansion of equations (3.92), (3.93), (3.98), and (3.99). Eigenvalues and mode shapes are obtained by following the procedure described at the end of section 3.10.

$$
\begin{array}{c}
\\
(3.92) \\
\\
\\
(3.98) \\
\\
\\
(3.93) \\
\\
\\
(3.99) \\
\\
\end{array}
\begin{array}{c}
\begin{array}{cccc}
\text{SRSV} & \text{SRWR} & \text{SVSR} & \text{WRSR}
\end{array} \\
\begin{bmatrix}
a_1 & 0 & 0 & b_{10} & b_{11} & b_{12} & c_1 & 0 & 0 & d_{10} & d_{11} & d_{12} \\
0 & a_2 & 0 & b_{20} & b_{21} & b_{22} & 0 & c_2 & 0 & d_{20} & d_{21} & d_{22} \\
0 & 0 & a_3 & b_{30} & b_{31} & b_{32} & 0 & 0 & c_3 & d_{30} & d_{31} & d_{32} \\
e_{10} & e_{20} & e_{30} & f_0 & 0 & 0 & g_{10} & g_{20} & g_{30} & h_0 & 0 & 0 \\
e_{11} & e_{21} & e_{31} & 0 & f_1 & 0 & g_{11} & g_{21} & g_{31} & 0 & h_1 & 0 \\
e_{12} & e_{22} & e_{32} & 0 & 0 & f_2 & g_{12} & g_{22} & g_{32} & 0 & 0 & h_2 \\
i_1 & 0 & 0 & j_{10} & j_{11} & j_{12} & k_1 & 0 & 0 & l_{10} & l_{11} & l_{12} \\
0 & i_2 & 0 & j_{20} & j_{21} & j_{22} & 0 & k_2 & 0 & l_{20} & l_{21} & l_{22} \\
0 & 0 & i_3 & j_{30} & j_{31} & j_{32} & 0 & 0 & k_3 & l_{30} & l_{31} & l_{32} \\
s_{10} & s_{20} & s_{30} & t_0 & 0 & 0 & u_{10} & u_{20} & u_{30} & v_0 & 0 & 0 \\
s_{11} & s_{21} & s_{31} & 0 & t_1 & 0 & u_{11} & u_{21} & u_{31} & 0 & v_1 & 0 \\
s_{12} & s_{22} & s_{32} & 0 & 0 & t_2 & u_{12} & u_{22} & u_{32} & 0 & 0 & v_2
\end{bmatrix}
\end{array}
\begin{Bmatrix}
E_{m-1} \\ E_{m-2} \\ E_{m-3} \\ E_{n-0} \\ E_{n-1} \\ E_{n-2} \\ E_{p-1} \\ E_{p-2} \\ E_{p-3} \\ E_{q-0} \\ E_{q-1} \\ E_{q-2}
\end{Bmatrix}
=
\begin{Bmatrix}
0 \\ 0 \\ 0 \\ 0 \\ 0 \\ 0 \\ 0 \\ 0 \\ 0 \\ 0 \\ 0 \\ 0
\end{Bmatrix}
$$

Figure 3.17 A three term expansion of the algebraic equations for the CFCF plate.

3.13 The SCSF Plate

The SCSF plate shown in Figure 3.18 can be solved for by directly applying a Lévy-type solution since the edges at $\xi = 0$ and $\xi = 1$ are both pinned. However, robust mathematical expressions would be created in enforcing the boundary conditions at $\eta = 0$ and $\eta = 1$. The alternate formulation by the method of superposition becomes quite attractive since the required building block solutions are readily available. Figure 3.1 shows that the SSSV (section 3.2) and SWSR (section 3.4) plates are used to complete this task. The SCSF plate solution becomes

$$W(\xi,\eta) = W_{SSSV}(\xi,\eta) + W_{SWSR}(\xi,\eta)$$

or

$$W(\xi,\eta) = \sum_{m=1,2,3}^{\infty} Y_m(\eta)\sin(m\pi\xi) + \sum_{p=1,2,3}^{\infty} Y_p(1-\eta)\sin(p\pi\xi)\,. \qquad (3.100)$$

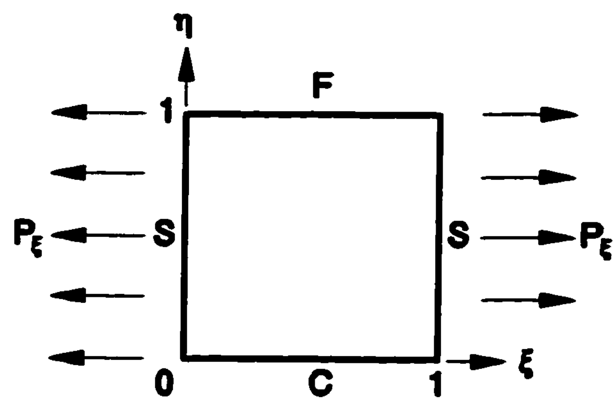

Figure 3.18 The SCSF plate under unilateral in-plane load.

Table 3.7 Boundary conditions summary of the SCSF plate and its building blocks.

	Boundary conditions at specified edge			
Plate	$\xi = 0$	$\eta = 0$	$\xi = 1$	$\eta = 1$
SSSV	$W = 0,\ M_\xi = 0$	$W = 0,\ M_\eta = 0$	$W = 0,\ M_\xi = 0$	$S_\eta \propto E_m,\ V_\eta = 0$
SWSR	$W = 0,\ M_\xi = 0$	$W = 0,\ M_\eta \propto E_p$	$W = 0,\ M_\xi = 0$	$S_\eta = 0,\ V_\eta = 0$
SCSF	$W = 0,\ M_\xi = 0$	$W = 0,\ S_\eta = 0$	$W = 0,\ M_\xi = 0$	$M_\eta = 0,\ V_\eta = 0$

Boundary conditions for the SSSV and SWSR building blocks and the SCSF plate are summarized in Table 3.7. Each building block has an edge driven by a sinusoidal slope or moment which controls its amplitude. The building block amplitudes are adjusted such that the slope at $\eta = 0$ and the bending moment at $\eta = 1$ vanish. Table 3.8 gives a summary of the building block case solutions and coefficient expressions.

The moment constraint at $\eta = 1$ is enforced by substituting solution (3.100) into

Table 3.8 Solutions summary for the SCSF building blocks.

Building block	Case solution		Solution coefficients (X)	
	Case	Equation	X = 0	X ≠ 0
SSSV Section 3.2 $Y_m(\eta)$	1	(3.8)	A_m, D_m	B_m (3.24), C_m (3.25)
	2	(3.12)	B_m, D_m	A_m (3.26), C_m (3.27)
	3	(3.16)	B_m, D_m	A_m (3.28), C_m (3.29)
SWSR Section 3.4 $Y_p(1-\eta)$	1	(3.8)*	B_p, C_p	A_p (3.53), D_p (3.54)
	2	(3.12)*	A_p, C_p	B_p (3.55), D_p (3.56)
	3	(3.16)*	A_p, C_p	B_p (3.57), D_p (3.58)

* Replace coordinate η with $1-\eta$.

equation (2.5), which in turn is set equal to zero. Simplifying and evaluating the resulting expression gives

$$\sum_{m=1,2,3}^{\infty}\left[Y_m''(1) - \nu(m\pi\phi)^2Y_m(1)\right]\sin(m\pi\xi) +$$

$$\sum_{p=1,2,3}^{\infty}\left[Y_p''(0) - \nu(p\pi\phi)^2Y_p(0)\right]\sin(p\pi\xi) = 0\ . \tag{3.101}$$

Both terms in the above equation are put under a single summation sign. Since the sine functions cannot equal zero for all values of ξ, equation (3.101) can be expressed as

$$\sum_{m,p=1,2,3}^{\infty}\left[Y_m''(1) - \nu(m\pi\phi)^2Y_m(1) + Y_p''(0) - \nu(p\pi\phi)^2Y_p(0)\right] = 0\ . \tag{3.102}$$

Equation (3.102) is expressed in terms of E factors as

$$\sum_{m,p=1,2,3}^{\infty}\left[\, a_mE_m + c_pE_p \,\right] = 0\ . \tag{3.103}$$

Attention is now drawn towards satisfying the zero slope condition at $\eta = 0$. The $W(\xi,\eta)$ parameter in slope equation (2.3) is replaced by equation (3.100). The resulting equation is equated to zero and evaluated at $\eta = 0$ to give

$$\sum_{m=1,2,3}^{\infty} Y_m'(0)\sin(m\pi\xi) + \sum_{p=1,2,3}^{\infty} Y_p'(1)\sin(p\pi\xi) = 0 \, . \tag{3.104}$$

Equation (3.104) is simplified to

$$\sum_{m,p=1,2,3}^{\infty} \left[Y_m'(0) + Y_p'(1) \right] = 0 \, , \tag{3.105}$$

which can also be expressed as

$$\sum_{m,p=1,2,3}^{\infty} \left[l_m E_m + k_p E_p \right] = 0 \, . \tag{3.106}$$

$$\begin{array}{c} \\ (3.103) \\ \\ (3.106) \end{array}
\begin{array}{c}
\begin{array}{cc} \text{SSSV} & \text{SWSR} \end{array} \\
\begin{bmatrix} a_1 & 0 & 0 & c_1 & 0 & 0 \\ 0 & a_2 & 0 & 0 & c_2 & 0 \\ 0 & 0 & a_3 & 0 & 0 & c_3 \\ l_1 & 0 & 0 & k_1 & 0 & 0 \\ 0 & l_2 & 0 & 0 & k_2 & 0 \\ 0 & 0 & l_3 & 0 & 0 & k_3 \end{bmatrix}
\end{array}
\begin{Bmatrix} E_{m=1} \\ E_{m=2} \\ E_{m=3} \\ E_{p=1} \\ E_{p=2} \\ E_{p=3} \end{Bmatrix} = \begin{Bmatrix} 0 \\ 0 \\ 0 \\ 0 \\ 0 \\ 0 \end{Bmatrix}$$

Figure 3.19 A three term expansion of the algebraic equations for the SCSF plate.

Equations (3.103) and (3.106) are expanded by k terms, producing 2k linear homogeneous equations with 2k unknown plate amplitudes E. Figure 3.19 portrays the system of equations, in matrix form, resulting from a three term expansion. The elements within the coefficient matrix correspond to building block contributions for each boundary condition equation in the expansion and are defined in appendix A. Eigenvalues and mode shapes are obtained by following the procedure given in section 3.10.

3.14 The SSCF Plate

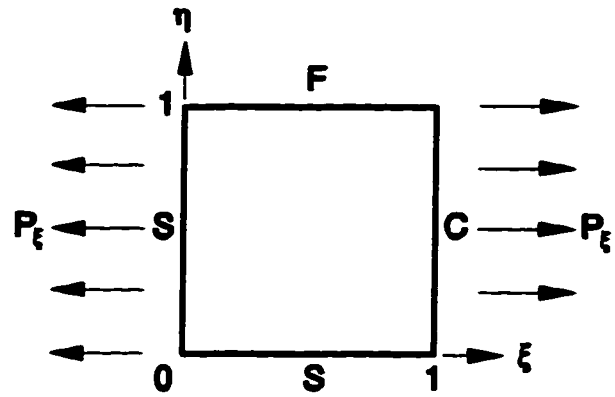

Figure 3.20 The SSCF plate under unilateral in-plane load.

Table 3.9 Boundary conditions summary of the SSCF plate and its building blocks.

	Boundary conditions at specified edge			
Plate	$\xi = 0$	$\eta = 0$	$\xi = 1$	$\eta = 1$
SSSV	$W = 0,\ M_\xi = 0$	$W = 0,\ M_\eta = 0$	$W = 0,\ M_\xi = 0$	$S_\eta \propto E_m,\ V_\eta = 0$
SSWR	$W = 0,\ M_\xi = 0$	$W = 0,\ M_\eta = 0$	$W = 0,\ M_\xi \propto E_n$	$S_\eta = 0,\ V_\eta = 0$
SSCF	$W = 0,\ M_\xi = 0$	$W = 0,\ M_\eta = 0$	$W = 0,\ S_\xi = 0$	$M_\eta = 0,\ V_\eta = 0$

The SSSV and SSWR building blocks are superimposed (as shown in Figure 3.1) to obtain an analytical solution for the SSCF plate shown in Figure 3.20. The SSCF plate solution becomes

$$W(\xi,\eta) = W_{SSSV}(\xi,\eta) + W_{SSWR}(\xi,\eta)$$

or

Table 3.10 Solutions summary for the SSCF building blocks.

Building block	Case solution		Solution coefficients (X)	
	Case	Equation	X = 0	X ≠ 0
SSSV Section 3.2 $Y_m(\eta)$	1	(3.8)	A_m, D_m	B_m (3.24), C_m (3.25)
	2	(3.12)	B_m, D_m	A_m (3.26), C_m (3.27)
	3	(3.16)	B_m, D_m	A_m (3.28), C_m (3.29)
SSWR Section 3.3 $Y_n(\xi)$	1	(3.37)	A_n, D_n	B_n (3.38), C_n (3.39)
	2	(3.40)	B_n, D_n	A_n (3.41), C_n (3.42)
	3	(3.43)	B_n, D_n	A_n (3.44), C_n (3.45)
	4	(3.46)	B_n, D_n	A_n (3.47), C_n (3.48)

$$W(\xi,\eta) = \sum_{m=1,2,3}^{\infty} Y_m(\eta)\sin(m\pi\xi) + \sum_{n=1,3,5}^{\infty} Y_n(\xi)\sin\left(\frac{n\pi\eta}{2}\right) . \tag{3.107}$$

Boundary conditions for the plates involved are listed in Table 3.9. The harmonic slope of the SSSV building block is adjusted to eliminate the overall bending moment at $\eta = 1$ of the superimposed solution. Similarly, the sinusoidally driven moment of the SSWR plate will induce the slope at $\xi = 1$ to vanish. Table 3.10 summarizes the building block case solutions and coefficient expressions.

The zero moment at $\eta = 1$ is enforced by substituting solution (3.107) into equation (2.5). Upon evaluation, the resulting equation becomes

$$\sum_{m=1,2,3}^{\infty} \left[Y_m''(1) - \nu(m\pi\phi)^2 Y_m(1)\right]\sin(m\pi\xi) +$$

$$\sum_{n=1,3,5}^{\infty} \left[\nu\phi^2 Y_n''(\xi) - \left(\frac{n\pi}{2}\right)^2 Y_n(\xi)\right]\sin\left(\frac{n\pi}{2}\right) = 0 . \tag{3.108}$$

Expanding $Y_n''(\xi)$ and $Y_n(\xi)$ into Fourier $\sin(m\pi\xi)$ series and simplifying produces

$$\sum_{m=1,2,3}^{\infty}\ \sum_{n=1,3,5}^{\infty}\left\{Y_m''(1) - \nu(m\pi\phi)^2 Y_m(1) + 2(-1)^{\left(\frac{n-1}{2}\right)}\left[\nu\phi^2\int_0^1 Y_n''(\xi)\sin(m\pi\xi)d\xi - \left(\frac{n\pi}{2}\right)\int_0^1 Y_n(\xi)\sin(m\pi\xi)d\xi\right]\right\}\sin(m\pi\xi) = 0 . \tag{3.109}$$

Equation (3.109) is expressed in terms of E factors as

$$\sum_{m=1,2,3}^{\infty}\ \sum_{n=1,3,5}^{\infty}\left[\, a_m E_m + b_{mn} E_n \,\right] = 0 . \tag{3.110}$$

Attention is now drawn towards satisfying the zero slope condition at $\xi = 1$. The $W(\xi,\eta)$ parameter in slope equation (2.2) is replaced by solution (3.107). The resulting equation is equated to zero and evaluated to give

$$\sum_{m=1,2,3}^{\infty}(m\pi)Y_m(\eta)\cos(m\pi) + \sum_{n=1,3,5}^{\infty} Y_n'(1)\sin\left(\frac{n\pi\eta}{2}\right) = 0 . \tag{3.111}$$

Expanding the $Y_m(\eta)$ term into a Fourier $\sin(n\pi\eta/2)$ series results in

$$\sum_{m=1,2,3}^{\infty}\ \sum_{n=1,3,5}^{\infty}\left\{2m\pi(-1)^m\int_0^1 Y_m(\eta)\sin\left(\frac{n\pi\eta}{2}\right)d\eta + Y_n'(1)\right\}\sin\left(\frac{n\pi\eta}{2}\right) = 0 , \tag{3.112}$$

which can also be expressed as

$$\sum_{m=1,2,3}^{\infty}\ \sum_{n=1,3,5}^{\infty}\left[\, e_{mn} E_m + f_p E_p \,\right] = 0 . \tag{3.113}$$

Equations (3.110) and (3.113) are used to generate a system of linear equations with unknown E factors. Figure 3.21 shows a three term expansion of the equations in matrix form. Elements within the coefficient matrix are building block contributions as defined in appendix A. Eigenvalues and mode shapes are obtained by following the procedure given in section 3.10.

$$
\begin{array}{l}
\\
(3.110) \\
\\
\\
(3.113) \\
\\
\end{array}
\begin{array}{c}
\begin{array}{cc} \text{SSSV} & \text{SSWR} \end{array} \\
\begin{bmatrix}
a_1 & 0 & 0 & b_{11} & b_{13} & b_{15} \\
0 & a_2 & 0 & b_{21} & b_{23} & b_{25} \\
0 & 0 & a_3 & b_{31} & b_{33} & b_{35} \\
e_{11} & e_{21} & e_{31} & f_1 & 0 & 0 \\
e_{13} & e_{23} & e_{33} & 0 & f_3 & 0 \\
e_{15} & e_{25} & e_{35} & 0 & 0 & f_5
\end{bmatrix}
\end{array}
\begin{Bmatrix}
E_{m-1} \\ E_{m-2} \\ E_{m-3} \\ E_{n-1} \\ E_{n-3} \\ E_{n-5}
\end{Bmatrix}
=
\begin{Bmatrix}
0 \\ 0 \\ 0 \\ 0 \\ 0 \\ 0
\end{Bmatrix}
$$

Figure 3.21 A three term expansion of the algebraic equations for a SCSF plate.

3.15 The SCCF Plate

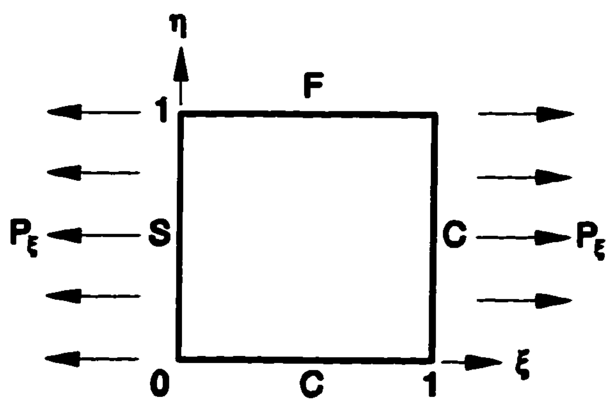

Figure 3.22 The SCCF plate under unilateral in-plane load.

An analytical-type solution for the SCCF plate is obtained by superimposing the SSSV, SSWR, and SWSR building blocks, as shown in Figure 3.1. The number of building blocks used in a solution is directly governed by the sum of clamped and free edges present. Each building block possesses an adjustable edge load which is used to correct a boundary condition that the superimposed solution violates. Specifically, harmonic slopes are used to regulate moments for a free edge and harmonic moments

Table 3.11 Boundary conditions summary of the SCCF plate and its building blocks.

	Boundary conditions at specified edge			
Plate	$\xi = 0$	$\eta = 0$	$\xi = 1$	$\eta = 1$
SSSV	$W = 0,\ M_\xi = 0$	$W = 0,\ M_\eta = 0$	$W = 0,\ M_\xi = 0$	$S_\eta \propto E_m,\ V_\eta = 0$
SSWR	$W = 0,\ M_\xi = 0$	$W = 0,\ M_\eta = 0$	$W = 0,\ M_\xi \propto E_n$	$S_\eta = 0,\ V_\eta = 0$
SWSR	$W = 0,\ M_\xi = 0$	$W = 0,\ M_\eta \propto E_p$	$W = 0,\ M_\xi = 0$	$S_\eta = 0,\ V_\eta = 0$
SCCF	$W = 0,\ M_\xi = 0$	$W = 0,\ S_\eta = 0$	$W = 0,\ S_\xi = 0$	$M_\eta = 0,\ V_\eta = 0$

are used to regulate slopes for a clamped edge. This is clearly shown in Table 3.11.

The superimposed SCCF solution is

$$W(\xi,\eta) = W_{SSSV}(\xi,\eta) + W_{SSWR}(\xi,\eta) + W_{SWSR}(\xi,\eta)$$

or

$$W(\xi,\eta) = \sum_{m=1,2,3}^{\infty} Y_m(\eta)\sin(m\pi\xi) + \sum_{n=1,3,5}^{\infty} Y_n(\xi)\sin\left(\frac{n\pi\eta}{2}\right)$$

$$+ \sum_{p=1,2,3}^{\infty} Y_p(1-\eta)\sin(p\pi\xi)\ . \tag{3.114}$$

The details of functions $Y_m(\eta)$, $Y_n(\xi)$, and $Y_p(1-\eta)$ above are given in Table 3.12.

The zero bending moment along the free edge is defined as

$$\sum_{m=1,2,3}^{\infty}\left[Y_m''(1) - \nu(m\pi\phi)^2 Y_m(1)\right]\sin(m\pi\xi) +$$

$$\sum_{n=1,3,5}^{\infty}\left[\nu\phi^2 Y_n''(\xi) - \left(\frac{n\pi}{2}\right)^2 Y_n(\xi)\right]\cos\left(\frac{n\pi}{2}\right) +$$

$$\sum_{p=1,2,3}^{\infty}\left[Y_p''(0) - \nu(p\pi\phi)^2 Y_p(0)\right]\sin(p\pi\xi) = 0\ . \tag{3.115}$$

Equation (3.115) was derived by substituting solution (3.114) into moment equation (2.5),

Table 3.12 Solutions summary for the SCCF building blocks.

Building block	Case solution		Solution coefficients (X)	
	Case	Equation	X = 0	X ≠ 0
SSSV Section 3.2 $Y_m(\eta)$	1	(3.8)	A_m, D_m	B_m (3.24), C_m (3.25)
	2	(3.12)	B_m, D_m	A_m (3.26), C_m (3.27)
	3	(3.16)	B_m, D_m	A_m (3.28), C_m (3.29)
SSWR Section 3.3 $Y_n(\xi)$	1	(3.37)	A_n, D_n	B_n (3.38), C_n (3.39)
	2	(3.40)	B_n, D_n	A_n (3.41), C_n (3.42)
	3	(3.43)	B_n, D_n	A_n (3.44), C_n (3.45)
	4	(3.46)	B_n, D_n	A_n (3.47), C_n (3.48)
SWSR Section 3.4 $Y_p(1-\eta)$	1	(3.8)*	B_p, C_p	A_p (3.53), D_p (3.54)
	2	(3.12)*	A_p, C_p	B_p (3.55), D_p (3.56)
	3	(3.16)*	A_p, C_p	B_p (3.57), D_p (3.58)

* Replace coordinate η with $1-\eta$.

setting the result to zero, and evaluating η equal to 1. Note that indices m and p are assigned to a single summation sign since they consist of the same sequence of numbers. The $Y_n(\xi)$ and $Y_n''(\xi)$ terms in equation (3.115) are expanded into Fourier $\sin(m\pi\xi)$ series, giving

$$\sum_{m,p=1,2,3}^{\infty}\ \sum_{n=1,3,5}^{\infty}\left\{Y_m''(1) - \nu(m\pi\phi)^2 Y_m(1) - 2\left(\frac{n\pi}{2}\right)^2(-1)^{\left(\frac{n-1}{2}\right)}\int_0^1 Y_n(\xi)\sin(m\pi\xi)\,d\xi\right.$$

$$\left. + 2\nu\phi^2(-1)^{\left(\frac{n-1}{2}\right)}\int_0^1 Y_n''(\xi)\sin(m\pi\xi)\,d\xi + Y_p''(0) - \nu(p\pi\phi)^2 Y_p(0)\right\}\sin(m\pi\xi) = 0\ . \qquad (3.116)$$

Equation (3.116) is rewritten as

$$\sum_{m,p=1,2,3}^{\infty}\ \sum_{n=1,3,5}^{\infty}\left[\, a_m E_m + b_{mn} E_n + c_p E_p \,\right] = 0\ . \qquad (3.117)$$

The coefficient leading each E factor (or plate amplitude) is defined in appendix A and can be described as a building block contribution in the superimposed solution.

Slope along a clamped edge is defined by either equation (2.2) or (2.3). Once again, the superimposed solution, given by equation (3.114), is used for $W(\xi,\eta)$ in these expressions. Evaluation for each clamped edge results in

$$\sum_{m=1,2,3}^{\infty}(m\pi)Y_m(\eta)\cos(m\pi) + \sum_{n=1,3,5}^{\infty}Y_n'(1)\sin\left(\frac{n\pi\eta}{2}\right) +$$

$$\sum_{p=1,2,3}^{\infty}(p\pi)Y_p(1-\eta)\cos(p\pi) = 0 \tag{3.118}$$

for $\xi = 1$ and

$$\sum_{m=1,2,3}^{\infty}Y_m'(0)\sin(m\pi\xi) + \sum_{n=1,3,5}^{\infty}\left(\frac{n\pi}{2}\right)Y_n(\xi) -$$

$$\sum_{p=1,2,3}^{\infty}Y_p'(1)\sin(p\pi\xi) = 0 \tag{3.119}$$

for $\eta = 0$. The first and third terms in equation (3.118) are expanding into Fourier $\sin(n\pi\eta/2)$ series while the second term in equation (3.119) is expanded into Fourier $\sin(m\pi\xi)$ series. The above two equations respectively become

$$\sum_{m,p=1,2,3}^{\infty}\sum_{n=1,3,5}^{\infty}\left\{2m\pi(-1)^m\int_0^1 Y_m(\eta)\sin\left(\frac{n\pi\eta}{2}\right)d\eta + Y_n'(1)\right.$$

$$\left. + 2p\pi(-1)^p\int_0^1 Y_p(1-\eta)\sin\left(\frac{n\pi\eta}{2}\right)d\eta\right\}\sin\left(\frac{n\pi\eta}{2}\right) = 0 \tag{3.120}$$

and

$$\sum_{m,p=1,2,3}^{\infty}\sum_{n=1,3,5}^{\infty}\left\{Y_m'(0) + n\pi\int_0^1 Y_n(\xi)\sin(m\pi\xi)\,d\xi - Y_p'(1)\right\}\sin(m\pi\xi) = 0\ . \tag{3.121}$$

The slope equations are reduced to

$$\sum_{m,p=1,2,3}^{\infty} \sum_{n=1,3,5}^{\infty} [\, e_{mn}E_m + f_nE_n + g_{pn}E_p \,] = 0 \tag{3.122}$$

for the edge at $\xi = 1$ and

$$\sum_{m,p=1,2,3}^{\infty} \sum_{n=1,3,5}^{\infty} [\, i_mE_m + j_{mn}E_n + k_pE_p \,] = 0 \tag{3.123}$$

for the edge at $\eta = 0$. The building block contributions are listed in appendix A.

$$\begin{array}{c c}
 & \begin{array}{ccc} \text{SSSV} & \text{SSWR} & \text{SWSR} \end{array} \\
\begin{array}{c} (3.117) \\ \\ \\ (3.122) \\ \\ \\ (3.123) \\ \\ \\ \end{array} &
\left[\begin{array}{ccc ccc ccc}
a_1 & 0 & 0 & b_{11} & b_{13} & b_{15} & c_1 & 0 & 0 \\
0 & a_2 & 0 & b_{21} & b_{23} & b_{25} & 0 & c_2 & 0 \\
0 & 0 & a_3 & b_{31} & b_{33} & b_{35} & 0 & 0 & c_3 \\
e_{11} & e_{21} & e_{31} & f_1 & 0 & 0 & g_{11} & g_{21} & g_{31} \\
e_{13} & e_{23} & e_{33} & 0 & f_3 & 0 & g_{13} & g_{23} & g_{33} \\
e_{15} & e_{25} & e_{35} & 0 & 0 & f_5 & g_{15} & g_{25} & g_{35} \\
i_1 & 0 & 0 & j_{11} & j_{13} & j_{15} & k_1 & 0 & 0 \\
0 & i_2 & 0 & j_{21} & j_{23} & j_{25} & 0 & k_2 & 0 \\
0 & 0 & i_3 & j_{31} & j_{33} & j_{35} & 0 & 0 & k_3
\end{array}\right]
\left\{\begin{array}{c}
E_{m=1} \\ E_{m=2} \\ E_{m=3} \\ E_{n=1} \\ E_{n=3} \\ E_{n=5} \\ E_{p=1} \\ E_{p=2} \\ E_{p=3}
\end{array}\right\}
=
\left\{\begin{array}{c}
0 \\ 0 \\ 0 \\ 0 \\ 0 \\ 0 \\ 0 \\ 0 \\ 0
\end{array}\right\}
\end{array}$$

Figure 3.23 A three term expansion of the algebraic equations for the SCCF plate.

Figure 3.23 portrays the system of equations, in matrix form, resulting from a three term expansion of equations (3.117), (3.122), and (3.123). Coefficients leading each E factor are building block contributions and are defined in appendix A. Any integrals used are listed in appendix B. Eigenvalues and mode shapes are obtained by following the same procedure presented in section 3.10 for the SFSF plate.

3.16 The CSCF Plate

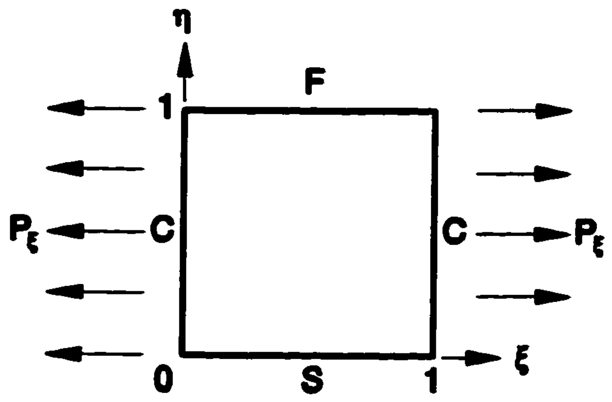

Figure 3.24 The CSCF plate under unilateral in-plane load.

Table 3.13 Boundary conditions summary of the CSCF plate and its building blocks.

	Boundary conditions at specified edge			
Plate	$\xi = 0$	$\eta = 0$	$\xi = 1$	$\eta = 1$
SSSV	$W = 0,\ M_\xi = 0$	$W = 0,\ M_\eta = 0$	$W = 0,\ M_\xi = 0$	$S_\eta \propto E_m,\ V_\eta = 0$
SSWR	$W = 0,\ M_\xi = 0$	$W = 0,\ M_\eta = 0$	$W = 0,\ M_\xi \propto E_n$	$S_\eta = 0,\ V_\eta = 0$
WSSR	$W = 0,\ M_\xi \propto E_q$	$W = 0,\ M_\eta = 0$	$W = 0,\ M_\xi = 0$	$S_\eta = 0,\ V_\eta = 0$
CSCF	$W = 0,\ S_\xi = 0$	$W = 0,\ M_\eta = 0$	$W = 0,\ S_\xi = 0$	$M_\eta = 0,\ V_\eta = 0$

An analytical-type solution for the CSCF plate is obtained by superimposing the SSSV, SSWR, and WSSR building blocks, as shown in Figure 3.1. Each building block possesses a distinct harmonic boundary condition which regulates its amplitude, as shown in Table 3.13. The final solution is achieved once the harmonic rotations and moments are adequately adjusted such that the remaining boundary conditions become satisfied. Specifically, harmonic slopes cause moments for a free edge to vanish and harmonic moments cause slopes for a clamped edge to vanish.

The superimposed CSCF solution is

$$W(\xi,\eta) = W_{SSSV}(\xi,\eta) + W_{SSWR}(\xi,\eta) + W_{WSSR}(\xi,\eta)$$

or

$$W(\xi,\eta) = \sum_{m=1,2,3}^{\infty} Y_m(\eta)\sin(m\pi\xi) + \sum_{n=1,3,5}^{\infty} Y_n(\xi)\sin\left(\frac{n\pi\eta}{2}\right)$$

$$+ \sum_{q=1,3,5}^{\infty} Y_q(1-\xi)\sin\left(\frac{q\pi\eta}{2}\right). \tag{3.124}$$

The details of functions $Y_m(\eta)$, $Y_p(1-\eta)$, and $Y_q(1-\xi)$ above are given in Table 3.14.

The bending moment along the free edge is defined by equation (2.5) and is set equal to zero. Superimposed solution (3.124) is substituted for $W(\xi,\eta)$ in the expression. Evaluation at $\eta = 1$ gives

$$\sum_{m=1,2,3}^{\infty}\left[Y_m''(1) - \nu(m\pi\phi)^2 Y_m(1)\right]\sin(m\pi\xi) +$$

$$\sum_{n=1,3,5}^{\infty}\left[\nu\phi^2 Y_n''(\xi) - \left(\frac{n\pi}{2}\right)^2 Y_n(\xi)\right]\cos\left(\frac{n\pi}{2}\right) +$$

$$\sum_{q=1,3,5}^{\infty}\left[\nu\phi^2 Y_q''(1-\xi) - \left(\frac{q\pi}{2}\right)^2 Y_q(1-\xi)\right]\cos\left(\frac{q\pi}{2}\right) = 0. \tag{3.125}$$

The $Y_n(\xi)$, $Y_n''(\xi)$, $Y_q(1-\xi)$, and $Y_q''(1-\xi)$ terms are expanded into $\sin(m\pi\xi)$ series, giving

$$\sum_{m=1,2,3}^{\infty}\sum_{n,q=1,3,5}^{\infty}\left\{Y_m''(1) - \nu(m\pi\phi)^2 Y_m(1) - 2\left(\frac{n\pi}{2}\right)^2(-1)^{\left(\frac{n-1}{2}\right)}\int_0^1 Y_n(\xi)\sin(m\pi\xi)\,d\xi\right.$$

$$+ 2\nu\phi^2(-1)^{\left(\frac{n-1}{2}\right)}\int_0^1 Y_n''(\xi)\sin(m\pi\xi)\,d\xi \tag{3.126}$$

$$\left.- 2\left(\frac{q\pi}{2}\right)^2(-1)^{\left(\frac{q-1}{2}\right)}\int_0^1 Y_q(1-\xi)\sin(m\pi\xi)\,d\xi + 2\nu\phi^2(-1)^{\left(\frac{q-1}{2}\right)}\int_0^1 Y_q''(1-\xi)\sin(m\pi\xi)\,d\xi\right\}\sin(m\pi\xi) = 0.$$

Table 3.14 Solutions summary for the CSCF building blocks.

Building block	Case solution		Solution coefficients (X)	
	Case	Equation	X = 0	X ≠ 0
SSSV Section 3.2 $Y_m(\eta)$	1	(3.8)	A_m, D_m	B_m (3.24), C_m (3.25)
	2	(3.12)	B_m, D_m	A_m (3.26), C_m (3.27)
	3	(3.16)	B_m, D_m	A_m (3.28), C_m (3.29)
SSWR Section 3.3 $Y_n(\xi)$	1	(3.37)	A_n, D_n	B_n (3.38), C_n (3.39)
	2	(3.40)	B_n, D_n	A_n (3.41), C_n (3.42)
	3	(3.43)	B_n, D_n	A_n (3.44), C_n (3.45)
	4	(3.46)	B_n, D_n	A_n (3.47), C_n (3.48)
WSSR Section 3.5 $Y_q(1-\xi)$	1	(3.37)*	A_n, D_n	B_n (3.38), C_n (3.39)
	2	(3.40)*	B_n, D_n	A_n (3.41), C_n (3.42)
	3	(3.43)*	B_n, D_n	A_n (3.44), C_n (3.45)
	4	(3.46)*	B_n, D_n	A_n (3.47), C_n (3.48)

* Replace coordinate ξ with $1-\xi$.

Equation (3.126) is rewritten as

$$\sum_{m=1,2,3}^{\infty} \sum_{n,q=1,3,5}^{\infty} [\, a_m E_m + b_{mn} E_n + d_{mq} E_q \,] = 0 \,. \tag{3.127}$$

The coefficient leading each E factor (or plate amplitude) is defined in appendix A and can be labelled as a building block contribution in the superimposed solution.

Slope along the clamped edges are defined by equation (2.2). Once again, the superimposed solution, given by equation (3.124), is used for $W(\xi,\eta)$ in this expression. Evaluation results in

$$\sum_{m=1,2,3}^{\infty} (m\pi) Y_m(\eta) \cos(m\pi) + \sum_{n=1,3,5}^{\infty} Y_n'(1) \sin\left(\frac{n\pi\eta}{2}\right) -$$

$$\sum_{q=1,3,5}^{\infty} Y_q'(0) \sin\left(\frac{q\pi\eta}{2}\right) = 0 \tag{3.128}$$

for $\xi = 1$ and

$$\sum_{m=1,2,3}^{\infty} (m\pi) Y_m(\eta) + \sum_{n=1,3,5}^{\infty} Y_n'(0) \sin\left(\frac{n\pi\eta}{2}\right) -$$

$$\sum_{q=1,3,5}^{\infty} Y_q'(1) \sin\left(\frac{q\pi\eta}{2}\right) = 0 \tag{3.129}$$

for $\xi = 0$. The first term in the above equations is expanded into Fourier $\sin(n\pi\eta/2)$ series, respectively becoming

$$\sum_{m=1,2,3}^{\infty} \sum_{n,q=1,3,5}^{\infty} \left\{ 2m\pi(-1)^m \int_0^1 Y_m(\eta) \sin\left(\frac{n\pi\eta}{2}\right) d\eta + Y_n'(1) - Y_q'(0) \right\} \sin\left(\frac{n\pi\eta}{2}\right) = 0 \tag{3.130}$$

and

$$\sum_{m=1,2,3}^{\infty} \sum_{n,q=1,3,5}^{\infty} \left\{ 2m\pi \int_0^1 Y_m(\eta) \sin\left(\frac{n\pi\eta}{2}\right) d\eta + Y_n'(0) - Y_q'(1) \right\} \sin\left(\frac{n\pi\eta}{2}\right) = 0\,. \tag{3.131}$$

The slope equations are reduced to

$$\sum_{m=1,2,3}^{\infty} \sum_{n,q=1,3,5}^{\infty} [\, e_{mn} E_m + f_n E_n + h_q E_q \,] = 0 \tag{3.132}$$

for the edge at $\xi = 1$ and

$$\sum_{m=1,2,3}^{\infty} \sum_{n,q=1,3,5}^{\infty} [\, s_{mn} E_m + t_n E_n + v_q E_q \,] = 0 \tag{3.133}$$

for the edge at $\xi = 0$. The building block contributions are listed in appendix A.

Figure 3.25 portrays the system of equations, in matrix form, resulting from a three term expansion of equations (3.127), (3.132), and (3.133). Coefficients leading each E factor are building block contributions and are defined in appendix A. Any integrals used are listed in appendix B. Eigenvalues and mode shapes are obtained by following the same procedure presented in section 3.10 for the SFSF plate.

$$
\begin{array}{c c}
 & \begin{array}{ccc} \text{SSSV} \qquad & \text{SSWR} \qquad & \text{WSSR} \end{array} \\
\begin{array}{c} \\ (3.127) \\ \\ \\ (3.132) \\ \\ \\ (3.133) \\ \\ \end{array} &
\left[\begin{array}{ccccccccc}
a_1 & 0 & 0 & b_{11} & b_{13} & b_{15} & d_{11} & d_{13} & d_{15} \\
0 & a_2 & 0 & b_{21} & b_{23} & b_{25} & d_{21} & d_{23} & d_{25} \\
0 & 0 & a_3 & b_{31} & b_{33} & b_{35} & d_{31} & d_{33} & d_{35} \\
e_{11} & e_{21} & e_{31} & f_1 & 0 & 0 & h_1 & 0 & 0 \\
e_{13} & e_{23} & e_{33} & 0 & f_3 & 0 & 0 & h_3 & 0 \\
e_{15} & e_{25} & e_{35} & 0 & 0 & f_5 & 0 & 0 & h_5 \\
s_{11} & s_{21} & s_{31} & t_1 & 0 & 0 & v_1 & 0 & 0 \\
s_{13} & s_{23} & s_{33} & 0 & t_3 & 0 & 0 & v_3 & 0 \\
s_{15} & s_{25} & s_{35} & 0 & 0 & t_5 & 0 & 0 & v_5
\end{array}\right]
\left\{\begin{array}{c}
E_{m-1} \\ E_{m-2} \\ E_{m-3} \\ E_{n-1} \\ E_{n-3} \\ E_{n-5} \\ E_{q-1} \\ E_{q-3} \\ E_{q-5}
\end{array}\right\}
=
\left\{\begin{array}{c}
0 \\ 0 \\ 0 \\ 0 \\ 0 \\ 0 \\ 0 \\ 0 \\ 0
\end{array}\right\}
\end{array}
$$

Figure 3.25 A three term expansion of the algebraic equations for the CSCF plate.

3.17 The CCCF Plate

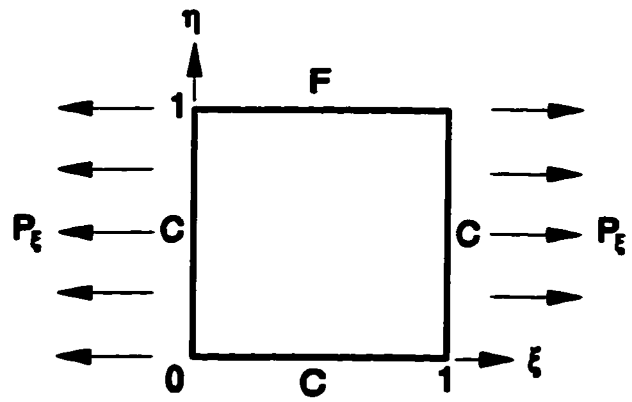

Figure 3.26 The CCCF thin rectangular plate under unilateral in-plane load.

Consider the plate presented in Figure 3.26, where none of the edges are either simply supported or slip shear. The superimposed solution of the CCCF plate consists of the SSSV, SSWR, SWSR, and WSSR building blocks, as shown in Figure 3.1. The building block solutions are derived in sections 3.2 through 3.5 inclusively. The CCCF plate solution becomes

$$W(\xi,\eta) = W_{SSSV}(\xi,\eta) + W_{SSWR}(\xi,\eta) + W_{SWSR}(\xi,\eta) + W_{WSSR}(\xi,\eta)$$

or

$$W(\xi,\eta) = \sum_{m=1,2,3}^{\infty} Y_m(\eta)\sin(m\pi\xi) + \sum_{n=1,3,5}^{\infty} Y_n(\xi)\sin\left(\frac{n\pi\eta}{2}\right)$$

$$+ \sum_{p=1,2,3}^{\infty} Y_p(1-\eta)\sin(p\pi\xi) + \sum_{q=1,3,5}^{\infty} Y_q(1-\xi)\sin\left(\frac{q\pi\eta}{2}\right). \qquad (3.134)$$

Table 3.15 Boundary conditions summary of the CCCF plate and its building blocks.

	Boundary conditions at specified edge			
Plate	$\xi = 0$	$\eta = 0$	$\xi = 1$	$\eta = 1$
SSSV	$W = 0,\ M_\xi = 0$	$W = 0,\ M_\eta = 0$	$W = 0,\ M_\xi = 0$	$S_\eta \propto E_m,\ V_\eta = 0$
SSWR	$W = 0,\ M_\xi = 0$	$W = 0,\ M_\eta = 0$	$W = 0,\ M_\xi \propto E_n$	$S_\eta = 0,\ V_\eta = 0$
SWSR	$W = 0,\ M_\xi = 0$	$W = 0,\ M_\eta \propto E_p$	$W = 0,\ M_\xi = 0$	$S_\eta = 0,\ V_\eta = 0$
WSSR	$W = 0,\ M_\xi \propto E_q$	$W = 0,\ M_\eta = 0$	$W = 0,\ M_\xi = 0$	$S_\eta = 0,\ V_\eta = 0$
CCCF	$W = 0,\ S_\xi = 0$	$W = 0,\ S_\eta = 0$	$W = 0,\ S_\xi = 0$	$M_\eta = 0,\ V_\eta = 0$

Table 3.16 summarizes the building block solutions. Each building block possesses a distinct harmonic boundary condition which regulates its amplitude, as shown in Table 3.15. The final solution is achieved once the harmonic rotations and moments are adequately adjusted such that the remaining boundary conditions become satisfied.

The bending moment along the free edge is defined by equation (2.5) and is set equal to zero. Superimposed solution (3.134) is substituted for $W(\xi,\eta)$ in the expression. Evaluation at $\eta = 1$ gives

Table 3.16 Solutions summary for the CFCF building blocks.

Building block	Case solution		Solution coefficients (X)	
	Case	Equation	X = 0	X ≠ 0
SSSV Section 3.2 $Y_m(\eta)$	1	(3.8)	A_m, D_m	B_m (3.24), C_m (3.25)
	2	(3.12)	B_m, D_m	A_m (3.26), C_m (3.27)
	3	(3.16)	B_m, D_m	A_m (3.28), C_m (3.29)
SSWR Section 3.3 $Y_n(\xi)$	1	(3.37)	A_n, D_n	B_n (3.38), C_n (3.39)
	2	(3.40)	B_n, D_n	A_n (3.41), C_n (3.42)
	3	(3.43)	B_n, D_n	A_n (3.44), C_n (3.45)
	4	(3.46)	B_n, D_n	A_n (3.47), C_n (3.48)
SWSR Section 3.4 $Y_p(1-\eta)$	1	(3.8)*	B_p, C_p	A_p (3.53), D_p (3.54)
	2	(3.12)*	A_p, C_p	B_p (3.55), D_p (3.56)
	3	(3.16)*	A_p, C_p	B_p (3.57), D_p (3.58)
WSSR Section 3.5 $Y_q(1-\xi)$	1	(3.37)**	A_n, D_n	B_n (3.38), C_n (3.39)
	2	(3.40)**	B_n, D_n	A_n (3.41), C_n (3.42)
	3	(3.43)**	B_n, D_n	A_n (3.44), C_n (3.45)
	4	(3.46)**	B_n, D_n	A_n (3.47), C_n (3.48)

* Replace coordinate η with $1-\eta$.
** Replace coordinate ξ with $1-\xi$.

$$\sum_{m=1,2,3}^{\infty}\left[Y_m''(1)-\nu(m\pi\phi)^2Y_m(1)\right]\sin(m\pi\xi)\ +$$

$$\sum_{n=1,3,5}^{\infty}\left[\nu\phi^2Y_n''(\xi)-\left(\frac{n\pi}{2}\right)^2Y_n(\xi)\right]\cos\left(\frac{n\pi}{2}\right)\ +$$

$$\sum_{p=1,2,3}^{\infty}\left[Y_p''(0)-\nu(p\pi\phi)^2Y_p(0)\right]\sin(p\pi\xi)\ +$$

$$\sum_{q=1,3,5}^{\infty}\left[\nu\phi^2Y_q''(1-\xi)-\left(\frac{q\pi}{2}\right)^2Y_q(1-\xi)\right]\cos\left(\frac{q\pi}{2}\right)=0\ . \qquad (3.135)$$

$$
\begin{array}{c}
\begin{array}{cccc} \qquad\quad \text{SSSV} & \qquad\qquad \text{SSWR} & \qquad\qquad \text{SWSR} & \qquad\qquad \text{WSSR} \end{array} \\
\begin{array}{c}
\\ (3.137) \\ \\ \\ (3.144) \\ \\ \\ (3.145) \\ \\ \\ (3.146) \\ \\
\end{array}
\left[
\begin{array}{ccc ccc ccc ccc}
a_1 & 0 & 0 & b_{11} & b_{13} & b_{15} & c_1 & 0 & 0 & d_{11} & d_{13} & d_{15} \\
0 & a_2 & 0 & b_{21} & b_{23} & b_{25} & 0 & c_2 & 0 & d_{21} & d_{23} & d_{25} \\
0 & 0 & a_3 & b_{31} & b_{33} & b_{35} & 0 & 0 & c_3 & d_{31} & d_{33} & d_{35} \\
e_{11} & e_{21} & e_{31} & f_1 & 0 & 0 & g_{11} & g_{21} & g_{31} & h_1 & 0 & 0 \\
e_{13} & e_{23} & e_{33} & 0 & f_3 & 0 & g_{13} & g_{23} & g_{33} & 0 & h_3 & 0 \\
e_{15} & e_{25} & e_{35} & 0 & 0 & f_5 & g_{15} & g_{25} & g_{35} & 0 & 0 & h_5 \\
i_1 & 0 & 0 & j_{11} & j_{13} & j_{15} & k_1 & 0 & 0 & l_{11} & l_{13} & l_{15} \\
0 & i_2 & 0 & j_{21} & j_{23} & j_{25} & 0 & k_2 & 0 & l_{21} & l_{23} & l_{25} \\
0 & 0 & i_3 & j_{31} & j_{33} & j_{35} & 0 & 0 & k_3 & l_{31} & l_{33} & l_{35} \\
s_{11} & s_{21} & s_{31} & t_1 & 0 & 0 & u_{11} & u_{21} & u_{31} & v_1 & 0 & 0 \\
s_{13} & s_{23} & s_{33} & 0 & t_3 & 0 & u_{13} & u_{23} & u_{33} & 0 & v_3 & 0 \\
s_{15} & s_{25} & s_{35} & 0 & 0 & t_5 & u_{15} & u_{25} & u_{35} & 0 & 0 & v_5
\end{array}
\right]
\left\{
\begin{array}{c}
E_{m=1} \\ E_{m=2} \\ E_{m=3} \\ E_{n=1} \\ E_{n=3} \\ E_{n=5} \\ E_{p=1} \\ E_{p=2} \\ E_{p=3} \\ E_{q=1} \\ E_{q=3} \\ E_{q=5}
\end{array}
\right\}
=
\left\{
\begin{array}{c}
0 \\ 0 \\ 0 \\ 0 \\ 0 \\ 0 \\ 0 \\ 0 \\ 0 \\ 0 \\ 0 \\ 0
\end{array}
\right\}
\end{array}
$$

Figure 3.27 A three term expansion of the algebraic equations for the CCCF plate.

Indices consisting of the same sequence of numbers are grouped together. The $Y_n(\xi)$, $Y_n''(\xi)$, $Y_q(1-\xi)$, and $Y_q''(1-\xi)$ terms in the above equation are expanded into Fourier $\sin(m\pi\xi)$ series, giving

$$
\begin{aligned}
\sum_{m,p=1,2,3}^{\infty} \sum_{n,q=1,3,5}^{\infty} \Bigg\{ & Y_m''(1) - \nu(m\pi\phi)^2 Y_m(1) - 2\left(\frac{n\pi}{2}\right)^2 (-1)^{\left(\frac{n-1}{2}\right)} \int_0^1 Y_n(\xi)\sin(m\pi\xi)\,d\xi \\
& + 2\nu\phi^2(-1)^{\left(\frac{n-1}{2}\right)} \int_0^1 Y_n''(\xi)\sin(m\pi\xi)\,d\xi + Y_p''(0) - \nu(p\pi\phi)^2 Y_p(0) \qquad (3.136) \\
- 2\left(\frac{q\pi}{2}\right)^2 (-1)^{\left(\frac{q-1}{2}\right)} & \int_0^1 Y_q(1-\xi)\sin(m\pi\xi)\,d\xi + 2\nu\phi^2(-1)^{\left(\frac{q-1}{2}\right)} \int_0^1 Y_q''(1-\xi)\sin(m\pi\xi)\,d\xi \Bigg\} \sin(m\pi\xi) = 0 \,.
\end{aligned}
$$

Equation (3.136) is rewritten as

$$
\sum_{m,p=1,2,3}^{\infty} \sum_{n,q=1,3,5}^{\infty} \left[a_m E_m + b_{mn} E_n + c_p E_p + d_{mq} E_q \right] = 0 \,. \qquad (3.137)
$$

The coefficient leading each E factor (or plate amplitude) is defined in appendix A and can be described as a building block contribution in the superimposed solution.

Slope along a clamped edge is defined by either equation (2.2) or (2.3). Once again, the superimposed solution, given by equation (3.134), is used for $W(\xi,\eta)$ in these expressions. Evaluation for each edge results in

$$\sum_{m=1,2,3}^{\infty}(m\pi)Y_m(\eta)\cos(m\pi) + \sum_{n=1,3,5}^{\infty}Y_n'(1)\sin\left(\frac{n\pi\eta}{2}\right) +$$

$$\sum_{p=1,2,3}^{\infty}(p\pi)Y_p(1-\eta)\cos(p\pi) - \sum_{q=1,3,5}^{\infty}Y_q'(0)\sin\left(\frac{q\pi\eta}{2}\right) = 0 \qquad (3.138)$$

for $\xi = 1$,

$$\sum_{m=1,2,3}^{\infty}Y_m'(0)\sin(m\pi\xi) + \sum_{n=1,3,5}^{\infty}\left(\frac{n\pi}{2}\right)Y_n(\xi) -$$

$$\sum_{p=1,2,3}^{\infty}Y_p'(1)\sin(p\pi\xi) + \sum_{q=1,3,5}^{\infty}\left(\frac{q\pi}{2}\right)Y_q(1-\xi) = 0 \qquad (3.139)$$

for $\eta = 0$, and

$$\sum_{m=1,2,3}^{\infty}(m\pi)Y_m(\eta) + \sum_{n=1,3,5}^{\infty}Y_n'(0)\sin\left(\frac{n\pi\eta}{2}\right) +$$

$$\sum_{p=1,2,3}^{\infty}(p\pi)Y_p(1-\eta) - \sum_{q=1,3,5}^{\infty}Y_q'(1)\sin\left(\frac{q\pi\eta}{2}\right) = 0 \qquad (3.140)$$

for $\xi = 0$. The first and third terms in equations (3.138) and (3.140) are expanded into Fourier $\sin(n\pi\eta/2)$ series while the second and fourth terms in equation (3.139) are expanded into Fourier $\sin(m\pi\xi)$ series. The above three equations respectively become

$$\sum_{m,p=1,2,3}^{\infty}\sum_{n,q=1,3,5}^{\infty}\left\{2m\pi(-1)^m\int_0^1 Y_m(\eta)\sin\left(\frac{n\pi\eta}{2}\right)d\eta + Y_n'(1)\right.$$

$$\left. + 2p\pi(-1)^p\int_0^1 Y_p(1-\eta)\sin\left(\frac{n\pi\eta}{2}\right)d\eta - Y_q'(0)\right\}\sin\left(\frac{n\pi\eta}{2}\right) = 0\,, \qquad (3.141)$$

$$\sum_{m,p=1,2,3}^{\infty} \sum_{n,q=1,3,5}^{\infty} \left\{ Y_m'(0) + n\pi \int_0^1 Y_n(\xi)\sin(m\pi\xi)\,d\xi \right.$$

$$\left. - Y_p'(1) + q\pi \int_0^1 Y_q(1-\xi)\sin(m\pi\xi)\,d\xi \right\} \sin(m\pi\xi) = 0 \,, \tag{3.142}$$

and

$$\sum_{m,p=1,2,3}^{\infty} \sum_{n,q=1,3,5}^{\infty} \left\{ 2m\pi \int_0^1 Y_m(\eta)\sin\left(\frac{n\pi\eta}{2}\right)d\eta + Y_n'(0) \right.$$

$$\left. + 2p\pi \int_0^1 Y_p(1-\eta)\sin\left(\frac{n\pi\eta}{2}\right)d\eta - Y_q'(1) \right\} \sin\left(\frac{n\pi\eta}{2}\right) = 0 \,. \tag{3.143}$$

The slope equations are reduced to

$$\sum_{m,p=1,2,3}^{\infty} \sum_{n,q=1,3,5}^{\infty} [\, e_{mn}E_m + f_nE_n + g_{pn}E_p + h_qE_q \,] = 0 \tag{3.144}$$

for the edge at $\xi = 1$,

$$\sum_{m,p=1,2,3}^{\infty} \sum_{n,q=1,3,5}^{\infty} [\, i_mE_m + j_{mn}E_n + k_pE_p + l_{mq}E_q \,] = 0 \tag{3.145}$$

for the edge at $\eta = 0$, and

$$\sum_{m,p=1,2,3}^{\infty} \sum_{n,q=1,3,5}^{\infty} [\, s_{mn}E_m + t_nE_n + u_{pn}E_p + v_qE_q \,] = 0 \tag{3.146}$$

for the edge at $\xi = 0$. The building block contributions are listed in appendix A.

Figure 3.27 is a matrix representation of the linear equations resulting from a three term expansion of equations (3.137), (3.144), (3.145), and (3.146). Eigenvalues and mode shapes are obtained by following the procedure described at the end of section 3.10.

4 Presentation of Results

Free vibration analysis results are presented for thin rectangular plates subjected to evenly distributed unilateral in-plane loads. The magnitude of each in-plane load used is a specified percentage of the critical buckling load for the plate being analyzed. Thus, plate stability is analyzed prior to free vibration. Buckling loads are presented for each plate under investigation. Eigenvalues and associated eigenvectors are then presented for the first eight modes of free vibration. Mode shape migrations are traced in eigenvalue curves. The following plate configurations are analyzed: SSSF, SFSF, SFCF, CFCF, SCSF, SSCF, SCCF, CSCF, and CCCF. Nine aspect ratios are considered for each plate: 1/3, 2/5, 1/2, 2/3, 1/1, 3/2, 2/1, 5/2, and 3/1. Buckling load curves are also presented for each plate. All calculated results are presented in dimensionless form.

4.1 Buckling Analysis Results

Equation (2.1) can be modified to analyze plate buckling due to in-plane loads. Setting parameter λ^2 equal to zero eliminates the dynamic characteristics of free vibration from the governing equation. The resulting differential equation,

$$\frac{\partial^4 W(\xi,\eta)}{\partial\eta^4} + 2\phi^2\frac{\partial^4 W(\xi,\eta)}{\partial\eta^2\partial\xi^2} + \phi^4\frac{\partial^4 W(\xi,\eta)}{\partial\xi^4} + P_\xi\phi^2\frac{\partial^2 W(\xi,\eta)}{\partial\xi^2} = 0, \tag{4.1}$$

is used to determine transverse plate displacement due to a unilateral load. The first value of P_ξ to satisfy equation (4.1) for a given plate is a critical buckling load.

The free vibration solutions presented in section 3 can be used to obtain buckling loads. In a free vibration analysis, natural frequencies are determined by examining the effect of λ^2 on the determinant of a coefficient matrix comprised of building block contributions. The λ^2 value which makes the determinant equal to zero is a dimensionless natural frequency. For plate buckling, λ^2 is set equal to zero and the effect of P_ξ on the determinant is examined instead.

Timoshenko [17] used Lévy-type solutions to obtain buckling loads for the SSSF and SCSF plates. Buckling k factor results are reproduced in Tables 4.1 and 4.2 so that comparisons can be made with results obtained using the present solution, where

$$k = \frac{-P_\xi}{\pi^2} . \qquad (4.2)$$

Calculated k factors were within 0.5% of the published results.

Table 4.1 Buckling k factors, SSSF plate, $\nu = 0.25$, $k = -N_x b^2 / (\pi^2 D)$.

ϕ	Lévy-type solution [17]	Present solution	Percent difference
1/3	0.564	0.563	-0.17%
1/2	0.698	0.698	-0.01%
1/1	1.440	1.434	-0.40%
2/1	4.400	4.404	0.08%

Table 4.2 Buckling k factors, SCSF plate, $\nu = 0.25$, $k = -N_x b^2 / (\pi^2 D)$.

ϕ	Lévy-type solution [17]	Present solution	Percent difference
1/2	1.38	1.386	0.45%
2/3	1.34	1.339	-0.06%
1/1	1.70	1.698	-0.10%

Timoshenko [17] also reviews column buckling solutions which satisfy

$$\frac{d^4y}{dx^4} + \frac{P_x}{EI}\frac{d^2y}{dx^2} = 0 . \qquad (4.3)$$

Results are presented as k factors. Beams having a rectangular cross-section can be approximated as long, slender plates. Published beam results are compared to those derived using the present solution, where

$$k = \frac{-P_{\xi}}{\pi^2 \phi^2 (1 - v^2)} . \qquad (4.4)$$

Specifically, the simple-simple, simple-clamped, and clamped-clamped beams are compared to the SFSF, SFCF, and CFCF plates respectively. Tables 4.3, 4.4, and 4.5 show that beam results are approached by the plate solution as the plate becomes long and slender. A Poisson ratio of 0.333 was used in the plate solutions.

Table 4.3 Buckling k factors, SS beam, $k = - P_x a^2 / (\pi^2 E I)$.

ϕ	Beam solution [17]	Plate solution	Percent difference
1/10	1.000	1.002	0.17%
1/3	1.000	1.013	1.31%
1/2	1.000	1.025	2.53%
1/1	1.000	1.057	5.71%

Table 4.4 Buckling k factors, CC beam, $k = - P_x a^2 / (\pi^2 E I)$.

ϕ	Beam solution [17]	Plate solution	Percent difference
1/10	4.000	4.089	2.22%
1/3	4.000	4.251	6.27%
1/2	4.000	4.306	7.66%
1/1	4.000	4.382	9.54%

Table 4.5 Buckling k factors, SC beam, $k = - P_x a^2 / (\pi^2 E I)$.

ϕ	Beam solution [17]	Plate solution	Percent difference
1/10	2.047	2.068	1.06%
1/3	2.047	2.126	3.88%
1/2	2.047	2.157	5.40%
1/1	2.047	2.210	8.00%

Comparisons are also made to results generated using the approximate formula proposed by Dickinson [11]. Coefficients used in buckling formula (1.2) were derived using characteristic beam functions in Rayleigh's method and are taken directly from the paper. Results of the study are listed in Table 4.6. Relative error in the approximate results is as high as 11%.

Table 4.6 Approximate buckling loads, $P_\xi = - N_x b^2 / D$.

ϕ	SSSF	SFSF	SFCF	CFCF	SCSF	SSCF	SCCF	CSCF	CCCF
					Approximate formula [11]				
1/3	5.10	1.10	2.30	4.52	12.84	6.30	14.69	8.52	17.25
1/1	13.87	9.87	20.69	40.68	16.75	24.69	27.40	44.68	47.31
3/1	92.83	88.83	186.21	366.12	94.60	190.21	191.96	370.13	371.86
					Present solution				
1/3	5.06	0.99	2.07	4.15	12.41	6.18	13.45	8.28	16.27
1/1	13.59	9.28	19.40	38.45	15.98	23.75	25.81	42.81	44.74
3/1	91.22	86.67	178.83	351.49	91.83	183.37	183.87	355.98	356.42
					Percent difference				
1/3	0.8%	11.1%	11.1%	8.9%	3.5%	1.9%	9.2%	2.9%	6.0%
1/1	2.1%	6.4%	6.6%	5.8%	4.8%	4.0%	6.2%	4.4%	5.7%
3/1	1.8%	2.5%	4.1%	4.2%	3.0%	3.7%	4.4%	4.0%	4.3%

Unilateral in-plane buckling loads for all plates of interest are calculated using the present method and are listed in Table 4.7. Comparisons are made to numerical results obtained using the general purpose finite element program ANSYS [18]. The difference in P_ξ between the two solution methods did not exceed 0.3%. Details of the FEM model and analysis are given in appendix C. Buckling load versus aspect ratio graphs are shown in Figures 4.1 to 4.9.

Table 4.7 Buckling loads, $P_\xi = - N_x b^2 / D$.

ϕ	SSSF	SFSF	SFCF	CFCF	SCSF	SSCF	SCCF	CSCF	CCCF
					Plate				
					Present solution				
1/3	5.062	0.988	2.073	4.145	12.413	6.179	13.450	8.276	16.271
2/5	5.529	1.429	3.004	6.005	13.344	7.140	13.994	10.165	17.057
1/2	6.390	2.249	4.732	9.447	12.846	8.912	14.178	13.648	18.637
2/3	8.253	4.046	8.502	16.928	12.413	12.749	16.270	21.191	24.498
1/1	13.593	9.276	19.397	38.451	15.980	23.748	25.807	42.810	44.736
3/2	25.659	21.235	44.142	87.158	27.095	48.590	49.829	91.602	92.745
2/1	42.611	38.122	78.963	155.568	43.620	83.466	84.328	160.054	160.835
5/2	64.462	59.932	123.858	243.677	65.226	128.391	129.035	248.179	248.751
3/1	91.220	86.665	178.826	351.486	91.825	183.371	183.873	355.984	356.420
					Finite element solution [18]				
1/3	5.061	0.989	2.077	4.156	12.409	6.179	13.450	8.279	16.289
2/5	5.529	1.430	3.009	6.020	13.347	7.142	13.994	10.172	17.065
1/2	6.391	2.251	4.739	9.467	12.844	8.916	14.180	13.663	18.653
2/3	8.256	4.048	8.512	16.956	12.414	12.758	16.280	21.218	24.529
1/1	13.600	9.281	19.411	38.488	15.987	23.766	25.828	42.852	44.788
3/2	25.673	21.243	44.160	87.185	27.111	48.617	49.862	91.643	92.804
2/1	42.636	38.140	78.992	155.570	43.648	83.506	84.378	160.082	160.890
5/2	64.510	59.970	123.913	243.673	65.278	128.463	129.120	248.218	248.825
3/1	91.305	86.736	178.932	351.510	91.914	183.504	184.023	356.100	356.580
					Percent difference				
1/3	-0.01%	0.09%	0.17%	0.28%	-0.03%	0.00%	0.00%	0.04%	0.11%
2/5	0.00%	0.08%	0.16%	0.25%	0.02%	0.02%	0.00%	0.07%	0.05%
1/2	0.02%	0.08%	0.14%	0.21%	-0.02%	0.05%	0.02%	0.11%	0.09%
2/3	0.04%	0.06%	0.11%	0.17%	0.01%	0.07%	0.06%	0.13%	0.13%
1/1	0.05%	0.05%	0.07%	0.10%	0.05%	0.07%	0.08%	0.10%	0.12%
3/2	0.05%	0.04%	0.04%	0.03%	0.06%	0.06%	0.07%	0.04%	0.06%
2/1	0.06%	0.05%	0.04%	0.00%	0.06%	0.05%	0.06%	0.02%	0.03%
5/2	0.07%	0.06%	0.04%	0.00%	0.08%	0.06%	0.07%	0.02%	0.03%
3/1	0.09%	0.08%	0.06%	0.01%	0.10%	0.07%	0.08%	0.03%	0.05%

Figure 4.1 Buckling load curves, SSSF plate, $\phi = b / a$, $P_\xi = - N_x b^2 / D$.

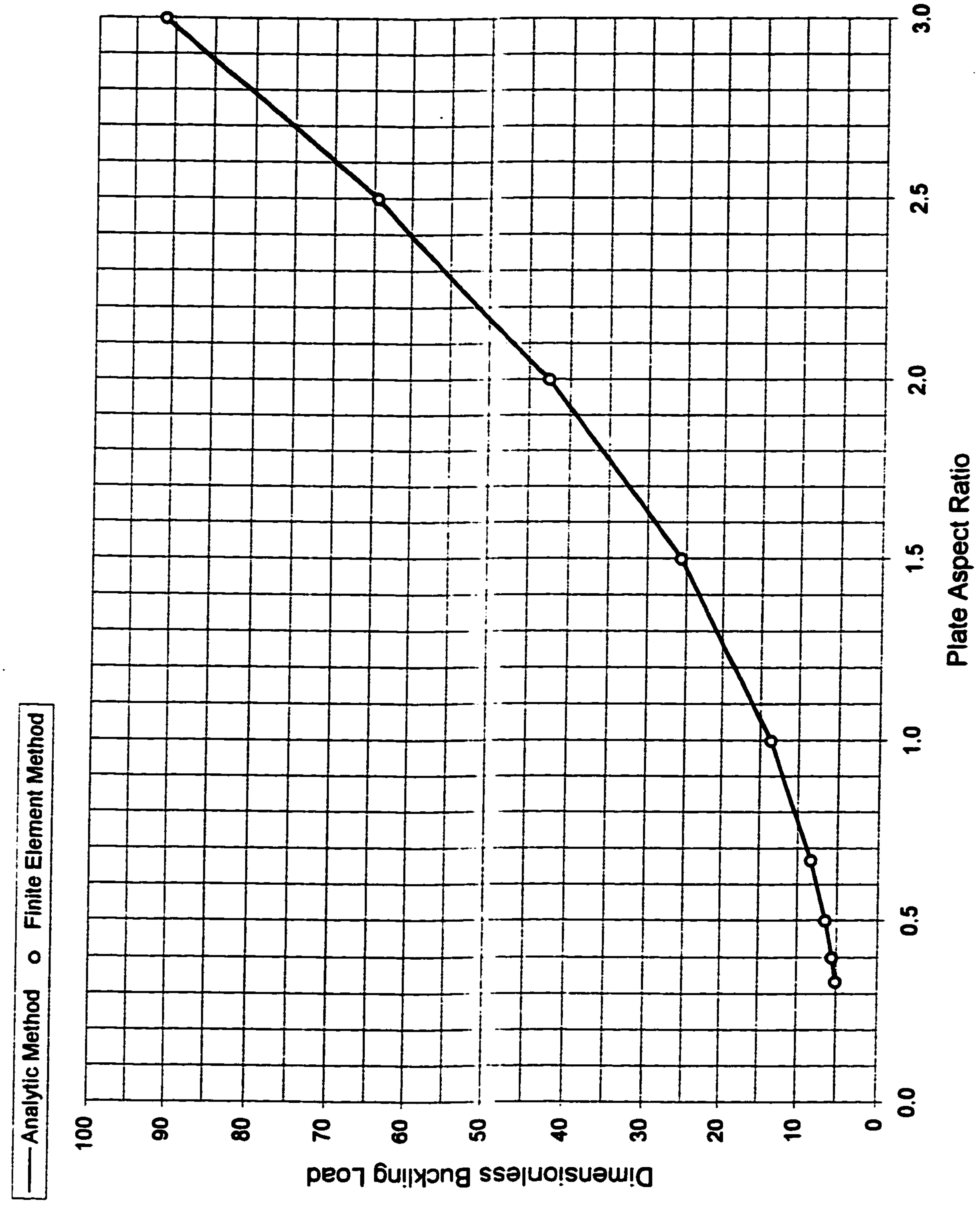

Figure 4.2 Buckling load curves, SFSF plate, $\phi = b / a$, $P_\xi = - N_x b^2 / D$.

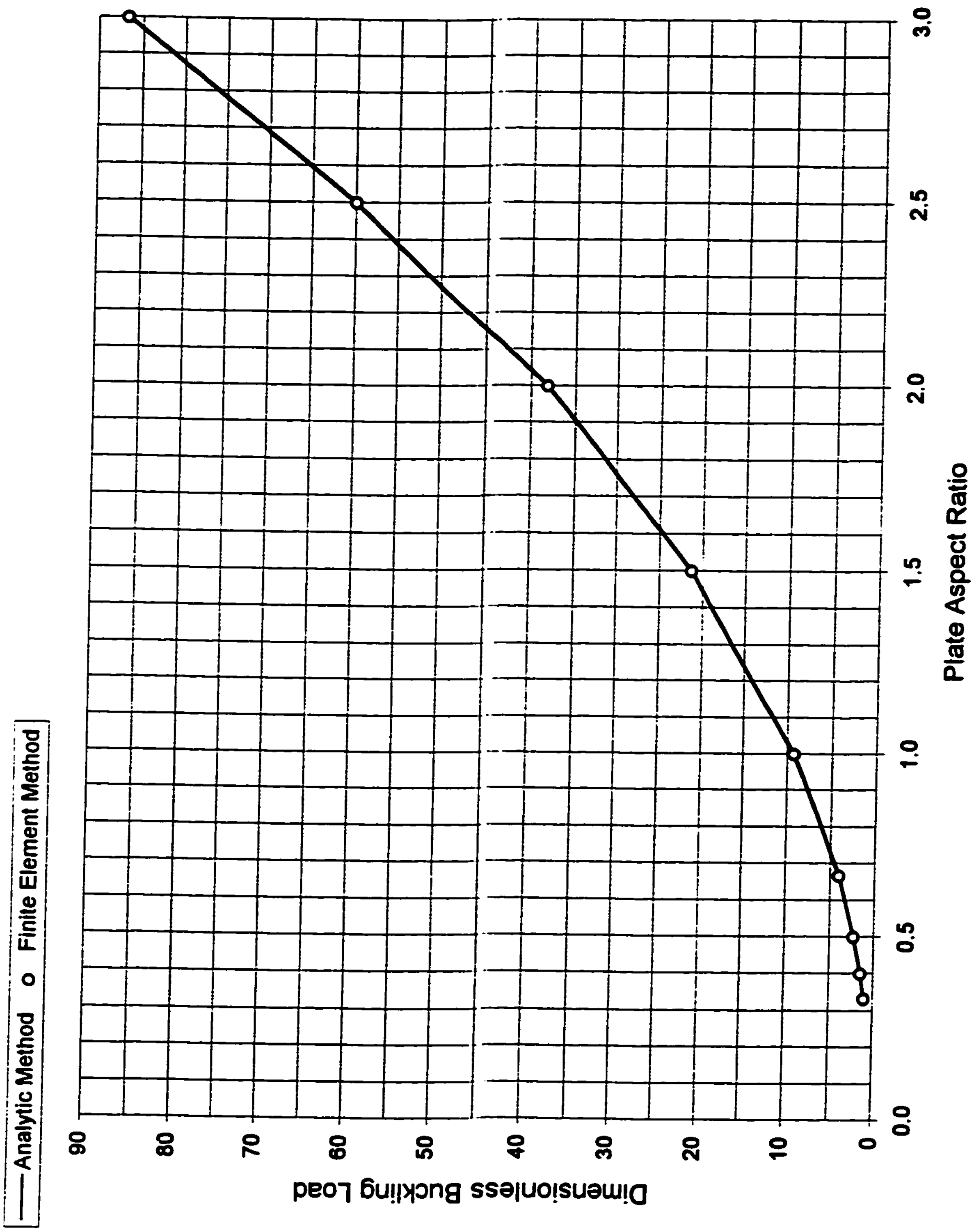

Figure 4.3 Buckling load curves, SFCF plate, $\phi = b / a$, $P_\xi = - N_x b^2 / D$.

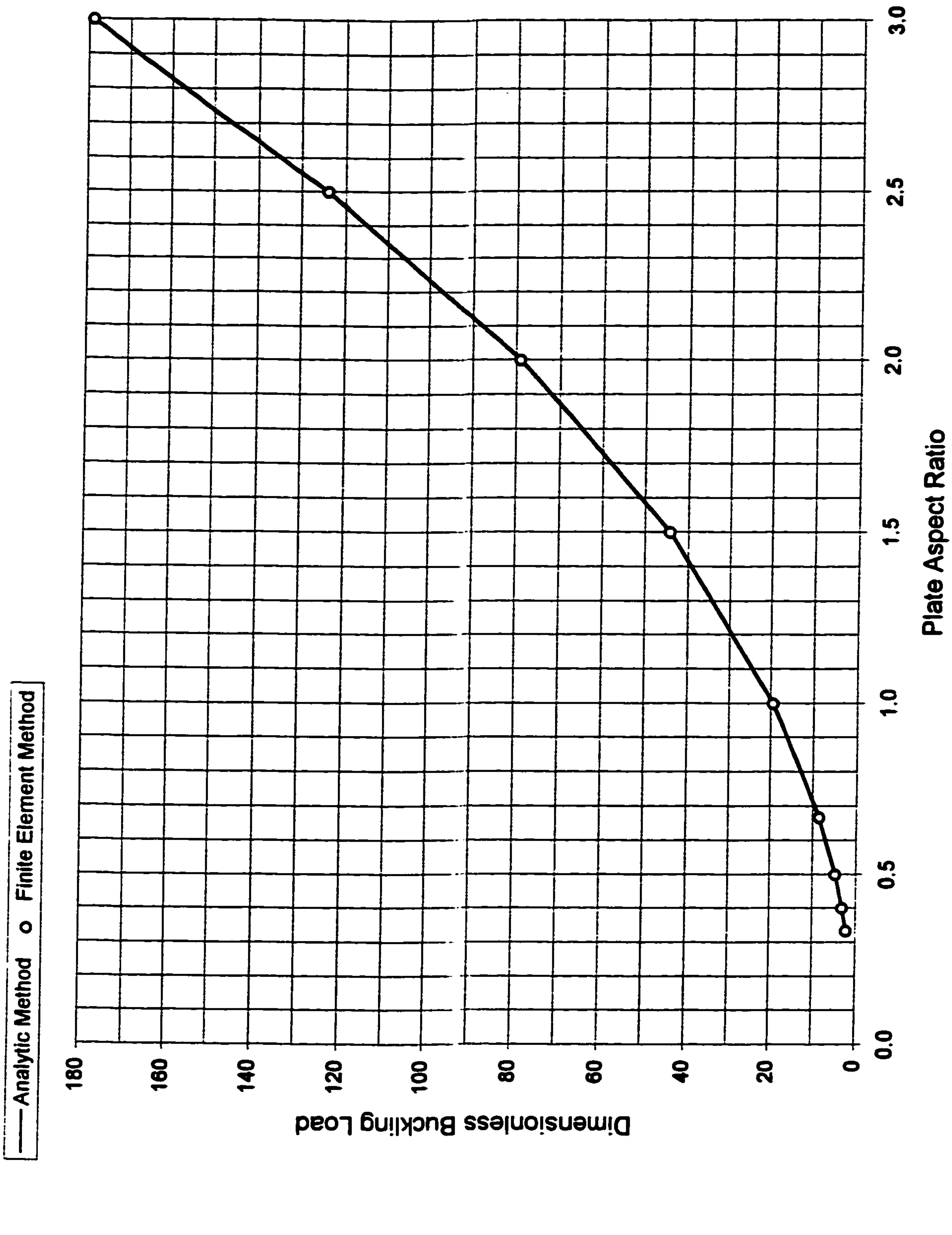

Figure 4.4 Buckling load curves, CFCF plate, $\phi = b / a$, $P_\xi = - N_x b^2 / D$.

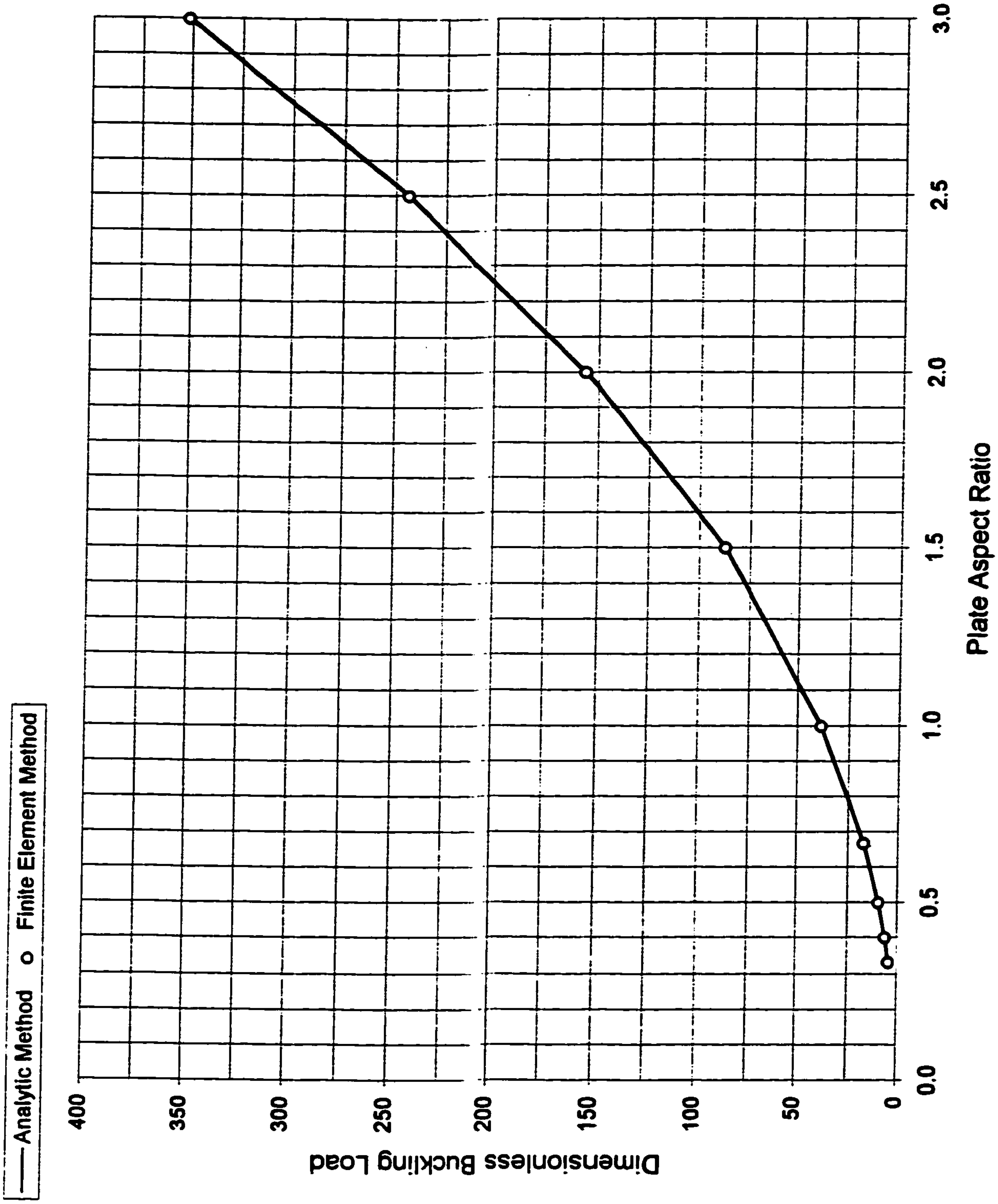

Figure 4.5 Buckling load curves, SCSF plate, $\phi = b / a$, $P_\xi = - N_x b^2 / D$.

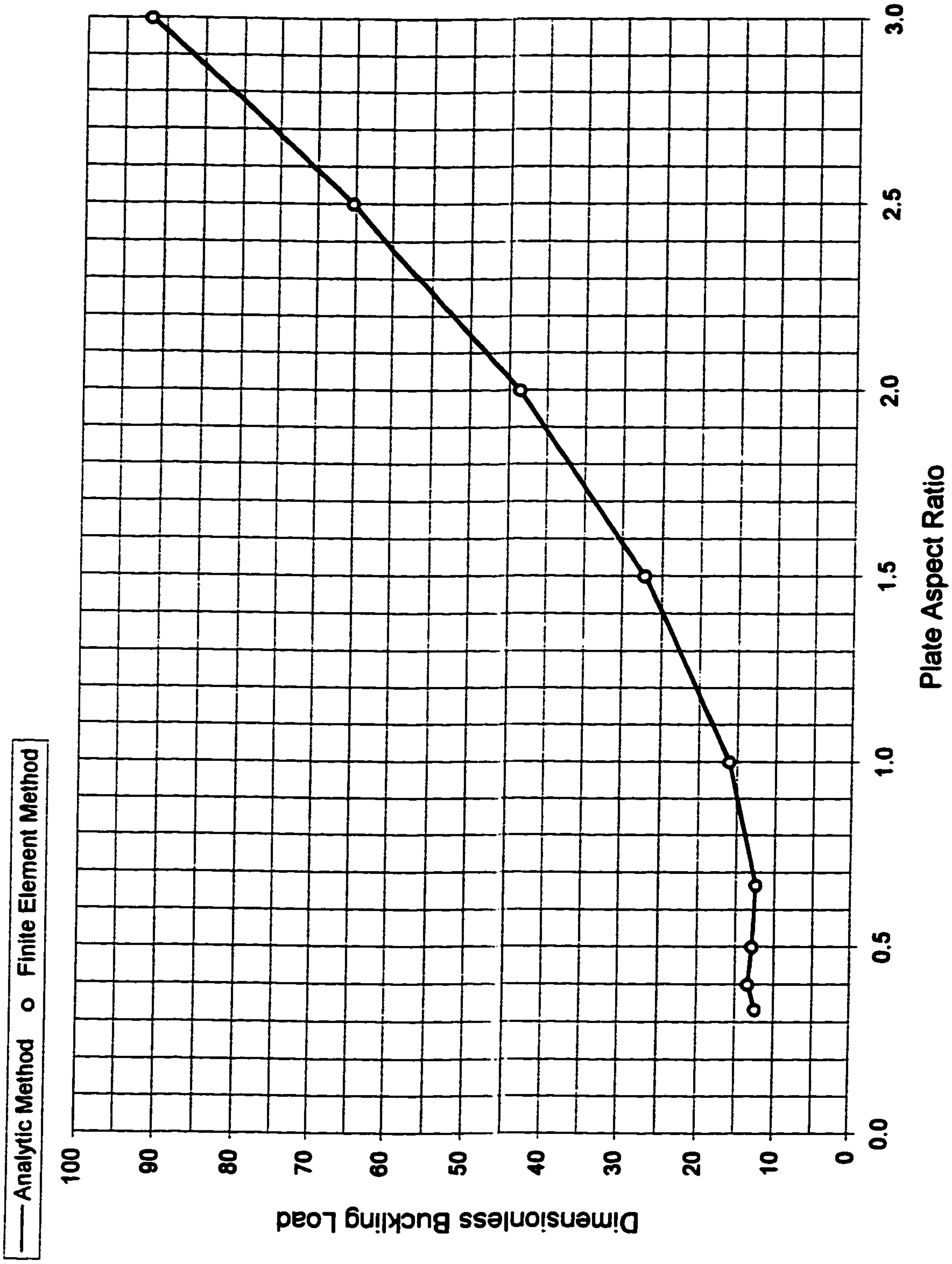

Figure 4.6 Buckling load curves, SSCF plate, $\phi = b / a$, $P_\xi = - N_x b^2 / D$.

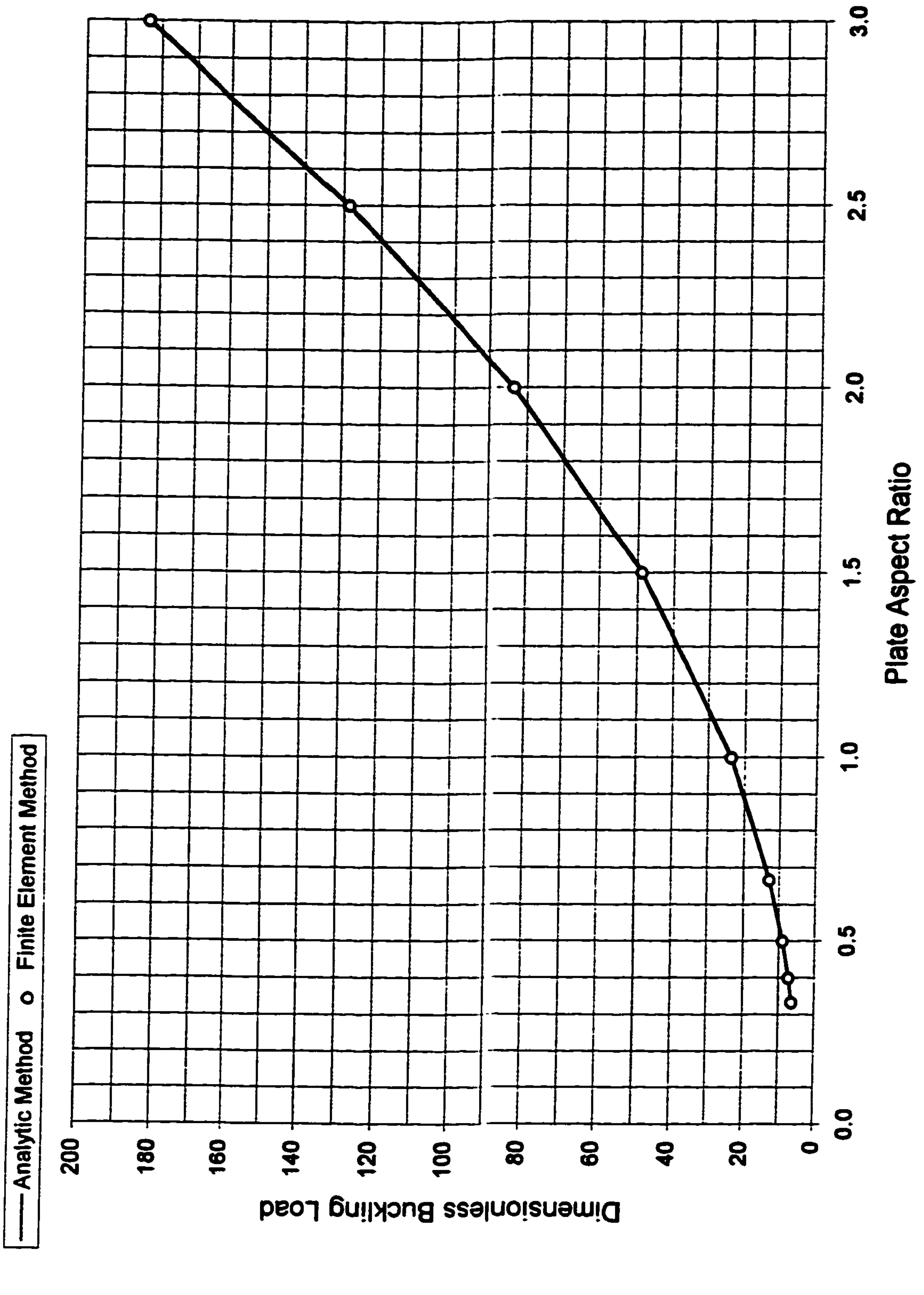

Figure 4.7 Buckling load curves, SCCF plate, $\phi = b / a$, $P_\xi = - N_x b^2 / D$.

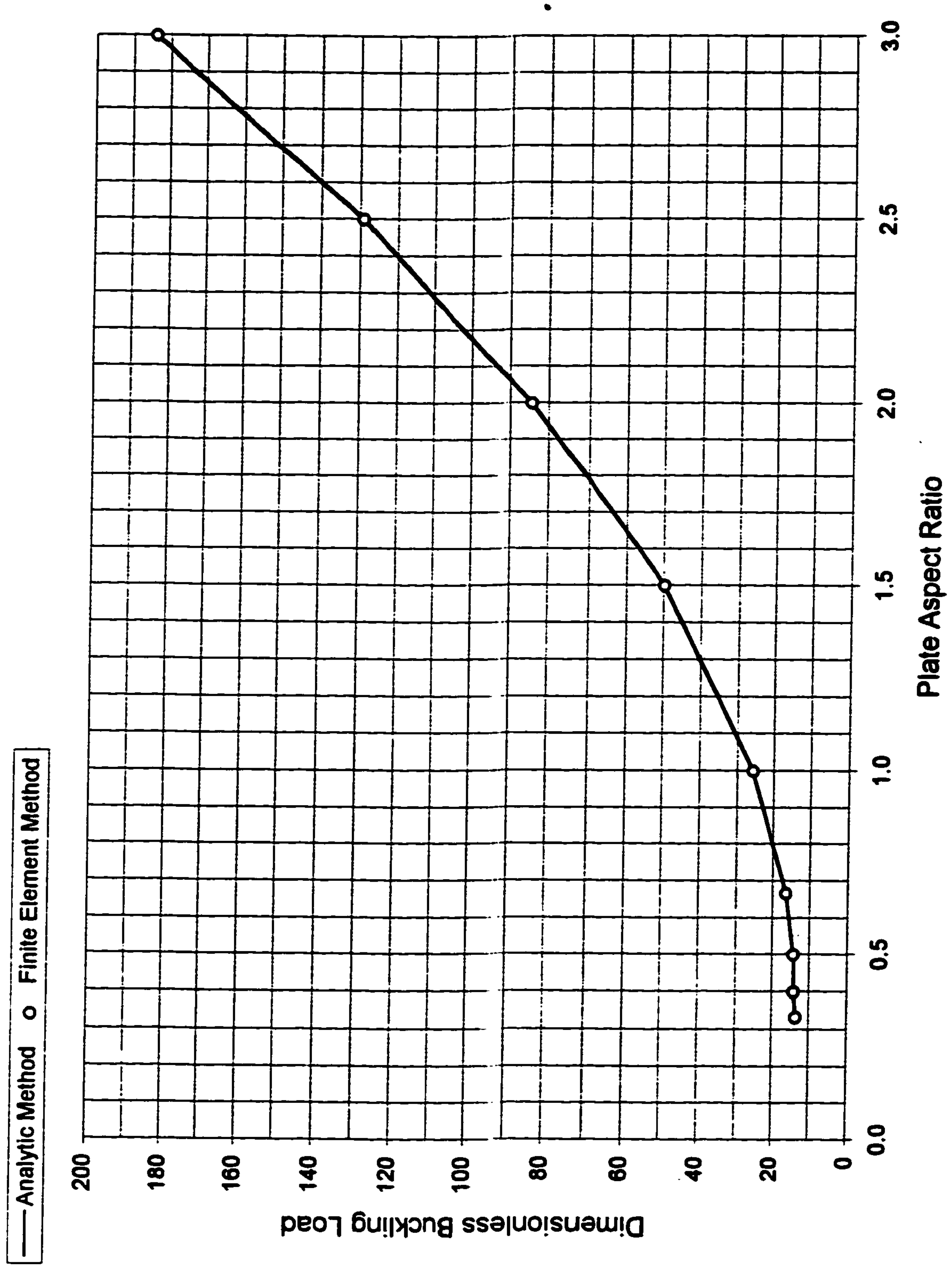

Figure 4.8 Buckling load curves, CSCF plate, $\phi = b / a$, $P_\xi = - N_x b^2 / D$.

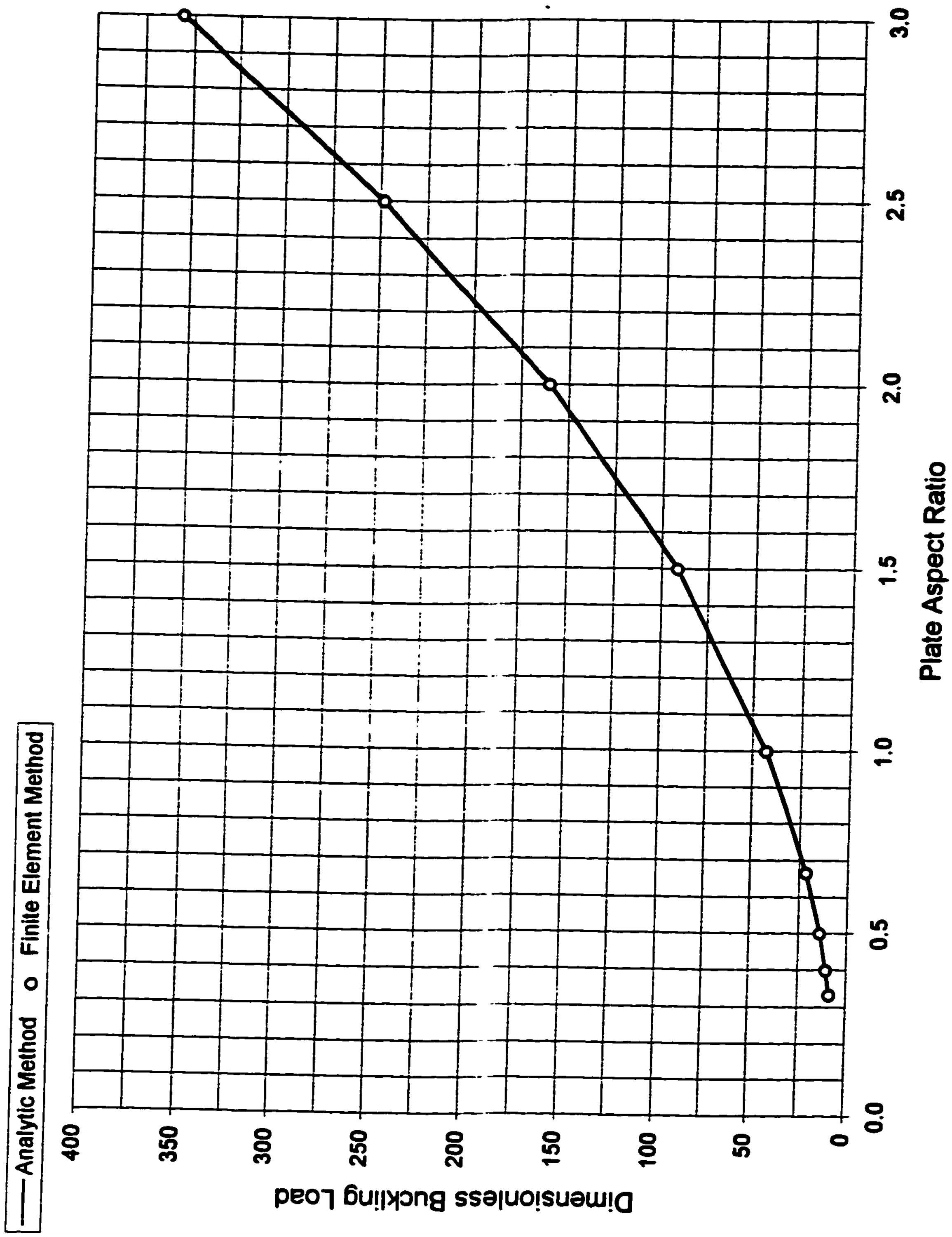

Figure 4.9 Buckling load curves, CCCF plate, $\phi = b / a$, $P_\xi = - N_x b^2 / D$.

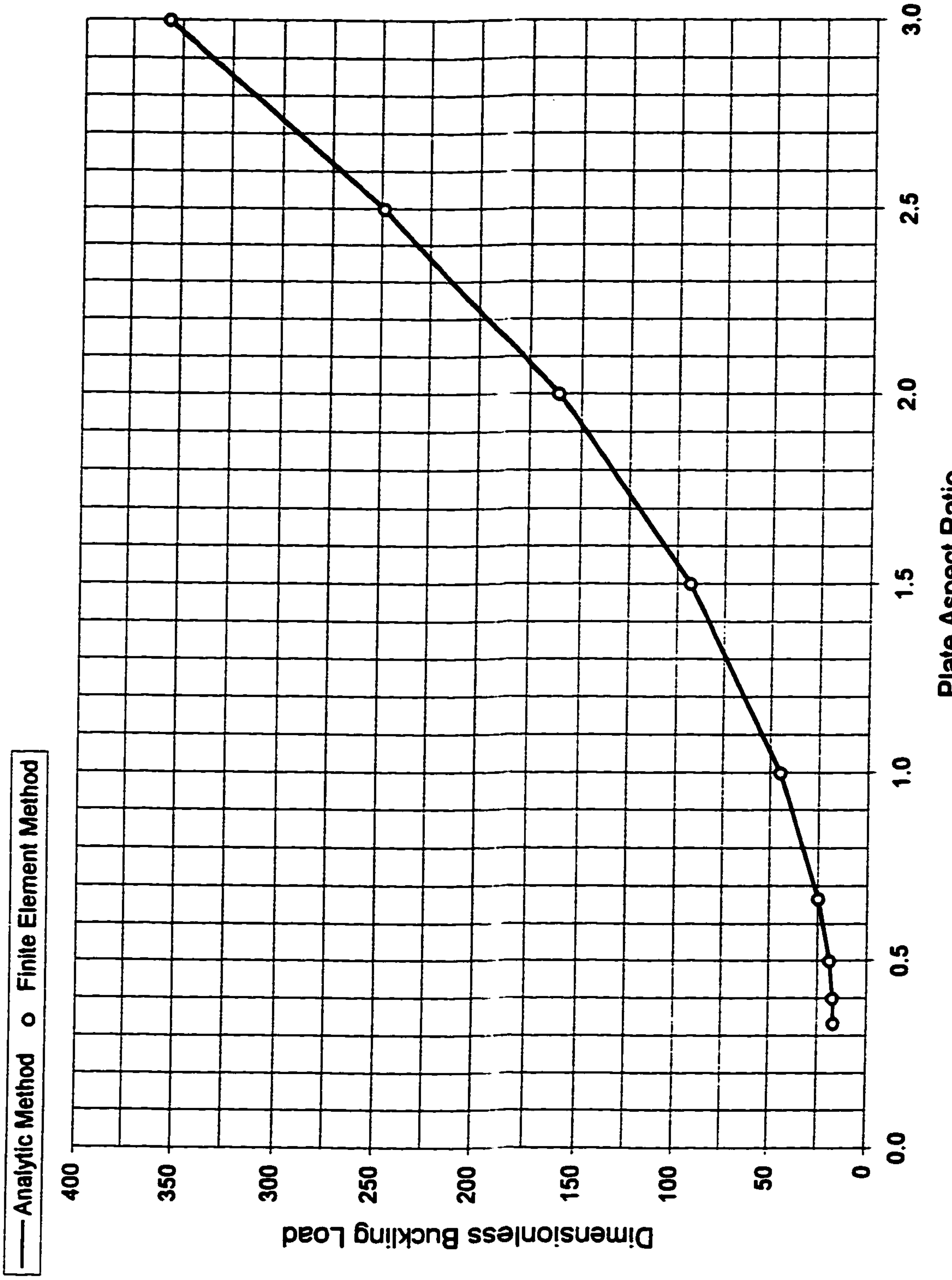

4.2 Free Vibration Analysis Results

An approximate frequency formula is used to generate free vibration results for comparison purposes. Eigenvalues for the first and second modes are obtained by using equation (1.1) with coefficients tabulated in Dickinson's paper [11]. Unloaded plates of aspect ratio 1/3, 1/1, and 3/1 are examined. Results are listed in Tables 4.8 to 4.10. The maximum relative error between the two methods exceeds 5%.

The present solution is used to calculate eigenvalues and mode shapes for plates subject to in-plane forces. Results were obtained for eight modes of free vibration. Comparisons are made to calculated ANSYS [18] finite element results. Relative differences in eigenvalues averaged at 0.2%. Eigenvalues are listed in Tables 4.11 to 4.91. Details of the FEM model and analysis are given in appendix C.

Only analytic-type results are used to generate the eigenvalue curves presented. Each plotted line represents the eigenvalues associated with a specific deflected shape. This allows the reader to trace how stiffness for a specific mode shape will be affected by in-plane load. Deflected shapes are labelled according to the mode shapes of the plate under zero in-plane load. The mode shapes themselves are also illustrated.

Table 4.8 Approximate eigenvalues, $\phi = 1/3$, $\lambda^2 = \omega a^2 (\rho / D)^{1/2}$.

Mode	Plate								
	SSSF	SFSF	SFCF	CFCF	SCSF	SSCF	SCCF	CSCF	CCCF
	Approximate formula [11]								
1	21.28	9.87	15.42	22.39	40.00	25.53	42.69	30.74	46.12
2	54.59	38.98	43.52	47.70	67.54	63.57	75.31	73.90	84.48
	Present solution								
1	21.20	9.37	14.87	21.82	39.85	25.23	42.28	30.41	45.65
2	54.15	37.91	42.45	46.58	66.41	63.02	74.00	73.24	83.02
	Percent difference								
1	0.4%	5.3%	3.7%	2.6%	0.4%	1.2%	1.0%	1.1%	1.0%
2	0.8%	2.8%	2.5%	2.4%	1.7%	0.9%	1.8%	0.9%	1.8%

Table 4.9 Approximate eigenvalues, $\phi = 1 / 1$, $\lambda^2 = \omega a^2 (\rho / D)^{1/2}$.

Mode	Plate								
	SSSF	SFSF	SFCF	CFCF	SCSF	SSCF	SCCF	CSCF	CCCF
	Approximate formula [11]								
1	11.70	9.87	15.42	22.39	12.86	16.85	17.75	23.46	24.14
2	27.73	15.98	20.54	26.42	33.12	31.32	36.36	35.78	40.35
	Present solution								
1	11.58	9.57	15.13	22.11	12.56	16.70	17.42	23.28	23.81
2	27.59	15.88	20.34	26.19	32.89	30.95	35.85	35.41	39.83
	Percent difference								
1	1.0%	3.1%	1.9%	1.3%	2.4%	0.9%	1.9%	0.8%	1.4%
2	0.5%	0.6%	1.0%	0.9%	0.7%	1.2%	1.4%	1.0%	1.3%

Table 4.10 Approximate eigenvalues, $\phi = 3 / 1$, $\lambda^2 = \omega a^2 (\rho / D)^{1/2}$.

Mode	Plate								
	SSSF	SFSF	SFCF	CFCF	SCSF	SSCF	SCCF	CSCF	CCCF
	Approximate formula [11]								
1	10.09	9.87	15.42	22.39	10.19	15.59	15.66	22.51	22.56
2	12.19	10.72	16.07	22.87	12.67	17.23	17.62	23.75	24.05
	Present solution								
1	10.00	9.75	15.30	22.26	10.03	15.49	15.51	22.40	22.42
2	12.07	10.61	15.94	22.72	12.39	17.11	17.35	23.63	23.81
	Percent difference								
1	0.9%	1.2%	0.8%	0.6%	1.6%	0.6%	1.0%	0.5%	0.6%
2	1.0%	1.0%	0.8%	0.7%	2.3%	0.7%	1.6%	0.5%	1.0%

Table 4.11 Eigenvalues, SSSF plate, $\phi = 1 / 3$, $\lambda^2 = \omega a^2 (\rho / D)^{1/2}$.

Mode	In-plane load as a percentage of buckling load								
	-100%	-50%	0%	20%	40%	60%	80%	90%	99%
	Present solution								
1	29.99	25.97	21.20	18.97	16.42	13.41	9.48	6.71	2.12
2	68.78	61.90	54.15	50.72	47.04	43.05	38.65	36.24	33.94
3	122.12	113.53	104.24	100.29	96.17	91.86	87.35	85.00	82.83
4	153.95	153.22	152.48	152.19	151.89	151.59	151.30	151.15	151.02
5	192.81	183.24	173.15	168.94	164.63	160.20	155.64	153.32	151.19
6	195.19	192.87	190.52	189.58	188.63	187.67	186.71	186.23	185.79
7	256.36	252.38	248.34	246.71	245.06	243.40	241.73	240.90	239.15
8	282.06	271.92	261.38	257.04	252.63	248.14	243.57	241.25	240.14
	Finite element solution [18]								
1	29.99	25.97	21.20	18.96	16.42	13.41	9.48	6.70	2.12
2	68.79	61.91	54.16	50.73	47.05	43.06	38.66	36.26	33.95
3	122.20	113.63	104.34	100.39	96.27	91.97	87.46	85.12	82.95
4	153.86	153.12	152.39	152.09	151.79	151.49	151.20	151.06	150.92
5	193.14	183.59	173.52	169.32	165.02	160.60	156.06	153.74	151.61
6	194.92	192.60	190.26	189.31	188.36	187.40	186.43	185.95	185.52
7	255.73	251.75	247.70	246.06	244.41	242.75	241.07	240.24	239.48
8	282.97	272.86	262.36	258.04	253.65	249.17	244.62	242.32	240.22
	Percent difference								
1	-0.01%	-0.01%	0.00%	-0.01%	-0.01%	-0.01%	-0.01%	-0.01%	-0.02%
2	0.01%	0.01%	0.02%	0.02%	0.02%	0.03%	0.04%	0.04%	0.05%
3	0.06%	0.08%	0.09%	0.10%	0.11%	0.12%	0.13%	0.14%	0.15%
4	-0.06%	-0.06%	-0.06%	-0.06%	-0.06%	-0.07%	-0.06%	-0.06%	-0.07%
5	0.17%	0.19%	0.21%	0.22%	0.24%	0.25%	0.27%	0.27%	0.28%
6	-0.13%	-0.14%	-0.14%	-0.14%	-0.14%	-0.14%	-0.15%	-0.15%	-0.15%
7	-0.24%	-0.25%	-0.26%	-0.26%	-0.26%	-0.27%	-0.27%	-0.27%	0.14%
8	0.32%	0.35%	0.37%	0.39%	0.40%	0.42%	0.43%	0.44%	0.03%

Figure 4.10 Eigenvalue curves, SSSF plate, $\phi = 1 / 3$,

$P_\xi = - N_x b^2 / D$, $\lambda^2 = \omega a^2 (\rho / D)^{1/2}$.

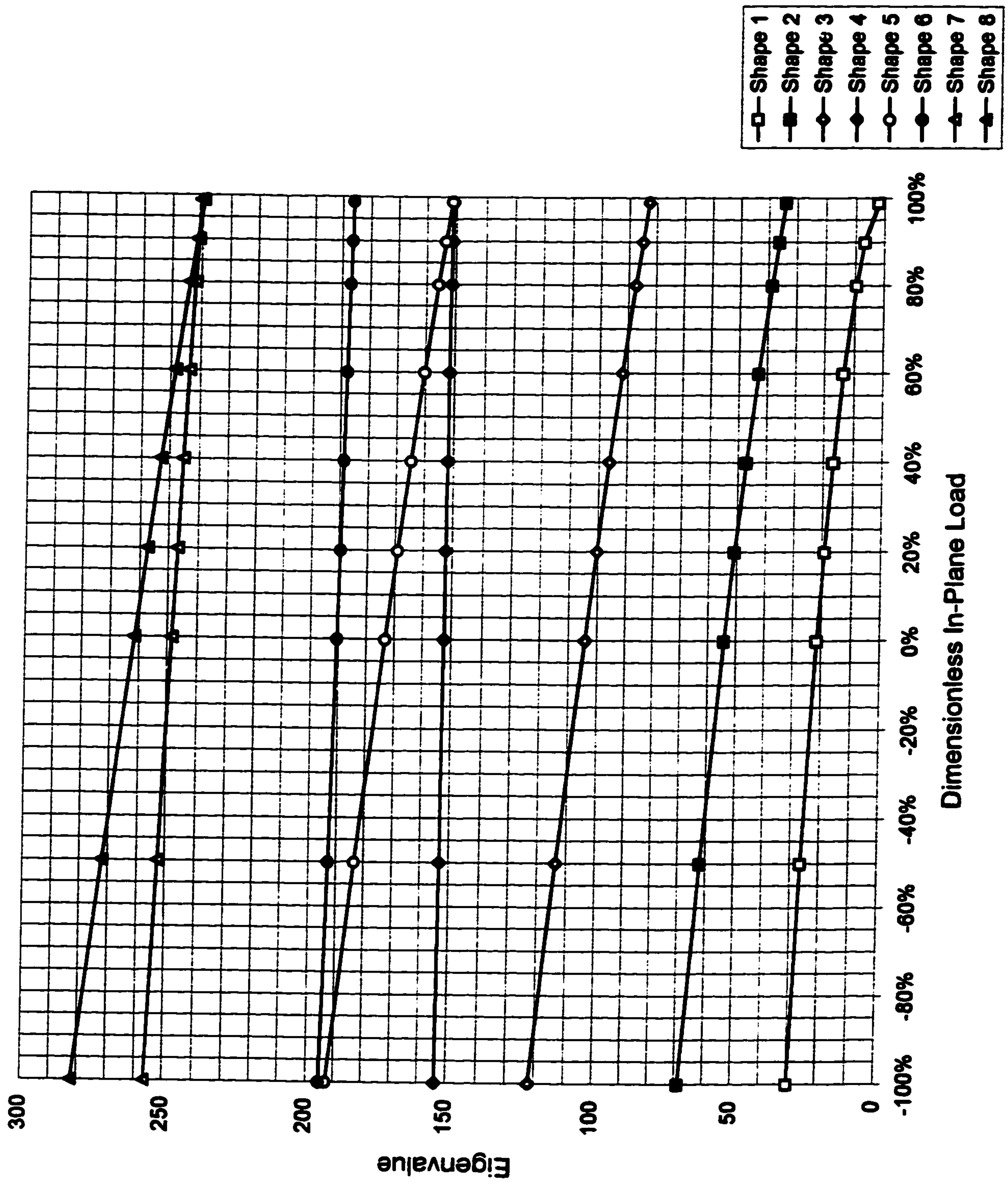

Figure 4.11 Mode shapes, SSSF plate, $\phi = 1 / 3$.

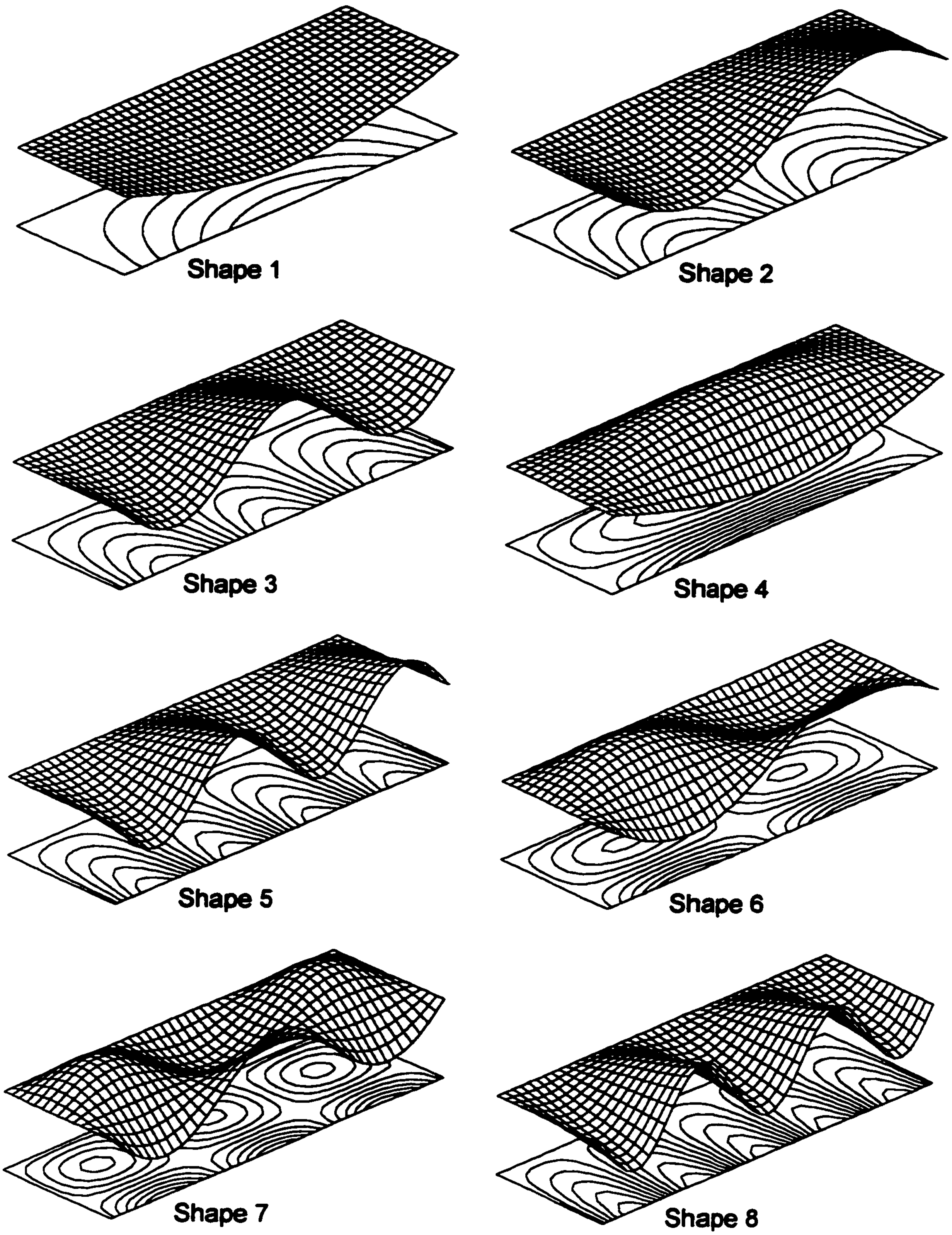

Table 4.12 Eigenvalues, SSSF plate, $\phi = 2 / 5$, $\lambda^2 = \omega a^2 (\rho / D)^{1/2}$.

Mode	In-plane load as a percentage of buckling load								
	-100%	-50%	0%	20%	40%	60%	80%	90%	99%
	Present solution								
1	26.12	22.62	18.47	16.52	14.30	11.68	8.26	5.84	2.33
2	62.16	56.41	50.00	47.19	44.20	41.00	37.53	35.66	40.11
3	111.48	106.94	99.50	96.37	93.13	89.77	86.29	84.49	93.84
4	113.89	110.71	109.94	109.63	109.32	109.01	108.69	108.54	109.52
5	151.41	149.14	146.84	145.90	144.97	144.02	143.07	142.59	146.12
6	183.69	176.10	168.18	164.90	161.56	158.14	154.66	152.88	167.10
7	209.97	206.28	202.53	201.01	199.47	197.93	196.37	195.59	202.69
8	272.46	264.53	256.34	252.99	249.60	246.16	242.67	240.91	260.02
	Finite element solution [18]								
1	26.12	22.62	18.47	16.52	14.30	11.68	8.26	5.84	1.85
2	62.17	56.42	50.01	47.21	44.22	41.02	37.55	35.69	33.92
3	111.42	107.04	99.62	96.49	93.25	89.90	86.42	84.62	82.98
4	113.99	110.65	109.88	109.57	109.26	108.95	108.63	108.48	108.33
5	151.23	148.96	146.66	145.72	144.78	143.83	142.89	142.41	141.97
6	184.05	176.48	168.57	165.31	161.97	158.57	155.09	153.31	151.71
7	209.55	205.85	202.09	200.57	199.03	197.48	195.92	195.13	194.43
8	273.40	265.49	257.33	253.99	250.62	247.19	243.72	241.97	240.37
	Percent difference								
1	0.00%	0.00%	0.00%	0.00%	0.00%	0.00%	0.00%	0.00%	-20.62%
2	0.02%	0.03%	0.03%	0.04%	0.04%	0.05%	0.06%	0.07%	-15.44%
3	-0.06%	0.10%	0.12%	0.13%	0.13%	0.14%	0.16%	0.16%	-11.58%
4	0.09%	-0.06%	-0.05%	-0.06%	-0.06%	-0.05%	-0.06%	-0.05%	-1.09%
5	-0.12%	-0.12%	-0.12%	-0.12%	-0.13%	-0.13%	-0.13%	-0.13%	-2.84%
6	0.20%	0.22%	0.24%	0.25%	0.26%	0.27%	0.28%	0.28%	-9.21%
7	-0.20%	-0.21%	-0.22%	-0.22%	-0.22%	-0.23%	-0.23%	-0.23%	-4.07%
8	0.34%	0.36%	0.39%	0.40%	0.41%	0.42%	0.43%	0.44%	-7.55%

Figure 4.12 Eigenvalue curves, SSSF plate, $\phi = 2 / 5$,
$P_\xi = - N_x b^2 / D$, $\lambda^2 = \omega a^2 (\rho / D)^{1/2}$.

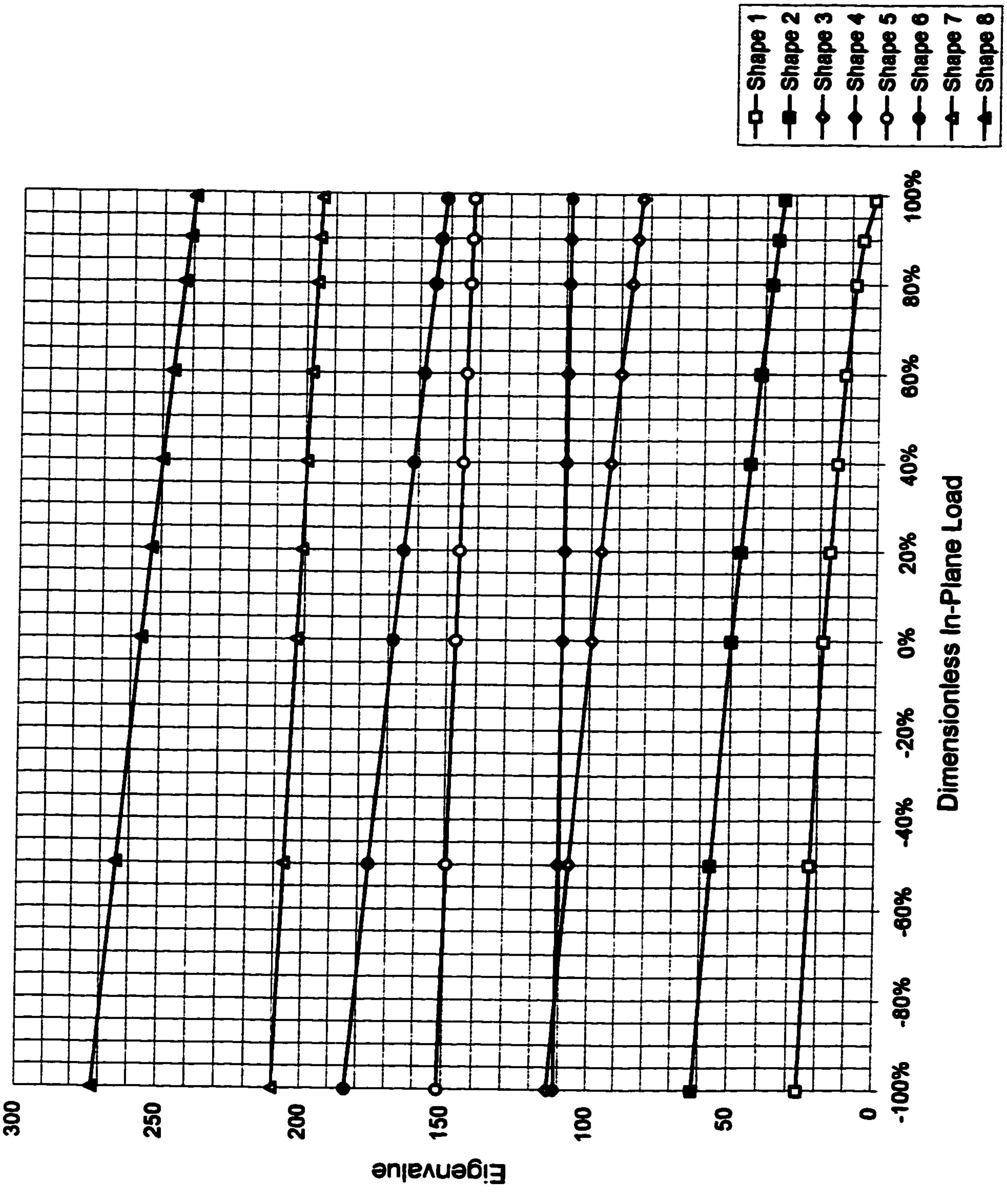

Figure 4.13 Mode shapes, SSSF plate, $\phi = 2 / 5$.

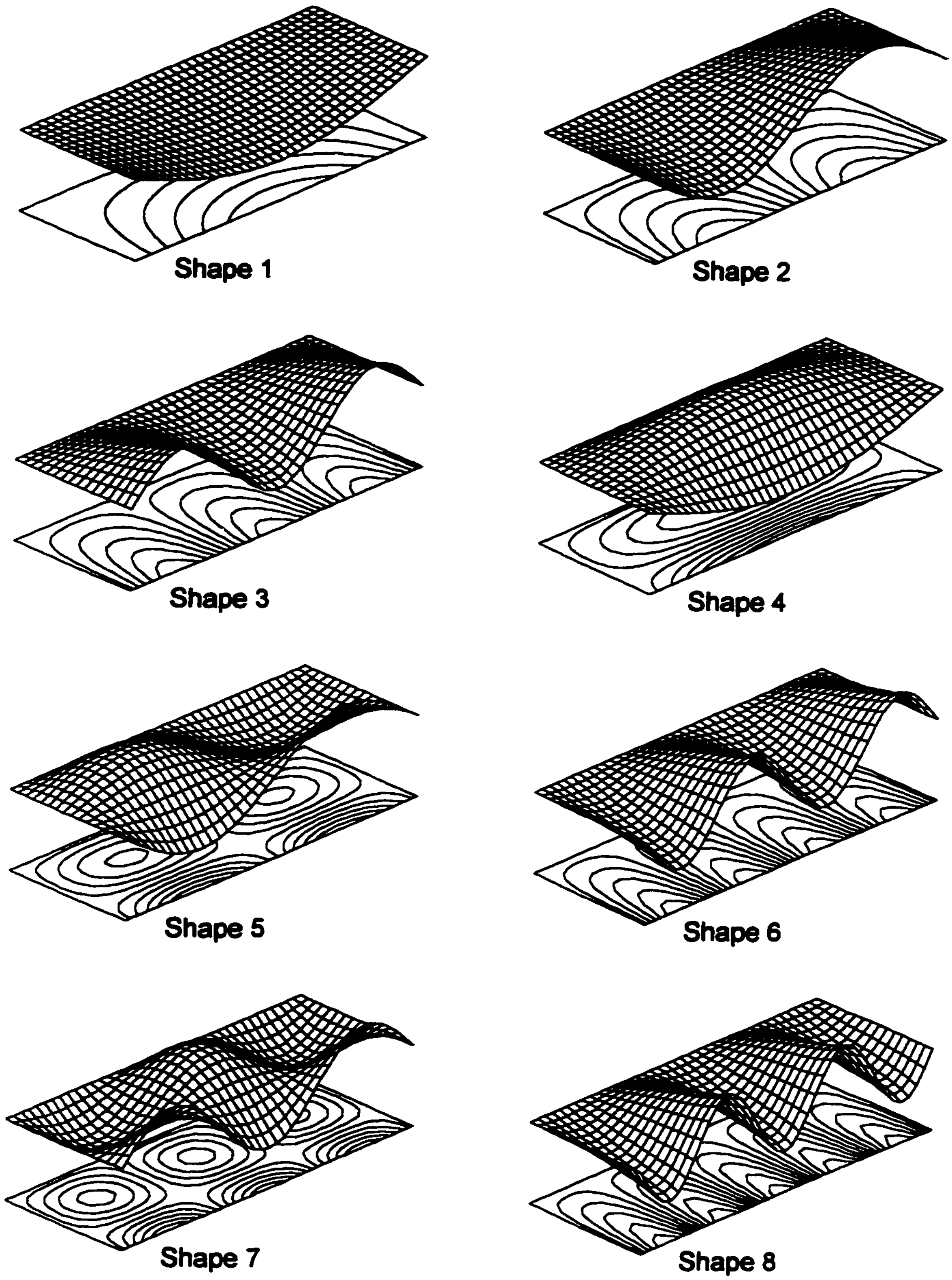

Table 4.13 Eigenvalues, SSSF plate, $\phi = 1/2$, $\lambda^2 = \omega a^2 (\rho / D)^{1/2}$.

Mode	In-plane load as a percentage of buckling load								
	-100%	-50%	0%	20%	40%	60%	80%	90%	99%
					Present solution				
1	22.46	19.45	15.88	14.21	12.30	10.05	7.10	5.02	1.59
2	56.17	51.49	46.33	44.10	41.75	39.26	36.60	35.19	33.88
3	76.68	75.86	75.02	74.68	74.35	74.01	73.66	73.49	73.34
4	106.71	101.25	95.48	93.07	90.60	88.06	85.44	84.10	82.88
5	114.85	112.64	110.37	109.46	108.53	107.60	106.65	106.18	105.75
6	170.58	167.22	163.79	161.58	159.06	156.50	153.90	152.59	151.39
7	175.93	170.10	164.06	162.40	160.99	159.58	158.15	157.43	156.78
8	212.52	212.23	211.93	211.81	211.69	211.57	211.45	211.39	211.34
					Finite element solution [18]				
1	22.46	19.45	15.88	14.21	12.30	10.05	7.10	5.02	1.59
2	56.20	51.51	46.35	44.12	41.77	39.28	36.63	35.22	33.91
3	76.65	75.82	74.98	74.65	74.31	73.97	73.63	73.46	73.30
4	106.82	101.37	95.61	93.20	90.73	88.19	85.58	84.24	83.02
5	114.75	112.53	110.27	109.35	108.42	107.48	106.55	106.07	105.64
6	170.35	166.98	163.55	161.98	159.46	156.91	154.32	153.00	151.81
7	176.29	170.47	164.45	162.15	160.74	159.33	157.90	157.17	156.52
8	212.26	211.97	211.66	211.55	211.43	211.31	211.19	211.13	211.08
					Percent difference				
1	0.01%	0.01%	0.01%	0.01%	0.01%	0.01%	0.01%	0.01%	0.03%
2	0.04%	0.04%	0.05%	0.06%	0.06%	0.07%	0.08%	0.08%	0.09%
3	-0.04%	-0.05%	-0.05%	-0.05%	-0.05%	-0.05%	-0.05%	-0.05%	-0.05%
4	0.11%	0.12%	0.13%	0.14%	0.14%	0.15%	0.16%	0.16%	0.17%
5	-0.09%	-0.09%	-0.10%	-0.10%	-0.10%	-0.10%	-0.10%	-0.11%	-0.10%
6	-0.14%	-0.14%	-0.15%	0.24%	0.25%	0.26%	0.27%	0.27%	0.28%
7	0.21%	0.22%	0.24%	-0.15%	-0.15%	-0.16%	-0.16%	-0.16%	-0.16%
8	-0.12%	-0.12%	-0.12%	-0.13%	-0.12%	-0.12%	-0.12%	-0.12%	-0.12%

Figure 4.14 Eigenvalue curves, SSSF plate, $\phi = 1 / 2$,
$P_\xi = - N_x b^2 / D$, $\lambda^2 = \omega a^2 (\rho / D)^{1/2}$.

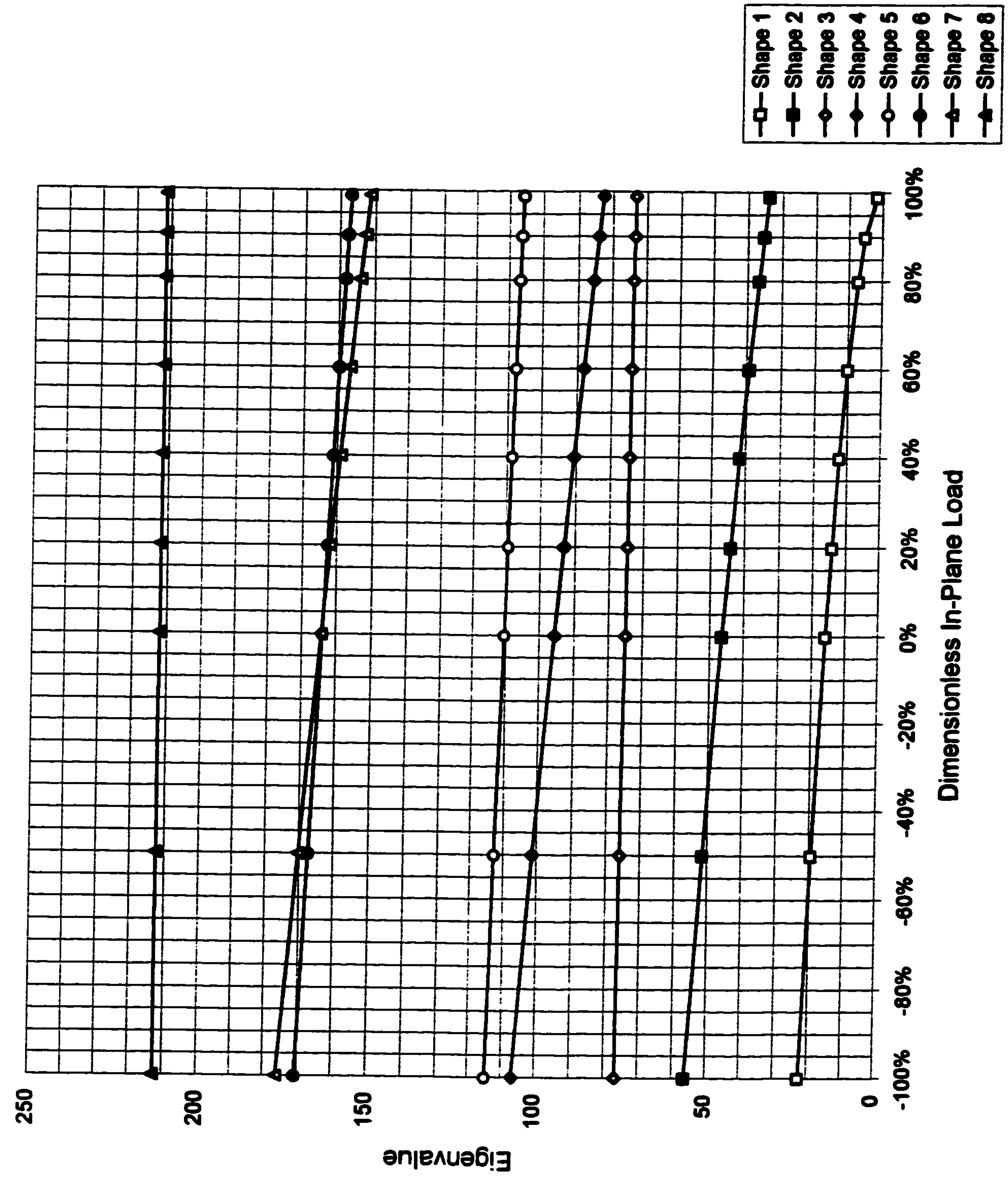

Figure 4.15 Mode shapes, SSSF plate, $\phi = 1 / 2$.

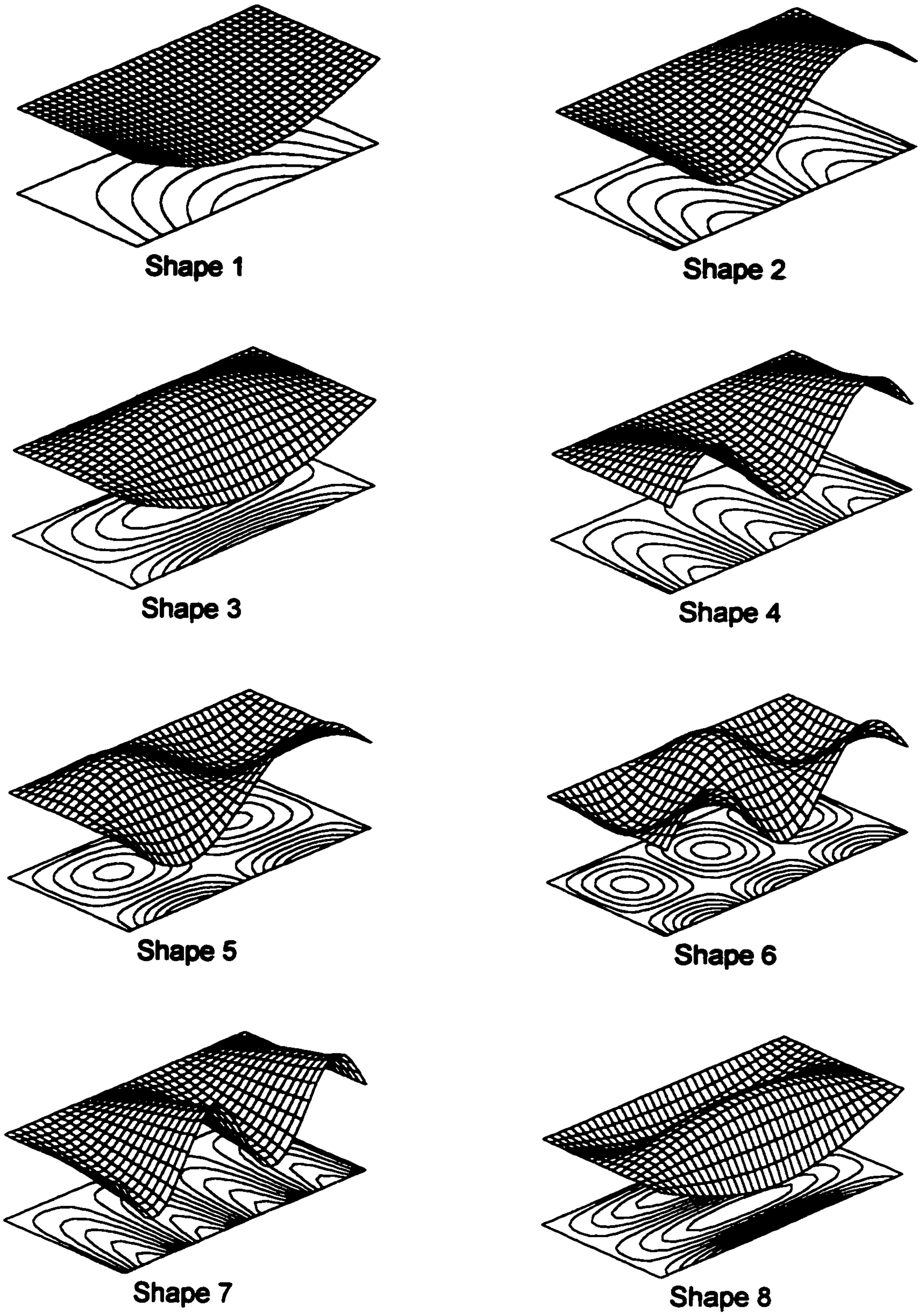

Table 4.14 Eigenvalues, SSSF plate, $\phi = 2/3$, $\lambda^2 = \omega a^2 (\rho / D)^{1/2}$.

Mode	In-plane load as a percentage of buckling load								
	-100%	-50%	0%	20%	40%	60%	80%	90%	99%
	Present solution								
1	19.15	16.58	13.54	12.11	10.49	8.56	6.05	4.28	1.35
2	49.52	47.33	43.29	41.56	39.76	37.87	35.88	34.84	33.88
3	51.06	48.58	47.63	47.24	46.85	46.46	46.07	45.87	45.69
4	85.41	83.24	81.01	80.10	79.18	78.25	77.30	76.83	76.40
5	100.82	96.65	92.28	90.48	88.64	86.76	84.83	83.86	82.97
6	125.13	124.77	124.40	124.25	124.10	123.96	123.81	123.73	123.67
7	138.39	135.38	132.30	131.04	129.78	128.50	127.21	126.56	125.97
8	160.73	159.58	158.43	157.97	157.18	155.31	153.41	152.45	151.58
	Finite element solution [18]								
1	19.15	16.58	13.54	12.11	10.49	8.56	6.06	4.28	1.35
2	49.50	47.36	43.31	41.59	39.78	37.90	35.91	34.87	33.91
3	51.08	48.57	47.61	47.23	46.84	46.45	46.05	45.85	45.67
4	85.37	83.20	80.96	80.05	79.13	78.20	77.26	76.78	76.35
5	100.93	96.76	92.40	90.59	88.75	86.87	84.95	83.98	83.09
6	125.03	124.66	124.29	124.14	123.99	123.85	123.70	123.63	123.56
7	138.31	135.30	132.21	130.96	129.69	128.41	127.12	126.47	125.88
8	160.52	159.37	158.22	157.75	157.29	155.64	153.74	152.78	151.92
	Percent difference								
1	0.02%	0.02%	0.02%	0.02%	0.02%	0.02%	0.02%	0.01%	0.03%
2	-0.03%	0.06%	0.06%	0.06%	0.07%	0.08%	0.08%	0.08%	0.09%
3	0.05%	-0.03%	-0.03%	-0.03%	-0.03%	-0.03%	-0.03%	-0.03%	-0.04%
4	-0.05%	-0.05%	-0.06%	-0.05%	-0.06%	-0.06%	-0.06%	-0.06%	-0.06%
5	0.11%	0.11%	0.12%	0.13%	0.13%	0.14%	0.14%	0.14%	0.15%
6	-0.09%	-0.09%	-0.09%	-0.09%	-0.09%	-0.09%	-0.09%	-0.09%	-0.09%
7	-0.06%	-0.06%	-0.06%	-0.07%	-0.07%	-0.07%	-0.07%	-0.07%	-0.07%
8	-0.13%	-0.13%	-0.14%	-0.14%	0.07%	0.22%	0.22%	0.22%	0.22%

Figure 4.16 Eigenvalue curves, SSSF plate, $\phi = 2/3$,

$P_\xi = -N_x b^2/D$, $\lambda^2 = \omega a^2 (\rho/D)^{1/2}$.

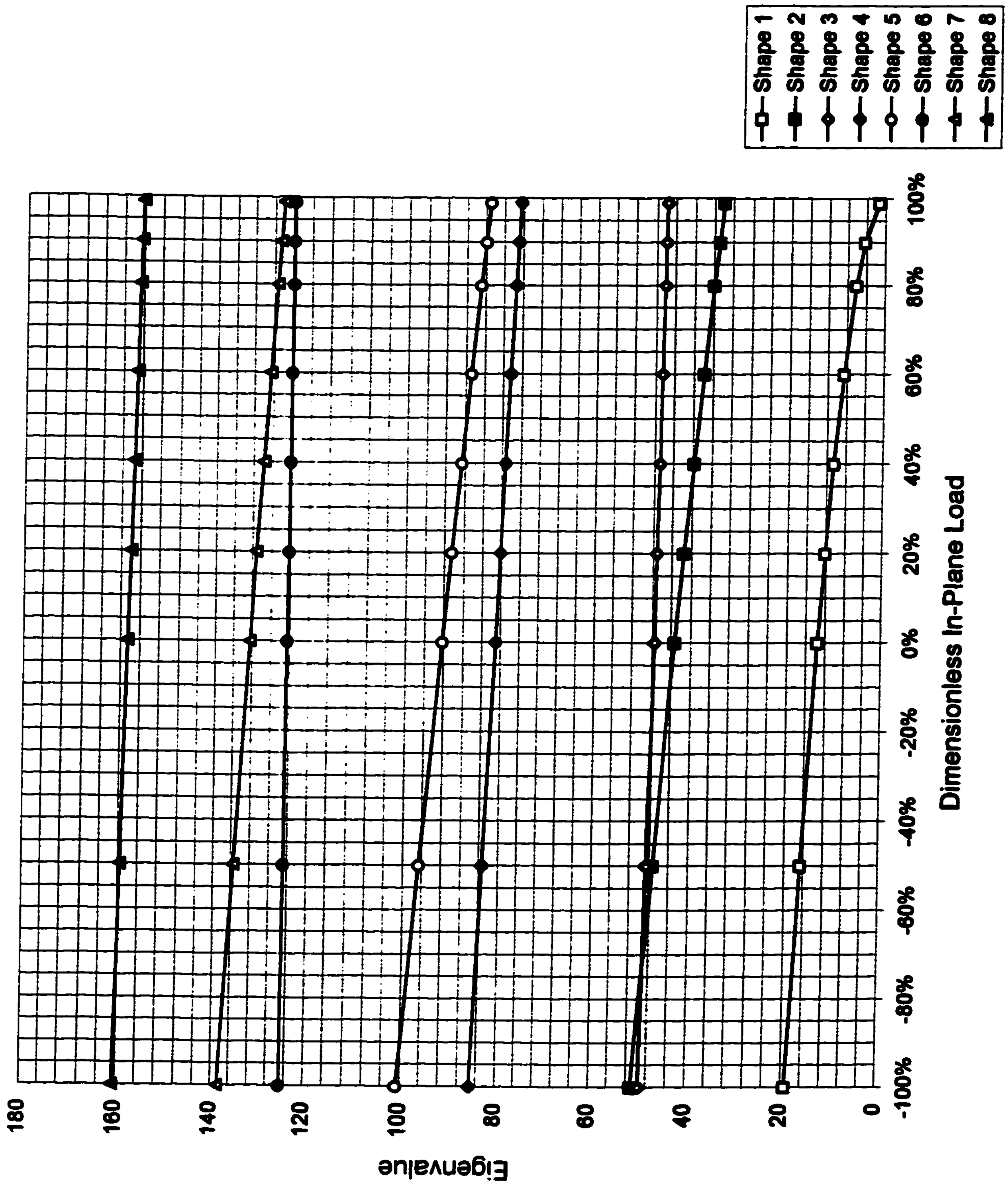

Figure 4.17 Mode shapes, SSSF plate, $\phi = 2 / 3$.

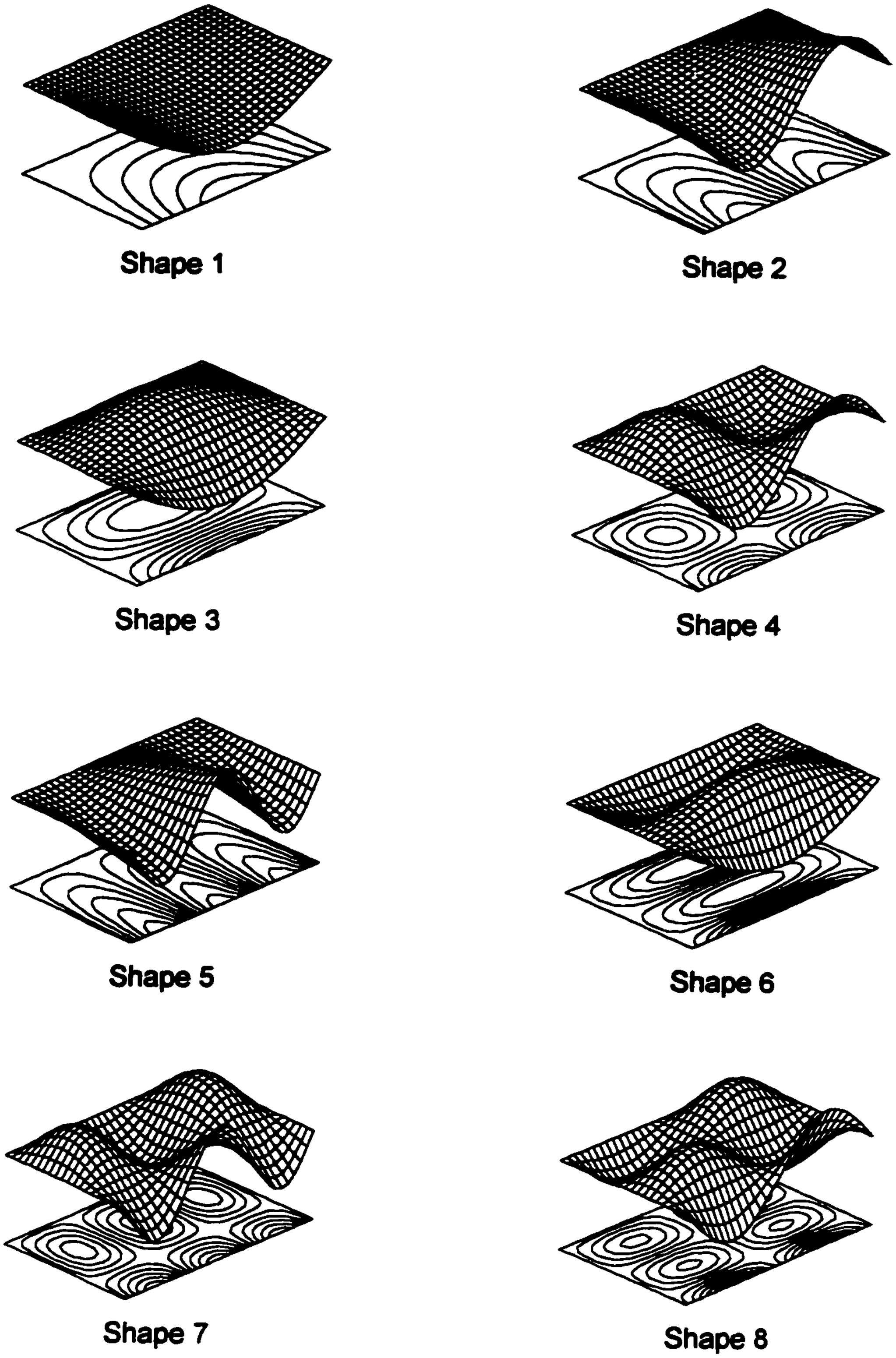

Table 4.15 Eigenvalues, SSSF plate, $\phi = 1 / 1$, $\lambda^2 = \omega a^2 (\rho / D)^{1/2}$.

Mode	In-plane load as a percentage of buckling load								
	-100%	-50%	0%	20%	40%	60%	80%	90%	99%
	Present solution								
1	16.38	14.19	11.58	10.36	8.97	7.33	5.18	3.66	1.16
2	29.93	28.78	27.59	27.10	26.60	26.09	25.57	25.31	25.07
3	47.10	44.16	41.01	39.68	38.31	36.88	35.40	34.63	33.93
4	62.79	61.04	58.80	57.88	56.94	55.99	55.03	54.54	54.09
5	63.20	62.26	61.72	61.50	61.28	61.06	60.84	60.73	60.63
6	96.49	93.31	90.02	88.66	87.29	85.90	84.48	83.76	83.11
7	96.96	95.56	94.15	93.58	93.00	92.42	91.84	91.55	91.29
8	114.02	111.34	108.59	107.47	106.34	105.20	104.05	103.47	102.94
	Finite element solution [18]								
1	16.38	14.19	11.59	10.36	8.97	7.33	5.18	3.66	1.16
2	29.92	28.78	27.59	27.10	26.60	26.09	25.57	25.31	25.07
3	47.13	44.19	41.04	39.71	38.33	36.90	35.42	34.65	33.95
4	62.76	61.03	58.79	57.87	56.94	55.98	55.02	54.53	54.08
5	63.19	62.23	61.68	61.47	61.25	61.03	60.81	60.70	60.60
6	96.55	93.37	90.08	88.73	87.36	85.96	84.55	83.83	83.18
7	96.88	95.48	94.07	93.50	92.92	92.34	91.76	91.46	91.20
8	114.00	111.32	108.58	107.46	106.33	105.19	104.03	103.45	102.92
	Percent difference								
1	0.02%	0.03%	0.02%	0.02%	0.02%	0.02%	0.02%	0.02%	-0.01%
2	-0.01%	-0.01%	-0.02%	-0.02%	-0.02%	-0.02%	-0.02%	-0.02%	-0.02%
3	0.04%	0.05%	0.05%	0.05%	0.05%	0.06%	0.06%	0.06%	0.06%
4	-0.05%	-0.01%	-0.01%	-0.01%	-0.01%	-0.02%	-0.02%	-0.02%	-0.02%
5	-0.01%	-0.05%	-0.05%	-0.05%	-0.05%	-0.05%	-0.06%	-0.06%	-0.06%
6	0.07%	0.07%	0.07%	0.07%	0.07%	0.08%	0.08%	0.08%	0.08%
7	-0.08%	-0.08%	-0.09%	-0.09%	-0.09%	-0.09%	-0.09%	-0.10%	-0.10%
8	-0.01%	-0.01%	-0.01%	-0.01%	-0.01%	-0.01%	-0.02%	-0.02%	-0.02%

Figure 4.18 Eigenvalue curves, SSSF plate, $\phi = 1 / 1$,

$P_\xi = - N_x b^2 / D$, $\lambda^2 = \omega a^2 (\rho / D)^{1/2}$.

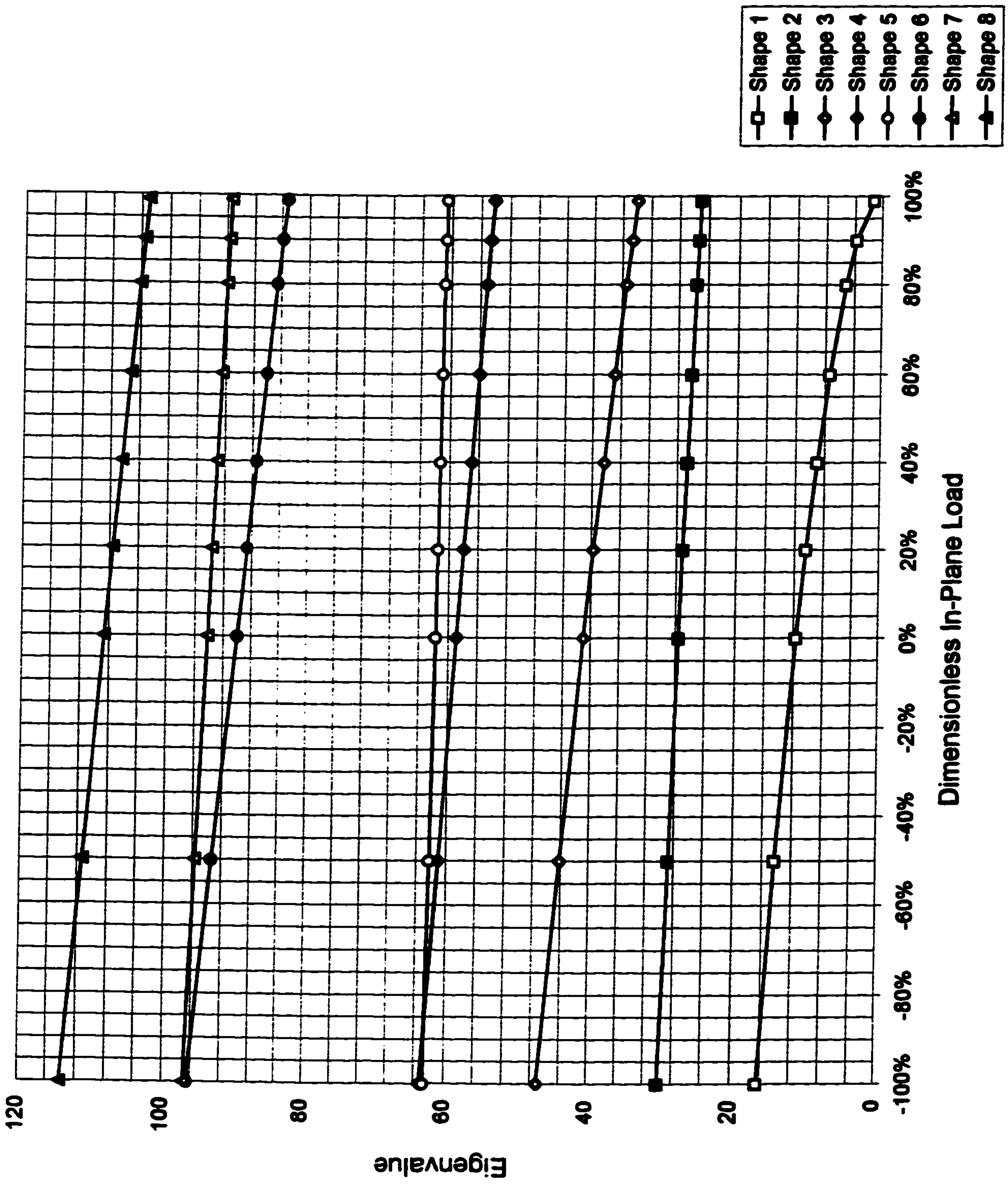

Figure 4.19 Mode shapes, SSSF plate, $\phi = 1 / 1$.

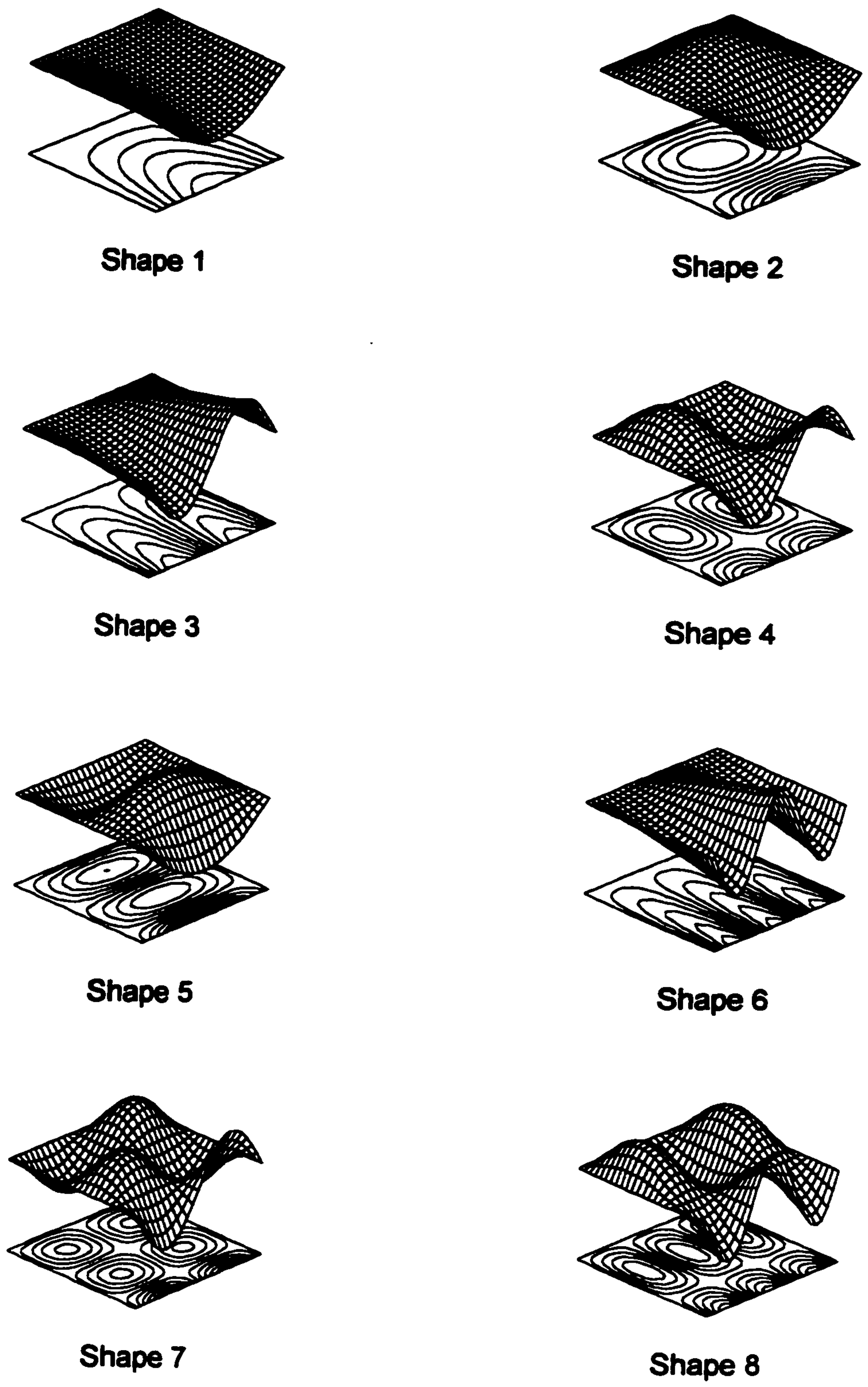

Table 4.16 Eigenvalues, SSSF plate, $\phi = 3/2$, $\lambda^2 = \omega a^2 (\rho / D)^{1/2}$.

Mode	In-plane load as a percentage of buckling load								
	-100%	-50%	0%	20%	40%	60%	80%	90%	99%
	Present solution								
1	15.00	12.99	10.61	9.49	8.22	6.71	4.74	3.35	1.06
2	21.07	19.68	18.20	17.57	16.92	16.24	15.53	15.16	14.82
3	35.22	34.41	33.59	33.25	32.91	32.57	32.22	32.04	31.88
4	45.29	42.73	40.01	38.87	37.69	36.48	35.22	34.57	33.98
5	52.72	50.54	48.26	47.32	46.36	45.38	44.37	43.86	43.40
6	58.46	57.98	57.49	57.30	57.10	56.90	56.71	56.61	56.52
7	67.93	66.26	64.53	63.83	63.12	62.41	61.68	61.31	60.98
8	90.80	90.22	88.96	87.93	86.77	85.59	84.40	83.80	83.25
	Finite element solution [18]								
1	15.01	13.00	10.61	9.49	8.22	6.71	4.75	3.36	1.06
2	21.07	19.68	18.20	17.57	16.91	16.23	15.53	15.16	14.82
3	35.20	34.40	33.57	33.23	32.89	32.54	32.20	32.02	31.86
4	45.30	42.74	40.02	38.88	37.70	36.49	35.23	34.58	33.99
5	52.72	50.54	48.26	47.32	46.35	45.37	44.37	43.86	43.39
6	58.42	57.94	57.45	57.25	57.05	56.86	56.66	56.56	56.47
7	67.88	66.20	64.48	63.78	63.07	62.35	61.62	61.26	60.92
8	90.74	90.06	88.80	87.93	86.77	85.59	84.40	83.80	83.25
	Percent difference								
1	0.03%	0.03%	0.03%	0.03%	0.03%	0.03%	0.02%	0.02%	-0.02%
2	0.00%	0.00%	0.00%	-0.01%	-0.01%	-0.02%	-0.02%	-0.02%	-0.03%
3	-0.05%	-0.06%	-0.06%	-0.06%	-0.06%	-0.06%	-0.07%	-0.07%	-0.07%
4	0.03%	0.03%	0.03%	0.03%	0.03%	0.03%	0.03%	0.03%	0.03%
5	0.00%	-0.01%	-0.01%	-0.01%	-0.01%	-0.01%	-0.02%	-0.02%	-0.02%
6	-0.08%	-0.08%	-0.08%	-0.08%	-0.08%	-0.08%	-0.08%	-0.08%	-0.08%
7	-0.07%	-0.08%	-0.08%	-0.09%	-0.09%	-0.09%	-0.10%	-0.10%	-0.10%
8	-0.07%	-0.18%	-0.19%	0.00%	0.00%	0.00%	0.00%	0.00%	0.00%

Figure 4.20 Eigenvalue curves, SSSF plate, $\phi = 3 / 2$,

$P_\xi = - N_x b^2 / D$, $\lambda^2 = \omega a^2 (\rho / D)^{1/2}$.

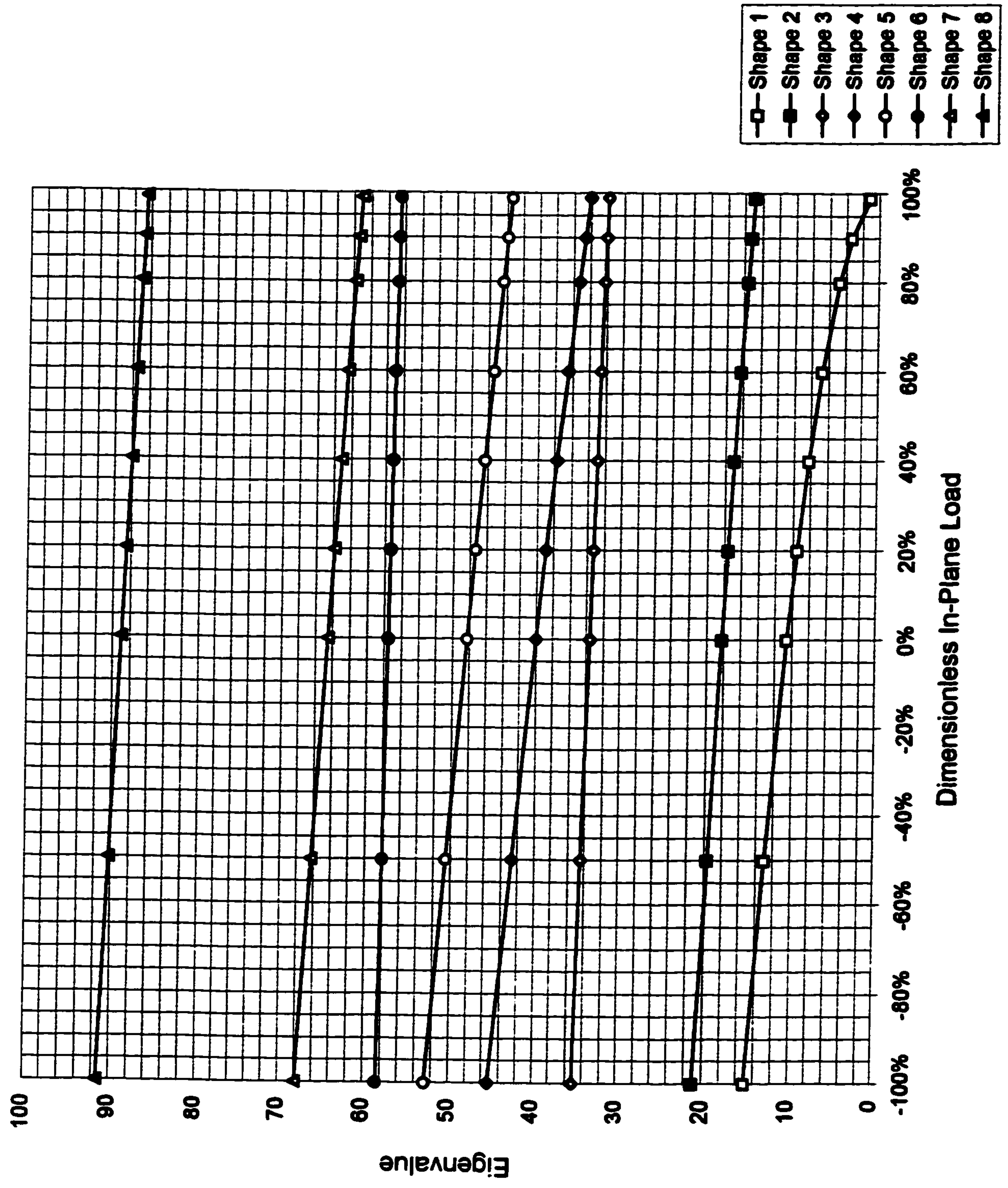

Figure 4.21 Mode shapes, SSSF plate, $\phi = 3 / 2$.

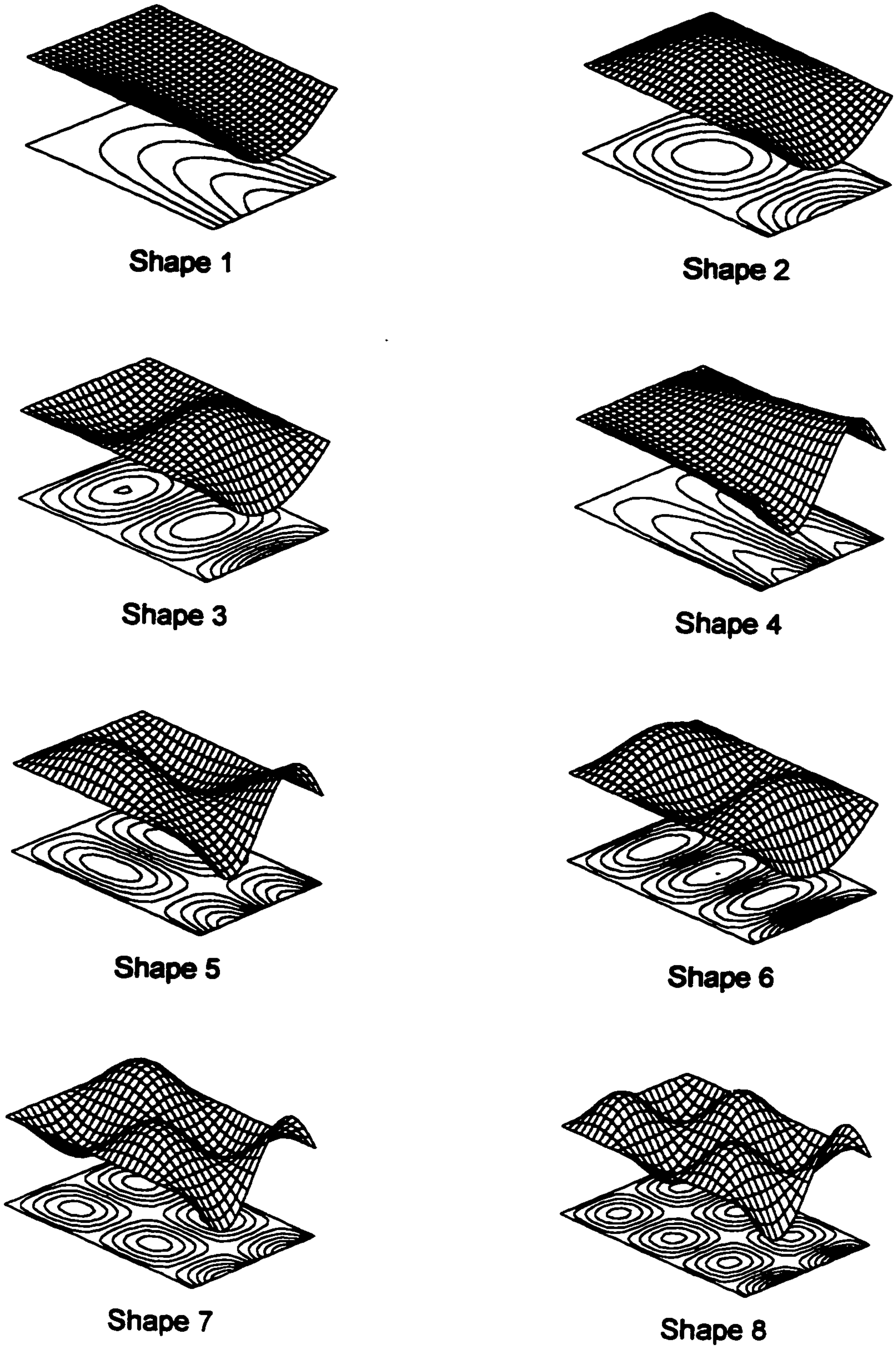

Table 4.17 Eigenvalues, SSSF plate, $\phi = 2 / 1$, $\lambda^2 = \omega\, a^2 (\rho / D)^{1/2}$.

Mode	In-plane load as a percentage of buckling load								
	-100%	-50%	0%	20%	40%	60%	80%	90%	99%
	Present solution								
1	14.50	12.56	10.25	9.17	7.94	6.49	4.59	3.24	1.03
2	17.92	16.39	14.70	13.97	13.19	12.37	11.49	11.02	10.58
3	25.67	24.63	23.54	23.09	22.63	22.16	21.68	21.43	21.21
4	38.44	37.75	37.04	36.76	36.47	36.18	35.18	34.57	34.02
5	44.66	42.24	39.67	38.60	37.49	36.35	35.89	35.74	35.61
6	48.93	46.73	44.43	43.47	42.49	41.49	40.46	39.94	39.46
7	56.36	55.70	53.78	52.99	52.19	51.38	50.55	50.13	49.76
8	57.55	55.89	55.42	55.23	55.04	54.85	54.66	54.56	54.47
	Finite element solution [18]								
1	14.51	12.56	10.26	9.17	7.94	6.49	4.59	3.24	1.03
2	17.92	16.39	14.70	13.96	13.19	12.37	11.48	11.02	10.58
3	25.66	24.61	23.52	23.07	22.61	22.14	21.66	21.41	21.19
4	38.39	37.70	36.99	36.71	36.42	36.13	35.18	34.58	34.03
5	44.67	42.25	39.68	38.61	37.50	36.36	35.84	35.69	35.56
6	48.92	46.73	44.42	43.46	42.48	41.48	40.45	39.93	39.45
7	56.29	55.65	53.72	52.93	52.13	51.32	50.49	50.07	49.69
8	57.51	55.82	55.34	55.15	54.96	54.77	54.58	54.48	54.40
	Percent difference								
1	0.03%	0.03%	0.03%	0.03%	0.03%	0.03%	0.03%	0.03%	0.02%
2	0.01%	0.00%	0.00%	-0.01%	-0.01%	-0.02%	-0.03%	-0.03%	-0.03%
3	-0.06%	-0.07%	-0.08%	-0.09%	-0.09%	-0.09%	-0.10%	-0.10%	-0.11%
4	-0.12%	-0.13%	-0.13%	-0.14%	-0.14%	-0.14%	0.02%	0.02%	0.02%
5	0.02%	0.02%	0.02%	0.02%	0.02%	0.02%	-0.15%	-0.15%	-0.15%
6	-0.02%	-0.02%	-0.02%	-0.03%	-0.03%	-0.03%	-0.04%	-0.04%	-0.04%
7	-0.13%	-0.09%	-0.10%	-0.11%	-0.11%	-0.12%	-0.12%	-0.12%	-0.12%
8	-0.08%	-0.14%	-0.14%	-0.14%	-0.14%	-0.14%	-0.14%	-0.14%	-0.14%

Figure 4.22 Eigenvalue curves, SSSF plate, $\phi = 2 / 1$,

$P_\xi = - N_x b^2 / D$, $\lambda^2 = \omega a^2 (\rho / D)^{1/2}$.

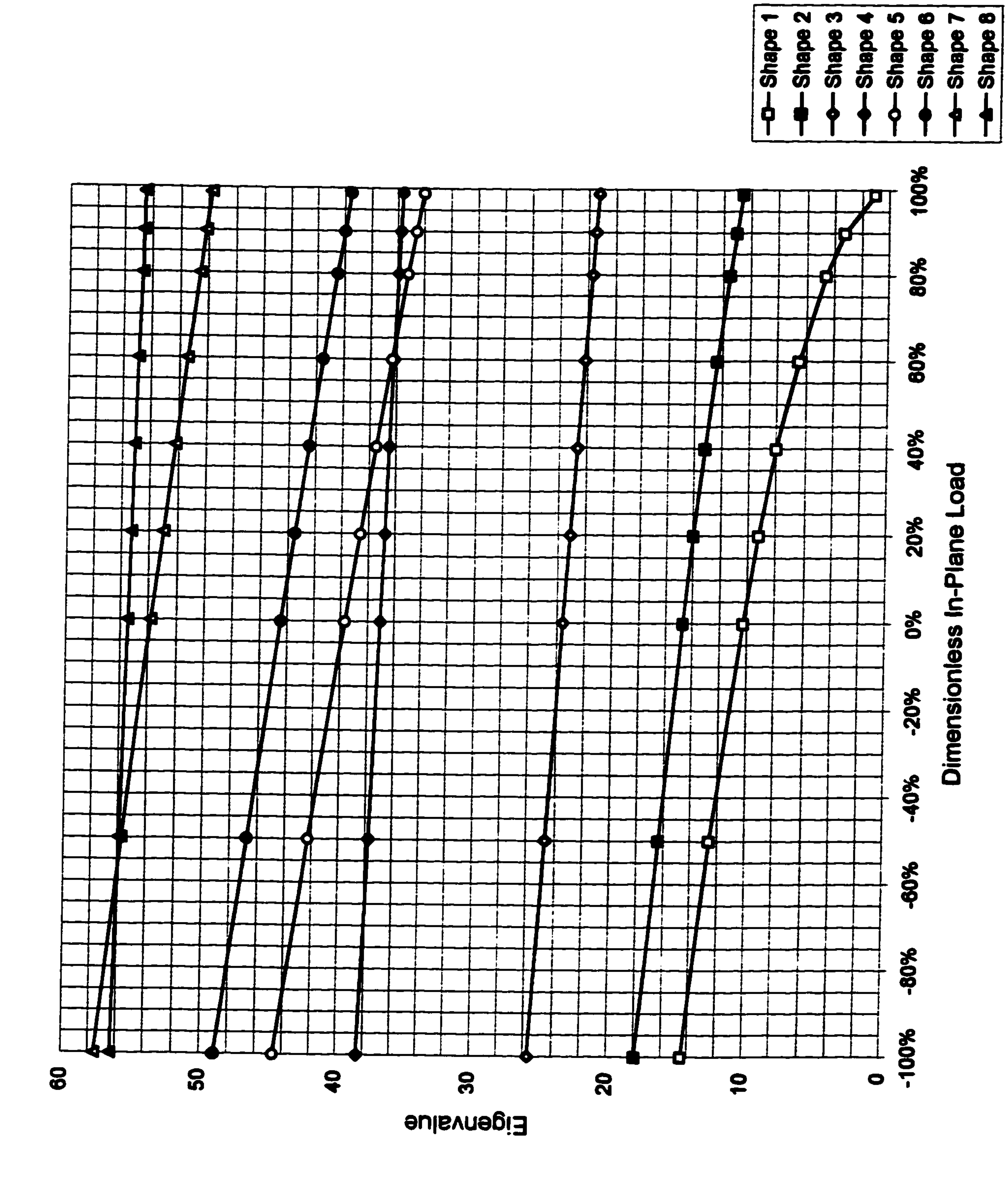

Figure 4.23 Mode shapes, SSSF plate, $\phi = 2 / 1$.

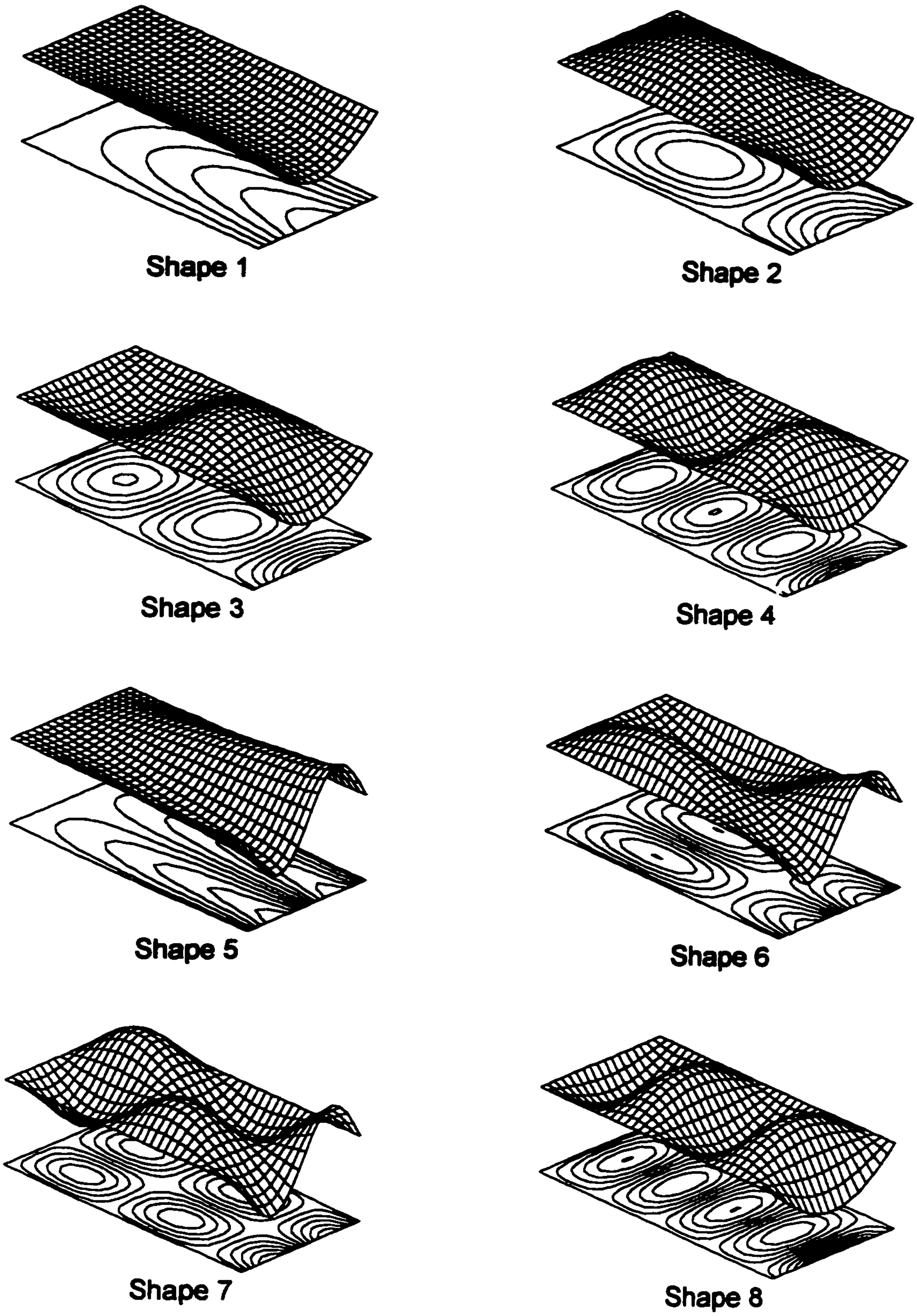

Table 4.18 Eigenvalues, SSSF plate, $\phi = 5 / 2$, $\lambda^2 = \omega a^2 (\rho / D)^{1/2}$.

Mode	In-plane load as a percentage of buckling load								
	-100%	-50%	0%	20%	40%	60%	80%	90%	99%
				Present solution					
1	14.27	12.36	10.09	9.02	7.82	6.38	4.51	3.19	1.01
2	16.46	14.84	13.01	12.20	11.34	10.40	9.37	8.81	8.27
3	21.32	20.09	18.78	18.23	17.66	17.07	16.47	16.15	15.87
4	29.28	28.40	27.49	27.12	26.74	26.36	25.97	25.77	25.59
5	40.55	39.91	39.27	38.49	37.41	36.31	35.17	34.58	34.05
6	44.38	42.03	39.53	39.01	38.75	38.49	38.22	38.08	37.60
7	47.16	44.95	42.62	41.66	40.67	39.66	38.62	38.09	37.97
8	52.70	50.73	48.69	47.84	46.98	46.11	45.22	44.76	44.35
				Finite element solution [18]					
1	14.27	12.36	10.09	9.03	7.82	6.38	4.51	3.19	1.01
2	16.47	14.84	13.01	12.20	11.34	10.40	9.37	8.81	8.27
3	21.30	20.07	18.76	18.21	17.64	17.05	16.44	16.13	15.84
4	29.24	28.35	27.44	27.06	26.68	26.30	25.91	25.71	25.53
5	40.46	39.82	39.18	38.50	37.42	36.32	35.18	34.59	34.06
6	44.40	42.04	39.54	38.92	38.65	38.39	38.12	37.99	37.58
7	47.15	44.94	42.61	41.64	40.65	39.64	38.60	38.06	37.87
8	52.65	50.68	48.63	47.79	46.92	46.05	45.15	44.70	44.29
				Percent difference					
1	0.04%	0.04%	0.04%	0.04%	0.04%	0.04%	0.04%	0.03%	-0.02%
2	0.01%	0.01%	0.00%	-0.01%	-0.02%	-0.02%	-0.04%	-0.05%	-0.06%
3	-0.06%	-0.08%	-0.10%	-0.10%	-0.11%	-0.12%	-0.14%	-0.14%	-0.15%
4	-0.16%	-0.18%	-0.19%	-0.20%	-0.21%	-0.21%	-0.22%	-0.22%	-0.23%
5	-0.22%	-0.23%	-0.24%	0.03%	0.03%	0.03%	0.03%	0.03%	0.03%
6	0.03%	0.03%	0.03%	-0.24%	-0.25%	-0.25%	-0.25%	-0.25%	-0.06%
7	-0.02%	-0.03%	-0.03%	-0.04%	-0.04%	-0.04%	-0.05%	-0.06%	-0.26%
8	-0.09%	-0.10%	-0.11%	-0.12%	-0.13%	-0.13%	-0.14%	-0.14%	-0.15%

Figure 4.24 Eigenvalue curves, SSSF plate, $\phi = 5 / 2$,
$P_\xi = - N_x b^2 / D$, $\lambda^2 = \omega a^2 (\rho / D)^{1/2}$.

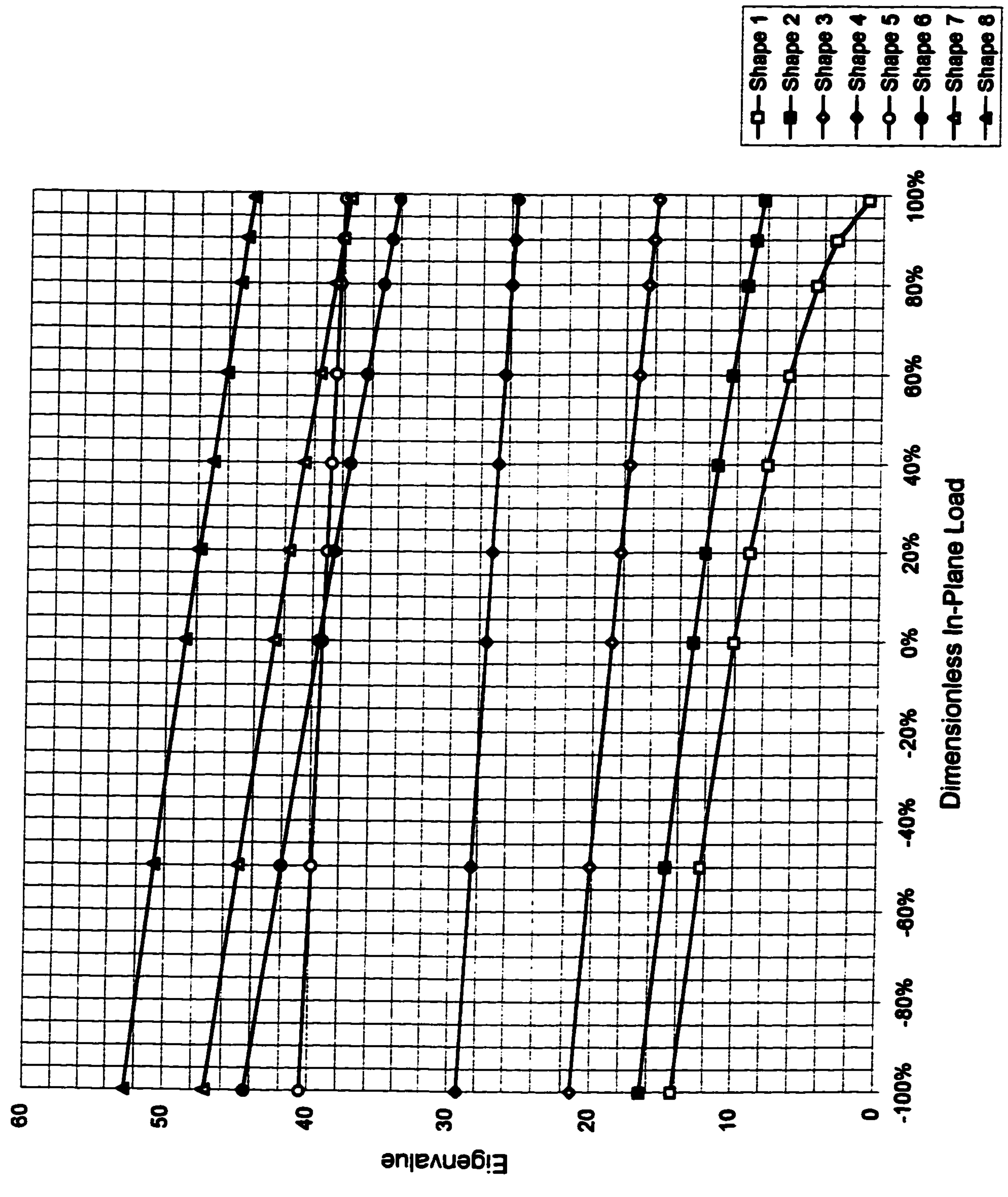

Figure 4.25 Mode shapes, SSSF plate, $\phi = 5 / 2$.

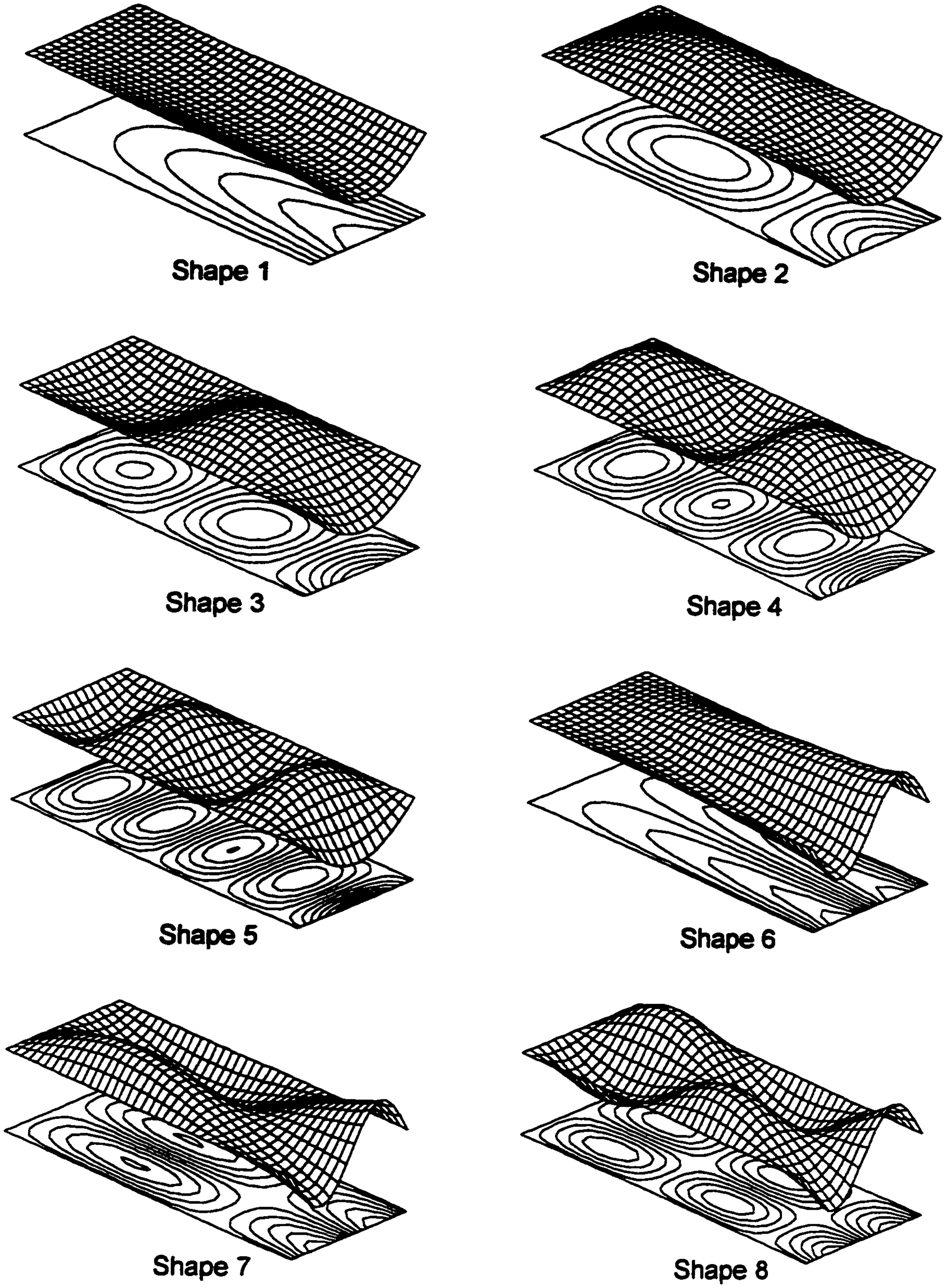

Table 4.19 Eigenvalues, SSSF plate, $\phi = 3 / 1$, $\lambda^2 = \omega a^2 (\rho / D)^{1/2}$.

Mode	In-plane load as a percentage of buckling load								
	-100%	-50%	0%	20%	40%	60%	80%	90%	99%
	Present solution								
1	14.14	12.25	10.00	8.95	7.75	6.33	4.47	3.16	1.00
2	15.67	13.99	12.07	11.21	10.27	9.25	8.10	7.45	6.82
3	18.98	17.62	16.13	15.50	14.84	14.15	13.43	13.05	12.70
4	24.39	23.34	22.24	21.79	21.32	20.85	20.36	20.12	19.89
5	32.05	31.26	30.45	30.12	29.79	29.45	29.11	28.94	28.78
6	42.03	41.43	39.46	38.43	37.37	36.29	35.17	34.59	34.07
7	44.24	41.92	40.82	40.57	39.67	38.65	37.60	37.06	36.58
8	46.20	43.98	41.64	40.67	40.33	40.08	39.83	39.70	39.59
	Finite element solution [18]								
1	14.15	12.26	10.01	8.95	7.75	6.33	4.48	3.16	1.00
2	15.68	13.99	12.07	11.21	10.27	9.25	8.09	7.45	6.82
3	18.97	17.60	16.12	15.48	14.82	14.13	13.40	13.02	12.67
4	24.34	23.29	22.19	21.73	21.27	20.79	20.30	20.06	19.83
5	31.96	31.17	30.35	30.02	29.68	29.35	29.00	28.83	28.67
6	41.89	41.28	39.48	38.45	37.39	36.31	35.19	34.61	34.09
7	44.26	41.94	40.67	40.43	39.65	38.63	37.58	37.04	36.55
8	46.19	43.97	41.63	40.65	40.18	39.93	39.68	39.55	39.44
	Percent difference								
1	0.04%	0.05%	0.05%	0.05%	0.05%	0.05%	0.05%	0.05%	-0.02%
2	0.02%	0.02%	0.00%	0.00%	-0.01%	-0.03%	-0.05%	-0.07%	-0.10%
3	-0.06%	-0.08%	-0.10%	-0.12%	-0.13%	-0.15%	-0.17%	-0.18%	-0.20%
4	-0.19%	-0.21%	-0.23%	-0.24%	-0.26%	-0.27%	-0.29%	-0.29%	-0.30%
5	-0.29%	-0.31%	-0.33%	-0.34%	-0.35%	-0.36%	-0.37%	-0.37%	-0.38%
6	-0.34%	-0.35%	0.05%	0.05%	0.05%	0.05%	0.05%	0.05%	0.05%
7	0.05%	0.05%	-0.36%	-0.37%	-0.04%	-0.05%	-0.06%	-0.06%	-0.06%
8	-0.02%	-0.03%	-0.04%	-0.04%	-0.37%	-0.38%	-0.38%	-0.39%	-0.39%

Figure 4.26 Eigenvalue curves, SSSF plate, $\phi = 3 / 1$,
$P_\xi = - N_x \, b^2 / D$, $\lambda^2 = \omega \, a^2 (\rho / D)^{1/2}$.

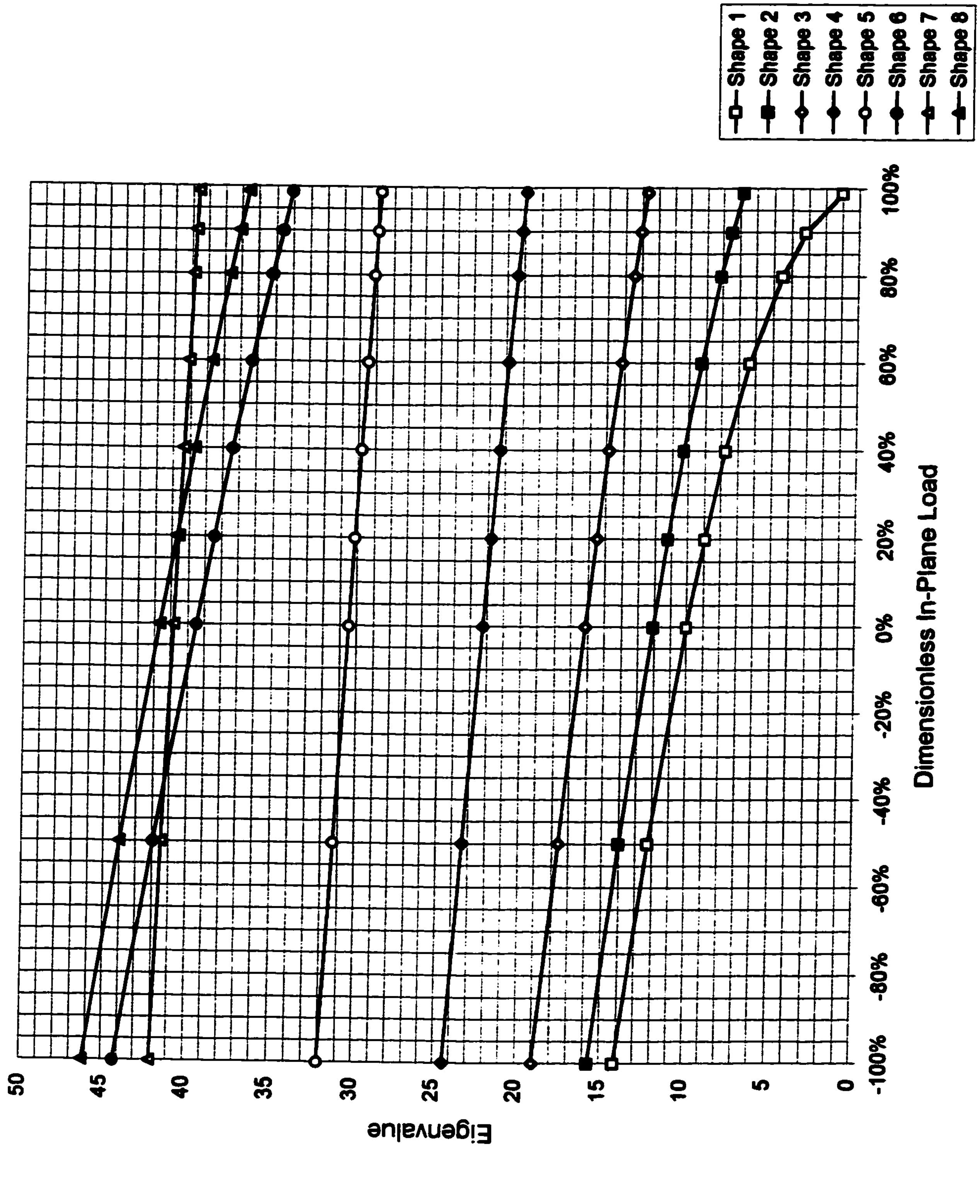

Figure 4.27 Mode shapes, SSSF plate, $\phi = 3 / 1$.

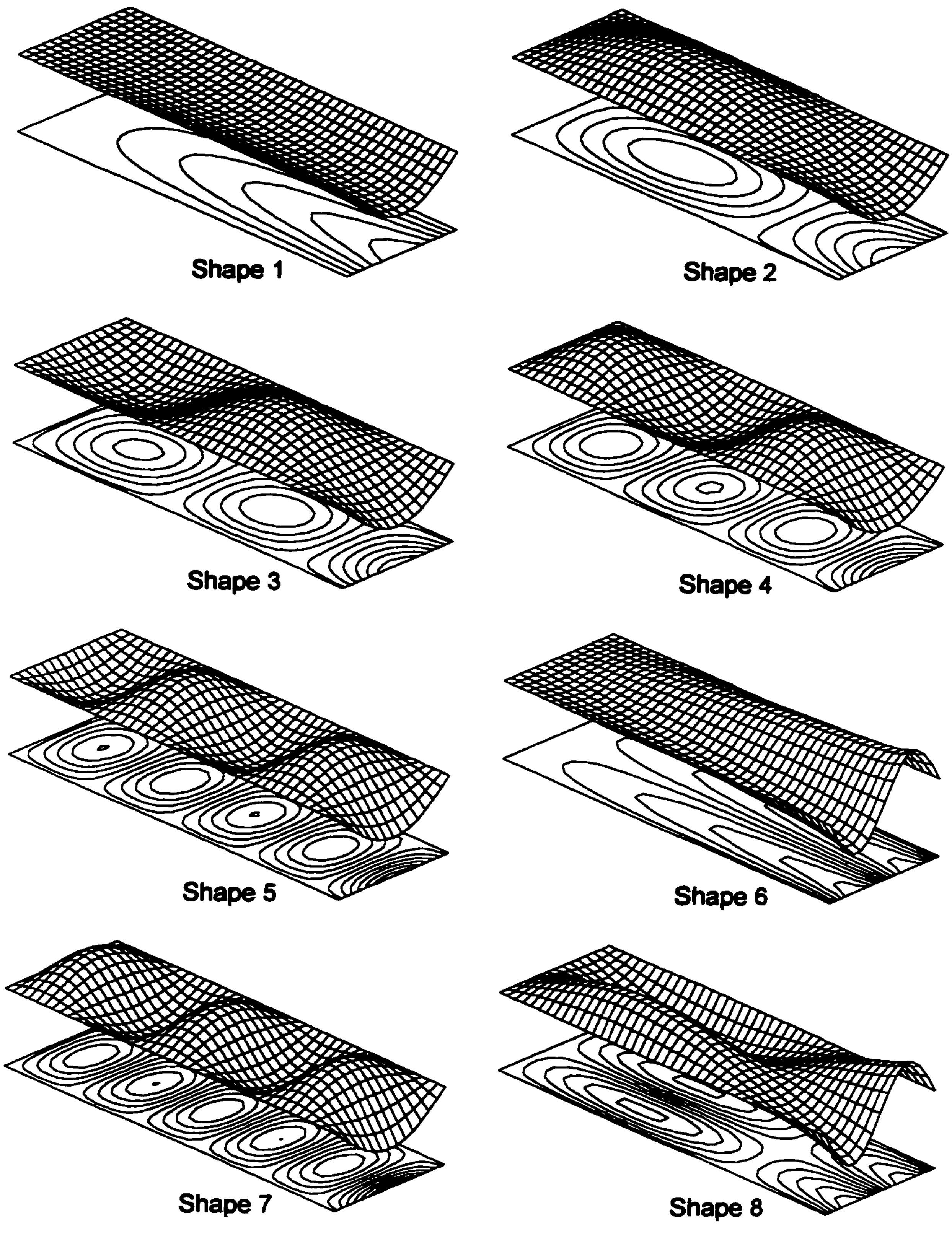

Table 4.20 Eigenvalues, SFSF plate, $\phi = 1 / 3$, $\lambda^2 = \omega a^2 (\rho / D)^{1/2}$.

Mode	In-plane load as a percentage of buckling load								
	-100%	-50%	0%	20%	40%	60%	80%	90%	99%
	Present solution								
1	13.25	11.47	9.37	8.38	7.26	5.92	4.19	2.96	0.94
2	40.05	39.49	37.91	36.98	36.02	35.03	34.01	33.49	33.02
3	42.29	40.16	38.94	38.71	38.48	38.25	38.02	37.91	37.80
4	86.86	85.85	84.82	84.40	83.99	83.32	82.36	81.88	81.45
5	90.58	88.38	86.11	85.19	84.26	83.57	83.15	82.93	82.74
6	145.68	144.32	142.94	142.39	141.83	141.28	140.72	140.43	140.18
7	158.55	156.32	154.06	153.15	152.23	151.30	150.37	149.91	149.48
8	217.53	217.43	216.60	215.95	215.30	214.65	213.99	213.67	213.37
	Finite element solution [18]								
1	13.25	11.48	9.37	8.38	7.26	5.93	4.19	2.96	0.94
2	40.04	39.49	37.97	37.03	36.07	35.08	34.07	33.55	33.07
3	42.34	40.21	38.93	38.70	38.48	38.25	38.02	37.90	37.80
4	86.84	85.82	84.80	84.38	83.96	83.54	82.60	82.12	81.69
5	90.81	88.60	86.35	85.43	84.49	83.55	83.12	82.91	82.72
6	145.67	144.31	142.93	142.38	141.82	141.26	140.70	140.42	140.16
7	159.19	156.96	154.71	153.80	152.88	151.96	151.04	150.57	150.15
8	217.40	217.30	216.74	216.08	215.43	214.78	214.13	213.80	213.50
	Percent difference								
1	0.04%	0.04%	0.04%	0.04%	0.04%	0.04%	0.03%	0.02%	-0.17%
2	-0.01%	-0.01%	0.14%	0.15%	0.15%	0.16%	0.16%	0.17%	0.17%
3	0.12%	0.13%	-0.01%	-0.01%	-0.01%	-0.01%	-0.01%	-0.01%	-0.02%
4	-0.02%	-0.02%	-0.03%	-0.03%	-0.03%	0.27%	0.29%	0.29%	0.29%
5	0.25%	0.26%	0.27%	0.27%	0.28%	-0.02%	-0.03%	-0.03%	-0.03%
6	0.00%	-0.01%	-0.01%	-0.01%	-0.01%	-0.01%	-0.01%	-0.01%	-0.01%
7	0.40%	0.41%	0.42%	0.42%	0.43%	0.44%	0.44%	0.44%	0.45%
8	-0.06%	-0.06%	0.06%	0.06%	0.06%	0.06%	0.06%	0.06%	0.06%

Figure 4.28 Eigenvalue curves, SFSF plate, $\phi = 1 / 3$,
$P_\xi = - N_x b^2 / D$, $\lambda^2 = \omega a^2 (\rho / D)^{1/2}$.

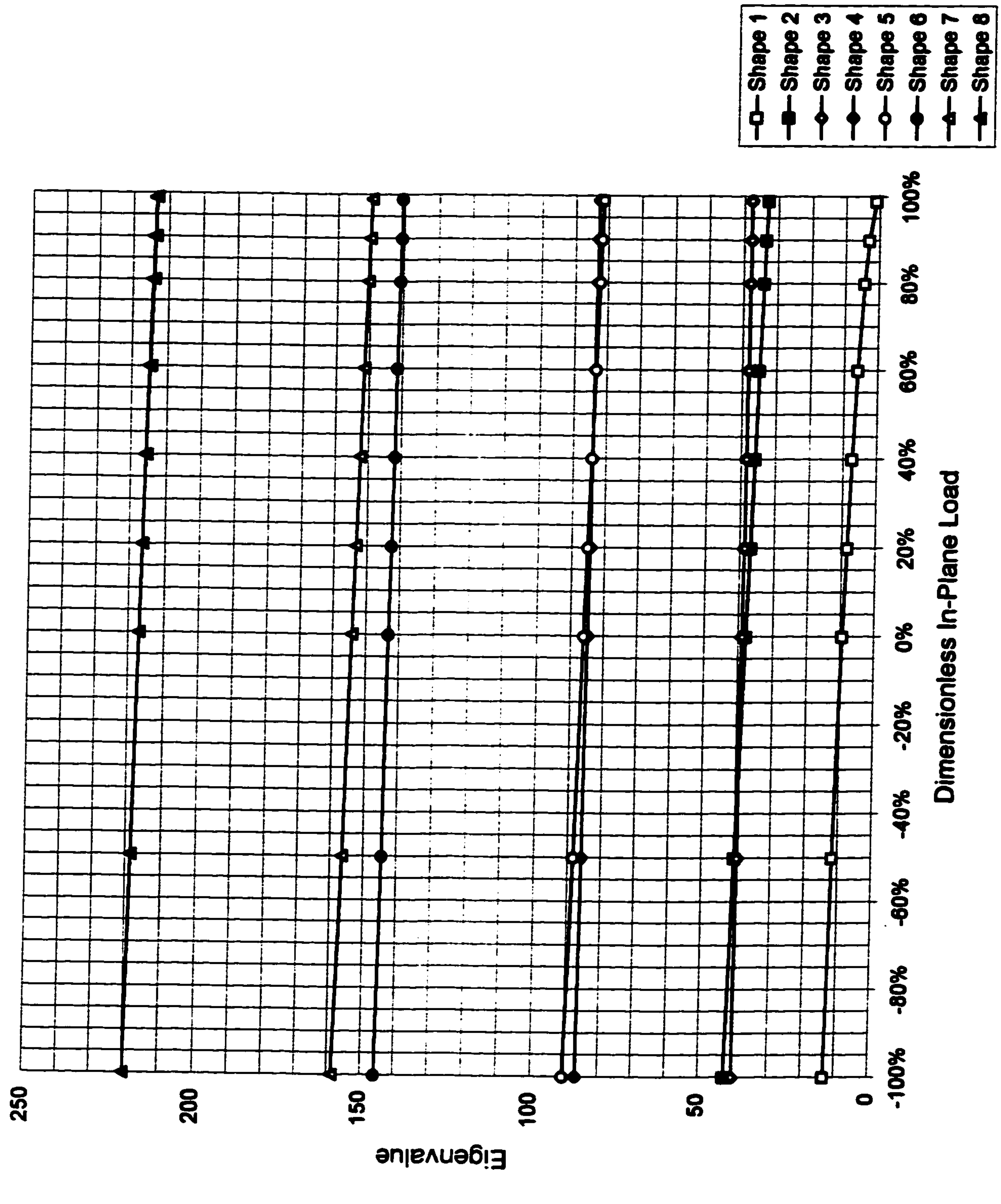

Figure 4.29 Mode shapes, SFSF plate, $\phi = 1 / 3$.

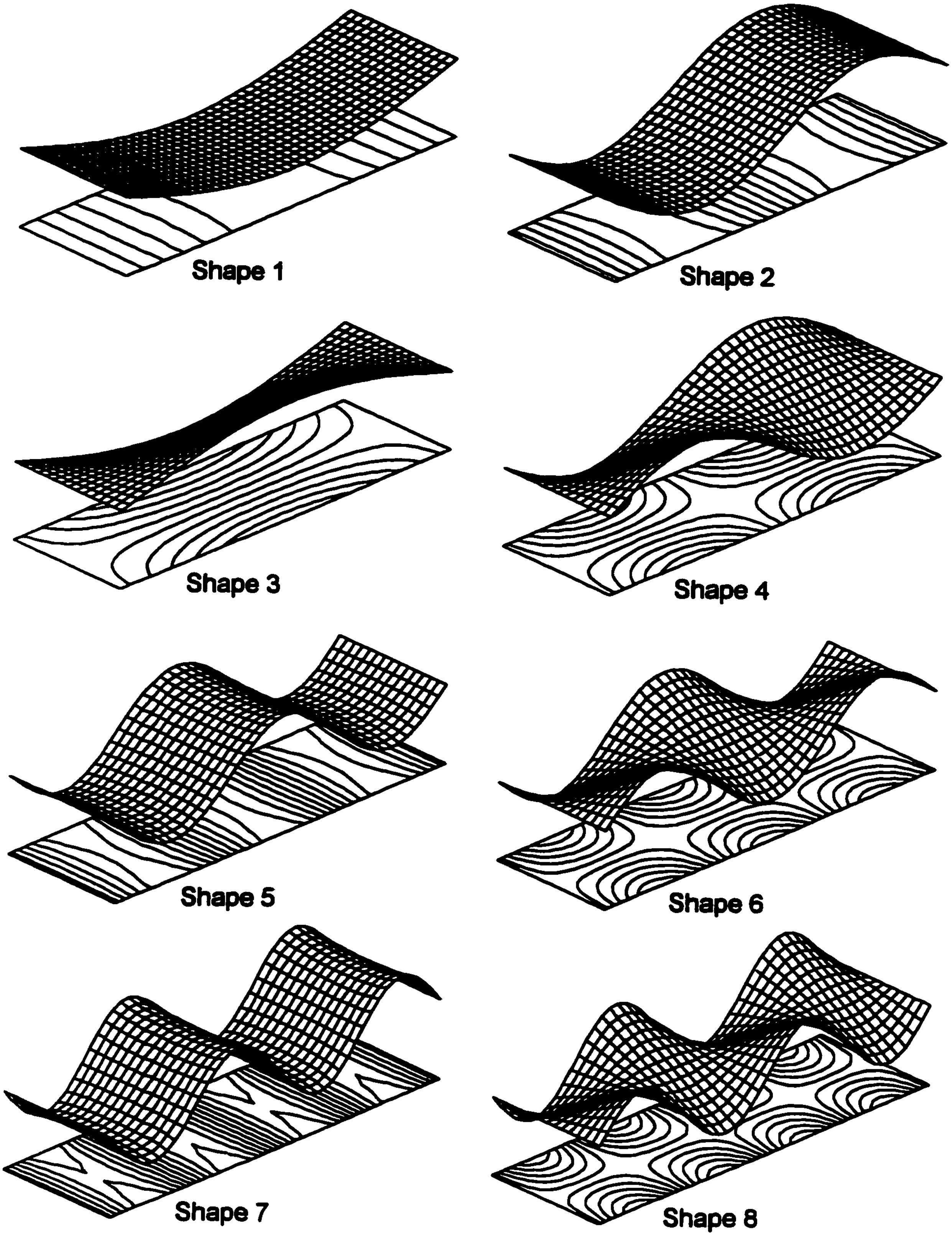

Table 4.21 Eigenvalues, SFSF plate, $\phi = 2 / 5$, $\lambda^2 = \omega a^2 (\rho / D)^{1/2}$.

Mode	In-plane load as a percentage of buckling load								
	-100%	-50%	0%	20%	40%	60%	80%	90%	99%
					Present solution				
1	13.28	11.50	9.39	8.40	7.27	5.94	4.20	2.97	0.94
2	34.20	33.55	32.89	32.62	32.35	32.07	31.80	31.66	31.53
3	42.45	40.32	38.07	37.14	36.17	35.19	34.17	33.65	33.17
4	76.22	75.05	73.87	73.39	72.91	72.42	71.94	71.69	71.47
5	90.94	88.73	86.47	85.55	84.61	83.67	82.72	82.24	81.80
6	131.61	130.10	128.56	127.95	127.32	126.70	126.07	125.76	125.47
7	155.93	155.79	154.60	153.69	152.77	151.84	150.91	150.44	150.02
8	159.10	156.87	155.65	155.59	155.53	155.48	155.42	155.39	155.37
					Finite element solution [18]				
1	13.28	11.50	9.39	8.40	7.28	5.94	4.20	2.97	0.94
2	34.20	33.55	32.89	32.62	32.34	32.07	31.79	31.65	31.53
3	42.50	40.37	38.12	37.18	36.22	35.24	34.22	33.70	33.23
4	76.22	75.05	73.87	73.39	72.91	72.42	71.93	71.69	71.47
5	91.14	88.93	86.68	85.76	84.82	83.88	82.93	82.45	82.01
6	131.67	130.15	128.62	128.00	127.38	126.75	126.12	125.81	125.53
7	155.84	155.70	155.18	154.27	153.36	152.43	151.50	151.04	150.62
8	159.67	157.44	155.56	155.50	155.45	155.39	155.33	155.30	155.28
					Percent difference				
1	0.04%	0.04%	0.04%	0.04%	0.04%	0.05%	0.05%	0.06%	0.15%
2	0.00%	0.00%	0.00%	-0.01%	-0.01%	-0.01%	-0.01%	-0.01%	-0.01%
3	0.11%	0.12%	0.13%	0.13%	0.14%	0.14%	0.15%	0.15%	0.16%
4	0.00%	0.00%	0.00%	0.00%	0.00%	0.00%	-0.01%	0.00%	0.00%
5	0.22%	0.23%	0.24%	0.25%	0.25%	0.25%	0.26%	0.26%	0.26%
6	0.04%	0.04%	0.05%	0.04%	0.04%	0.04%	0.04%	0.04%	0.05%
7	-0.06%	-0.06%	0.37%	0.38%	0.38%	0.39%	0.39%	0.40%	0.40%
8	0.36%	0.36%	-0.06%	-0.06%	-0.06%	-0.06%	-0.06%	-0.06%	-0.06%

Figure 4.30 Eigenvalue curves, SFSF plate, $\phi = 2 / 5$,

$P_\xi = - N_x b^2 / D$, $\lambda^2 = \omega a^2 (\rho / D)^{1/2}$.

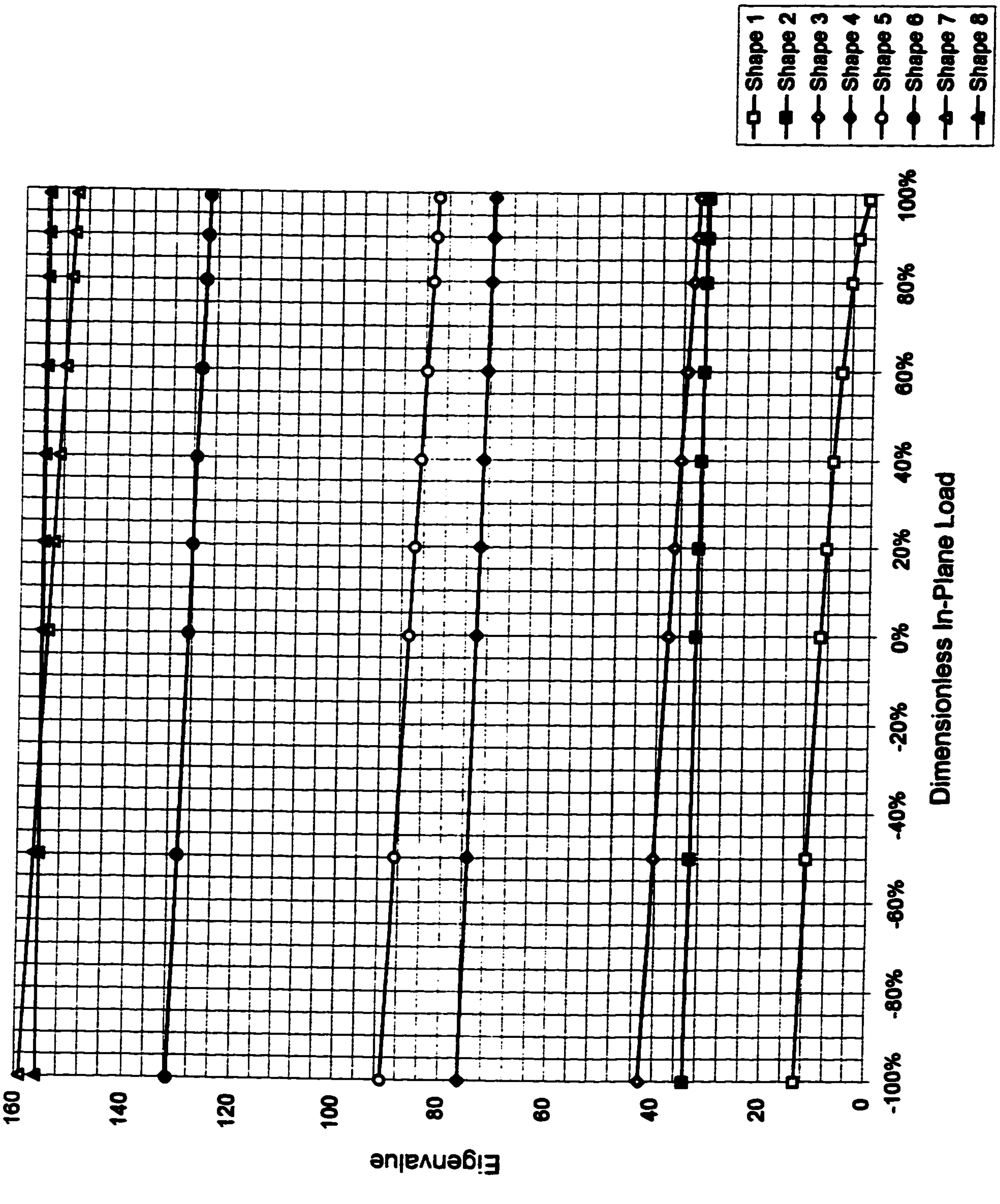

Figure 4.31 Mode shapes, SFSF plate, $\phi = 2 / 5$.

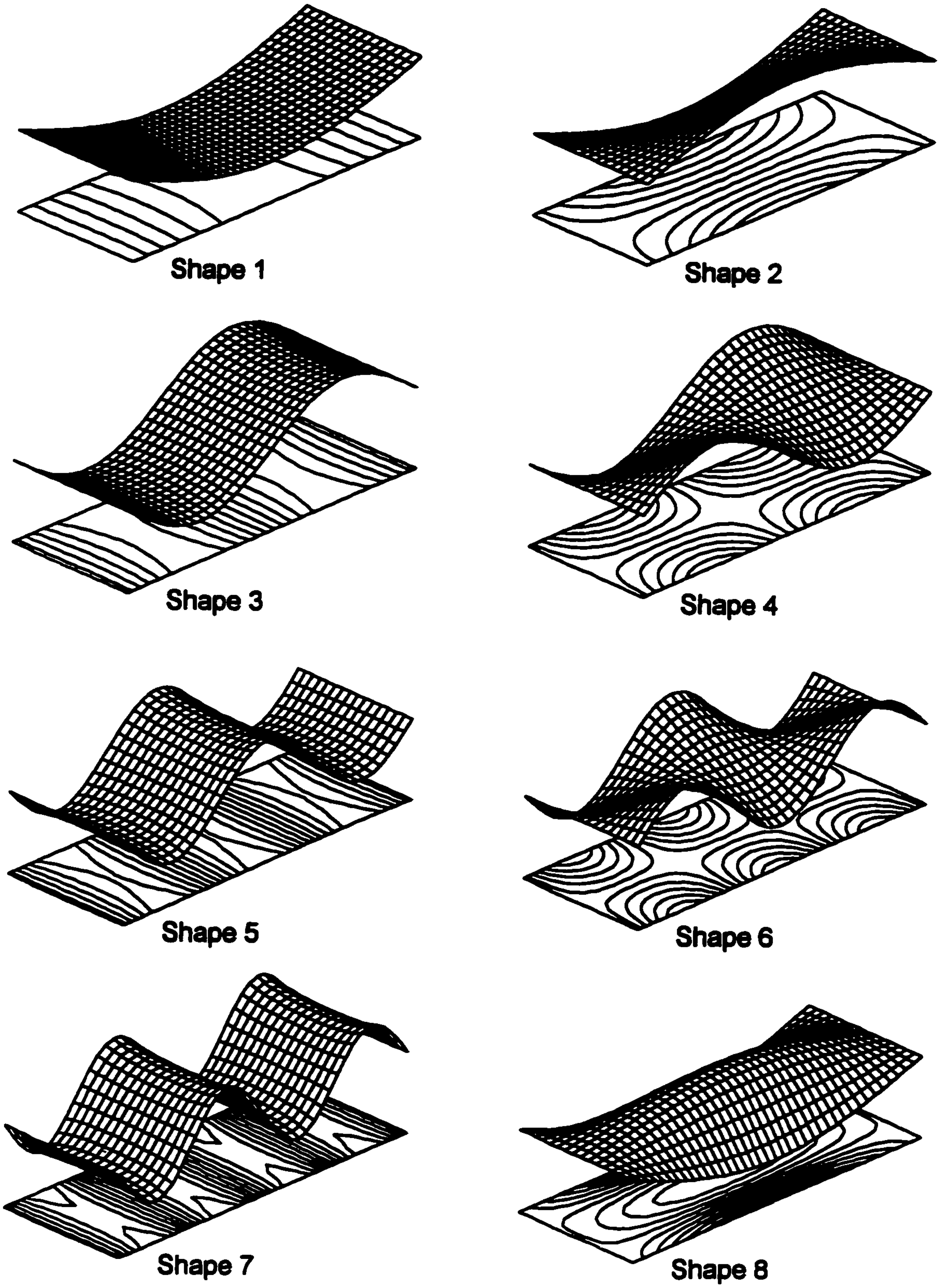

Table 4.22 Eigenvalues, SFSF plate, $\phi = 1 / 2$, $\lambda^2 = \omega a^2 (\rho / D)^{1/2}$.

Mode	In-plane load as a percentage of buckling load								
	-100%	-50%	0%	20%	40%	60%	80%	90%	99%
	Present solution								
1	13.33	11.54	9.42	8.43	7.30	5.96	4.21	2.98	0.94
2	28.55	27.76	26.95	26.61	26.28	25.94	25.59	25.42	25.26
3	42.66	40.53	38.27	37.33	36.37	35.38	34.36	33.84	33.36
4	66.27	64.91	63.53	62.97	62.40	61.83	61.25	60.96	60.70
5	91.35	89.13	86.86	85.94	85.00	84.06	83.10	82.62	82.18
6	105.46	105.25	105.04	104.96	104.87	104.79	104.70	104.66	104.62
7	118.91	117.21	115.50	114.80	114.10	113.40	112.69	112.34	112.02
8	146.90	146.29	145.68	145.44	145.19	144.95	144.70	144.58	144.47
	Finite element solution [18]								
1	13.33	11.55	9.43	8.43	7.30	5.96	4.22	2.98	0.94
2	28.55	27.76	26.95	26.62	26.28	25.94	25.59	25.42	25.26
3	42.70	40.57	38.32	37.38	36.41	35.42	34.41	33.88	33.41
4	66.29	64.93	63.55	62.99	62.42	61.85	61.27	60.98	60.72
5	91.52	89.31	87.04	86.11	85.18	84.24	83.28	82.80	82.36
6	105.42	105.20	104.99	104.91	104.82	104.74	104.65	104.61	104.57
7	119.02	117.33	115.61	114.92	114.22	113.52	112.81	112.45	112.14
8	146.77	146.16	145.56	145.31	145.07	144.82	144.58	144.45	144.34
	Percent difference								
1	0.04%	0.04%	0.04%	0.03%	0.04%	0.04%	0.04%	0.03%	-0.07%
2	0.01%	0.01%	0.01%	0.00%	0.00%	0.00%	0.00%	0.00%	0.00%
3	0.10%	0.10%	0.11%	0.11%	0.12%	0.12%	0.13%	0.13%	0.14%
4	0.04%	0.03%	0.04%	0.03%	0.03%	0.04%	0.03%	0.04%	0.03%
5	0.19%	0.20%	0.21%	0.21%	0.21%	0.22%	0.22%	0.22%	0.22%
6	-0.04%	-0.05%	-0.05%	-0.05%	-0.05%	-0.05%	-0.05%	-0.05%	-0.05%
7	0.09%	0.10%	0.10%	0.10%	0.10%	0.10%	0.10%	0.10%	0.10%
8	-0.09%	-0.09%	-0.09%	-0.09%	-0.09%	-0.09%	-0.09%	-0.09%	-0.09%

Figure 4.32 Eigenvalue curves, SFSF plate, $\phi = 1 / 2$,
$P_\xi = - N_x b^2 / D$, $\lambda^2 = \omega a^2 (\rho / D)^{1/2}$.

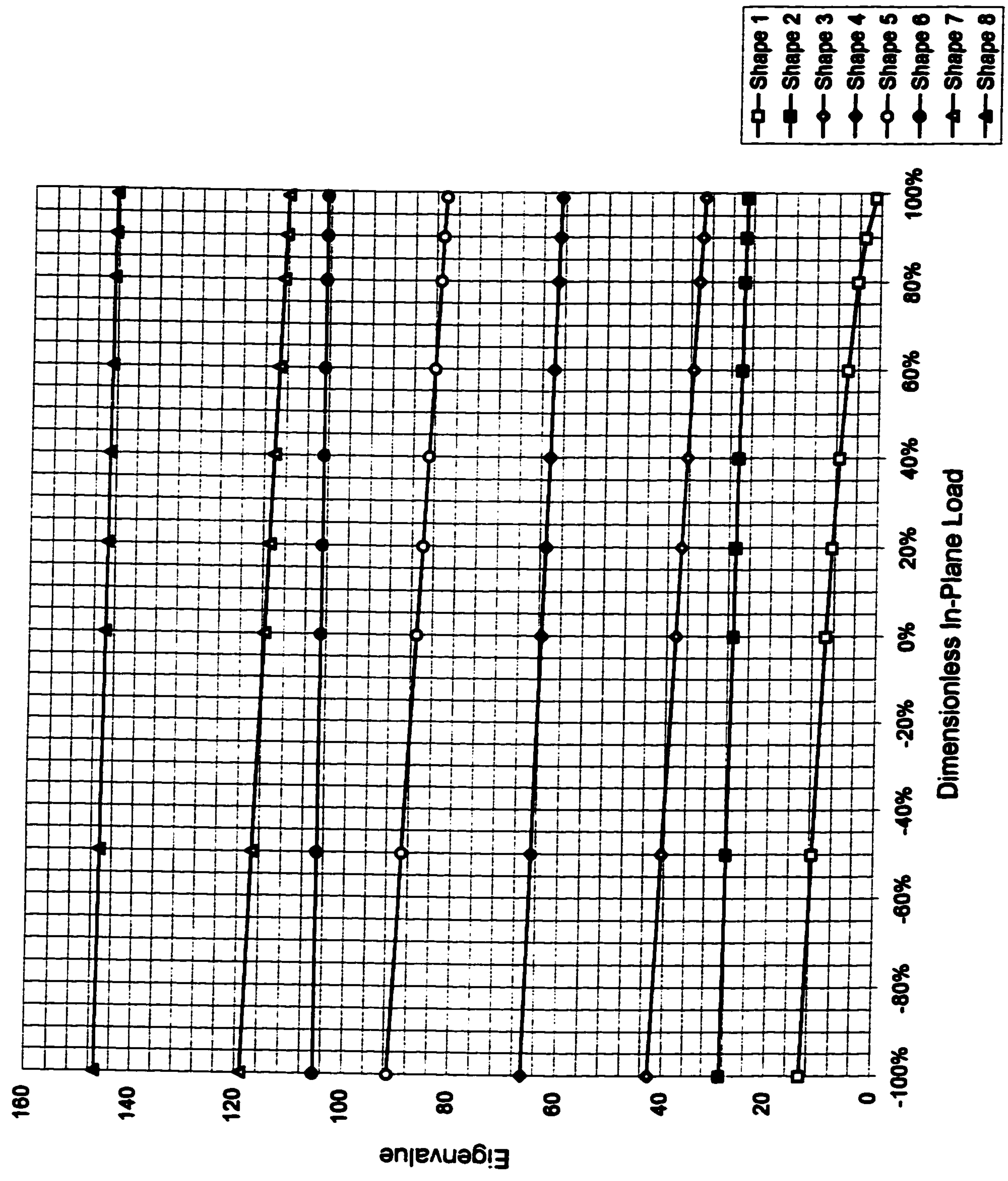

Figure 4.33 Mode shapes, SFSF plate, $\phi = 1 / 2$.

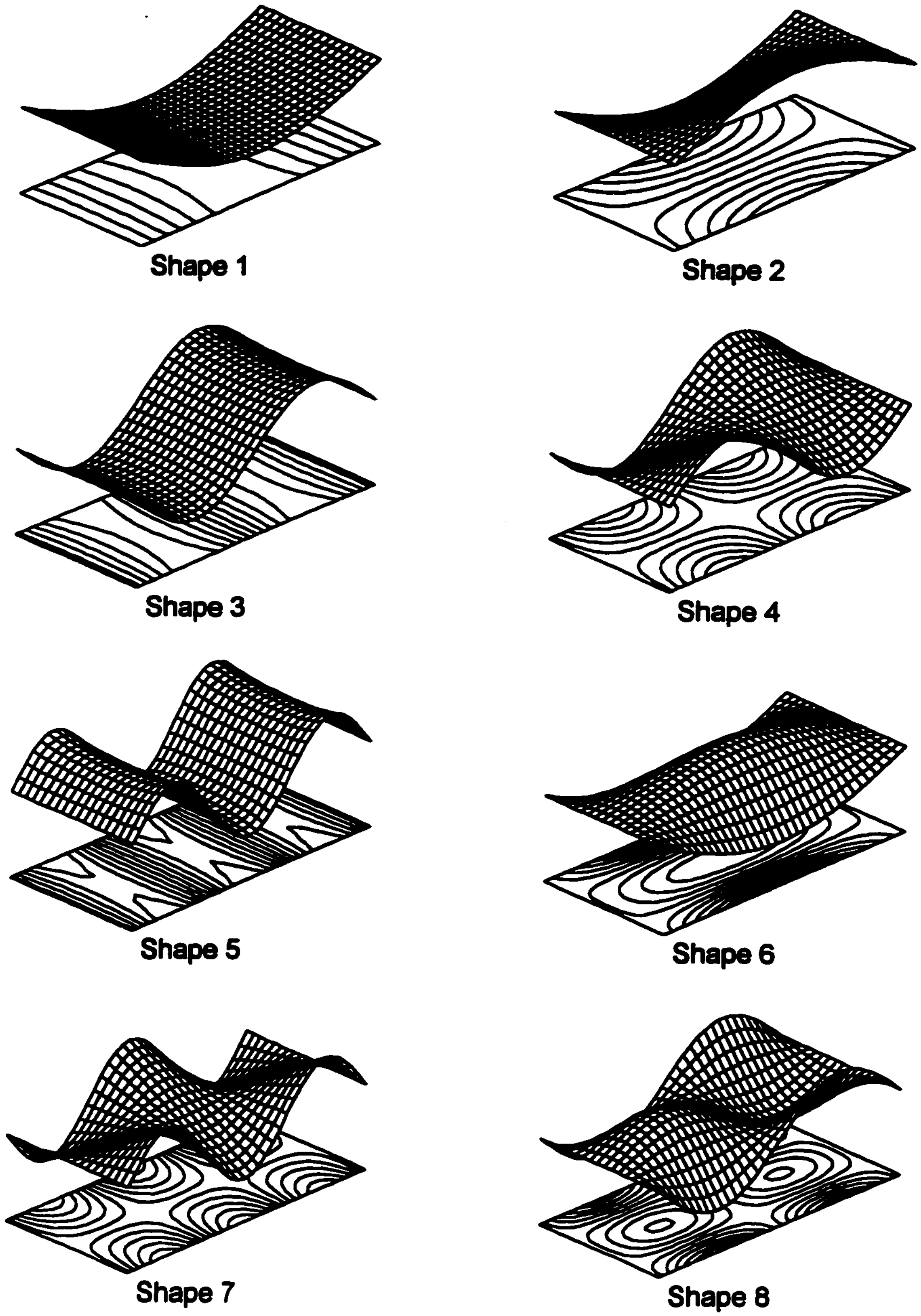

Table 4.23 Eigenvalues, SFSF plate, $\phi = 2/3$, $\lambda^2 = \omega a^2 (\rho / D)^{1/2}$.

Mode	In-plane load as a percentage of buckling load								
	-100%	-50%	0%	20%	40%	60%	80%	90%	99%
					Present solution				
1	13.40	11.61	9.48	8.48	7.34	5.99	4.24	3.00	0.95
2	23.23	22.24	21.20	20.78	20.34	19.89	19.44	19.20	18.99
3	42.93	40.78	38.52	37.57	36.60	35.61	34.58	34.06	33.58
4	57.37	55.79	54.15	53.48	52.81	52.12	51.43	51.08	50.76
5	66.08	65.74	65.39	65.26	65.12	64.98	64.84	64.77	64.71
6	91.80	89.57	87.29	86.36	85.41	84.46	83.50	83.01	82.57
7	104.76	103.90	103.03	102.68	102.33	101.89	101.09	100.69	100.33
8	108.05	106.17	104.24	103.47	102.68	101.98	101.63	101.45	101.29
					Finite element solution [18]				
1	13.41	11.61	9.48	8.48	7.34	6.00	4.24	3.00	0.95
2	23.23	22.24	21.21	20.78	20.34	19.90	19.44	19.21	18.99
3	42.96	40.82	38.55	37.60	36.64	35.64	34.62	34.09	33.62
4	57.41	55.82	54.19	53.52	52.84	52.16	51.47	51.11	50.80
5	66.06	65.72	65.37	65.24	65.10	64.96	64.82	64.75	64.69
6	91.93	89.71	87.42	86.49	85.55	84.60	83.64	83.15	82.71
7	104.72	103.86	102.99	102.64	102.29	101.94	101.25	100.84	100.48
8	108.20	106.31	104.39	103.62	102.83	102.04	101.59	101.41	101.25
					Percent difference				
1	0.03%	0.03%	0.03%	0.03%	0.03%	0.03%	0.03%	0.02%	-0.04%
2	0.02%	0.02%	0.02%	0.02%	0.02%	0.02%	0.02%	0.02%	0.02%
3	0.08%	0.08%	0.09%	0.09%	0.09%	0.10%	0.10%	0.10%	0.10%
4	0.07%	0.07%	0.07%	0.07%	0.07%	0.07%	0.08%	0.07%	0.08%
5	-0.03%	-0.03%	-0.03%	-0.03%	-0.03%	-0.03%	-0.03%	-0.03%	-0.03%
6	0.14%	0.15%	0.15%	0.16%	0.16%	0.16%	0.16%	0.17%	0.17%
7	-0.04%	-0.04%	-0.04%	-0.04%	-0.04%	0.05%	0.15%	0.15%	0.15%
8	0.14%	0.14%	0.14%	0.14%	0.15%	0.06%	-0.04%	-0.04%	-0.04%

Figure 4.34 Eigenvalue curves, SFSF plate, $\phi = 2 / 3$,

$P_{\xi} = - N_x b^2 / D$, $\lambda^2 = \omega a^2 (\rho / D)^{1/2}$.

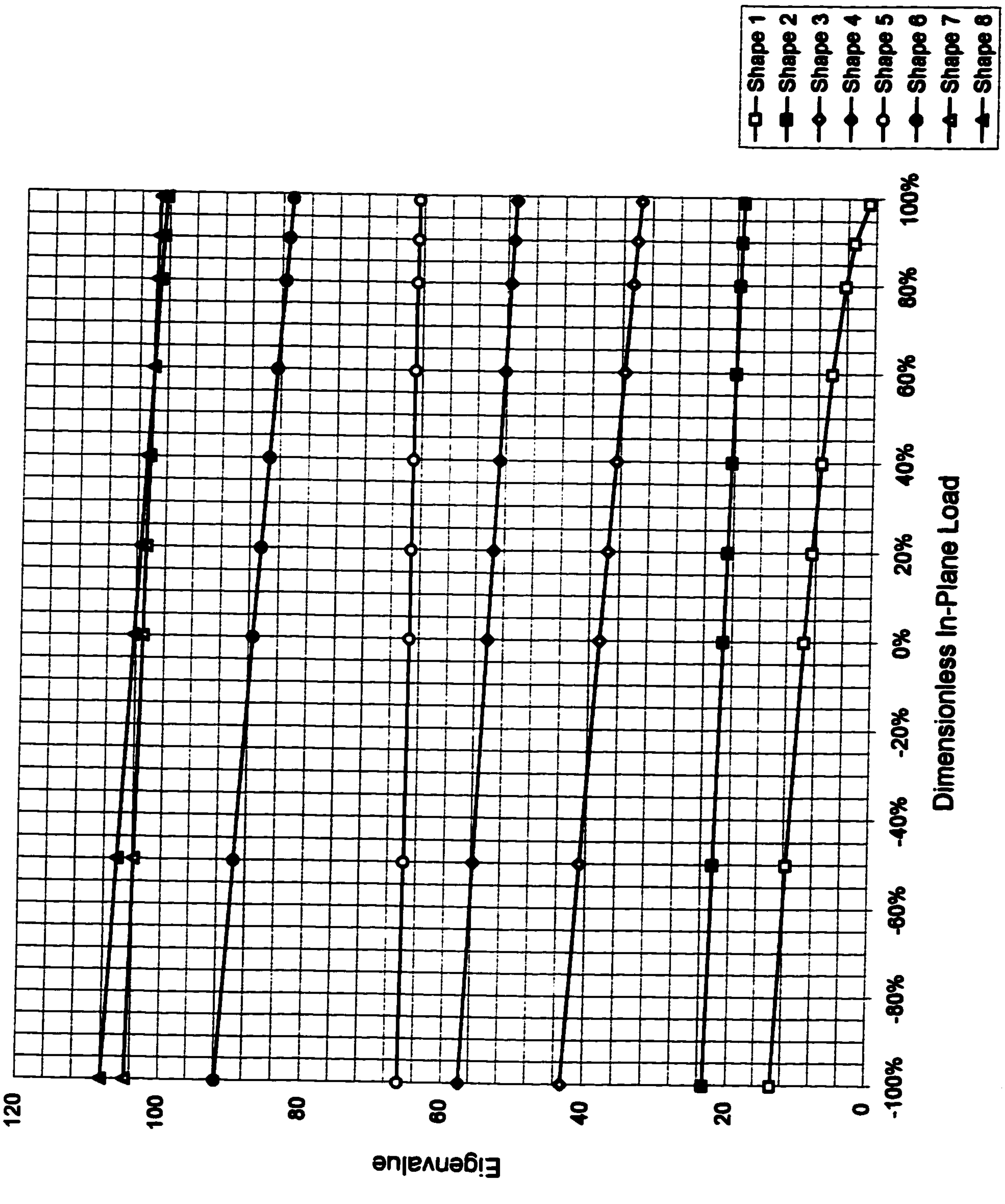

Figure 4.35 Mode shapes, SFSF plate, $\phi = 2 / 3$.

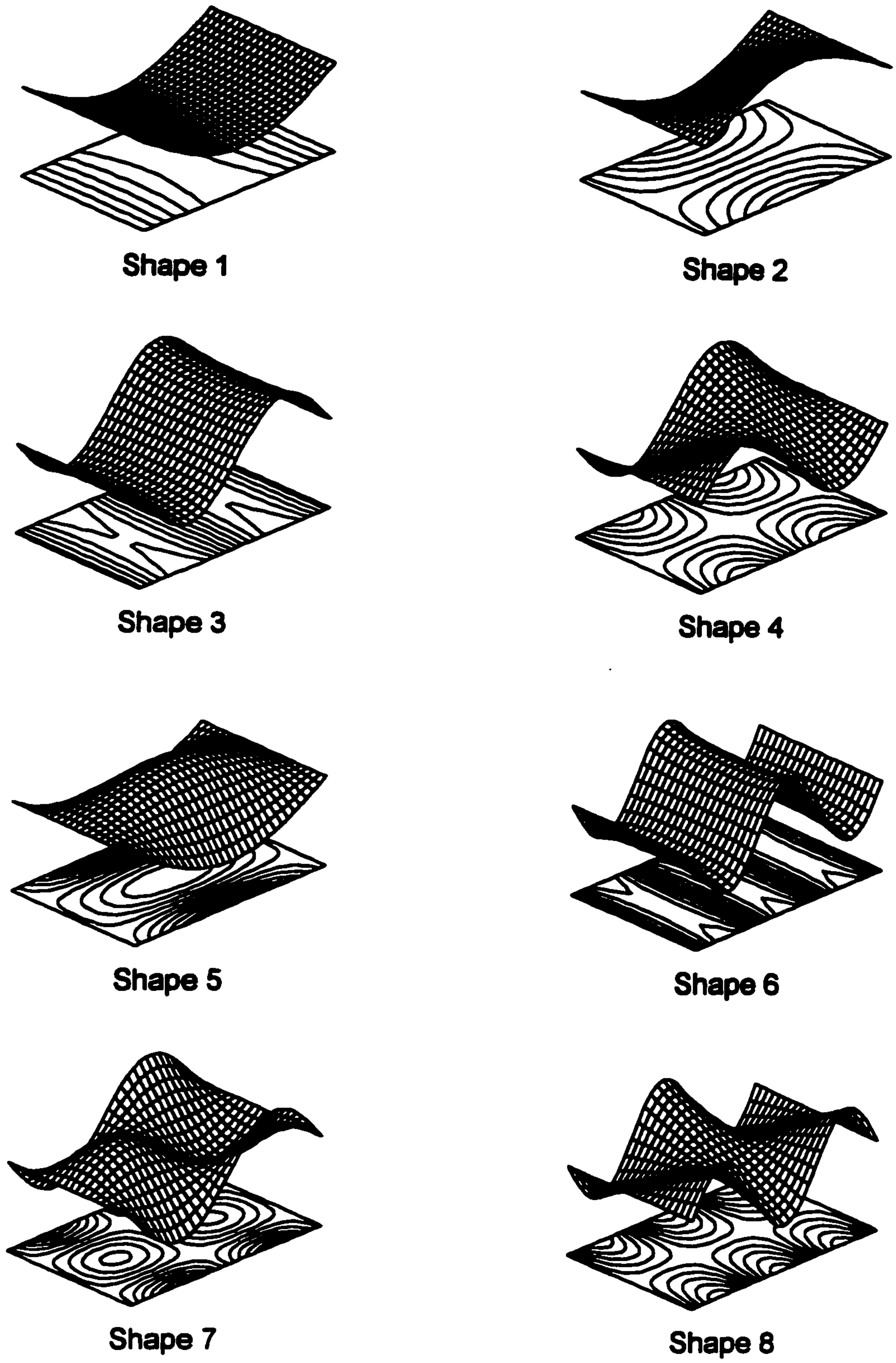

Table 4.24 Eigenvalues, SFSF plate, $\phi = 1 / 1$, $\lambda^2 = \omega a^2 (\rho / D)^{1/2}$.

Mode	In-plane load as a percentage of buckling load								
	-100%	-50%	0%	20%	40%	60%	80%	90%	99%
	Present solution								
1	13.53	11.72	9.57	8.56	7.41	6.05	4.28	3.03	0.96
2	18.54	17.26	15.88	15.30	14.68	14.05	13.38	13.03	12.71
3	37.66	37.04	36.42	36.17	35.91	35.66	34.81	34.28	33.80
4	43.26	41.09	38.79	37.84	36.86	35.85	35.40	35.27	35.15
5	50.13	48.27	46.33	45.53	44.72	43.90	43.05	42.63	42.24
6	72.73	71.46	70.16	69.64	69.11	68.58	68.04	67.77	67.53
7	75.63	75.33	75.02	74.90	74.78	74.65	74.53	74.47	74.41
8	92.32	90.06	87.74	86.79	85.84	84.88	83.90	83.41	82.96
	Finite element solution [18]								
1	13.54	11.72	9.57	8.56	7.41	6.05	4.28	3.03	0.96
2	18.55	17.27	15.89	15.30	14.69	14.05	13.39	13.04	12.72
3	37.65	37.04	36.42	36.16	35.91	35.65	34.83	34.30	33.82
4	43.28	41.11	38.81	37.86	36.88	35.87	35.40	35.27	35.15
5	50.17	48.31	46.38	45.58	44.77	43.94	43.10	42.67	42.29
6	72.75	71.48	70.19	69.66	69.13	68.60	68.06	67.79	67.55
7	75.59	75.29	74.98	74.86	74.74	74.62	74.49	74.43	74.38
8	92.38	90.12	87.80	86.86	85.91	84.94	83.96	83.47	83.03
	Percent difference								
1	0.03%	0.02%	0.02%	0.02%	0.03%	0.02%	0.03%	0.03%	0.05%
2	0.04%	0.04%	0.04%	0.05%	0.05%	0.05%	0.05%	0.06%	0.06%
3	-0.01%	-0.01%	-0.01%	-0.01%	-0.01%	-0.01%	0.06%	0.06%	0.06%
4	0.05%	0.05%	0.05%	0.05%	0.06%	0.06%	-0.01%	-0.01%	-0.01%
5	0.09%	0.09%	0.10%	0.10%	0.11%	0.11%	0.11%	0.11%	0.11%
6	0.03%	0.03%	0.03%	0.03%	0.03%	0.03%	0.03%	0.03%	0.03%
7	-0.05%	-0.05%	-0.05%	-0.05%	-0.05%	-0.05%	-0.05%	-0.05%	-0.05%
8	0.07%	0.07%	0.07%	0.07%	0.08%	0.08%	0.08%	0.08%	0.08%

Figure 4.36 Eigenvalue curves, SFSF plate, $\phi = 1 / 1$,
$P_\xi = - N_x b^2 / D$, $\lambda^2 = \omega a^2 (\rho / D)^{1/2}$.

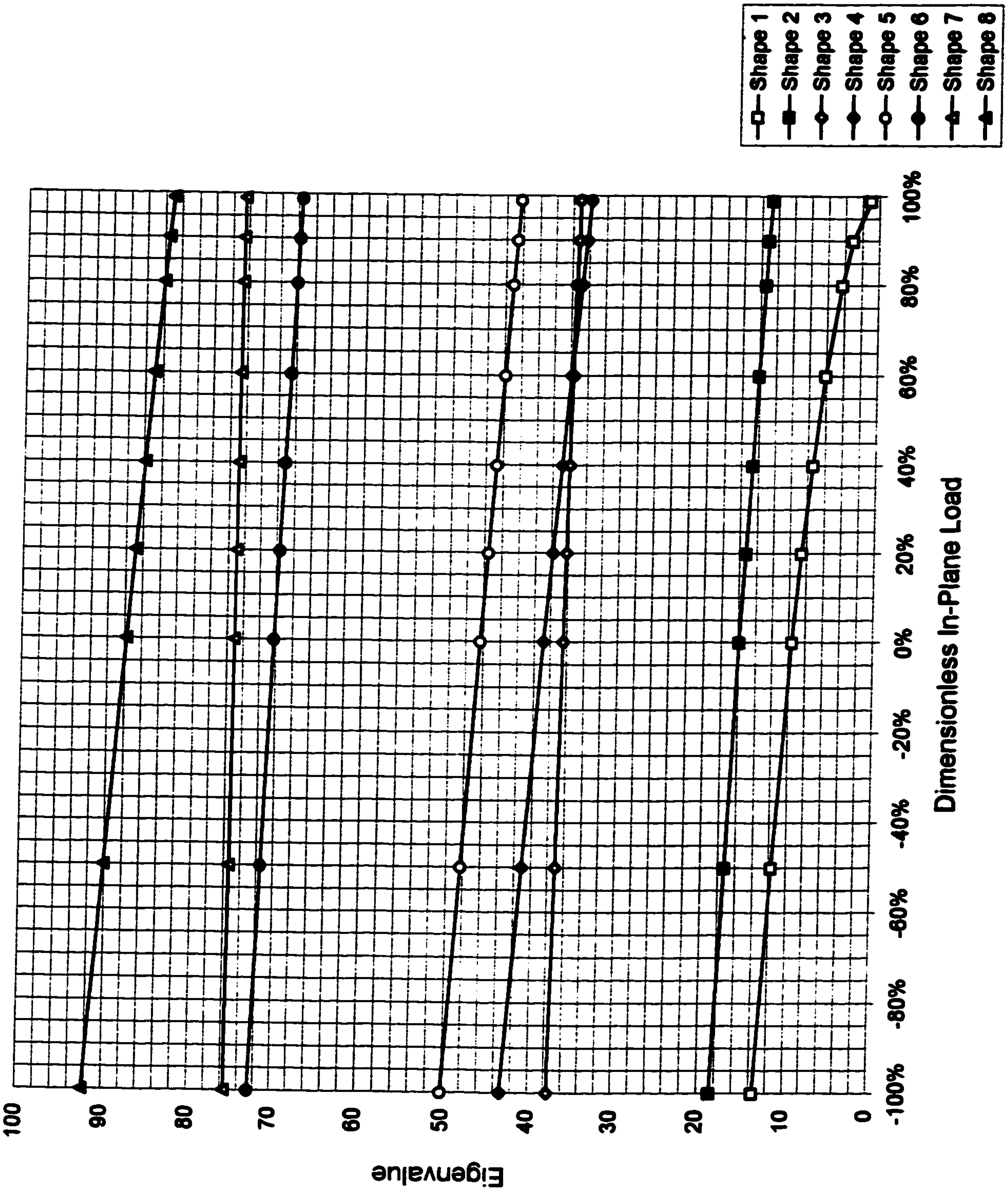

Figure 4.37 Mode shapes, SFSF plate, $\phi = 1 / 1$.

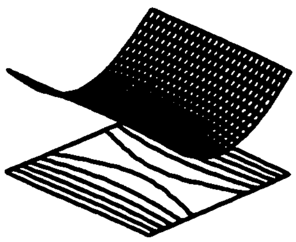

Shape 1

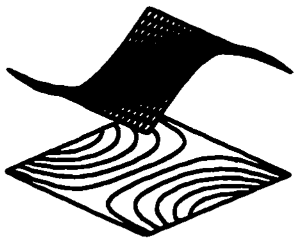

Shape 2

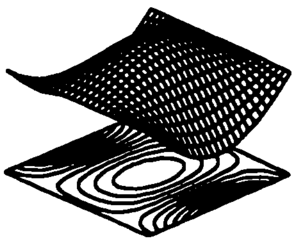

Shape 3

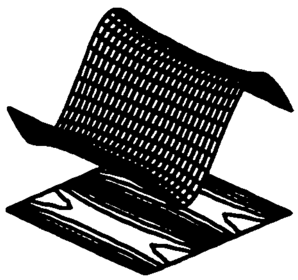

Shape 4

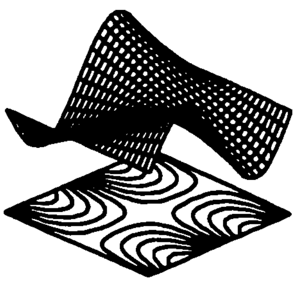

Shape 5

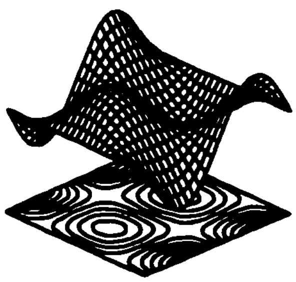

Shape 6

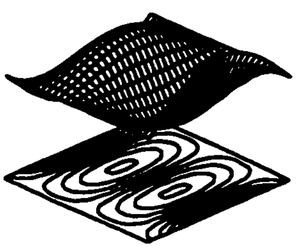

Shape 7

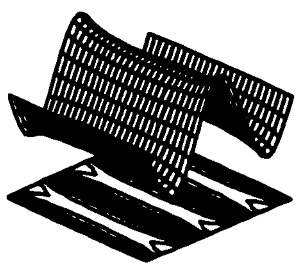

Shape 8

Table 4.25 Eigenvalues, SFSF plate, $\phi = 3 / 2$, $\lambda^2 = \omega a^2 (\rho / D)^{1/2}$.

Mode	In-plane load as a percentage of buckling load								
	-100%	-50%	0%	20%	40%	60%	80%	90%	99%
	Present solution								
1	13.65	11.82	9.65	8.63	7.48	6.10	4.32	3.05	0.96
2	16.06	14.53	12.83	12.09	11.29	10.43	9.50	8.99	8.51
3	24.71	23.75	22.75	22.33	21.91	21.48	21.05	20.82	20.62
4	41.29	40.72	39.00	38.03	37.04	36.01	34.97	34.43	33.94
5	43.51	41.31	40.15	39.91	39.68	39.44	38.77	38.28	37.84
6	46.62	44.58	42.44	41.55	40.64	39.71	39.21	39.09	38.98
7	57.27	55.62	53.92	53.22	52.51	51.80	51.08	50.71	50.38
8	66.75	66.40	66.04	65.90	65.76	65.62	65.48	65.41	65.34
	Finite element solution [18]								
1	13.65	11.82	9.65	8.63	7.48	6.11	4.32	3.05	0.97
2	16.07	14.54	12.84	12.09	11.30	10.44	9.51	9.00	8.52
3	24.71	23.75	22.75	22.34	21.92	21.49	21.05	20.83	20.62
4	41.27	40.70	39.00	38.04	37.04	36.02	34.97	34.44	33.95
5	43.52	41.32	40.13	39.89	39.66	39.43	38.81	38.33	37.89
6	46.66	44.62	42.48	41.59	40.69	39.76	39.19	39.07	38.96
7	57.30	55.65	53.95	53.26	52.55	51.84	51.11	50.75	50.41
8	66.70	66.35	66.00	65.86	65.72	65.57	65.43	65.36	65.30
	Percent difference								
1	0.02%	0.02%	0.02%	0.02%	0.02%	0.03%	0.03%	0.04%	0.21%
2	0.05%	0.06%	0.07%	0.08%	0.08%	0.09%	0.11%	0.12%	0.13%
3	0.01%	0.01%	0.01%	0.02%	0.01%	0.01%	0.01%	0.01%	0.01%
4	-0.04%	-0.05%	0.02%	0.02%	0.02%	0.02%	0.02%	0.02%	0.02%
5	0.02%	0.02%	-0.05%	-0.05%	-0.05%	-0.05%	0.12%	0.12%	0.13%
6	0.09%	0.10%	0.10%	0.11%	0.11%	0.12%	-0.05%	-0.05%	-0.05%
7	0.06%	0.06%	0.07%	0.07%	0.07%	0.07%	0.07%	0.07%	0.07%
8	-0.07%	-0.07%	-0.07%	-0.07%	-0.07%	-0.07%	-0.07%	-0.07%	-0.07%

Figure 4.38 Eigenvalue curves, SFSF plate, $\phi = 3 / 2$,

$P_{\xi} = - N_x b^2 / D$, $\lambda^2 = \omega a^2 (\rho / D)^{1/2}$.

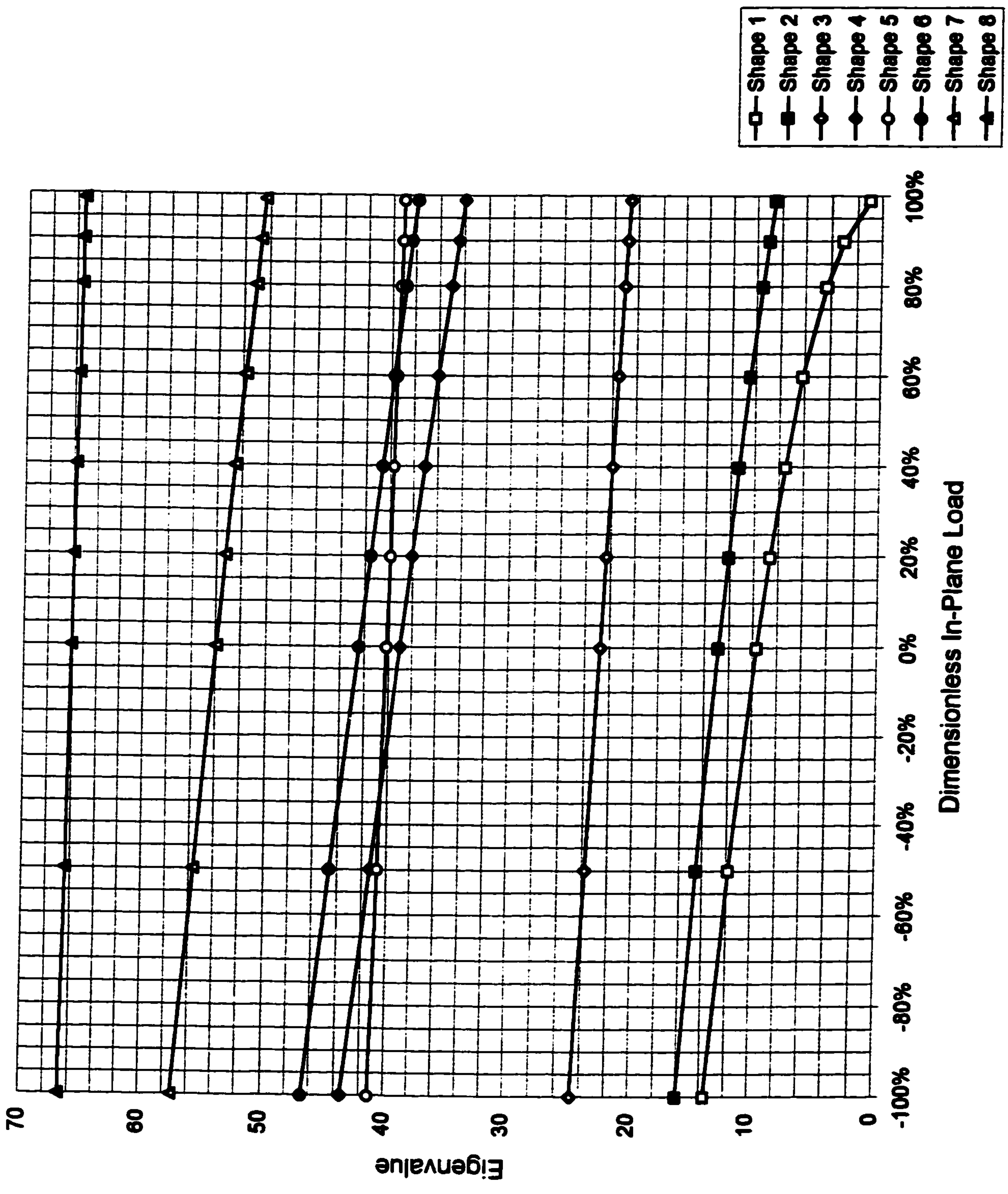

Figure 4.39 Mode shapes, SFSF plate, $\phi = 3 / 2$.

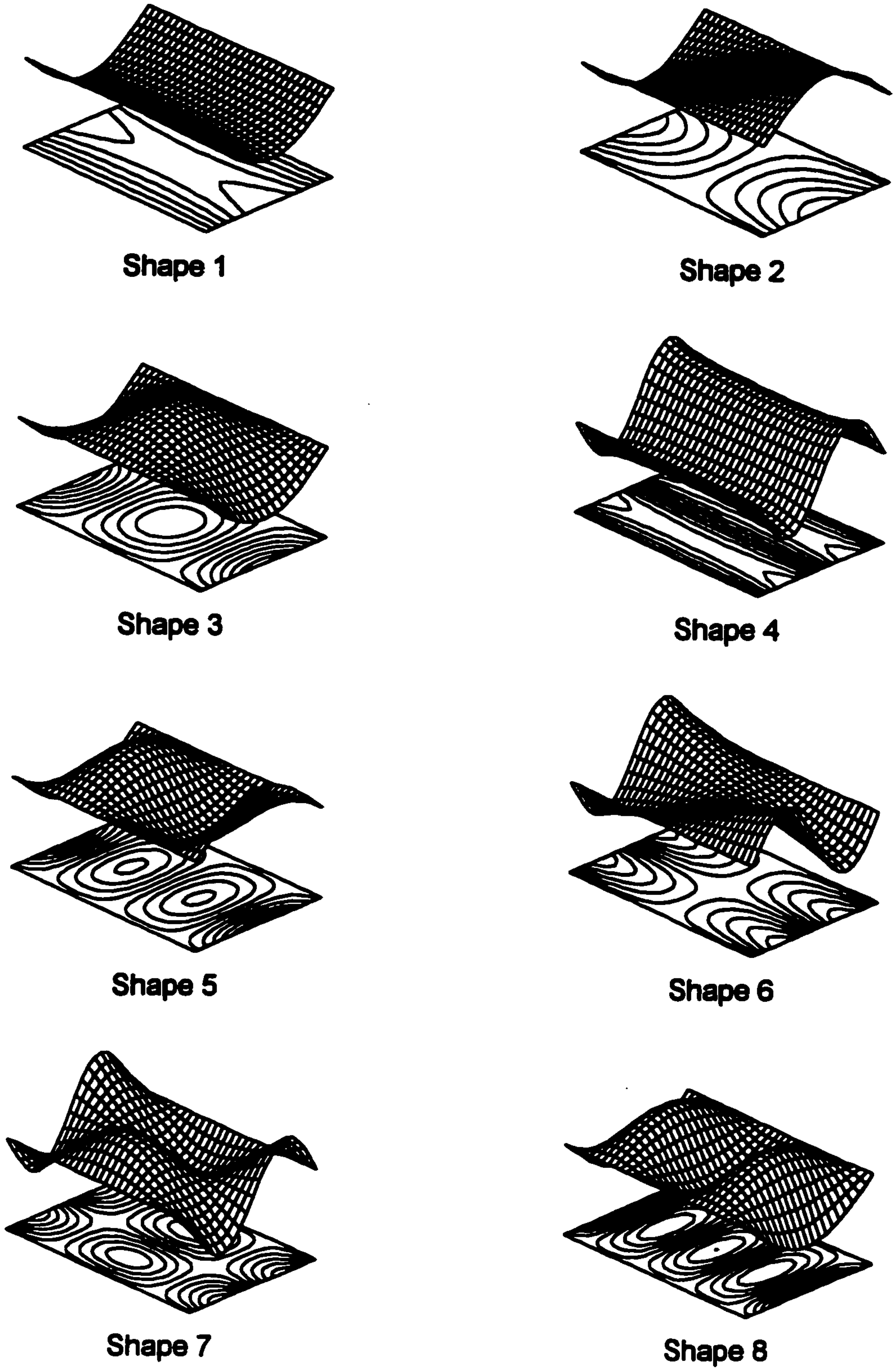

Table 4.26 Eigenvalues, SFSF plate, $\phi = 2 / 1$, $\lambda^2 = \omega a^2 (\rho / D)^{1/2}$.

Mode	In-plane load as a percentage of buckling load								
	-100%	-50%	0%	20%	40%	60%	80%	90%	99%
	Present solution								
1	13.72	11.88	9.70	8.67	7.51	6.13	4.34	3.07	0.97
2	15.11	13.46	11.58	10.74	9.83	8.82	7.68	7.04	6.41
3	20.04	18.83	17.54	17.00	16.43	15.85	15.25	14.93	14.65
4	29.25	28.43	27.59	27.25	26.90	26.55	26.19	26.01	25.85
5	43.33	41.44	39.10	38.12	37.12	36.10	35.04	34.50	34.00
6	43.65	42.78	41.01	40.09	39.14	38.16	37.16	36.65	36.19
7	45.37	43.25	42.23	42.00	41.78	41.55	41.33	41.21	41.11
8	51.54	49.68	47.75	46.96	46.15	45.33	44.49	44.06	43.68
	Finite element solution [18]								
1	13.72	11.88	9.70	8.68	7.51	6.14	4.34	3.07	0.97
2	15.12	13.47	11.59	10.75	9.84	8.83	7.69	7.05	6.42
3	20.05	18.84	17.55	17.00	16.44	15.86	15.25	14.94	14.65
4	29.23	28.42	27.58	27.23	26.89	26.53	26.18	26.00	25.83
5	43.28	41.44	39.11	38.13	37.13	36.10	35.04	34.50	34.01
6	43.65	42.73	41.06	40.14	39.19	38.21	37.21	36.70	36.24
7	45.41	43.29	42.18	41.95	41.73	41.50	41.28	41.16	41.06
8	51.58	49.72	47.79	46.99	46.19	45.36	44.53	44.10	43.72
	Percent difference								
1	0.02%	0.02%	0.02%	0.02%	0.03%	0.03%	0.03%	0.03%	0.06%
2	0.05%	0.07%	0.08%	0.09%	0.11%	0.12%	0.16%	0.18%	0.21%
3	0.03%	0.03%	0.03%	0.03%	0.04%	0.03%	0.04%	0.03%	0.04%
4	-0.05%	-0.05%	-0.06%	-0.06%	-0.06%	-0.06%	-0.07%	-0.07%	-0.07%
5	-0.11%	0.02%	0.02%	0.01%	0.01%	0.01%	0.01%	0.01%	0.01%
6	0.02%	-0.11%	0.12%	0.12%	0.12%	0.13%	0.13%	0.14%	0.14%
7	0.10%	0.11%	-0.11%	-0.12%	-0.12%	-0.12%	-0.12%	-0.12%	-0.12%
8	0.07%	0.07%	0.07%	0.08%	0.08%	0.08%	0.08%	0.08%	0.08%

Figure 4.40 Eigenvalue curves, SFSF plate, $\phi = 2 / 1$,

$P_{\xi} = - N_x b^2 / D$, $\lambda^2 = \omega a^2 (\rho / D)^{1/2}$.

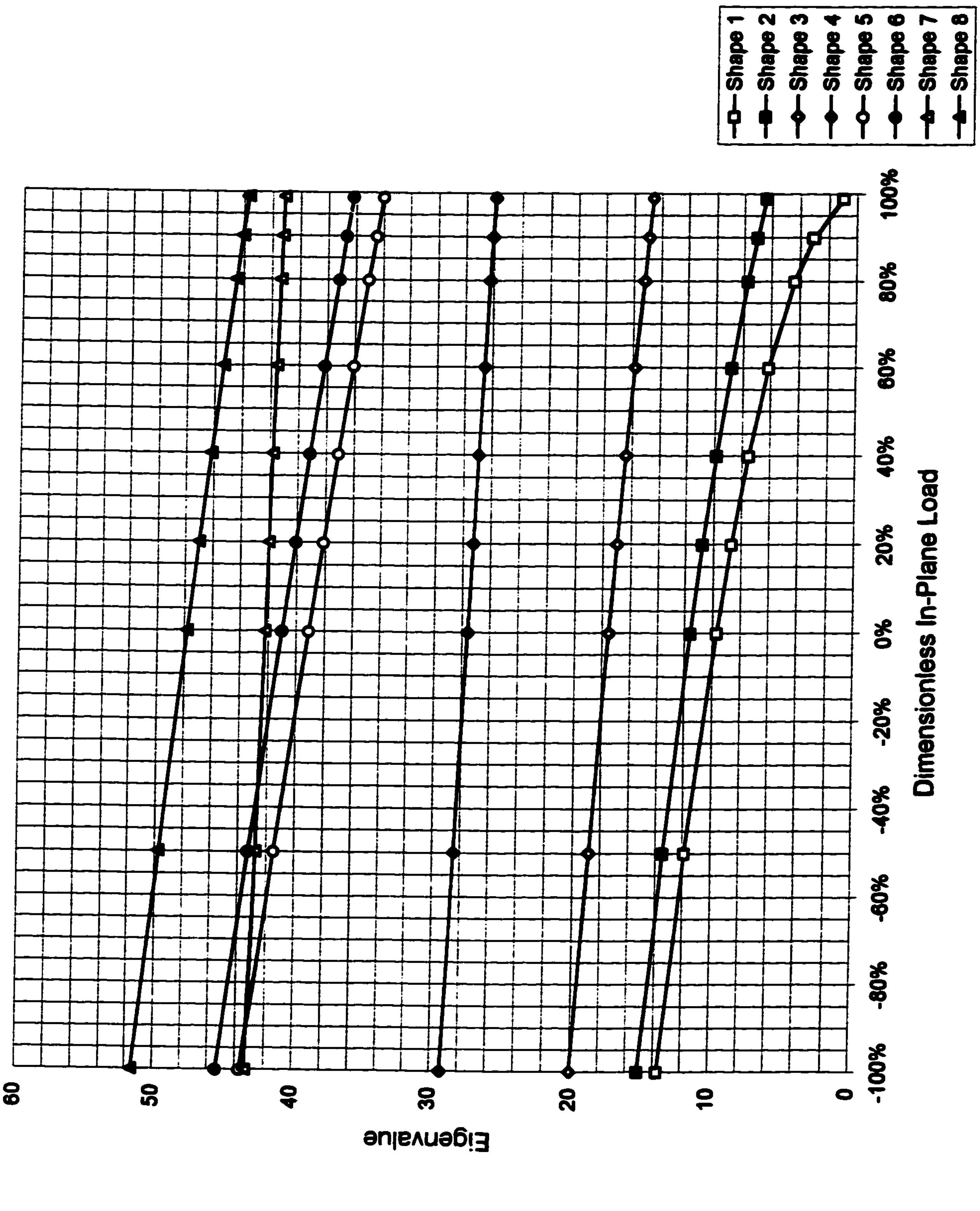

Figure 4.41 Mode shapes, SFSF plate, $\phi = 2 / 1$.

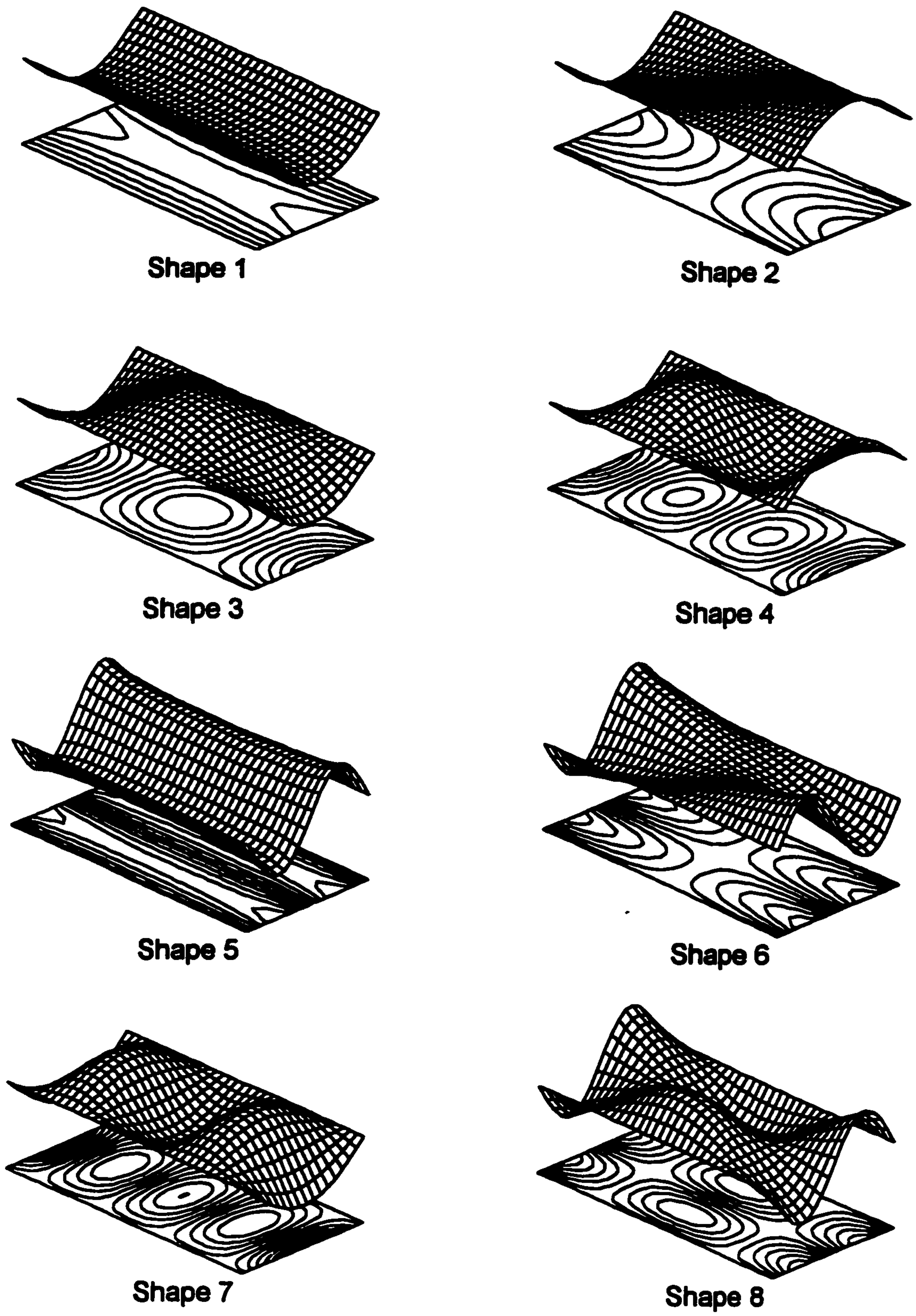

Table 4.27 Eigenvalues, SFSF plate, $\phi = 5 / 2$, $\lambda^2 = \omega a^2 (\rho / D)^{1/2}$.

Mode	In-plane load as a percentage of buckling load								
	-100%	-50%	0%	20%	40%	60%	80%	90%	99%
	Present solution								
1	13.76	11.91	9.73	8.70	7.54	6.15	4.35	3.08	0.97
2	14.65	12.94	10.96	10.06	9.07	7.96	6.66	5.91	5.14
3	17.84	16.46	14.96	14.31	13.63	12.92	12.17	11.77	11.40
4	23.67	22.65	21.58	21.14	20.68	20.22	19.75	19.51	19.29
5	32.53	31.80	31.04	30.74	30.43	30.12	29.80	29.64	29.50
6	43.73	41.51	39.16	38.18	37.18	36.15	35.08	34.54	34.04
7	44.62	42.64	40.36	39.41	38.44	37.44	36.41	35.89	35.41
8	44.80	44.08	43.54	43.33	43.06	42.17	41.27	40.80	40.38
	Finite element solution [18]								
1	13.76	11.92	9.73	8.70	7.54	6.15	4.35	3.08	0.97
2	14.66	12.95	10.97	10.07	9.08	7.97	6.68	5.93	5.16
3	17.85	16.47	14.96	14.32	13.64	12.93	12.17	11.78	11.41
4	23.66	22.64	21.57	21.12	20.67	20.21	19.73	19.49	19.27
5	32.49	31.75	30.99	30.69	30.38	30.06	29.75	29.59	29.44
6	43.74	41.52	39.17	38.19	37.19	36.15	35.09	34.55	34.05
7	44.53	42.69	40.41	39.46	38.49	37.50	36.47	35.95	35.47
8	44.86	43.99	43.45	43.23	43.01	42.21	41.30	40.84	40.42
	Percent difference								
1	0.03%	0.03%	0.03%	0.03%	0.03%	0.03%	0.03%	0.04%	0.03%
2	0.07%	0.08%	0.10%	0.11%	0.13%	0.16%	0.21%	0.26%	0.33%
3	0.04%	0.05%	0.05%	0.06%	0.06%	0.06%	0.06%	0.06%	0.06%
4	-0.04%	-0.05%	-0.06%	-0.06%	-0.07%	-0.07%	-0.08%	-0.08%	-0.08%
5	-0.14%	-0.15%	-0.16%	-0.16%	-0.17%	-0.17%	-0.18%	-0.18%	-0.18%
6	0.02%	0.02%	0.02%	0.02%	0.02%	0.02%	0.02%	0.02%	0.02%
7	-0.20%	0.13%	0.14%	0.14%	0.15%	0.15%	0.16%	0.16%	0.17%
8	0.12%	-0.20%	-0.21%	-0.21%	-0.11%	0.09%	0.09%	0.09%	0.10%

Figure 4.42 Eigenvalue curves, SFSF plate, $\phi = 5 / 2$,
$P_{\xi} = - N_x b^2 / D$, $\lambda^2 = \omega a^2 (\rho / D)^{1/2}$.

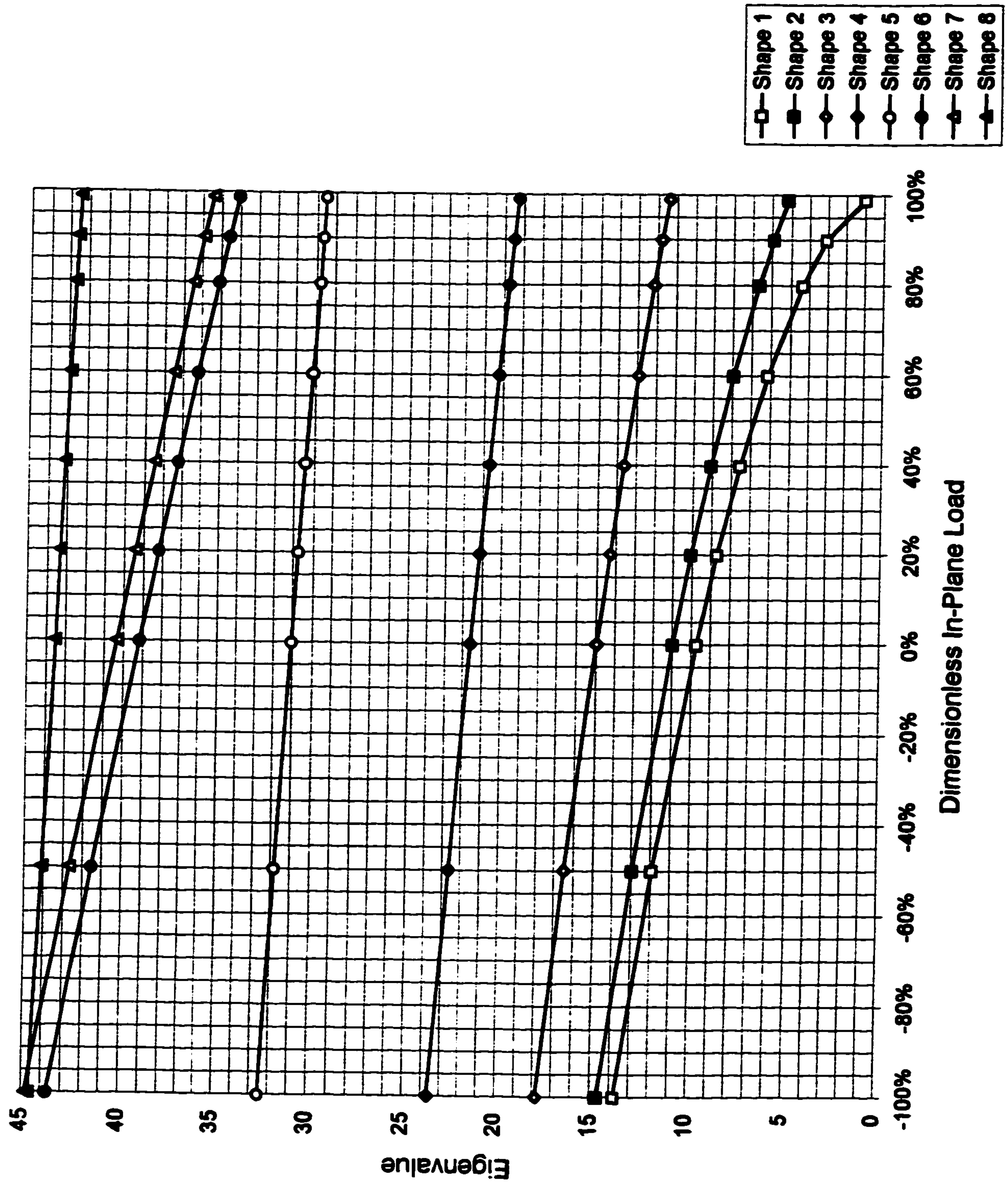

Figure 4.43 Mode shapes, SFSF plate, $\phi = 5 / 2$.

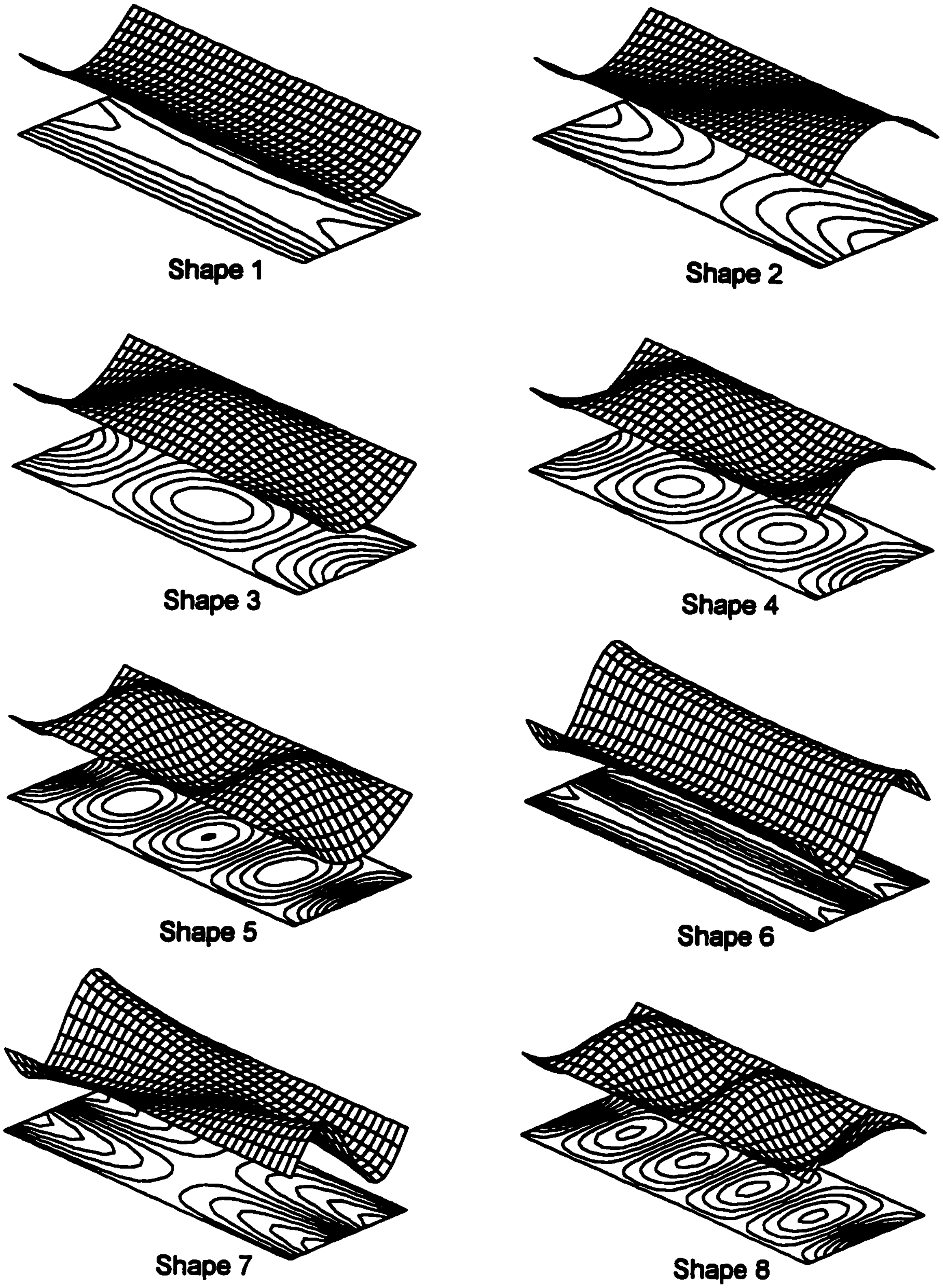

Table 4.28 Eigenvalues, SFSF plate, $\phi = 3 / 1$, $\lambda^2 = \omega a^2 (\rho / D)^{1/2}$.

Mode	In-plane load as a percentage of buckling load -100%	-50%	0%	20%	40%	60%	80%	90%	99%
	Present solution								
1	13.79	11.94	9.75	8.72	7.55	6.17	4.36	3.08	0.97
2	14.41	12.65	10.61	9.67	8.63	7.45	6.04	5.20	4.30
3	16.63	15.14	13.48	12.75	11.99	11.16	10.28	9.81	9.36
4	20.65	19.46	18.20	17.67	17.12	16.56	15.97	15.67	15.40
5	26.71	25.80	24.86	24.48	24.09	23.69	23.28	23.08	22.89
6	34.97	34.29	33.59	33.30	33.02	32.73	32.43	32.29	32.16
7	43.79	41.56	39.21	38.22	37.22	36.18	35.11	34.57	34.07
8	44.51	42.32	40.01	39.05	38.06	37.05	36.01	35.47	34.99
	Finite element solution [18]								
1	13.79	11.95	9.75	8.72	7.55	6.17	4.36	3.08	0.98
2	14.42	12.66	10.62	9.68	8.65	7.47	6.06	5.22	4.32
3	16.64	15.15	13.49	12.76	12.00	11.17	10.29	9.81	9.37
4	20.64	19.45	18.19	17.66	17.11	16.55	15.96	15.66	15.38
5	26.66	25.76	24.81	24.43	24.04	23.64	23.23	23.03	22.84
6	34.88	34.19	33.49	33.20	32.92	32.63	32.33	32.18	32.05
7	43.80	41.57	39.22	38.24	37.23	36.19	35.13	34.58	34.08
8	44.57	42.38	40.07	39.11	38.13	37.12	36.08	35.55	35.06
	Percent difference								
1	0.04%	0.05%	0.04%	0.04%	0.04%	0.04%	0.05%	0.04%	0.05%
2	0.08%	0.09%	0.12%	0.13%	0.16%	0.19%	0.27%	0.35%	0.49%
3	0.06%	0.06%	0.07%	0.07%	0.08%	0.08%	0.08%	0.09%	0.09%
4	-0.03%	-0.04%	-0.05%	-0.06%	-0.06%	-0.07%	-0.08%	-0.09%	-0.09%
5	-0.16%	-0.18%	-0.19%	-0.20%	-0.21%	-0.22%	-0.22%	-0.23%	-0.24%
6	-0.27%	-0.28%	-0.29%	-0.30%	-0.30%	-0.31%	-0.32%	-0.32%	-0.32%
7	0.04%	0.04%	0.04%	0.04%	0.04%	0.04%	0.04%	0.04%	0.04%
8	0.15%	0.16%	0.17%	0.17%	0.18%	0.19%	0.20%	0.20%	0.21%

Figure 4.44 Eigenvalue curves, SFSF plate, $\phi = 3 / 1$,
$P_\xi = - N_x b^2 / D$, $\lambda^2 = \omega a^2 (\rho / D)^{1/2}$.

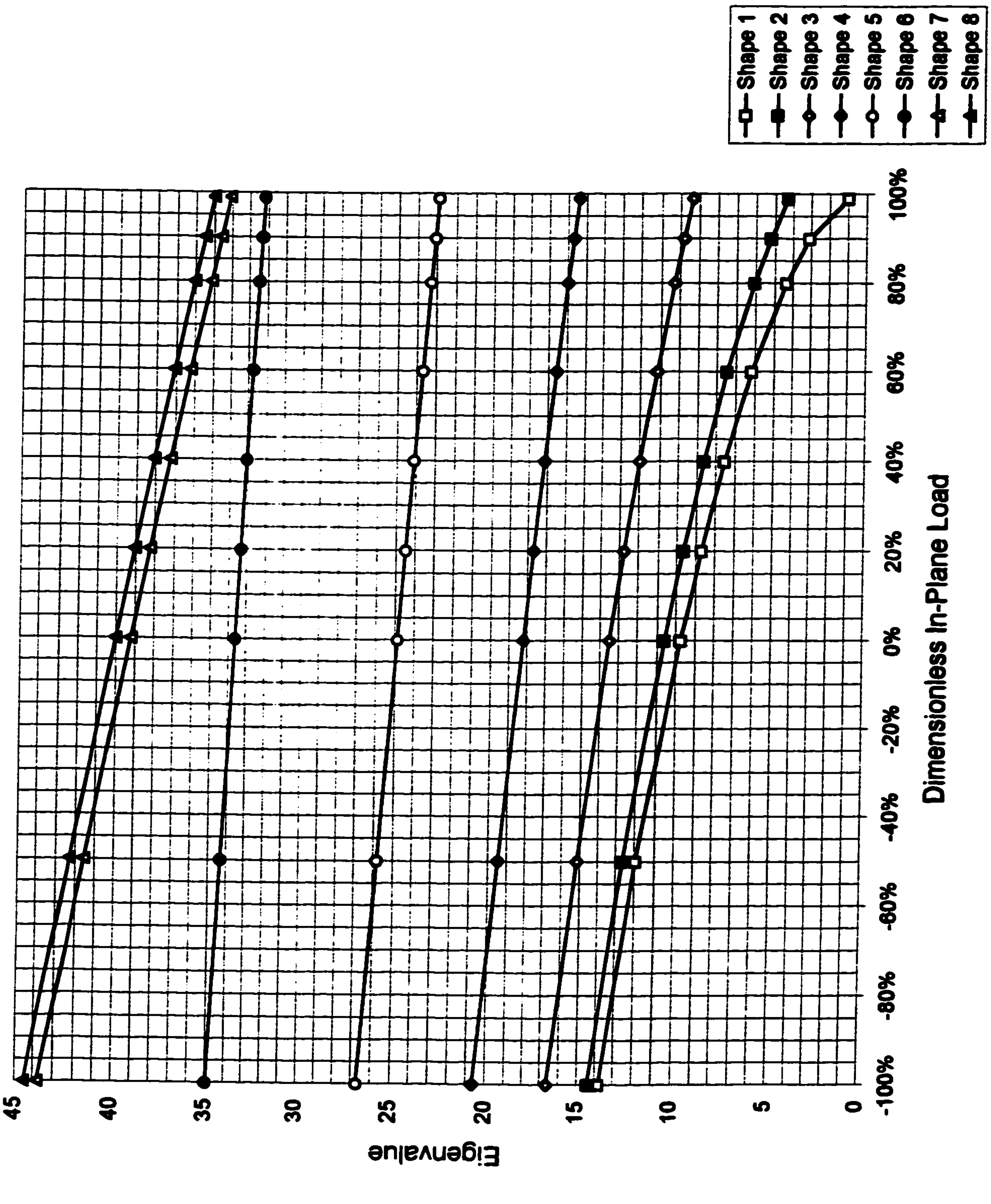

Figure 4.45 Mode shapes, SFSF plate, ϕ = 3 / 1.

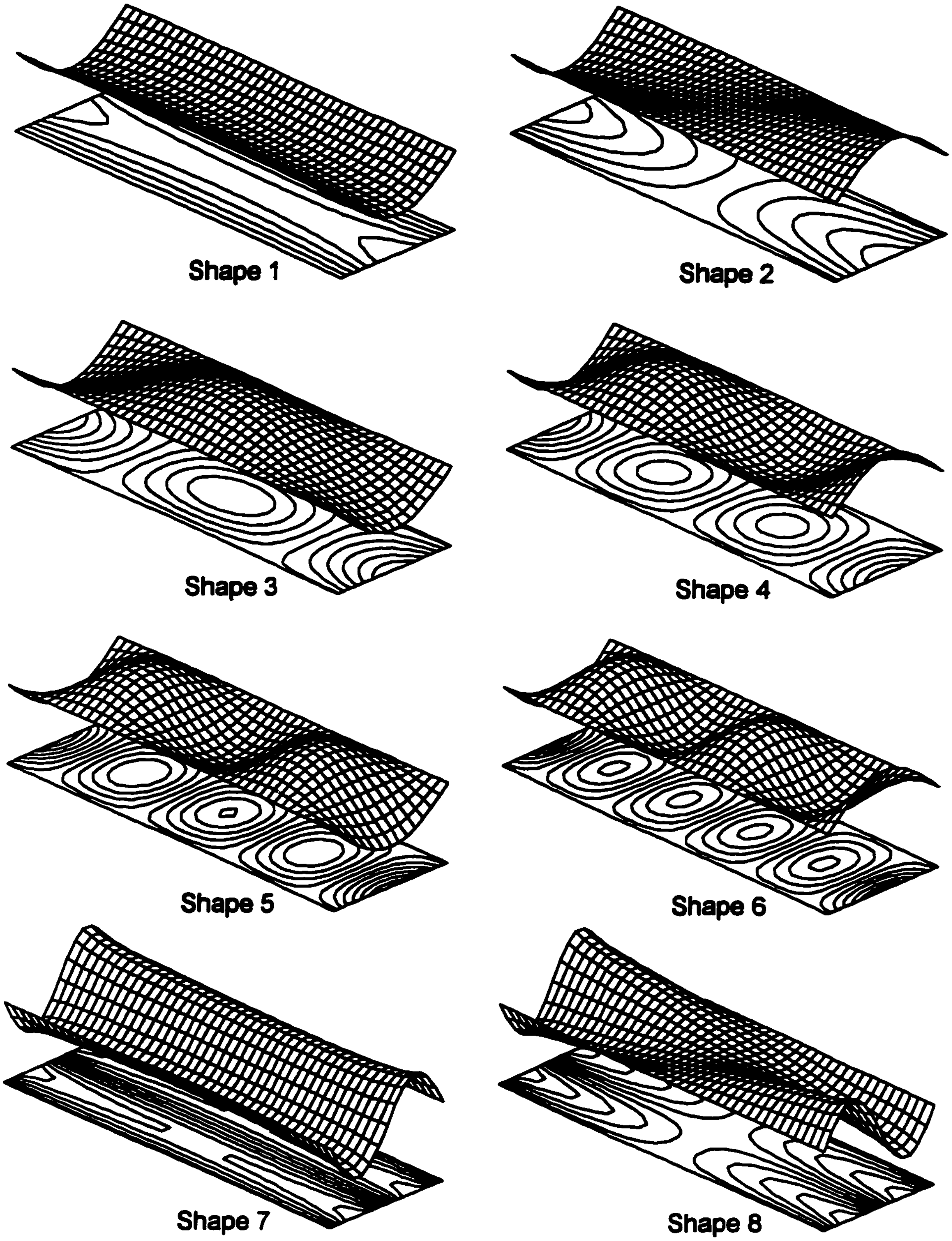

Table 4.29 Eigenvalues, SFCF plate, $\phi = 1/3$, $\lambda^2 = \omega a^2 (\rho / D)^{1/2}$.

Mode	In-plane load as a percentage of buckling load								
	-100%	-50%	0%	20%	40%	60%	80%	90%	99%
	Present solution								
1	20.83	18.11	14.87	13.33	11.57	9.48	6.72	4.76	1.51
2	44.71	43.60	42.45	41.98	41.50	41.02	40.53	40.26	39.36
3	56.07	52.38	48.40	46.72	44.97	43.15	41.25	40.29	40.06
4	96.51	94.46	92.37	91.52	90.66	89.79	88.91	88.47	88.07
5	109.88	105.81	101.57	99.83	98.05	96.25	94.40	93.47	92.62
6	160.61	157.88	155.09	153.97	152.83	151.69	150.53	149.95	149.43
7	183.08	178.83	174.47	172.70	170.91	169.10	167.26	166.34	165.51
8	219.03	218.81	218.59	218.50	218.41	218.33	218.24	218.19	218.16
	Finite element solution [18]								
1	20.85	18.13	14.88	13.34	11.58	9.48	6.73	4.77	1.51
2	44.71	43.59	42.44	41.97	41.49	41.01	40.52	40.28	39.45
3	56.16	52.47	48.50	46.81	45.06	43.24	41.34	40.36	40.05
4	96.50	94.45	92.35	91.50	90.64	89.77	88.89	88.44	88.04
5	110.21	106.14	101.92	100.17	98.40	96.60	94.76	93.82	92.98
6	160.66	157.92	155.13	154.01	152.87	151.72	150.57	149.98	149.46
7	183.94	179.70	175.35	173.59	171.79	169.99	168.17	167.25	166.41
8	218.86	218.64	218.42	218.34	218.25	218.16	218.07	218.03	217.99
	Percent difference								
1	0.09%	0.09%	0.08%	0.08%	0.08%	0.08%	0.08%	0.07%	0.00%
2	-0.01%	-0.01%	-0.02%	-0.02%	-0.02%	-0.03%	-0.03%	0.03%	0.25%
3	0.17%	0.18%	0.19%	0.20%	0.21%	0.22%	0.23%	0.18%	-0.03%
4	-0.01%	-0.01%	-0.02%	-0.02%	-0.02%	-0.02%	-0.02%	-0.03%	-0.03%
5	0.30%	0.32%	0.34%	0.34%	0.35%	0.36%	0.37%	0.38%	0.38%
6	0.03%	0.03%	0.02%	0.03%	0.03%	0.02%	0.02%	0.02%	0.02%
7	0.47%	0.49%	0.50%	0.51%	0.52%	0.53%	0.54%	0.55%	0.55%
8	-0.08%	-0.08%	-0.08%	-0.07%	-0.07%	-0.08%	-0.08%	-0.07%	-0.07%

Figure 4.46 Eigenvalue curves, SFCF plate, $\phi = 1 / 3$,
$P_\xi = - N_x b^2 / D$, $\lambda^2 = \omega a^2 (\rho / D)^{1/2}$.

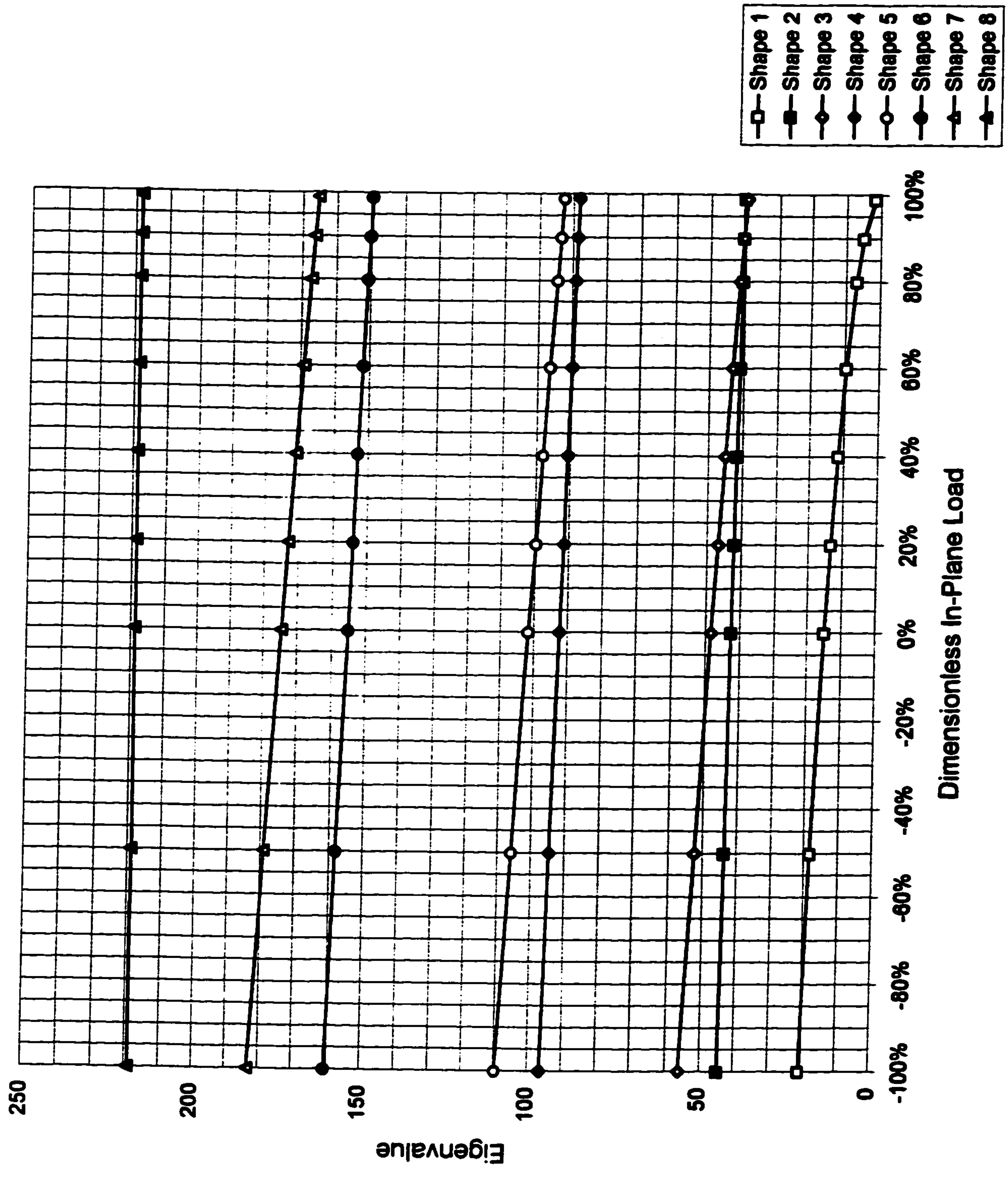

Figure 4.47 Mode shapes, SFCF plate, $\phi = 1 / 3$.

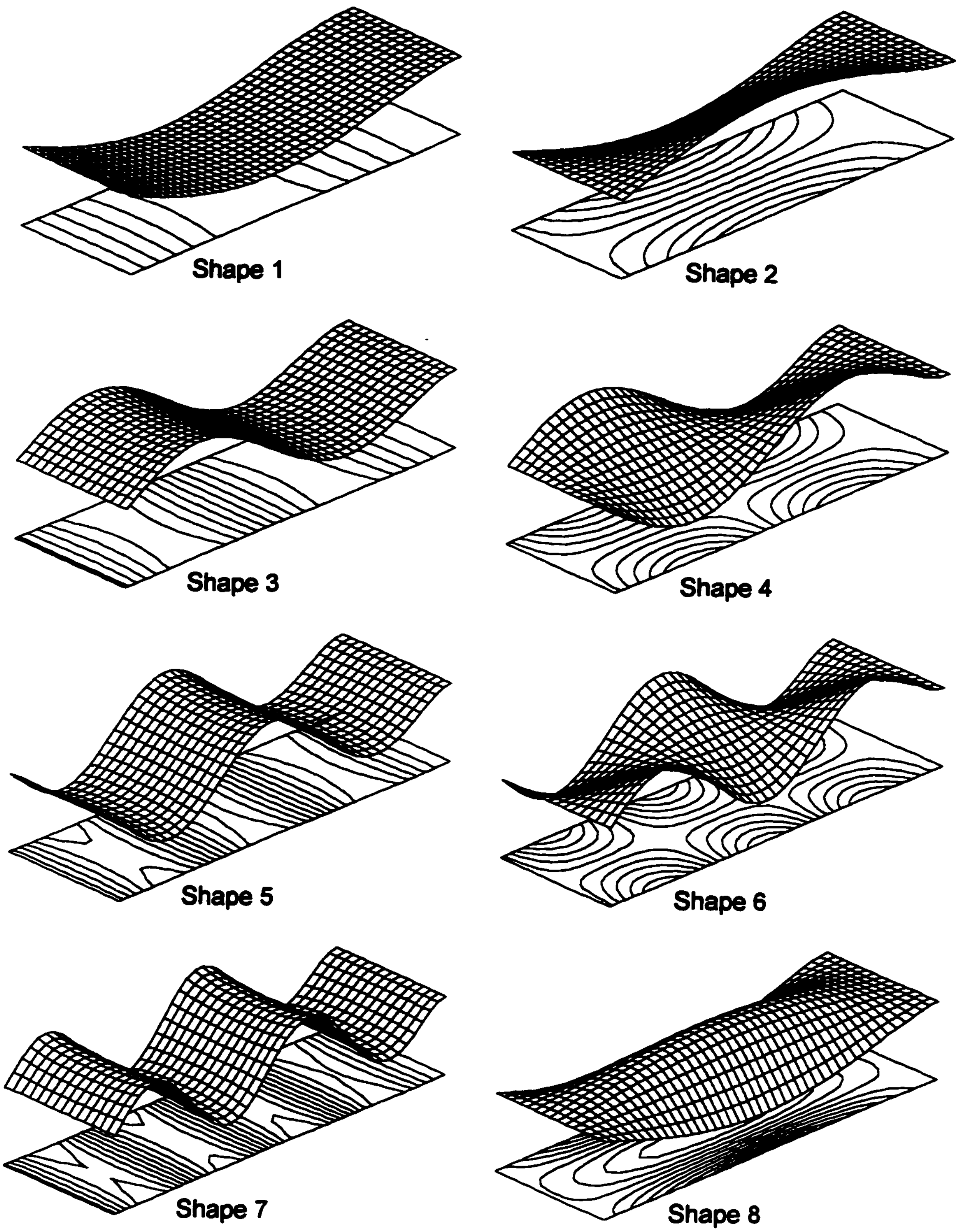

Table 4.30 Eigenvalues, SFCF plate, $\phi = 2 / 5$, $\lambda^2 = \omega a^2 (\rho / D)^{1/2}$.

Mode	In-plane load as a percentage of buckling load								
	-100%	-50%	0%	20%	40%	60%	80%	90%	99%
	Present solution								
1	20.89	18.17	14.91	13.37	11.61	9.50	6.74	4.77	1.51
2	39.15	37.85	36.50	35.94	35.38	34.80	34.21	33.92	33.65
3	56.26	52.56	48.58	46.89	45.13	43.31	41.40	40.42	39.51
4	86.44	84.12	81.74	80.76	79.77	78.77	77.76	77.24	76.78
5	110.25	106.17	101.93	100.18	98.40	96.59	94.74	93.80	92.95
6	147.33	144.32	141.24	139.99	138.73	137.45	136.17	135.52	134.94
7	157.75	157.44	157.13	157.01	156.89	156.76	156.64	156.58	156.52
8	183.65	179.38	175.01	173.23	171.43	169.62	167.78	166.85	166.02
	Finite element solution [18]								
1	20.91	18.18	14.92	13.38	11.61	9.51	6.75	4.78	1.51
2	39.16	37.85	36.50	35.94	35.37	34.80	34.21	33.91	33.64
3	56.35	52.65	48.66	46.97	45.22	43.39	41.49	40.50	39.60
4	86.46	84.14	81.75	80.78	79.79	78.78	77.76	77.25	76.79
5	110.55	106.48	102.24	100.48	98.71	96.90	95.05	94.12	93.27
6	147.45	144.44	141.36	140.10	138.84	137.57	136.28	135.63	135.04
7	157.65	157.34	157.02	156.91	156.78	156.66	156.53	156.47	156.42
8	184.42	180.16	175.80	174.02	172.23	170.42	168.59	167.66	166.83
	Percent difference								
1	0.08%	0.08%	0.08%	0.08%	0.08%	0.07%	0.08%	0.08%	0.15%
2	0.01%	0.00%	0.00%	-0.01%	-0.01%	-0.01%	-0.01%	-0.02%	-0.02%
3	0.15%	0.16%	0.18%	0.18%	0.19%	0.20%	0.21%	0.22%	0.22%
4	0.03%	0.02%	0.02%	0.02%	0.02%	0.01%	0.01%	0.01%	0.01%
5	0.27%	0.29%	0.30%	0.31%	0.32%	0.32%	0.33%	0.34%	0.34%
6	0.08%	0.08%	0.08%	0.08%	0.08%	0.08%	0.08%	0.08%	0.08%
7	-0.06%	-0.07%	-0.07%	-0.07%	-0.07%	-0.07%	-0.07%	-0.07%	-0.07%
8	0.42%	0.43%	0.45%	0.46%	0.46%	0.47%	0.48%	0.48%	0.49%

Figure 4.48 Eigenvalue curves, SFCF plate, $\phi = 2 / 5$,
$P_\xi = - N_x b^2 / D$, $\lambda^2 = \omega a^2 (\rho / D)^{1/2}$.

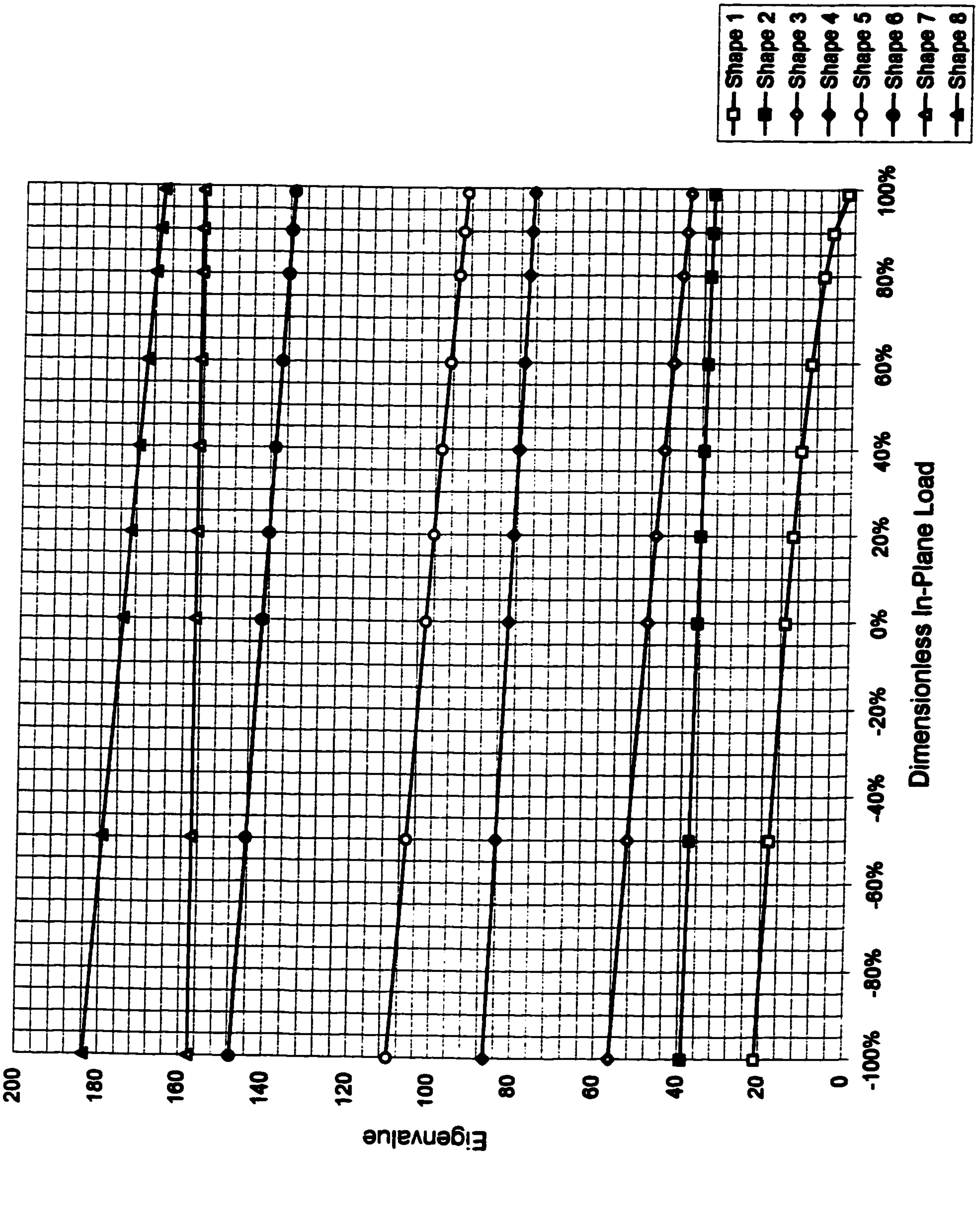

Figure 4.49 Mode shapes, SFCF plate, $\phi = 2 / 5$.

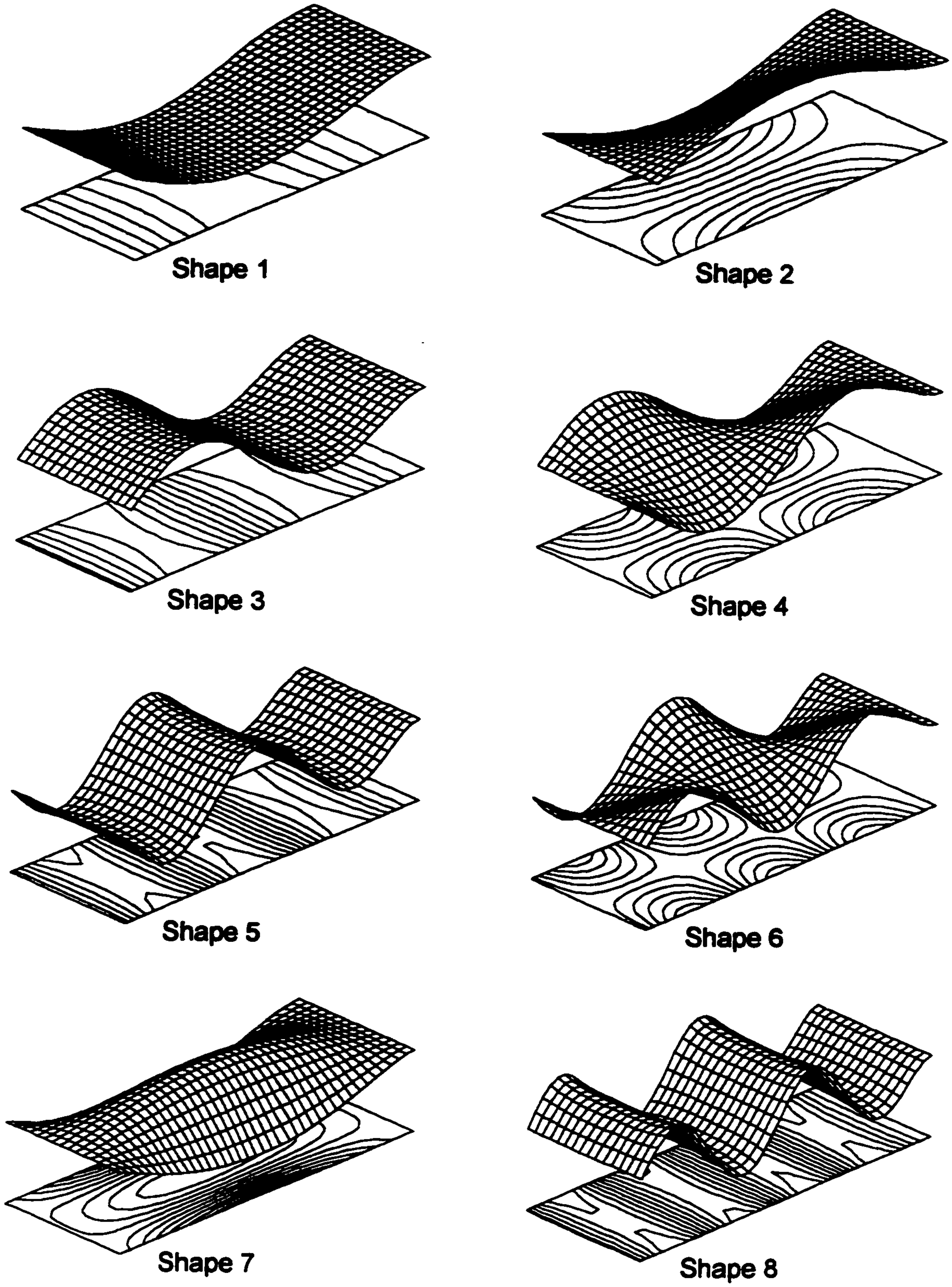

Table 4.31 Eigenvalues, SFCF plate, $\phi = 1 / 2$, $\lambda^2 = \omega a^2 (\rho / D)^{1/2}$.

Mode	In-plane load as a percentage of buckling load								
	-100%	-50%	0%	20%	40%	60%	80%	90%	99%
					Present solution				
1	20.96	18.23	14.96	13.41	11.65	9.54	6.77	4.79	1.52
2	33.89	32.34	30.71	30.04	29.34	28.63	27.89	27.52	27.18
3	56.50	52.78	48.78	47.09	45.33	43.49	41.58	40.59	39.68
4	77.21	74.57	71.83	70.70	69.55	68.38	67.20	66.59	66.05
5	107.76	106.56	102.31	100.56	98.77	96.95	95.10	94.16	93.30
6	110.68	107.32	106.85	106.66	106.48	106.29	106.11	106.01	105.93
7	135.51	132.20	128.79	127.41	126.01	124.59	123.15	122.43	121.78
8	153.89	152.61	151.32	150.80	150.28	149.76	149.23	148.97	148.73
					Finite element solution [18]				
1	20.98	18.25	14.97	13.42	11.66	9.54	6.77	4.79	1.52
2	33.90	32.35	30.72	30.04	29.34	28.63	27.89	27.52	27.17
3	56.57	52.86	48.86	47.16	45.40	43.57	41.66	40.67	39.76
4	77.26	74.61	71.87	70.74	69.59	68.42	67.23	66.63	66.08
5	107.71	106.80	102.57	100.82	99.03	97.22	95.36	94.42	93.57
6	110.93	107.28	106.79	106.61	106.42	106.24	106.05	105.96	105.87
7	135.69	132.38	128.97	127.59	126.18	124.77	123.33	122.61	121.95
8	153.75	152.47	151.18	150.65	150.13	149.60	149.08	148.82	148.58
					Percent difference				
1	0.07%	0.07%	0.07%	0.07%	0.07%	0.07%	0.06%	0.06%	0.02%
2	0.03%	0.02%	0.01%	0.01%	0.01%	0.01%	0.00%	0.00%	0.00%
3	0.13%	0.14%	0.15%	0.16%	0.16%	0.17%	0.18%	0.18%	0.19%
4	0.06%	0.06%	0.06%	0.05%	0.05%	0.05%	0.05%	0.05%	0.05%
5	-0.05%	0.22%	0.25%	0.26%	0.27%	0.27%	0.28%	0.28%	0.29%
6	0.23%	-0.04%	-0.05%	-0.05%	-0.05%	-0.05%	-0.05%	-0.05%	-0.05%
7	0.13%	0.14%	0.14%	0.14%	0.14%	0.14%	0.14%	0.15%	0.15%
8	-0.09%	-0.09%	-0.10%	-0.10%	-0.10%	-0.10%	-0.10%	-0.10%	-0.10%

Figure 4.50 Eigenvalue curves, SFCF plate, $\phi = 1 / 2$,

$P_\xi = - N_x b^2 / D$, $\lambda^2 = \omega a^2 (\rho / D)^{1/2}$.

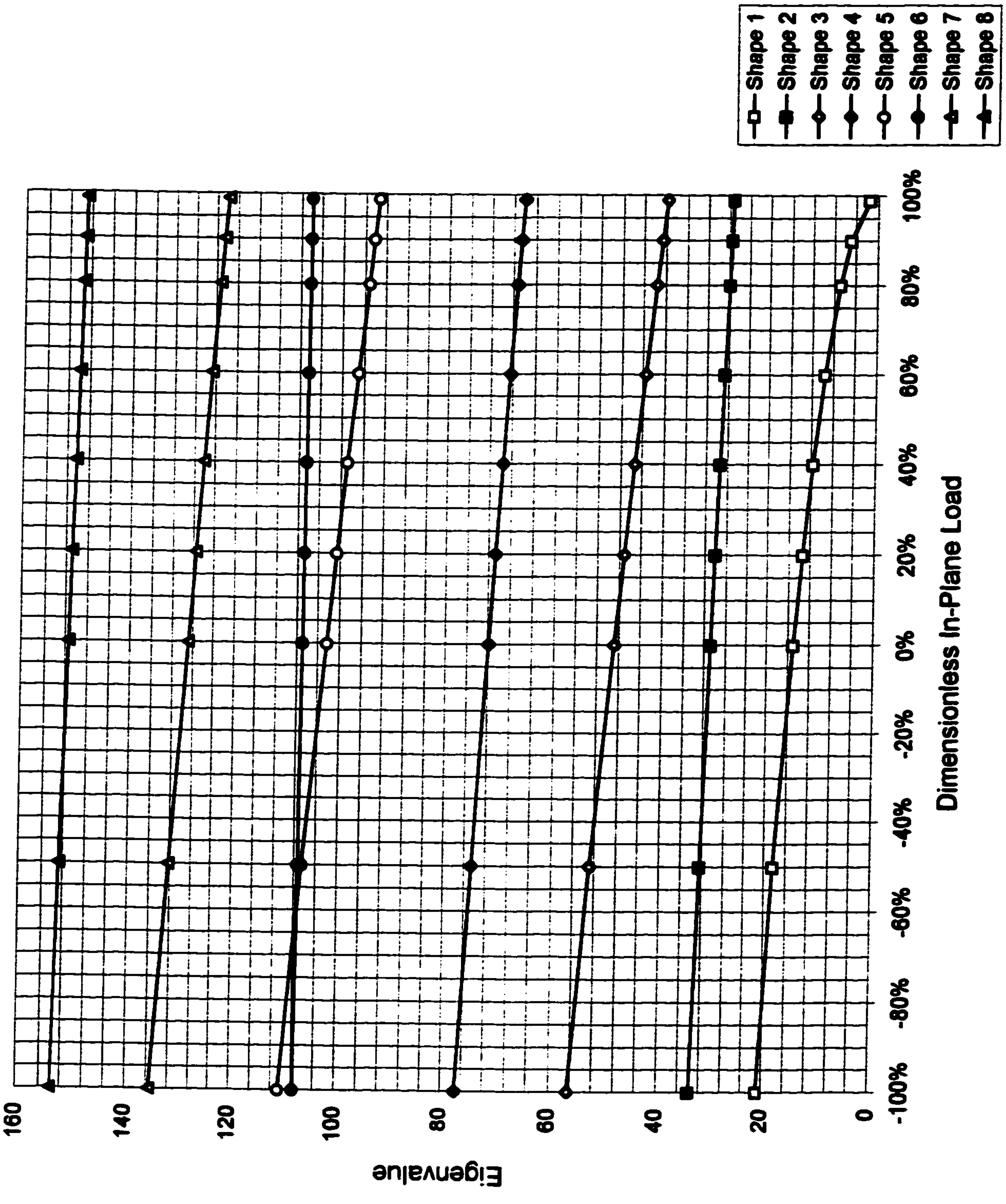

Figure 4.51 Mode shapes, SFCF plate, $\phi = 1 / 2$.

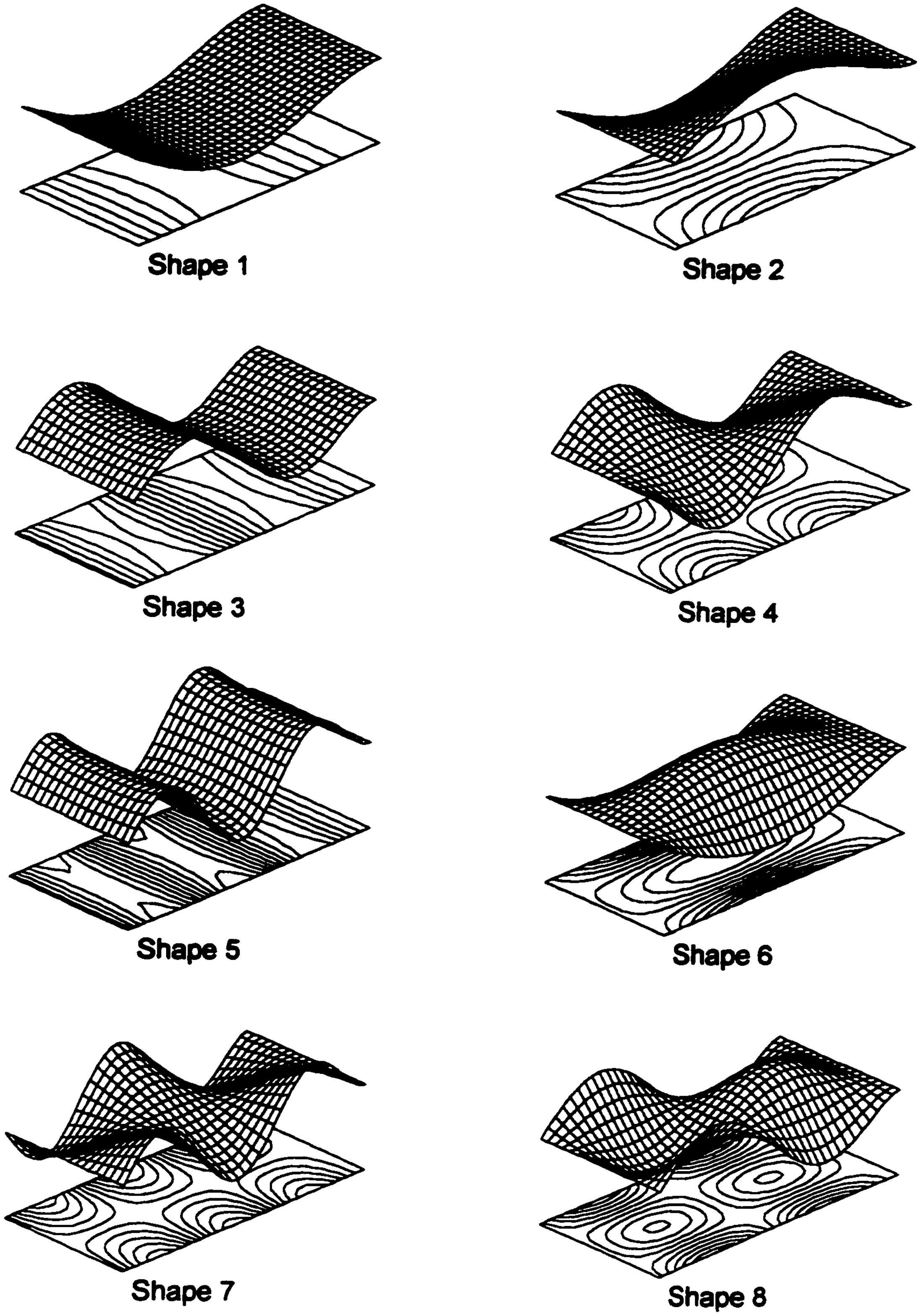

Table 4.32 Eigenvalues, SFCF plate, $\phi = 2 / 3$, $\lambda^2 = \omega a^2 (\rho / D)^{1/2}$.

Mode	In-plane load as a percentage of buckling load								
	-100%	-50%	0%	20%	40%	60%	80%	90%	99%
				Present solution					
1	21.07	18.32	15.03	13.48	11.70	9.58	6.80	4.81	1.53
2	29.10	27.24	25.23	24.38	23.49	22.56	21.59	21.09	20.63
3	56.78	53.05	49.02	47.32	45.55	43.71	41.79	40.79	39.87
4	69.15	66.17	63.02	61.71	60.37	59.00	57.60	56.88	56.23
5	69.18	68.41	67.67	67.37	67.07	66.77	66.46	66.31	66.17
6	111.15	107.02	102.73	100.97	99.17	97.34	95.47	94.52	93.66
7	113.19	111.41	109.59	108.86	108.12	107.38	106.63	106.25	105.91
8	125.60	121.98	118.24	116.71	115.16	113.59	111.99	111.19	110.45
				Finite element solution [18]					
1	21.08	18.33	15.04	13.49	11.71	9.59	6.80	4.82	1.53
2	29.11	27.25	25.24	24.39	23.50	22.57	21.60	21.10	20.63
3	56.83	53.10	49.08	47.37	45.60	43.76	41.84	40.85	39.93
4	69.13	66.23	63.07	61.77	60.43	59.06	57.65	56.94	56.29
5	69.24	68.39	67.65	67.35	67.05	66.74	66.44	66.28	66.15
6	111.33	107.21	102.92	101.16	99.36	97.53	95.66	94.72	93.86
7	113.15	111.37	109.55	108.82	108.08	107.33	106.58	106.20	105.86
8	125.80	122.18	118.44	116.91	115.36	113.79	112.20	111.39	110.66
				Percent difference					
1	0.06%	0.05%	0.05%	0.05%	0.05%	0.05%	0.05%	0.05%	0.03%
2	0.05%	0.04%	0.04%	0.04%	0.03%	0.03%	0.03%	0.03%	0.03%
3	0.10%	0.10%	0.11%	0.11%	0.12%	0.13%	0.13%	0.13%	0.14%
4	-0.03%	0.09%	0.09%	0.09%	0.10%	0.10%	0.10%	0.10%	0.10%
5	0.08%	-0.03%	-0.03%	-0.03%	-0.03%	-0.03%	-0.03%	-0.04%	-0.04%
6	0.16%	0.17%	0.18%	0.19%	0.19%	0.20%	0.20%	0.20%	0.21%
7	-0.03%	-0.03%	-0.04%	-0.04%	-0.04%	-0.04%	-0.04%	-0.05%	-0.04%
8	0.16%	0.16%	0.17%	0.17%	0.18%	0.18%	0.18%	0.19%	0.19%

Figure 4.52 Eigenvalue curves, SFCF plate, $\phi = 2 / 3$,

$P_\xi = - N_x b^2 / D$, $\lambda^2 = \omega a^2 (\rho / D)^{1/2}$.

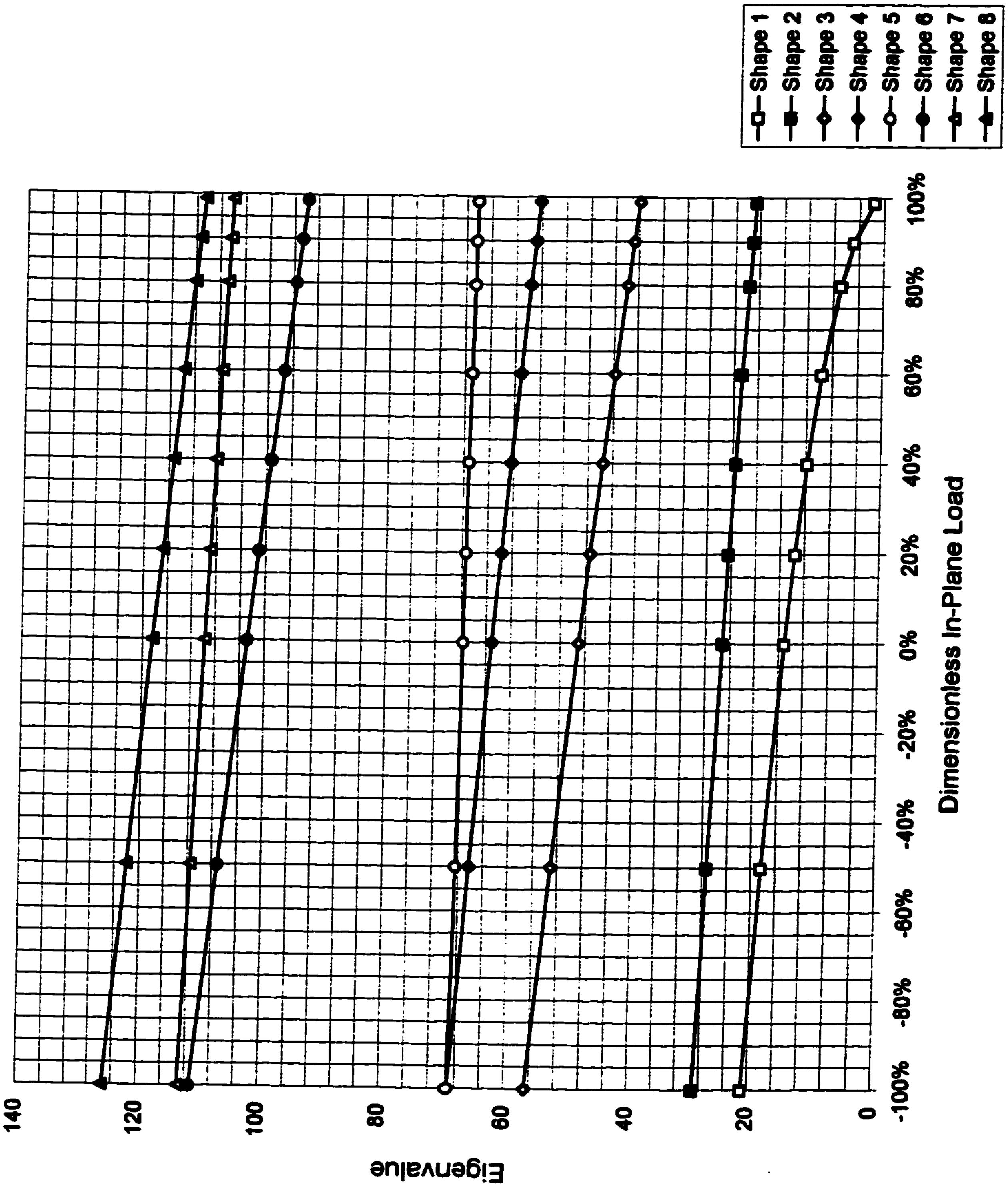

Figure 4.53 Mode shapes, SFCF plate, $\phi = 2 / 3$.

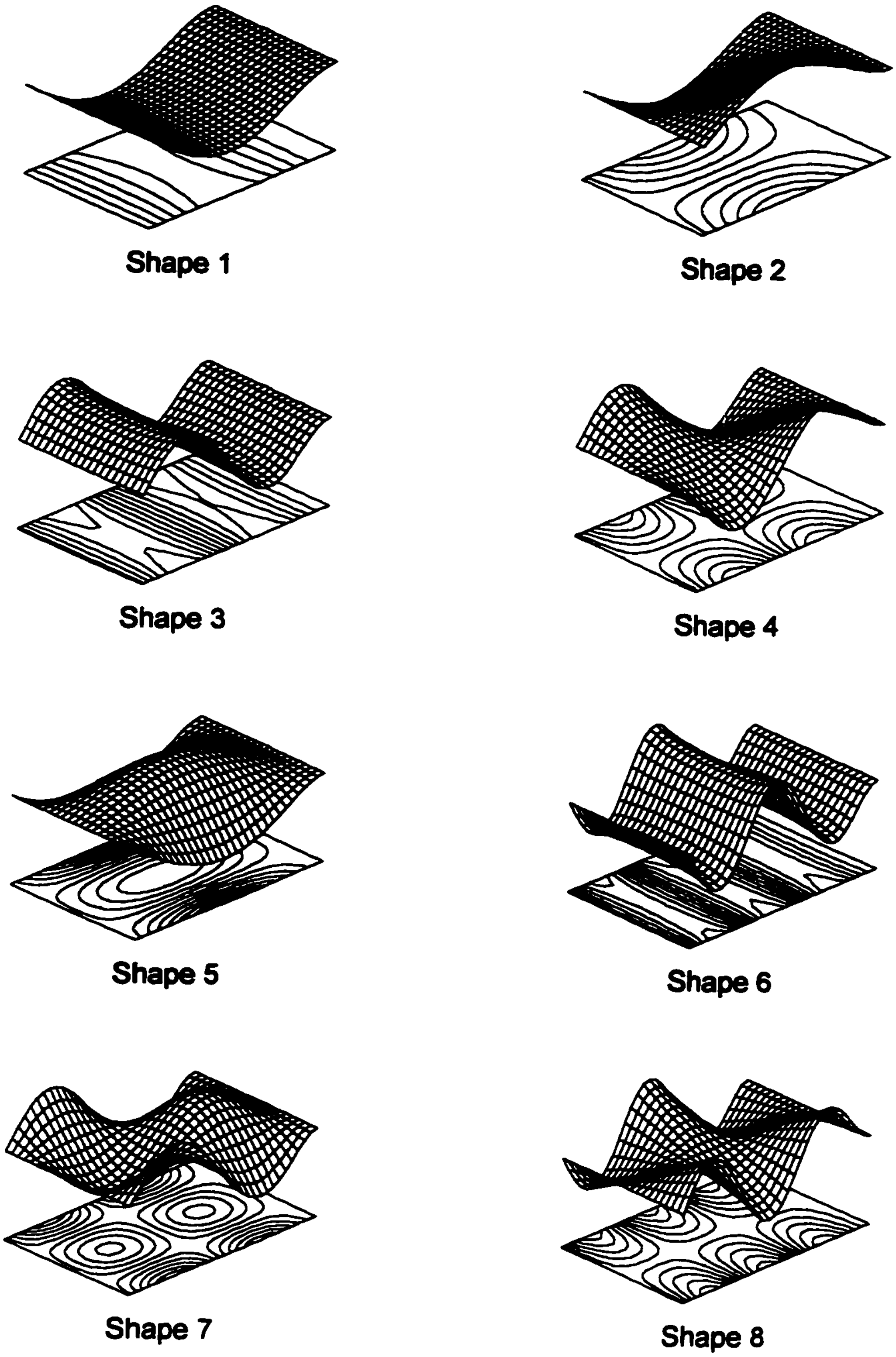

Table 4.33 Eigenvalues, SFCF plate, $\phi = 1 / 1$, $\lambda^2 = \omega a^2 (\rho / D)^{1/2}$.

Mode	In-plane load as a percentage of buckling load								
	-100%	-50%	0%	20%	40%	60%	80%	90%	99%
	Present solution								
1	21.20	18.44	15.13	13.56	11.78	9.64	6.84	4.84	1.53
2	25.11	22.86	20.34	19.24	18.06	16.79	15.40	14.66	13.95
3	42.00	40.73	39.42	38.89	38.34	37.79	37.22	36.94	36.68
4	57.11	53.35	49.30	47.58	45.79	43.94	42.00	40.99	40.07
5	62.87	59.48	55.88	54.38	52.82	51.23	49.57	48.73	47.95
6	78.37	77.71	77.05	76.78	75.83	74.73	73.62	73.06	72.55
7	83.06	80.56	77.97	76.91	76.52	76.25	75.98	75.84	75.72
8	111.67	107.51	103.18	101.39	99.58	97.73	95.84	94.88	94.01
	Finite element solution [18]								
1	21.21	18.44	15.13	13.57	11.78	9.65	6.84	4.85	1.54
2	25.12	22.87	20.36	19.25	18.07	16.80	15.42	14.67	13.97
3	42.00	40.73	39.42	38.89	38.34	37.79	37.22	36.94	36.68
4	57.13	53.37	49.32	47.60	45.82	43.96	42.02	41.02	40.09
5	62.92	59.53	55.94	54.43	52.88	51.28	49.63	48.79	48.01
6	78.33	77.67	77.01	76.74	75.85	74.76	73.65	73.08	72.57
7	83.09	80.58	77.99	76.93	76.48	76.21	75.94	75.80	75.68
8	111.72	107.56	103.24	101.45	99.64	97.79	95.90	94.94	94.08
	Percent difference								
1	0.03%	0.03%	0.03%	0.03%	0.03%	0.03%	0.03%	0.03%	0.05%
2	0.05%	0.05%	0.06%	0.06%	0.07%	0.07%	0.09%	0.09%	0.10%
3	0.00%	0.00%	0.00%	0.00%	0.00%	0.00%	0.00%	-0.01%	-0.01%
4	0.04%	0.04%	0.04%	0.05%	0.05%	0.05%	0.05%	0.05%	0.06%
5	0.08%	0.09%	0.10%	0.10%	0.11%	0.11%	0.12%	0.12%	0.12%
6	-0.05%	-0.05%	-0.05%	-0.05%	0.03%	0.03%	0.03%	0.03%	0.03%
7	0.03%	0.03%	0.03%	0.03%	-0.05%	-0.05%	-0.05%	-0.05%	-0.05%
8	0.05%	0.05%	0.06%	0.06%	0.06%	0.06%	0.06%	0.06%	0.06%

Figure 4.54 Eigenvalue curves, SFCF plate, $\phi = 1 / 1$, $P_\xi = - N_x b^2 / D$, $\lambda^2 = \omega a^2 (\rho / D)^{1/2}$.

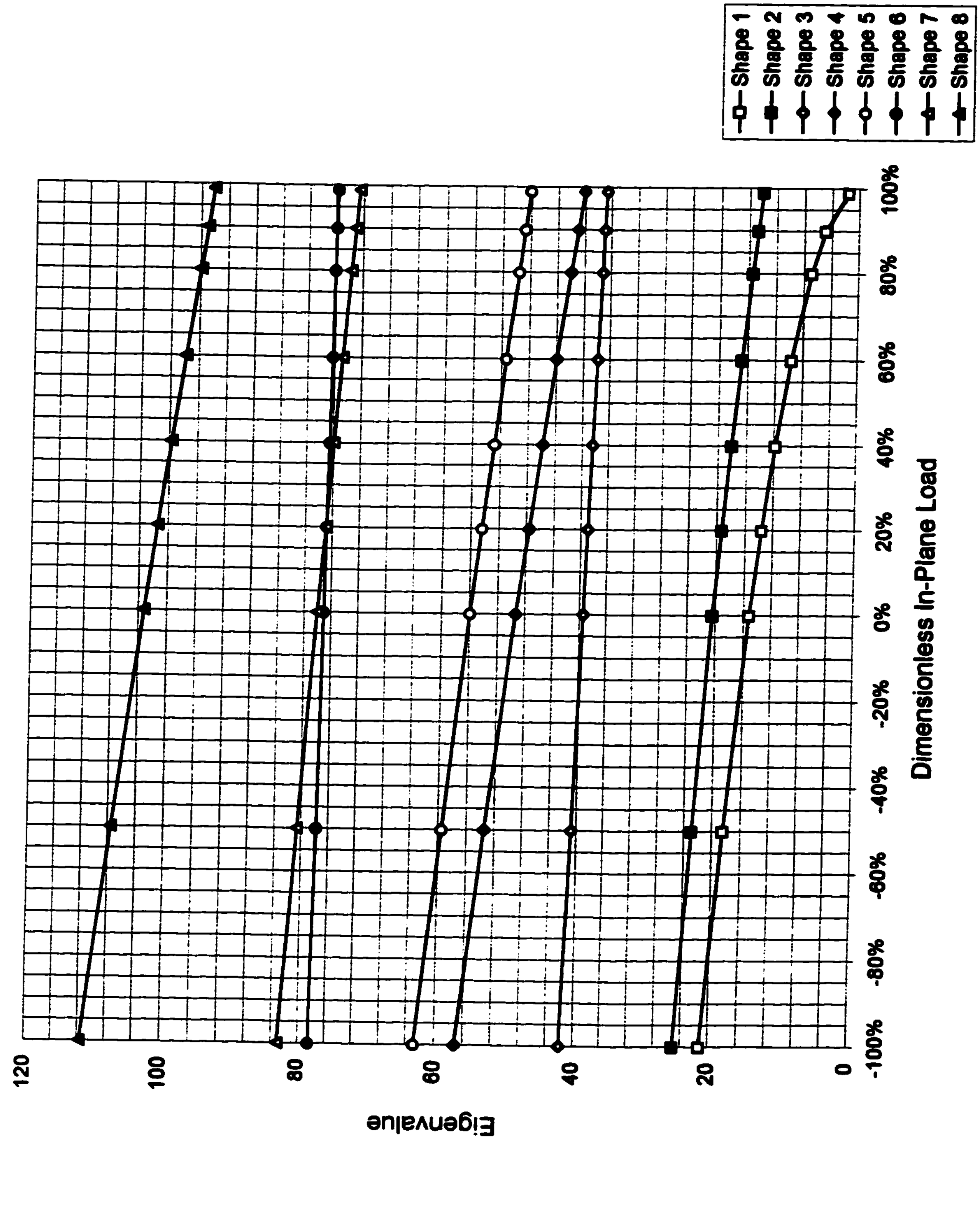

Figure 4.55 Mode shapes, SFCF plate, $\phi = 1 / 1$.

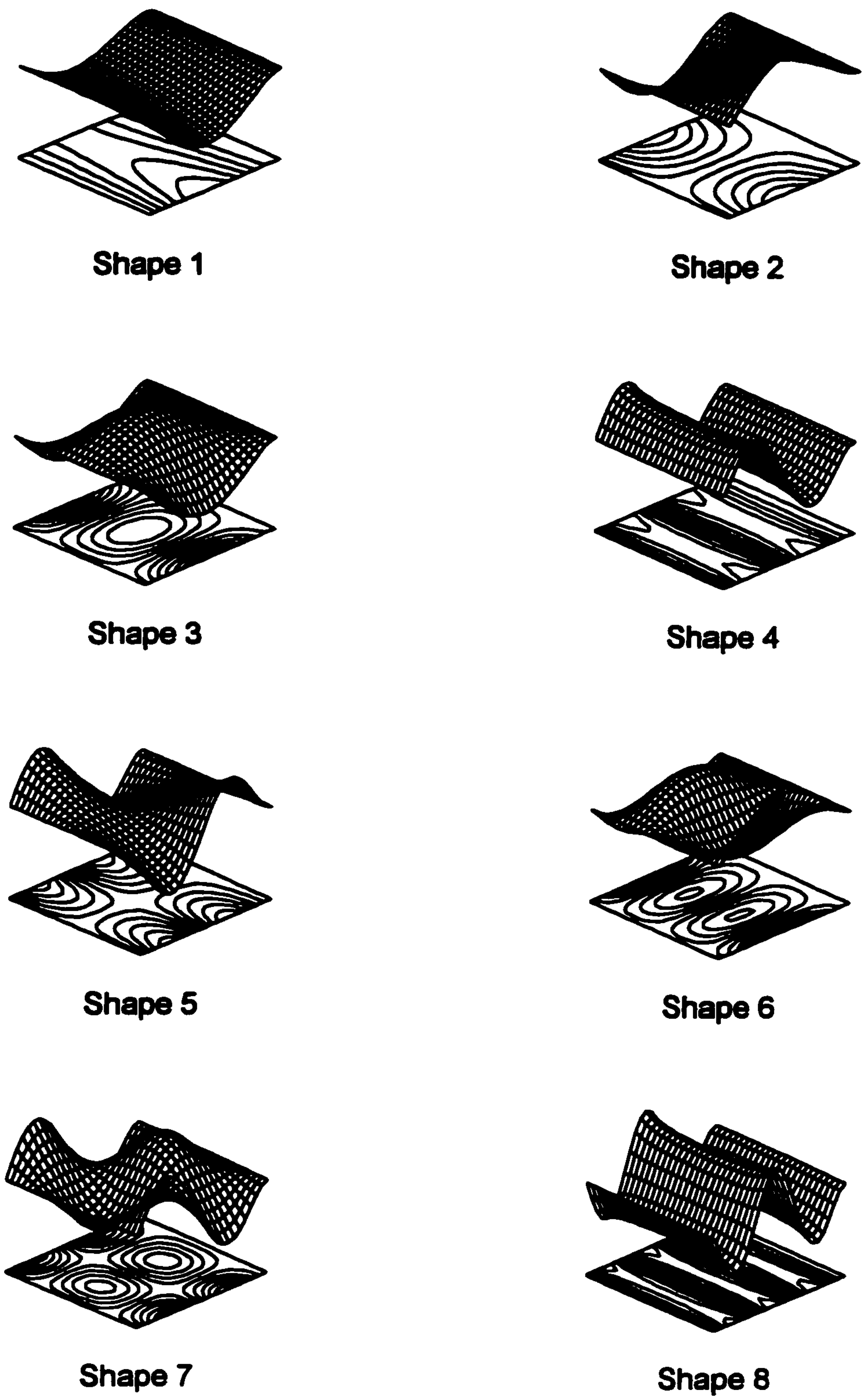

Table 4.34 Eigenvalues, SFCF plate, $\phi = 3/2$, $\lambda^2 = \omega a^2 (\rho / D)^{1/2}$.

Mode	In-plane load as a percentage of buckling load								
	-100%	-50%	0%	20%	40%	60%	80%	90%	99%
	Present solution								
1	21.31	18.54	15.21	13.64	11.84	9.69	6.88	4.87	1.54
2	23.12	20.61	17.71	16.40	14.96	13.35	11.51	10.46	9.41
3	30.29	28.46	26.49	25.65	24.78	23.88	22.94	22.45	22.00
4	45.33	44.15	42.93	42.43	41.93	41.42	40.90	40.64	40.19
5	57.36	53.57	49.49	47.76	45.96	44.09	42.14	41.13	40.40
6	59.92	56.31	52.44	50.81	49.13	47.38	45.57	44.64	43.78
7	69.10	66.03	62.78	61.43	60.05	58.64	57.19	56.45	55.78
8	69.69	68.92	68.16	67.85	67.54	67.23	66.92	66.77	66.62
	Finite element solution [18]								
1	21.31	18.54	15.21	13.64	11.84	9.69	6.88	4.87	1.54
2	23.13	20.62	17.73	16.41	14.97	13.37	11.53	10.48	9.43
3	30.30	28.46	26.49	25.66	24.79	23.89	22.95	22.46	22.01
4	45.31	44.13	42.91	42.42	41.91	41.40	40.88	40.62	40.18
5	57.35	53.56	49.48	47.75	45.95	44.08	42.12	41.11	40.38
6	59.94	56.34	52.48	50.85	49.16	47.42	45.61	44.68	43.82
7	69.12	66.04	62.80	61.45	60.07	58.66	57.21	56.48	55.80
8	69.64	68.87	68.11	67.80	67.49	67.18	66.87	66.71	66.57
	Percent difference								
1	0.00%	0.01%	0.01%	0.01%	0.01%	0.01%	0.01%	0.02%	0.08%
2	0.03%	0.04%	0.07%	0.07%	0.10%	0.12%	0.15%	0.19%	0.24%
3	0.02%	0.02%	0.02%	0.02%	0.03%	0.03%	0.03%	0.04%	0.04%
4	-0.04%	-0.04%	-0.04%	-0.04%	-0.04%	-0.04%	-0.04%	-0.04%	-0.03%
5	-0.02%	-0.02%	-0.02%	-0.02%	-0.03%	-0.03%	-0.03%	-0.03%	-0.04%
6	0.04%	0.05%	0.06%	0.07%	0.07%	0.08%	0.09%	0.09%	0.10%
7	0.03%	0.03%	0.03%	0.04%	0.04%	0.04%	0.05%	0.05%	0.05%
8	-0.07%	-0.07%	-0.07%	-0.07%	-0.07%	-0.07%	-0.08%	-0.08%	-0.08%

Figure 4.56 Eigenvalue curves, SFCF plate, $\phi = 3/2$,
$P_\xi = -N_x b^2/D$, $\lambda^2 = \omega a^2 (\rho/D)^{1/2}$.

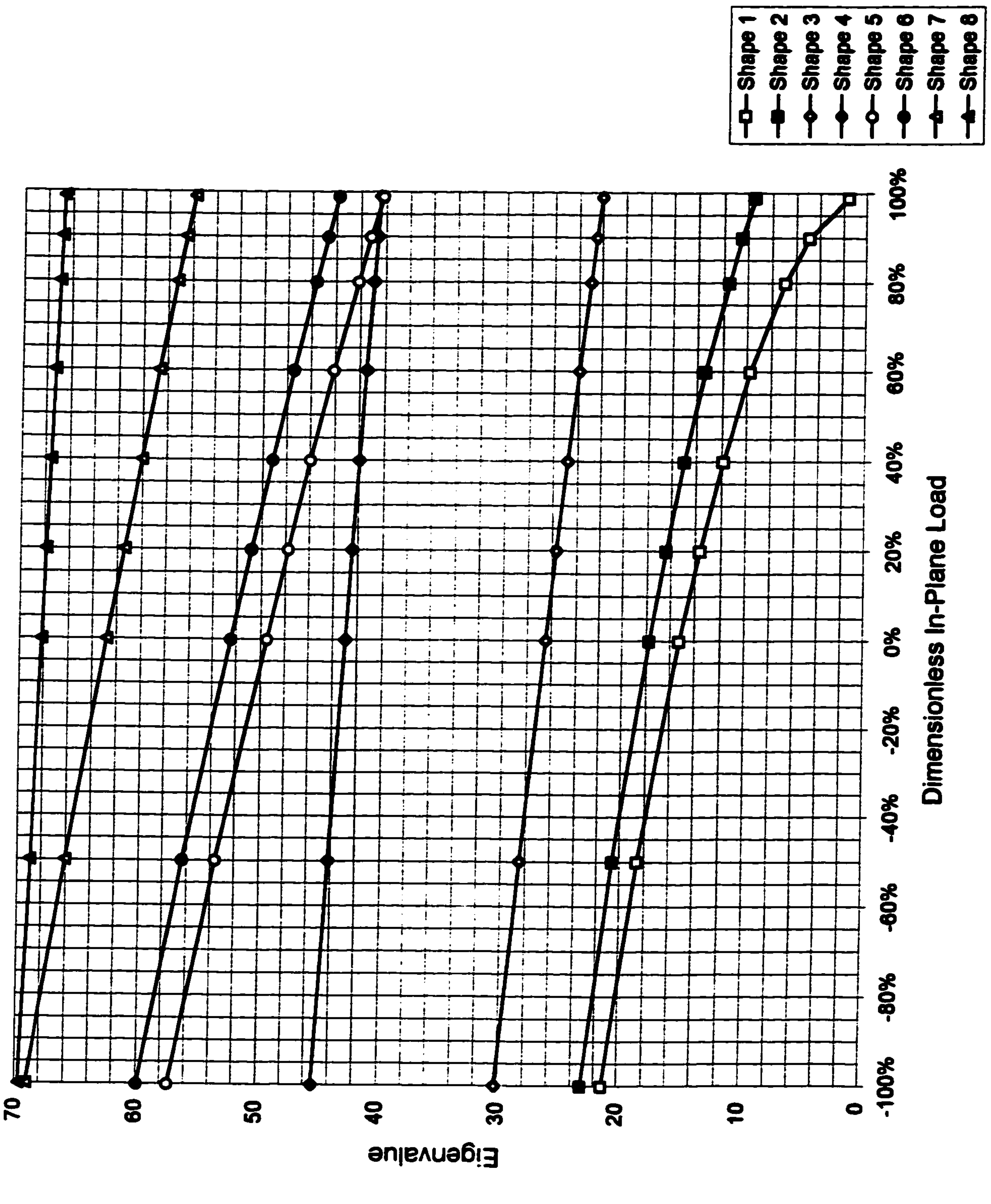

Figure 4.57 Mode shapes, SFCF plate, $\phi = 3 / 2$.

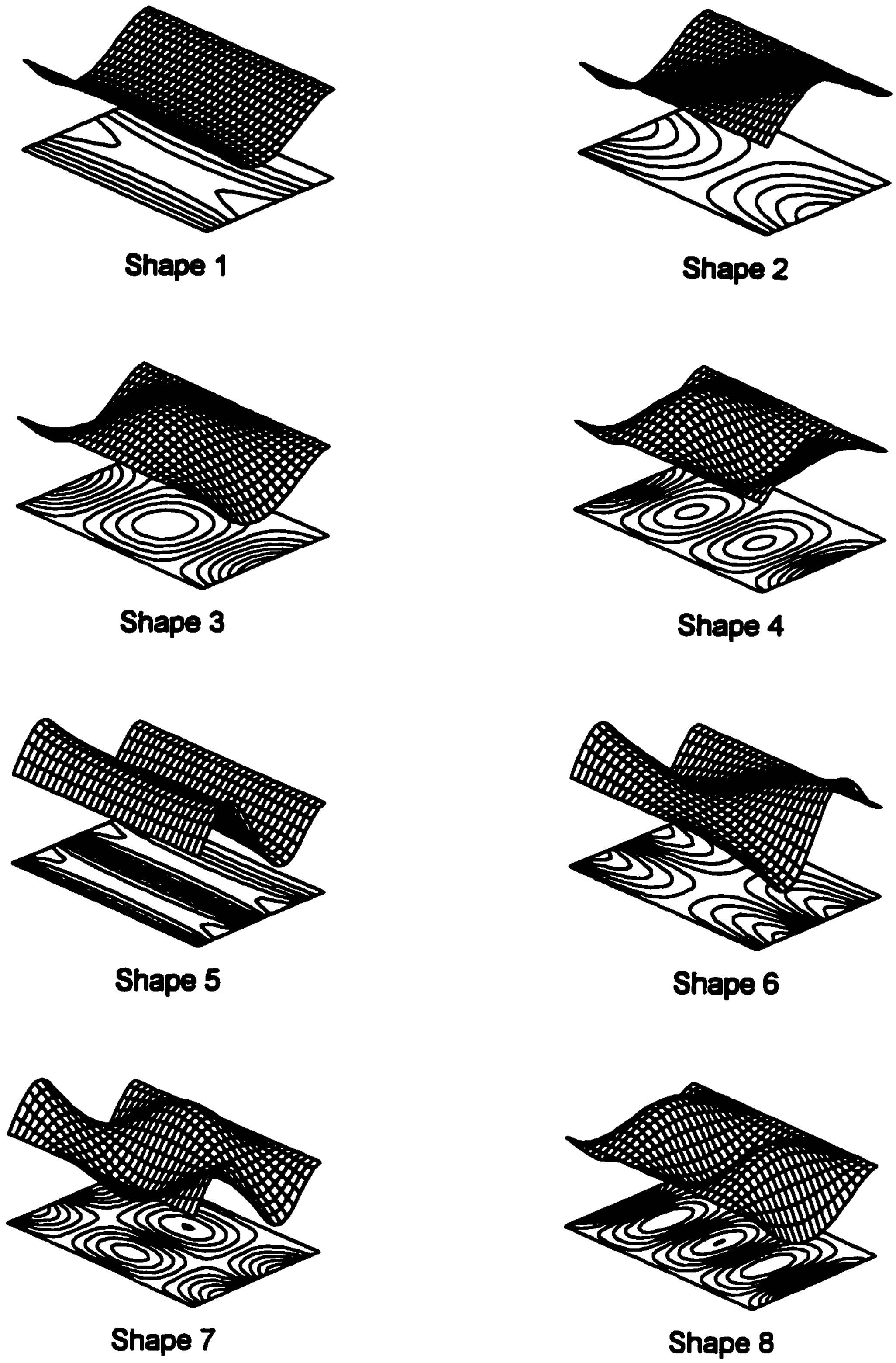

Table 4.35 Eigenvalues, SFCF plate, $\phi = 2 / 1$, $\lambda^2 = \omega a^2 (\rho / D)^{1/2}$.

Mode	In-plane load as a percentage of buckling load								
	-100%	-50%	0%	20%	40%	60%	80%	90%	99%
	Present solution								
1	21.38	18.59	15.25	13.68	11.87	9.72	6.90	4.88	1.55
2	22.40	19.77	16.70	15.28	13.70	11.90	9.76	8.47	7.11
3	26.33	24.16	21.76	20.71	19.61	18.42	17.15	16.48	15.85
4	34.26	32.65	30.95	30.24	29.51	28.76	27.98	27.59	27.23
5	47.21	46.07	44.89	44.42	43.93	43.44	42.20	41.19	40.25
6	57.49	53.69	49.59	47.85	46.05	44.17	42.94	42.69	42.24
7	58.89	55.19	51.22	49.53	47.79	45.98	44.10	43.13	42.46
8	64.14	60.77	57.19	55.70	54.16	52.57	50.93	50.10	49.33
	Finite element solution [18]								
1	21.37	18.59	15.25	13.68	11.87	9.72	6.90	4.88	1.55
2	22.41	19.78	16.71	15.29	13.72	11.92	9.78	8.50	7.14
3	26.33	24.17	21.77	20.72	19.61	18.43	17.17	16.49	15.86
4	34.25	32.64	30.94	30.23	29.50	28.74	27.97	27.57	27.21
5	47.16	46.02	44.84	44.36	43.88	43.39	42.17	41.16	40.22
6	57.46	53.66	49.56	47.82	46.02	44.14	42.89	42.64	42.27
7	58.91	55.21	51.24	49.56	47.82	46.01	44.13	43.16	42.41
8	64.14	60.77	57.20	55.70	54.16	52.58	50.95	50.11	49.34
	Percent difference								
1	-0.01%	-0.01%	0.00%	0.00%	-0.01%	0.00%	0.00%	0.00%	-0.02%
2	0.02%	0.04%	0.07%	0.08%	0.10%	0.15%	0.22%	0.30%	0.43%
3	0.01%	0.03%	0.04%	0.04%	0.05%	0.06%	0.07%	0.07%	0.08%
4	-0.04%	-0.04%	-0.04%	-0.05%	-0.05%	-0.05%	-0.05%	-0.05%	-0.05%
5	-0.10%	-0.11%	-0.11%	-0.12%	-0.12%	-0.12%	-0.07%	-0.08%	-0.08%
6	-0.05%	-0.06%	-0.06%	-0.06%	-0.06%	-0.07%	-0.12%	-0.12%	0.08%
7	0.02%	0.03%	0.04%	0.05%	0.05%	0.06%	0.07%	0.07%	-0.12%
8	0.00%	0.00%	0.01%	0.01%	0.01%	0.02%	0.02%	0.02%	0.03%

Figure 4.58 Eigenvalue curves, SFCF plate, $\phi = 2 / 1$,
$P_\xi = - N_x b^2 / D$, $\lambda^2 = \omega a^2 (\rho / D)^{1/2}$.

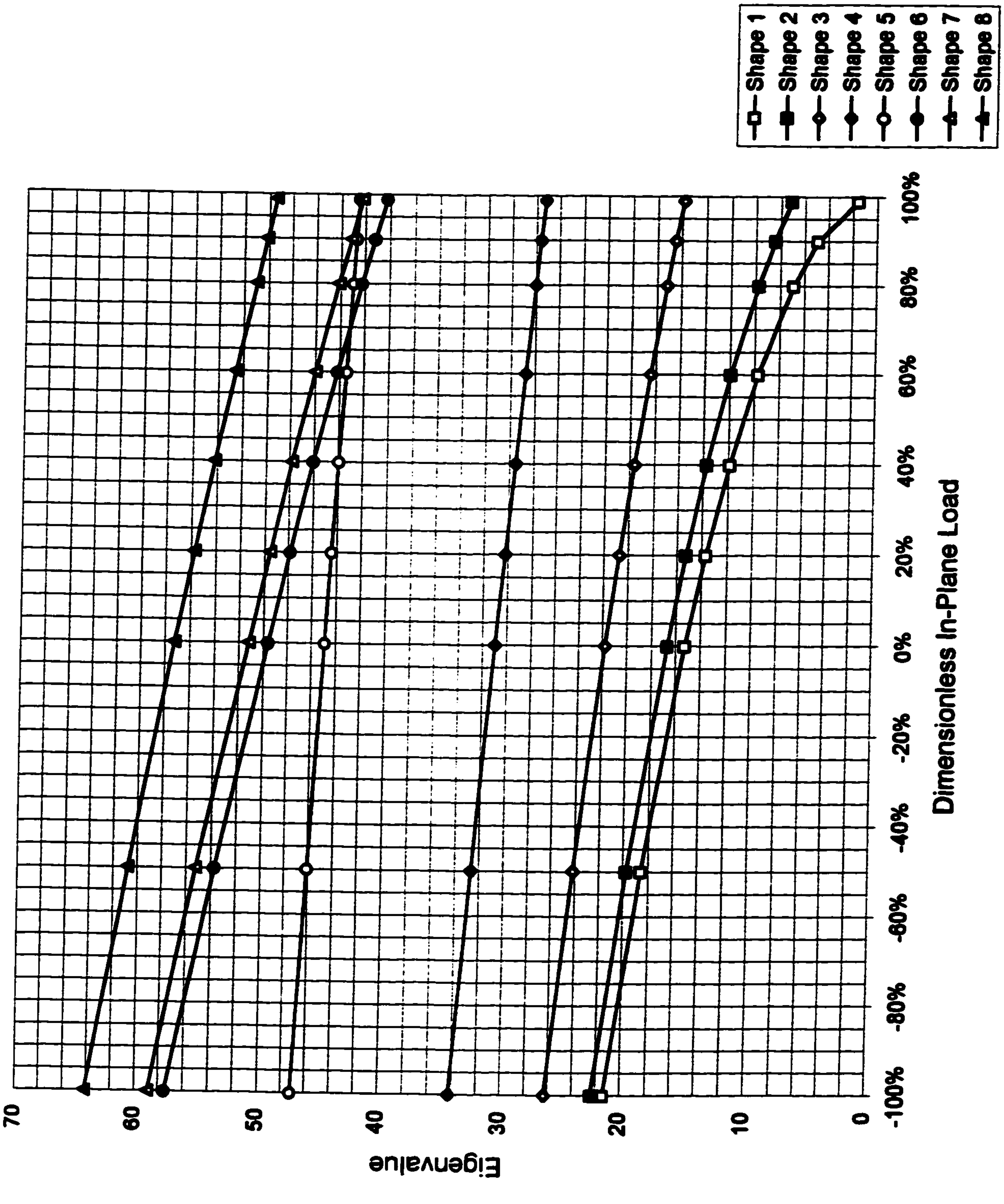

Figure 4.59 Mode shapes, SFCF plate, $\phi = 2 / 1$.

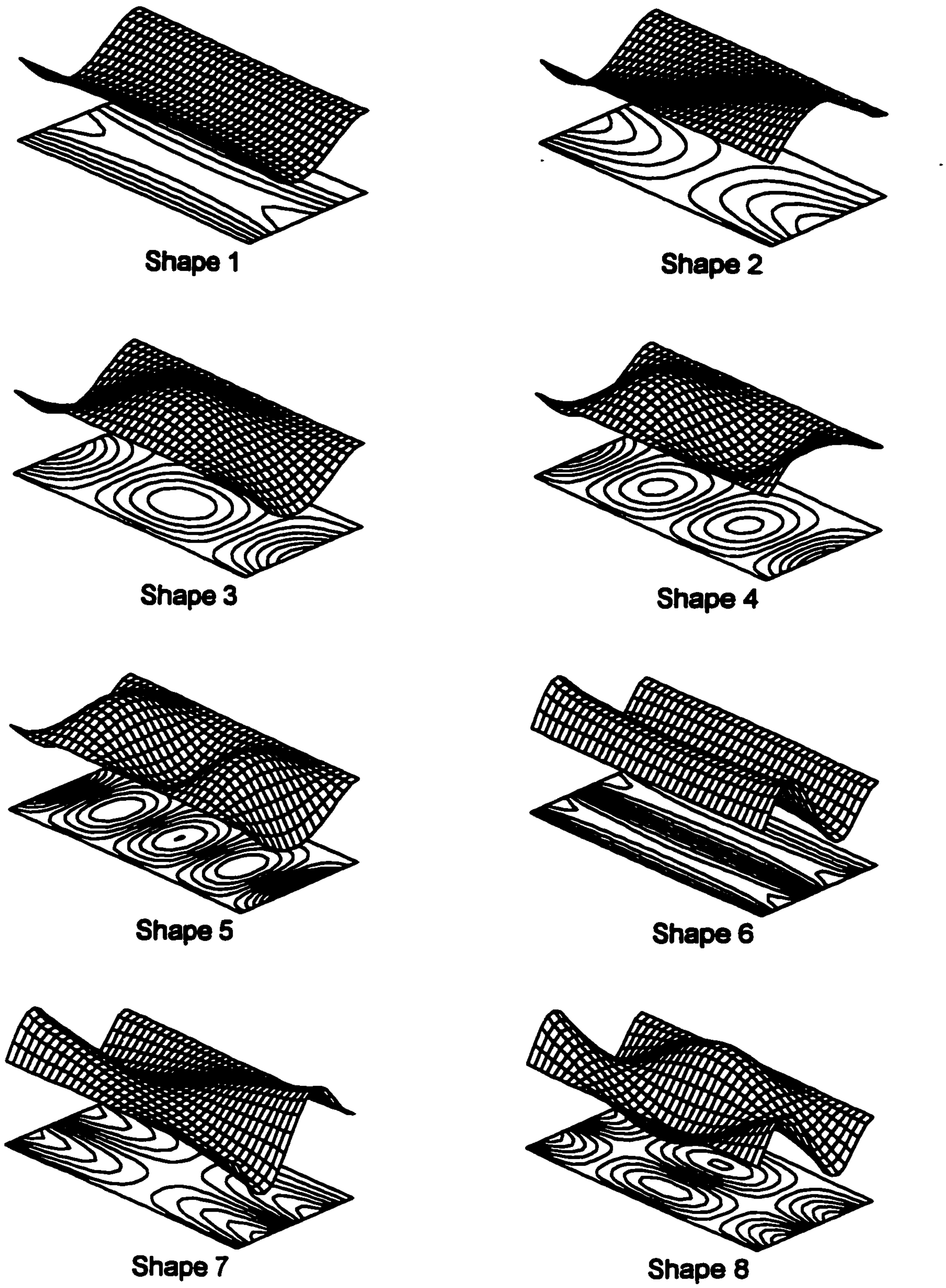

Table 4.36 Eigenvalues, SFCF plate, $\phi = 5 / 2$, $\lambda^2 = \omega a^2 (\rho / D)^{1/2}$.

	In-plane load as a percentage of buckling load								
Mode	-100%	-50%	0%	20%	40%	60%	80%	90%	99%
				Present solution					
1	21.39	18.62	15.28	13.70	11.90	9.74	6.91	4.89	1.55
2	22.07	19.38	16.21	14.73	13.08	11.17	8.82	7.37	5.74
3	24.54	22.18	19.50	18.31	17.03	15.64	14.10	13.26	12.44
4	29.37	27.45	25.37	24.48	23.56	22.59	21.58	21.05	20.57
5	37.20	35.72	34.18	33.53	32.88	32.20	31.52	31.17	30.85
6	48.40	47.29	46.14	45.67	45.20	44.21	42.25	41.23	40.29
7	57.57	53.76	49.65	47.91	46.10	44.72	43.42	42.43	41.52
8	58.44	54.69	50.66	48.95	47.18	45.34	44.24	43.99	43.77
				Finite element solution [18]					
1	21.41	18.62	15.28	13.70	11.90	9.74	6.91	4.89	1.55
2	22.07	19.39	16.22	14.75	13.09	11.19	8.85	7.40	5.78
3	24.55	22.19	19.51	18.32	17.05	15.65	14.11	13.27	12.46
4	29.36	27.44	25.36	24.47	23.55	22.58	21.57	21.04	20.55
5	37.15	35.68	34.12	33.48	32.82	32.15	31.46	31.11	30.79
6	48.31	47.19	46.04	45.58	45.10	44.18	42.21	41.19	40.25
7	57.53	53.73	49.62	47.87	46.06	44.62	43.45	42.46	41.55
8	58.45	54.70	50.68	48.97	47.20	45.37	44.14	43.89	43.67
				Percent difference					
1	0.10%	-0.01%	-0.01%	-0.01%	0.00%	0.00%	0.00%	0.00%	-0.02%
2	0.02%	0.04%	0.07%	0.09%	0.12%	0.17%	0.29%	0.42%	0.70%
3	0.01%	0.02%	0.04%	0.05%	0.06%	0.08%	0.10%	0.11%	0.13%
4	-0.04%	-0.04%	-0.04%	-0.05%	-0.05%	-0.05%	-0.05%	-0.06%	-0.06%
5	-0.13%	-0.14%	-0.15%	-0.15%	-0.16%	-0.17%	-0.17%	-0.17%	-0.18%
6	-0.20%	-0.21%	-0.21%	-0.22%	-0.22%	-0.08%	-0.09%	-0.09%	-0.09%
7	-0.06%	-0.07%	-0.07%	-0.07%	-0.08%	-0.23%	0.07%	0.08%	0.08%
8	0.02%	0.03%	0.04%	0.05%	0.06%	0.07%	-0.23%	-0.23%	-0.24%

Figure 4.60 Eigenvalue curves, SFCF plate, $\phi = 5 / 2$,
$P_\xi = - N_x b^2 / D$, $\lambda^2 = \omega a^2 (\rho / D)^{1/2}$.

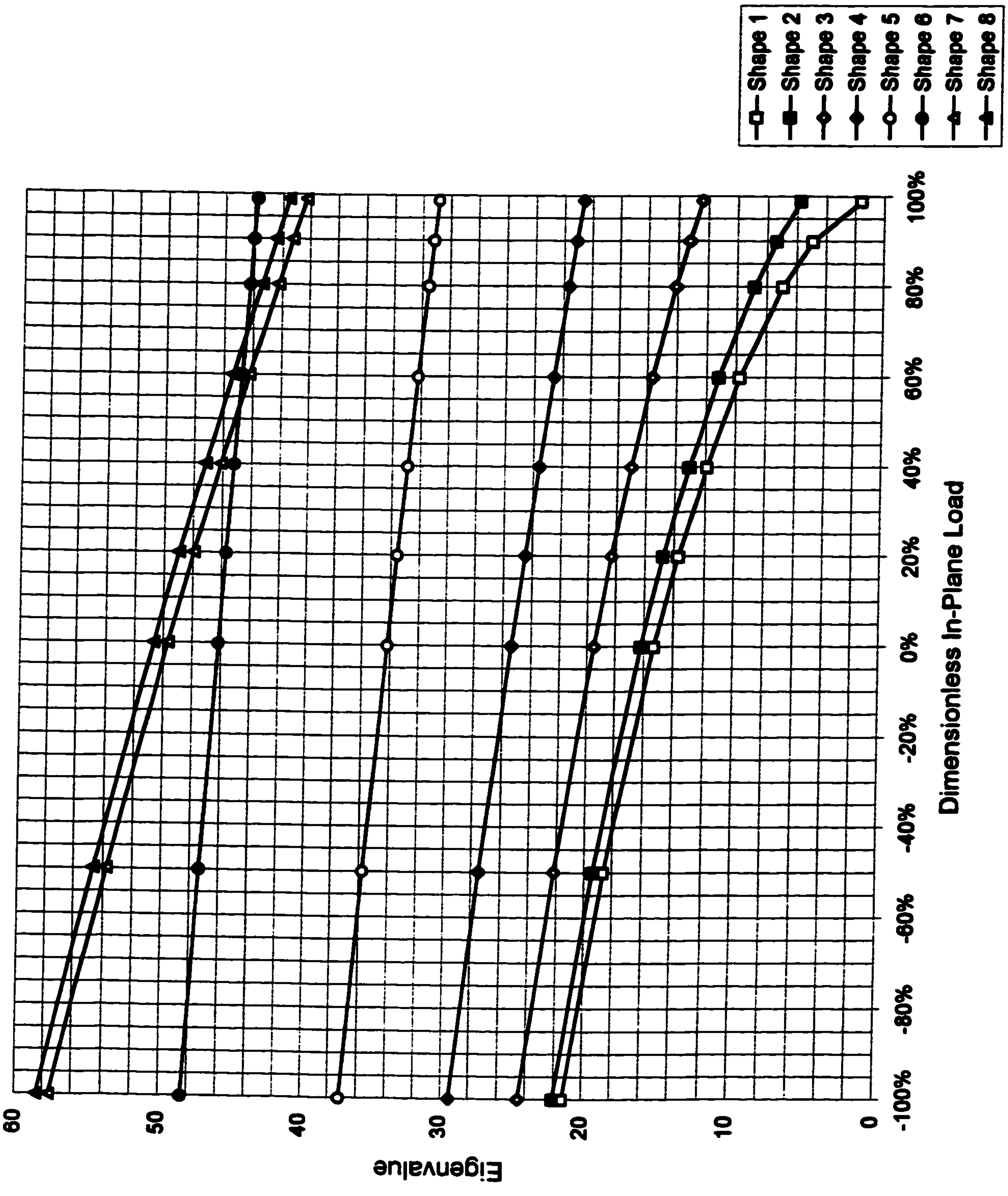

Figure 4.61 Mode shapes, SFCF plate, $\phi = 5 / 2$.

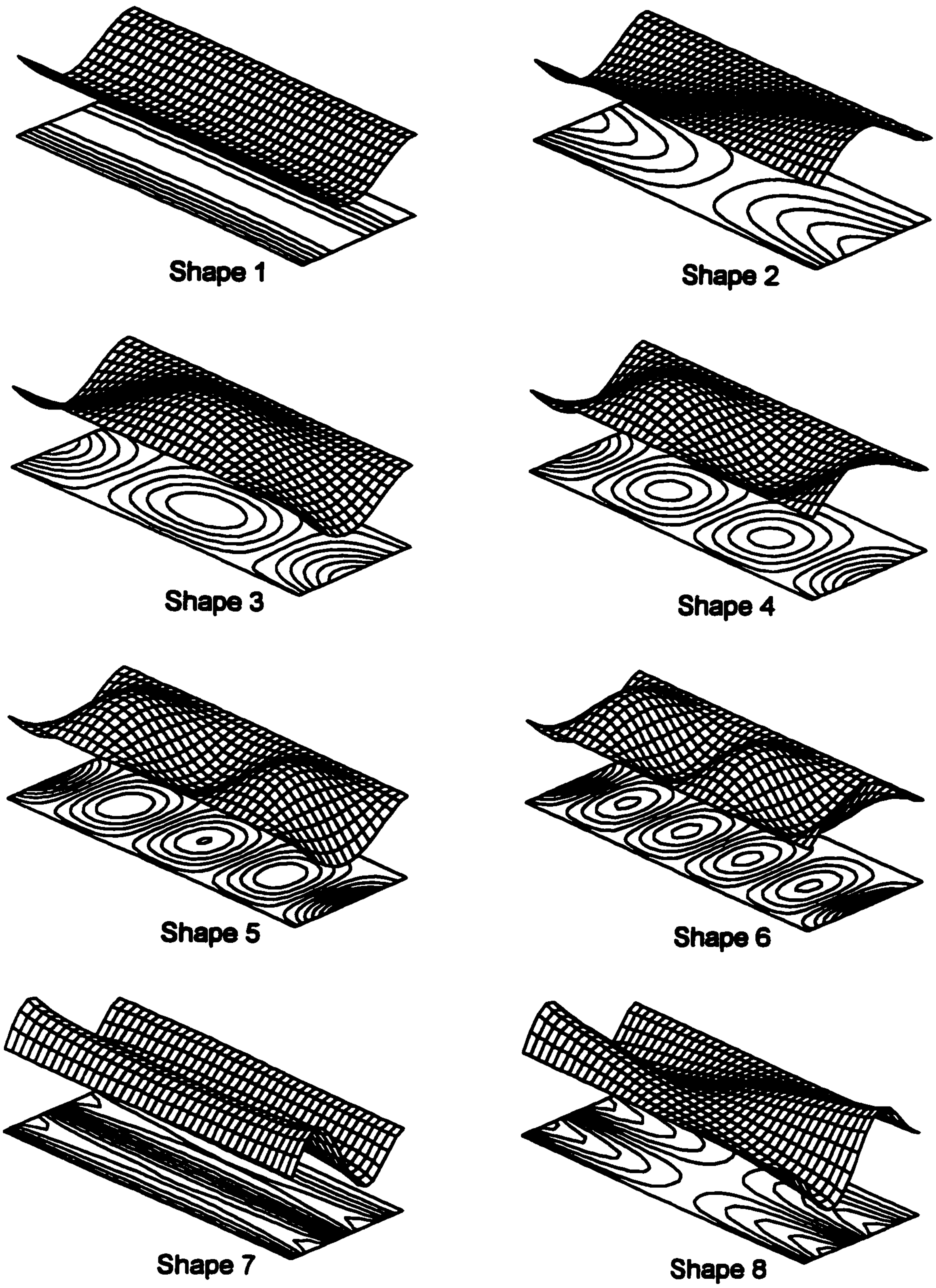

Table 4.37 Eigenvalues, SFCF plate, $\phi = 3 / 1$, $\lambda^2 = \omega a^2 (\rho / D)^{1/2}$.

Mode	In-plane load as a percentage of buckling load								
	-100%	-50%	0%	20%	40%	60%	80%	90%	99%
	Present solution								
1	21.44	18.65	15.30	13.72	11.91	9.75	6.92	4.90	1.55
2	21.89	19.17	15.94	14.43	12.73	10.75	8.27	6.69	4.82
3	23.59	21.11	18.26	16.97	15.57	14.01	12.25	11.26	10.28
4	26.82	24.69	22.32	21.30	20.22	19.07	17.84	17.18	16.57
5	31.99	30.24	28.37	27.58	26.77	25.93	25.06	24.61	24.19
6	39.41	38.02	36.57	35.97	35.36	34.73	34.10	33.77	33.48
7	49.23	48.13	47.00	46.54	46.07	44.25	42.27	41.25	40.31
8	57.63	53.81	49.69	47.95	46.14	44.99	43.05	42.05	41.13
	Finite element solution [18]								
1	21.44	18.65	15.30	13.72	11.91	9.75	6.92	4.90	1.55
2	21.90	19.17	15.95	14.44	12.75	10.77	8.30	6.72	4.87
3	23.60	21.11	18.26	16.98	15.58	14.03	12.27	11.28	10.30
4	26.81	24.68	22.31	21.29	20.21	19.06	17.83	17.17	16.56
5	31.95	30.20	28.32	27.54	26.72	25.88	25.00	24.55	24.14
6	39.32	37.92	36.47	35.86	35.25	34.63	33.99	33.66	33.37
7	49.07	47.97	46.84	46.38	45.91	44.21	42.24	41.22	40.28
8	57.59	53.77	49.66	47.91	46.10	45.03	43.09	42.09	41.17
	Percent difference								
1	-0.01%	-0.01%	0.00%	0.00%	0.00%	0.00%	0.00%	0.01%	0.01%
2	0.02%	0.05%	0.08%	0.10%	0.13%	0.20%	0.35%	0.54%	1.05%
3	0.02%	0.02%	0.04%	0.06%	0.07%	0.09%	0.12%	0.15%	0.18%
4	-0.04%	-0.04%	-0.04%	-0.04%	-0.04%	-0.05%	-0.05%	-0.06%	-0.06%
5	-0.14%	-0.15%	-0.17%	-0.18%	-0.19%	-0.20%	-0.21%	-0.22%	-0.23%
6	-0.25%	-0.27%	-0.28%	-0.29%	-0.30%	-0.31%	-0.32%	-0.33%	-0.34%
7	-0.31%	-0.32%	-0.34%	-0.35%	-0.36%	-0.08%	-0.09%	-0.09%	-0.09%
8	-0.06%	-0.07%	-0.07%	-0.07%	-0.07%	0.08%	0.09%	0.10%	0.11%

Figure 4.62 Eigenvalue curves, SFCF plate, $\phi = 3 / 1$,

$P_\xi = - N_x b^2 / D$, $\lambda^2 = \omega a^2 (\rho / D)^{1/2}$.

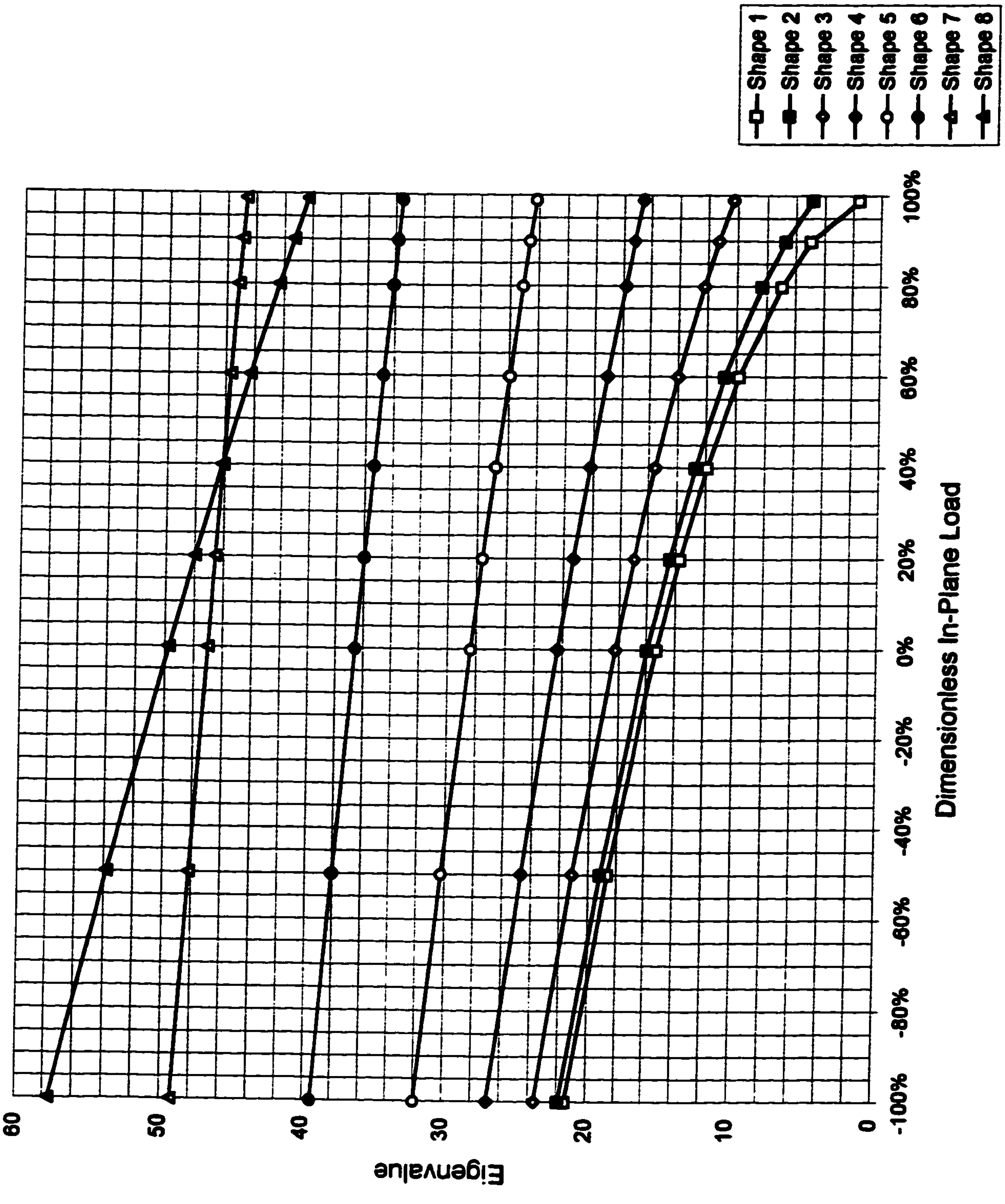

Figure 4.63 Mode shapes, SFCF plate, $\phi = 3 / 1$.

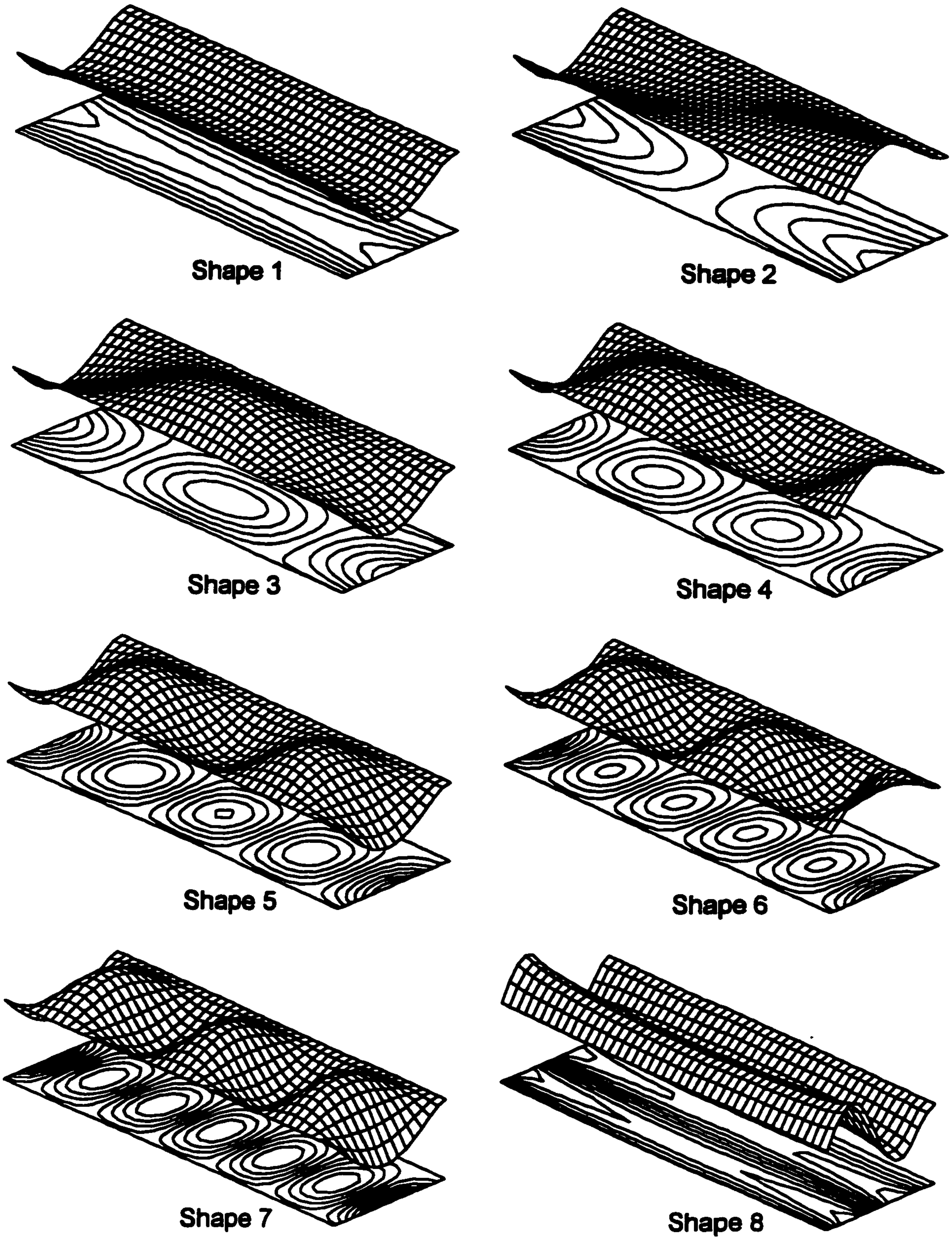

Table 4.38 Eigenvalues, CFCF plate, $\phi = 1 / 3$, $\lambda^2 = \omega a^2 (\rho / D)^{1/2}$.

Mode	In-plane load as a percentage of buckling load								
	-100%	-50%	0%	20%	40%	60%	80%	90%	99%
	Present solution								
1	30.47	26.54	21.82	19.58	17.01	13.94	9.90	7.02	2.22
2	50.87	48.78	46.58	45.66	44.73	43.77	42.79	42.29	41.83
3	72.99	66.90	60.14	57.20	54.08	50.76	47.19	45.30	43.52
4	108.79	104.95	100.95	99.30	97.62	95.90	94.16	93.27	92.47
5	132.96	125.84	118.28	115.11	111.85	108.49	105.02	103.25	101.62
6	178.95	173.81	168.50	166.32	164.11	161.88	159.61	158.46	157.42
7	211.82	204.12	196.12	192.83	189.47	186.06	182.58	180.82	179.21
8	220.89	220.45	220.00	219.82	219.64	219.46	219.27	219.18	219.10
	Finite element solution [18]								
1	30.51	26.58	21.85	19.60	17.03	13.96	9.91	7.02	2.22
2	50.88	48.77	46.56	45.65	44.71	43.75	42.77	42.26	41.81
3	73.15	67.05	60.29	57.35	54.23	50.91	47.35	45.45	43.67
4	108.82	104.97	100.95	99.29	97.61	95.89	94.14	93.25	92.44
5	133.44	126.32	118.76	115.60	112.34	108.98	105.52	103.75	102.13
6	179.10	173.94	168.60	166.42	164.21	161.97	159.69	158.54	157.49
7	212.96	205.28	197.29	194.01	190.66	187.25	183.78	182.03	180.42
8	220.70	220.26	219.81	219.63	219.45	219.26	219.08	218.99	218.91
	Percent difference								
1	0.14%	0.13%	0.13%	0.12%	0.12%	0.12%	0.11%	0.10%	0.10%
2	0.01%	-0.01%	-0.02%	-0.03%	-0.04%	-0.05%	-0.06%	-0.06%	-0.07%
3	0.23%	0.24%	0.26%	0.27%	0.28%	0.30%	0.32%	0.34%	0.35%
4	0.03%	0.02%	0.00%	0.00%	-0.01%	-0.02%	-0.02%	-0.03%	-0.03%
5	0.36%	0.38%	0.41%	0.43%	0.44%	0.45%	0.48%	0.49%	0.50%
6	0.08%	0.07%	0.06%	0.06%	0.06%	0.06%	0.05%	0.05%	0.05%
7	0.54%	0.57%	0.60%	0.61%	0.63%	0.64%	0.66%	0.67%	0.68%
8	-0.09%	-0.09%	-0.09%	-0.09%	-0.09%	-0.09%	-0.09%	-0.09%	-0.09%

Figure 4.64 Eigenvalue curves, CFCF plate, $\phi = 1 / 3$,
$P_\xi = - N_x b^2 / D$, $\lambda^2 = \omega a^2 (\rho / D)^{1/2}$.

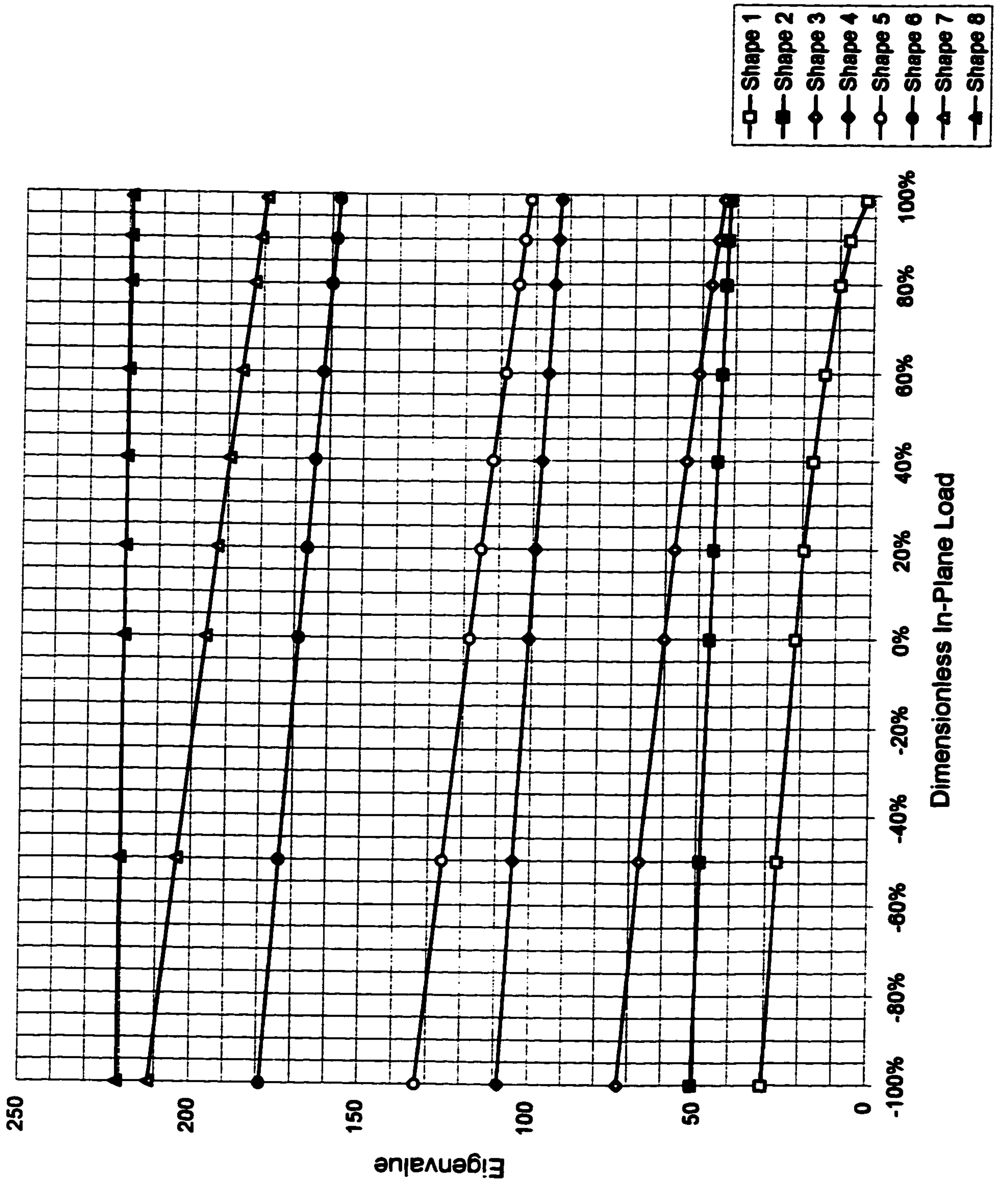

Figure 4.65 Mode shapes, CFCF plate, $\phi = 1 / 3$.

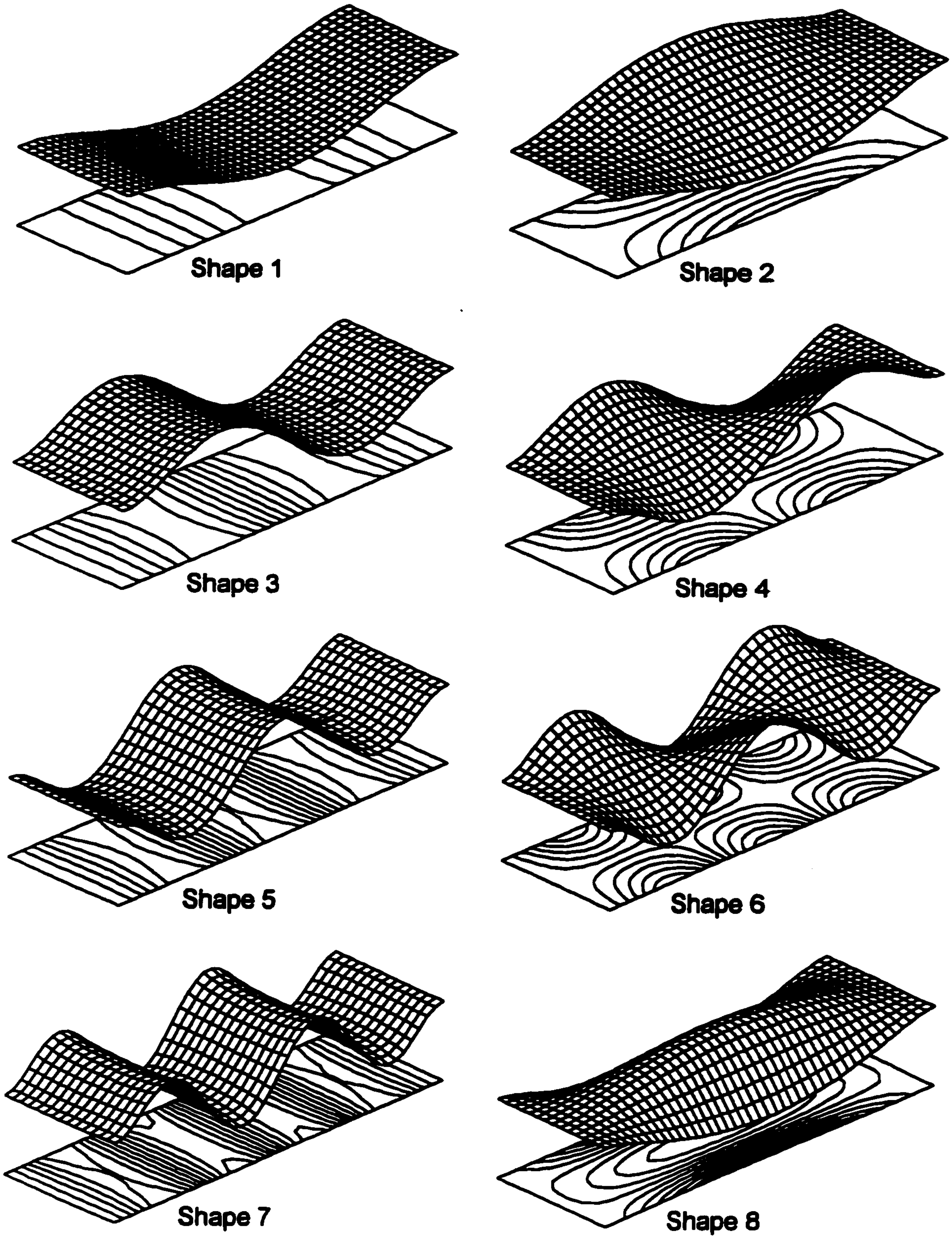

Table 4.39 Eigenvalues, CFCF plate, $\phi = 2 / 5$, $\lambda^2 = \omega a^2 (\rho / D)^{1/2}$.

Mode	In-plane load as a percentage of buckling load								
	-100%	-50%	0%	20%	40%	60%	80%	90%	99%
	Free Vibration Eigenvalue by the Method of Superposition								
1	30.55	26.61	21.88	19.63	17.06	13.98	9.92	7.03	2.23
2	45.79	43.40	40.86	39.79	38.69	37.55	36.37	35.76	35.21
3	73.20	67.09	60.32	57.36	54.24	50.91	47.34	45.44	43.65
4	99.53	95.25	90.75	88.89	86.97	85.02	83.01	81.98	81.05
5	133.35	126.21	118.63	115.45	112.18	108.81	105.34	103.55	101.92
6	160.10	159.47	155.23	152.85	150.42	147.95	145.43	144.16	143.00
7	166.64	161.04	158.83	158.58	158.32	158.07	157.81	157.68	157.57
8	212.25	204.67	196.65	193.34	189.98	186.55	183.06	181.29	179.68
	Free Vibration Eigenvalue by the Finite Element Method								
1	30.59	26.64	21.90	19.65	17.08	13.99	9.93	7.04	2.23
2	45.80	43.41	40.86	39.79	38.68	37.54	36.36	35.75	35.19
3	73.35	67.23	60.45	57.50	54.38	51.05	47.47	45.58	43.79
4	99.59	95.30	90.80	88.92	87.00	85.04	83.03	82.00	81.07
5	133.79	126.64	119.06	115.89	112.62	109.25	105.79	104.00	102.37
6	159.98	159.34	155.44	153.04	150.61	148.13	145.61	144.34	143.18
7	166.86	161.26	158.71	158.45	158.19	157.94	157.68	157.56	157.44
8	212.25	205.69	197.69	194.39	191.04	187.62	184.14	182.37	180.77
	Free Vibration Eigenvalue by the Finite Element Method								
1	0.13%	0.12%	0.12%	0.12%	0.11%	0.11%	0.10%	0.10%	0.13%
2	0.03%	0.02%	0.00%	-0.01%	-0.02%	-0.03%	-0.04%	-0.04%	-0.05%
3	0.21%	0.21%	0.23%	0.24%	0.25%	0.27%	0.29%	0.30%	0.32%
4	0.06%	0.05%	0.05%	0.04%	0.03%	0.03%	0.03%	0.02%	0.02%
5	0.32%	0.34%	0.36%	0.38%	0.39%	0.40%	0.43%	0.43%	0.44%
6	-0.07%	-0.08%	0.13%	0.13%	0.13%	0.13%	0.12%	0.13%	0.12%
7	0.13%	0.13%	-0.08%	-0.08%	-0.08%	-0.08%	-0.08%	-0.08%	-0.08%
8	0.00%	0.50%	0.53%	0.55%	0.56%	0.57%	0.59%	0.60%	0.60%

Figure 4.66 Eigenvalue curves, CFCF plate, $\phi = 2 / 5$,

$P_\xi = - N_x b^2 / D$, $\lambda^2 = \omega a^2 (\rho / D)^{1/2}$.

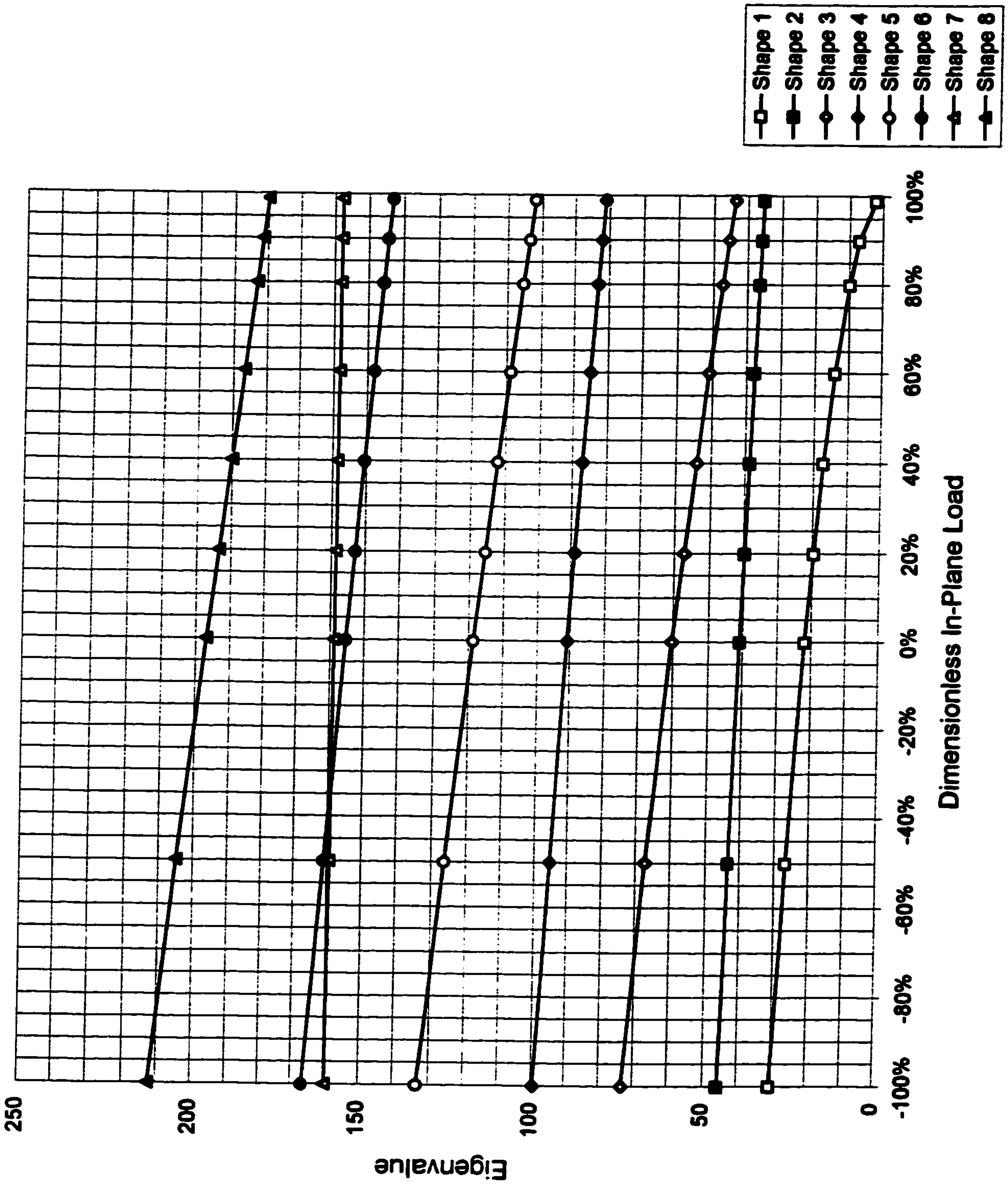

Figure 4.67 Mode shapes, CFCF plate, $\phi = 2 / 5$.

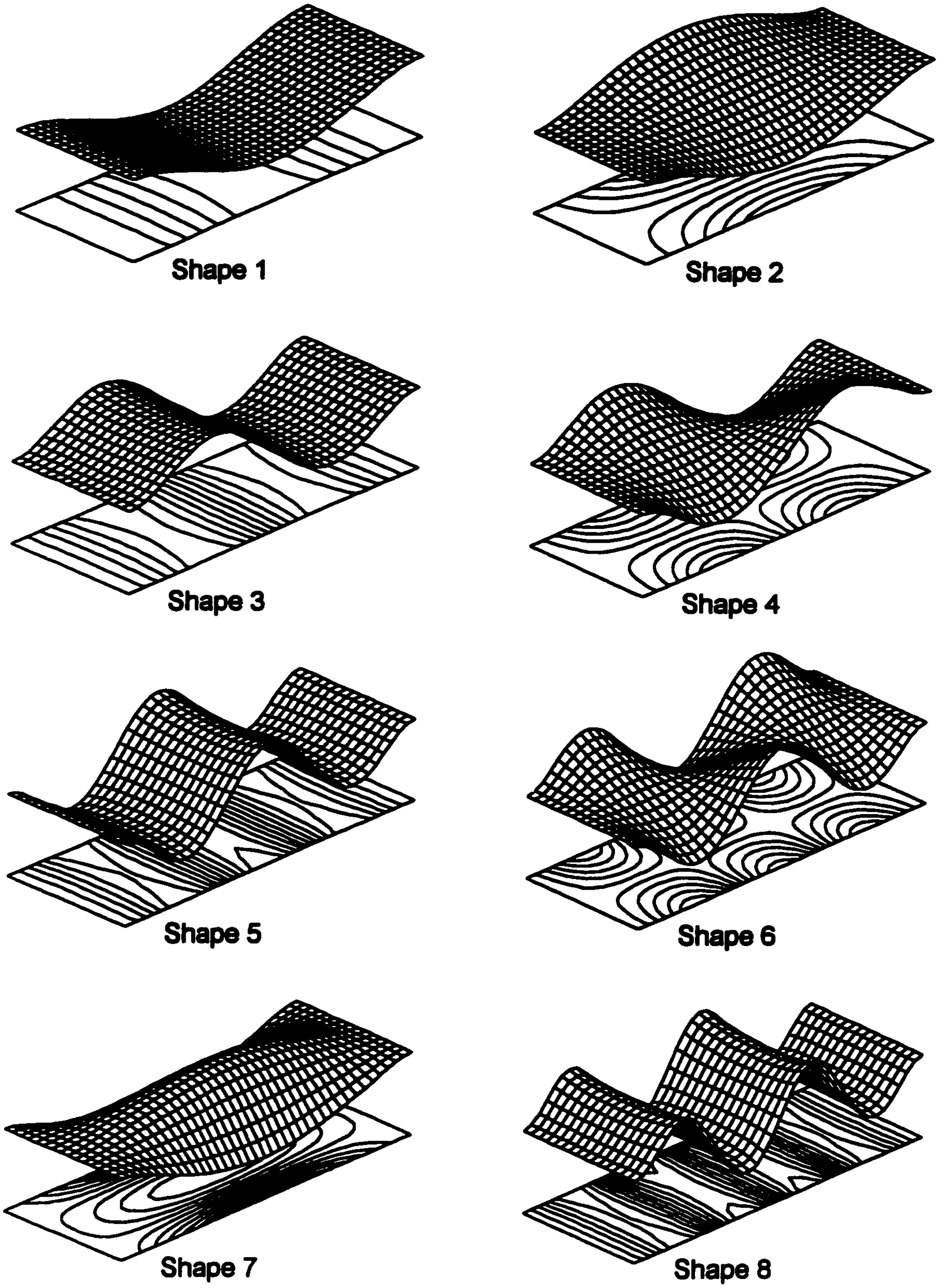

Table 4.40 Eigenvalues, CFCF plate, $\phi = 1/2$, $\lambda^2 = \omega a^2 (\rho / D)^{1/2}$.

Mode	-100%	-50%	0%	20%	40%	60%	80%	90%	99%
	In-plane load as a percentage of buckling load								
	Present solution								
1	30.64	26.69	21.94	19.69	17.11	14.02	9.95	7.05	2.24
2	41.11	38.38	35.40	34.13	32.81	31.42	29.95	29.19	28.49
3	73.44	67.32	60.52	57.56	54.43	51.09	47.51	45.60	43.81
4	91.21	86.45	81.39	79.27	77.08	74.83	72.50	71.30	70.20
5	110.84	109.91	108.96	108.58	108.19	107.78	105.64	103.87	102.24
6	133.79	126.62	119.02	115.83	112.56	109.21	107.47	107.26	107.08
7	155.85	149.79	143.46	140.84	138.17	135.45	132.67	131.25	129.97
8	162.82	160.29	157.72	156.68	155.63	154.57	153.50	152.96	152.48
	Finite element solution [18]								
1	30.67	26.72	21.96	19.70	17.12	14.03	9.96	7.06	2.24
2	41.13	38.39	35.41	34.14	32.81	31.42	29.95	29.19	28.48
3	73.57	67.44	60.64	57.68	54.54	51.21	47.62	45.72	43.93
4	91.30	86.54	81.46	79.34	77.15	74.89	72.55	71.36	70.26
5	110.78	109.84	108.89	108.51	108.12	107.71	105.99	104.23	102.61
6	134.15	126.99	119.38	116.20	112.93	109.58	107.42	107.20	107.01
7	156.13	150.06	143.72	141.11	138.43	135.71	132.93	131.51	130.23
8	162.67	160.13	157.55	156.50	155.45	154.38	153.32	152.78	152.29
	Percent difference								
1	0.11%	0.10%	0.10%	0.10%	0.09%	0.09%	0.09%	0.09%	0.10%
2	0.05%	0.04%	0.03%	0.02%	0.01%	0.00%	-0.01%	-0.01%	-0.02%
3	0.17%	0.18%	0.19%	0.20%	0.21%	0.22%	0.24%	0.25%	0.27%
4	0.10%	0.09%	0.09%	0.09%	0.09%	0.09%	0.08%	0.08%	0.08%
5	-0.06%	-0.06%	-0.06%	-0.07%	-0.07%	-0.06%	0.34%	0.35%	0.36%
6	0.27%	0.29%	0.31%	0.32%	0.33%	0.34%	-0.05%	-0.06%	-0.07%
7	0.18%	0.18%	0.19%	0.19%	0.19%	0.19%	0.19%	0.20%	0.20%
8	-0.09%	-0.10%	-0.11%	-0.11%	-0.12%	-0.12%	-0.12%	-0.12%	-0.13%

Figure 4.68 Eigenvalue curves, CFCF plate, $\phi = 1 / 2$,
$P_\xi = - N_x b^2 / D$, $\lambda^2 = \omega a^2 (\rho / D)^{1/2}$.

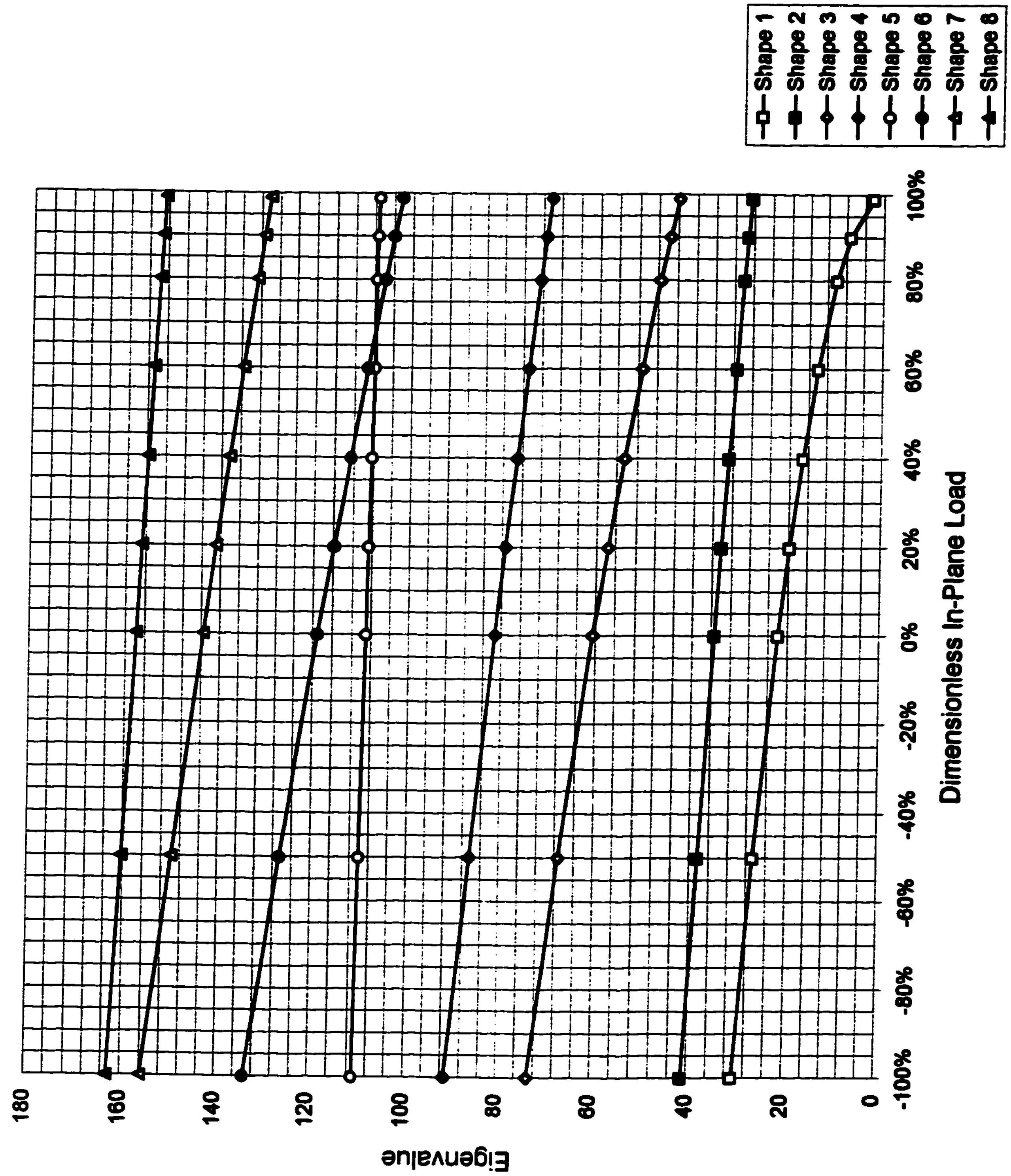

Figure 4.69 Mode shapes, CFCF plate, $\phi = 1 / 2$.

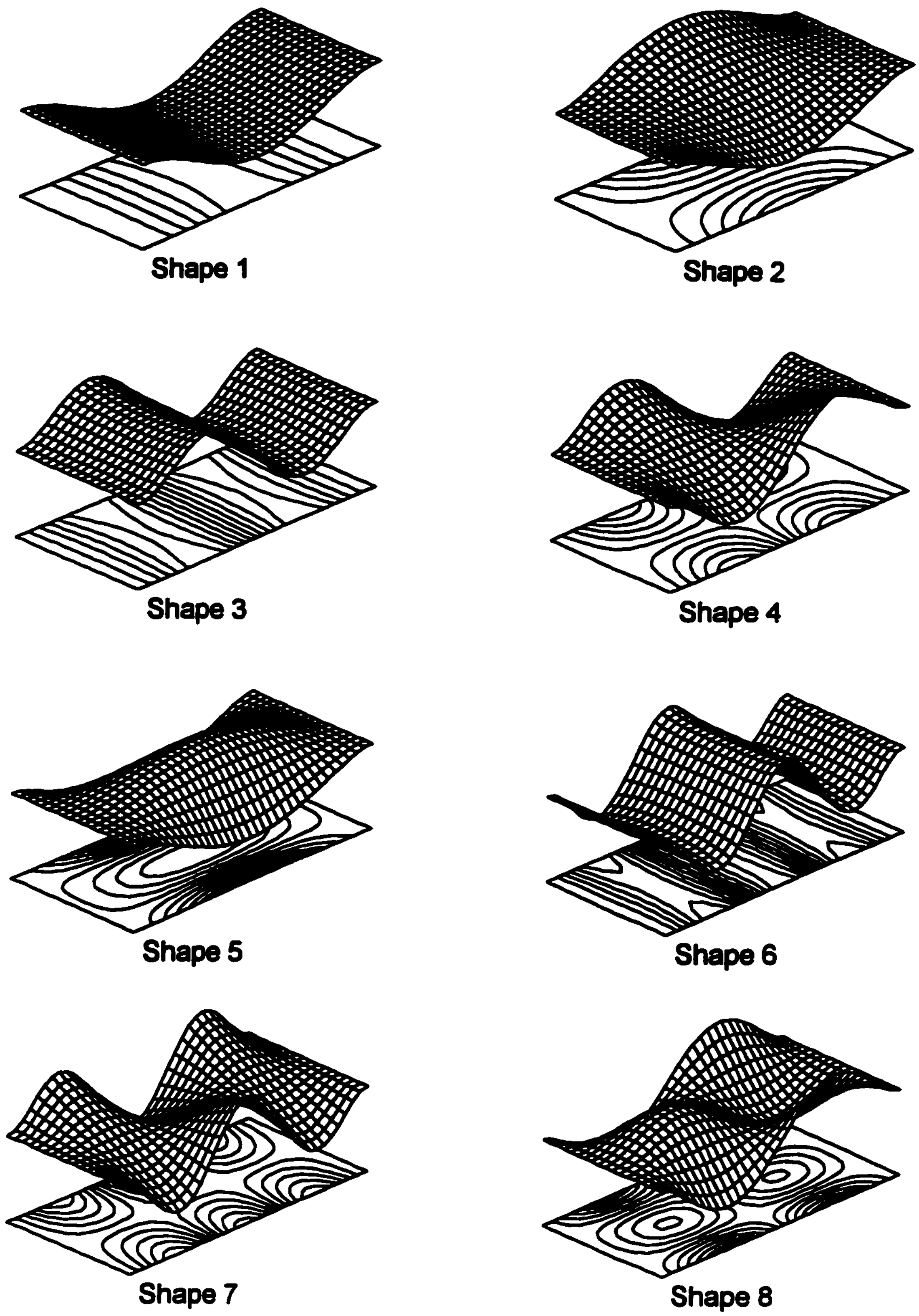

Table 4.41 Eigenvalues, CFCF plate, $\phi = 2 / 3$, $\lambda^2 = \omega a^2 (\rho / D)^{1/2}$.

Mode	In-plane load as a percentage of buckling load								
	-100%	-50%	0%	20%	40%	60%	80%	90%	99%
	Present solution								
1	30.74	26.78	22.01	19.75	17.16	14.07	9.99	7.08	2.24
2	37.03	33.90	30.40	28.87	27.24	25.49	23.60	22.59	21.63
3	73.40	67.58	60.76	57.79	54.65	51.30	47.70	45.79	44.00
4	73.72	71.94	70.45	69.84	68.33	65.72	63.01	61.60	60.30
5	84.17	78.91	73.23	70.83	69.22	68.60	67.97	67.65	67.36
6	124.10	120.68	117.16	115.71	112.93	109.53	106.03	104.23	102.59
7	134.26	127.06	119.42	116.22	114.25	112.77	111.26	110.50	109.81
8	146.97	140.45	133.60	130.75	127.84	124.86	121.81	120.25	118.83
	Finite element solution [18]								
1	30.77	26.80	22.03	19.77	17.18	14.07	9.99	7.08	2.24
2	37.06	33.92	30.42	28.89	27.26	25.51	23.61	22.60	21.64
3	73.38	67.66	60.84	57.87	54.73	51.38	47.78	45.87	44.08
4	73.81	71.92	70.42	69.81	68.41	65.81	63.09	61.68	60.38
5	84.26	79.00	73.32	70.91	69.19	68.57	67.94	67.62	67.33
6	124.07	120.65	117.12	115.67	113.18	109.79	106.29	104.49	102.85
7	134.51	127.31	119.67	116.47	114.20	112.72	111.21	110.44	109.75
8	147.23	140.71	133.87	131.02	128.12	125.14	122.08	120.53	119.11
	Percent difference								
1	0.08%	0.08%	0.07%	0.07%	0.07%	0.07%	0.07%	0.06%	0.01%
2	0.07%	0.06%	0.06%	0.05%	0.05%	0.05%	0.04%	0.04%	0.04%
3	-0.03%	0.13%	0.13%	0.14%	0.15%	0.16%	0.17%	0.18%	0.19%
4	0.12%	-0.03%	-0.03%	-0.04%	0.12%	0.13%	0.13%	0.14%	0.14%
5	0.11%	0.11%	0.12%	0.12%	-0.04%	-0.04%	-0.05%	-0.05%	-0.04%
6	-0.02%	-0.03%	-0.04%	-0.04%	0.23%	0.23%	0.25%	0.25%	0.25%
7	0.19%	0.20%	0.21%	0.22%	-0.04%	-0.04%	-0.05%	-0.05%	-0.05%
8	0.18%	0.19%	0.20%	0.21%	0.21%	0.22%	0.23%	0.23%	0.23%

Figure 4.70 Eigenvalue curves, CFCF plate, $\phi = 2 / 3$,

$P_\xi = - N_x b^2 / D$, $\lambda^2 = \omega a^2 (\rho / D)^{1/2}$.

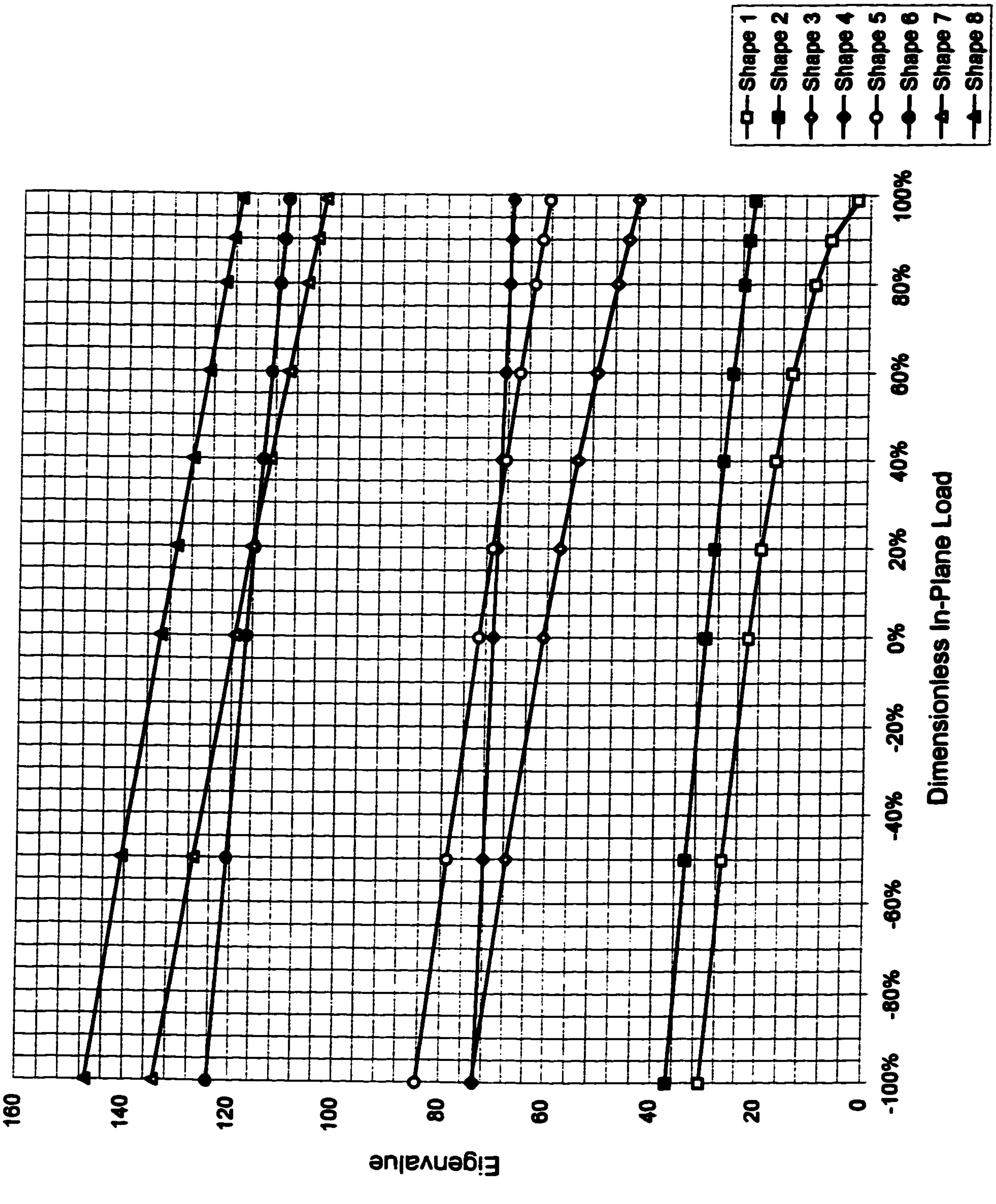

Figure 4.71 Mode shapes, CFCF plate, $\phi = 2 / 3$.

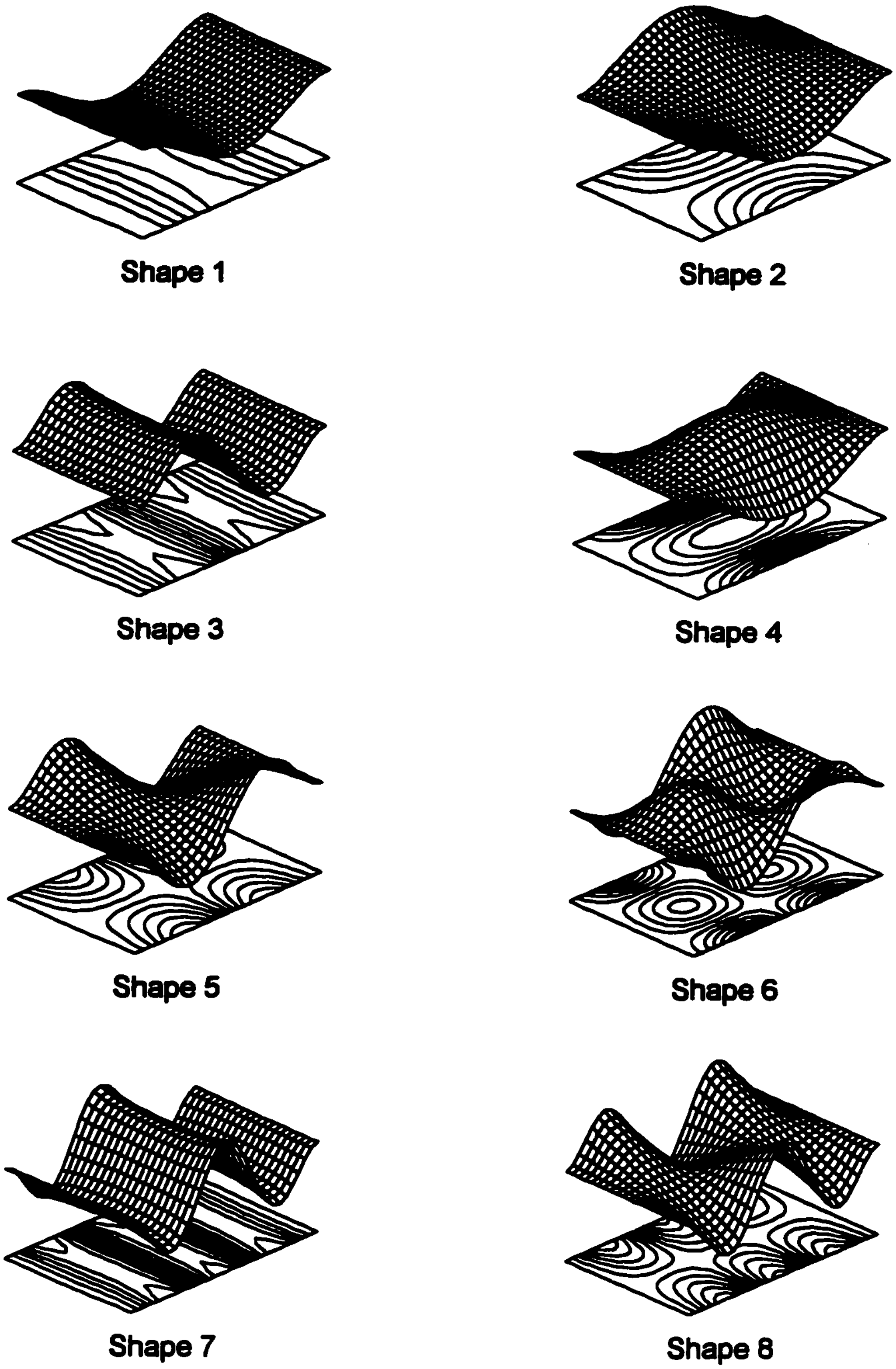

Table 4.42 Eigenvalues, CFCF plate, $\phi = 1 / 1$, $\lambda^2 = \omega a^2 (\rho / D)^{1/2}$.

Mode	In-plane load as a percentage of buckling load								
	-100%	-50%	0%	20%	40%	60%	80%	90%	99%
	Present solution								
1	30.88	26.89	22.11	19.83	17.23	14.12	10.03	7.11	2.25
2	33.82	30.27	26.19	24.34	22.32	20.07	17.51	16.06	14.63
3	48.12	45.78	43.29	42.24	41.16	40.05	38.90	38.31	37.77
4	74.05	67.87	61.02	58.04	54.88	51.52	47.90	45.98	44.18
5	78.80	73.07	66.79	64.10	61.27	58.30	55.16	53.52	51.99
6	82.19	80.87	79.54	78.99	78.44	77.89	77.33	77.05	76.53
7	96.42	91.87	87.05	85.04	82.97	80.85	78.67	77.55	76.80
8	130.45	127.18	119.85	116.63	113.32	109.90	106.38	104.57	102.92
	Finite element solution [18]								
1	30.88	26.90	22.11	19.84	17.24	14.13	10.03	7.11	2.25
2	33.83	30.29	26.20	24.36	22.33	20.09	17.53	16.09	14.66
3	48.13	45.78	43.29	42.24	41.17	40.05	38.90	38.31	37.77
4	74.07	67.89	61.04	58.06	54.90	51.54	47.92	46.00	44.20
5	78.86	73.12	66.85	64.16	61.34	58.37	55.23	53.59	52.06
6	82.15	80.83	79.50	78.95	78.40	77.85	77.29	77.01	76.55
7	96.44	91.89	87.07	85.06	82.99	80.87	78.69	77.57	76.75
8	130.37	127.10	119.89	116.67	113.36	109.95	106.43	104.62	102.97
	Percent difference								
1	0.03%	0.03%	0.03%	0.03%	0.03%	0.03%	0.03%	0.02%	-0.03%
2	0.05%	0.05%	0.07%	0.08%	0.08%	0.10%	0.13%	0.16%	0.19%
3	0.01%	0.01%	0.01%	0.01%	0.01%	0.01%	0.00%	0.00%	0.00%
4	0.03%	0.03%	0.03%	0.04%	0.04%	0.04%	0.04%	0.04%	0.05%
5	0.07%	0.08%	0.09%	0.10%	0.10%	0.11%	0.13%	0.13%	0.14%
6	-0.05%	-0.05%	-0.05%	-0.05%	-0.05%	-0.05%	-0.05%	-0.05%	0.03%
7	0.02%	0.02%	0.02%	0.02%	0.02%	0.03%	0.03%	0.03%	-0.06%
8	-0.06%	-0.06%	0.04%	0.04%	0.04%	0.04%	0.04%	0.04%	0.05%

Figure 4.72 Eigenvalue curves, CFCF plate, $\phi = 1 / 1$,

$P_\xi = - N_x b^2 / D$, $\lambda^2 = \omega a^2 (\rho / D)^{1/2}$.

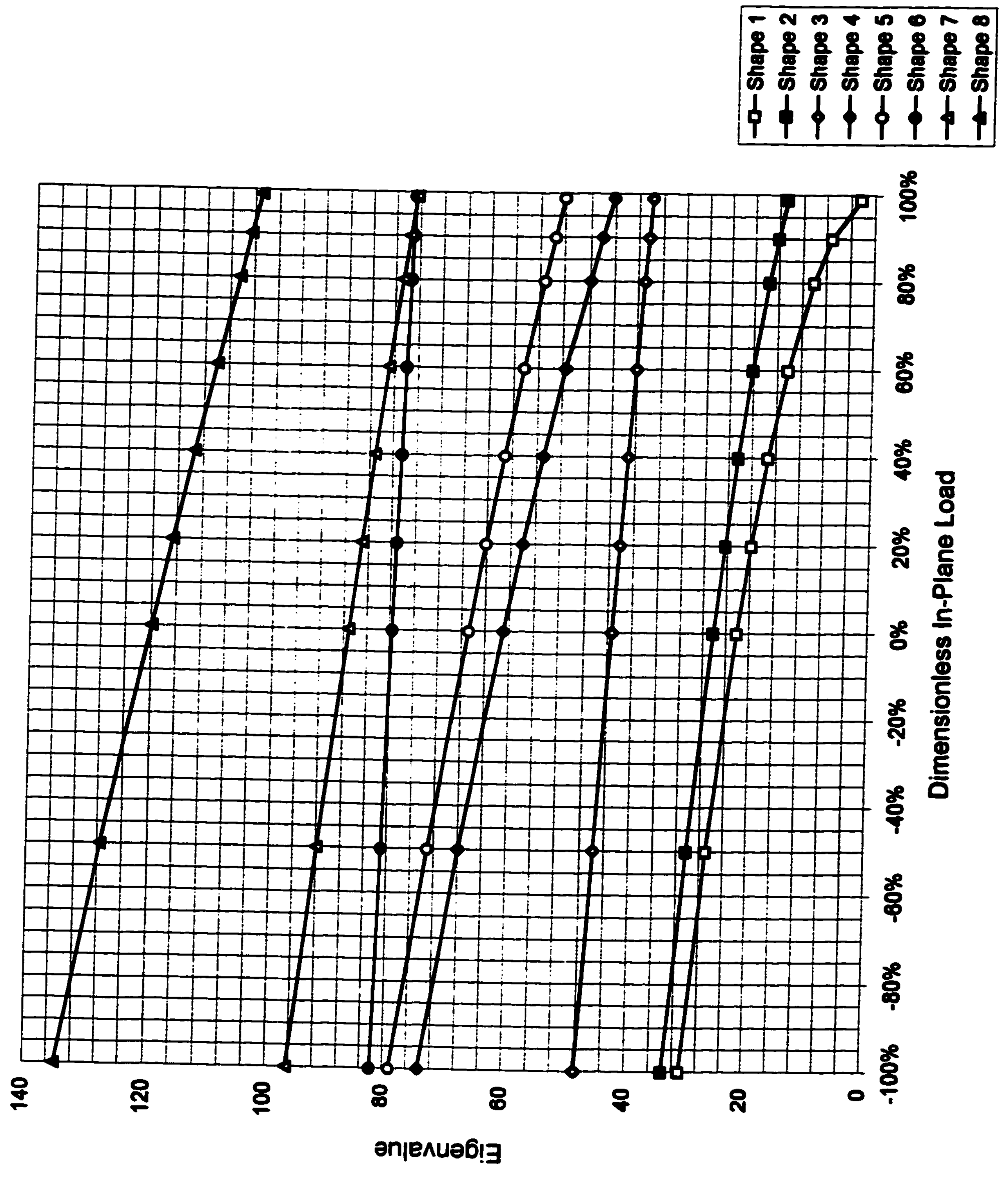

Figure 4.73 Mode shapes, CFCF plate, $\phi = 1 / 1$.

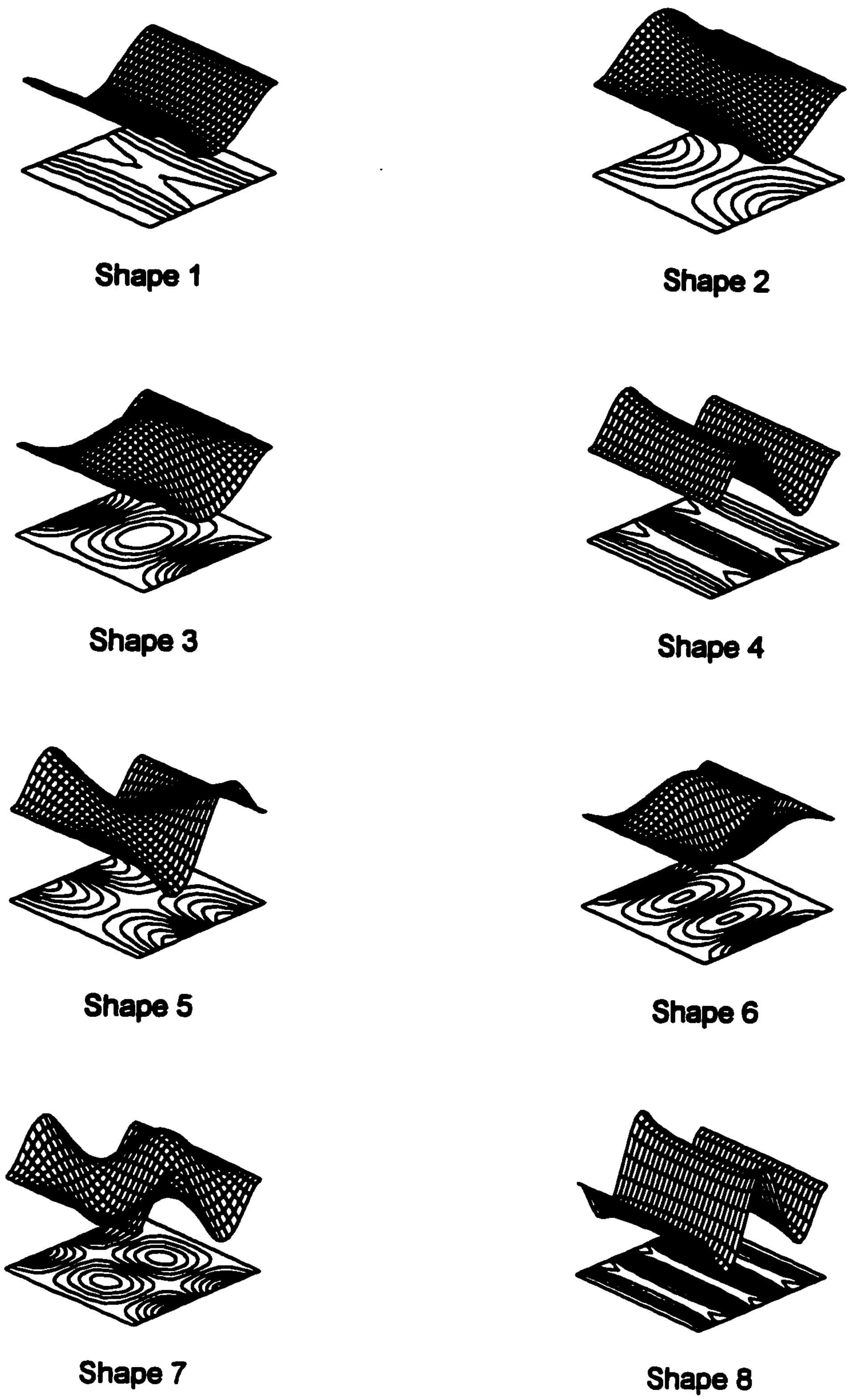

Table 4.43 Eigenvalues, CFCF plate, $\phi = 3 / 2$, $\lambda^2 = \omega a^2 (\rho / D)^{1/2}$.

Mode	In-plane load as a percentage of buckling load								
	-100%	-50%	0%	20%	40%	60%	80%	90%	99%
	Present solution								
1	30.98	26.98	22.18	19.90	17.29	14.17	10.06	7.13	2.26
2	32.31	28.52	24.06	22.00	19.70	17.05	13.87	11.95	9.88
3	38.00	34.90	31.44	29.93	28.33	26.62	24.77	23.79	22.86
4	51.09	48.88	46.54	45.56	44.56	43.53	42.47	41.92	41.43
5	73.81	68.09	61.21	58.21	55.04	51.67	48.04	46.11	44.30
6	74.29	70.37	63.76	60.90	57.88	54.69	51.29	49.49	47.82
7	76.37	72.32	70.80	70.18	68.02	65.35	62.57	61.12	59.79
8	84.17	78.82	73.03	70.57	69.55	68.91	68.27	67.94	67.65
	Finite element solution [18]								
1	30.97	26.97	22.18	19.90	17.29	14.17	10.06	7.13	2.26
2	32.31	28.52	24.07	22.01	19.71	17.08	13.90	11.99	9.93
3	38.00	34.90	31.45	29.94	28.34	26.63	24.79	23.81	22.88
4	51.07	48.86	46.52	45.55	44.54	43.51	42.45	41.91	41.42
5	73.75	68.03	61.16	58.16	54.99	51.62	47.99	46.06	44.25
6	74.23	70.36	63.76	60.90	57.90	54.71	51.31	49.52	47.85
7	76.35	72.27	70.75	70.12	68.01	65.35	62.57	61.13	59.80
8	84.15	78.80	73.02	70.56	69.50	68.86	68.21	67.89	67.59
	Percent difference								
1	-0.03%	-0.03%	-0.03%	-0.02%	-0.02%	-0.02%	-0.01%	-0.01%	-0.03%
2	0.00%	0.01%	0.04%	0.06%	0.09%	0.14%	0.23%	0.32%	0.49%
3	0.00%	0.01%	0.03%	0.03%	0.04%	0.06%	0.07%	0.08%	0.09%
4	-0.04%	-0.04%	-0.04%	-0.03%	-0.03%	-0.03%	-0.03%	-0.03%	-0.03%
5	-0.07%	-0.08%	-0.08%	-0.09%	-0.09%	-0.10%	-0.10%	-0.11%	-0.11%
6	-0.08%	-0.01%	0.00%	0.01%	0.02%	0.03%	0.05%	0.05%	0.06%
7	-0.02%	-0.07%	-0.07%	-0.07%	-0.01%	0.00%	0.00%	0.01%	0.01%
8	-0.03%	-0.03%	-0.02%	-0.01%	-0.08%	-0.08%	-0.08%	-0.08%	-0.08%

Figure 4.74 Eigenvalue curves, CFCF plate, $\phi = 3 / 2$,

$P_\xi = - N_x b^2 / D$, $\lambda^2 = \omega a^2 (\rho / D)^{1/2}$.

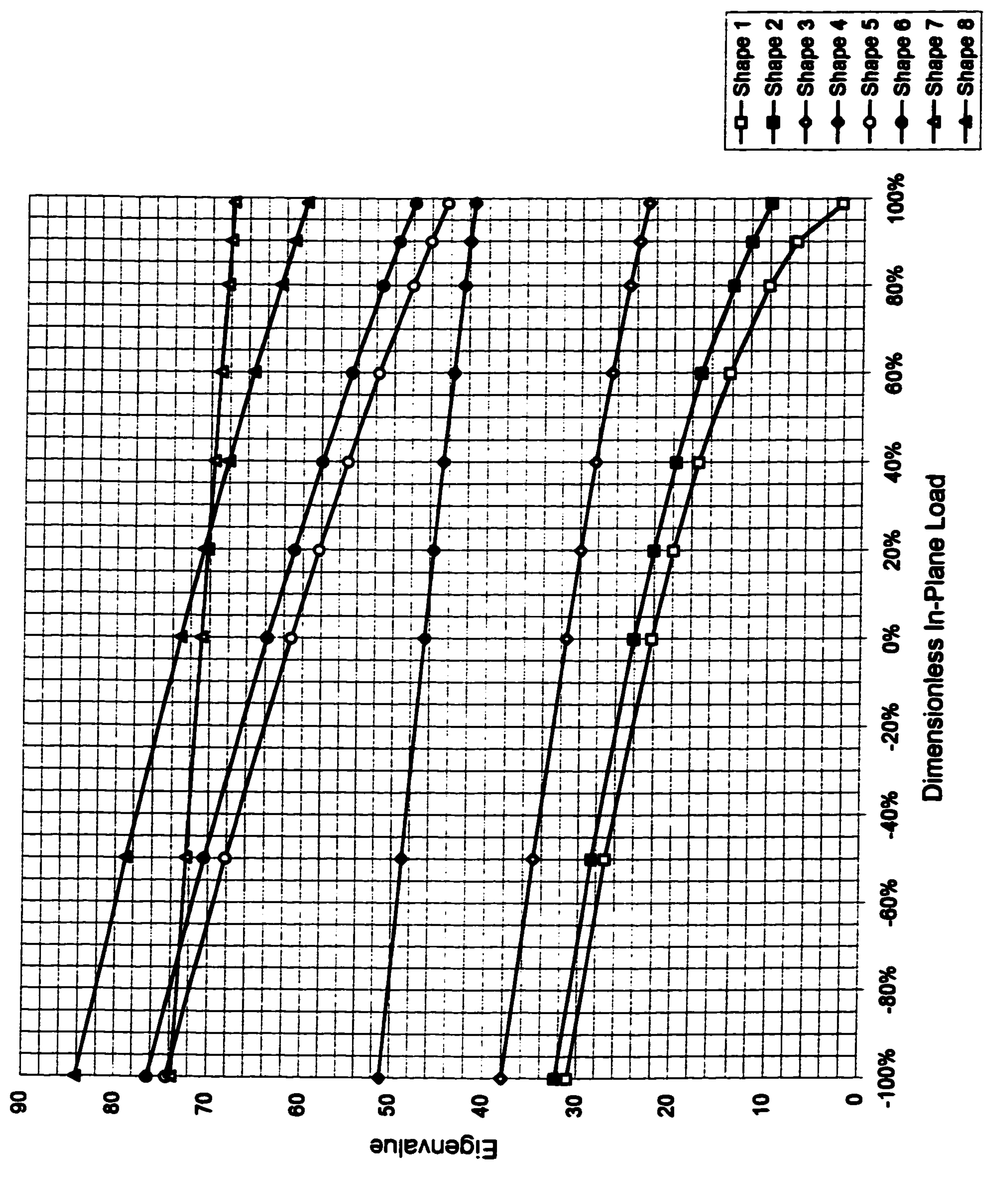

Figure 4.75 Mode shapes, CFCF plate, $\phi = 3 / 2$.

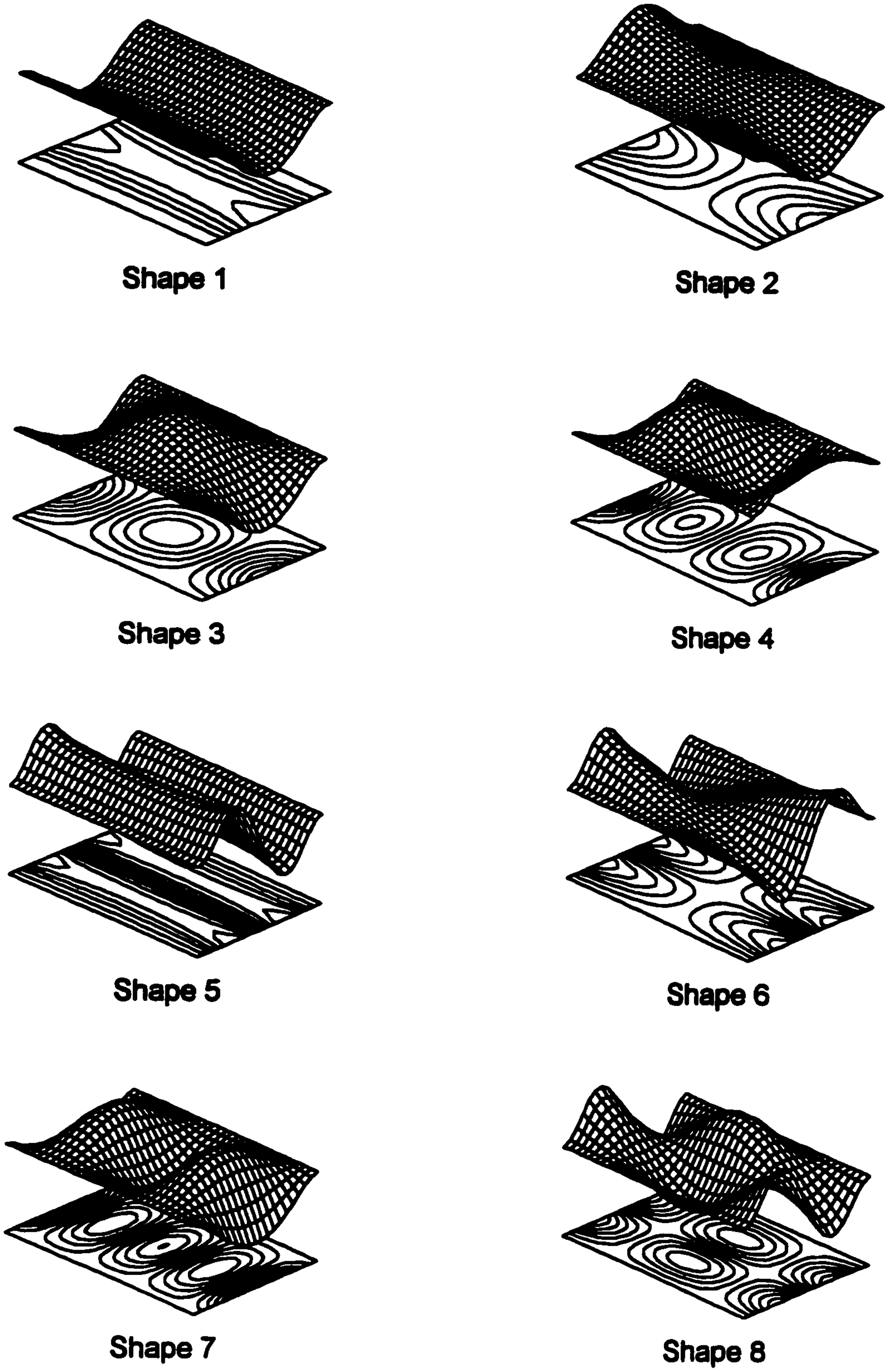

Table 4.44 Eigenvalues, CFCF plate, $\phi = 2 / 1$, $\lambda^2 = \omega a^2 (\rho / D)^{1/2}$.

Mode	In-plane load as a percentage of buckling load								
	-100%	-50%	0%	20%	40%	60%	80%	90%	99%
	Present solution								
1	31.04	27.03	22.22	19.94	17.32	14.20	10.08	7.14	2.26
2	31.78	27.89	23.28	21.12	18.69	15.85	12.33	10.10	7.51
3	34.80	31.33	27.37	25.59	23.66	21.53	19.15	17.83	16.54
4	41.33	38.50	35.41	34.09	32.70	31.23	29.69	28.88	28.13
5	52.78	50.63	48.37	47.43	46.46	45.47	44.45	43.93	43.46
6	69.83	68.20	61.31	58.30	55.13	51.74	48.10	46.17	44.35
7	74.41	68.24	62.69	59.77	56.68	53.39	49.88	48.03	46.29
8	75.54	69.44	66.61	65.32	62.53	59.59	56.49	54.87	53.37
	Finite element solution [18]								
1	31.01	27.01	22.21	19.93	17.32	14.19	10.08	7.14	2.26
2	31.76	27.89	23.29	21.13	18.71	15.88	12.37	10.14	7.58
3	34.79	31.33	27.37	25.59	23.67	21.55	19.17	17.85	16.57
4	41.31	38.48	35.40	34.07	32.69	31.22	29.68	28.87	28.12
5	52.72	50.58	48.31	47.37	46.41	45.42	44.40	43.88	43.41
6	69.73	68.10	61.21	58.21	55.04	51.65	48.01	46.08	44.26
7	74.31	68.15	62.66	59.74	56.66	53.38	49.88	48.02	46.29
8	75.48	69.39	66.52	65.28	62.48	59.55	56.46	54.84	53.34
	Percent difference								
1	-0.07%	-0.06%	-0.05%	-0.05%	-0.05%	-0.04%	-0.04%	-0.04%	-0.03%
2	-0.04%	-0.02%	0.02%	0.04%	0.08%	0.15%	0.30%	0.48%	0.93%
3	-0.03%	-0.02%	0.01%	0.03%	0.05%	0.08%	0.12%	0.15%	0.18%
4	-0.06%	-0.05%	-0.04%	-0.04%	-0.03%	-0.03%	-0.02%	-0.02%	-0.01%
5	-0.11%	-0.11%	-0.11%	-0.11%	-0.11%	-0.11%	-0.11%	-0.11%	-0.11%
6	-0.14%	-0.14%	-0.15%	-0.16%	-0.17%	-0.18%	-0.19%	-0.20%	-0.21%
7	-0.14%	-0.14%	-0.05%	-0.04%	-0.03%	-0.02%	-0.01%	0.00%	0.00%
8	-0.08%	-0.07%	-0.14%	-0.08%	-0.07%	-0.07%	-0.06%	-0.06%	-0.05%

Figure 4.76 Eigenvalue curves, CFCF plate, $\phi = 2 / 1$,

$P_\xi = - N_x b^2 / D$, $\lambda^2 = \omega a^2 (\rho / D)^{1/2}$.

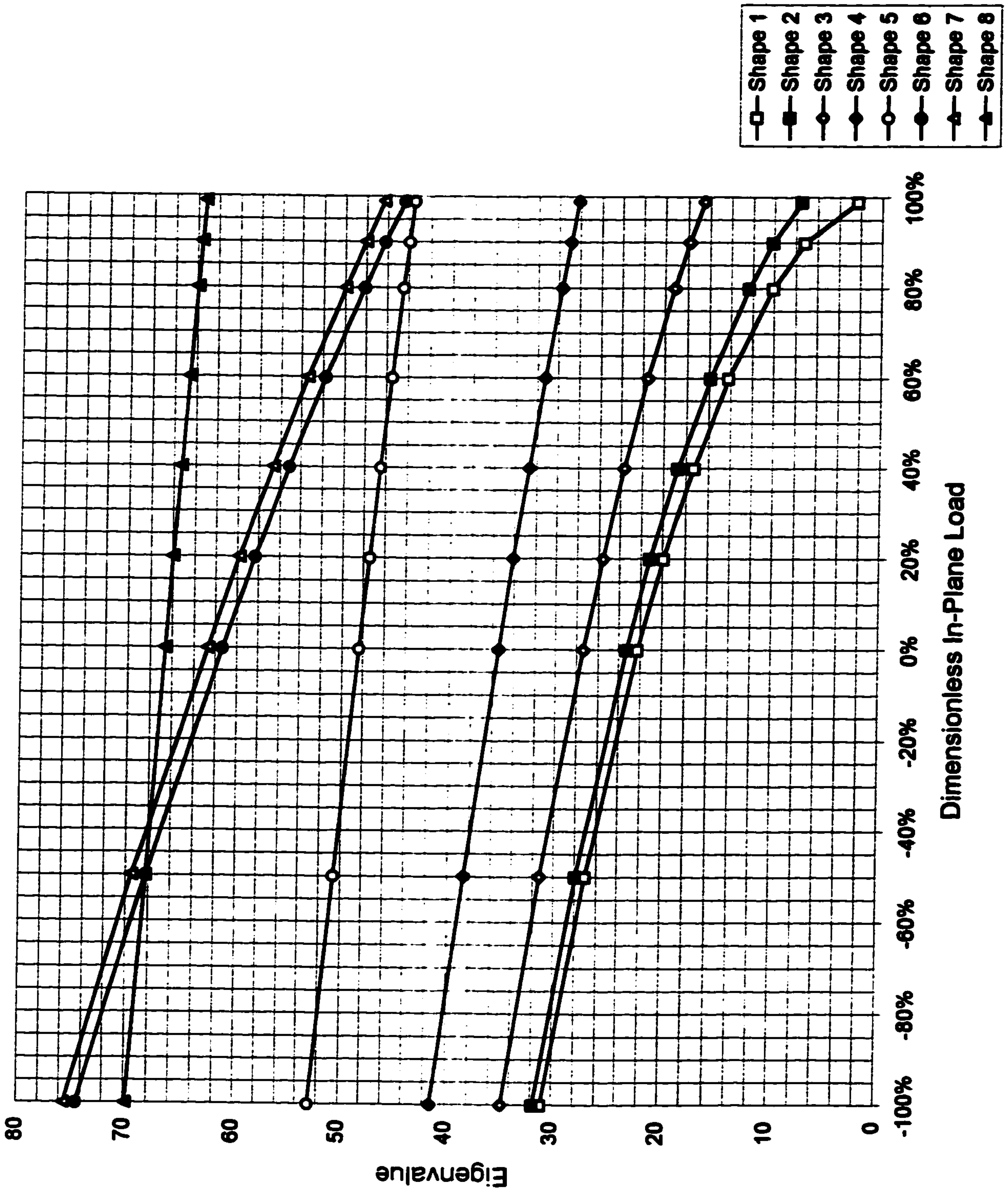

Figure 4.77 Mode shapes, CFCF plate, $\phi = 2 / 1$.

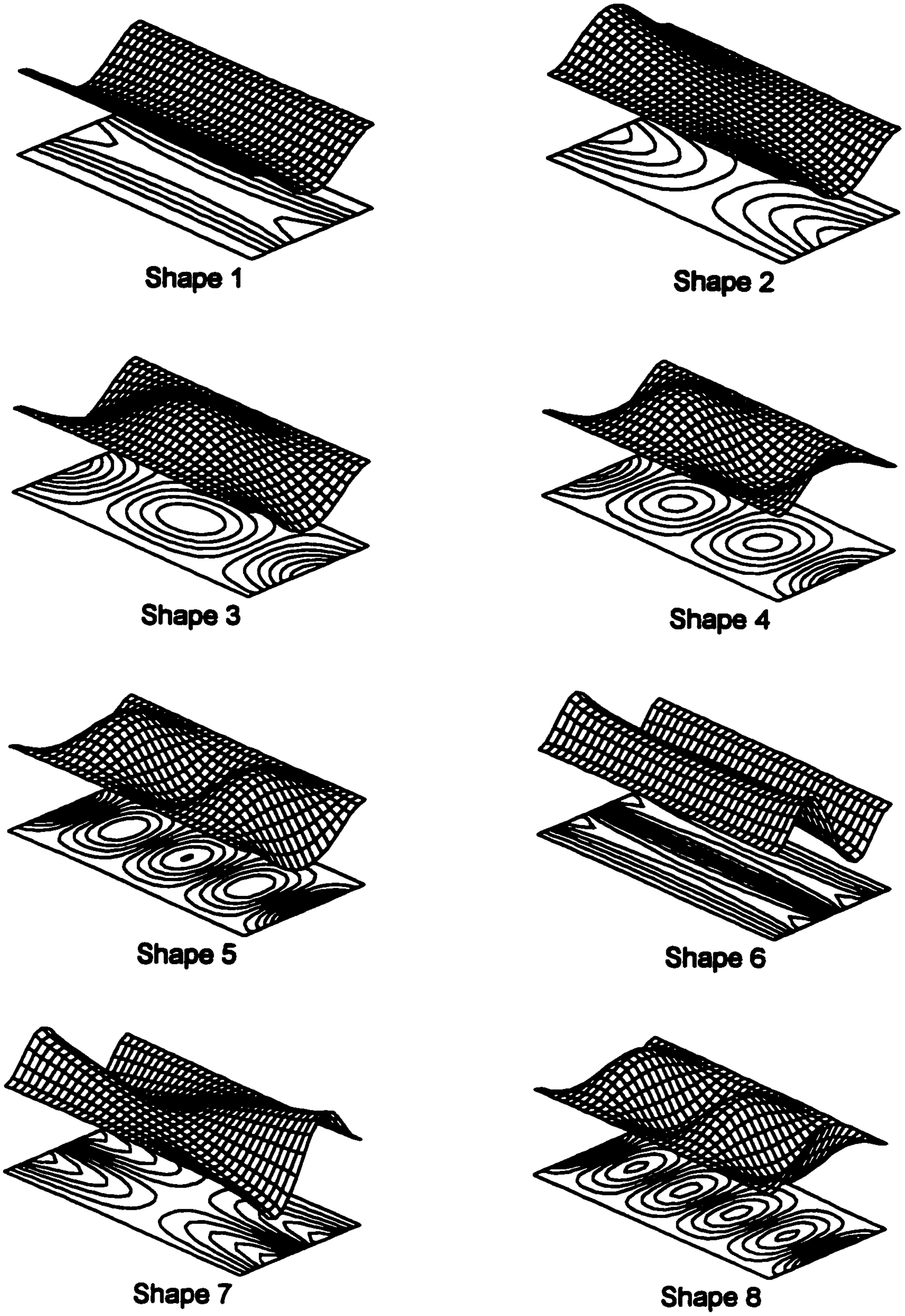

Table 4.45 Eigenvalues, CFCF plate, $\phi = 5 / 2$, $\lambda^2 = \omega a^2 (\rho / D)^{1/2}$.

Mode	In-plane load as a percentage of buckling load								
	-100%	-50%	0%	20%	40%	60%	80%	90%	99%
	Present solution								
1	31.07	27.06	22.25	19.96	17.34	14.21	10.09	7.15	2.27
2	31.54	27.60	22.92	20.71	18.21	15.27	11.55	9.11	6.10
3	33.41	29.76	25.51	23.57	21.44	19.04	16.26	14.65	13.03
4	37.25	34.04	30.45	28.87	27.19	25.38	23.41	22.35	21.35
5	43.86	41.21	38.34	37.12	35.85	34.53	33.14	32.42	31.76
6	53.86	51.75	49.53	48.61	47.67	46.70	45.71	45.20	44.39
7	67.50	65.85	61.37	58.36	55.18	51.79	48.14	46.21	44.74
8	74.49	68.27	62.21	59.25	56.13	52.80	49.23	47.34	45.57
	Finite element solution [18]								
1	31.04	27.04	22.23	19.95	17.33	14.21	10.09	7.15	2.27
2	31.52	27.59	22.92	20.72	18.23	15.30	11.59	9.17	6.19
3	33.39	29.74	25.51	23.57	21.45	19.05	16.28	14.68	13.07
4	37.22	34.02	30.44	28.86	27.18	25.37	23.41	22.35	21.35
5	43.80	41.15	38.28	37.07	35.80	34.48	33.09	32.37	31.71
6	53.75	51.64	49.43	48.51	47.56	46.59	45.60	45.09	44.27
7	67.35	65.70	61.25	58.25	55.06	51.67	48.03	46.09	44.63
8	74.36	68.14	62.17	59.21	56.09	52.78	49.22	47.33	45.57
	Percent difference								
1	-0.09%	-0.08%	-0.07%	-0.07%	-0.06%	-0.05%	-0.05%	-0.05%	-0.03%
2	-0.06%	-0.04%	0.01%	0.03%	0.08%	0.16%	0.36%	0.63%	1.52%
3	-0.06%	-0.04%	-0.01%	0.02%	0.04%	0.08%	0.15%	0.21%	0.29%
4	-0.08%	-0.07%	-0.05%	-0.05%	-0.03%	-0.02%	-0.01%	0.00%	0.00%
5	-0.14%	-0.14%	-0.14%	-0.14%	-0.15%	-0.15%	-0.15%	-0.15%	-0.16%
6	-0.20%	-0.21%	-0.21%	-0.22%	-0.22%	-0.23%	-0.23%	-0.24%	-0.25%
7	-0.22%	-0.23%	-0.19%	-0.19%	-0.20%	-0.22%	-0.23%	-0.24%	-0.24%
8	-0.17%	-0.18%	-0.08%	-0.07%	-0.06%	-0.05%	-0.03%	-0.02%	-0.01%

Figure 4.78 Eigenvalue curves, CFCF plate, $\phi = 5 / 2$,

$P_\xi = - N_x b^2 / D$, $\lambda^2 = \omega a^2 (\rho / D)^{1/2}$.

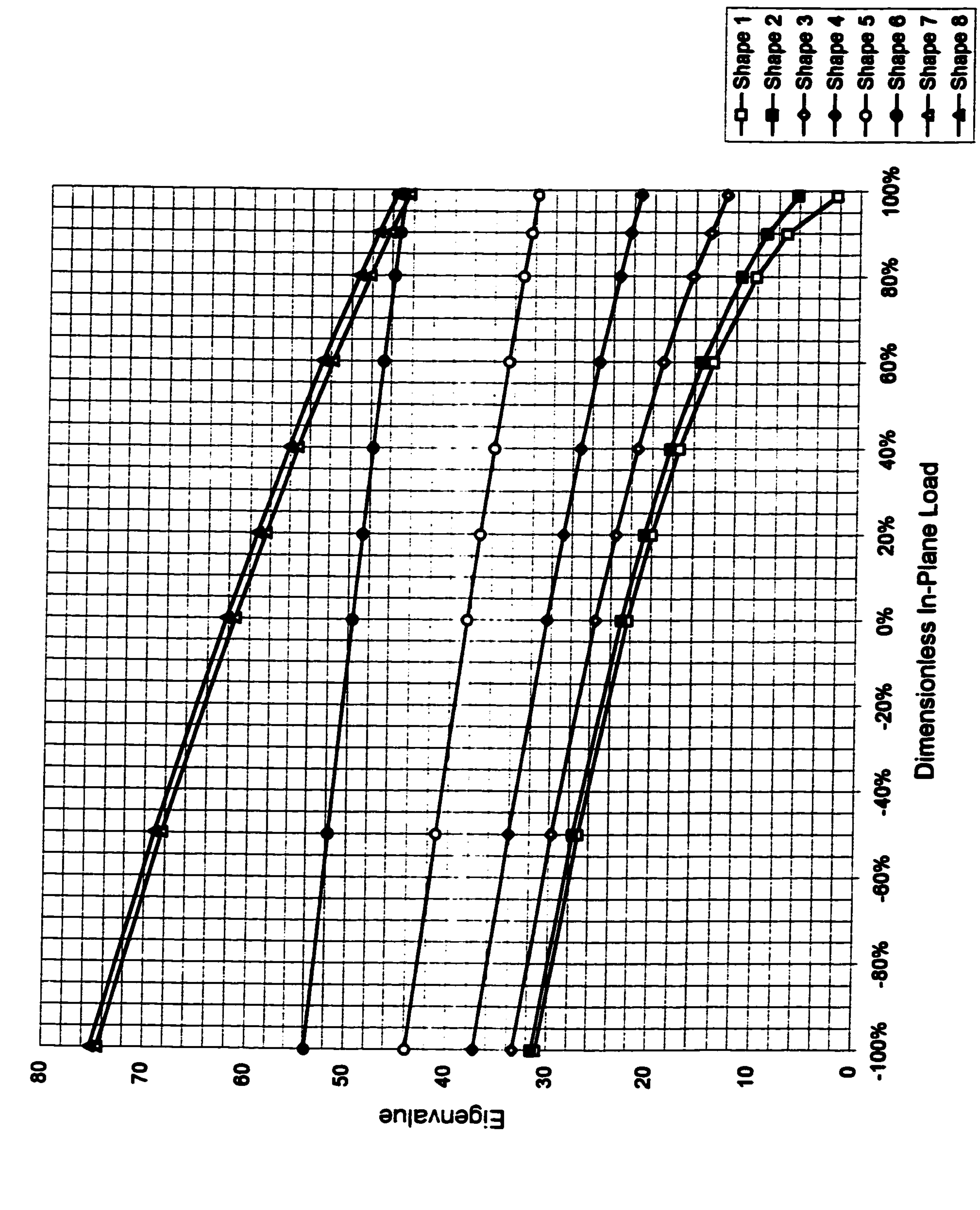

Figure 4.79 Mode shapes, CFCF plate, $\phi = 5 / 2$.

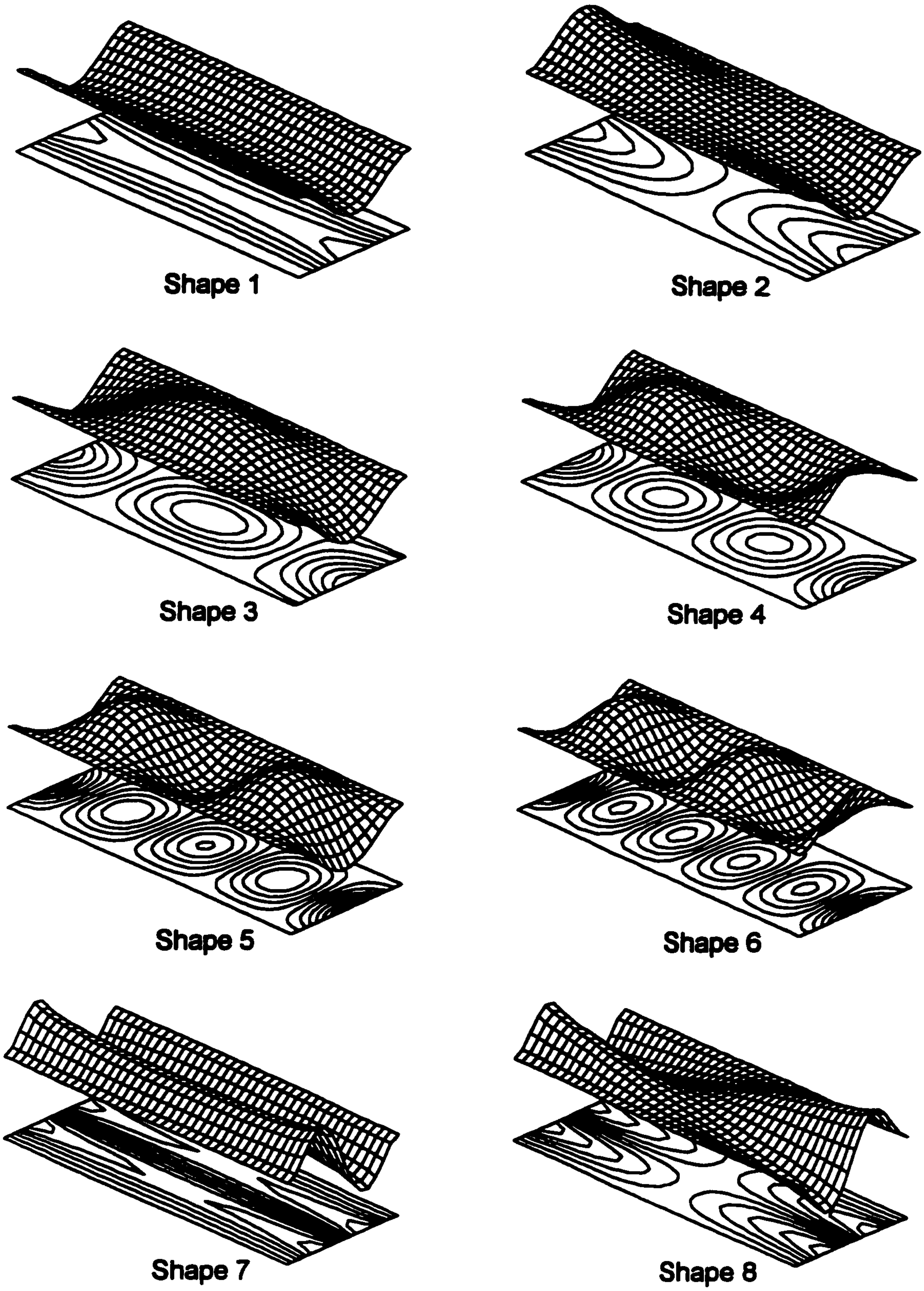

Table 4.46 Eigenvalues, CFCF plate, $\phi = 3 / 1$, $\lambda^2 = \omega a^2 (\rho / D)^{1/2}$.

Mode	In-plane load as a percentage of buckling load								
	-100%	-50%	0%	20%	40%	60%	80%	90%	99%
	Present solution								
1	31.09	27.08	22.26	19.97	17.36	14.22	10.10	7.16	2.27
2	31.41	27.45	22.72	20.49	17.95	14.95	11.11	8.53	5.18
3	32.69	28.93	24.51	22.48	20.21	17.63	14.56	12.73	10.80
4	35.20	31.76	27.84	26.09	24.19	22.11	19.79	18.51	17.27
5	39.41	36.41	33.09	31.64	30.12	28.51	26.79	25.87	25.02
6	45.79	43.25	40.54	39.39	38.20	36.96	35.67	35.00	34.39
7	54.61	52.52	50.34	49.43	48.50	47.55	46.57	46.07	44.41
8	65.98	64.28	61.40	58.40	55.21	51.82	48.17	46.23	45.19
	Finite element solution [18]								
1	31.06	27.06	22.25	19.96	17.35	14.22	10.09	7.15	2.27
2	31.39	27.44	22.72	20.49	17.96	14.97	11.15	8.60	5.30
3	32.66	28.91	24.51	22.48	20.22	17.65	14.58	12.76	10.84
4	35.16	31.73	27.82	26.07	24.18	22.10	19.79	18.51	17.27
5	39.35	36.35	33.03	31.59	30.07	28.46	26.74	25.82	24.97
6	45.67	43.14	40.43	39.27	38.08	36.85	35.56	34.89	34.28
7	54.43	52.35	50.16	49.25	48.32	47.37	46.39	45.90	44.29
8	65.75	64.06	61.28	58.27	55.09	51.70	48.05	46.11	45.19
	Percent difference								
1	-0.10%	-0.09%	-0.08%	-0.07%	-0.07%	-0.06%	-0.05%	-0.04%	0.13%
2	-0.07%	-0.04%	0.01%	0.04%	0.09%	0.18%	0.42%	0.79%	2.29%
3	-0.08%	-0.05%	-0.02%	0.01%	0.04%	0.08%	0.17%	0.26%	0.40%
4	-0.10%	-0.08%	-0.07%	-0.05%	-0.04%	-0.03%	0.00%	0.01%	0.03%
5	-0.16%	-0.16%	-0.16%	-0.16%	-0.17%	-0.17%	-0.18%	-0.19%	-0.19%
6	-0.25%	-0.26%	-0.27%	-0.28%	-0.29%	-0.30%	-0.32%	-0.33%	-0.33%
7	-0.32%	-0.33%	-0.34%	-0.35%	-0.36%	-0.37%	-0.38%	-0.39%	-0.27%
8	-0.33%	-0.34%	-0.20%	-0.21%	-0.22%	-0.23%	-0.25%	-0.26%	-0.01%

Figure 4.80 Eigenvalue curves, CFCF plate, $\phi = 3 / 1$,
$P_\xi = - N_x b^2 / D$, $\lambda^2 = \omega a^2 (\rho / D)^{1/2}$.

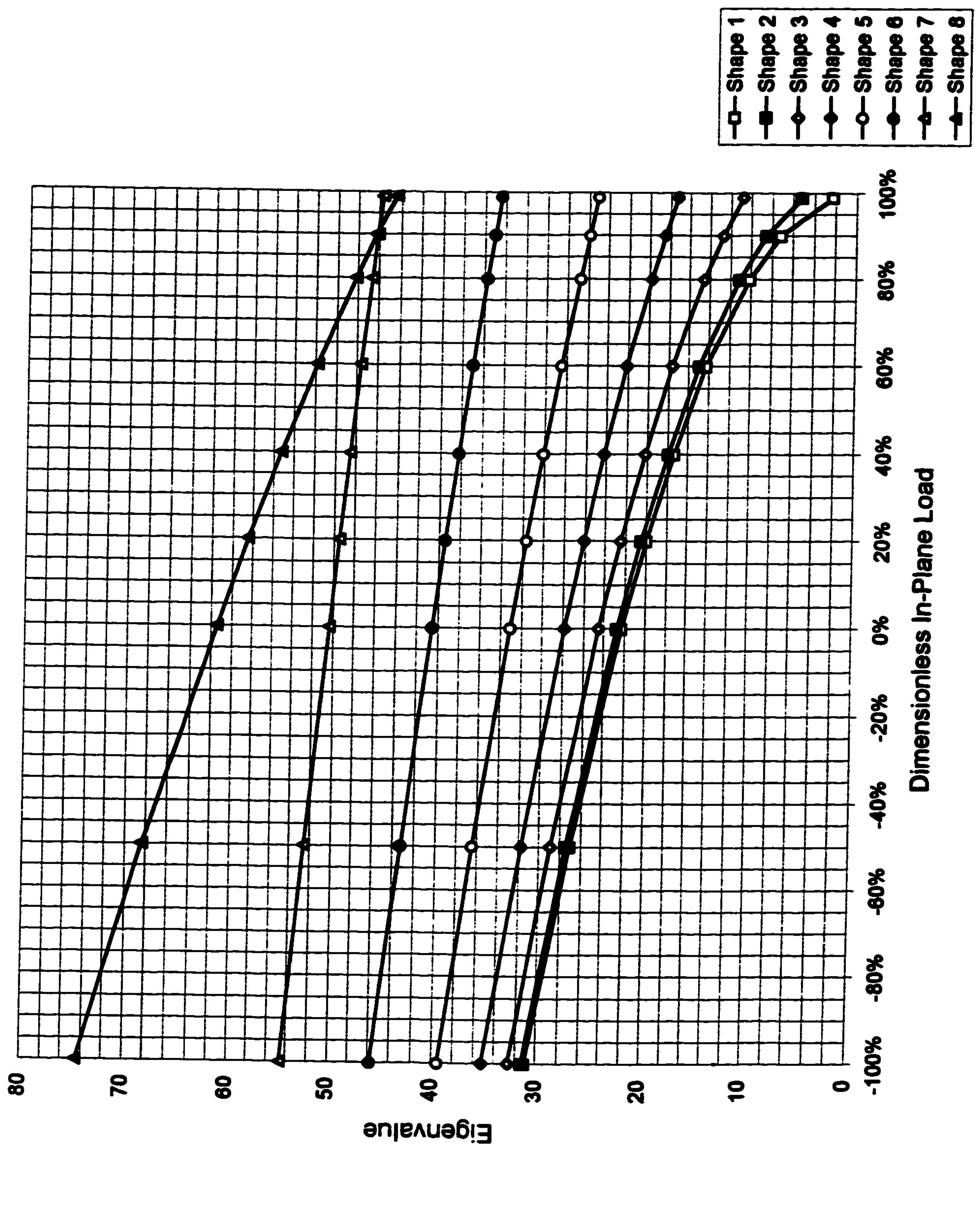

Figure 4.81 Mode shapes, CFCF plate, $\phi = 3 / 1$.

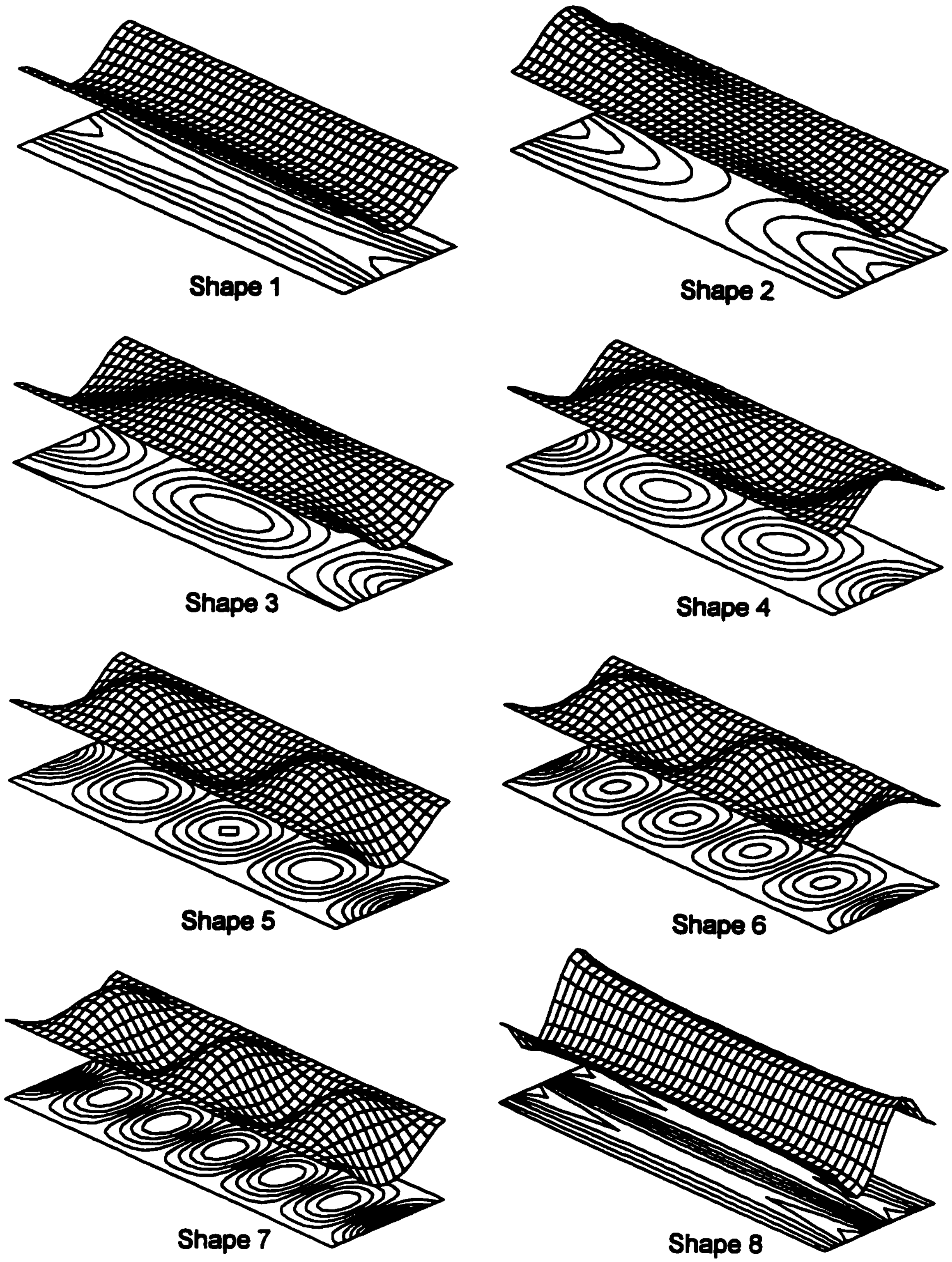

Table 4.47 Eigenvalues, SCSF plate, $\phi = 1/3$, $\lambda^2 = \omega a^2 (\rho / D)^{1/2}$.

Mode	In-plane load as a percentage of buckling load								
	-100%	-50%	0%	20%	40%	60%	80%	90%	99%
				Present solution					
1	51.87	46.25	39.85	36.97	33.86	30.43	26.56	21.00	6.64
2	93.92	81.34	66.41	59.40	51.44	42.00	29.70	24.40	22.27
3	150.66	133.18	113.02	103.87	93.84	82.59	69.54	62.00	54.32
4	212.46	202.88	179.83	169.74	159.01	147.50	135.01	128.31	121.96
5	223.56	211.16	209.85	209.32	208.79	208.27	207.74	207.47	207.23
6	252.09	247.68	243.19	241.37	239.53	233.63	221.52	215.21	209.37
7	312.36	291.38	266.69	256.14	245.15	237.69	235.82	234.89	234.04
8	314.15	304.31	296.05	292.68	289.27	285.82	282.32	280.56	278.96
				Finite element solution [18]					
1	51.85	46.24	39.83	36.96	33.85	30.42	26.55	21.00	6.63
2	93.90	81.32	66.40	59.39	51.43	41.99	29.69	24.38	22.26
3	150.70	133.23	113.10	103.95	93.93	82.69	69.67	62.15	54.49
4	212.18	203.17	180.17	170.11	159.40	147.93	135.48	128.80	122.48
5	223.83	210.88	209.57	209.04	208.52	207.99	207.45	207.19	206.95
6	251.62	247.19	242.70	240.87	239.03	234.72	222.68	216.41	210.60
7	311.47	292.26	267.64	257.14	246.19	237.19	235.31	234.38	233.53
8	314.95	303.40	295.12	291.73	288.31	284.85	281.34	279.58	277.97
				Percent difference					
1	-0.02%	-0.03%	-0.03%	-0.04%	-0.04%	-0.04%	-0.05%	-0.03%	-0.12%
2	-0.02%	-0.02%	-0.02%	-0.02%	-0.02%	-0.02%	-0.02%	-0.06%	-0.07%
3	0.03%	0.04%	0.06%	0.07%	0.10%	0.13%	0.19%	0.24%	0.32%
4	-0.13%	0.15%	0.19%	0.22%	0.25%	0.29%	0.35%	0.39%	0.43%
5	0.12%	-0.13%	-0.13%	-0.13%	-0.13%	-0.13%	-0.14%	-0.13%	-0.13%
6	-0.19%	-0.20%	-0.20%	-0.20%	-0.21%	0.47%	0.52%	0.56%	0.59%
7	-0.28%	0.30%	0.36%	0.39%	0.42%	-0.21%	-0.22%	-0.22%	-0.22%
8	0.26%	-0.30%	-0.32%	-0.32%	-0.33%	-0.34%	-0.35%	-0.35%	-0.35%

Figure 4.82 Eigenvalue curves, SCSF plate, $\phi = 1 / 3$, $P_\xi = - N_x b^2 / D$, $\lambda^2 = \omega a^2 (\rho / D)^{1/2}$.

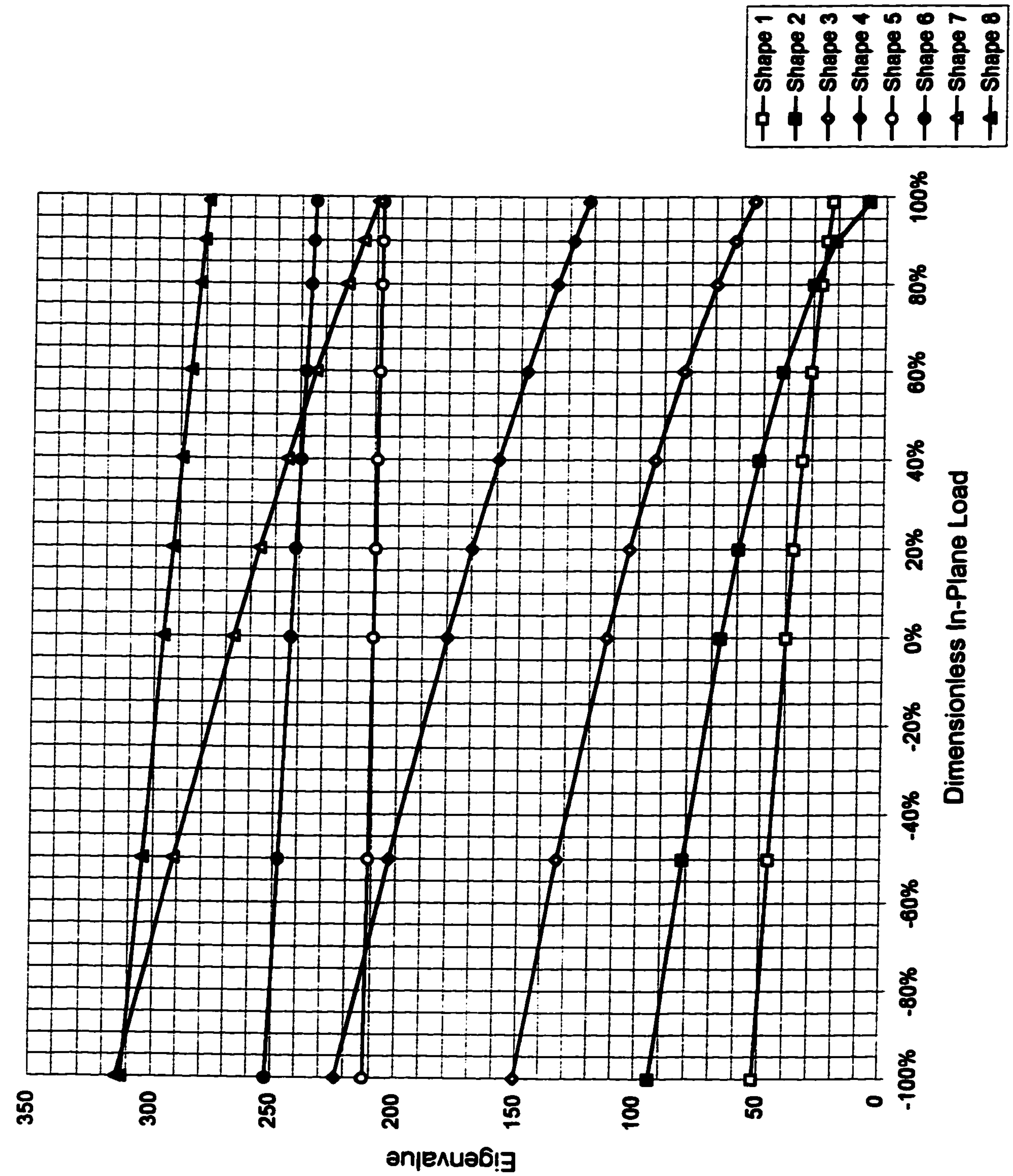

Figure 4.83 Mode shapes, SCŜF plate, $\phi = 1 / 3$.

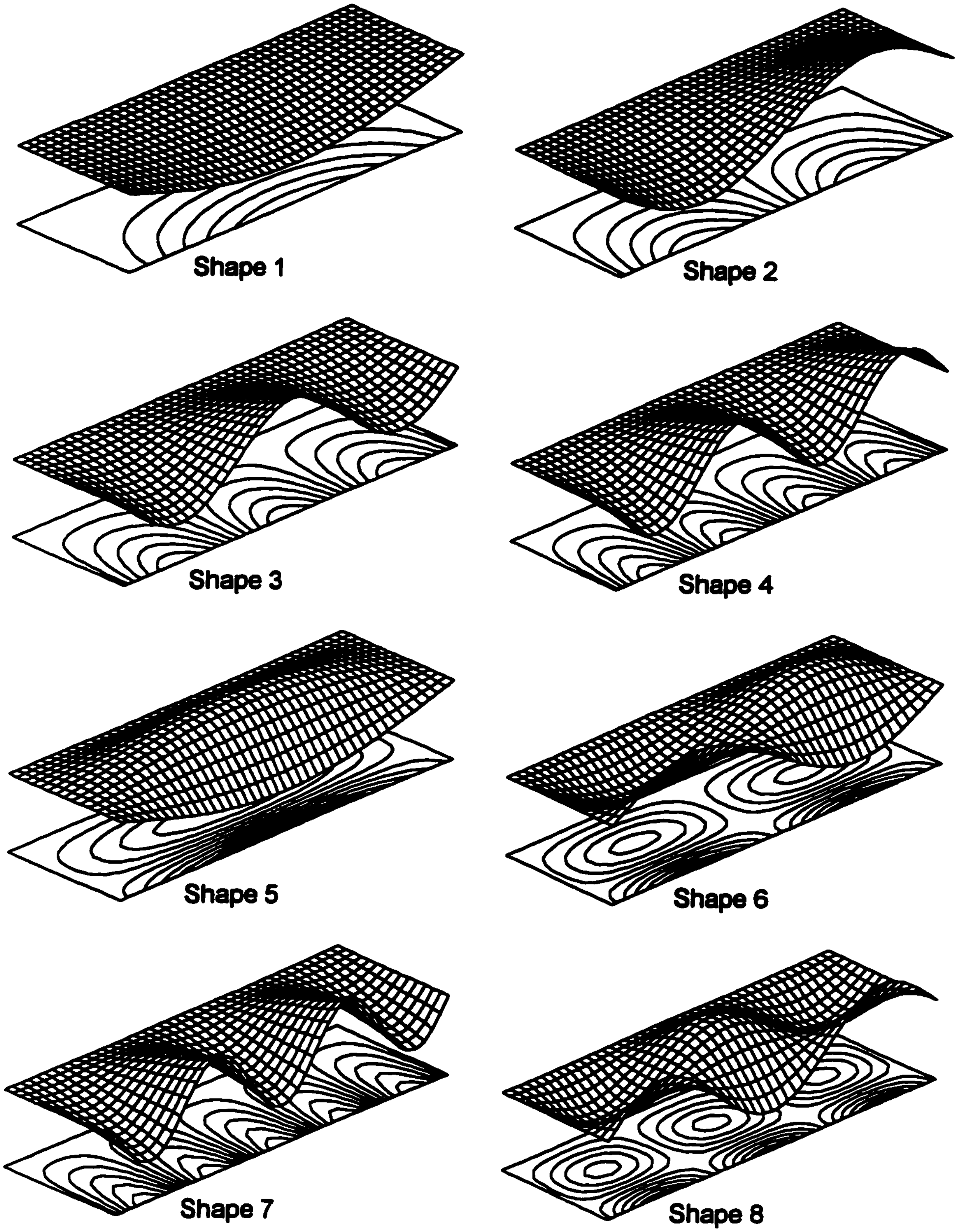

Table 4.48 Eigenvalues, SCSF plate, $\phi = 2 / 5$, $\lambda^2 = \omega a^2 (\rho / D)^{1/2}$.

Mode	In-plane load as a percentage of buckling load								
	-100%	-50%	0%	20%	40%	60%	80%	90%	99%
	Present solution								
1	41.71	36.45	30.28	27.42	24.24	20.56	16.07	13.26	5.74
2	81.15	70.28	57.38	51.32	44.45	36.29	25.66	18.15	10.09
3	135.50	121.06	104.65	97.31	89.38	80.66	70.89	65.45	60.15
4	151.93	150.57	149.20	148.65	148.09	147.28	138.05	133.19	128.67
5	190.84	186.48	172.03	164.19	155.97	147.54	146.98	146.70	146.44
6	206.79	190.21	182.01	180.19	178.35	176.50	174.62	173.68	172.82
7	249.06	241.51	233.72	230.53	227.29	224.01	220.68	218.99	216.55
8	296.39	278.49	259.36	251.30	242.97	234.35	225.40	220.79	217.46
	Finite element solution [18]								
1	41.71	36.44	30.27	27.42	24.23	20.55	16.05	13.24	5.73
2	81.16	70.28	57.39	51.33	44.45	36.29	25.66	18.15	10.06
3	135.58	121.16	104.75	97.43	89.49	80.79	71.03	65.61	60.31
4	151.76	150.39	149.02	148.47	147.92	147.36	138.52	133.68	129.17
5	190.53	186.16	172.42	164.60	156.39	147.72	146.80	146.52	146.26
6	207.12	190.56	181.68	179.86	178.02	176.16	174.28	173.34	172.48
7	248.48	240.91	233.09	229.89	226.64	223.35	220.01	218.32	216.79
8	297.26	279.41	260.35	252.32	244.02	235.43	226.53	221.93	217.72
	Percent difference								
1	-0.01%	-0.01%	-0.02%	-0.03%	-0.04%	-0.07%	-0.11%	-0.17%	-0.02%
2	0.01%	0.01%	0.01%	0.01%	0.01%	0.01%	0.01%	0.01%	-0.30%
3	0.06%	0.08%	0.10%	0.12%	0.13%	0.15%	0.20%	0.23%	0.28%
4	-0.12%	-0.12%	-0.12%	-0.12%	-0.12%	0.05%	0.34%	0.37%	0.39%
5	-0.16%	-0.17%	0.23%	0.24%	0.27%	0.13%	-0.12%	-0.12%	-0.12%
6	0.16%	0.19%	-0.18%	-0.18%	-0.19%	-0.19%	-0.19%	-0.20%	-0.20%
7	-0.23%	-0.25%	-0.27%	-0.28%	-0.28%	-0.29%	-0.30%	-0.31%	0.11%
8	0.29%	0.33%	0.38%	0.41%	0.43%	0.46%	0.50%	0.52%	0.12%

Figure 4.84 Eigenvalue curves, SCSF plate, $\phi = 2 / 5$,
$P_\xi = - N_x b^2 / D$, $\lambda^2 = \omega a^2 (\rho / D)^{1/2}$.

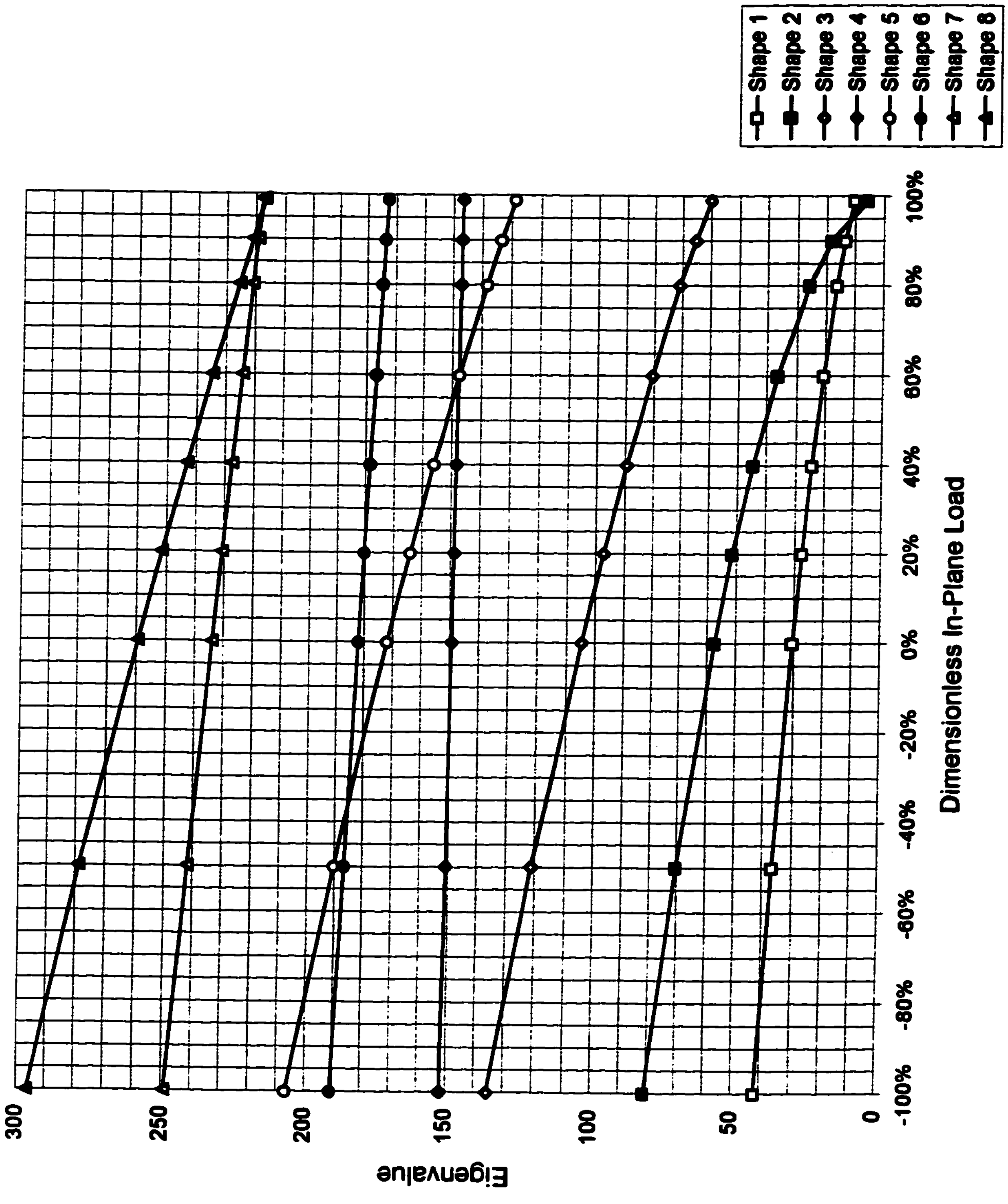

Figure 4.85 Mode shapes, SCSF plate, $\phi = 2 / 5$.

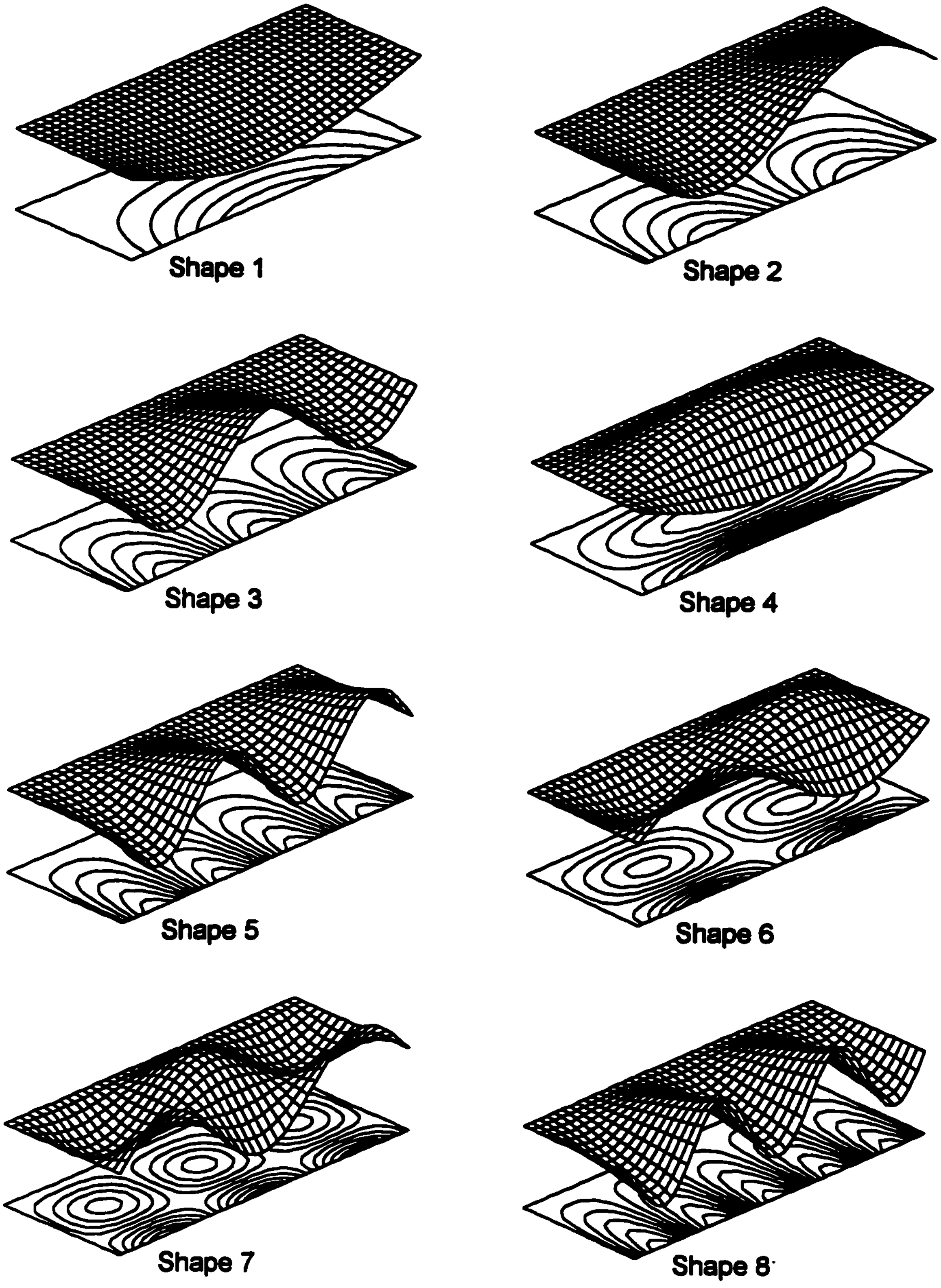

Table 4.49 Eigenvalues, SCSF plate, $\phi = 1/2$, $\lambda^2 = \omega a^2 (\rho / D)^{1/2}$.

Mode	In-plane load as a percentage of buckling load								
	-100%	-50%	0%	20%	40%	60%	80%	90%	99%
	Present solution								
1	31.85	27.58	22.52	20.14	17.44	14.24	10.07	7.12	2.25
2	67.47	59.48	50.23	46.02	41.38	36.14	30.01	26.41	22.69
3	102.05	100.80	98.12	93.35	88.32	83.00	77.30	74.29	71.47
4	119.13	109.13	99.53	99.02	98.51	97.99	97.47	97.21	96.98
5	139.07	135.38	131.58	130.03	128.46	126.87	125.26	124.45	123.71
6	188.86	177.79	165.99	161.03	155.91	150.61	145.12	142.30	139.71
7	194.15	188.18	182.02	179.49	176.93	174.33	171.69	170.36	169.15
8	258.43	257.94	250.86	247.61	243.52	238.26	232.88	230.14	227.65
	Finite element solution [18]								
1	31.84	27.58	22.52	20.14	17.44	14.24	10.07	7.12	2.25
2	67.48	59.50	50.25	46.04	41.40	36.17	30.05	26.46	22.75
3	101.95	100.70	98.24	93.48	88.46	83.14	77.46	74.46	71.64
4	119.23	109.24	99.43	98.92	98.41	97.89	97.37	97.11	96.88
5	138.90	135.19	131.39	129.84	128.27	126.68	125.06	124.25	123.51
6	189.20	178.15	166.38	161.43	156.32	151.04	145.57	142.76	140.18
7	193.82	187.84	181.67	179.14	176.57	173.96	171.33	169.99	168.77
8	257.90	257.40	250.32	247.06	243.75	239.26	233.90	231.17	228.69
	Percent difference								
1	-0.01%	-0.01%	-0.01%	-0.01%	-0.01%	-0.01%	-0.02%	-0.02%	-0.19%
2	0.02%	0.03%	0.04%	0.05%	0.06%	0.09%	0.13%	0.17%	0.23%
3	-0.09%	-0.10%	0.13%	0.14%	0.16%	0.18%	0.21%	0.23%	0.24%
4	0.08%	0.10%	-0.10%	-0.10%	-0.10%	-0.10%	-0.10%	-0.10%	-0.10%
5	-0.13%	-0.14%	-0.14%	-0.14%	-0.15%	-0.15%	-0.16%	-0.16%	-0.16%
6	0.18%	0.20%	0.24%	0.25%	0.27%	0.29%	0.31%	0.32%	0.34%
7	-0.17%	-0.18%	-0.19%	-0.20%	-0.20%	-0.21%	-0.21%	-0.22%	-0.22%
8	-0.21%	-0.21%	-0.22%	-0.22%	0.09%	0.42%	0.44%	0.45%	0.46%

Figure 4.86 Eigenvalue curves, SCSF plate, $\phi = 1 / 2$,
$P_\xi = - N_x b^2 / D$, $\lambda^2 = \omega a^2 (\rho / D)^{1/2}$.

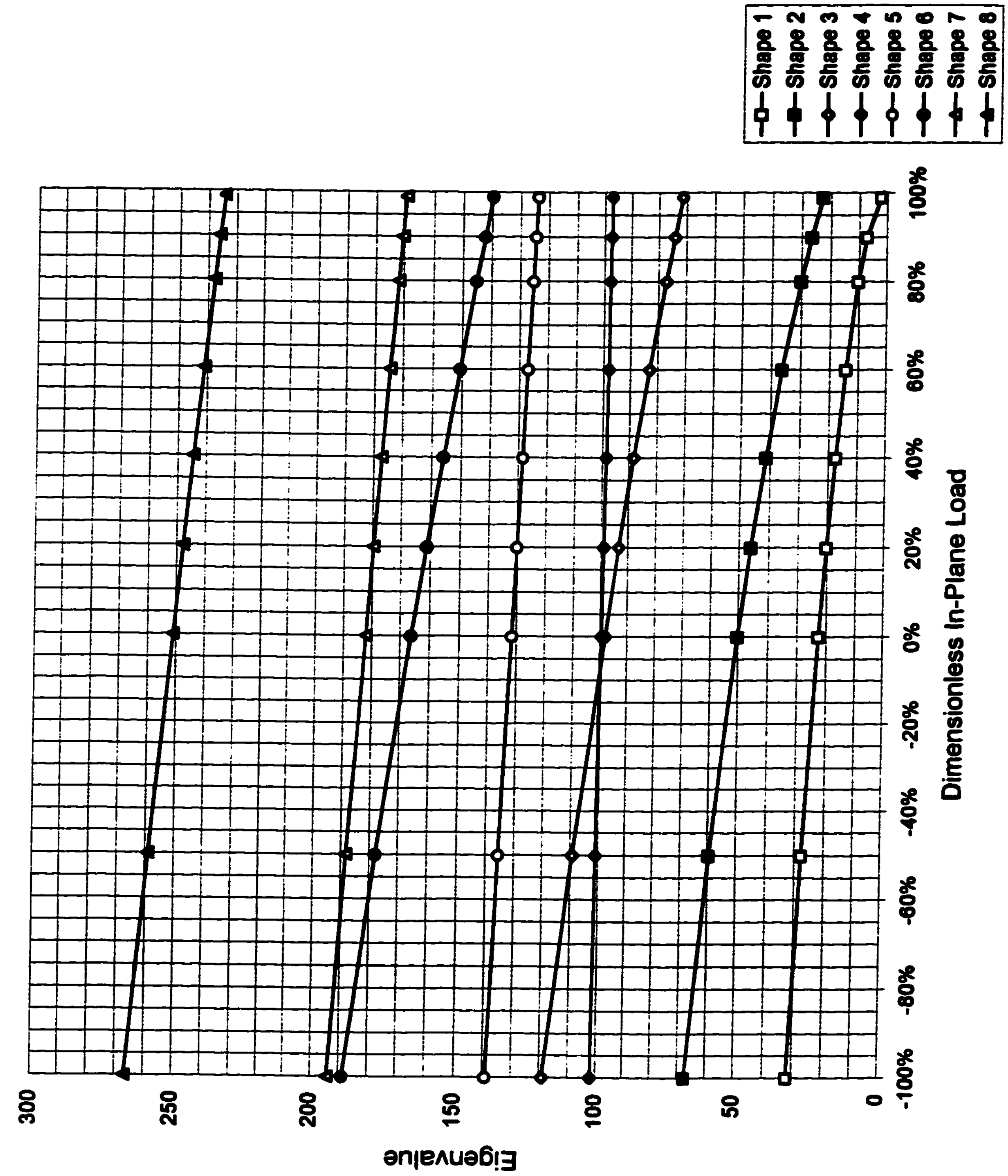

Figure 4.87 Mode shapes, SCSF plate, $\phi = 1 / 2$.

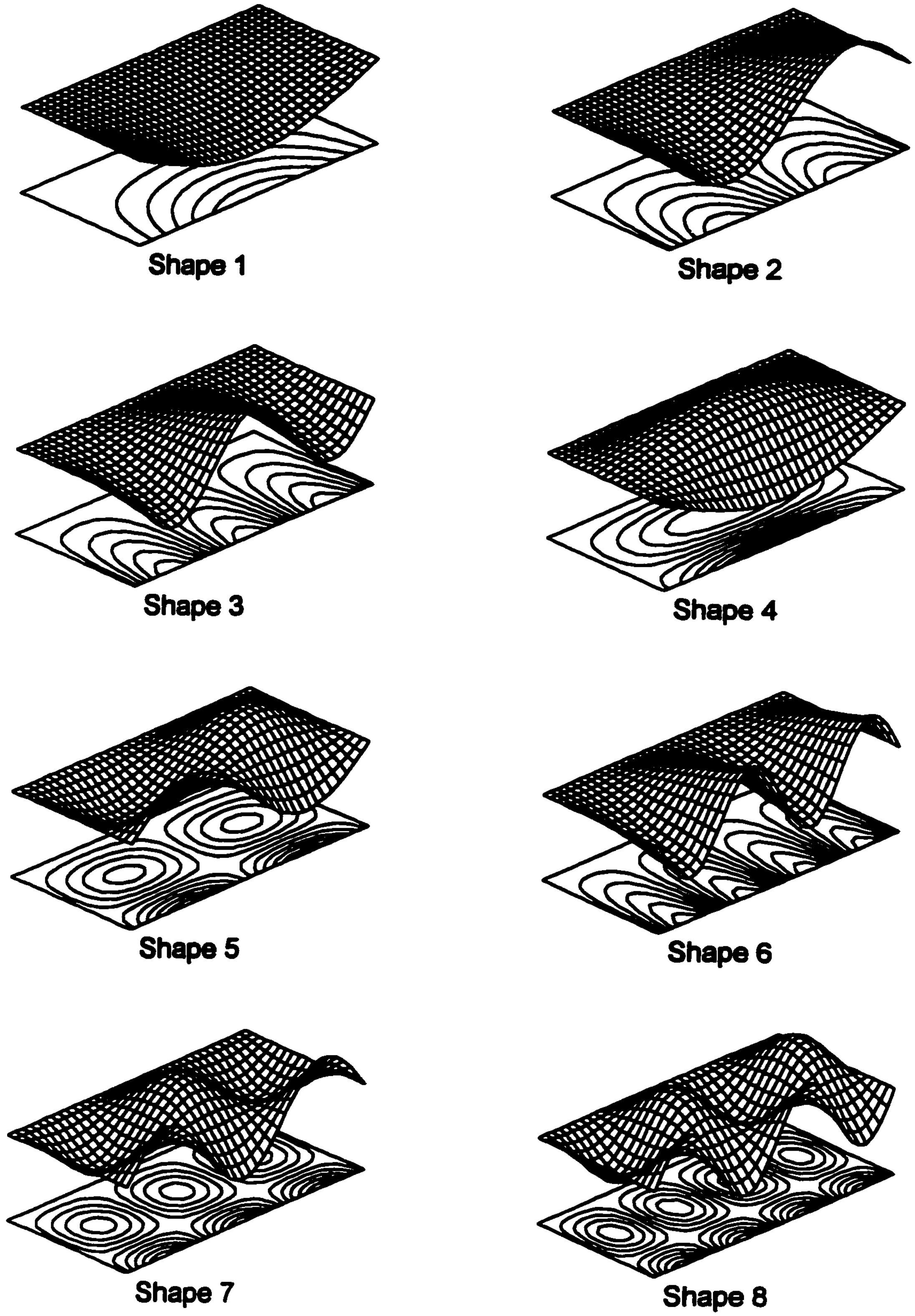

Table 4.50 Eigenvalues, SCSF plate, $\phi = 2/3$, $\lambda^2 = \omega a^2 (\rho / D)^{1/2}$.

Mode	In-plane load as a percentage of buckling load								
	-100%	-50%	0%	20%	40%	60%	80%	90%	99%
	Present solution								
1	23.48	20.33	16.60	14.85	12.86	10.50	7.42	5.25	1.66
2	55.89	50.72	44.96	42.43	39.75	36.87	33.75	32.08	30.49
3	63.02	61.92	60.80	60.34	59.88	59.42	58.96	58.72	58.51
4	97.61	94.75	91.79	90.58	87.89	85.03	82.06	80.53	79.13
5	105.82	99.79	93.37	90.67	89.36	88.12	86.86	86.22	85.64
6	149.64	145.44	141.11	139.34	137.55	135.73	133.89	132.96	132.12
7	150.37	149.91	149.45	149.27	149.08	148.90	148.71	148.62	147.52
8	174.76	168.33	161.65	158.89	156.09	153.24	150.34	148.86	148.54
	Finite element solution [18]								
1	23.48	20.34	16.60	14.85	12.86	10.50	7.43	5.25	1.66
2	55.91	50.74	44.98	42.46	39.78	36.90	33.79	32.11	30.53
3	62.98	61.88	60.76	60.30	59.84	59.38	58.91	58.68	58.47
4	97.54	94.67	91.71	90.50	88.02	85.15	82.19	80.66	79.27
5	105.93	99.90	93.49	90.79	89.28	88.03	86.77	86.13	85.56
6	149.52	145.31	140.98	139.21	137.41	135.59	133.75	132.82	131.98
7	150.16	149.70	149.24	149.05	148.87	148.68	148.50	148.40	147.88
8	175.06	168.65	161.98	159.23	156.43	153.59	150.69	149.22	148.32
	Percent difference								
1	0.01%	0.01%	0.01%	0.01%	0.01%	0.01%	0.01%	0.02%	0.18%
2	0.04%	0.05%	0.06%	0.07%	0.08%	0.08%	0.10%	0.11%	0.12%
3	-0.06%	-0.06%	-0.07%	-0.07%	-0.07%	-0.07%	-0.07%	-0.07%	-0.07%
4	-0.07%	-0.08%	-0.09%	-0.09%	0.14%	0.15%	0.16%	0.17%	0.17%
5	0.10%	0.11%	0.12%	0.13%	-0.09%	-0.10%	-0.10%	-0.10%	-0.10%
6	-0.08%	-0.09%	-0.09%	-0.10%	-0.10%	-0.10%	-0.11%	-0.11%	-0.11%
7	-0.14%	-0.14%	-0.14%	-0.14%	-0.14%	-0.14%	-0.15%	-0.15%	0.24%
8	0.18%	0.19%	0.21%	0.21%	0.22%	0.23%	0.24%	0.24%	-0.15%

Figure 4.88 Eigenvalue curves, SCSF plate, $\phi = 2 / 3$,

$P_\xi = - N_x b^2 / D$, $\lambda^2 = \omega a^2 (\rho / D)^{1/2}$.

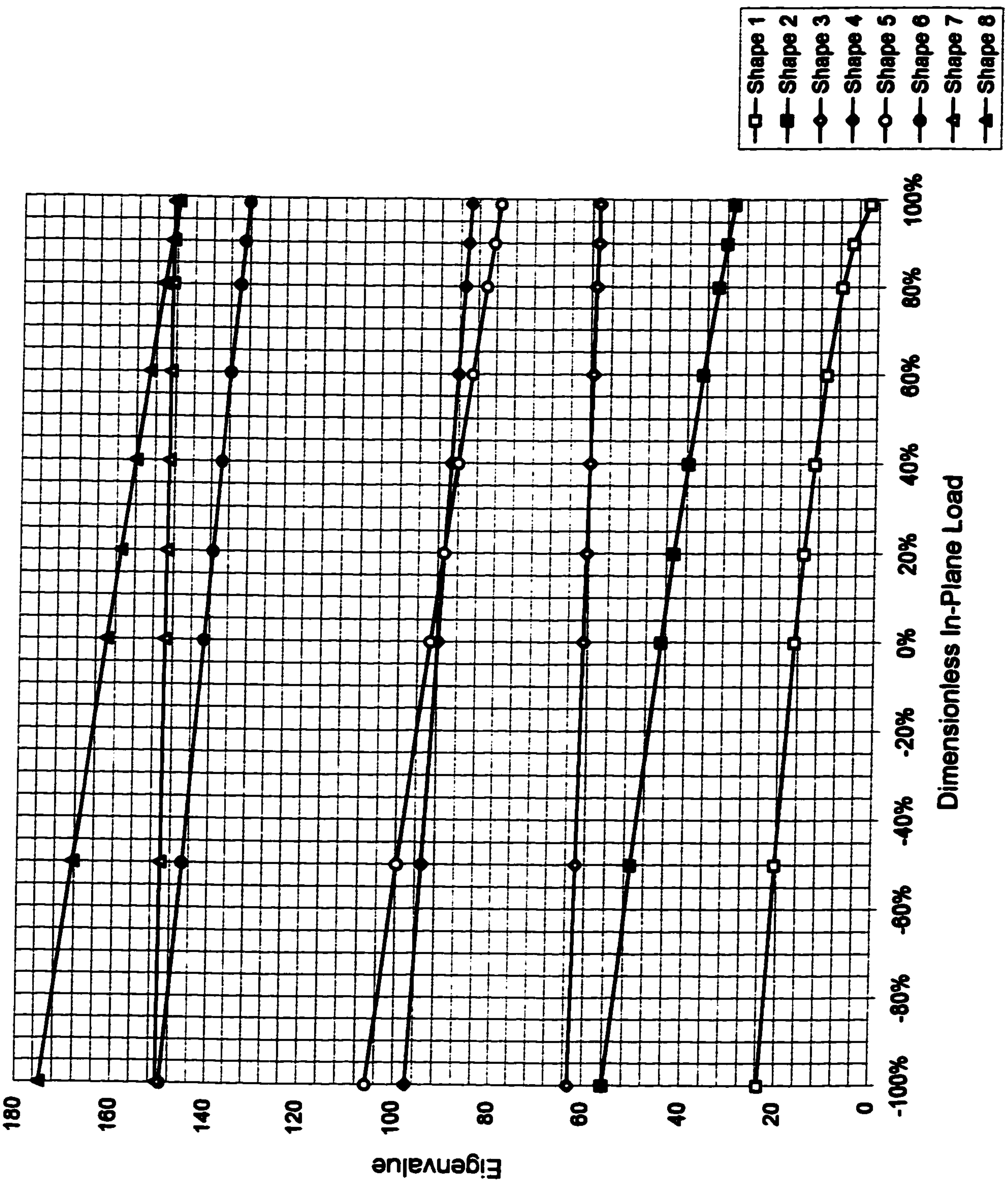

Figure 4.89 Mode shapes, SCSF plate, $\phi = 2 / 3$.

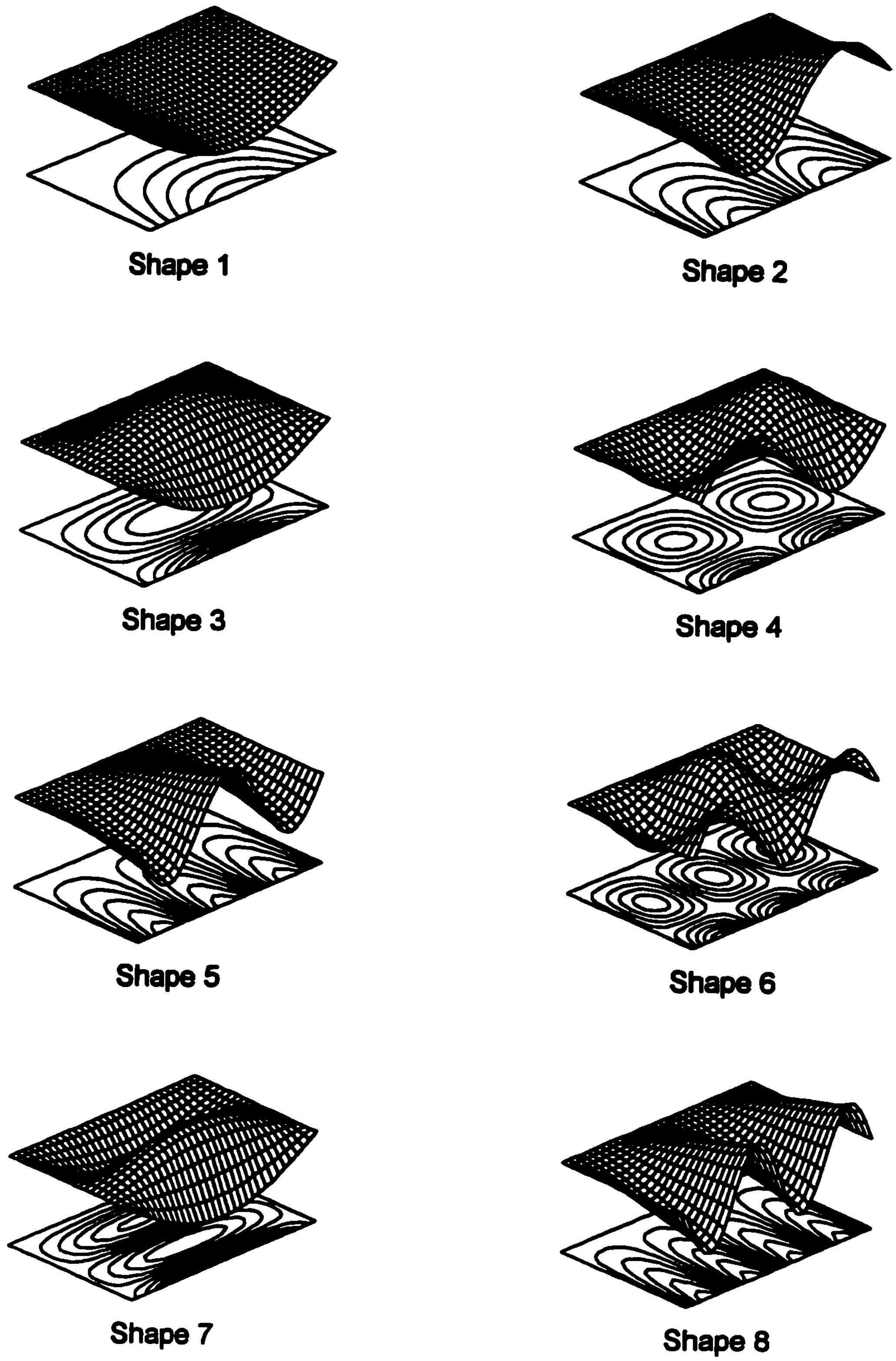

Table 4.51 Eigenvalues, SCSF plate, $\phi = 1 / 1$, $\lambda^2 = \omega a^2 (\rho / D)^{1/2}$.

Mode	In-plane load as a percentage of buckling load -100%	-50%	0%	20%	40%	60%	80%	90%	99%
					Present solution				
1	17.76	15.38	12.56	11.23	9.73	7.94	5.62	3.97	1.26
2	35.21	34.07	32.89	32.41	31.92	31.42	30.92	30.66	30.43
3	48.51	45.14	41.50	39.95	38.34	36.65	34.89	33.97	33.13
4	67.56	65.18	62.72	61.70	60.67	59.62	58.55	58.01	57.52
5	73.34	72.80	72.26	72.04	71.82	71.60	71.38	71.27	71.17
6	97.86	94.16	90.31	88.73	87.11	85.47	83.79	82.94	82.17
7	105.84	104.34	102.81	102.20	101.58	100.96	100.33	100.01	99.73
8	117.73	114.67	111.54	110.26	108.96	107.65	106.33	105.66	105.05
					Finite element solution [18]				
1	17.76	15.38	12.56	11.24	9.73	7.94	5.62	3.97	1.26
2	35.20	34.06	32.88	32.40	31.91	31.41	30.90	30.65	30.42
3	48.53	45.16	41.52	39.97	38.36	36.68	34.91	34.00	33.15
4	67.55	65.17	62.70	61.68	60.65	59.60	58.53	57.99	57.50
5	73.29	72.75	72.21	71.99	71.77	71.55	71.33	71.22	71.12
6	97.92	94.23	90.38	88.80	87.18	85.54	83.86	83.01	82.24
7	105.72	104.22	102.70	102.08	101.46	100.84	100.21	99.89	99.61
8	117.70	114.65	111.51	110.23	108.93	107.62	106.29	105.62	105.02
					Percent difference				
1	0.02%	0.02%	0.02%	0.03%	0.02%	0.02%	0.03%	0.03%	0.07%
2	-0.03%	-0.03%	-0.03%	-0.03%	-0.03%	-0.03%	-0.04%	-0.04%	-0.04%
3	0.04%	0.05%	0.05%	0.05%	0.06%	0.06%	0.06%	0.07%	0.07%
4	-0.02%	-0.02%	-0.03%	-0.03%	-0.03%	-0.03%	-0.03%	-0.03%	-0.04%
5	-0.07%	-0.07%	-0.07%	-0.07%	-0.07%	-0.07%	-0.07%	-0.07%	-0.07%
6	0.07%	0.07%	0.08%	0.08%	0.08%	0.08%	0.08%	0.09%	0.09%
7	-0.11%	-0.11%	-0.12%	-0.12%	-0.12%	-0.12%	-0.12%	-0.12%	-0.12%
8	-0.02%	-0.02%	-0.02%	-0.03%	-0.03%	-0.03%	-0.03%	-0.03%	-0.03%

Figure 4.90 Eigenvalue curves, SCSF plate, $\phi = 1 / 1$,
$P_\xi = - N_x b^2 / D$, $\lambda^2 = \omega a^2 (\rho / D)^{1/2}$.

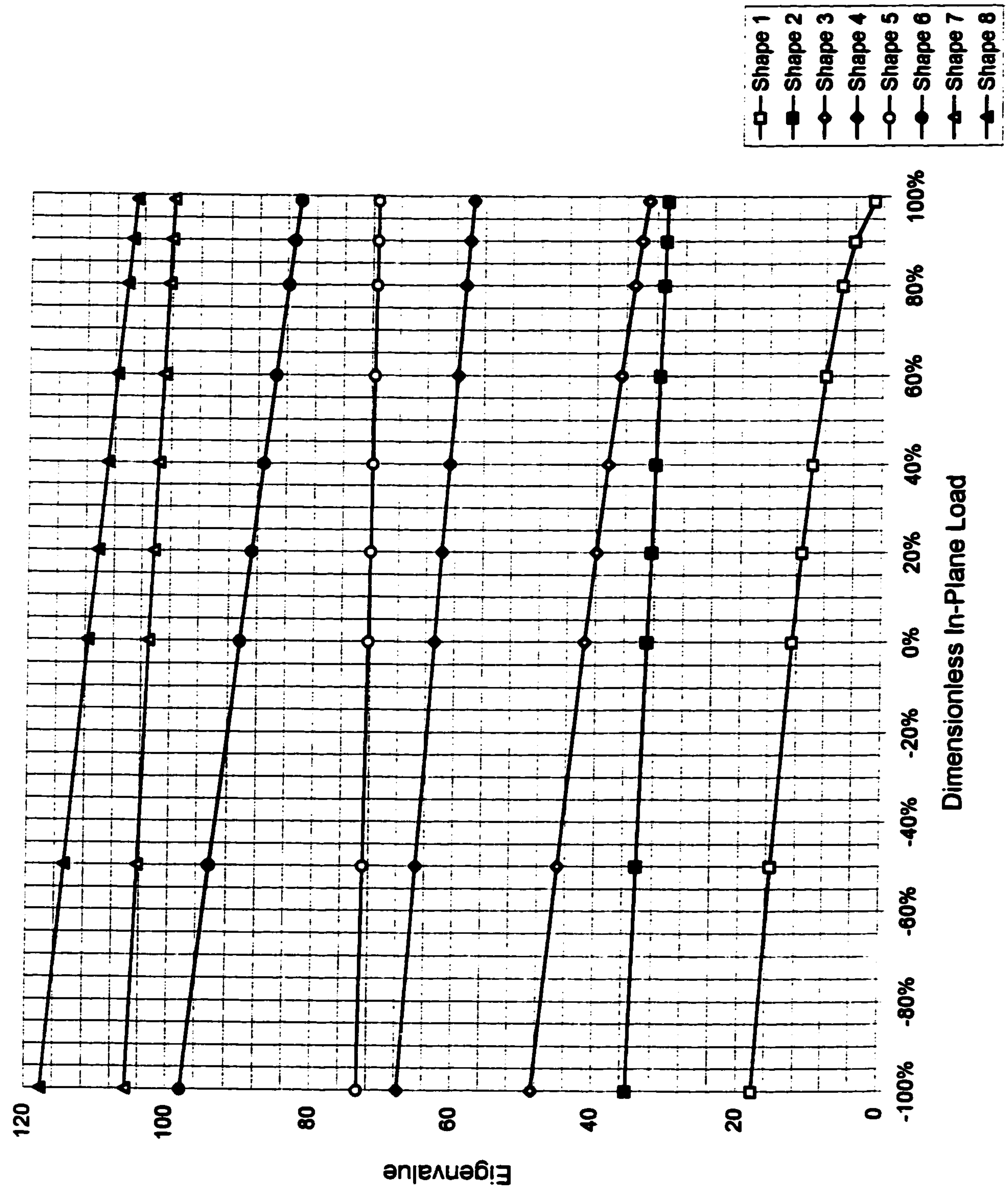

Figure 4.91 Mode shapes, SCSF plate, $\phi = 1 / 1$.

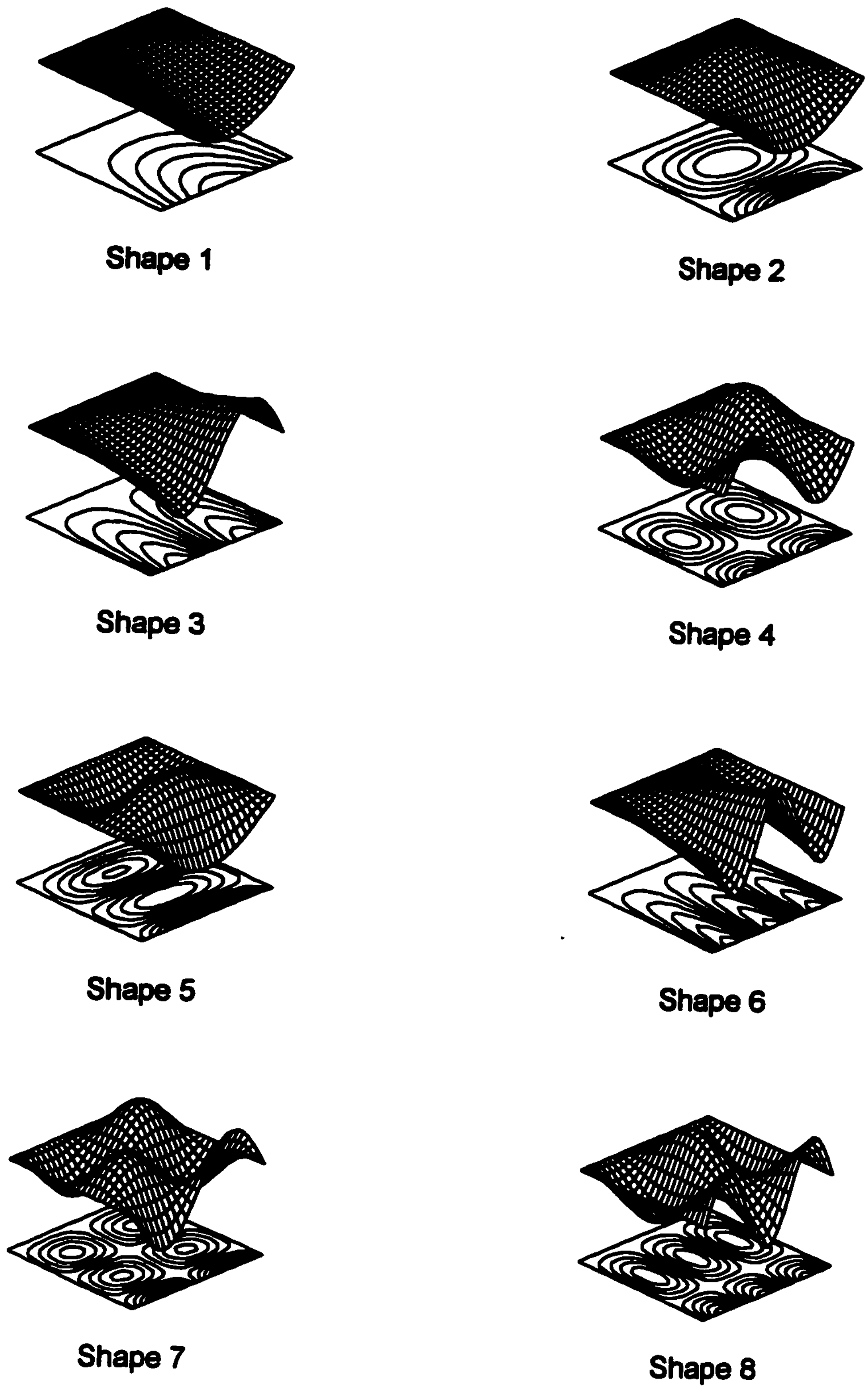

Table 4.52 Eigenvalues, SCSF plate, $\phi = 3/2$, $\lambda^2 = \omega a^2 (\rho / D)^{1/2}$.

Mode	In-plane load as a percentage of buckling load								
	-100%	-50%	0%	20%	40%	60%	80%	90%	99%
				Present solution					
1	15.42	13.35	10.90	9.75	8.44	6.89	4.88	3.45	1.09
2	22.98	21.64	20.22	19.63	19.01	18.38	17.72	17.38	17.07
3	39.38	38.62	37.84	37.53	37.21	36.41	35.08	34.40	33.77
4	45.68	43.00	40.14	38.94	37.70	36.89	36.57	36.40	36.26
5	54.16	51.91	49.57	48.60	47.62	46.61	45.57	45.05	44.57
6	65.01	64.55	64.09	63.91	63.72	63.53	63.35	63.25	63.17
7	71.12	69.43	67.69	66.99	66.27	65.55	64.82	64.45	64.12
8	94.96	92.10	89.15	87.94	86.72	85.47	84.21	83.57	83.00
				Finite element solution [18]					
1	15.42	13.36	10.91	9.75	8.45	6.90	4.88	3.45	1.09
2	22.97	21.64	20.22	19.62	19.01	18.37	17.71	17.37	17.06
3	39.36	38.60	37.82	37.50	37.19	36.42	35.09	34.41	33.78
4	45.69	43.01	40.15	38.95	37.71	36.87	36.54	36.38	36.23
5	54.15	51.91	49.56	48.59	47.60	46.59	45.56	45.04	44.56
6	64.97	64.51	64.05	63.86	63.68	63.49	63.30	63.21	63.12
7	71.05	69.36	67.62	66.91	66.20	65.48	64.75	64.38	64.04
8	94.97	92.11	89.15	87.95	86.72	85.48	84.22	83.58	83.00
				Percent difference					
1	0.03%	0.03%	0.03%	0.03%	0.03%	0.03%	0.03%	0.02%	-0.09%
2	-0.01%	-0.01%	-0.02%	-0.02%	-0.02%	-0.03%	-0.03%	-0.03%	-0.03%
3	-0.05%	-0.06%	-0.06%	-0.06%	-0.06%	0.03%	0.03%	0.03%	0.03%
4	0.03%	0.03%	0.03%	0.03%	0.03%	-0.06%	-0.07%	-0.07%	-0.07%
5	-0.01%	-0.02%	-0.02%	-0.02%	-0.02%	-0.02%	-0.03%	-0.03%	-0.03%
6	-0.06%	-0.06%	-0.07%	-0.07%	-0.07%	-0.07%	-0.07%	-0.07%	-0.07%
7	-0.09%	-0.10%	-0.10%	-0.11%	-0.11%	-0.11%	-0.12%	-0.12%	-0.12%
8	0.01%	0.01%	0.01%	0.01%	0.01%	0.01%	0.00%	0.00%	0.00%

Figure 4.92 Eigenvalue curves, SCSF plate, $\phi = 3 / 2$,

$P_\xi = - N_x b^2 / D$, $\lambda^2 = \omega a^2 (\rho / D)^{1/2}$.

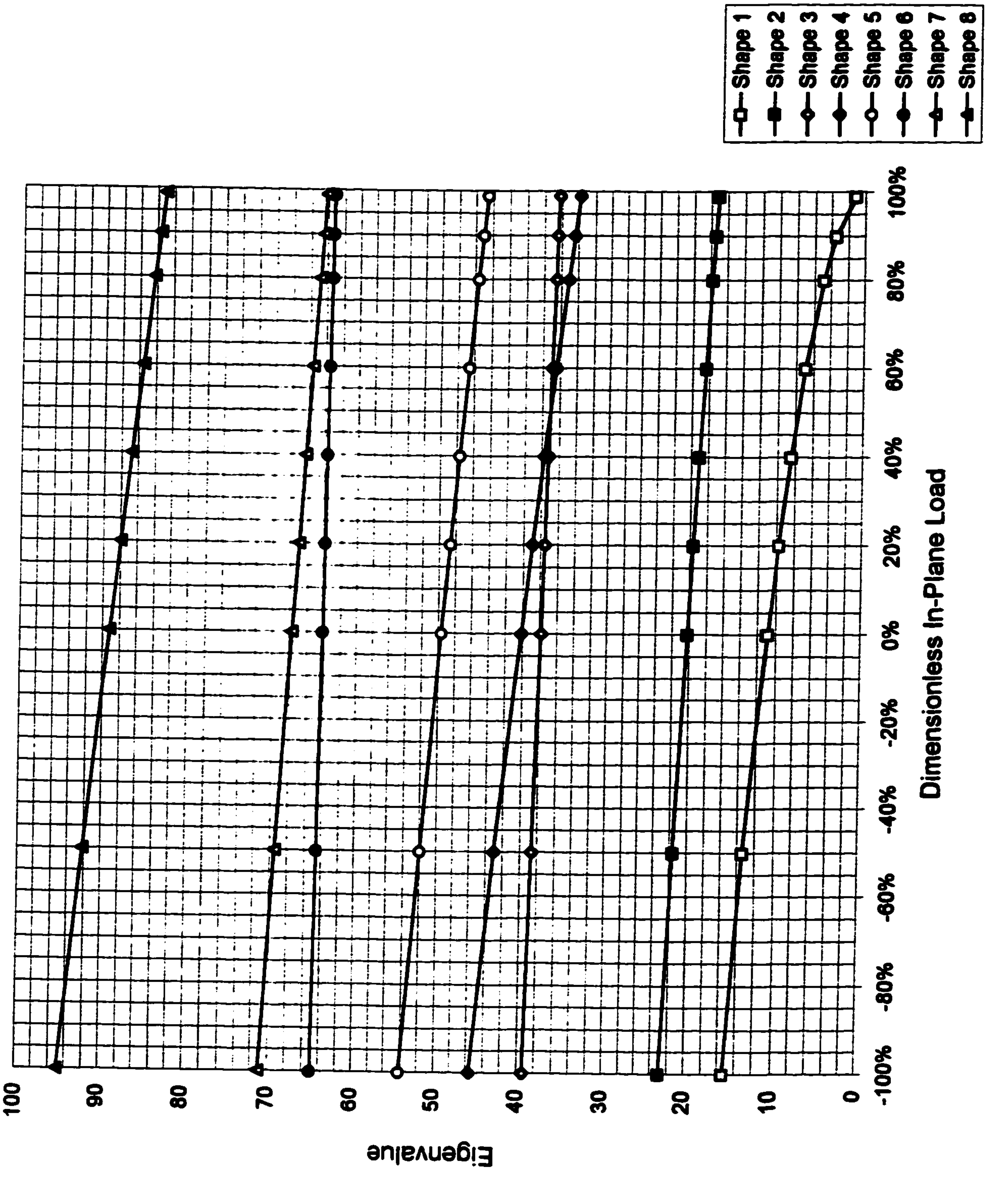

Figure 4.93 Mode shapes, SCSF plate, $\phi = 3 / 2$.

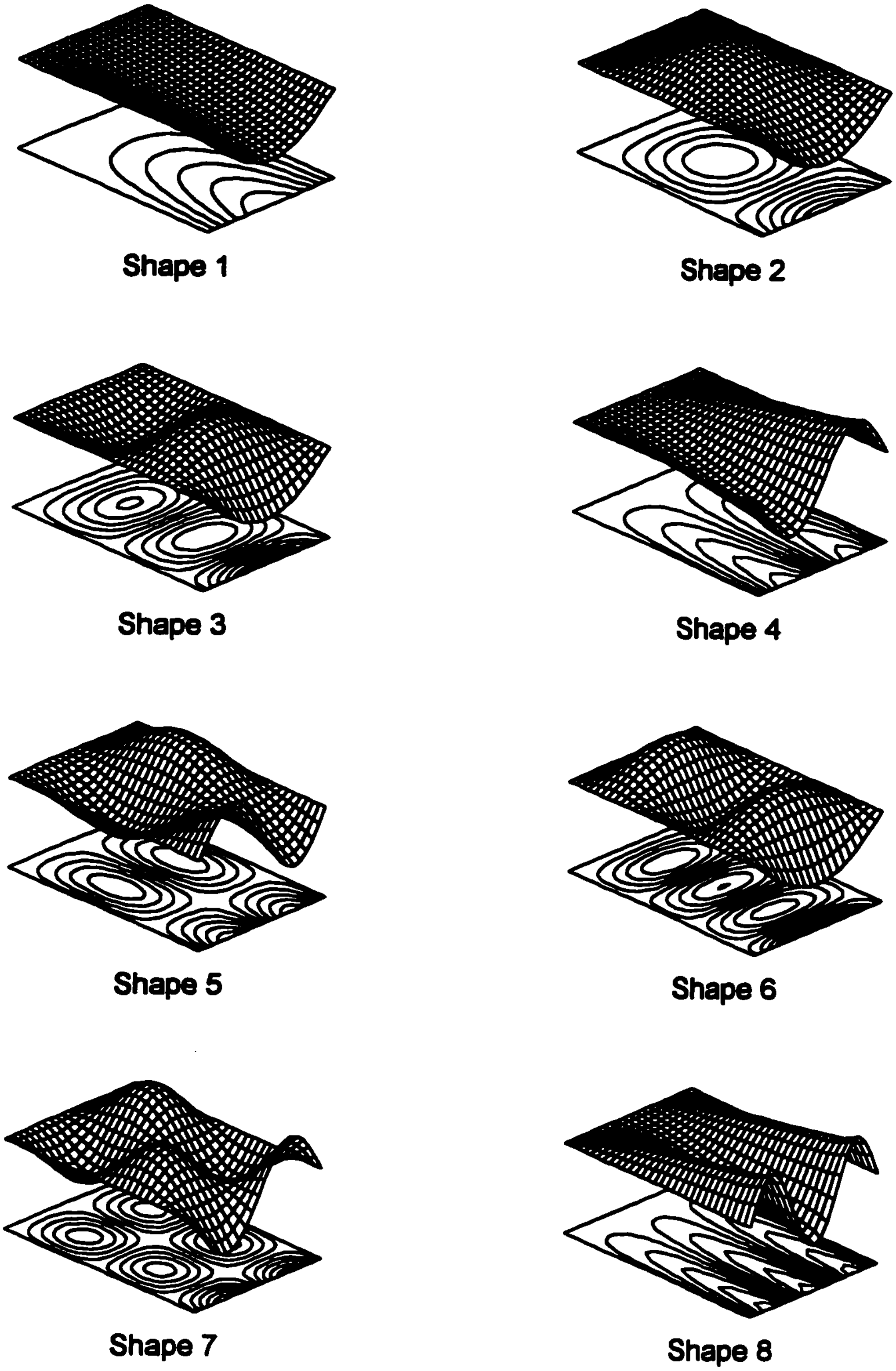

Table 4.53 Eigenvalues, SCSF plate, $\phi = 2 / 1$, $\lambda^2 = \omega a^2 (\rho / D)^{1/2}$.

Mode	In-plane load as a percentage of buckling load								
	-100%	-50%	0%	20%	40%	60%	80%	90%	99%
				Present solution					
1	14.67	12.71	10.37	9.28	8.04	6.56	4.64	3.28	1.04
2	18.80	17.31	15.68	14.98	14.24	13.46	12.64	12.21	11.80
3	27.72	26.73	25.70	25.28	24.85	24.42	23.97	23.74	23.54
4	41.82	41.17	39.72	38.62	37.49	36.33	35.12	34.50	33.94
5	44.82	42.35	40.51	40.24	39.97	39.70	39.43	39.30	39.17
6	49.56	47.33	45.00	44.04	43.05	42.04	41.00	40.47	39.99
7	59.02	57.16	55.25	54.47	53.67	52.86	52.04	51.62	51.25
8	61.10	60.65	60.21	60.03	59.85	59.67	59.49	59.40	59.32
				Finite element solution [18]					
1	14.68	12.71	10.38	9.28	8.04	6.56	4.64	3.28	1.04
2	18.80	17.31	15.68	14.97	14.24	13.46	12.63	12.20	11.80
3	27.70	26.71	25.68	25.26	24.83	24.39	23.95	23.72	23.51
4	41.77	41.12	39.73	38.63	37.50	36.34	35.13	34.51	33.95
5	44.83	42.36	40.46	40.19	39.93	39.66	39.38	39.25	39.12
6	49.55	47.32	44.99	44.02	43.03	42.02	40.98	40.45	39.97
7	58.96	57.10	55.18	54.39	53.60	52.79	51.96	51.55	51.17
8	61.04	60.60	60.15	59.97	59.79	59.61	59.43	59.34	59.26
				Percent difference					
1	0.04%	0.03%	0.03%	0.03%	0.03%	0.03%	0.03%	0.03%	0.04%
2	0.00%	-0.01%	-0.01%	-0.02%	-0.03%	-0.03%	-0.04%	-0.04%	-0.05%
3	-0.07%	-0.08%	-0.08%	-0.09%	-0.10%	-0.10%	-0.10%	-0.10%	-0.11%
4	-0.11%	-0.11%	0.03%	0.03%	0.03%	0.03%	0.02%	0.02%	0.02%
5	0.03%	0.03%	-0.12%	-0.12%	-0.12%	-0.12%	-0.13%	-0.13%	-0.13%
6	-0.02%	-0.03%	-0.03%	-0.04%	-0.04%	-0.04%	-0.05%	-0.05%	-0.05%
7	-0.11%	-0.11%	-0.13%	-0.13%	-0.14%	-0.14%	-0.15%	-0.15%	-0.15%
8	-0.09%	-0.10%	-0.10%	-0.10%	-0.10%	-0.10%	-0.10%	-0.10%	-0.10%

Figure 4.94 Eigenvalue curves, SCSF plate, $\phi = 2 / 1$,
$P_{\xi} = - N_x b^2 / D$, $\lambda^2 = \omega a^2 (\rho / D)^{1/2}$.

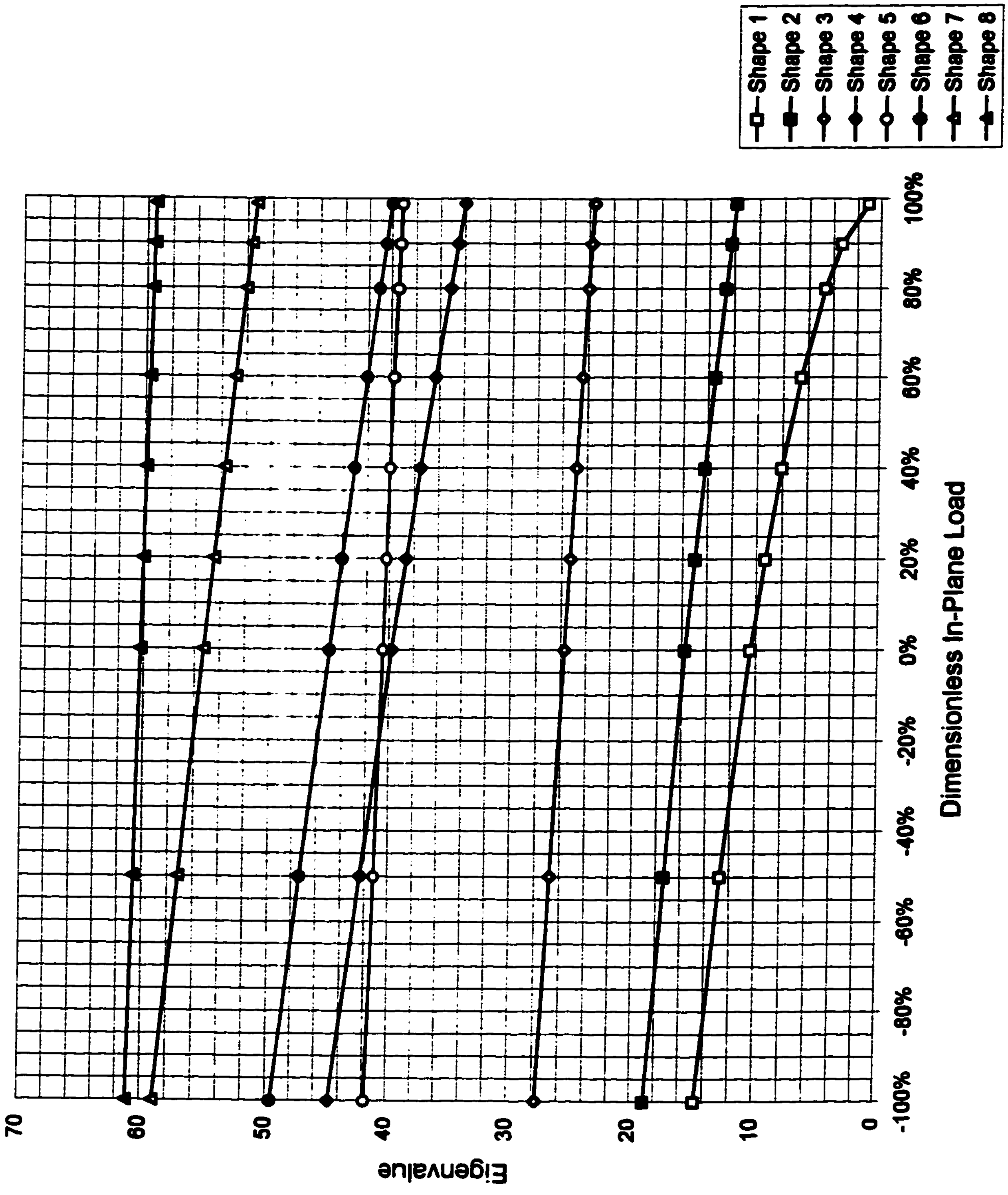

Figure 4.95 Mode shapes, SCSF plate, $\phi = 2 / 1$.

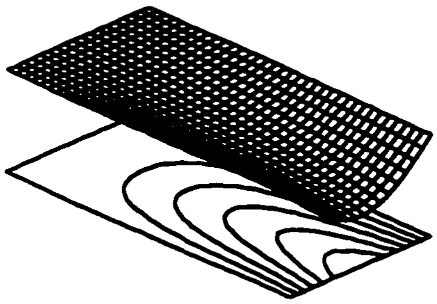

Shape 1

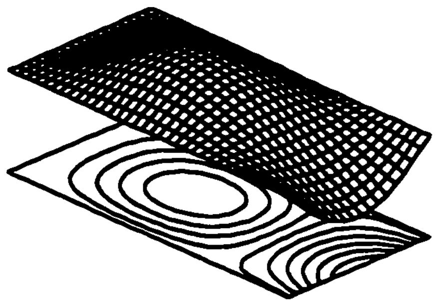

Shape 2

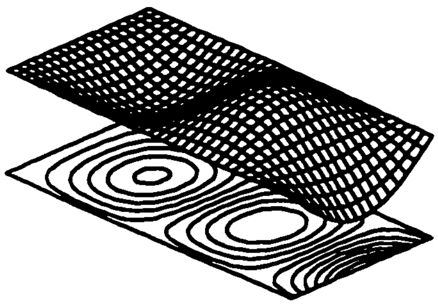

Shape 3

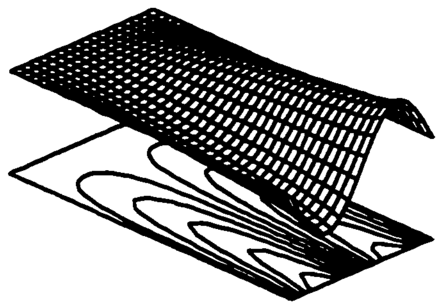

Shape 4

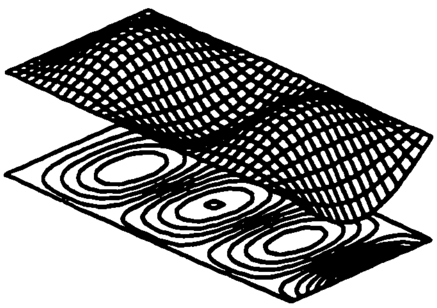

Shape 5

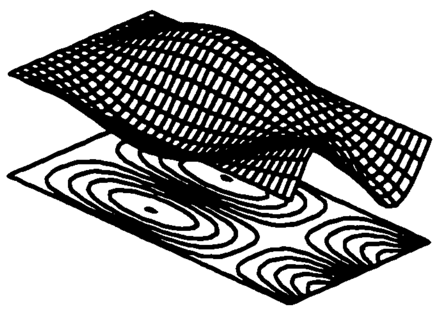

Shape 6

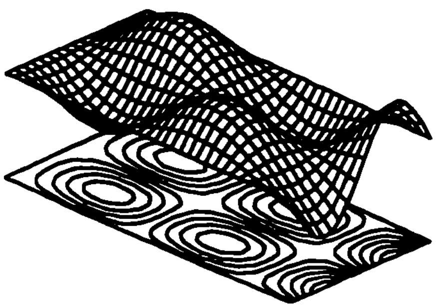

Shape 7

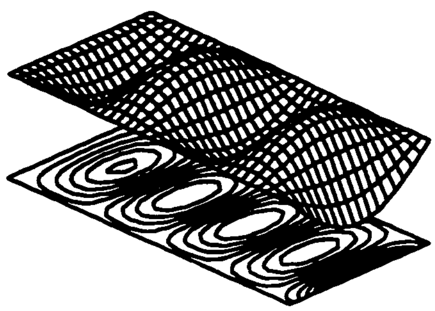

Shape 8

Table 4.54 Eigenvalues, SCSF plate, $\phi = 5 / 2$, $\lambda^2 = \omega a^2 (\rho / D)^{1/2}$.

Mode	In-plane load as a percentage of buckling load								
	-100%	-50%	0%	20%	40%	60%	80%	90%	99%
	Present solution								
1	14.35	12.43	10.15	9.08	7.86	6.42	4.54	3.21	1.01
2	16.93	15.33	13.55	12.77	11.93	11.04	10.06	9.54	9.04
3	22.45	21.28	20.03	19.51	18.97	18.42	17.86	17.56	17.30
4	31.25	30.41	29.55	29.20	28.85	28.49	28.12	27.94	27.77
5	43.38	42.08	39.55	38.50	37.41	36.29	35.14	34.55	34.01
6	44.46	42.78	42.18	41.93	40.96	39.94	38.90	38.36	37.88
7	47.48	45.26	42.92	41.95	41.69	41.44	41.19	41.06	40.95
8	53.48	51.52	49.48	48.64	47.79	46.92	46.03	45.58	45.17
	Finite element solution [18]								
1	14.36	12.43	10.15	9.08	7.86	6.42	4.54	3.21	1.02
2	16.93	15.33	13.55	12.77	11.93	11.03	10.05	9.53	9.03
3	22.44	21.26	20.01	19.49	18.95	18.40	17.83	17.54	17.27
4	31.20	30.36	29.50	29.15	28.79	28.43	28.06	27.88	27.71
5	43.30	42.09	39.57	38.51	37.42	36.31	35.15	34.56	34.02
6	44.47	42.70	42.09	41.85	40.94	39.92	38.87	38.34	37.85
7	47.47	45.25	42.91	41.93	41.60	41.35	41.10	40.97	40.86
8	53.42	51.45	49.41	48.57	47.71	46.84	45.95	45.50	45.09
	Percent difference								
1	0.04%	0.04%	0.04%	0.04%	0.04%	0.04%	0.04%	0.04%	0.02%
2	0.01%	0.00%	-0.02%	-0.02%	-0.03%	-0.04%	-0.06%	-0.07%	-0.08%
3	-0.08%	-0.09%	-0.11%	-0.12%	-0.13%	-0.13%	-0.15%	-0.15%	-0.16%
4	-0.16%	-0.17%	-0.18%	-0.19%	-0.20%	-0.20%	-0.21%	-0.21%	-0.22%
5	-0.19%	0.04%	0.03%	0.04%	0.03%	0.03%	0.03%	0.03%	0.03%
6	0.04%	-0.19%	-0.20%	-0.20%	-0.05%	-0.05%	-0.06%	-0.06%	-0.07%
7	-0.03%	-0.03%	-0.04%	-0.05%	-0.21%	-0.21%	-0.21%	-0.22%	-0.22%
8	-0.11%	-0.13%	-0.14%	-0.15%	-0.15%	-0.16%	-0.17%	-0.17%	-0.18%

Figure 4.96 Eigenvalue curves, SCSF plate, $\phi = 5 / 2$,
$P_\xi = - N_x b^2 / D$, $\lambda^2 = \omega a^2 (\rho / D)^{1/2}$.

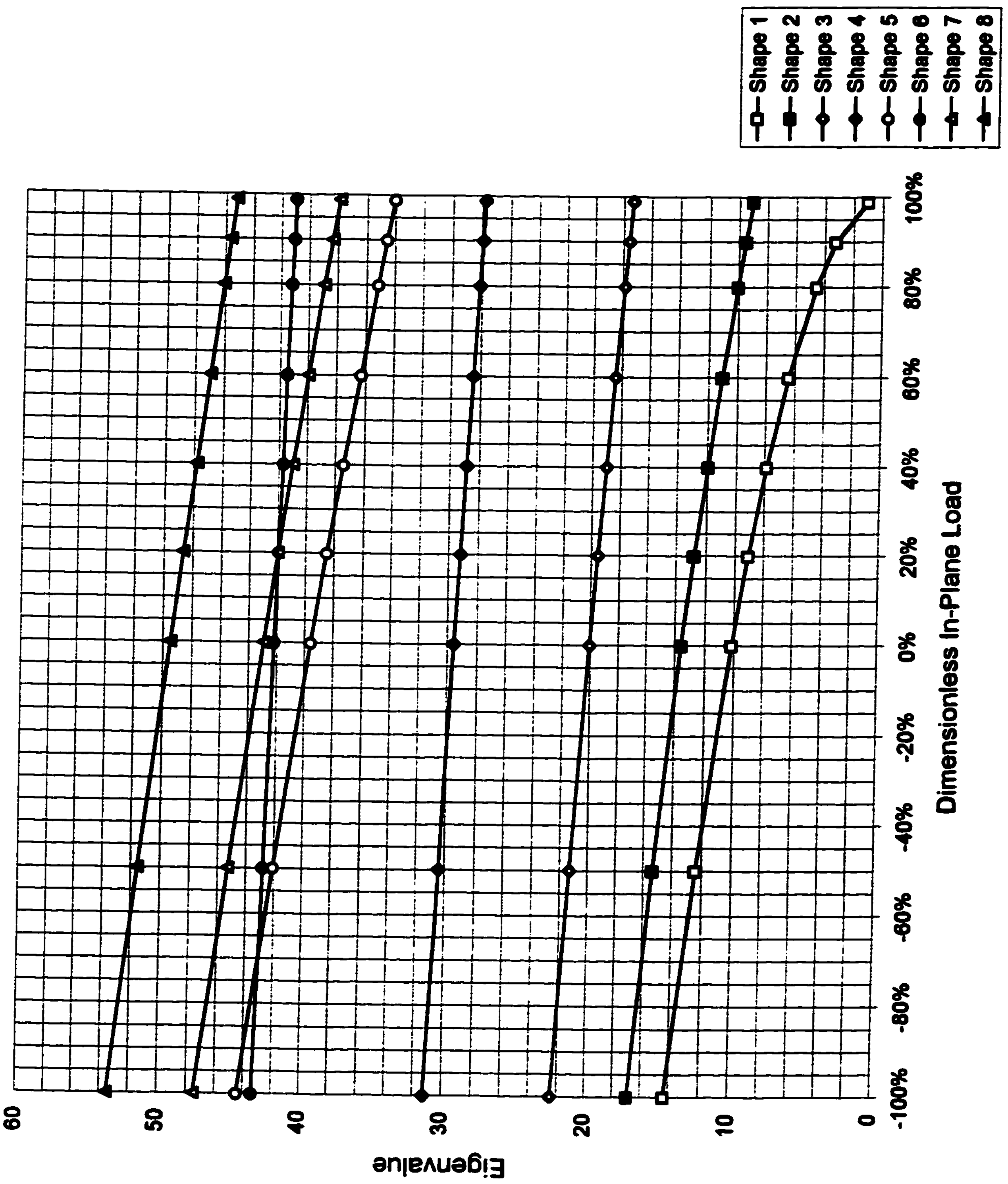

Figure 4.97 Mode shapes, SCSF plate, $\phi = 5 / 2$.

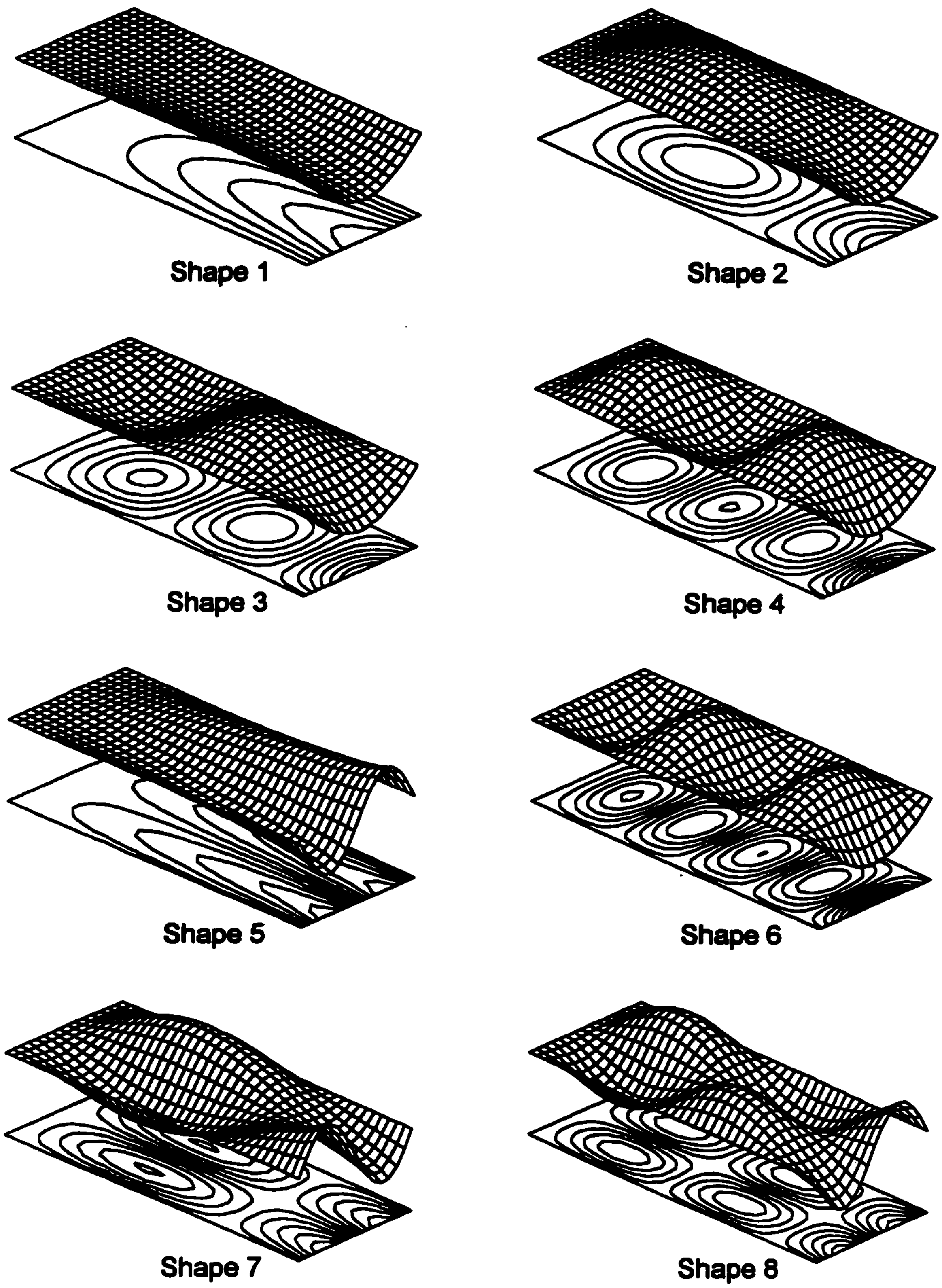

Table 4.55 Eigenvalues, SCSF plate, $\phi = 3 / 1$, $\lambda^2 = \omega a^2 (\rho / D)^{1/2}$.

	In-plane load as a percentage of buckling load								
Mode	-100%	-50%	0%	20%	40%	60%	80%	90%	99%
				Present solution					
1	14.19	12.29	10.03	8.98	7.77	6.35	4.49	3.17	1.00
2	15.95	14.28	12.39	11.55	10.64	9.65	8.55	7.93	7.34
3	19.67	18.35	16.92	16.32	15.69	15.03	14.35	13.99	13.66
4	25.62	24.62	23.57	23.14	22.70	22.25	21.80	21.56	21.35
5	33.88	33.13	32.36	32.05	31.73	31.41	31.09	30.93	30.78
6	44.28	41.94	39.47	38.44	37.37	36.28	35.15	34.57	34.05
7	44.46	43.89	41.81	40.84	39.84	38.82	37.76	37.23	36.74
8	46.38	44.16	43.32	43.08	42.85	42.61	42.38	42.24	41.84
				Finite element solution [18]					
1	14.20	12.30	10.04	8.98	7.78	6.35	4.49	3.17	1.00
2	15.95	14.28	12.39	11.55	10.64	9.65	8.54	7.93	7.33
3	19.66	18.33	16.90	16.29	15.66	15.01	14.32	13.96	13.63
4	25.57	24.56	23.52	23.08	22.64	22.19	21.73	21.50	21.29
5	33.78	33.03	32.26	31.95	31.63	31.31	30.98	30.82	30.67
6	44.30	41.97	39.49	38.46	37.39	36.30	35.17	34.59	34.06
7	44.33	43.76	41.79	40.82	39.82	38.79	37.74	37.20	36.71
8	46.37	44.14	43.18	42.95	42.71	42.48	42.24	42.12	41.76
				Percent difference					
1	0.05%	0.05%	0.05%	0.05%	0.05%	0.05%	0.05%	0.05%	0.05%
2	0.01%	0.01%	-0.01%	-0.02%	-0.03%	-0.05%	-0.08%	-0.10%	-0.12%
3	-0.08%	-0.09%	-0.12%	-0.14%	-0.15%	-0.17%	-0.19%	-0.20%	-0.22%
4	-0.20%	-0.22%	-0.24%	-0.25%	-0.26%	-0.28%	-0.29%	-0.30%	-0.30%
5	-0.28%	-0.29%	-0.31%	-0.31%	-0.32%	-0.33%	-0.34%	-0.34%	-0.35%
6	0.05%	0.05%	0.05%	0.05%	0.05%	0.05%	0.05%	0.05%	0.05%
7	-0.29%	-0.30%	-0.05%	-0.05%	-0.05%	-0.06%	-0.07%	-0.07%	-0.07%
8	-0.03%	-0.03%	-0.31%	-0.31%	-0.32%	-0.32%	-0.33%	-0.29%	-0.19%

Figure 4.98 Eigenvalue curves, SCSF plate, $\phi = 3 / 1$,

$P_{\xi} = - N_x b^2 / D$, $\lambda^2 = \omega a^2 (\rho / D)^{1/2}$.

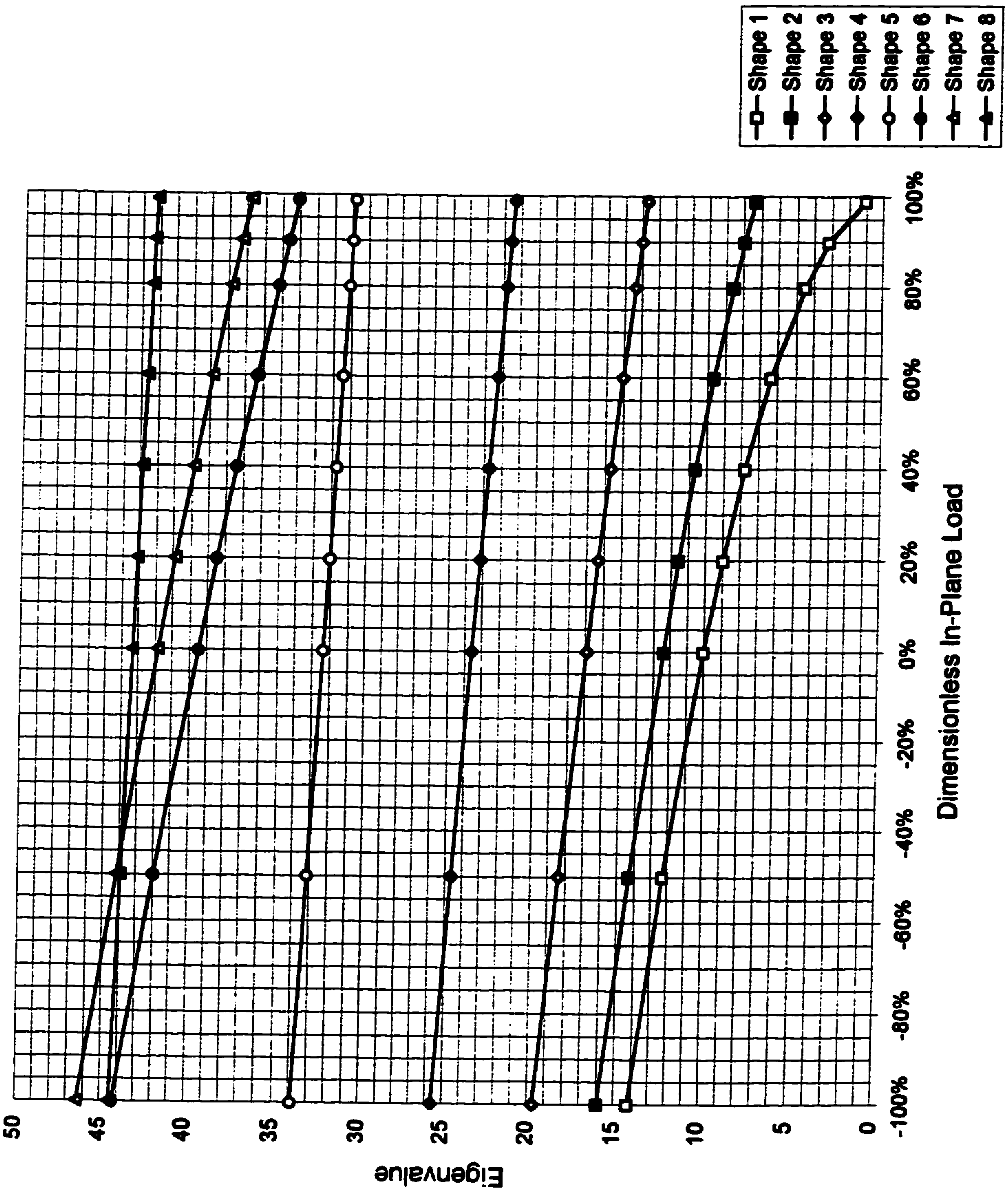

Figure 4.99 Mode shapes, SCSF plate, $\phi = 3 / 1$.

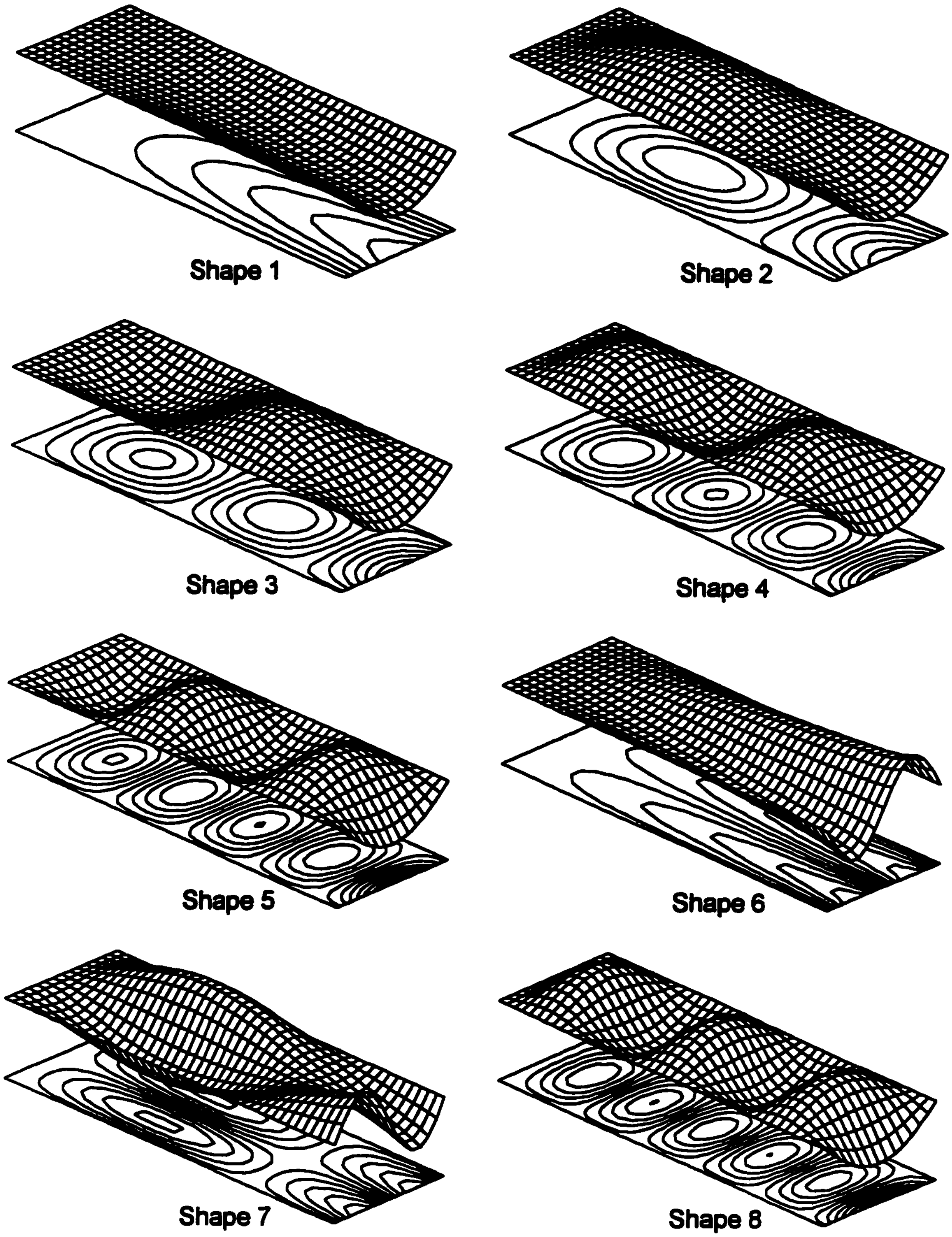

Table 4.56 Eigenvalues, SSCF plate, $\phi = 1/3$, $\lambda^2 = \omega a^2 (\rho / D)^{1/2}$.

Mode	In-plane load as a percentage of buckling load								
	-100%	-50%	0%	20%	40%	60%	80%	90%	99%
	Present solution								
1	35.25	30.68	25.23	22.65	19.70	16.17	11.51	8.18	2.60
2	79.57	71.79	63.02	59.13	54.96	50.43	45.45	42.74	40.14
3	138.55	128.80	118.24	113.73	109.04	104.13	98.98	96.30	93.82
4	155.75	154.83	153.89	153.52	153.14	152.77	152.39	152.20	152.03
5	201.12	198.25	192.29	187.46	182.50	177.40	172.15	169.47	167.01
6	214.81	203.86	195.34	194.16	192.97	191.78	190.57	189.97	189.42
7	267.25	262.41	257.47	255.46	253.44	251.40	249.35	248.31	247.38
8	309.52	297.82	285.64	280.62	275.51	270.30	264.99	262.29	259.84
	Finite element solution [18]								
1	35.25	30.69	25.23	22.65	19.70	16.17	11.51	8.18	2.60
2	79.60	71.82	63.05	59.16	54.99	50.47	45.49	42.78	40.19
3	138.71	128.97	118.42	113.91	109.23	104.33	99.18	96.51	94.04
4	155.64	154.71	153.78	153.41	153.03	152.65	152.27	152.08	151.91
5	200.80	197.93	192.86	188.04	183.09	178.01	172.78	170.10	167.66
6	215.32	204.40	195.01	193.83	192.64	191.45	190.24	189.63	189.08
7	266.54	261.69	256.73	254.72	252.69	250.65	248.59	247.55	246.60
8	310.78	299.13	286.99	282.00	276.91	271.73	266.43	263.75	261.31
	Percent difference								
1	0.01%	0.01%	0.00%	0.00%	0.00%	0.01%	0.00%	0.01%	0.03%
2	0.04%	0.04%	0.05%	0.06%	0.06%	0.08%	0.09%	0.10%	0.11%
3	0.11%	0.13%	0.15%	0.16%	0.18%	0.19%	0.21%	0.22%	0.23%
4	-0.07%	-0.07%	-0.08%	-0.07%	-0.08%	-0.08%	-0.08%	-0.08%	-0.08%
5	-0.16%	-0.16%	0.30%	0.31%	0.32%	0.34%	0.36%	0.37%	0.39%
6	0.24%	0.26%	-0.17%	-0.17%	-0.17%	-0.17%	-0.17%	-0.18%	-0.18%
7	-0.27%	-0.27%	-0.29%	-0.29%	-0.30%	-0.30%	-0.31%	-0.31%	-0.31%
8	0.41%	0.44%	0.47%	0.49%	0.51%	0.53%	0.55%	0.56%	0.57%

Figure 4.100 Eigenvalue curves, SSCF plate, $\phi = 1 / 3$,
$P_\xi = - N_x b^2 / D$, $\lambda^2 = \omega a^2 (\rho / D)^{1/2}$.

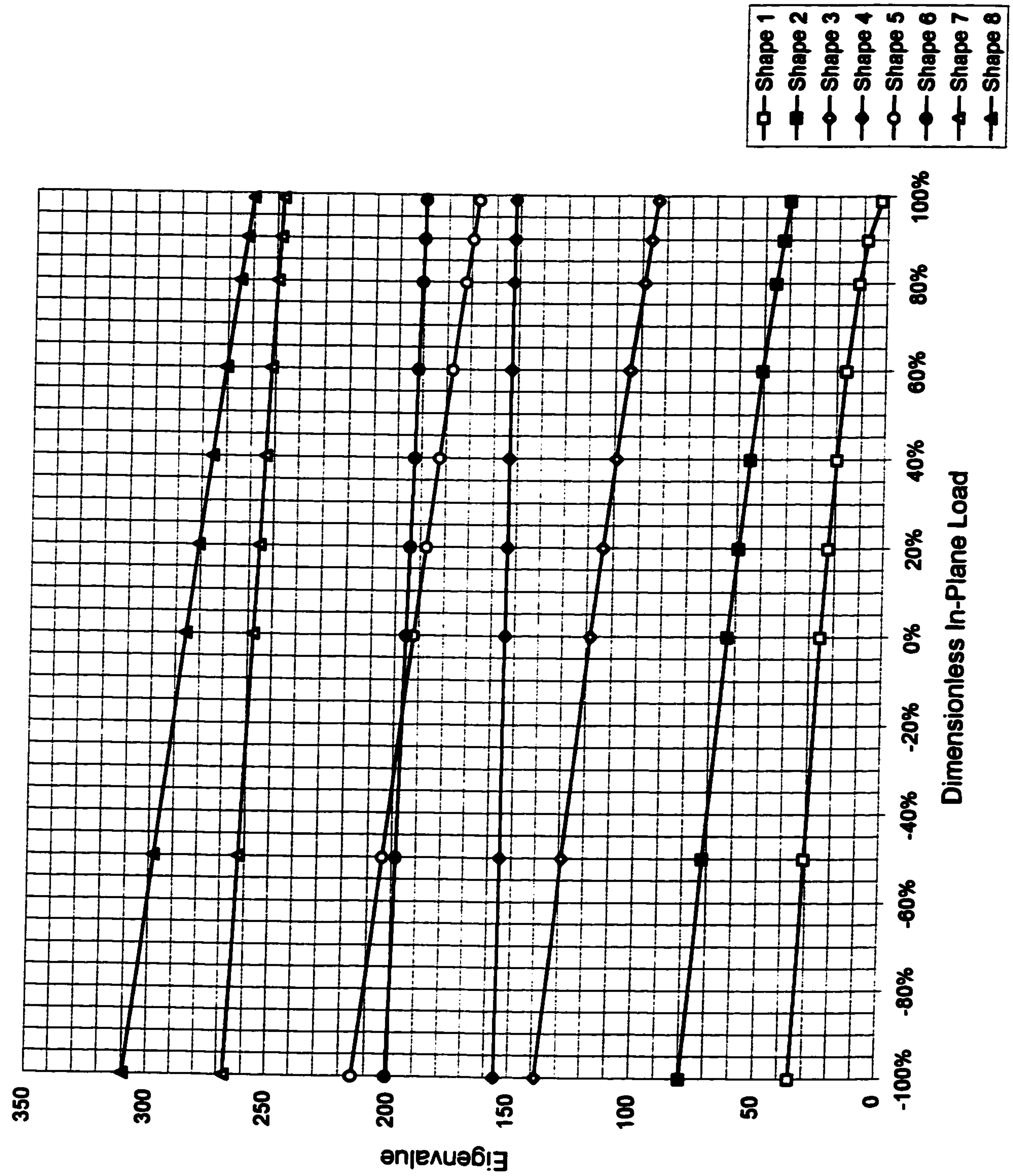

Figure 4.101 Mode shapes, SSCF plate, $\phi = 1 / 3$.

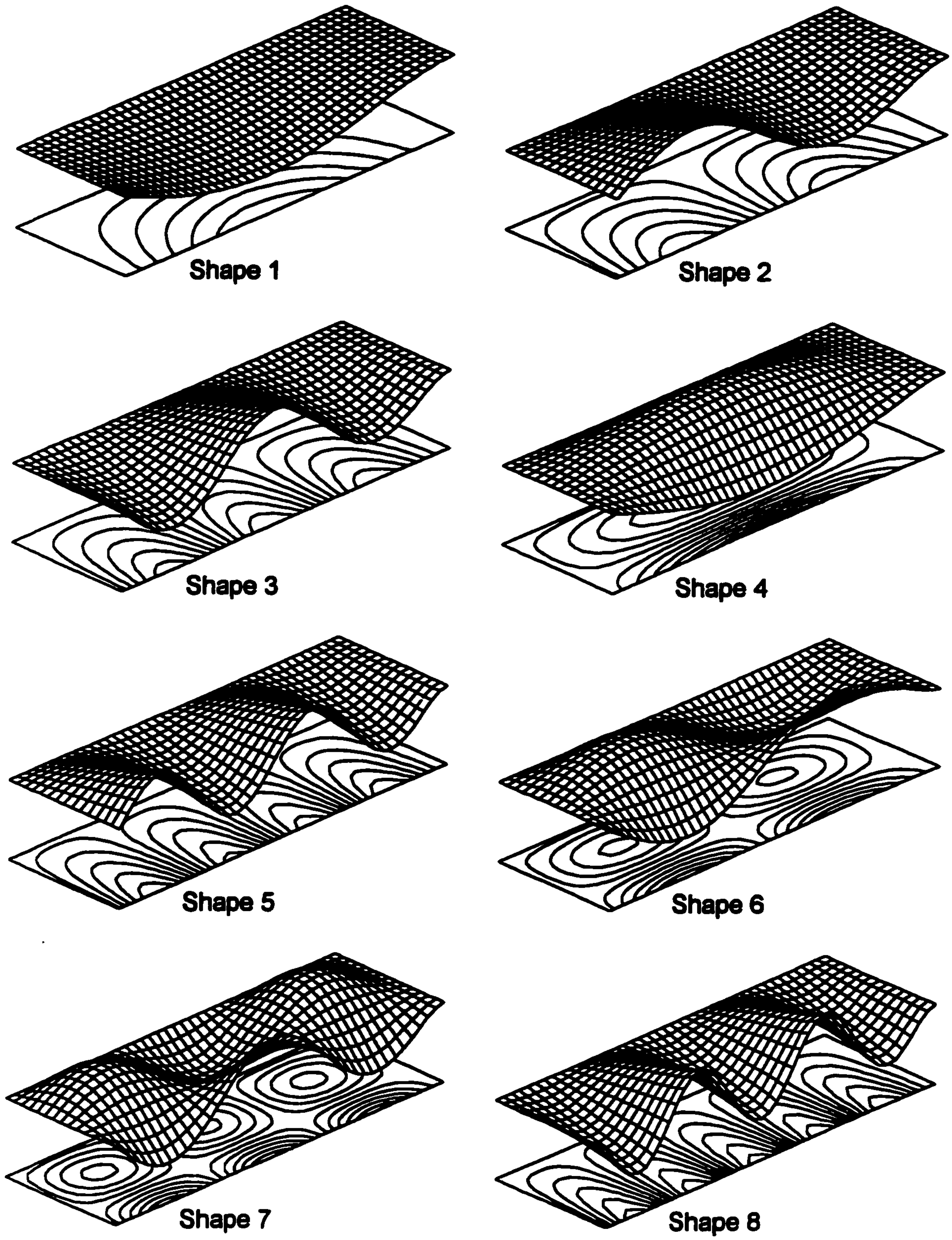

Table 4.57 Eigenvalues, SSCF plate, $\phi = 2 / 5$, $\lambda^2 = \omega a^2 (\rho / D)^{1/2}$.

Mode	In-plane load as a percentage of buckling load								
	-100%	-50%	0%	20%	40%	60%	80%	90%	99%
	Present solution								
1	31.70	27.59	22.68	20.36	17.70	14.52	10.33	7.33	2.33
2	73.51	66.75	59.20	55.88	52.34	48.55	44.42	42.21	40.11
3	113.68	112.65	111.61	110.10	106.22	102.19	98.00	95.83	93.84
4	130.96	122.71	113.85	111.20	110.77	110.35	109.93	109.71	109.52
5	158.24	155.29	152.28	151.06	149.82	148.58	147.32	146.69	146.12
6	206.32	197.21	187.65	183.68	179.63	175.48	171.24	169.07	167.10
7	222.09	217.38	212.57	210.61	208.63	206.64	204.62	203.60	202.69
8	300.51	290.87	280.89	276.80	272.65	268.43	264.15	261.98	260.02
	Finite element solution [18]								
1	31.71	27.60	22.69	20.36	17.71	14.53	10.33	7.33	2.33
2	73.55	66.80	59.24	55.92	52.39	48.59	44.47	42.26	40.17
3	113.61	112.57	111.54	110.30	106.43	102.41	98.22	96.06	94.07
4	131.14	122.90	114.05	111.12	110.70	110.28	109.85	109.64	109.45
5	158.03	155.07	152.06	150.84	149.60	148.35	147.09	146.46	145.89
6	206.86	197.76	188.23	184.28	180.24	176.10	171.86	169.71	167.74
7	221.63	216.91	212.08	210.12	208.14	206.13	204.11	203.09	202.17
8	301.77	292.17	282.24	278.16	274.02	269.83	265.56	263.40	261.45
	Percent difference								
1	0.02%	0.02%	0.02%	0.01%	0.02%	0.01%	0.02%	0.02%	0.06%
2	0.05%	0.06%	0.07%	0.08%	0.09%	0.10%	0.11%	0.12%	0.13%
3	-0.06%	-0.07%	-0.07%	0.18%	0.19%	0.21%	0.23%	0.23%	0.24%
4	0.14%	0.15%	0.17%	-0.07%	-0.07%	-0.07%	-0.07%	-0.07%	-0.07%
5	-0.13%	-0.14%	-0.14%	-0.14%	-0.15%	-0.15%	-0.16%	-0.16%	-0.16%
6	0.26%	0.28%	0.31%	0.32%	0.34%	0.35%	0.36%	0.38%	0.38%
7	-0.20%	-0.22%	-0.23%	-0.23%	-0.24%	-0.24%	-0.25%	-0.25%	-0.25%
8	0.42%	0.45%	0.48%	0.49%	0.50%	0.52%	0.53%	0.54%	0.55%

Figure 4.102 Eigenvalue curves, SSCF plate, $\phi = 2 / 5$,
$P_\xi = - N_x b^2 / D$, $\lambda^2 = \omega a^2 (\rho / D)^{1/2}$.

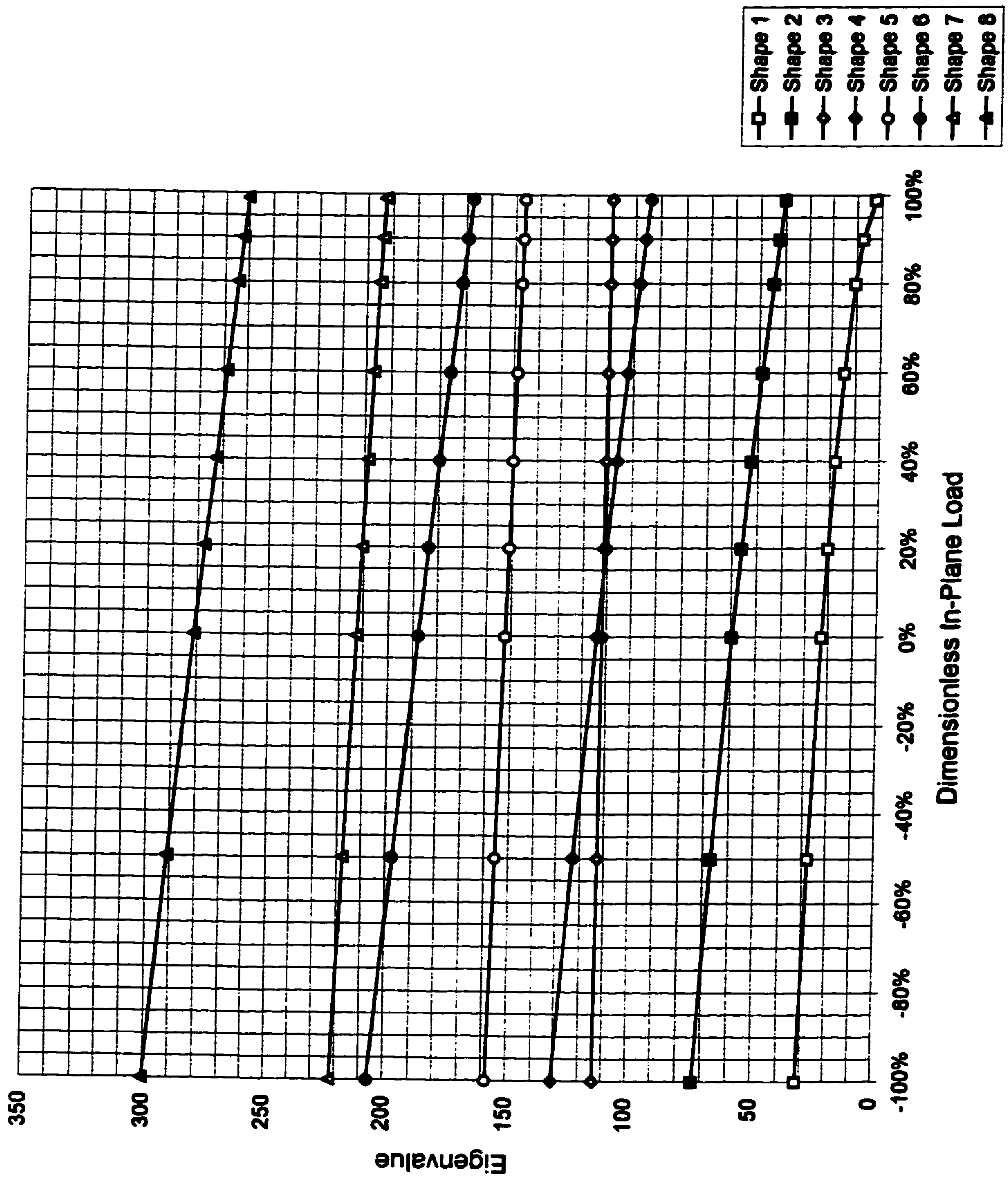

Figure 4.103 Mode shapes, SSCF plate, $\phi = 2 / 5$.

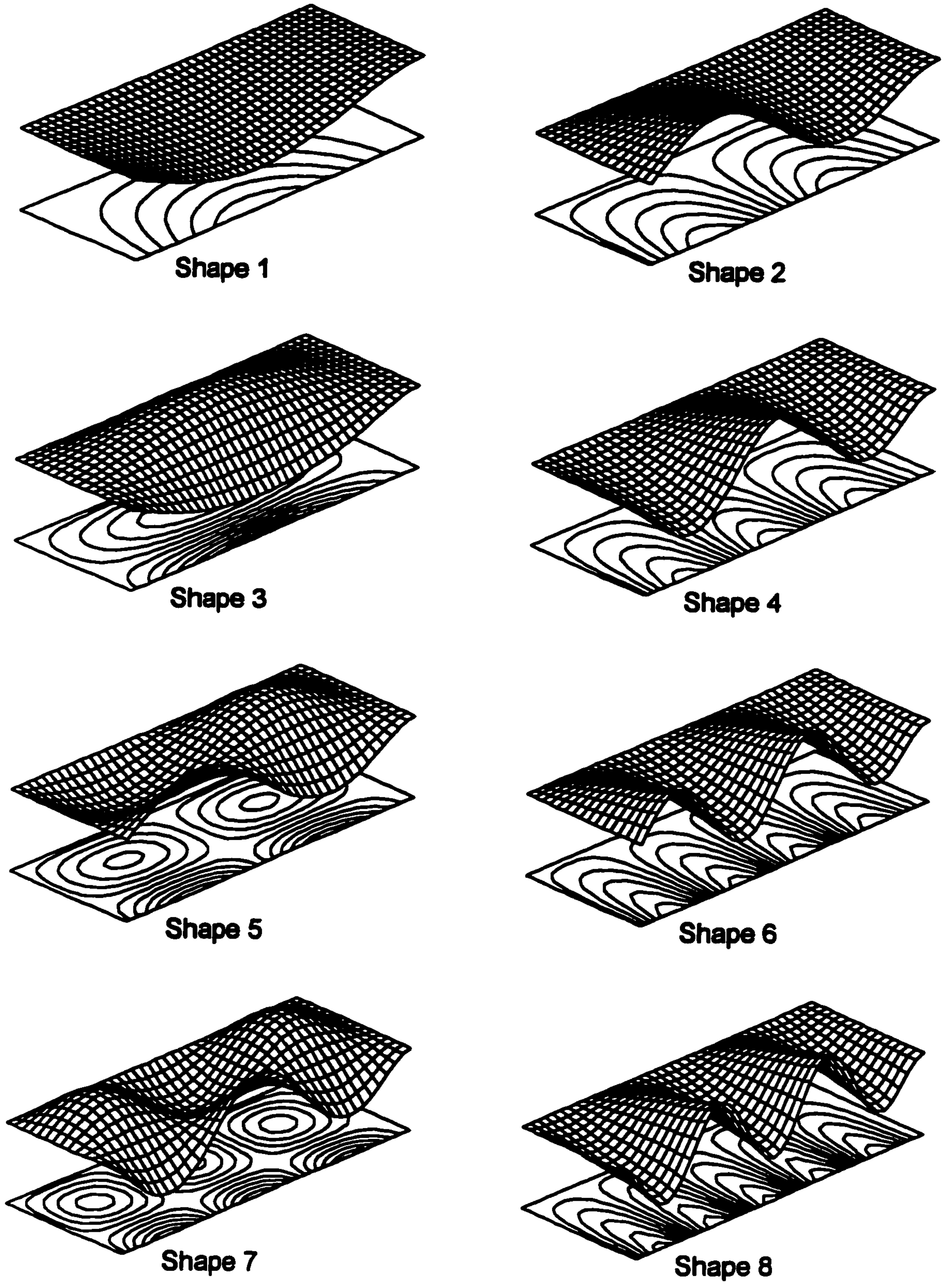

Table 4.58 Eigenvalues, SSCF plate, $\phi = 1 / 2$, $\lambda^2 = \omega a^2 (\rho / D)^{1/2}$.

Mode	In-plane load as a percentage of buckling load								
	-100%	-50%	0%	20%	40%	60%	80%	90%	99%
	Present solution								
1	28.45	24.76	20.35	18.26	15.87	13.01	9.25	6.56	2.08
2	68.15	62.33	55.88	53.08	50.12	46.96	43.58	41.79	40.11
3	79.45	78.26	77.05	76.56	76.07	75.57	75.07	74.81	74.58
4	122.82	117.52	110.16	107.08	103.90	100.62	97.23	95.49	93.89
5	124.44	119.76	116.60	115.32	114.01	112.70	111.36	110.69	110.08
6	184.15	179.59	174.91	173.00	171.06	169.11	167.13	166.13	165.23
7	199.17	191.65	183.82	180.60	177.31	173.96	170.55	168.81	167.24
8	213.92	213.49	213.05	212.88	212.71	212.54	212.36	212.28	212.20
	Finite element solution [18]								
1	28.46	24.77	20.35	18.26	15.87	13.01	9.25	6.56	2.08
2	68.20	62.38	55.93	53.13	50.17	47.01	43.63	41.84	40.16
3	79.41	78.22	77.01	76.52	76.02	75.52	75.02	74.77	74.54
4	122.71	117.71	110.36	107.28	104.11	100.83	97.44	95.70	94.11
5	124.62	119.64	116.48	115.19	113.88	112.56	111.22	110.55	109.94
6	183.92	179.35	174.65	172.74	170.80	168.84	166.86	165.86	164.95
7	199.69	192.18	184.37	181.15	177.87	174.53	171.13	169.40	167.83
8	213.64	213.21	212.78	212.60	212.43	212.25	212.08	212.00	211.92
	Percent difference								
1	0.03%	0.03%	0.03%	0.03%	0.03%	0.03%	0.02%	0.03%	0.07%
2	0.07%	0.08%	0.09%	0.09%	0.10%	0.11%	0.12%	0.13%	0.14%
3	-0.05%	-0.05%	-0.06%	-0.06%	-0.06%	-0.06%	-0.06%	-0.06%	-0.06%
4	-0.09%	0.16%	0.18%	0.19%	0.20%	0.21%	0.22%	0.23%	0.23%
5	0.15%	-0.10%	-0.11%	-0.11%	-0.11%	-0.12%	-0.12%	-0.12%	-0.12%
6	-0.13%	-0.14%	-0.15%	-0.15%	-0.16%	-0.16%	-0.16%	-0.17%	-0.17%
7	0.26%	0.28%	0.30%	0.31%	0.32%	0.33%	0.34%	0.35%	0.35%
8	-0.13%	-0.13%	-0.13%	-0.13%	-0.13%	-0.13%	-0.13%	-0.13%	-0.13%

Figure 4.104 Eigenvalue curves, SSCF plate, $\phi = 1 / 2$,
$P_\xi = - N_x b^2 / D$, $\lambda^2 = \omega a^2 (\rho / D)^{1/2}$.

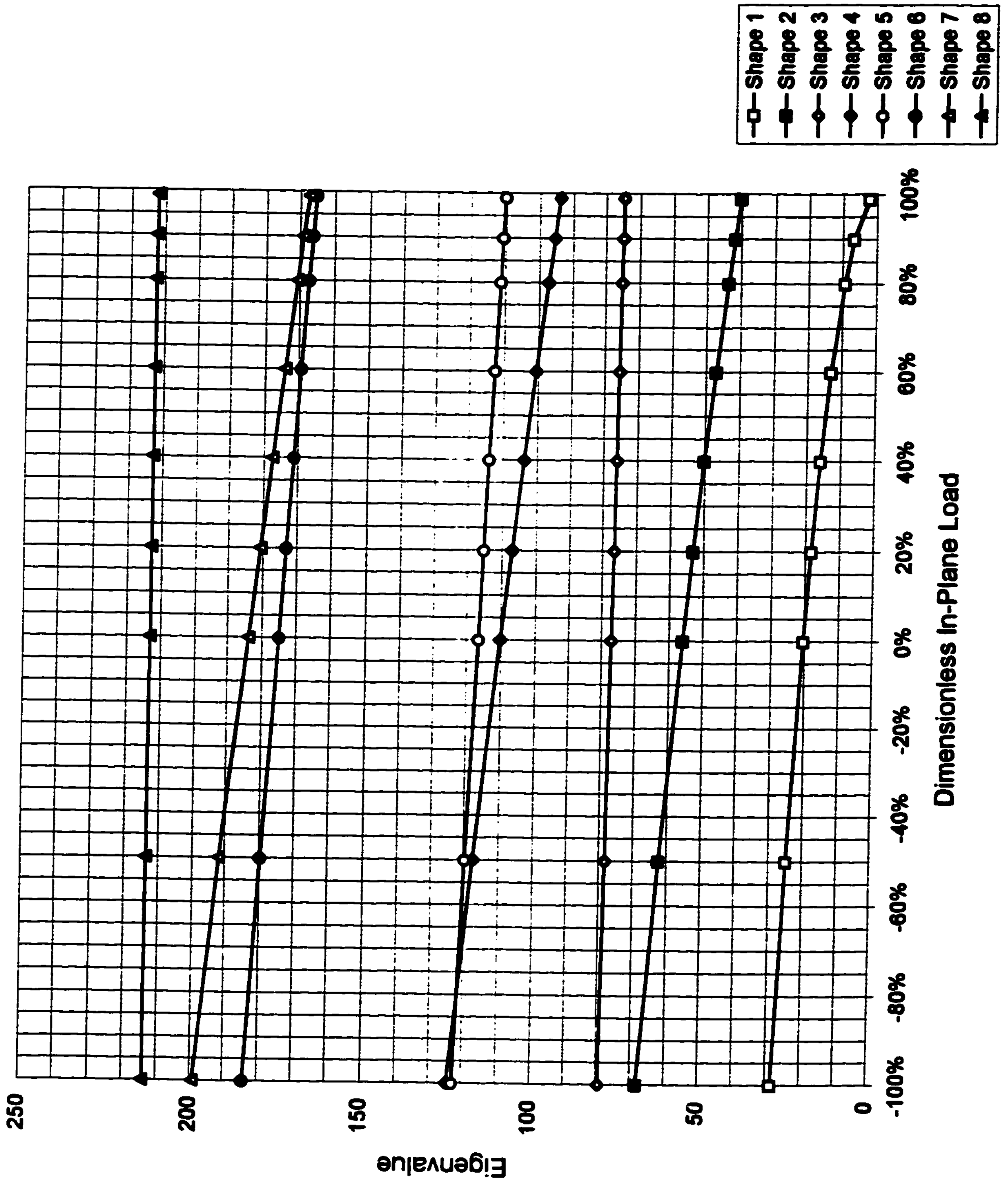

Figure 4.105 Mode shapes, SSCF plate, $\phi = 1 / 2$.

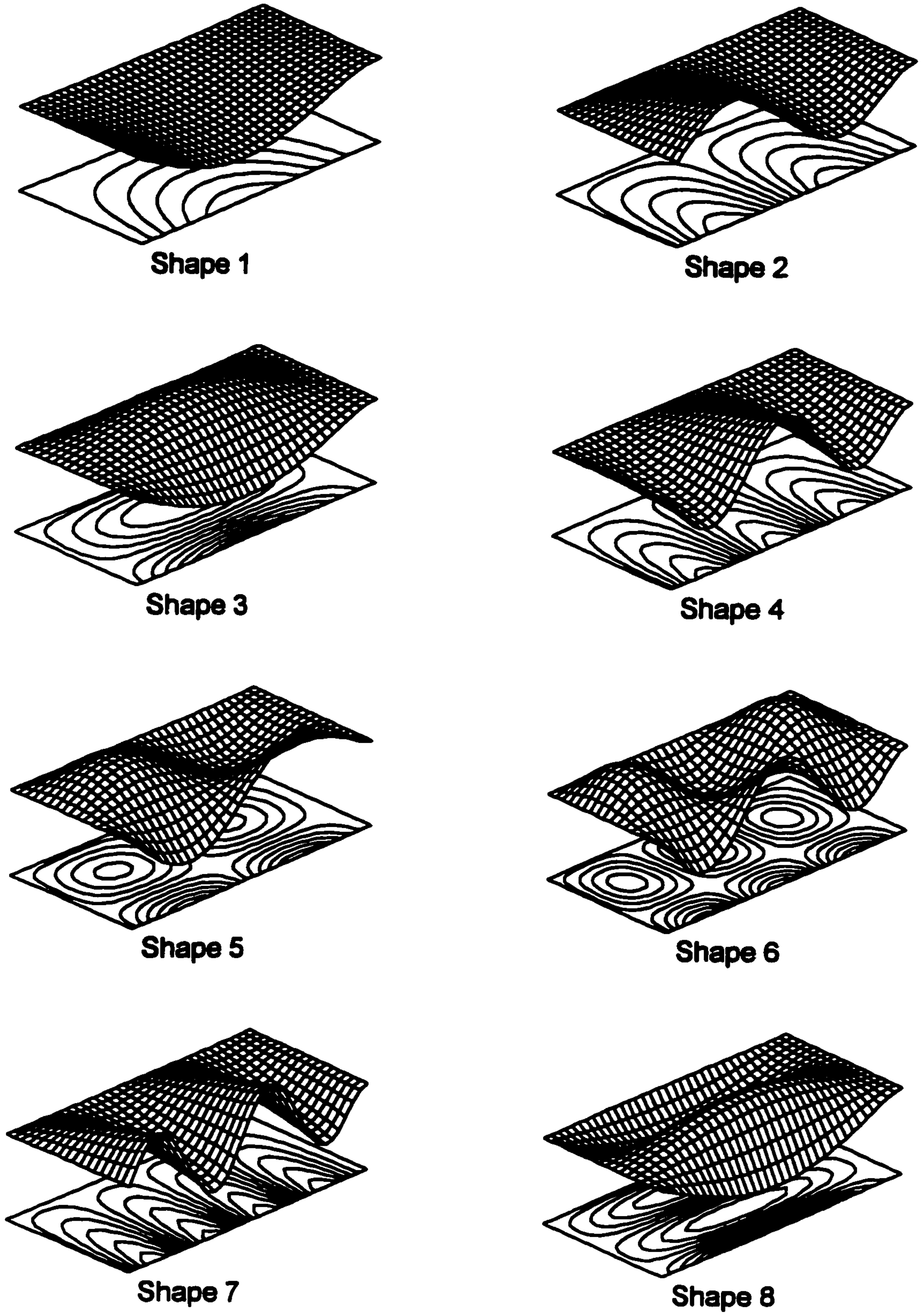

Table 4.59 Eigenvalues, SSCF plate, $\phi = 2/3$, $\lambda^2 = \omega a^2 (\rho / D)^{1/2}$.

Mode	In-plane load as a percentage of buckling load								
	-100%	-50%	0%	20%	40%	60%	80%	90%	99%
	Present solution								
1	25.61	22.29	18.31	16.42	14.27	11.69	8.30	5.88	1.87
2	53.16	51.69	50.18	49.57	48.33	45.72	42.94	41.48	40.12
3	63.68	58.68	53.19	50.82	48.94	48.30	47.66	47.33	47.03
4	94.84	91.60	88.23	86.85	85.44	84.01	82.55	81.81	81.14
5	119.17	113.38	107.26	104.72	102.11	99.43	96.68	95.27	93.99
6	127.07	126.48	125.89	125.65	125.41	125.17	124.93	124.81	124.70
7	153.67	149.24	144.68	142.81	140.92	139.00	137.05	136.07	135.17
8	167.13	165.34	163.53	162.80	162.07	161.33	160.59	160.22	159.88
	Finite element solution [18]								
1	25.62	22.30	18.31	16.43	14.27	11.70	8.31	5.89	1.87
2	53.14	51.68	50.17	49.55	48.38	45.76	42.99	41.53	40.17
3	63.73	58.72	53.23	50.87	48.92	48.28	47.63	47.31	47.01
4	94.80	91.55	88.18	86.80	85.39	83.95	82.49	81.75	81.08
5	119.33	113.53	107.43	104.88	102.27	99.60	96.85	95.45	94.16
6	126.95	126.36	125.77	125.53	125.29	125.05	124.81	124.69	124.58
7	153.60	149.17	144.60	142.72	140.83	138.91	136.96	135.97	135.08
8	166.89	165.10	163.28	162.55	161.82	161.08	160.34	159.96	159.63
	Percent difference								
1	0.03%	0.04%	0.03%	0.04%	0.04%	0.04%	0.04%	0.04%	0.13%
2	-0.03%	-0.03%	-0.04%	-0.04%	0.10%	0.10%	0.11%	0.11%	0.12%
3	0.07%	0.07%	0.08%	0.09%	-0.04%	-0.05%	-0.05%	-0.04%	-0.05%
4	-0.04%	-0.05%	-0.06%	-0.06%	-0.06%	-0.07%	-0.07%	-0.07%	-0.07%
5	0.13%	0.14%	0.15%	0.16%	0.16%	0.17%	0.18%	0.18%	0.19%
6	-0.09%	-0.09%	-0.10%	-0.09%	-0.10%	-0.10%	-0.10%	-0.10%	-0.10%
7	-0.05%	-0.05%	-0.06%	-0.06%	-0.06%	-0.07%	-0.07%	-0.07%	-0.07%
8	-0.14%	-0.15%	-0.15%	-0.15%	-0.16%	-0.16%	-0.16%	-0.16%	-0.16%

Figure 4.106 Eigenvalue curves, SSCF plate, $\phi = 2 / 3$,

$P_{\xi} = - N_x b^2 / D$, $\lambda^2 = \omega a^2 (\rho / D)^{1/2}$.

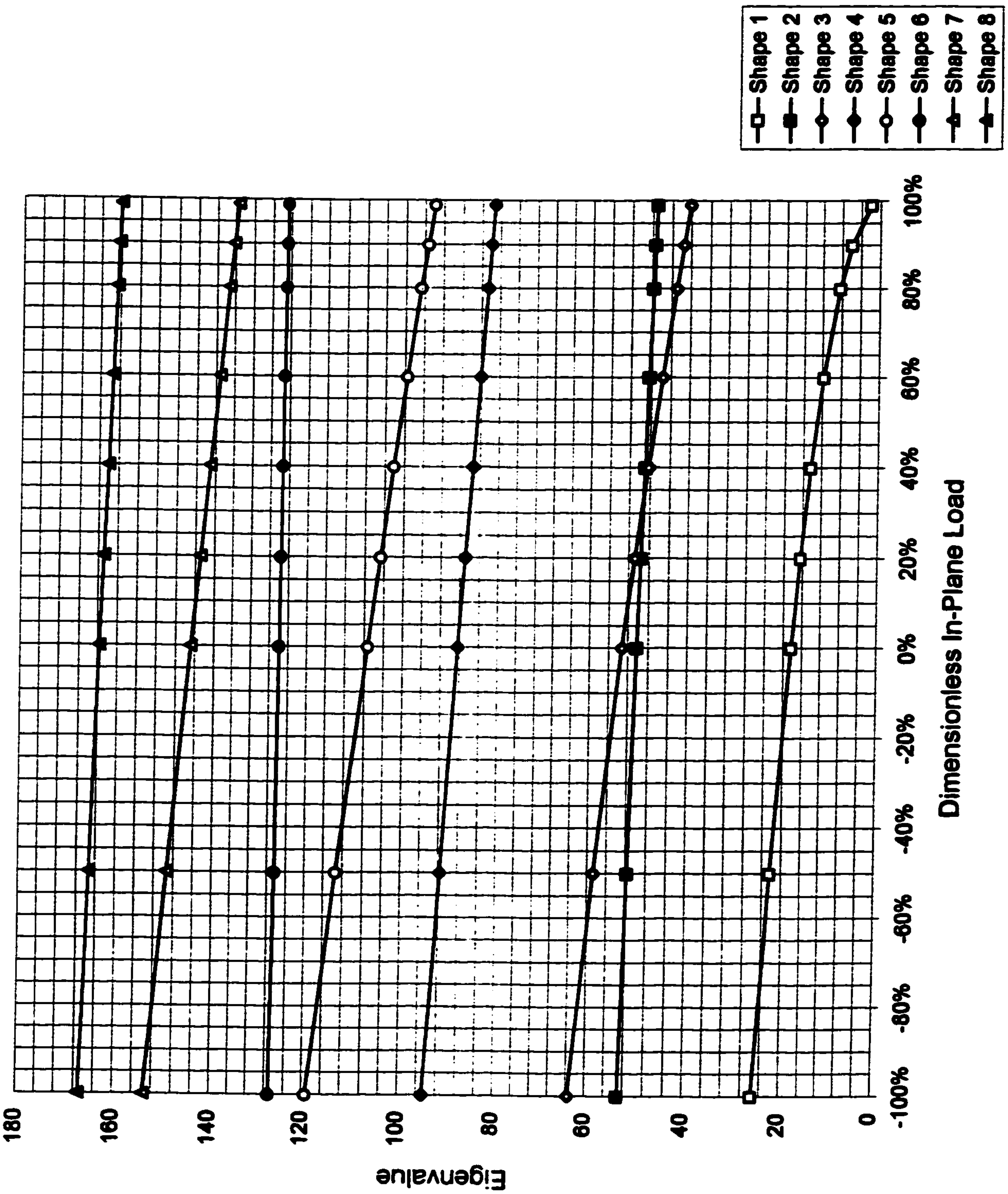

Figure 4.107 Mode shapes, SSCF plate, $\phi = 2 / 3$.

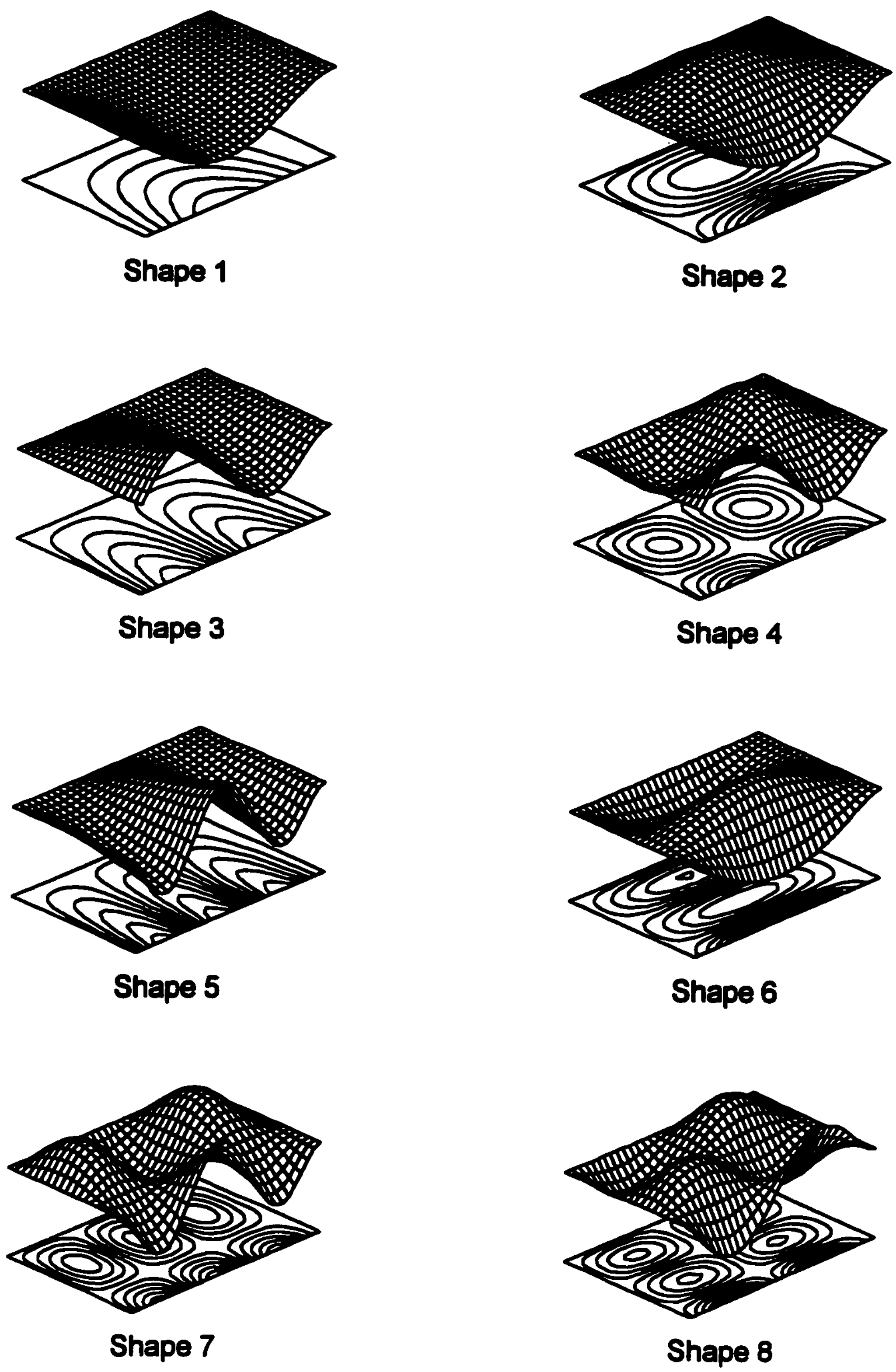

Table 4.60 Eigenvalues, SSCF plate, $\phi = 1 / 1$, $\lambda^2 = \omega a^2 (\rho / D)^{1/2}$.

Mode	In-plane load as a percentage of buckling load								
	-100%	-50%	0%	20%	40%	60%	80%	90%	99%
	Present solution								
1	23.38	20.34	16.70	14.97	13.00	10.65	7.56	5.36	1.70
2	34.89	32.99	30.95	30.09	29.21	28.29	27.34	26.85	26.40
3	60.33	55.96	51.22	49.19	47.07	44.85	42.51	41.30	40.17
4	65.82	64.86	63.87	63.47	63.06	62.48	60.93	60.10	59.34
5	74.40	70.93	67.28	65.76	64.21	62.79	62.28	62.07	61.89
6	105.62	103.23	100.78	99.79	98.78	97.76	96.37	95.20	94.14
7	115.35	110.41	105.23	103.09	100.90	98.66	96.73	96.21	95.74
8	118.15	117.62	117.09	116.88	116.66	116.44	114.81	113.84	112.95
	Finite element solution [18]								
1	23.39	20.34	16.70	14.98	13.01	10.66	7.56	5.36	1.70
2	34.89	32.98	30.95	30.09	29.20	28.28	27.33	26.84	26.39
3	60.35	55.99	51.24	49.21	47.09	44.87	42.53	41.32	40.19
4	65.79	64.82	63.83	63.43	63.02	62.46	60.92	60.08	59.32
5	74.39	70.92	67.27	65.75	64.19	62.75	62.24	62.03	61.85
6	105.52	103.13	100.68	99.68	98.67	97.65	96.43	95.26	94.20
7	115.41	110.47	105.29	103.15	100.96	98.72	96.62	96.10	95.63
8	118.05	117.51	116.98	116.77	116.55	116.34	114.77	113.79	112.91
	Percent difference								
1	0.03%	0.03%	0.03%	0.03%	0.03%	0.03%	0.03%	0.03%	0.02%
2	-0.01%	-0.01%	-0.01%	-0.02%	-0.02%	-0.03%	-0.03%	-0.03%	-0.03%
3	0.04%	0.04%	0.04%	0.04%	0.05%	0.05%	0.05%	0.05%	0.05%
4	-0.05%	-0.06%	-0.06%	-0.06%	-0.06%	-0.03%	-0.03%	-0.03%	-0.03%
5	-0.01%	-0.02%	-0.02%	-0.02%	-0.03%	-0.06%	-0.06%	-0.07%	-0.07%
6	-0.09%	-0.10%	-0.10%	-0.10%	-0.11%	-0.11%	0.06%	0.06%	0.06%
7	0.05%	0.05%	0.06%	0.06%	0.06%	0.06%	-0.11%	-0.11%	-0.12%
8	-0.08%	-0.09%	-0.09%	-0.09%	-0.10%	-0.08%	-0.04%	-0.04%	-0.04%

Figure 4.108 Eigenvalue curves, SSCF plate, $\phi = 1 / 1$,
$P_\xi = - N_x b^2 / D$, $\lambda^2 = \omega a^2 (\rho / D)^{1/2}$.

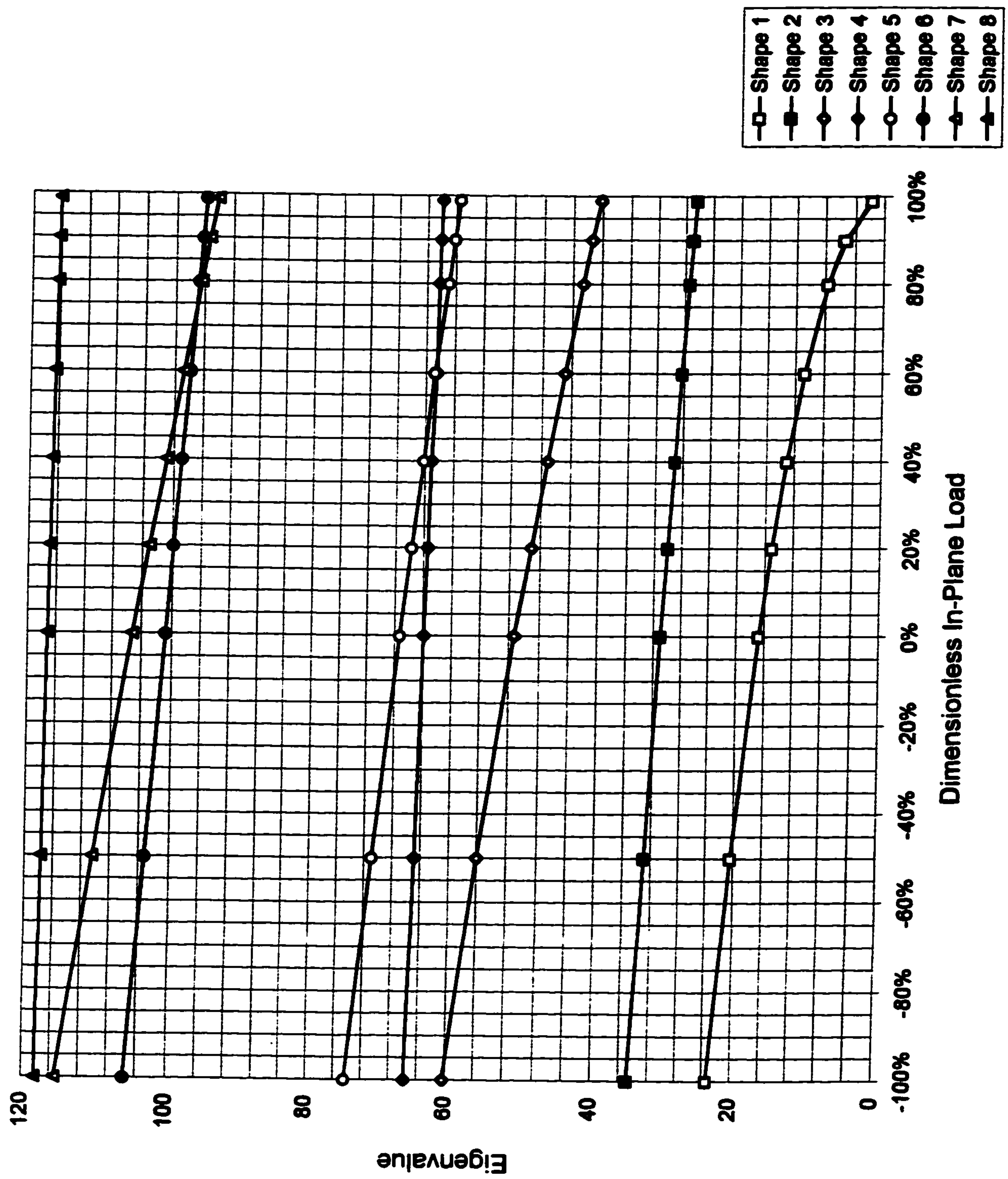

Figure 4.109 Mode shapes, SSCF plate, $\phi = 1 / 1$.

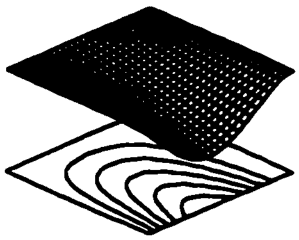

Shape 1

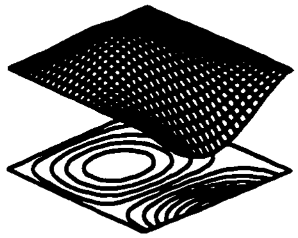

Shape 2

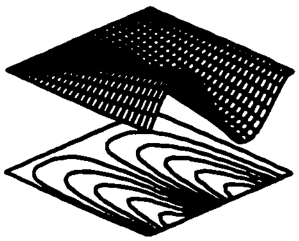

Shape 3

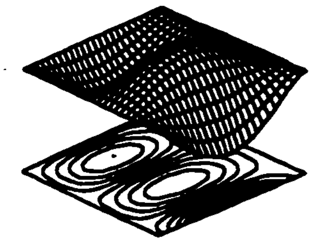

Shape 4

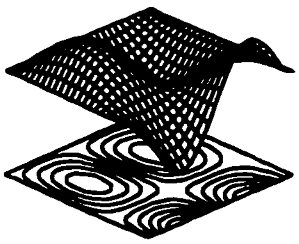

Shape 5

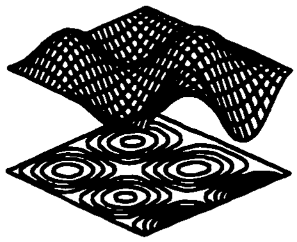

Shape 6

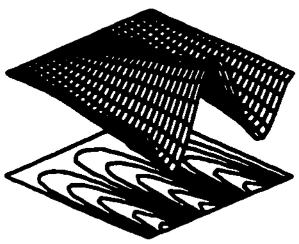

Shape 7

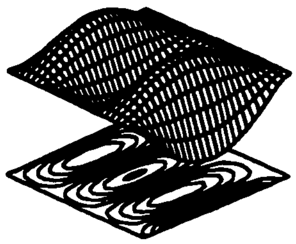

Shape 8

Table 4.61 Eigenvalues, SSCF plate, $\phi = 3/2$, $\lambda^2 = \omega a^2 (\rho / D)^{1/2}$.

Mode	In-plane load as a percentage of buckling load								
	-100%	-50%	0%	20%	40%	60%	80%	90%	99%
	Present solution								
1	22.33	19.42	15.94	14.29	12.41	10.16	7.21	5.11	1.62
2	27.17	24.88	22.32	21.21	20.02	18.76	17.39	16.66	15.97
3	39.65	38.15	36.57	35.92	35.25	34.57	33.87	33.52	33.20
4	58.83	54.76	50.36	48.49	46.53	44.50	42.36	41.25	40.23
5	61.61	60.66	57.66	56.03	54.36	52.63	50.84	49.92	49.07
6	65.17	61.53	59.70	59.32	58.92	58.53	58.13	57.93	57.75
7	78.65	75.69	72.60	71.32	70.02	68.69	67.34	66.65	66.03
8	93.13	92.51	91.89	91.64	91.39	91.14	90.88	90.75	90.61
	Finite element solution [18]								
1	22.33	19.42	15.94	14.29	12.41	10.16	7.21	5.11	1.62
2	27.17	24.88	22.32	21.20	20.02	18.75	17.38	16.65	15.96
3	39.63	38.12	36.55	35.89	35.23	34.54	33.85	33.49	33.17
4	58.82	54.76	50.35	48.48	46.52	44.49	42.35	41.24	40.22
5	61.55	60.61	57.63	56.00	54.32	52.59	50.80	49.88	49.04
6	65.14	61.50	59.65	59.26	58.87	58.47	58.07	57.87	57.69
7	78.57	75.60	72.51	71.23	69.93	68.60	67.25	66.56	65.93
8	93.05	92.44	91.82	91.57	91.32	91.06	90.80	90.67	90.51
	Percent difference								
1	0.01%	0.01%	0.01%	0.01%	0.02%	0.01%	0.02%	0.01%	0.00%
2	-0.01%	-0.01%	-0.02%	-0.01%	-0.02%	-0.02%	-0.03%	-0.03%	-0.03%
3	-0.06%	-0.06%	-0.07%	-0.07%	-0.07%	-0.08%	-0.08%	-0.08%	-0.08%
4	-0.02%	-0.02%	-0.02%	-0.02%	-0.02%	-0.02%	-0.02%	-0.03%	-0.03%
5	-0.09%	-0.09%	-0.05%	-0.06%	-0.06%	-0.06%	-0.07%	-0.07%	-0.07%
6	-0.04%	-0.05%	-0.09%	-0.10%	-0.10%	-0.10%	-0.10%	-0.10%	-0.10%
7	-0.10%	-0.11%	-0.12%	-0.12%	-0.13%	-0.13%	-0.14%	-0.14%	-0.14%
8	-0.08%	-0.08%	-0.08%	-0.08%	-0.09%	-0.08%	-0.09%	-0.09%	-0.11%

Figure 4.110 Eigenvalue curves, SSCF plate, $\phi = 3 / 2$,

$P_\xi = - N_x b^2 / D$, $\lambda^2 = \omega a^2 (\rho / D)^{1/2}$.

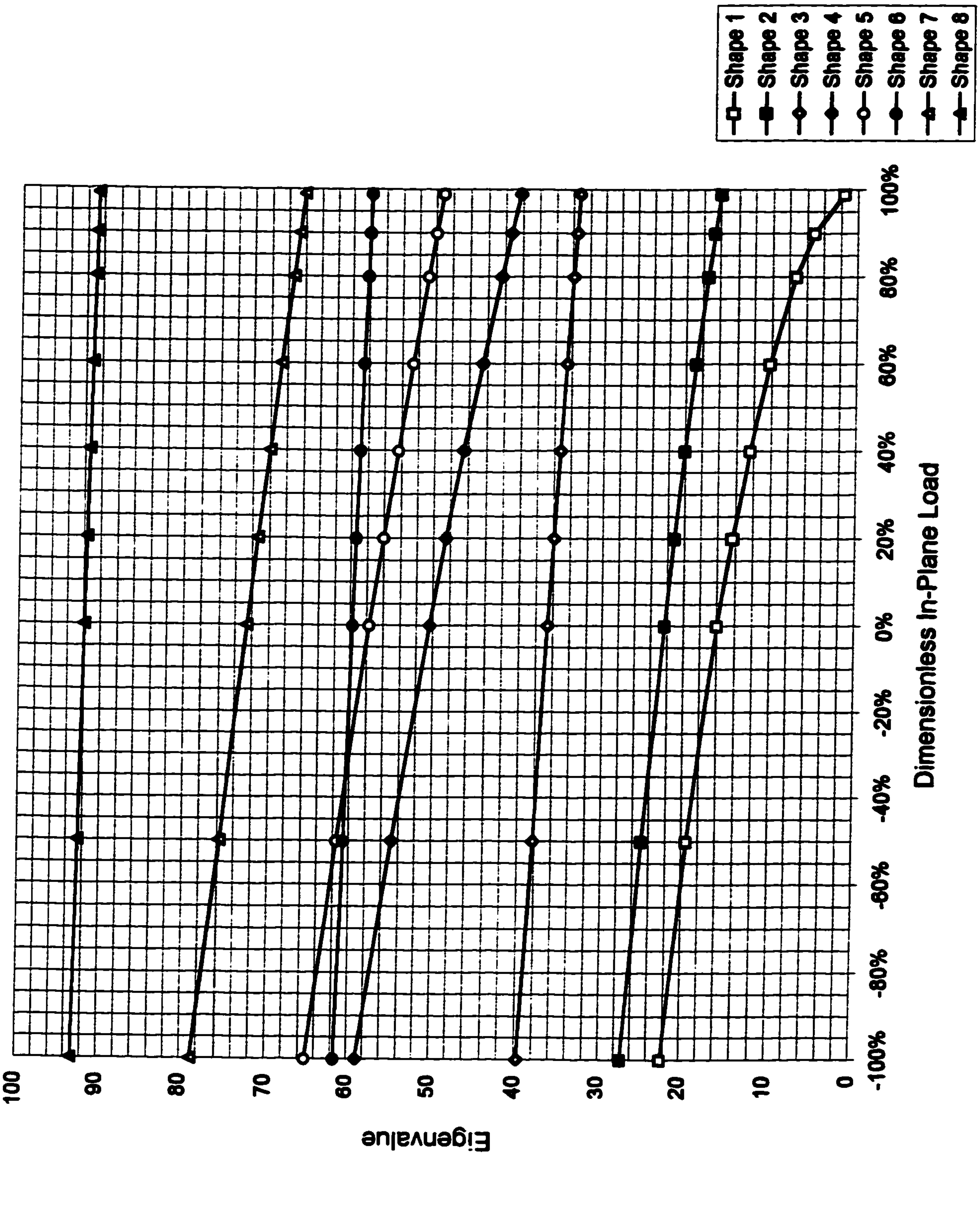

Figure 4.111 Mode shapes, SSCF plate, $\phi = 3 / 2$.

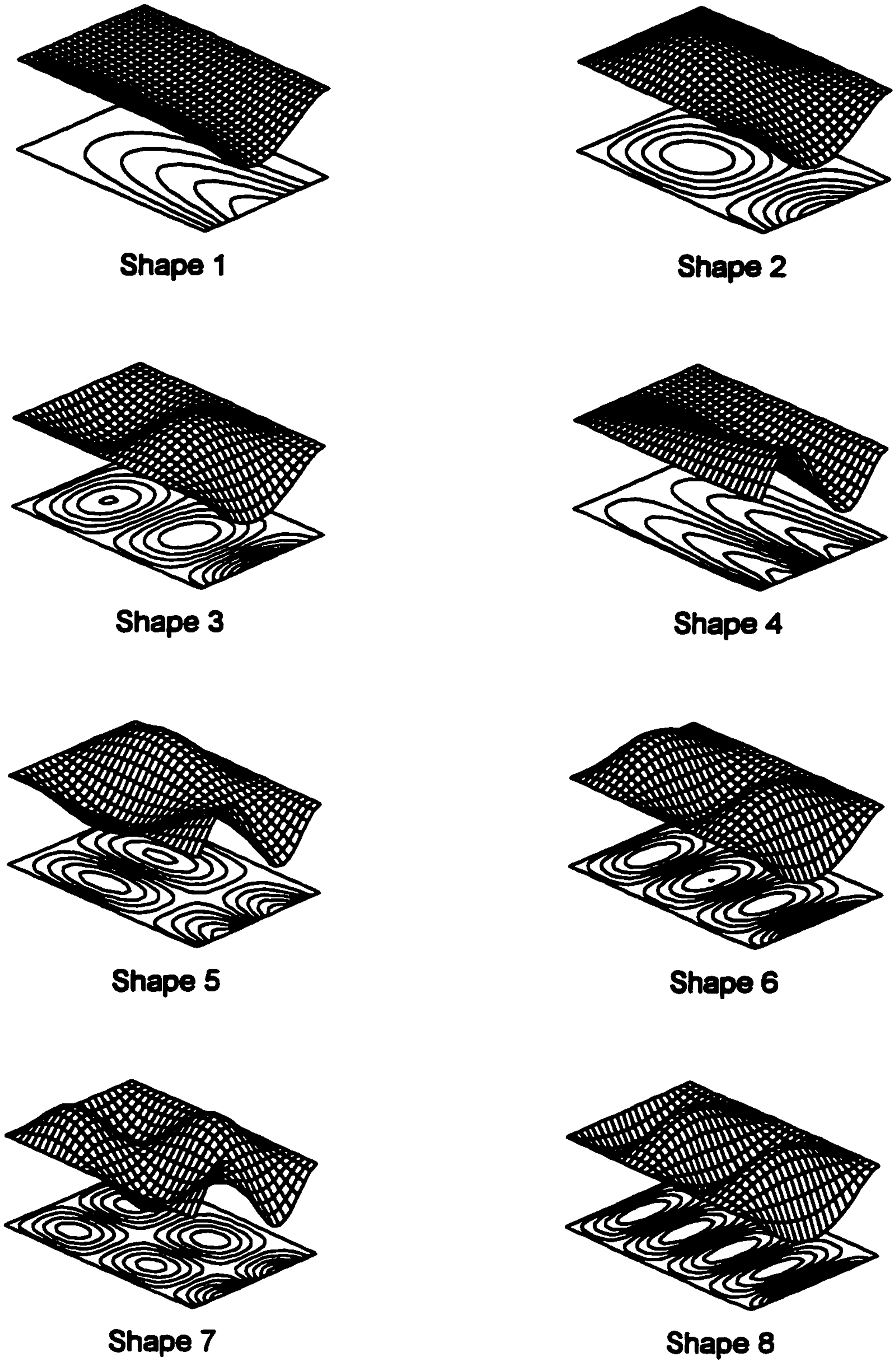

Table 4.62 Eigenvalues, SSCF plate, $\phi = 2 / 1$, $\lambda^2 = \omega a^2 (\rho / D)^{1/2}$.

Mode	In-plane load as a percentage of buckling load								
	-100%	-50%	0%	20%	40%	60%	80%	90%	99%
	Present solution								
1	21.96	19.10	15.67	14.05	12.20	9.99	7.09	5.02	1.59
2	24.61	22.12	19.28	18.01	16.63	15.12	13.42	12.48	11.56
3	31.09	29.18	27.13	26.26	25.36	24.42	23.44	22.93	22.46
4	42.60	41.25	39.85	39.27	38.69	38.09	37.49	37.18	36.90
5	58.33	54.37	50.08	48.26	46.37	44.39	42.33	41.26	40.27
6	59.56	58.22	54.25	52.57	50.84	49.05	47.19	46.23	45.35
7	61.93	58.62	57.66	57.27	56.87	56.48	56.07	55.81	55.14
8	69.39	66.11	62.65	61.21	59.74	58.23	56.68	55.81	55.70
	Finite element solution [18]								
1	21.96	19.10	15.67	14.05	12.20	9.99	7.09	5.02	1.59
2	24.60	22.12	19.28	18.00	16.62	15.11	13.41	12.47	11.55
3	31.06	29.16	27.11	26.24	25.34	24.39	23.41	22.90	22.43
4	42.54	41.19	39.79	39.21	38.63	38.03	37.42	37.11	36.83
5	58.30	54.34	50.06	48.23	46.34	44.37	42.30	41.23	40.24
6	59.47	58.17	54.19	52.52	50.79	48.99	47.13	46.17	45.29
7	61.88	58.53	57.56	57.17	56.78	56.38	55.97	55.71	55.03
8	69.29	66.01	62.55	61.11	59.64	58.12	56.57	55.83	55.60
	Percent difference								
1	-0.01%	0.00%	0.00%	0.00%	0.00%	0.00%	0.01%	0.01%	0.02%
2	-0.02%	-0.02%	-0.03%	-0.03%	-0.03%	-0.04%	-0.05%	-0.06%	-0.07%
3	-0.07%	-0.08%	-0.09%	-0.10%	-0.10%	-0.11%	-0.12%	-0.13%	-0.13%
4	-0.14%	-0.14%	-0.15%	-0.16%	-0.16%	-0.17%	-0.17%	-0.18%	-0.18%
5	-0.05%	-0.05%	-0.05%	-0.05%	-0.06%	-0.06%	-0.06%	-0.07%	-0.07%
6	-0.15%	-0.09%	-0.10%	-0.10%	-0.11%	-0.12%	-0.12%	-0.13%	-0.13%
7	-0.08%	-0.16%	-0.16%	-0.17%	-0.17%	-0.17%	-0.17%	-0.17%	-0.20%
8	-0.14%	-0.15%	-0.16%	-0.17%	-0.18%	-0.18%	-0.19%	0.04%	-0.18%

Figure 4.112 Eigenvalue curves, SSCF plate, $\phi = 2 / 1$,

$P_\xi = - N_x b^2 / D$, $\lambda^2 = \omega a^2 (\rho / D)^{1/2}$.

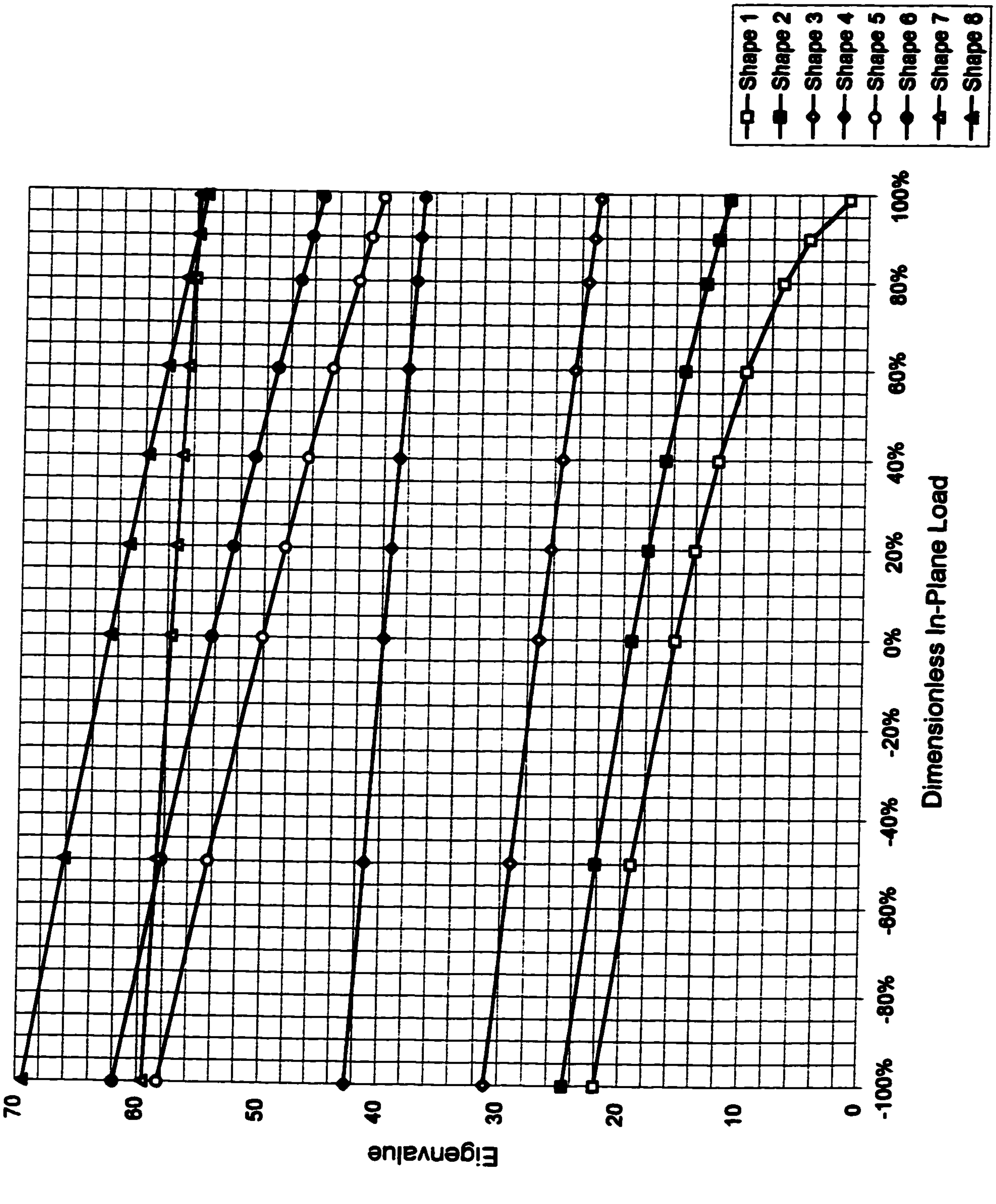

Figure 4.113 Mode shapes, SSCF plate, ϕ = 2 / 1.

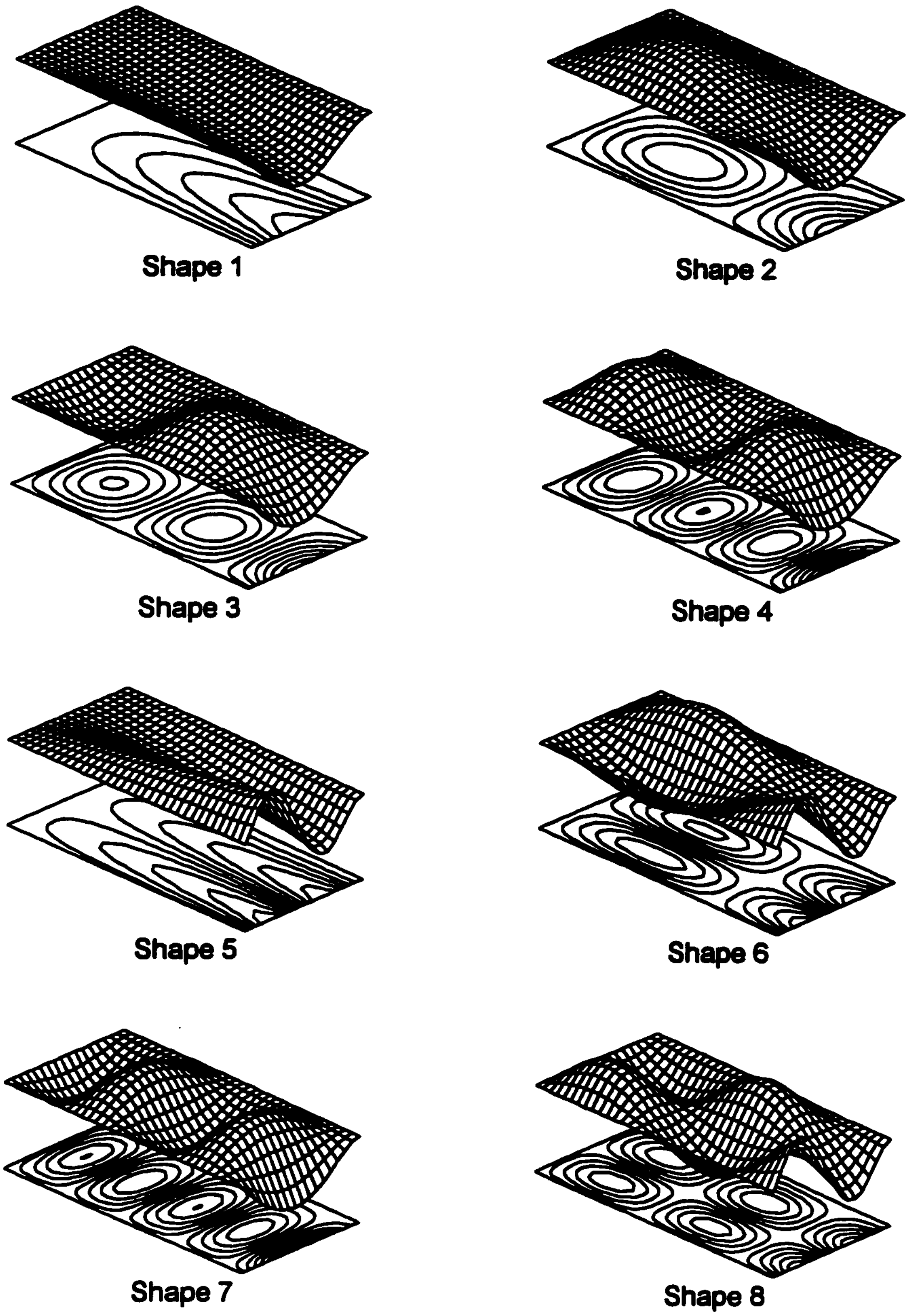

Table 4.63 Eigenvalues, SSCF plate, $\phi = 5 / 2$, $\lambda^2 = \omega a^2 (\rho / D)^{1/2}$.

	In-plane load as a percentage of buckling load								
Mode	-100%	-50%	0%	20%	40%	60%	80%	90%	99%
	Present solution								
1	21.79	18.95	15.55	13.94	12.11	9.91	7.03	4.98	1.58
2	23.46	20.87	17.87	16.50	15.00	13.32	11.38	10.26	9.13
3	27.37	25.21	22.82	21.78	20.69	19.53	18.29	17.63	17.02
4	34.25	32.57	30.79	30.04	29.27	28.48	27.66	27.24	26.86
5	44.55	43.28	41.97	41.44	40.89	40.34	39.78	39.49	39.23
6	58.11	54.19	49.97	48.17	46.30	44.36	42.32	41.27	40.29
7	58.36	56.69	52.67	50.97	49.21	47.38	45.48	44.50	43.60
8	60.44	57.41	56.44	56.05	54.93	53.30	51.62	50.76	49.98
	Finite element solution [18]								
1	21.79	18.95	15.55	13.94	12.11	9.91	7.03	4.98	1.58
2	23.46	20.87	17.86	16.50	15.00	13.31	11.37	10.25	9.11
3	27.35	25.18	22.79	21.76	20.66	19.50	18.26	17.60	16.98
4	34.19	32.51	30.72	29.97	29.20	28.41	27.59	27.17	26.78
5	44.44	43.17	41.86	41.32	40.78	40.22	39.66	39.37	39.11
6	58.07	54.16	49.93	48.14	46.27	44.32	42.29	41.23	40.26
7	58.22	56.62	52.60	50.90	49.14	47.31	45.41	44.43	43.52
8	60.37	57.26	56.29	55.90	54.81	53.18	51.50	50.64	49.85
	Percent difference								
1	-0.01%	-0.01%	0.00%	0.00%	0.00%	0.00%	0.00%	0.00%	0.00%
2	-0.03%	-0.03%	-0.04%	-0.04%	-0.05%	-0.06%	-0.08%	-0.10%	-0.13%
3	-0.08%	-0.09%	-0.11%	-0.12%	-0.13%	-0.15%	-0.17%	-0.18%	-0.20%
4	-0.17%	-0.19%	-0.21%	-0.22%	-0.23%	-0.24%	-0.26%	-0.26%	-0.27%
5	-0.24%	-0.25%	-0.27%	-0.28%	-0.28%	-0.29%	-0.30%	-0.30%	-0.31%
6	-0.06%	-0.06%	-0.06%	-0.06%	-0.07%	-0.07%	-0.08%	-0.08%	-0.08%
7	-0.25%	-0.12%	-0.13%	-0.14%	-0.14%	-0.15%	-0.16%	-0.17%	-0.18%
8	-0.11%	-0.26%	-0.26%	-0.27%	-0.21%	-0.23%	-0.24%	-0.25%	-0.25%

Figure 4.114 Eigenvalue curves, SSCF plate, $\phi = 5 / 2$,

$P_\xi = - N_x b^2 / D$, $\lambda^2 = \omega a^2 (\rho / D)^{1/2}$.

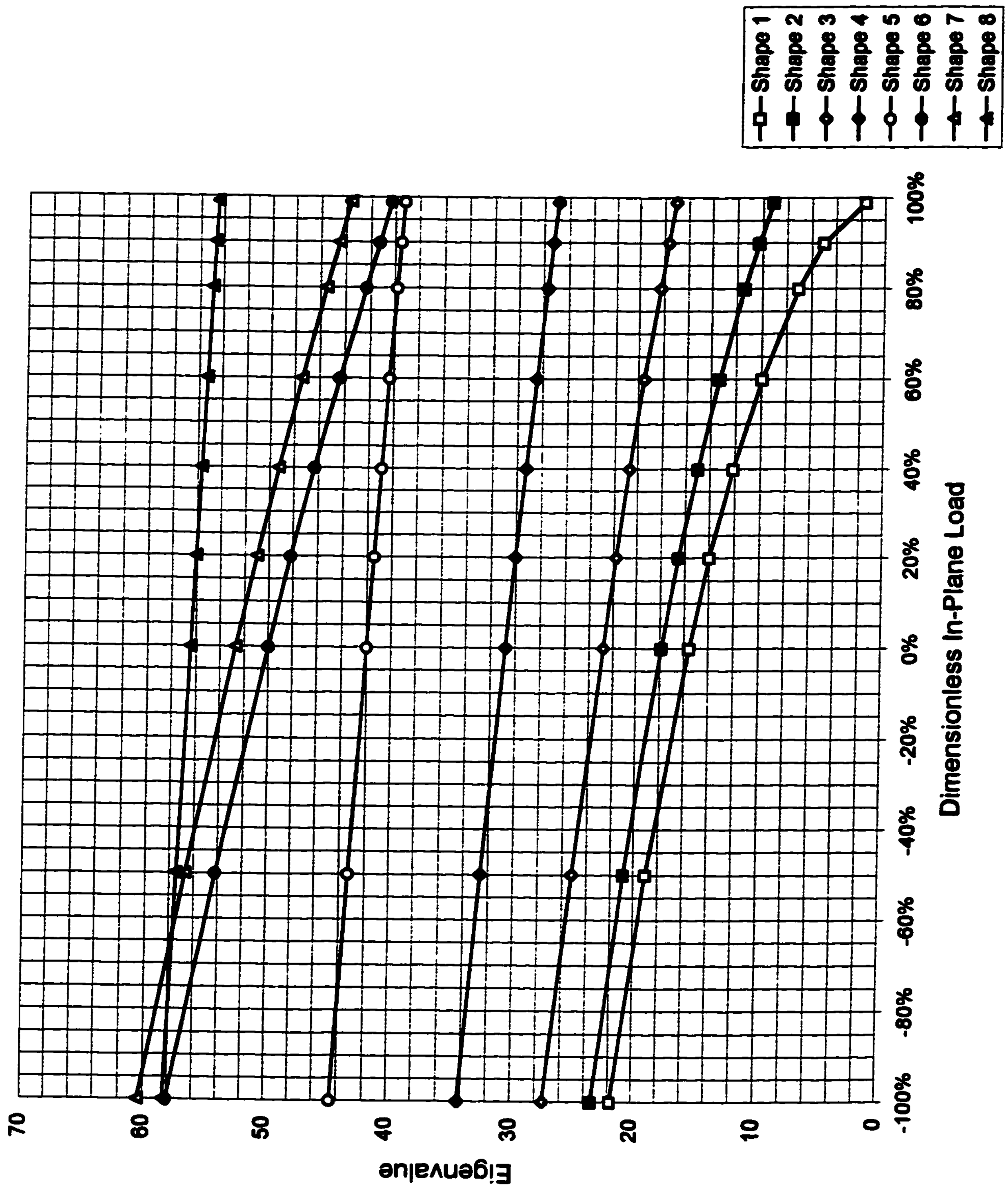

Figure 4.115 Mode shapes, SSCF plate, $\phi = 5 / 2$.

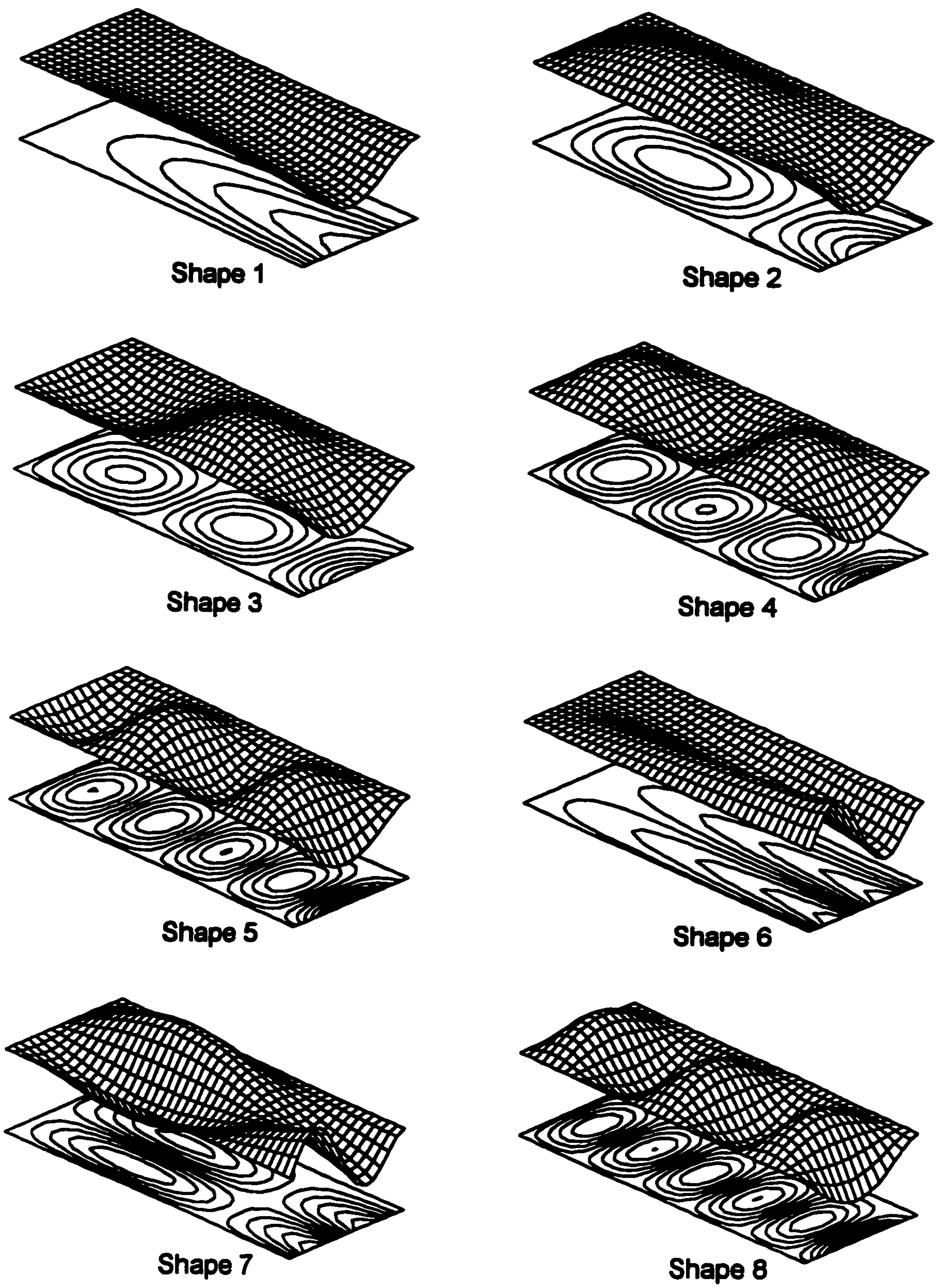

Table 4.64 Eigenvalues, SSCF plate, $\phi = 3 / 1$, $\lambda^2 = \omega a^2 (\rho / D)^{1/2}$.

	In-plane load as a percentage of buckling load								
Mode	-100%	-50%	0%	20%	40%	60%	80%	90%	99%
				Present solution					
1	21.70	18.88	15.49	13.89	12.06	9.87	7.00	4.96	1.57
2	22.86	20.20	17.11	15.68	14.10	12.30	10.17	8.91	7.59
3	25.46	23.12	20.50	19.34	18.10	16.77	15.30	14.51	13.75
4	29.96	28.03	25.93	25.04	24.11	23.14	22.12	21.59	21.10
5	36.73	35.18	33.56	32.88	32.19	31.48	30.76	30.38	30.05
6	45.92	44.71	43.46	42.94	42.42	41.89	41.36	41.09	40.31
7	57.57	54.11	49.91	48.12	46.27	44.34	42.32	41.28	40.84
8	58.00	55.87	51.81	50.10	48.32	46.48	44.55	43.56	42.65
				Finite element solution [18]					
1	21.70	18.88	15.49	13.89	12.06	9.87	7.00	4.96	1.57
2	22.85	20.20	17.10	15.67	14.09	12.29	10.16	8.89	7.57
3	25.44	23.10	20.48	19.32	18.08	16.74	15.27	14.47	13.71
4	29.90	27.97	25.87	24.97	24.04	23.07	22.05	21.51	21.02
5	36.62	35.07	33.44	32.76	32.07	31.36	30.62	30.25	29.91
6	45.75	44.54	43.28	42.76	42.24	41.71	41.17	40.90	40.28
7	57.35	54.08	49.88	48.10	46.24	44.31	42.29	41.25	40.65
8	57.97	55.79	51.73	50.02	48.24	46.39	44.47	43.47	42.56
				Percent difference					
1	-0.01%	0.00%	0.00%	0.00%	0.01%	0.01%	0.01%	0.01%	-0.01%
2	-0.03%	-0.03%	-0.04%	-0.04%	-0.06%	-0.08%	-0.12%	-0.16%	-0.23%
3	-0.09%	-0.10%	-0.12%	-0.14%	-0.16%	-0.18%	-0.22%	-0.24%	-0.27%
4	-0.19%	-0.21%	-0.25%	-0.26%	-0.29%	-0.31%	-0.34%	-0.36%	-0.38%
5	-0.30%	-0.33%	-0.36%	-0.37%	-0.39%	-0.41%	-0.43%	-0.44%	-0.45%
6	-0.37%	-0.39%	-0.41%	-0.42%	-0.43%	-0.44%	-0.46%	-0.46%	-0.08%
7	-0.37%	-0.05%	-0.06%	-0.06%	-0.06%	-0.07%	-0.07%	-0.07%	-0.46%
8	-0.05%	-0.13%	-0.15%	-0.16%	-0.17%	-0.18%	-0.19%	-0.20%	-0.21%

Figure 4.116 Eigenvalue curves, SSCF plate, $\phi = 3 / 1$,

$P_\xi = - N_x b^2 / D$, $\lambda^2 = \omega a^2 (\rho / D)^{1/2}$.

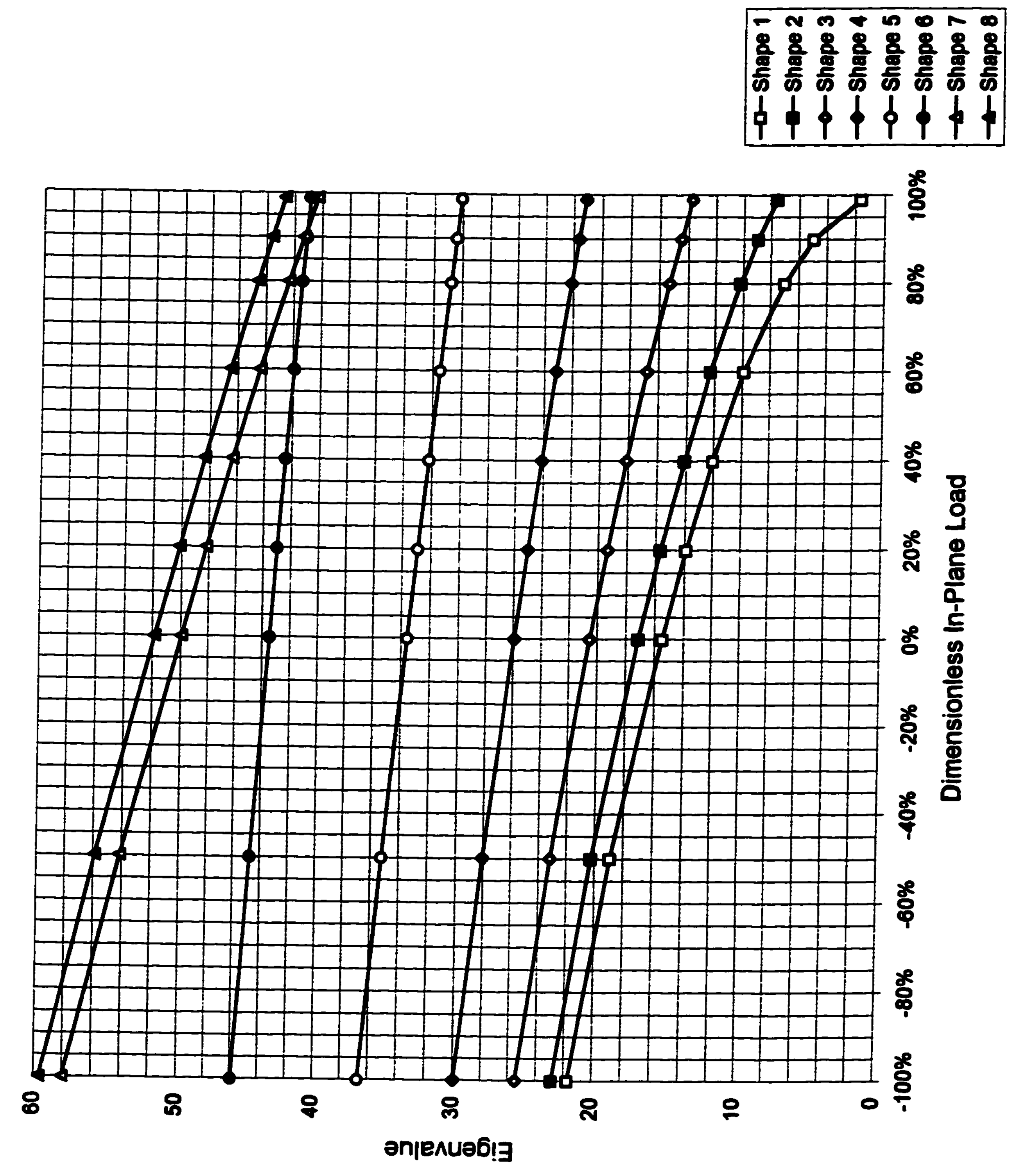

Figure 4.117 Mode shapes, SSCF plate, $\phi = 3 / 1$.

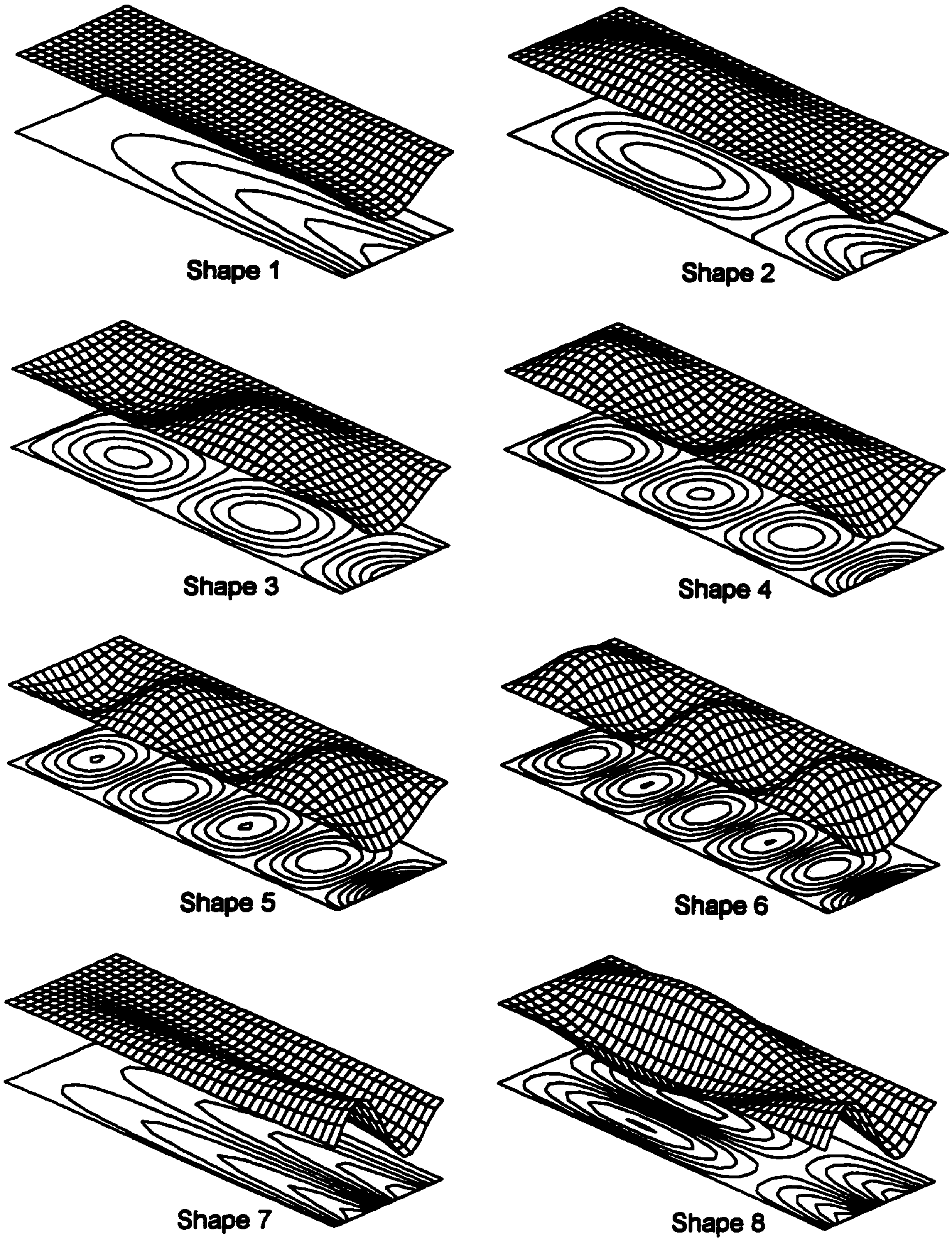

Table 4.65 Eigenvalues, SCCF plate, $\phi = 1 / 3$, $\lambda^2 = \omega a^2 (\rho / D)^{1/2}$.

	In-plane load as a percentage of buckling load								
Mode	-100%	-50%	0%	20%	40%	60%	80%	90%	99%
				Present solution					
1	55.56	49.43	42.28	38.99	35.29	30.94	24.96	19.55	6.71
2	102.88	89.67	74.00	66.65	58.34	48.60	36.63	29.85	24.37
3	165.07	146.95	126.17	116.80	106.60	95.31	82.51	75.32	68.25
4	213.88	212.42	198.40	188.07	177.13	165.46	152.92	146.24	139.97
5	243.50	222.12	210.95	210.36	209.76	209.16	208.56	208.26	207.99
6	257.06	252.18	247.19	245.16	243.12	241.05	238.94	237.45	231.88
7	321.88	313.07	290.55	279.70	268.41	256.62	244.15	238.31	237.01
8	339.62	316.08	304.07	300.37	296.62	292.82	288.97	287.03	285.26
				Finite element solution [18]					
1	55.55	49.42	42.27	38.97	35.27	30.92	24.94	19.53	6.71
2	102.90	89.69	74.01	66.66	58.35	48.61	36.65	29.87	24.38
3	165.21	147.09	126.32	116.96	106.78	95.51	82.73	75.56	68.52
4	213.59	212.12	198.94	188.63	177.72	166.09	153.60	146.95	140.71
5	243.97	222.62	210.66	210.06	209.46	208.86	208.26	207.96	207.69
6	256.53	251.64	246.64	244.61	242.56	240.48	238.38	237.28	233.48
7	320.92	312.09	291.88	281.07	269.83	258.10	245.83	239.51	236.46
8	340.80	317.31	303.04	299.32	295.55	291.75	287.88	285.93	284.15
				Percent difference					
1	-0.01%	-0.01%	-0.02%	-0.03%	-0.04%	-0.05%	-0.09%	-0.10%	0.00%
2	0.02%	0.02%	0.02%	0.02%	0.02%	0.03%	0.05%	0.07%	0.05%
3	0.08%	0.10%	0.12%	0.14%	0.17%	0.20%	0.27%	0.32%	0.39%
4	-0.14%	-0.14%	0.27%	0.30%	0.34%	0.38%	0.44%	0.48%	0.53%
5	0.19%	0.22%	-0.14%	-0.14%	-0.14%	-0.14%	-0.15%	-0.14%	-0.14%
6	-0.21%	-0.22%	-0.22%	-0.23%	-0.23%	-0.23%	-0.23%	-0.07%	0.69%
7	-0.30%	-0.32%	0.46%	0.49%	0.53%	0.58%	0.69%	0.50%	-0.23%
8	0.35%	0.39%	-0.34%	-0.35%	-0.36%	-0.37%	-0.38%	-0.38%	-0.39%

Figure 4.118 Eigenvalue curves, SCCF plate, $\phi = 1 / 3$,

$P_\xi = - N_x b^2 / D$, $\lambda^2 = \omega a^2 (\rho / D)^{1/2}$.

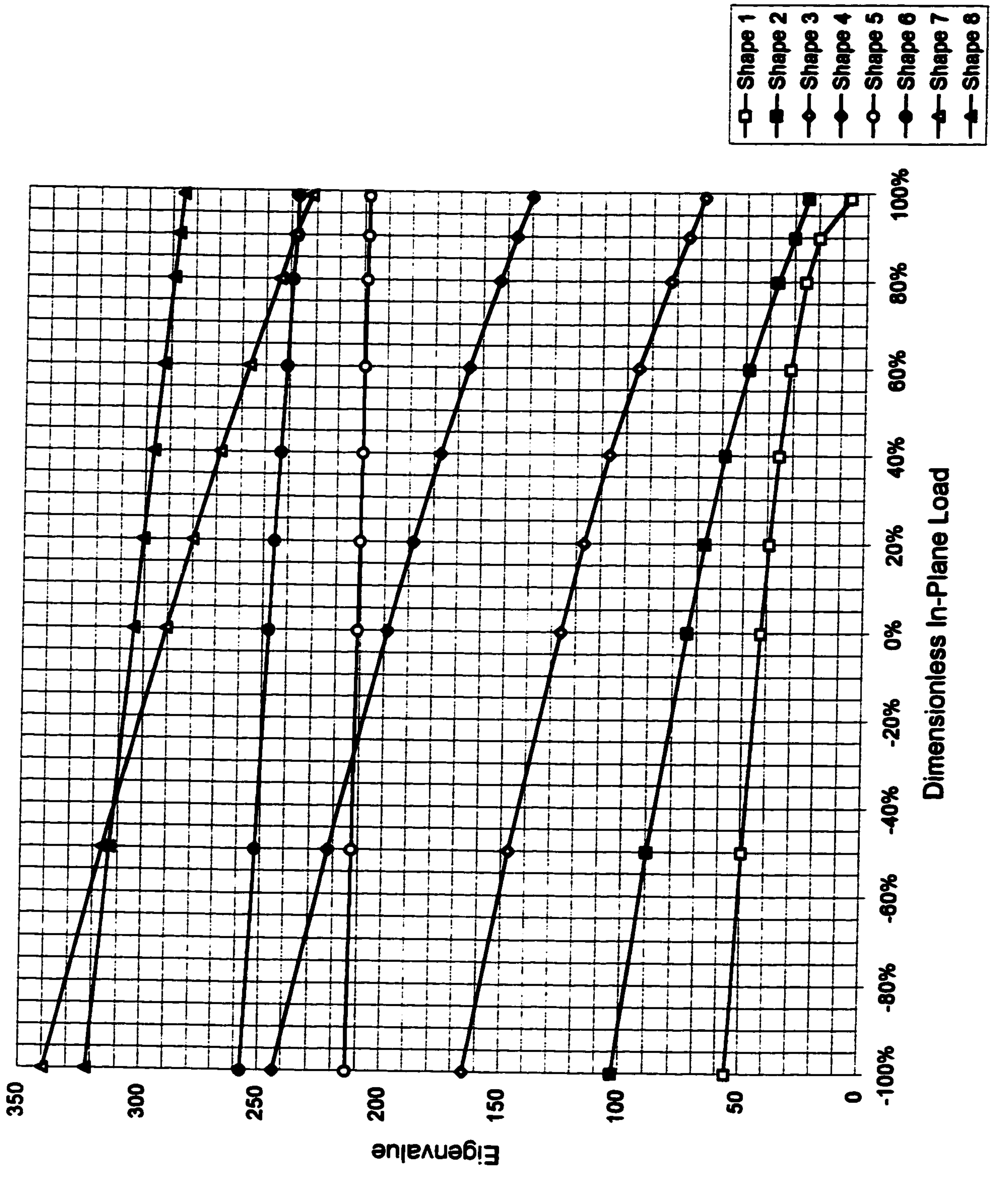

Figure 4.119 Mode shapes, SCCF plate, $\phi = 1 / 3$.

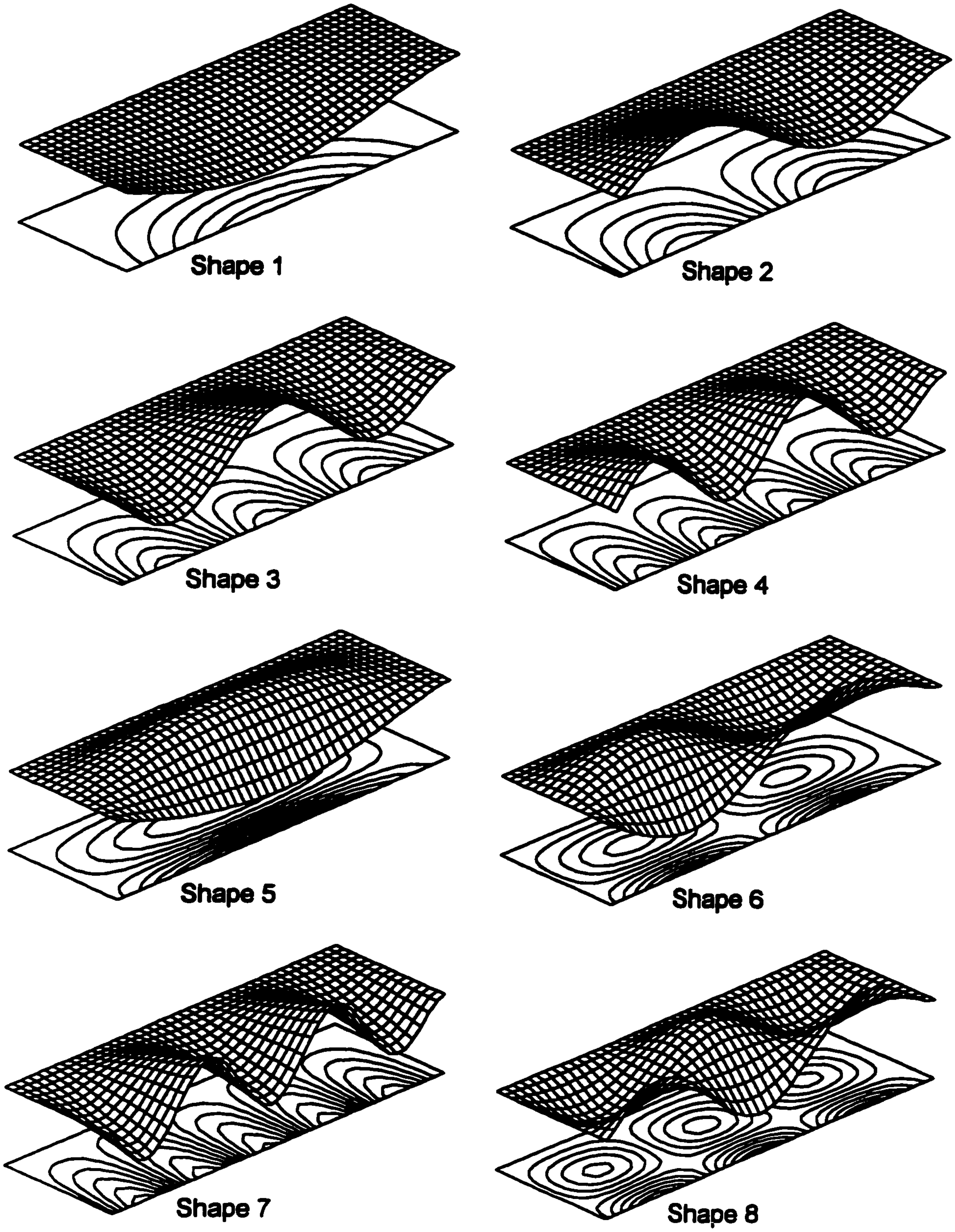

Table 4.66 Eigenvalues, SCCF plate, $\phi = 2 / 5$, $\lambda^2 = \omega a^2 (\rho / D)^{1/2}$.

Mode	In-plane load as a percentage of buckling load								
	-100%	-50%	0%	20%	40%	60%	80%	90%	99%
	Present solution								
1	45.25	39.73	33.16	30.07	26.54	22.30	16.57	12.21	4.07
2	89.56	78.57	65.68	59.71	53.05	45.41	36.25	30.80	25.20
3	149.09	134.66	118.44	111.28	103.63	95.35	86.29	81.39	76.71
4	153.51	152.02	150.52	149.91	149.30	148.69	148.06	147.75	147.43
5	196.09	191.43	186.63	183.37	175.38	166.96	158.09	153.46	149.21
6	225.72	209.16	191.17	184.77	182.73	180.73	178.70	177.68	176.75
7	258.89	250.95	242.75	239.39	235.97	232.50	228.98	227.19	225.58
8	320.65	302.73	283.67	275.68	267.45	258.96	250.17	245.67	241.54
	Finite element solution [18]								
1	45.25	39.72	33.16	30.07	26.54	22.30	16.56	12.20	4.07
2	89.59	78.61	65.71	59.74	53.09	45.45	36.30	30.86	25.27
3	149.25	134.84	118.63	111.48	103.83	95.57	86.53	81.65	76.99
4	153.32	151.83	150.33	149.72	149.11	148.49	147.88	147.56	147.26
5	195.75	191.07	186.27	183.85	176.00	167.61	158.76	154.16	149.90
6	226.22	209.69	191.74	184.52	182.36	180.35	178.32	177.29	176.37
7	258.26	250.30	242.07	238.69	235.27	231.79	228.25	226.46	224.84
8	321.85	303.99	285.01	277.05	268.86	260.40	251.67	247.18	243.08
	Percent difference								
1	0.00%	0.00%	-0.01%	-0.01%	-0.02%	-0.04%	-0.06%	-0.09%	-0.07%
2	0.04%	0.04%	0.05%	0.06%	0.07%	0.09%	0.14%	0.20%	0.28%
3	0.11%	0.13%	0.16%	0.18%	0.20%	0.23%	0.28%	0.32%	0.36%
4	-0.12%	-0.12%	-0.13%	-0.12%	-0.13%	-0.13%	-0.13%	-0.13%	-0.12%
5	-0.17%	-0.19%	-0.19%	0.26%	0.35%	0.39%	0.43%	0.45%	0.46%
6	0.22%	0.25%	0.30%	-0.14%	-0.20%	-0.21%	-0.21%	-0.22%	-0.22%
7	-0.24%	-0.26%	-0.28%	-0.29%	-0.30%	-0.31%	-0.32%	-0.32%	-0.33%
8	0.38%	0.42%	0.47%	0.50%	0.53%	0.56%	0.60%	0.62%	0.64%

Figure 4.120 Eigenvalue curves, SCCF plate, $\phi = 2 / 5$,

$P_\xi = - N_x b^2 / D$, $\lambda^2 = \omega a^2 (\rho / D)^{1/2}$.

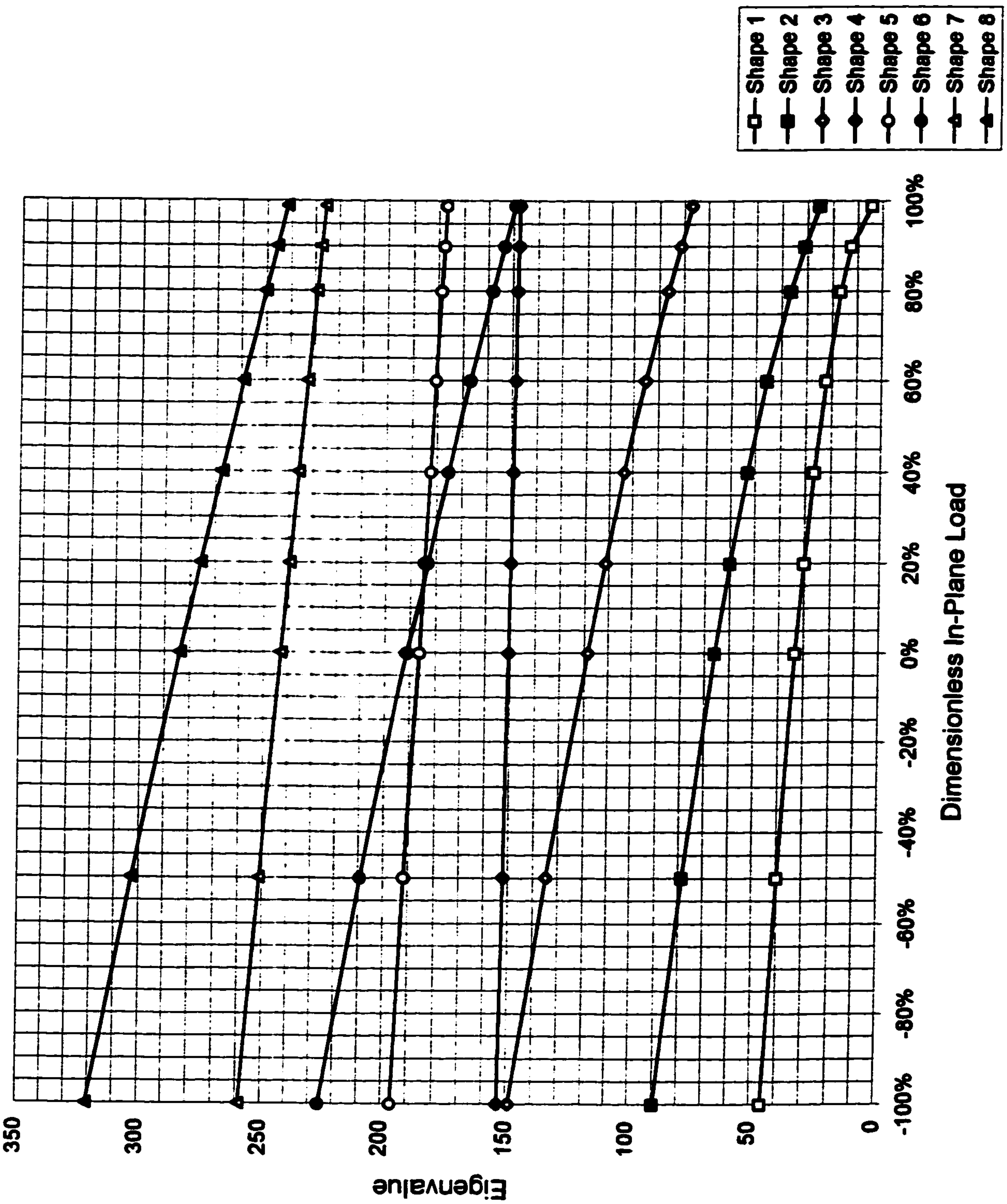

Figure 4.121 Mode shapes, SCCF plate, $\phi = 2 / 5$.

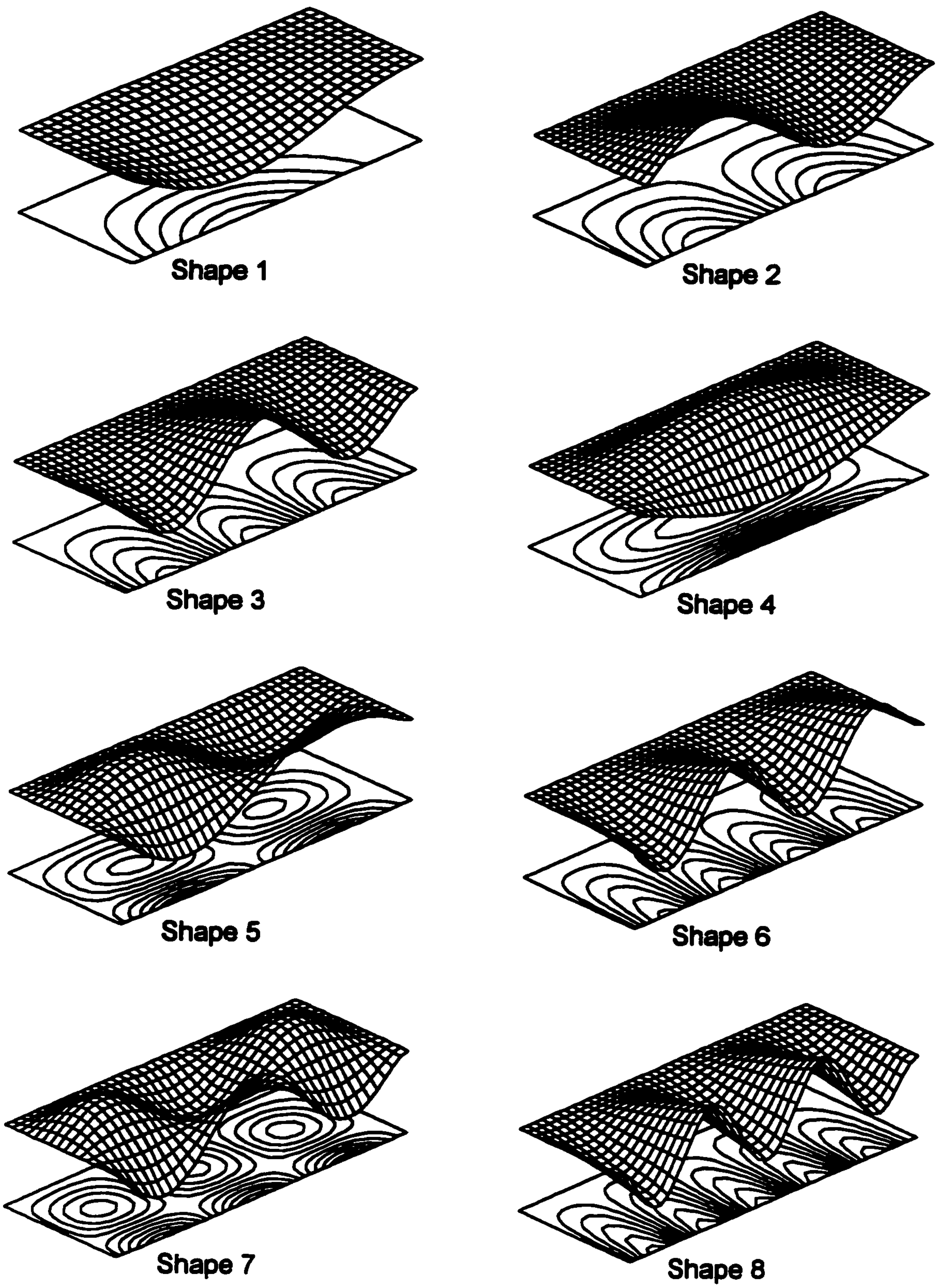

Table 4.67 Eigenvalues, SCCF plate, $\phi = 1/2$, $\lambda^2 = \omega a^2 (\rho / D)^{1/2}$.

Mode	In-plane load as a percentage of buckling load								
	-100%	-50%	0%	20%	40%	60%	80%	90%	99%
	Present solution								
1	36.02	31.45	25.98	23.38	20.41	16.84	12.08	8.63	2.76
2	76.96	68.70	59.23	54.98	50.35	45.25	39.50	36.30	33.18
3	104.06	102.62	101.16	100.56	99.95	97.19	91.56	88.60	85.85
4	134.08	123.77	112.49	107.65	102.59	99.40	98.78	98.47	98.19
5	145.42	141.30	137.05	135.31	133.55	131.75	129.94	129.02	128.18
6	205.55	197.74	185.56	180.45	175.19	169.76	164.16	161.29	158.65
7	209.26	199.07	192.31	189.54	186.73	183.87	180.97	179.50	178.17
8	259.53	258.96	258.39	258.16	257.88	255.61	251.96	250.11	248.42
	Finite element solution [18]								
1	36.03	31.45	25.98	23.39	20.42	16.84	12.08	8.63	2.76
2	77.00	68.74	59.28	55.02	50.40	45.31	39.57	36.37	33.25
3	103.96	102.52	101.05	100.46	99.85	97.41	91.79	88.84	86.10
4	134.26	123.95	112.69	107.85	102.79	99.30	98.67	98.36	98.09
5	145.22	141.10	136.84	135.10	133.33	131.54	129.71	128.79	127.96
6	205.22	198.22	186.11	181.02	175.77	170.36	164.77	161.91	159.29
7	209.75	198.76	191.94	189.16	186.34	183.48	180.57	179.10	177.76
8	258.98	258.41	257.84	257.60	257.33	255.06	251.40	249.54	247.85
	Percent difference								
1	0.01%	0.01%	0.01%	0.01%	0.01%	0.00%	0.00%	0.00%	0.12%
2	0.05%	0.06%	0.08%	0.08%	0.10%	0.13%	0.16%	0.18%	0.22%
3	-0.10%	-0.10%	-0.10%	-0.10%	-0.10%	0.22%	0.25%	0.27%	0.29%
4	0.13%	0.15%	0.17%	0.19%	0.20%	-0.10%	-0.11%	-0.11%	-0.11%
5	-0.13%	-0.14%	-0.15%	-0.16%	-0.16%	-0.16%	-0.17%	-0.17%	-0.17%
6	-0.16%	0.25%	0.30%	0.31%	0.33%	0.35%	0.37%	0.39%	0.40%
7	0.24%	-0.16%	-0.19%	-0.20%	-0.20%	-0.21%	-0.22%	-0.22%	-0.23%
8	-0.21%	-0.21%	-0.22%	-0.22%	-0.21%	-0.21%	-0.22%	-0.23%	-0.23%

Figure 4.122 Eigenvalue curves, SCCF plate, $\phi = 1 / 2$, $P_\xi = - N_x b^2 / D$, $\lambda^2 = \omega a^2 (\rho / D)^{1/2}$.

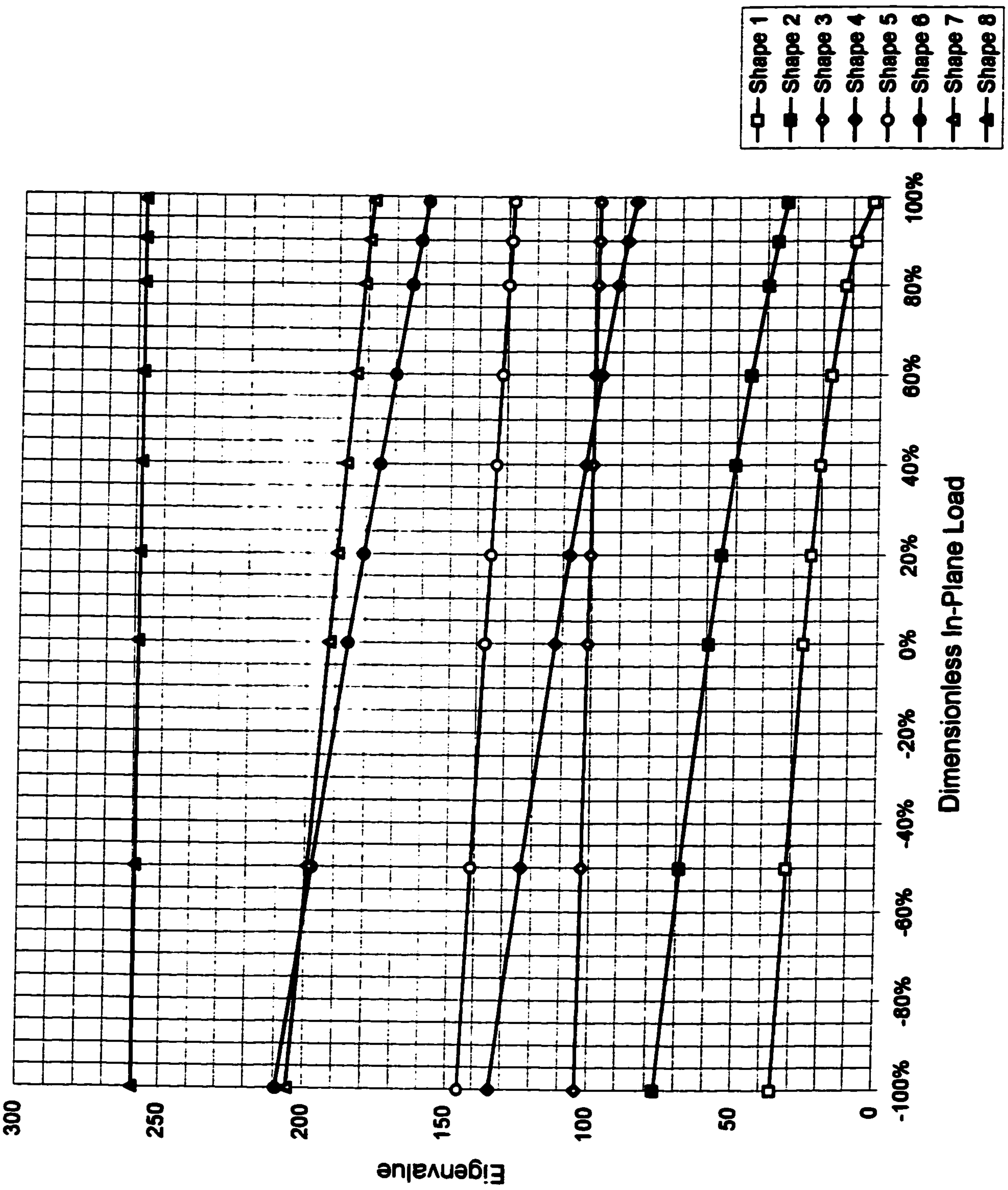

Figure 4.123 Mode shapes, SCCF plate, ϕ = 1 / 2.

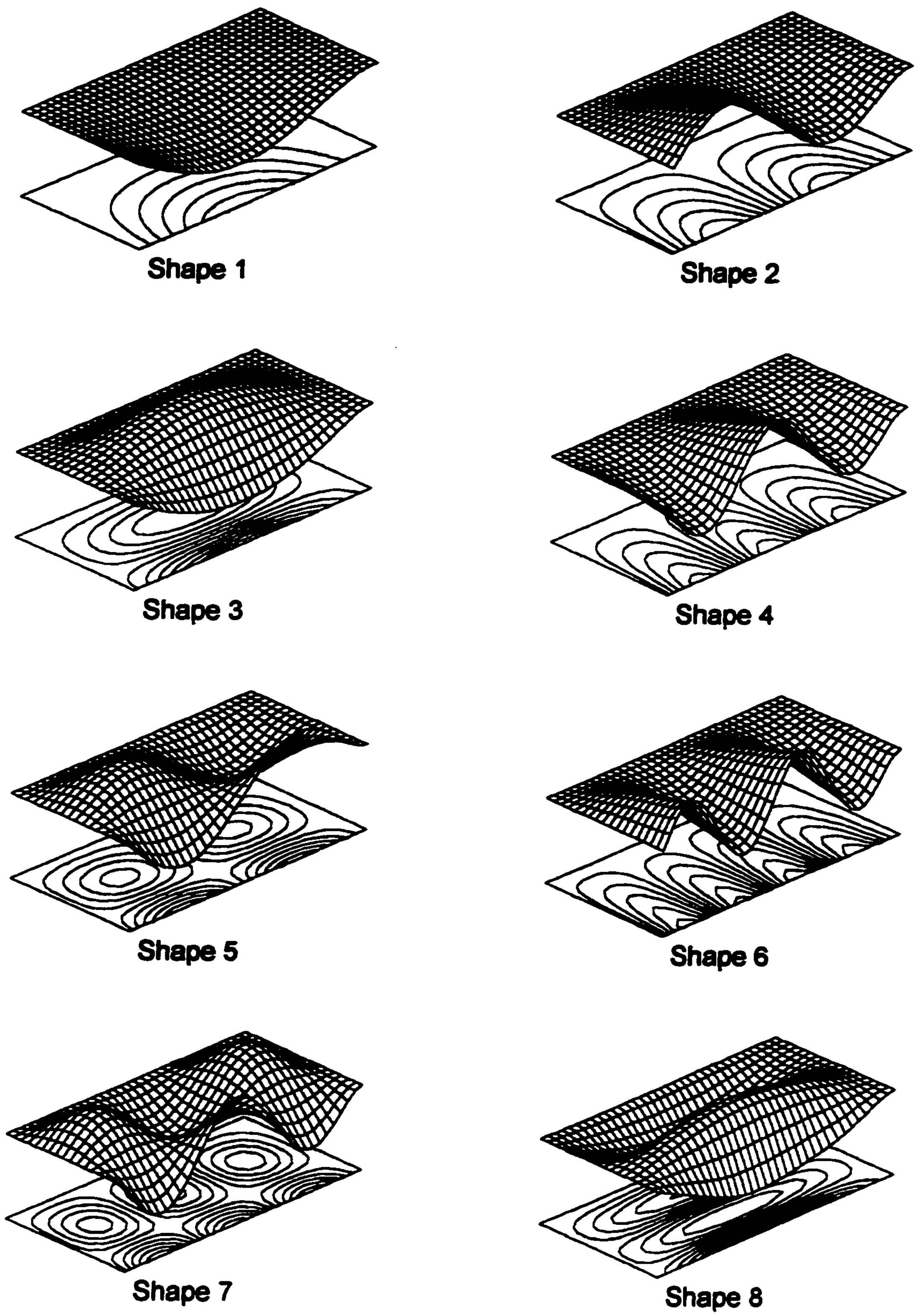

Table 4.68 Eigenvalues, SCCF plate, $\phi = 2/3$, $\lambda^2 = \omega a^2 (\rho / D)^{1/2}$.

Mode	-100%	-50%	0%	20%	40%	60%	80%	90%	99%
	In-plane load as a percentage of buckling load								
	Present solution								
1	28.95	25.22	20.75	18.63	16.21	13.31	9.47	6.72	2.13
2	65.93	61.34	54.58	51.63	48.49	45.13	41.50	39.56	37.73
3	67.42	64.46	62.92	62.30	61.66	61.02	60.37	60.04	59.74
4	105.92	102.23	98.39	96.80	95.19	93.55	91.87	91.01	90.22
5	123.09	115.89	108.22	104.99	101.65	98.21	94.64	92.81	91.16
6	151.98	151.35	150.69	150.25	148.31	146.00	143.64	142.45	141.36
7	163.72	158.42	152.95	150.88	150.27	149.99	149.73	149.60	149.48
8	189.35	187.33	181.57	178.22	174.80	171.31	167.75	165.94	164.29
	Finite element solution [18]								
1	28.96	25.23	20.76	18.64	16.21	13.31	9.47	6.72	2.13
2	65.89	61.38	54.63	51.67	48.53	45.18	41.55	39.61	37.78
3	67.46	64.42	62.88	62.25	61.62	60.97	60.32	59.99	59.70
4	105.85	102.15	98.30	96.72	95.10	93.46	91.78	90.92	90.13
5	123.24	116.05	108.38	105.15	101.83	98.38	94.82	92.99	91.33
6	151.76	151.13	150.47	150.06	148.17	145.86	143.50	142.30	141.21
7	163.60	158.30	152.81	150.71	150.05	149.77	149.50	149.37	149.26
8	188.98	186.96	182.01	178.66	175.24	171.76	168.21	166.40	164.76
	Percent difference								
1	0.03%	0.03%	0.03%	0.03%	0.03%	0.02%	0.02%	0.01%	-0.12%
2	-0.06%	0.08%	0.08%	0.09%	0.10%	0.11%	0.12%	0.14%	0.14%
3	0.06%	-0.06%	-0.07%	-0.07%	-0.07%	-0.08%	-0.08%	-0.08%	-0.08%
4	-0.07%	-0.08%	-0.09%	-0.09%	-0.09%	-0.10%	-0.10%	-0.10%	-0.09%
5	0.13%	0.14%	0.15%	0.16%	0.17%	0.18%	0.19%	0.19%	0.19%
6	-0.15%	-0.15%	-0.15%	-0.13%	-0.09%	-0.10%	-0.10%	-0.10%	-0.11%
7	-0.07%	-0.08%	-0.09%	-0.11%	-0.15%	-0.15%	-0.15%	-0.15%	-0.15%
8	-0.19%	-0.20%	0.24%	0.25%	0.26%	0.26%	0.27%	0.28%	0.28%

Figure 4.124 Eigenvalue curves, SCCF plate, $\phi = 2 / 3$,

$P_{\xi} = - N_x b^2 / D$, $\lambda^2 = \omega a^2 (\rho / D)^{1/2}$.

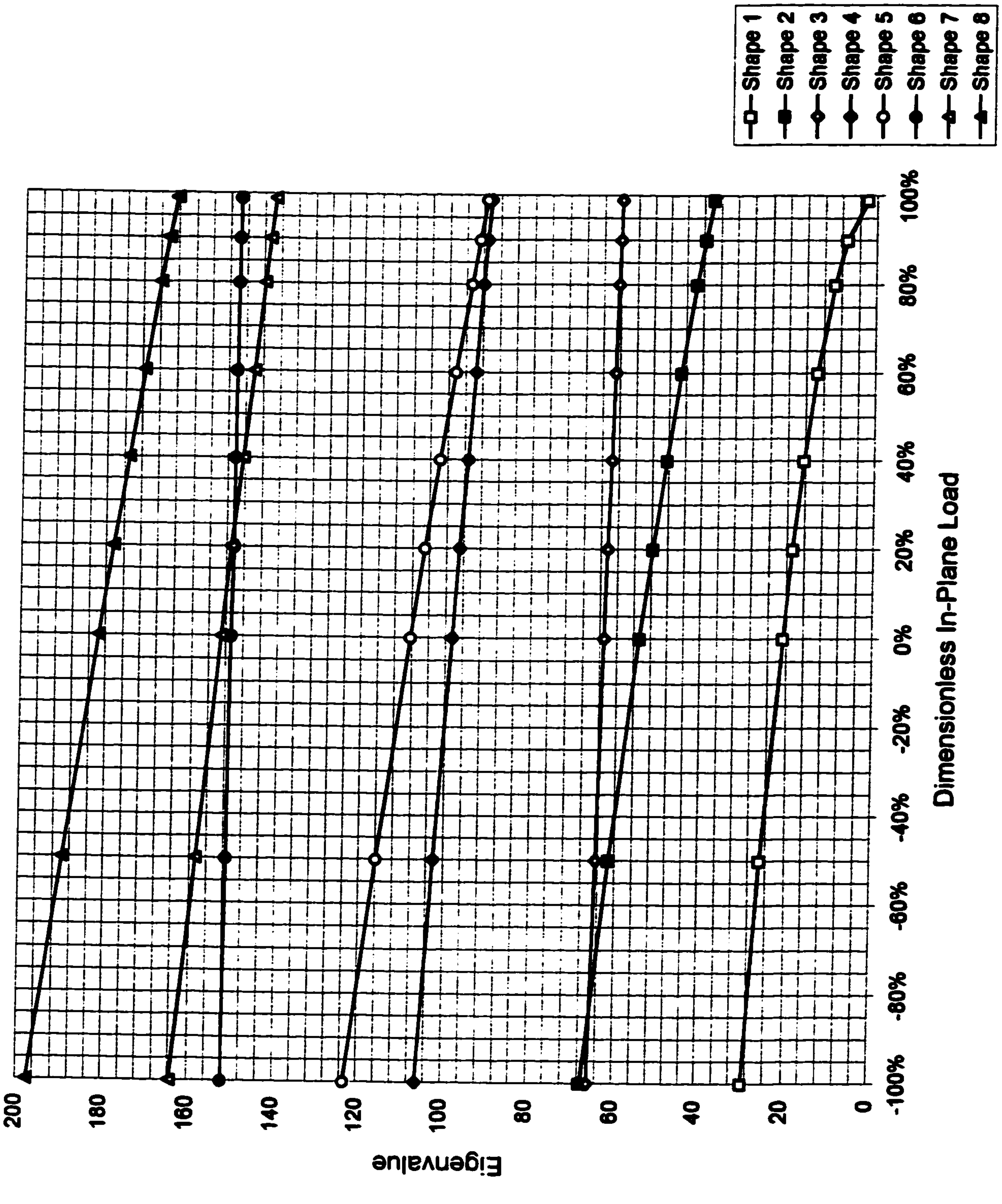

Figure 4.125 Mode shapes, SCCF plate, $\phi = 2 / 3$.

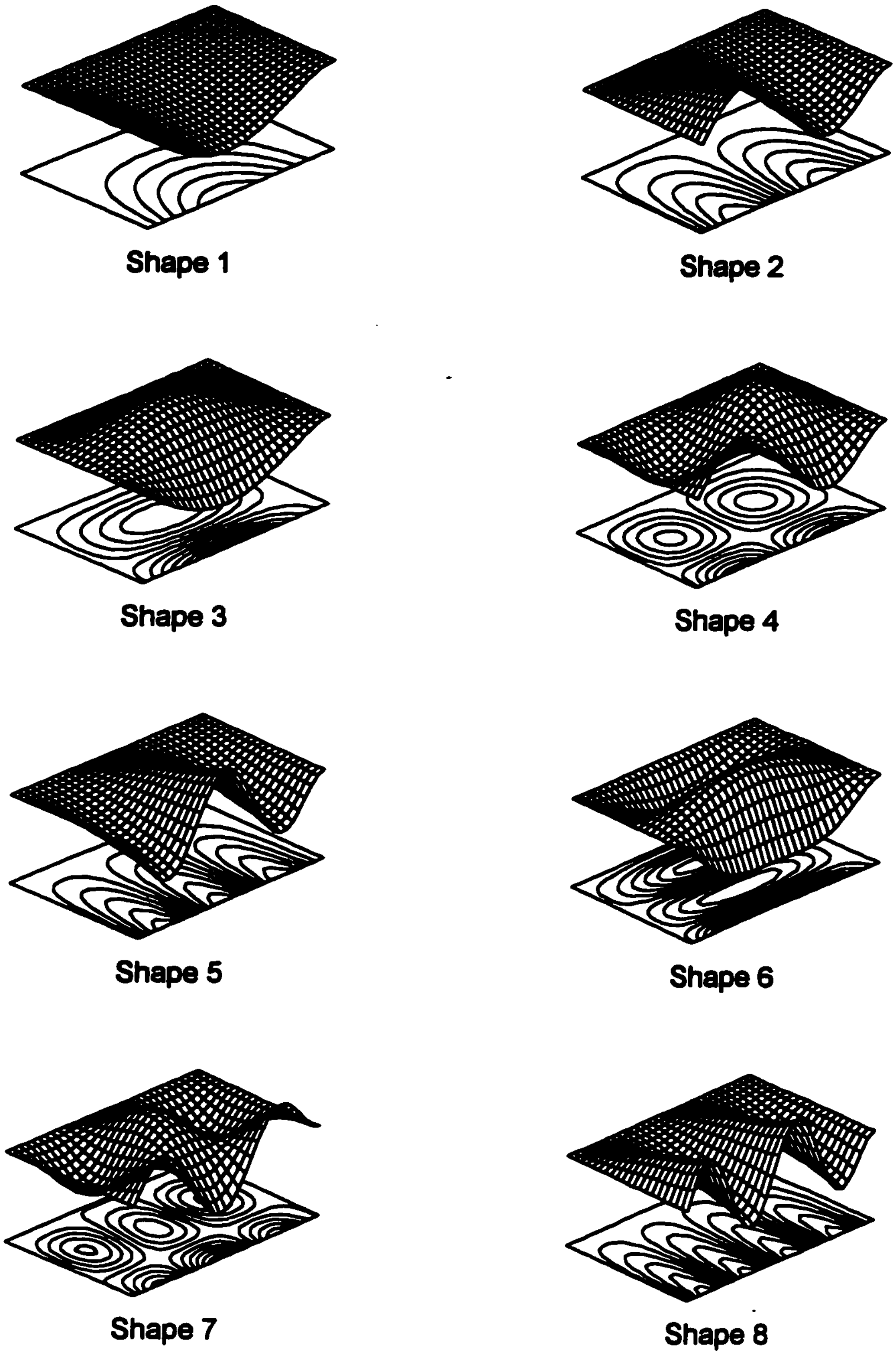

Table 4.69 Eigenvalues, SCCF plate, $\phi = 1 / 1$, $\lambda^2 = \omega a^2 (\rho / D)^{1/2}$.

Mode	In-plane load as a percentage of buckling load								
	-100%	-50%	0%	20%	40%	60%	80%	90%	99%
				Present solution					
1	24.37	21.21	17.42	15.62	13.57	11.12	7.90	5.60	1.77
2	39.58	37.77	35.85	35.05	34.23	33.38	32.51	32.06	31.66
3	61.39	56.72	51.61	49.42	47.12	44.71	42.16	40.82	39.58
4	75.96	74.49	70.79	69.22	67.62	65.97	64.28	63.42	62.63
5	78.19	75.18	74.18	73.80	73.43	73.05	72.67	72.48	72.31
6	113.88	111.09	105.49	103.16	100.78	98.34	95.84	94.57	93.40
7	116.42	111.48	109.01	108.01	107.00	105.98	104.95	104.43	103.96
8	133.70	129.77	125.02	123.07	121.08	119.06	117.01	115.97	115.03
				Finite element solution [18]					
1	24.38	21.21	17.42	15.63	13.58	11.13	7.90	5.60	1.77
2	39.57	37.76	35.84	35.04	34.22	33.37	32.50	32.05	31.64
3	61.41	56.74	51.64	49.44	47.15	44.73	42.18	40.85	39.61
4	75.91	74.46	70.77	69.20	67.59	65.94	64.25	63.39	62.60
5	78.17	75.12	74.12	73.75	73.37	72.99	72.61	72.42	72.25
6	113.75	111.14	105.55	103.22	100.85	98.41	95.91	94.63	93.47
7	116.48	111.36	108.88	107.88	106.86	105.84	104.81	104.29	103.81
8	133.55	129.73	124.97	123.02	121.02	119.01	116.95	115.91	114.97
				Percent difference					
1	0.03%	0.03%	0.04%	0.04%	0.04%	0.04%	0.03%	0.03%	0.00%
2	-0.02%	-0.02%	-0.03%	-0.03%	-0.03%	-0.04%	-0.04%	-0.05%	-0.05%
3	0.04%	0.04%	0.05%	0.05%	0.05%	0.05%	0.06%	0.06%	0.06%
4	-0.07%	-0.03%	-0.03%	-0.04%	-0.04%	-0.04%	-0.05%	-0.05%	-0.05%
5	-0.02%	-0.07%	-0.08%	-0.08%	-0.08%	-0.08%	-0.08%	-0.08%	-0.08%
6	-0.11%	0.04%	0.06%	0.06%	0.06%	0.07%	0.07%	0.07%	0.07%
7	0.05%	-0.11%	-0.12%	-0.13%	-0.13%	-0.13%	-0.14%	-0.14%	-0.14%
8	-0.11%	-0.03%	-0.04%	-0.04%	-0.05%	-0.05%	-0.05%	-0.05%	-0.05%

Figure 4.126 Eigenvalue curves, SCCF plate, $\phi = 1 / 1$,
$P_\xi = - N_x b^2 / D$, $\lambda^2 = \omega a^2 (\rho / D)^{1/2}$.

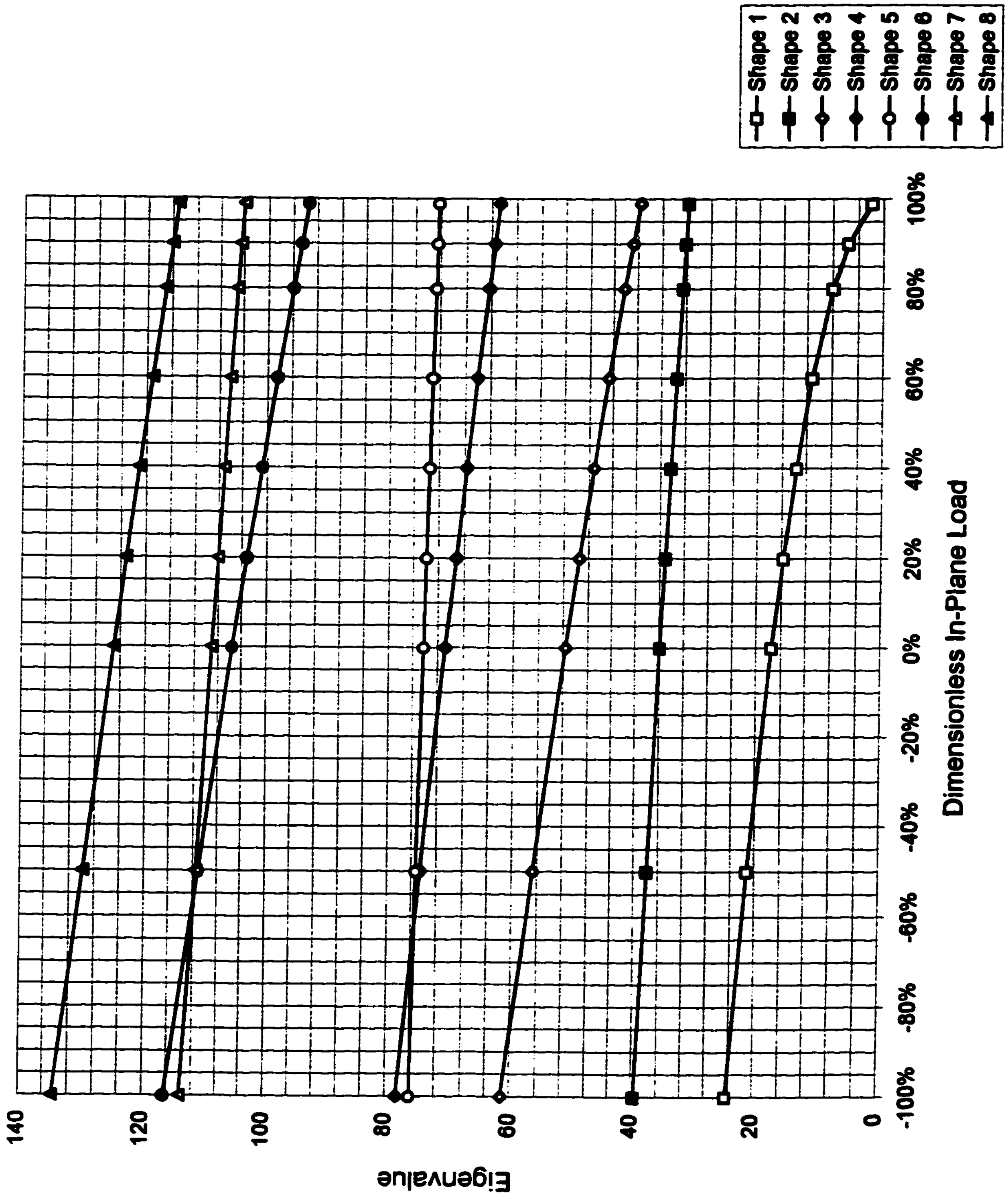

Figure 4.127 Mode shapes, SCCF plate, $\phi = 1 / 1$.

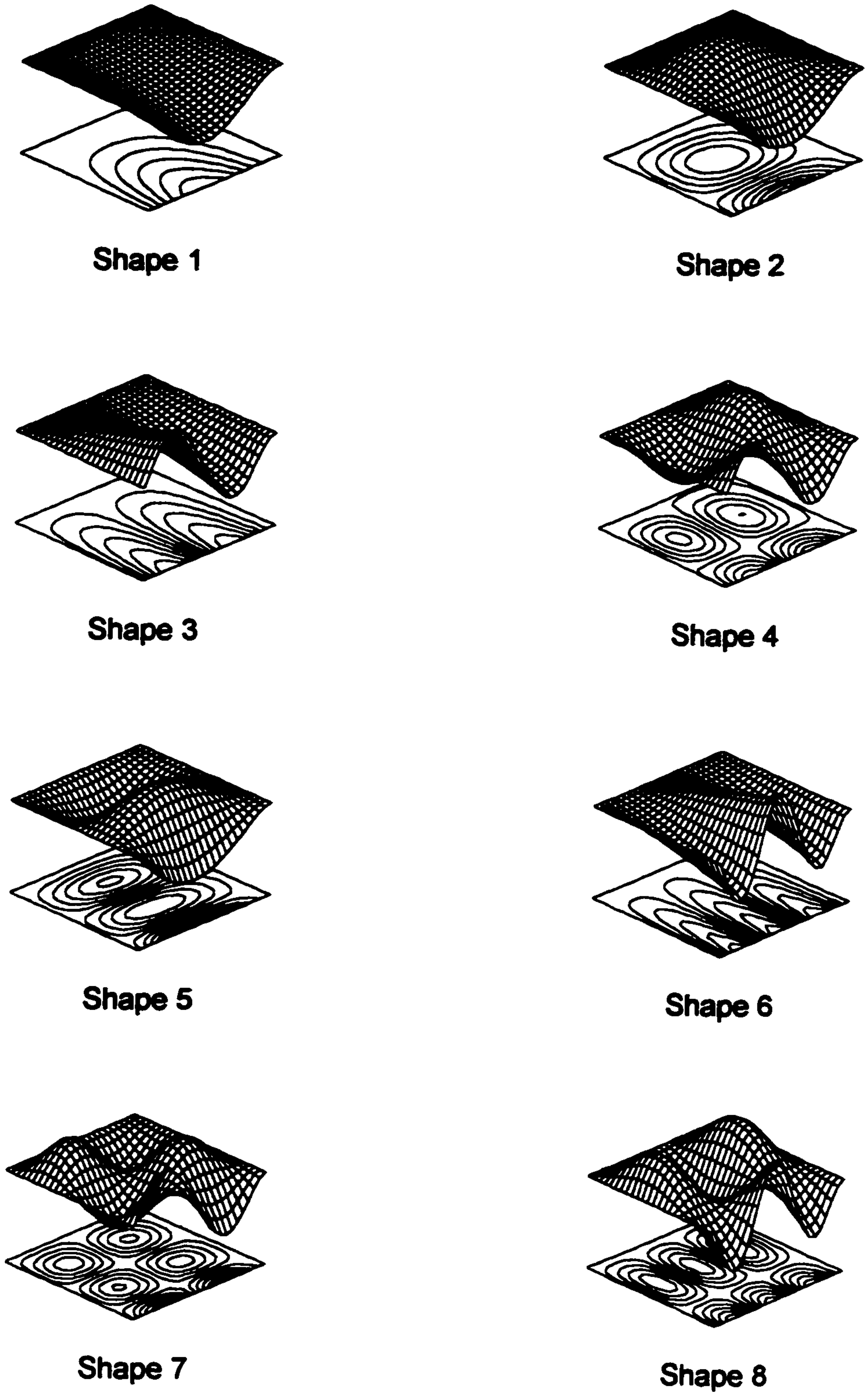

Table 4.70 Eigenvalues, SCCF plate, $\phi = 3/2$, $\lambda^2 = \omega a^2 (\rho / D)^{1/2}$.

Mode	In-plane load as a percentage of buckling load								
	-100%	-50%	0%	20%	40%	60%	80%	90%	99%
					Present solution				
1	22.61	19.67	16.14	14.48	12.57	10.30	7.31	5.18	1.64
2	28.72	26.50	24.06	23.01	21.89	20.71	19.45	18.79	18.17
3	43.43	42.02	40.56	39.96	39.35	38.73	38.09	37.77	37.48
4	59.12	54.97	50.47	48.55	46.55	44.46	42.26	41.12	40.07
5	66.35	62.69	58.79	57.16	55.47	53.74	51.94	51.02	50.17
6	67.88	67.00	66.11	65.75	65.39	65.02	64.65	64.47	64.30
7	81.46	78.53	75.48	74.22	72.94	71.64	70.31	69.64	69.03
8	101.84	101.25	100.55	99.80	98.89	97.95	96.16	95.07	94.07
					Finite element solution [18]				
1	22.61	19.67	16.15	14.48	12.57	10.30	7.31	5.18	1.64
2	28.72	26.50	24.06	23.00	21.89	20.71	19.45	18.78	18.16
3	43.40	42.00	40.54	39.93	39.32	38.70	38.06	37.74	37.44
4	59.12	54.96	50.46	48.54	46.54	44.45	42.26	41.11	40.06
5	66.31	62.65	58.76	57.12	55.44	53.70	51.90	50.97	50.13
6	67.83	66.95	66.06	65.70	65.34	64.97	64.60	64.41	64.24
7	81.37	78.43	75.38	74.12	72.84	71.53	70.20	69.53	68.92
8	101.78	101.20	100.41	99.58	98.66	97.71	96.08	94.99	94.00
					Percent difference				
1	0.01%	0.02%	0.02%	0.02%	0.02%	0.02%	0.02%	0.03%	0.08%
2	-0.01%	-0.02%	-0.02%	-0.02%	-0.03%	-0.03%	-0.04%	-0.04%	-0.04%
3	-0.06%	-0.06%	-0.07%	-0.07%	-0.07%	-0.08%	-0.08%	-0.08%	-0.08%
4	-0.01%	-0.01%	-0.02%	-0.02%	-0.02%	-0.02%	-0.02%	-0.02%	-0.02%
5	-0.05%	-0.05%	-0.06%	-0.06%	-0.07%	-0.07%	-0.08%	-0.08%	-0.08%
6	-0.07%	-0.08%	-0.08%	-0.08%	-0.08%	-0.08%	-0.08%	-0.08%	-0.09%
7	-0.12%	-0.12%	-0.13%	-0.14%	-0.14%	-0.15%	-0.15%	-0.16%	-0.16%
8	-0.06%	-0.06%	-0.13%	-0.22%	-0.23%	-0.24%	-0.08%	-0.08%	-0.08%

Figure 4.128 Eigenvalue curves, SCCF plate, $\phi = 3 / 2$,
$P_\xi = - N_x b^2 / D$, $\lambda^2 = \omega a^2 (\rho / D)^{1/2}$.

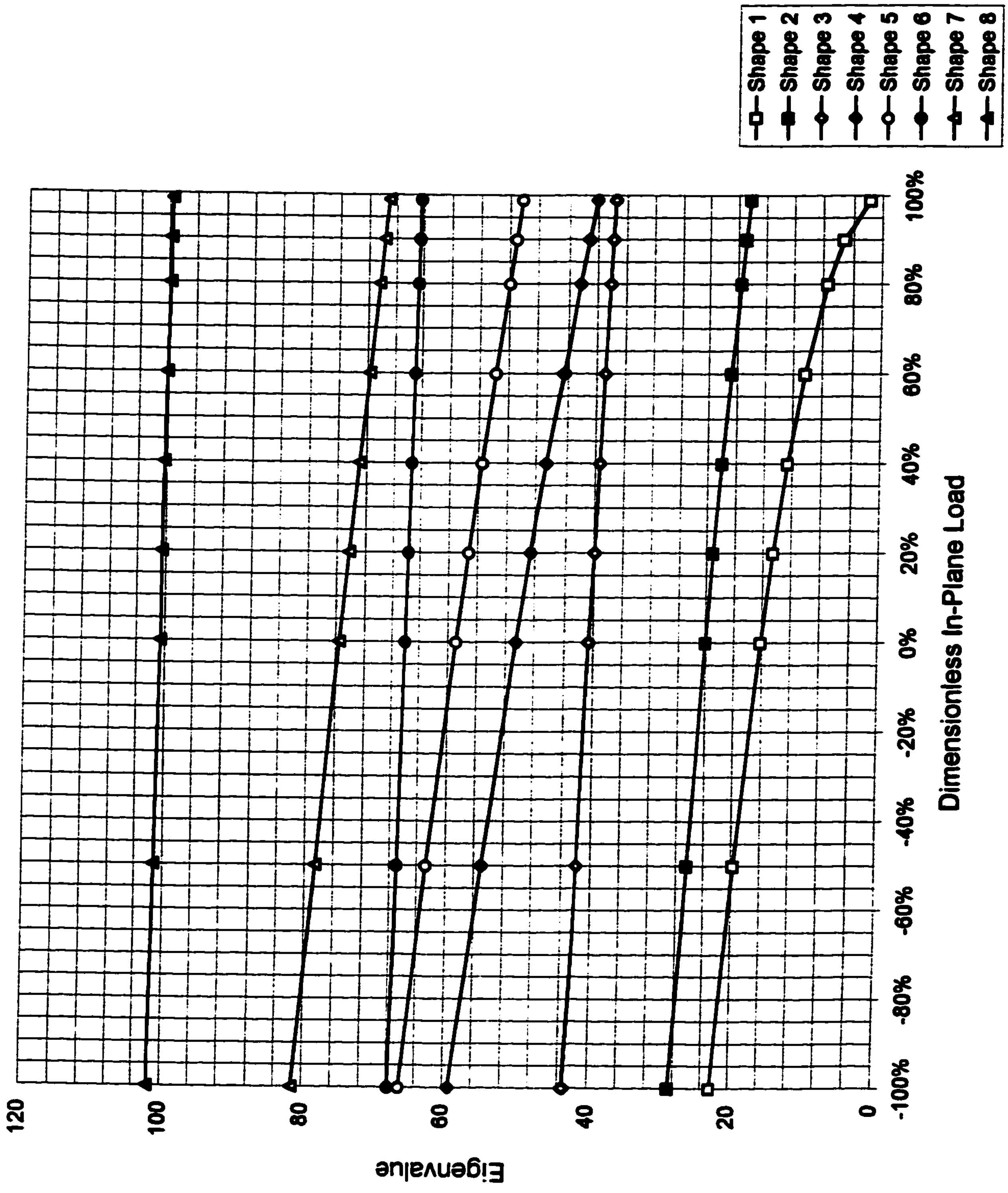

Figure 4.129 Mode shapes, SCCF plate, $\phi = 3 / 2$.

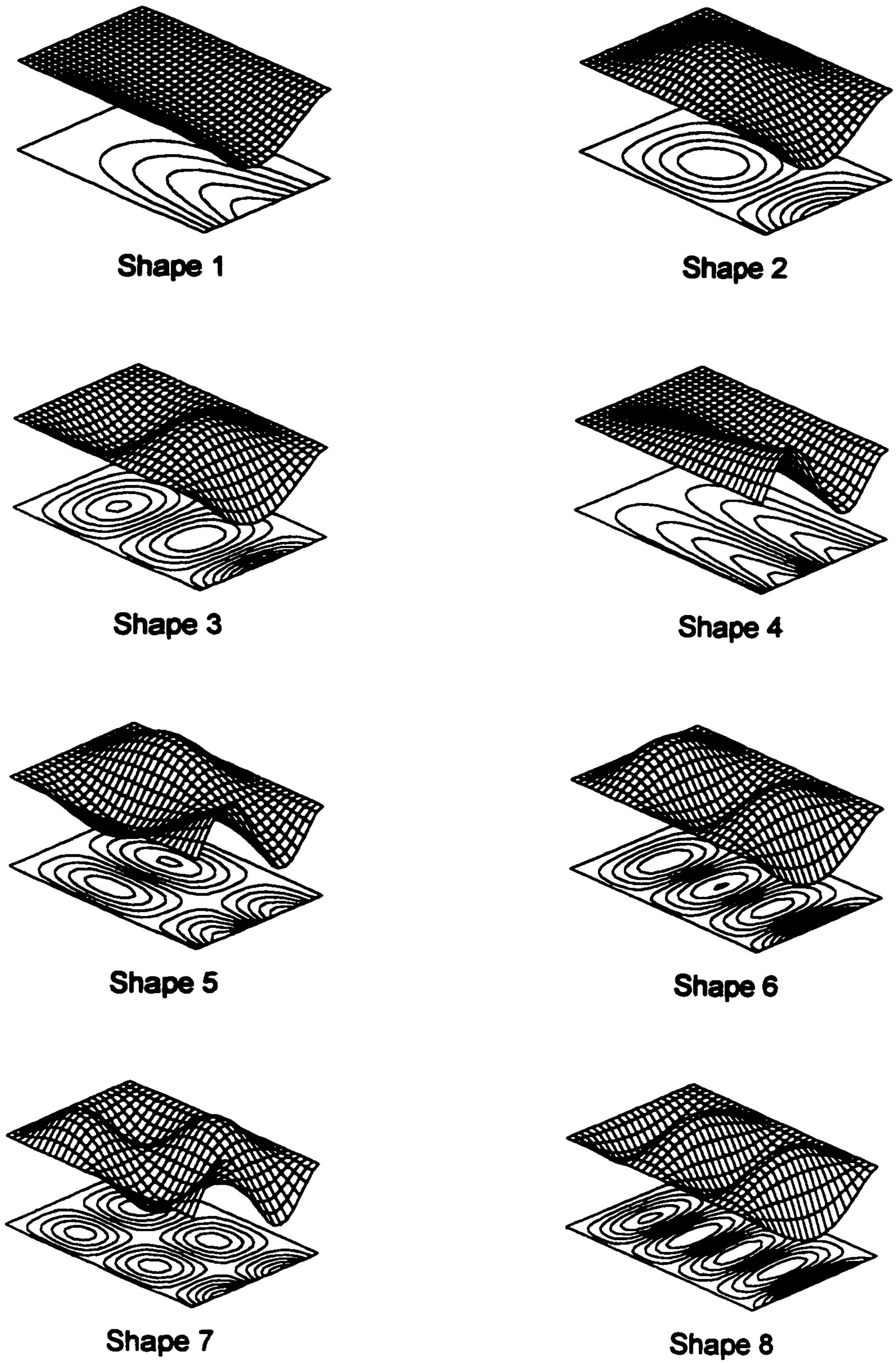

Table 4.71 Eigenvalues, SCCF plate, $\phi = 2 / 1$, $\lambda^2 = \omega a^2 (\rho / D)^{1/2}$.

Mode	In-plane load as a percentage of buckling load -100%	-50%	0%	20%	40%	60%	80%	90%	99%
				Present solution					
1	22.07	19.20	15.76	14.13	12.27	10.04	7.13	5.05	1.60
2	25.28	22.84	20.07	18.84	17.52	16.07	14.47	13.60	12.75
3	32.83	31.01	29.08	28.26	27.41	26.54	25.63	25.16	24.73
4	45.70	44.43	43.12	42.59	42.04	41.49	40.93	40.65	40.20
5	58.44	54.44	50.12	48.28	46.37	44.38	42.29	41.20	40.39
6	62.43	58.71	54.73	53.06	51.33	49.53	47.67	46.71	45.83
7	64.08	63.20	62.30	61.93	61.07	59.58	58.05	57.26	56.55
8	70.63	67.38	63.95	62.53	61.57	61.20	60.82	60.64	60.47
				Finite element solution [18]					
1	22.07	19.20	15.76	14.13	12.27	10.05	7.13	5.05	1.60
2	25.27	22.83	20.07	18.84	17.51	16.07	14.46	13.59	12.74
3	32.80	30.99	29.05	28.23	27.38	26.51	25.60	25.13	24.70
4	45.64	44.37	43.07	42.53	41.98	41.43	40.87	40.58	40.18
5	58.42	54.42	50.10	48.26	46.35	44.35	42.26	41.18	40.32
6	62.37	58.66	54.68	53.00	51.27	49.47	47.61	46.65	45.77
7	64.01	63.12	62.22	61.86	60.95	59.46	57.92	57.14	56.42
8	70.52	67.27	63.84	62.42	61.49	61.12	60.74	60.56	60.39
				Percent difference					
1	0.00%	0.00%	0.01%	0.01%	0.01%	0.01%	0.01%	0.01%	0.02%
2	-0.02%	-0.02%	-0.03%	-0.03%	-0.04%	-0.05%	-0.06%	-0.07%	-0.08%
3	-0.08%	-0.09%	-0.09%	-0.10%	-0.11%	-0.12%	-0.12%	-0.13%	-0.13%
4	-0.12%	-0.13%	-0.14%	-0.14%	-0.15%	-0.15%	-0.15%	-0.16%	-0.06%
5	-0.04%	-0.04%	-0.05%	-0.05%	-0.05%	-0.06%	-0.06%	-0.06%	-0.16%
6	-0.08%	-0.09%	-0.10%	-0.11%	-0.12%	-0.12%	-0.13%	-0.14%	-0.14%
7	-0.12%	-0.12%	-0.13%	-0.13%	-0.19%	-0.20%	-0.21%	-0.22%	-0.22%
8	-0.15%	-0.16%	-0.18%	-0.19%	-0.13%	-0.13%	-0.13%	-0.13%	-0.13%

Figure 4.130 Eigenvalue curves, SCCF plate, $\phi = 2 / 1$,

$P_\xi = - N_x b^2 / D$, $\lambda^2 = \omega a^2 (\rho / D)^{1/2}$.

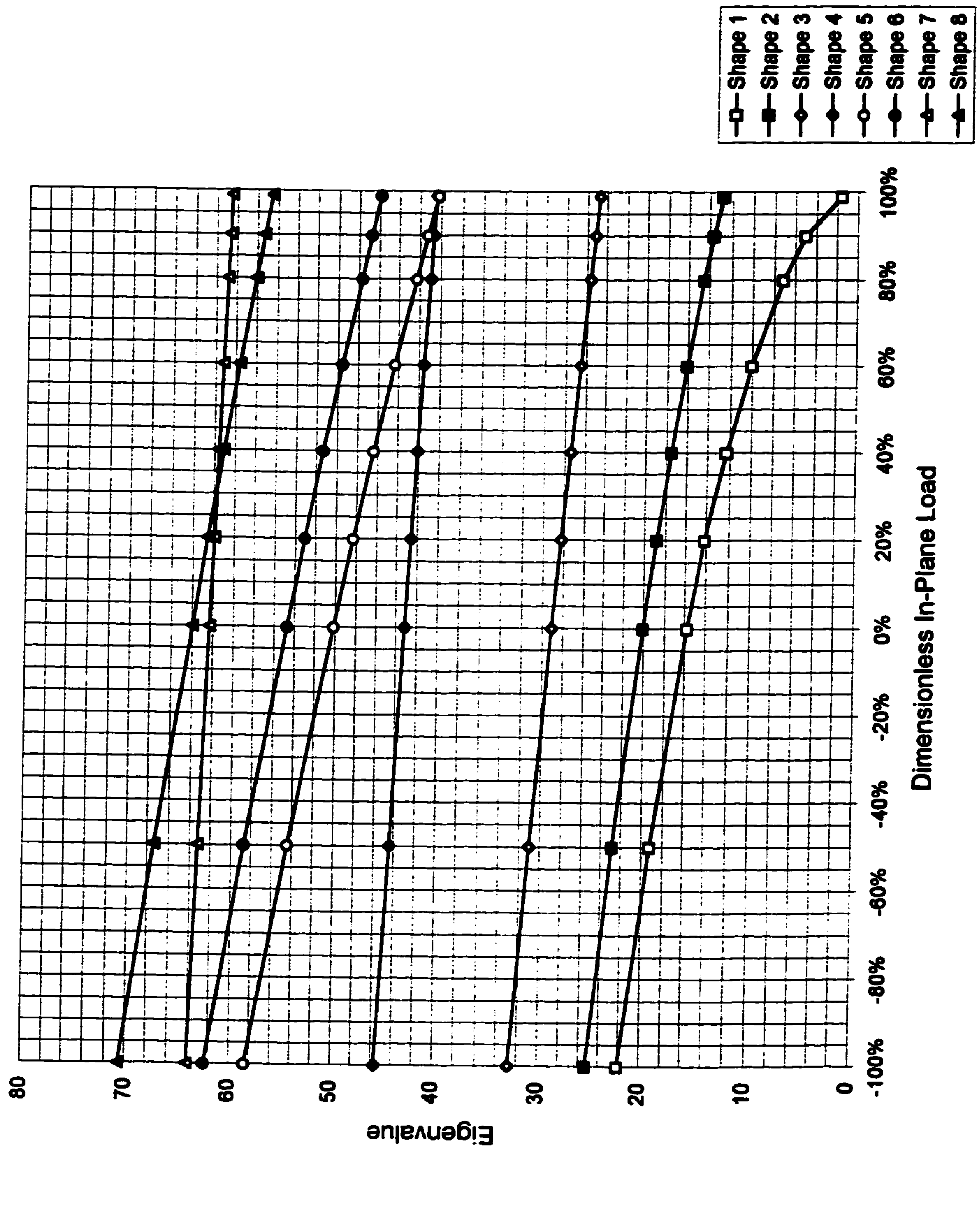

Figure 4.131 Mode shapes, SCCF plate, $\phi = 2 / 1$.

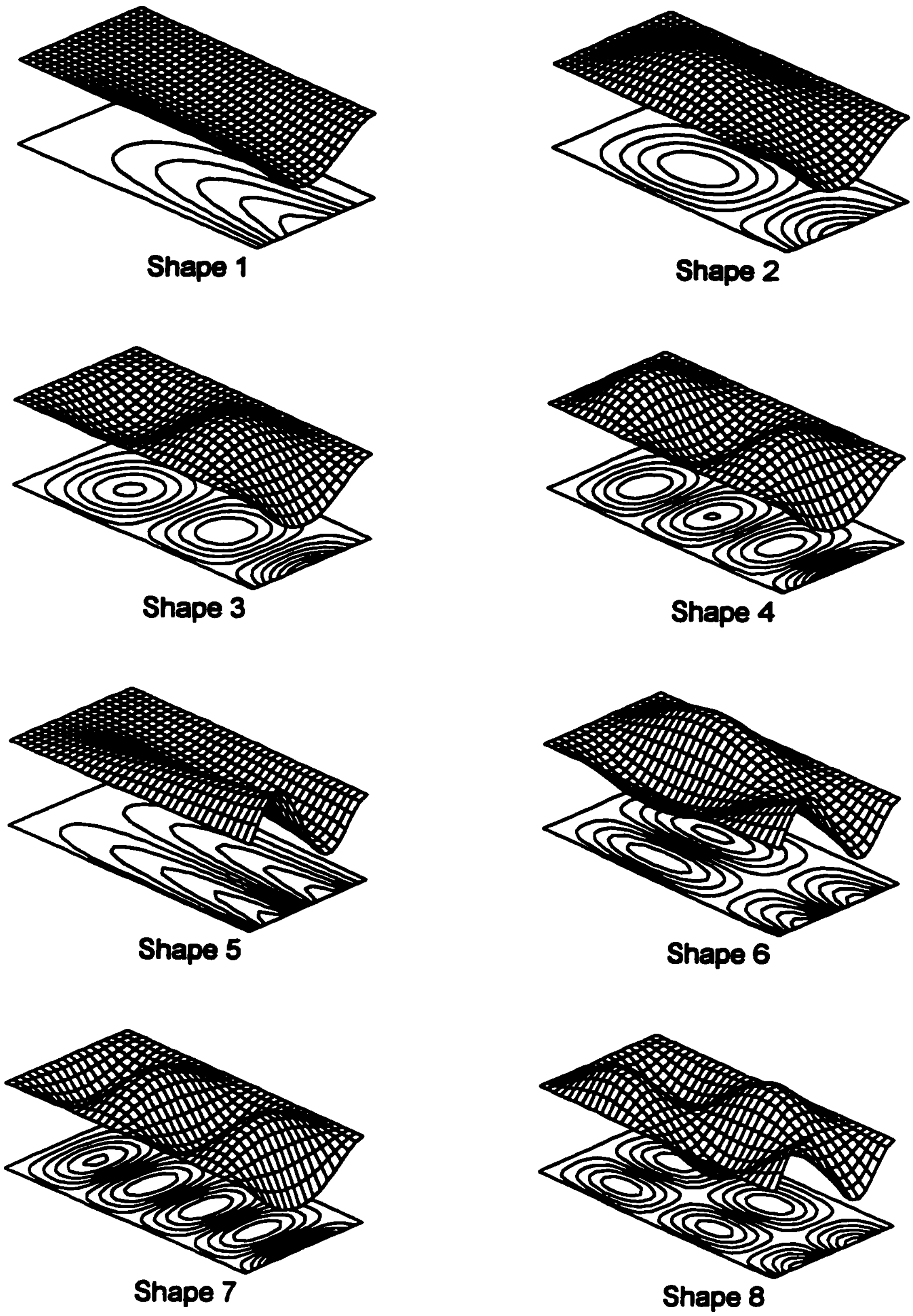

Table 4.72 Eigenvalues, SCCF plate, $\phi = 5 / 2$, $\lambda^2 = \omega a^2 (\rho / D)^{1/2}$.

Mode	In-plane load as a percentage of buckling load								
	-100%	-50%	0%	20%	40%	60%	80%	90%	99%
	Present solution								
1	21.85	19.00	15.59	13.98	12.14	9.94	7.05	4.99	1.58
2	23.81	21.24	18.29	16.95	15.49	13.86	11.99	10.93	9.87
3	28.29	26.19	23.90	22.90	21.86	20.76	19.60	18.98	18.41
4	35.97	34.37	32.67	31.97	31.24	30.50	29.74	29.35	28.99
5	47.16	45.96	44.73	44.22	43.71	43.19	42.30	41.24	40.26
6	58.16	54.23	49.98	48.18	46.30	44.35	42.67	42.40	42.16
7	60.69	56.94	52.92	51.22	49.46	47.63	45.73	44.76	43.86
8	61.89	60.99	58.73	57.21	55.64	54.03	52.36	51.51	50.73
	Finite element solution [18]								
1	21.85	19.00	15.59	13.98	12.14	9.94	7.05	5.00	1.58
2	23.80	21.24	18.28	16.94	15.48	13.85	11.98	10.92	9.86
3	28.26	26.17	23.87	22.88	21.83	20.73	19.56	18.95	18.37
4	35.91	34.30	32.61	31.90	31.17	30.43	29.66	29.27	28.91
5	47.06	45.86	44.62	44.12	43.60	43.08	42.26	41.21	40.23
6	58.13	54.20	49.95	48.15	46.27	44.32	42.56	42.29	42.05
7	60.63	56.87	52.85	51.14	49.38	47.56	45.65	44.67	43.77
8	61.77	60.86	58.60	57.08	55.51	53.89	52.23	51.37	50.59
	Percent difference								
1	0.00%	0.00%	0.00%	0.00%	0.01%	0.01%	0.01%	0.01%	0.00%
2	-0.03%	-0.03%	-0.04%	-0.05%	-0.06%	-0.07%	-0.10%	-0.12%	-0.15%
3	-0.09%	-0.10%	-0.12%	-0.13%	-0.14%	-0.16%	-0.18%	-0.19%	-0.21%
4	-0.17%	-0.19%	-0.20%	-0.21%	-0.22%	-0.24%	-0.25%	-0.25%	-0.26%
5	-0.22%	-0.23%	-0.24%	-0.24%	-0.25%	-0.26%	-0.08%	-0.08%	-0.08%
6	-0.05%	-0.06%	-0.06%	-0.06%	-0.06%	-0.07%	-0.25%	-0.26%	-0.27%
7	-0.11%	-0.12%	-0.13%	-0.14%	-0.15%	-0.16%	-0.17%	-0.18%	-0.19%
8	-0.19%	-0.20%	-0.21%	-0.22%	-0.24%	-0.25%	-0.26%	-0.27%	-0.28%

Figure 4.132 Eigenvalue curves, SCCF plate, $\phi = 5 / 2$,

$P_\xi = - N_x b^2 / D$, $\lambda^2 = \omega a^2 (\rho / D)^{1/2}$.

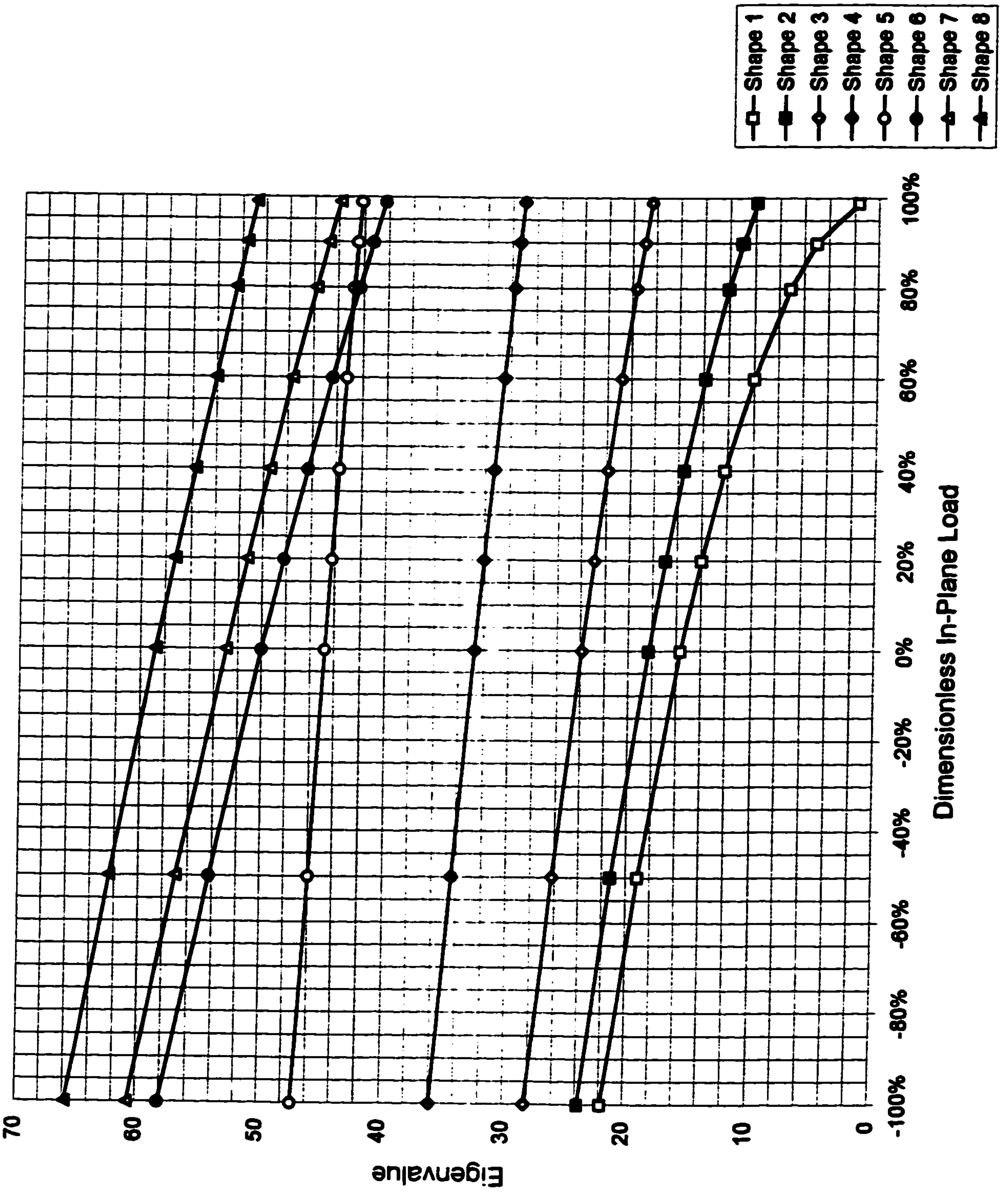

Figure 4.133 Mode shapes, SCCF plate, $\phi = 5 / 2$.

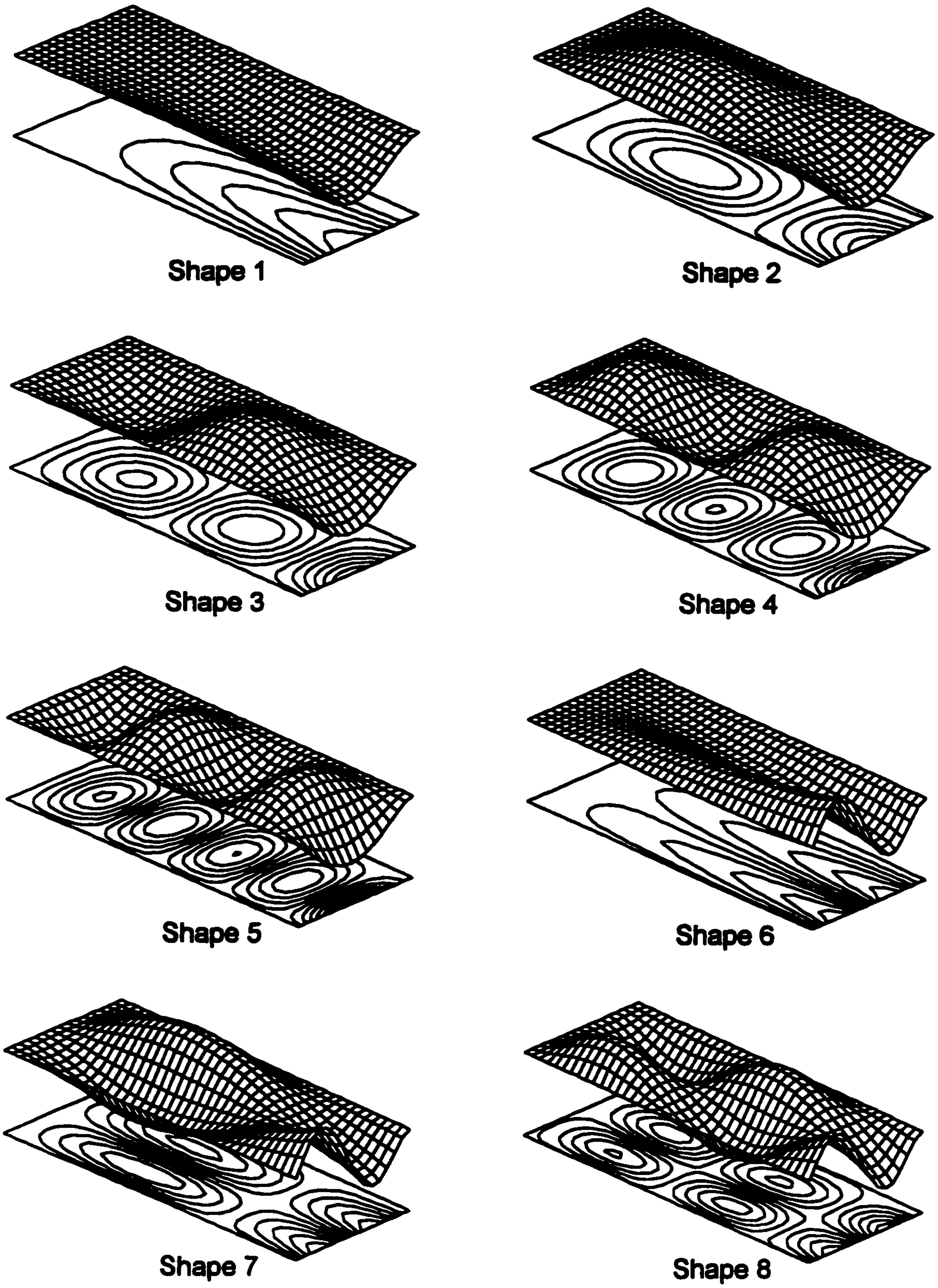

Table 4.73 Eigenvalues, SCCF plate, $\phi = 3 / 1$, $\lambda^2 = \omega a^2 (\rho / D)^{1/2}$.

Mode	In-plane load as a percentage of buckling load								
	-100%	-50%	0%	20%	40%	60%	80%	90%	99%
					Present solution				
1	21.73	18.90	15.51	13.91	12.08	9.89	7.01	4.97	1.57
2	23.05	20.42	17.35	15.94	14.39	12.63	10.56	9.35	8.09
3	25.99	23.71	21.15	20.03	18.83	17.55	16.15	15.40	14.69
4	30.99	29.12	27.11	26.26	25.37	24.45	23.48	22.99	22.53
5	38.35	36.87	35.32	34.68	34.03	33.35	32.67	32.32	32.00
6	48.18	47.02	45.83	45.34	44.85	44.33	42.31	41.26	40.29
7	58.03	54.13	49.92	48.13	46.27	44.35	43.84	43.58	42.79
8	59.78	56.01	51.96	50.24	48.46	46.62	44.70	43.58	43.35
					Finite element solution [18]				
1	21.73	18.90	15.51	13.91	12.08	9.89	7.02	4.97	1.57
2	23.05	20.41	17.34	15.94	14.38	12.62	10.55	9.33	8.07
3	25.97	23.68	21.12	20.00	18.80	17.51	16.11	15.36	14.65
4	30.93	29.06	27.04	26.18	25.30	24.37	23.40	22.90	22.44
5	38.24	36.76	35.20	34.56	33.90	33.23	32.54	32.18	31.86
6	48.02	46.86	45.66	45.17	44.68	44.17	42.28	41.23	40.26
7	58.00	54.10	49.89	48.10	46.24	44.31	43.66	43.40	42.70
8	59.71	55.93	51.88	50.16	48.38	46.54	44.61	43.62	43.18
					Percent difference				
1	0.00%	0.00%	0.00%	0.01%	0.01%	0.01%	0.02%	0.02%	0.02%
2	-0.03%	-0.03%	-0.05%	-0.05%	-0.07%	-0.09%	-0.14%	-0.18%	-0.25%
3	-0.10%	-0.11%	-0.14%	-0.15%	-0.17%	-0.20%	-0.24%	-0.26%	-0.29%
4	-0.20%	-0.22%	-0.25%	-0.27%	-0.29%	-0.32%	-0.34%	-0.36%	-0.38%
5	-0.29%	-0.31%	-0.34%	-0.35%	-0.37%	-0.39%	-0.40%	-0.41%	-0.42%
6	-0.33%	-0.35%	-0.36%	-0.37%	-0.38%	-0.36%	-0.07%	-0.07%	-0.07%
7	-0.05%	-0.05%	-0.05%	-0.06%	-0.06%	-0.09%	-0.40%	-0.41%	-0.22%
8	-0.12%	-0.13%	-0.15%	-0.16%	-0.17%	-0.18%	-0.20%	0.10%	-0.40%

Figure 4.134 Eigenvalue curves, SCCF plate, $\phi = 3 / 1$,
$P_\xi = - N_x b^2 / D$, $\lambda^2 = \omega a^2 (\rho / D)^{1/2}$.

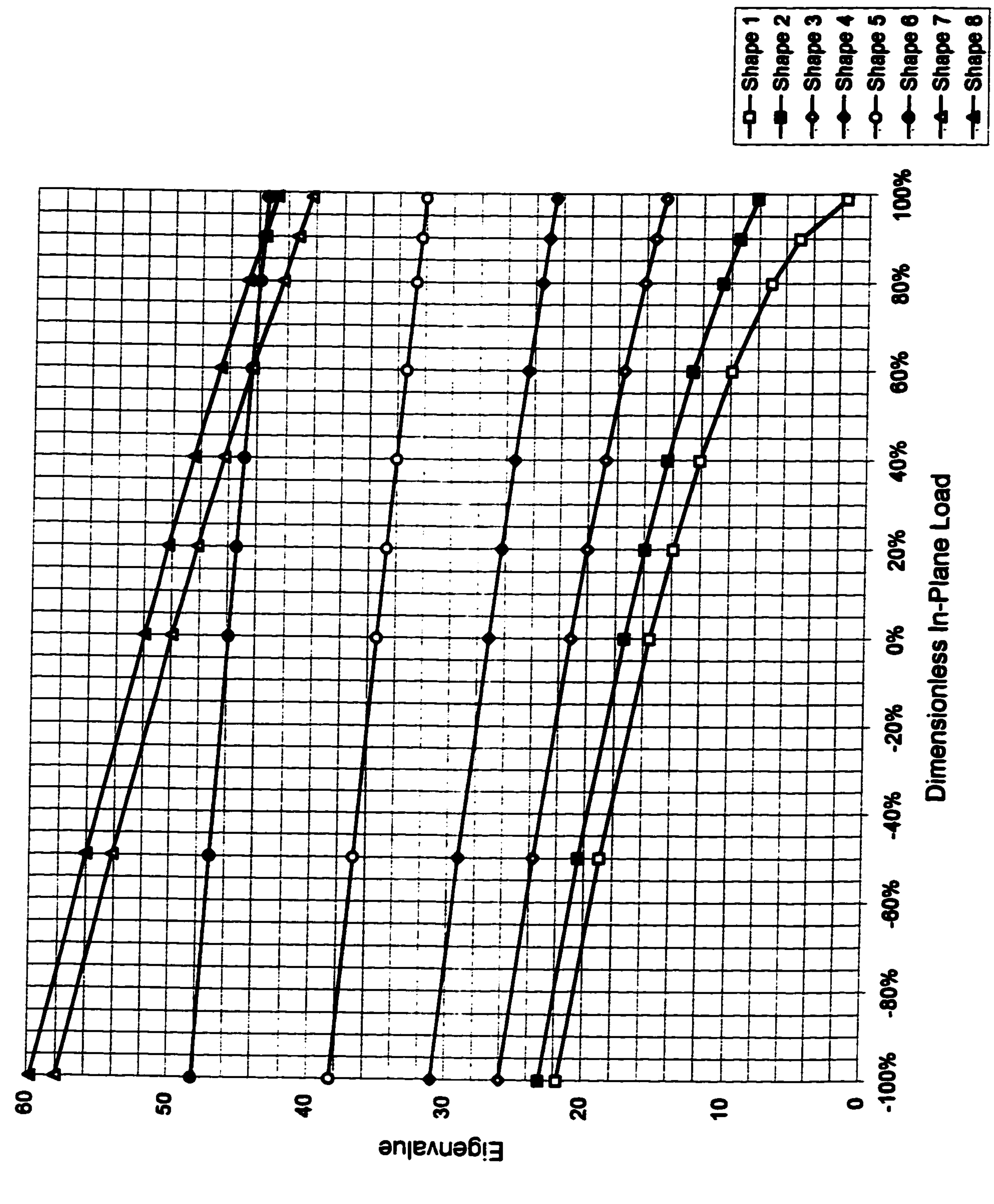

Figure 4.135 Mode shapes, SCCF plate, $\phi = 3 / 1$.

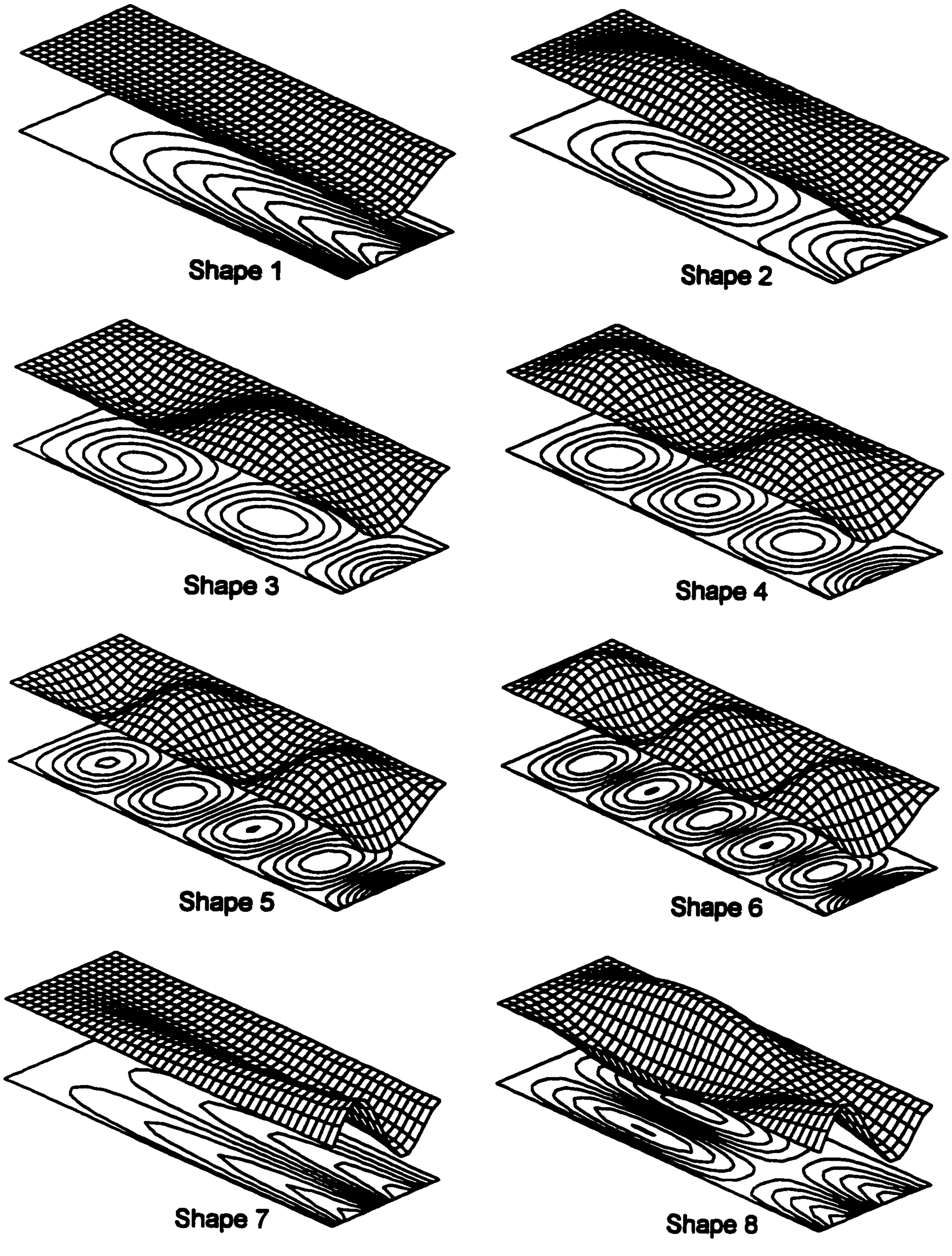

Table 4.74 Eigenvalues, CSCF plate, $\phi = 1 / 3$, $\lambda^2 = \omega a^2 (\rho / D)^{1/2}$.

	In-plane load as a percentage of buckling load								
Mode	-100%	-50%	0%	20%	40%	60%	80%	90%	99%
					Present solution				
1	42.31	36.90	30.41	27.32	23.78	19.53	13.90	9.87	3.13
2	93.35	83.95	73.24	68.44	63.25	57.56	51.20	47.67	44.25
3	158.07	146.68	133.60	127.98	122.09	115.89	109.33	105.90	102.71
4	158.67	156.82	155.53	155.01	154.49	153.96	153.44	153.17	152.93
5	208.56	204.70	200.76	199.16	197.53	193.90	187.19	183.74	180.58
6	240.89	227.28	212.78	206.69	200.41	195.93	194.27	193.44	192.68
7	280.54	274.12	267.54	264.85	262.14	259.39	256.62	255.22	253.95
8	341.34	326.64	311.23	304.84	298.32	291.65	284.82	281.35	278.18
					Finite element solution [18]				
1	42.33	36.91	30.41	27.32	23.78	19.53	13.91	9.87	3.13
2	93.42	84.02	73.31	68.51	63.33	57.64	51.28	47.76	44.34
3	157.95	146.97	133.90	128.27	122.39	116.21	109.66	106.23	103.05
4	158.94	156.69	155.39	154.87	154.35	153.83	153.30	153.03	152.79
5	208.20	204.32	200.37	198.76	197.14	194.75	188.09	184.65	181.50
6	241.65	228.07	213.60	207.52	201.26	195.53	193.86	193.02	192.27
7	279.77	273.32	266.70	264.00	261.28	258.52	255.73	254.33	253.05
8	343.04	328.39	313.03	306.68	300.18	293.54	286.74	283.29	280.14
					Percent difference				
1	0.04%	0.03%	0.02%	0.02%	0.02%	0.01%	0.01%	0.01%	-0.02%
2	0.08%	0.09%	0.10%	0.11%	0.12%	0.14%	0.16%	0.18%	0.20%
3	-0.07%	0.19%	0.22%	0.23%	0.25%	0.28%	0.30%	0.32%	0.33%
4	0.17%	-0.08%	-0.09%	-0.09%	-0.09%	-0.09%	-0.09%	-0.09%	-0.09%
5	-0.17%	-0.19%	-0.19%	-0.20%	-0.20%	0.44%	0.48%	0.49%	0.51%
6	0.32%	0.35%	0.38%	0.40%	0.42%	-0.20%	-0.21%	-0.22%	-0.21%
7	-0.28%	-0.29%	-0.31%	-0.32%	-0.33%	-0.34%	-0.34%	-0.35%	-0.35%
8	0.50%	0.54%	0.58%	0.60%	0.62%	0.65%	0.67%	0.69%	0.70%

Figure 4.136 Eigenvalue curves, CSCF plate, $\phi = 1/3$,

$P_\xi = -N_x b^2 / D$, $\lambda^2 = \omega a^2 (\rho / D)^{1/2}$.

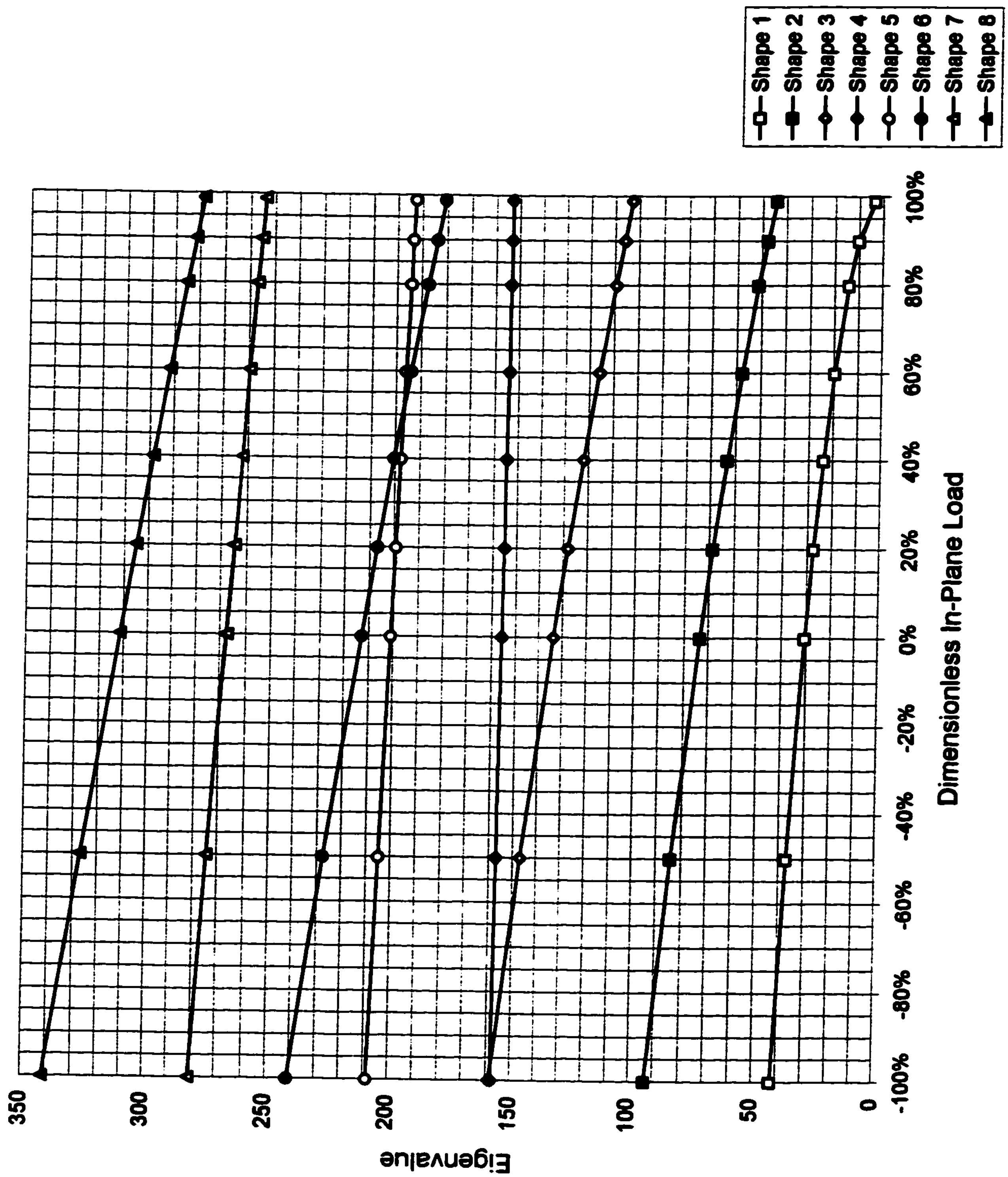

Figure 4.137 Mode shapes, CSCF plate, $\phi = 1 / 3$.

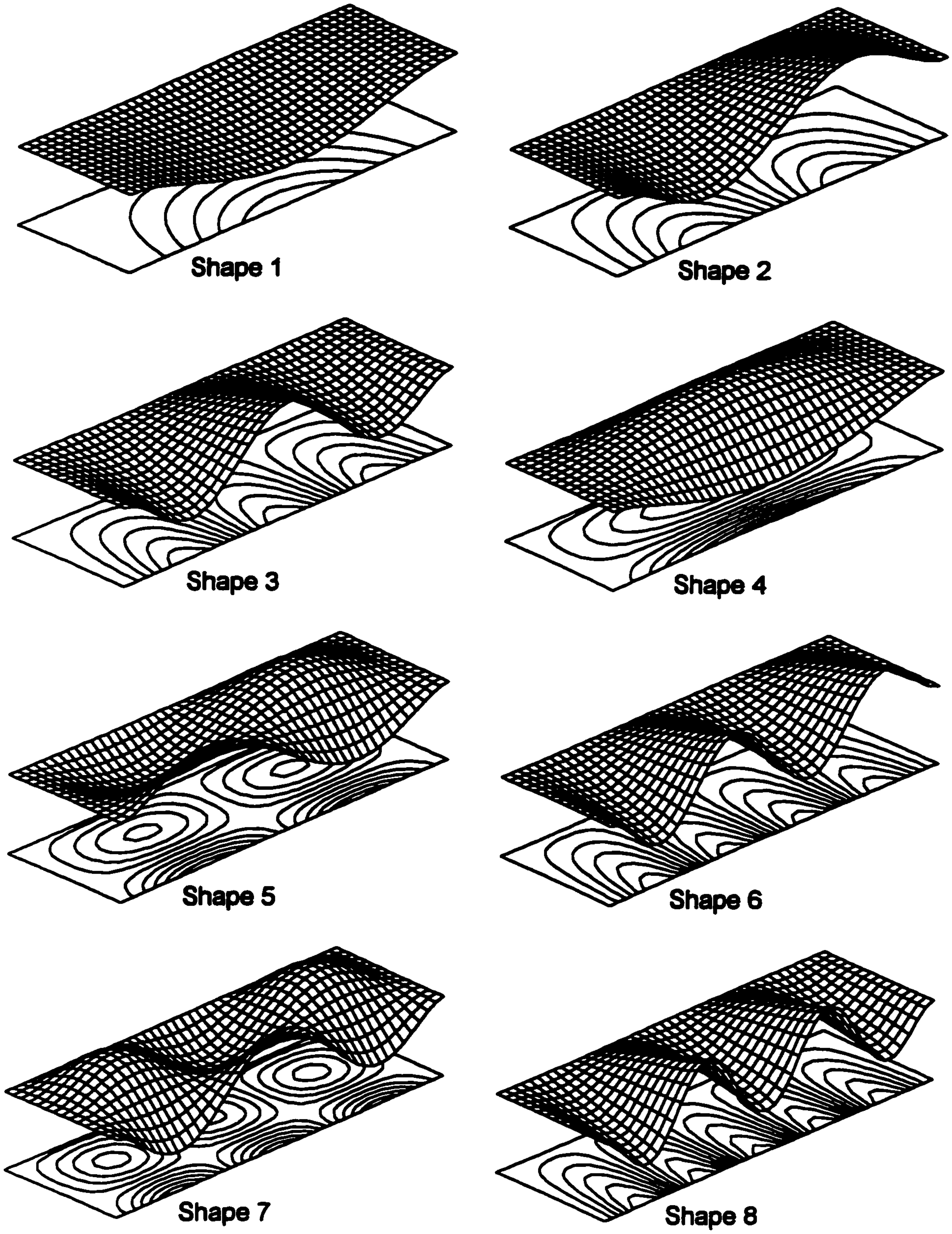

Table 4.75 Eigenvalues, CSCF plate, $\phi = 2 / 5$, $\lambda^2 = \omega a^2 (\rho / D)^{1/2}$.

Mode	In-plane load as a percentage of buckling load								
	-100%	-50%	0%	20%	40%	60%	80%	90%	99%
				Present solution					
1	39.23	34.21	28.17	25.30	22.01	18.07	12.86	9.12	2.89
2	87.96	79.43	69.76	65.46	60.83	55.79	50.21	47.16	44.22
3	116.61	115.11	113.59	112.97	112.35	111.72	108.40	105.46	102.73
4	151.78	141.12	129.55	124.61	119.46	114.08	111.11	110.79	110.50
5	166.95	162.79	158.50	156.74	154.97	153.17	151.35	150.42	149.59
6	233.09	221.12	208.44	203.14	197.70	192.10	186.33	183.38	180.68
7	236.99	230.45	223.70	220.94	218.14	215.30	212.43	210.97	209.65
8	324.31	315.91	306.75	301.23	295.61	289.88	284.03	281.06	278.35
				Finite element solution [18]					
1	39.25	34.22	28.18	25.31	22.02	18.08	12.86	9.12	2.90
2	88.05	79.52	69.85	65.55	60.92	55.88	50.30	47.25	44.32
3	116.52	115.02	113.50	112.88	112.26	111.63	108.73	105.80	103.08
4	152.08	141.42	129.85	124.92	119.78	114.40	111.01	110.69	110.40
5	166.72	162.54	158.24	156.48	154.70	152.89	151.07	150.14	149.30
6	233.86	221.91	209.25	203.97	198.54	192.95	187.20	184.26	181.57
7	236.51	229.94	223.17	220.40	217.59	214.74	211.85	210.39	209.06
8	323.58	315.13	306.46	302.91	297.41	291.70	285.88	282.92	280.24
				Percent difference					
1	0.05%	0.04%	0.04%	0.04%	0.03%	0.03%	0.03%	0.04%	0.19%
2	0.10%	0.11%	0.12%	0.13%	0.14%	0.15%	0.18%	0.20%	0.22%
3	-0.08%	-0.08%	-0.08%	-0.08%	-0.09%	-0.08%	0.31%	0.33%	0.34%
4	0.19%	0.21%	0.23%	0.25%	0.27%	0.28%	-0.09%	-0.09%	-0.09%
5	-0.14%	-0.15%	-0.17%	-0.17%	-0.17%	-0.18%	-0.18%	-0.19%	-0.19%
6	0.33%	0.36%	0.39%	0.41%	0.42%	0.44%	0.47%	0.48%	0.49%
7	-0.20%	-0.22%	-0.24%	-0.24%	-0.25%	-0.26%	-0.27%	-0.28%	-0.28%
8	-0.23%	-0.25%	-0.10%	0.56%	0.61%	0.63%	0.65%	0.66%	0.68%

Figure 4.138 Eigenvalue curves, CSCF plate, $\phi = 2 / 5$,
$P_\xi = - N_x b^2 / D$, $\lambda^2 = \omega a^2 (\rho / D)^{1/2}$.

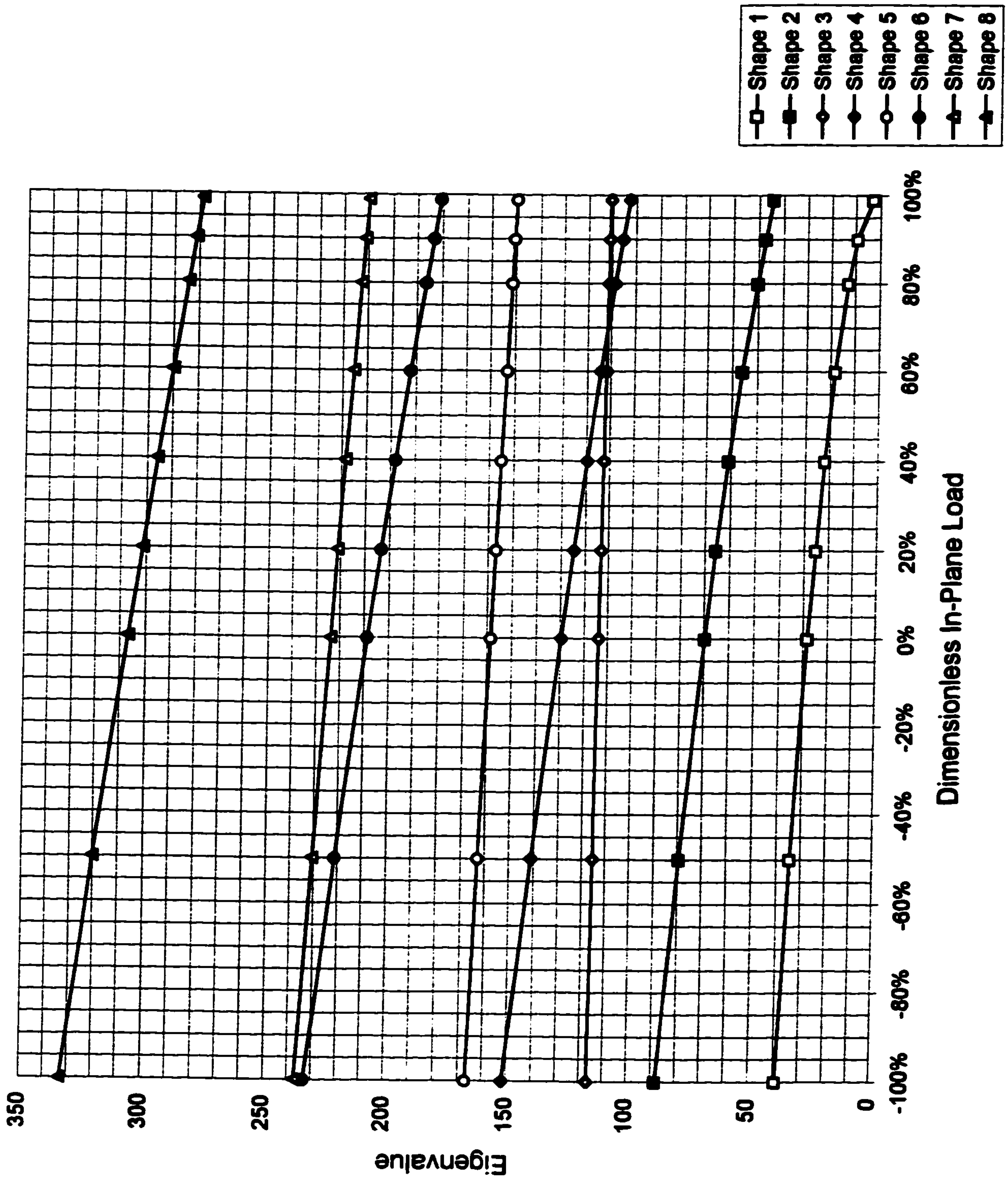

Figure 4.139 Mode shapes, CSCF plate, $\phi = 2 / 5$.

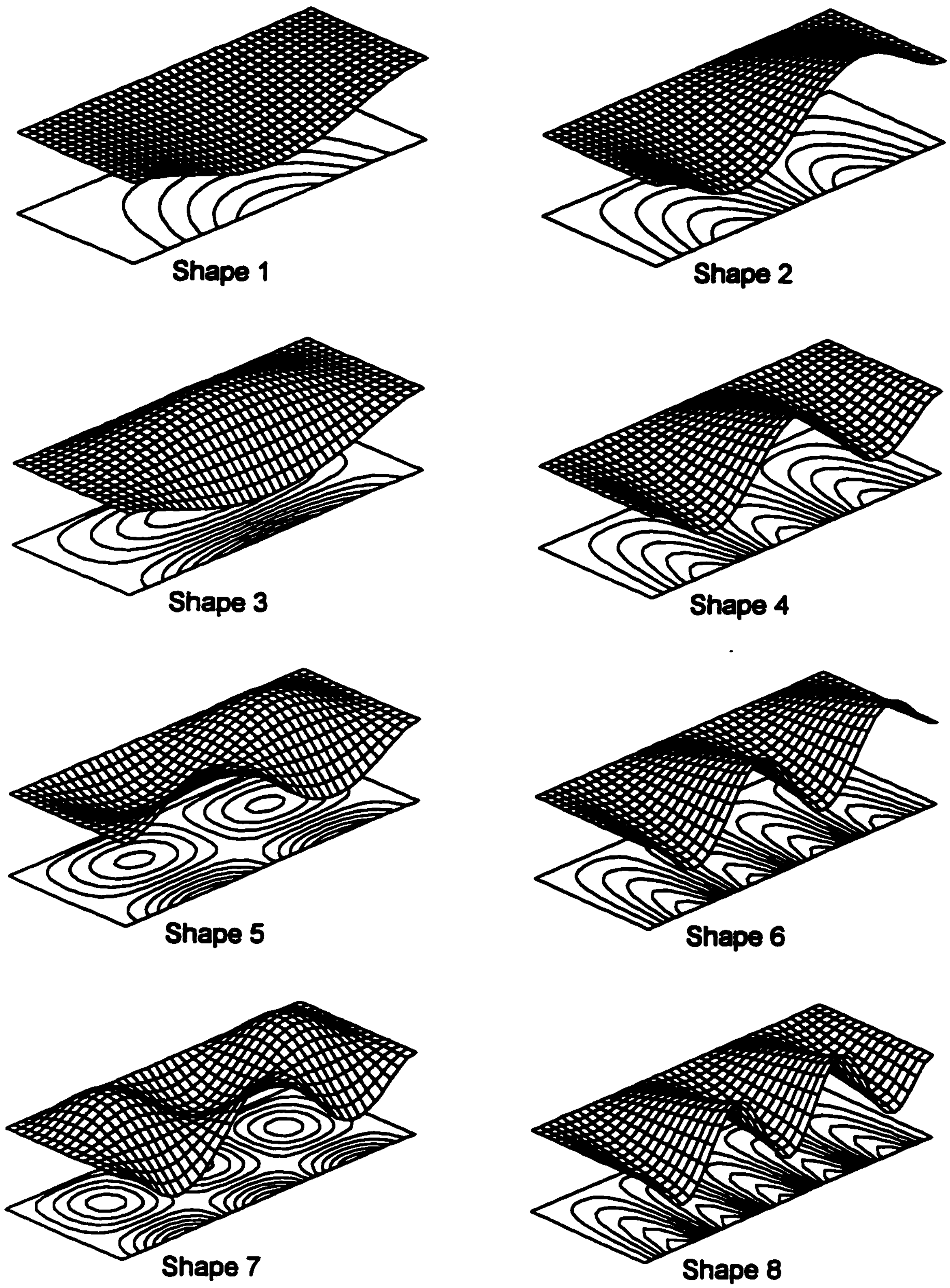

Table 4.76 Eigenvalues, CSCF plate, $\phi = 1/2$, $\lambda^2 = \omega a^2 (\rho / D)^{1/2}$.

Mode	In-plane load as a percentage of buckling load								
	-100%	-50%	0%	20%	40%	60%	80%	90%	99%
	Present solution								
1	36.50	31.82	26.19	23.51	20.45	16.78	11.93	8.46	2.68
2	83.27	75.53	66.79	62.93	58.79	54.32	49.41	46.75	44.21
3	83.30	81.43	79.54	78.76	77.98	77.19	76.38	75.97	75.61
4	133.13	128.56	123.81	121.82	117.30	112.60	107.68	105.14	102.79
5	145.95	136.44	126.18	121.85	119.86	117.83	115.75	114.70	113.74
6	200.92	194.23	187.27	184.41	181.50	178.55	175.53	174.01	172.62
7	215.71	215.03	204.88	200.26	195.52	190.67	185.68	183.14	180.82
8	226.58	216.01	214.35	214.07	213.80	213.52	213.25	213.11	212.98
	Finite element solution [18]								
1	36.52	31.83	26.20	23.53	20.46	16.78	11.93	8.46	2.68
2	83.22	75.62	66.88	63.01	58.88	54.40	49.50	46.84	44.30
3	83.39	81.38	79.48	78.71	77.92	77.13	76.32	75.91	75.54
4	133.01	128.43	123.67	121.70	117.60	112.90	107.99	105.45	103.11
5	146.23	136.72	126.47	122.11	119.70	117.66	115.59	114.53	113.57
6	200.70	193.99	187.01	184.14	181.22	178.26	175.24	173.70	172.31
7	215.41	214.73	205.63	201.01	196.29	191.44	186.47	183.93	181.62
8	227.29	216.74	214.04	213.77	213.49	213.22	212.94	212.80	212.68
	Percent difference								
1	0.06%	0.06%	0.05%	0.05%	0.05%	0.04%	0.04%	0.03%	-0.05%
2	-0.06%	0.12%	0.13%	0.13%	0.14%	0.16%	0.18%	0.19%	0.20%
3	0.11%	-0.06%	-0.07%	-0.07%	-0.07%	-0.08%	-0.08%	-0.08%	-0.08%
4	-0.09%	-0.10%	-0.12%	-0.10%	0.26%	0.27%	0.29%	0.30%	0.31%
5	0.19%	0.21%	0.23%	0.21%	-0.13%	-0.14%	-0.14%	-0.15%	-0.15%
6	-0.11%	-0.12%	-0.14%	-0.15%	-0.15%	-0.16%	-0.17%	-0.18%	-0.18%
7	-0.14%	-0.14%	0.36%	0.38%	0.39%	0.41%	0.42%	0.43%	0.44%
8	0.31%	0.34%	-0.14%	-0.14%	-0.14%	-0.14%	-0.14%	-0.14%	-0.14%

Figure 4.140 Eigenvalue curves, CSCF plate, $\phi = 1 / 2$,

$P_\xi = - N_x b^2 / D$, $\lambda^2 = \omega a^2 (\rho / D)^{1/2}$.

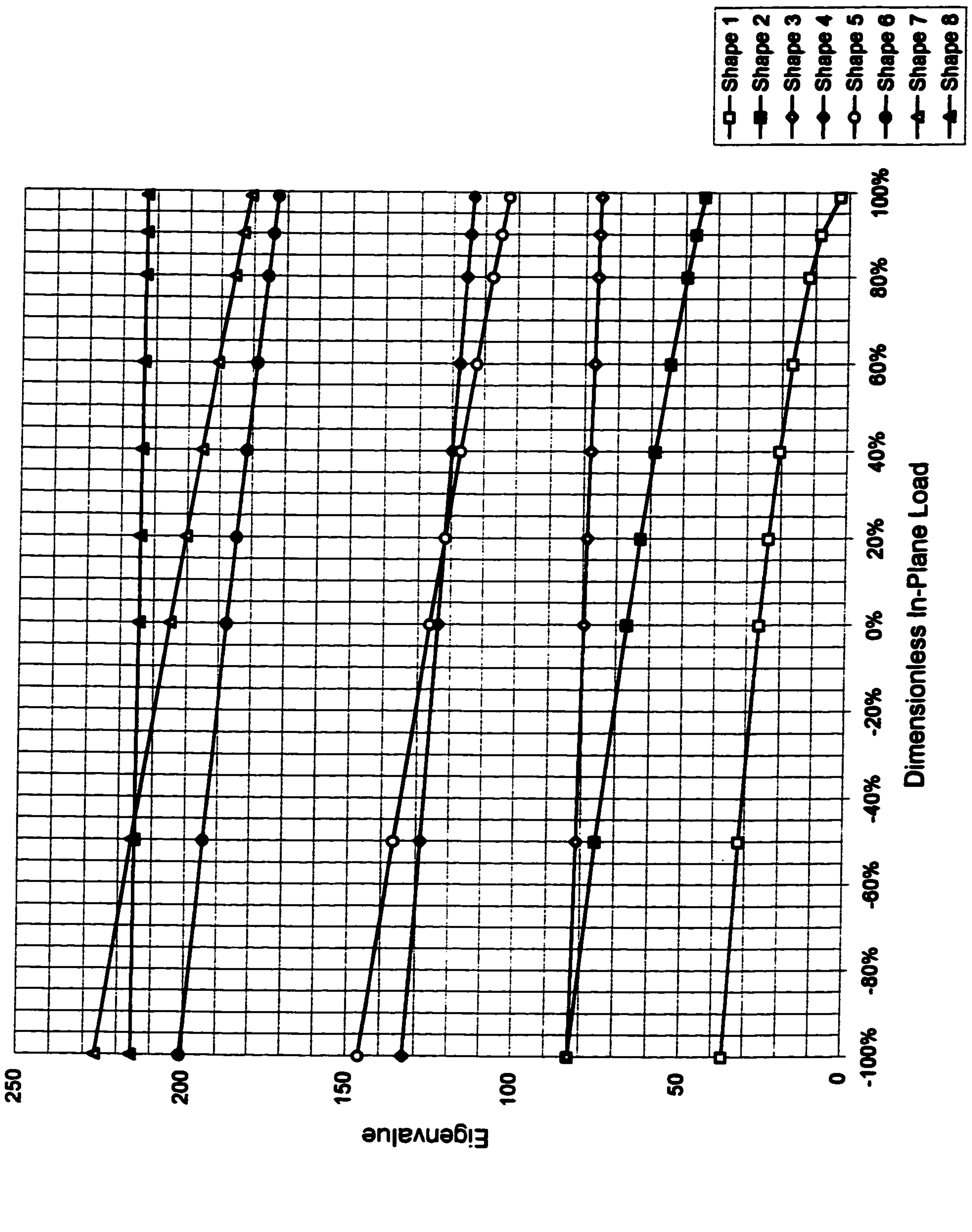

Figure 4.141 Mode shapes, CSCF plate, $\phi = 1 / 2$.

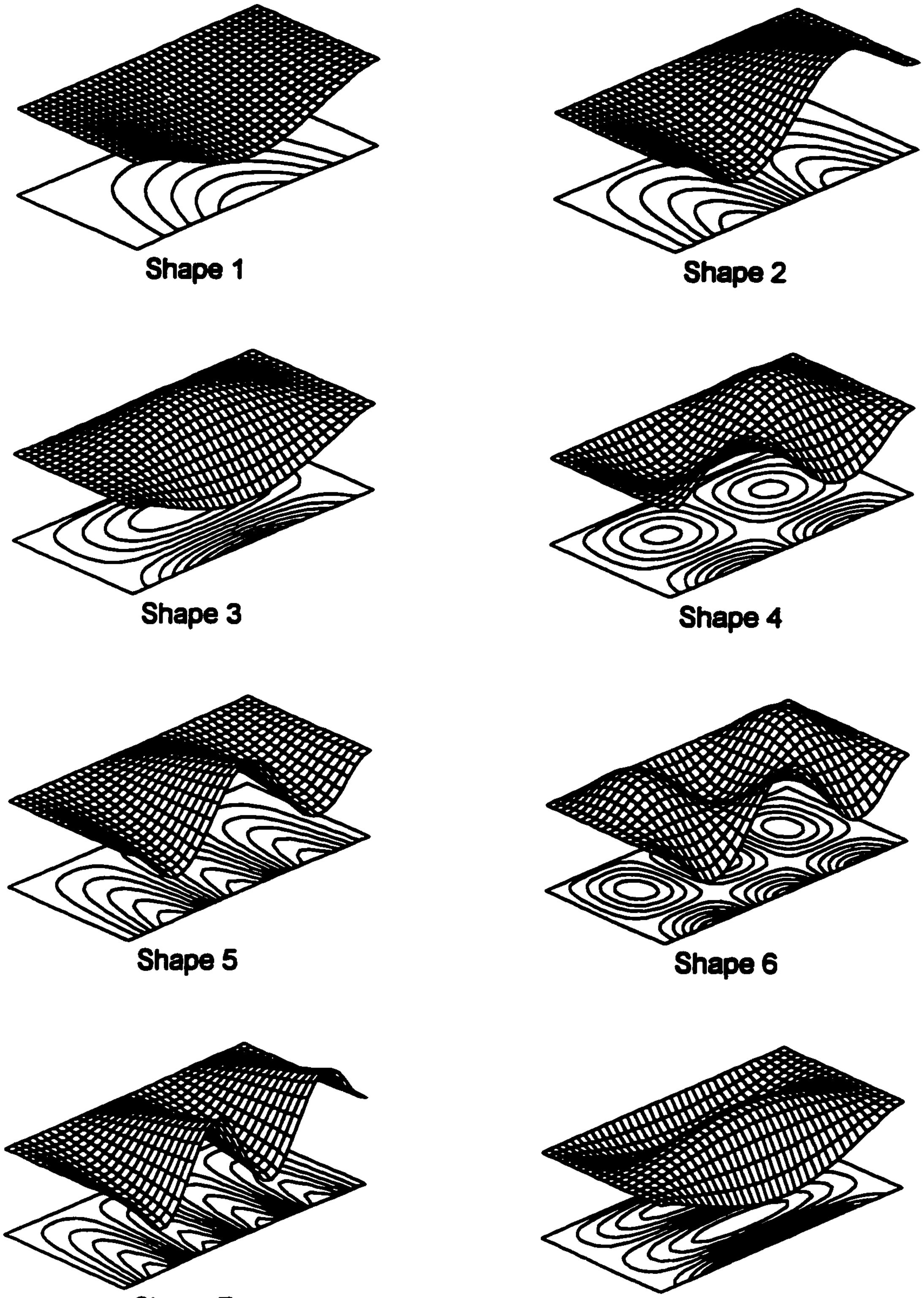

Table 4.77 Eigenvalues, CSCF plate, $\phi = 2/3$, $\lambda^2 = \omega a^2 (\rho / D)^{1/2}$.

Mode	In-plane load as a percentage of buckling load								
	-100%	-50%	0%	20%	40%	60%	80%	90%	99%
	Present solution								
1	34.22	29.82	24.53	22.02	19.14	15.70	11.15	7.91	2.51
2	58.30	55.94	53.45	52.41	51.35	50.26	48.80	46.45	44.23
3	79.49	72.38	64.41	60.91	57.18	53.16	49.14	48.57	48.04
4	107.07	102.02	96.67	94.44	92.14	89.79	87.36	86.12	84.98
5	129.68	128.67	123.54	119.66	115.65	111.49	107.17	104.94	102.89
6	141.31	132.73	127.66	127.24	126.83	126.41	126.00	125.79	125.60
7	172.51	165.62	158.42	155.44	152.41	149.30	146.13	144.51	143.04
8	175.37	172.40	169.38	168.15	166.91	165.66	164.40	163.77	163.19
	Finite element solution [18]								
1	34.24	29.83	24.55	22.03	19.15	15.71	11.16	7.91	2.51
2	58.28	55.92	53.42	52.39	51.32	50.23	48.87	46.52	44.30
3	79.57	72.45	64.48	60.98	57.24	53.23	49.11	48.53	48.01
4	107.04	101.97	96.61	94.38	92.08	89.72	87.28	86.04	84.90
5	129.56	128.54	123.76	119.89	115.88	111.72	107.40	105.17	103.13
6	141.52	132.95	127.52	127.11	126.70	126.28	125.86	125.65	125.46
7	172.46	165.57	158.35	155.37	152.32	149.21	146.03	144.41	142.94
8	175.10	172.12	169.09	167.86	166.62	165.36	164.10	163.46	162.89
	Percent difference								
1	0.06%	0.05%	0.05%	0.05%	0.05%	0.05%	0.04%	0.04%	-0.03%
2	-0.03%	-0.04%	-0.05%	-0.05%	-0.05%	-0.06%	0.14%	0.15%	0.16%
3	0.09%	0.10%	0.11%	0.11%	0.12%	0.13%	-0.06%	-0.07%	-0.07%
4	-0.03%	-0.04%	-0.06%	-0.06%	-0.07%	-0.08%	-0.09%	-0.09%	-0.09%
5	-0.10%	-0.10%	0.18%	0.19%	0.20%	0.21%	0.22%	0.22%	0.23%
6	0.15%	0.17%	-0.10%	-0.10%	-0.10%	-0.11%	-0.11%	-0.11%	-0.11%
7	-0.03%	-0.04%	-0.05%	-0.05%	-0.06%	-0.06%	-0.07%	-0.07%	-0.07%
8	-0.15%	-0.16%	-0.17%	-0.17%	-0.18%	-0.18%	-0.18%	-0.19%	-0.19%

Figure 4.142 Eigenvalue curves, CSCF plate, $\phi = 2 / 3$,

$P_\xi = - N_x b^2 / D$, $\lambda^2 = \omega a^2 (\rho / D)^{1/2}$.

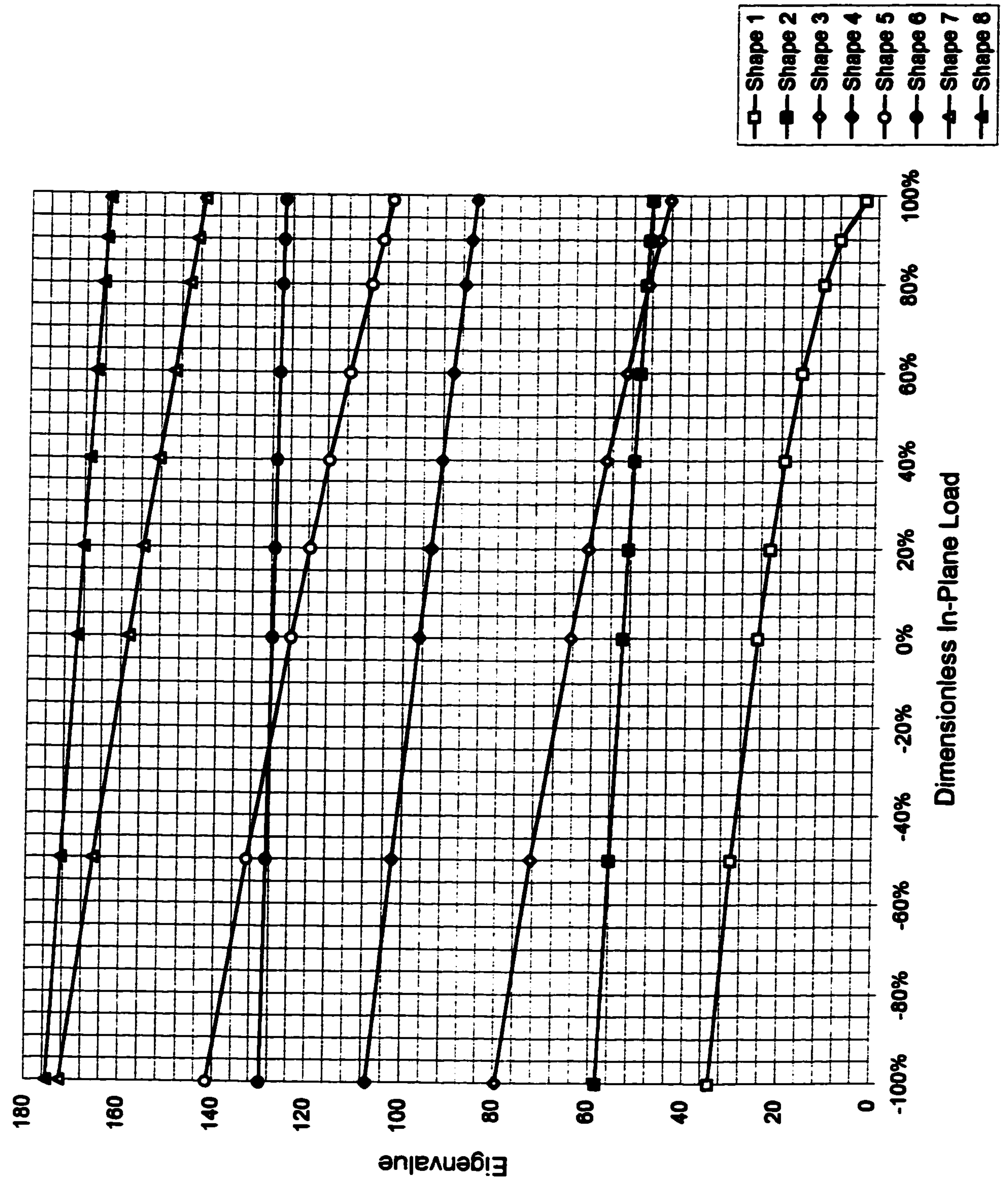

Figure 4.143 Mode shapes, CSCF plate, $\phi = 2 / 3$.

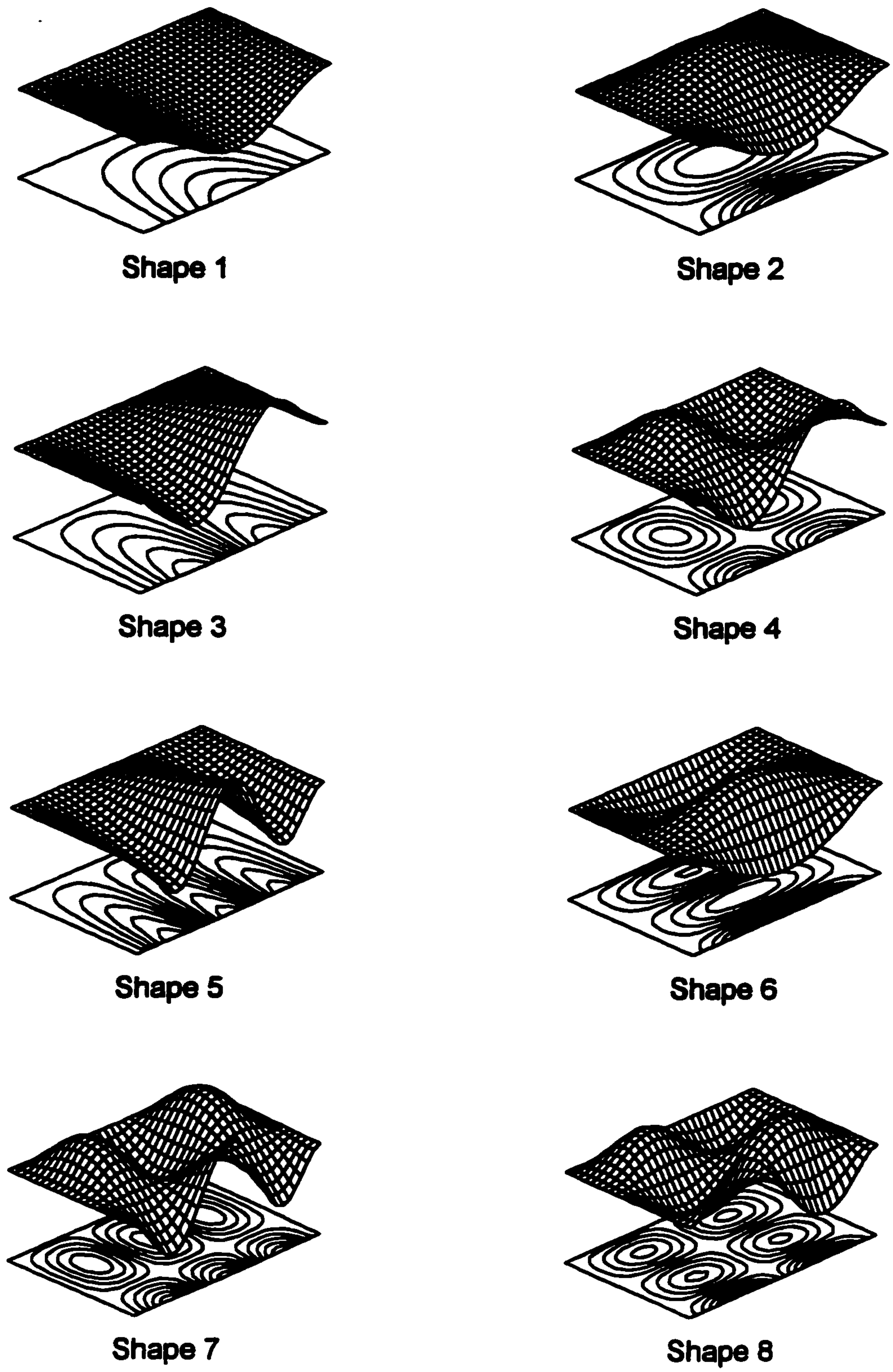

Table 4.78 Eigenvalues, CSCF plate, $\phi = 1 / 1$, $\lambda^2 = \omega a^2 (\rho / D)^{1/2}$.

Mode	In-plane load as a percentage of buckling load								
	-100%	-50%	0%	20%	40%	60%	80%	90%	99%
	Present solution								
1	32.50	28.31	23.28	20.89	18.16	14.89	10.57	7.49	2.38
2	41.88	38.80	35.41	33.95	32.41	30.78	29.04	28.12	27.27
3	70.14	68.40	62.70	59.47	56.03	52.36	48.40	46.28	44.28
4	76.71	70.08	66.61	65.87	65.13	64.37	63.60	63.21	62.86
5	88.76	83.16	77.13	74.56	71.90	69.13	66.23	64.72	63.34
6	116.94	112.83	108.54	106.77	104.97	103.13	101.26	100.31	99.44
7	120.87	119.90	118.91	118.17	114.54	110.77	106.87	104.87	103.03
8	137.99	130.12	121.72	118.52	118.11	117.71	117.30	117.10	116.91
	Finite element solution [18]								
1	32.51	28.32	23.29	20.90	18.17	14.89	10.58	7.50	2.38
2	41.87	38.80	35.41	33.94	32.40	30.77	29.03	28.11	27.25
3	70.10	68.36	62.72	59.48	56.05	52.38	48.41	46.29	44.30
4	76.73	70.10	66.56	65.83	65.08	64.32	63.55	63.16	62.81
5	88.74	83.14	77.10	74.53	71.87	69.09	66.19	64.68	63.30
6	116.83	112.71	108.41	106.64	104.84	103.00	101.12	100.17	99.30
7	120.76	119.78	118.79	118.20	114.58	110.82	106.92	104.92	103.08
8	138.03	130.16	121.75	118.42	117.99	117.59	117.18	116.98	116.79
	Percent difference								
1	0.03%	0.03%	0.03%	0.03%	0.03%	0.03%	0.03%	0.03%	0.05%
2	-0.01%	-0.01%	-0.02%	-0.02%	-0.03%	-0.04%	-0.04%	-0.05%	-0.05%
3	-0.06%	-0.06%	0.03%	0.03%	0.03%	0.04%	0.04%	0.04%	0.04%
4	0.03%	0.03%	-0.07%	-0.07%	-0.07%	-0.07%	-0.08%	-0.08%	-0.08%
5	-0.02%	-0.03%	-0.03%	-0.04%	-0.04%	-0.05%	-0.06%	-0.06%	-0.06%
6	-0.10%	-0.11%	-0.12%	-0.12%	-0.13%	-0.13%	-0.14%	-0.14%	-0.14%
7	-0.09%	-0.09%	-0.10%	0.02%	0.04%	0.04%	0.04%	0.04%	0.04%
8	0.03%	0.03%	0.03%	-0.08%	-0.10%	-0.10%	-0.10%	-0.10%	-0.10%

Figure 4.144 Eigenvalue curves, CSCF plate, $\phi = 1 / 1$,

$P_\xi = - N_x b^2 / D$, $\lambda^2 = \omega a^2 (\rho / D)^{1/2}$.

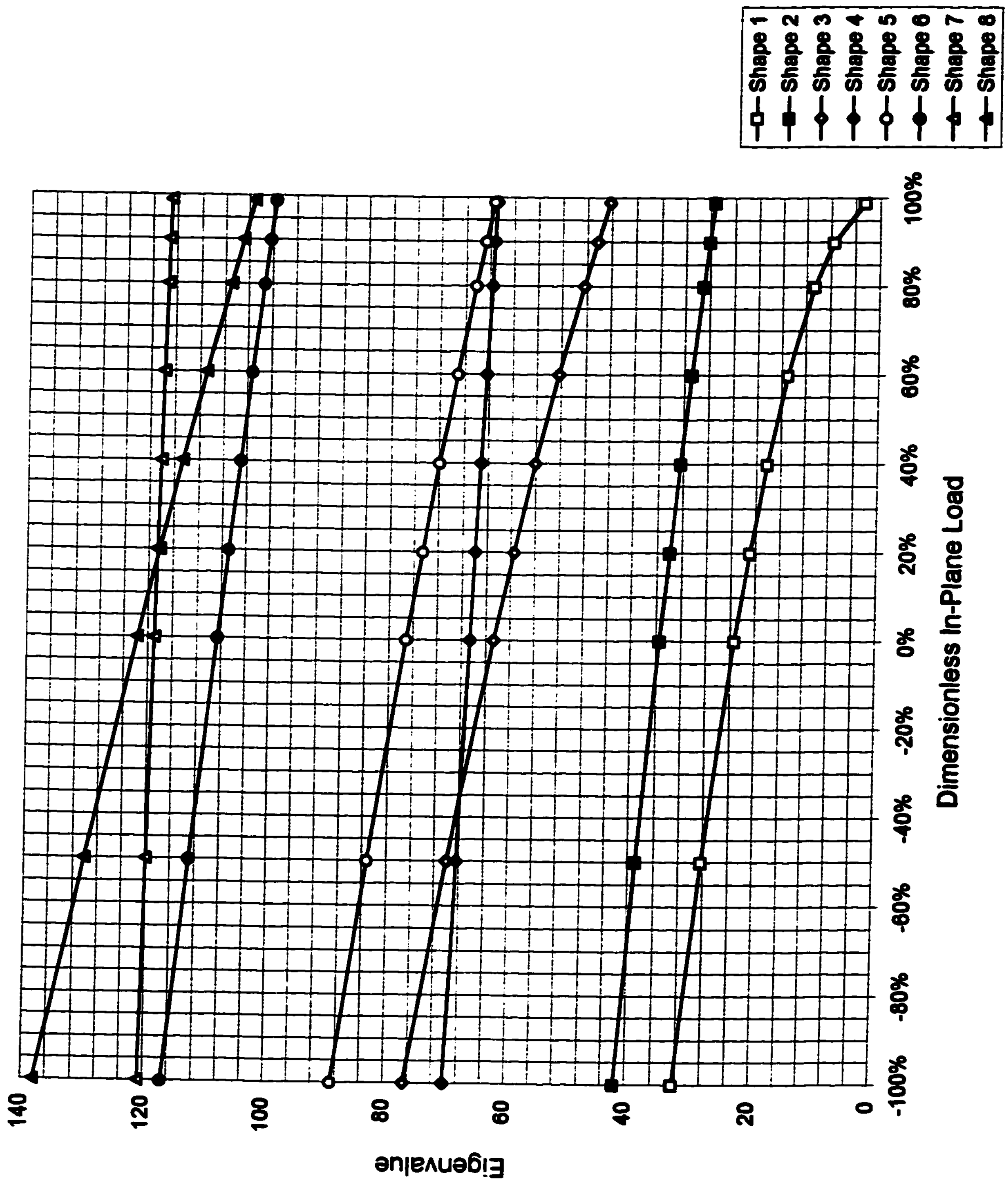

Figure 4.145 Mode shapes, CSCF plate, $\phi = 1 / 1$.

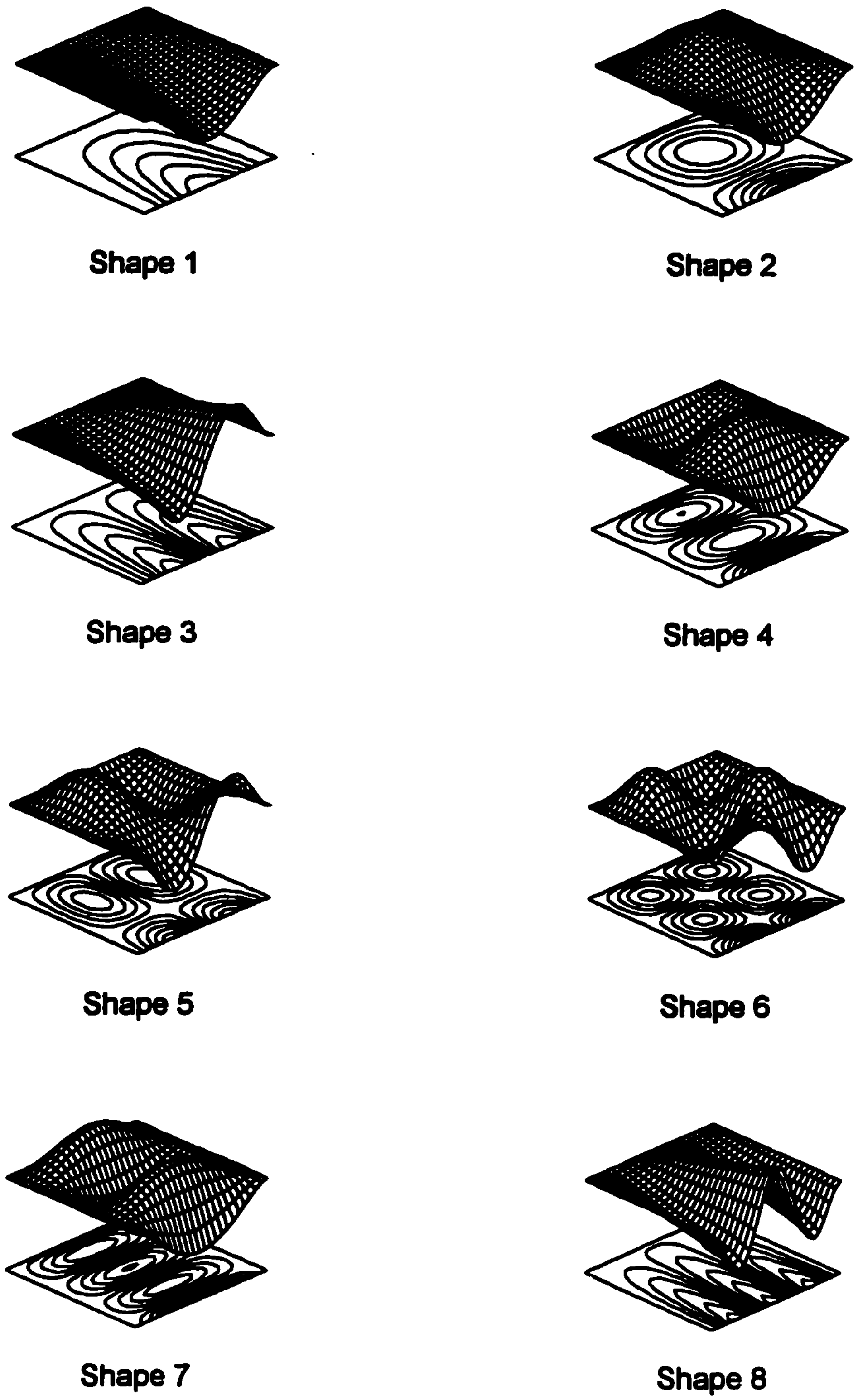

Table 4.79 Eigenvalues, CSCF plate, $\phi = 3/2$, $\lambda^2 = \omega a^2 (\rho / D)^{1/2}$.

Mode	In-plane load as a percentage of buckling load								
	-100%	-50%	0%	20%	40%	60%	80%	90%	99%
					Present solution				
1	31.72	27.63	22.72	20.39	17.72	14.52	10.31	7.31	2.32
2	35.47	31.91	27.84	26.01	24.02	21.83	19.36	17.99	16.65
3	46.00	43.37	40.54	39.34	38.09	36.80	35.45	34.75	34.10
4	66.13	64.36	61.97	58.86	55.56	52.04	48.25	46.23	44.33
5	75.50	69.09	62.54	61.79	61.02	59.66	56.42	54.71	53.13
6	80.81	74.90	68.43	65.64	62.73	60.25	59.46	59.06	58.70
7	92.49	87.42	82.01	79.73	77.38	74.95	72.43	71.13	69.94
8	96.39	95.21	94.01	93.52	93.03	92.54	92.04	91.79	91.57
					Finite element solution [18]				
1	31.72	27.63	22.72	20.38	17.72	14.52	10.31	7.31	2.32
2	35.46	31.90	27.83	26.00	24.01	21.82	19.35	17.98	16.64
3	45.96	43.33	40.50	39.31	38.06	36.77	35.41	34.71	34.07
4	66.06	64.29	61.92	58.81	55.51	51.99	48.20	46.18	44.28
5	75.44	69.04	62.47	61.72	60.95	59.58	56.33	54.63	53.05
6	80.73	74.82	68.35	65.57	62.65	60.18	59.39	58.99	58.63
7	92.36	87.29	81.87	79.59	77.24	74.81	72.29	70.99	69.80
8	96.29	95.11	93.91	93.43	92.94	92.44	91.95	91.69	91.47
					Percent difference				
1	-0.03%	-0.02%	-0.02%	-0.02%	-0.01%	-0.01%	-0.01%	0.00%	0.01%
2	-0.04%	-0.04%	-0.04%	-0.04%	-0.04%	-0.05%	-0.05%	-0.06%	-0.06%
3	-0.07%	-0.08%	-0.08%	-0.08%	-0.09%	-0.09%	-0.10%	-0.10%	-0.10%
4	-0.11%	-0.11%	-0.08%	-0.08%	-0.08%	-0.09%	-0.10%	-0.10%	-0.11%
5	-0.07%	-0.07%	-0.11%	-0.11%	-0.11%	-0.13%	-0.14%	-0.15%	-0.16%
6	-0.10%	-0.10%	-0.11%	-0.12%	-0.12%	-0.12%	-0.12%	-0.12%	-0.12%
7	-0.14%	-0.15%	-0.17%	-0.17%	-0.18%	-0.19%	-0.20%	-0.20%	-0.21%
8	-0.10%	-0.10%	-0.10%	-0.10%	-0.10%	-0.11%	-0.11%	-0.11%	-0.11%

Figure 4.146 Eigenvalue curves, CSCF plate, $\phi = 3 / 2$,
$P_\xi = - N_x b^2 / D$, $\lambda^2 = \omega a^2 (\rho / D)^{1/2}$.

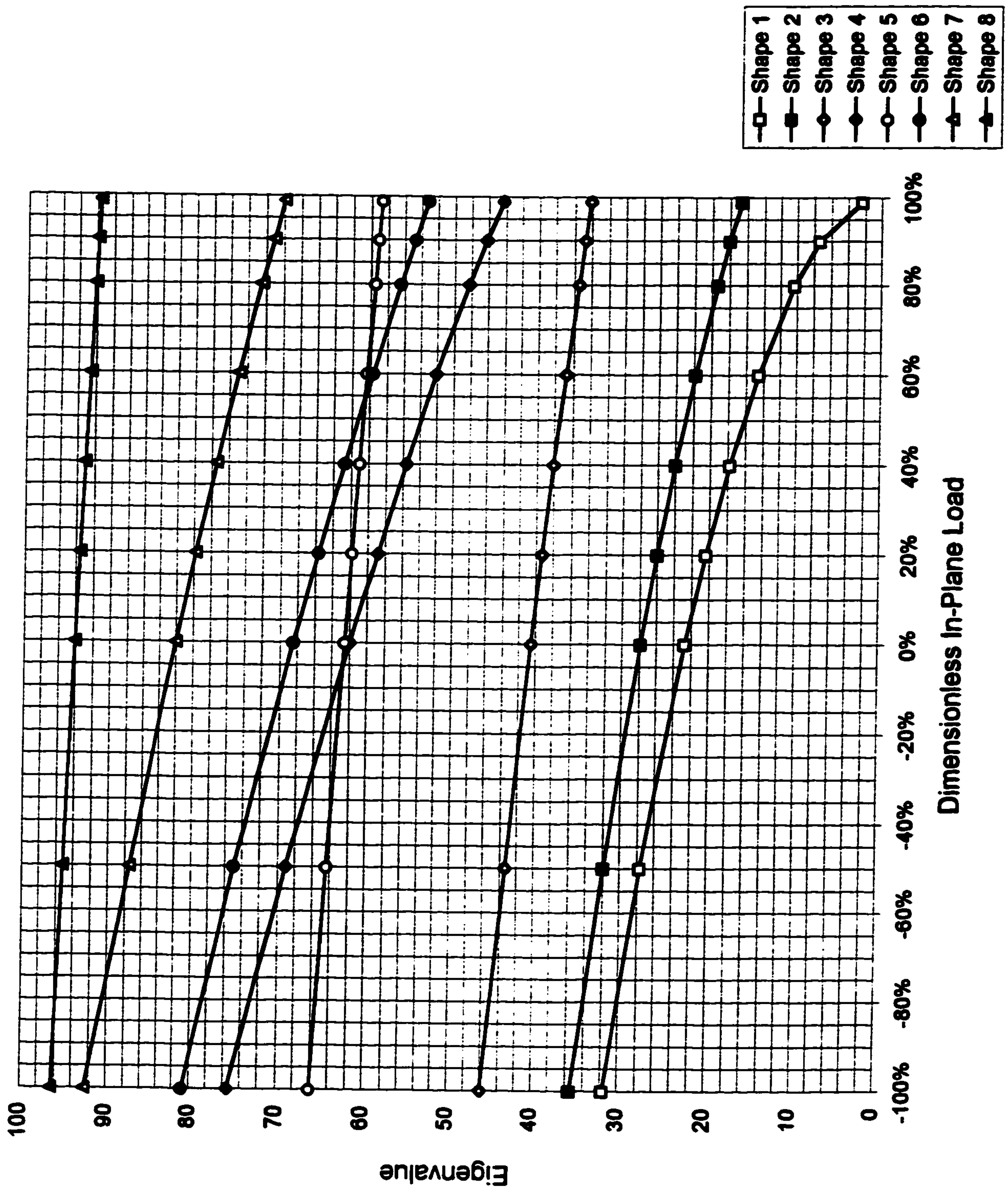

Figure 4.147 Mode shapes, CSCF plate, $\phi = 3 / 2$.

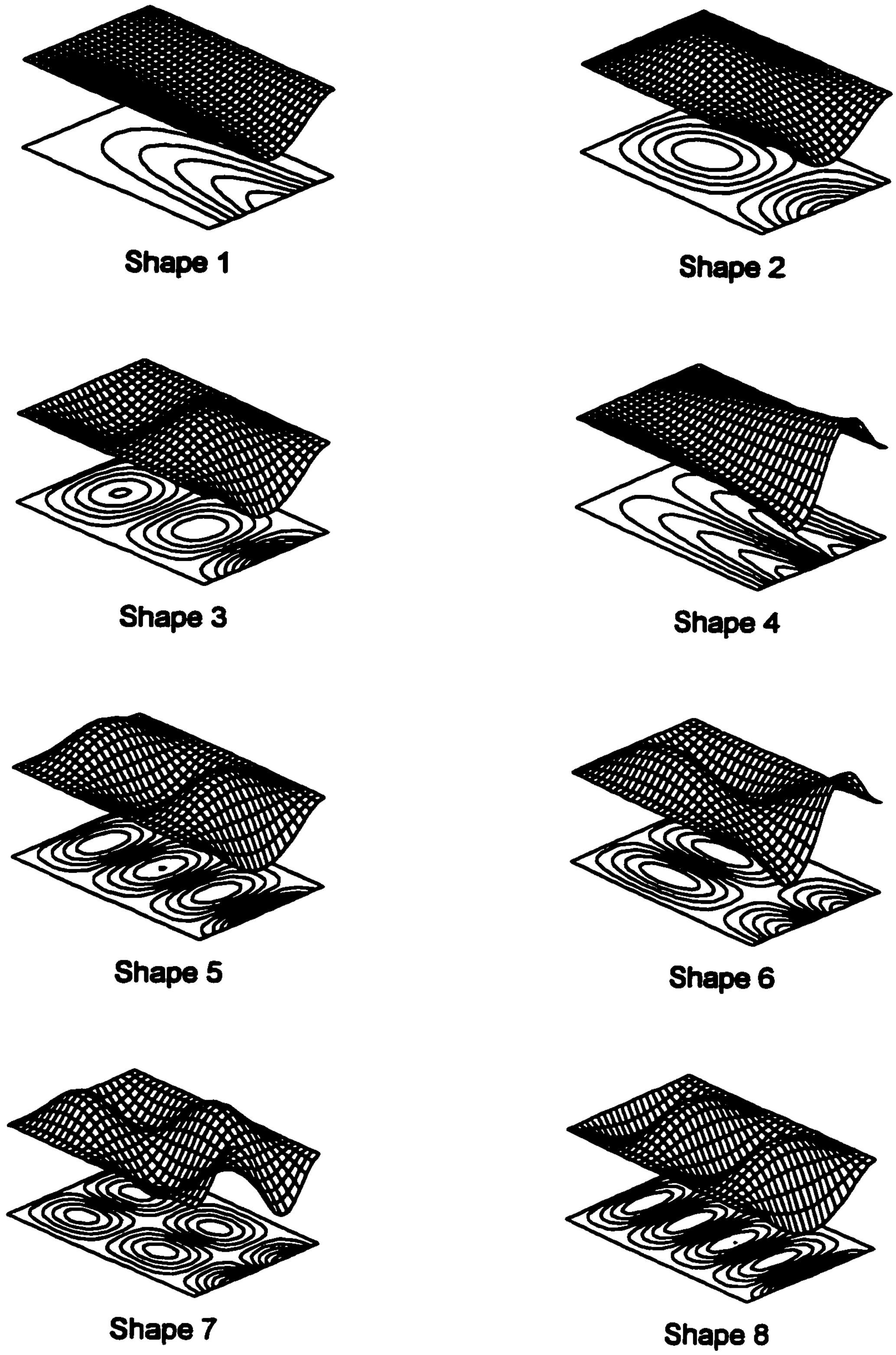

Table 4.80 Eigenvalues, CSCF plate, $\phi = 2 / 1$, $\lambda^2 = \omega a^2 (\rho / D)^{1/2}$.

Mode	In-plane load as a percentage of buckling load -100%	-50%	0%	20%	40%	60%	80%	90%	99%
	Present solution								
1	31.46	27.40	22.53	20.21	17.57	14.40	10.22	7.24	2.30
2	33.46	29.71	25.33	23.33	21.10	18.59	15.64	13.91	12.14
3	38.65	35.50	31.98	30.45	28.82	27.08	25.20	24.19	23.25
4	48.60	46.17	43.58	42.49	41.36	40.20	39.00	38.38	37.81
5	64.19	62.40	60.54	58.66	55.41	51.95	48.22	46.23	44.37
6	75.10	68.76	61.73	59.78	59.00	56.31	52.90	51.11	49.44
7	78.10	72.05	65.40	62.53	59.50	58.21	57.41	57.00	56.63
8	84.42	78.90	72.92	70.37	67.72	64.95	62.05	60.55	59.16
	Finite element solution [18]								
1	31.44	27.39	22.52	20.21	17.56	14.39	10.22	7.24	2.30
2	33.44	29.69	25.32	23.31	21.09	18.58	15.62	13.90	12.12
3	38.61	35.46	31.95	30.41	28.78	27.04	25.16	24.16	23.21
4	48.52	46.09	43.50	42.41	41.29	40.12	38.92	38.30	37.73
5	64.07	62.28	60.42	58.58	55.33	51.86	48.13	46.15	44.28
6	75.00	68.67	61.64	59.66	58.88	56.18	52.77	50.98	49.30
7	77.97	71.92	65.27	62.40	59.38	58.09	57.29	56.88	56.51
8	84.24	78.72	72.74	70.19	67.54	64.77	61.87	60.36	58.97
	Percent difference								
1	-0.06%	-0.06%	-0.05%	-0.04%	-0.04%	-0.04%	-0.03%	-0.03%	-0.01%
2	-0.08%	-0.07%	-0.07%	-0.07%	-0.07%	-0.08%	-0.09%	-0.11%	-0.14%
3	-0.11%	-0.11%	-0.12%	-0.12%	-0.13%	-0.14%	-0.15%	-0.16%	-0.17%
4	-0.16%	-0.17%	-0.18%	-0.18%	-0.19%	-0.20%	-0.21%	-0.21%	-0.21%
5	-0.19%	-0.19%	-0.20%	-0.15%	-0.16%	-0.17%	-0.18%	-0.19%	-0.20%
6	-0.13%	-0.14%	-0.14%	-0.20%	-0.20%	-0.23%	-0.25%	-0.26%	-0.27%
7	-0.17%	-0.18%	-0.19%	-0.20%	-0.21%	-0.21%	-0.21%	-0.21%	-0.21%
8	-0.21%	-0.22%	-0.24%	-0.25%	-0.27%	-0.28%	-0.30%	-0.31%	-0.32%

Figure 4.148 Eigenvalue curves, CSCF plate, $\phi = 2 / 1$,
$P_\xi = - N_x b^2 / D$, $\lambda^2 = \omega a^2 (\rho / D)^{1/2}$.

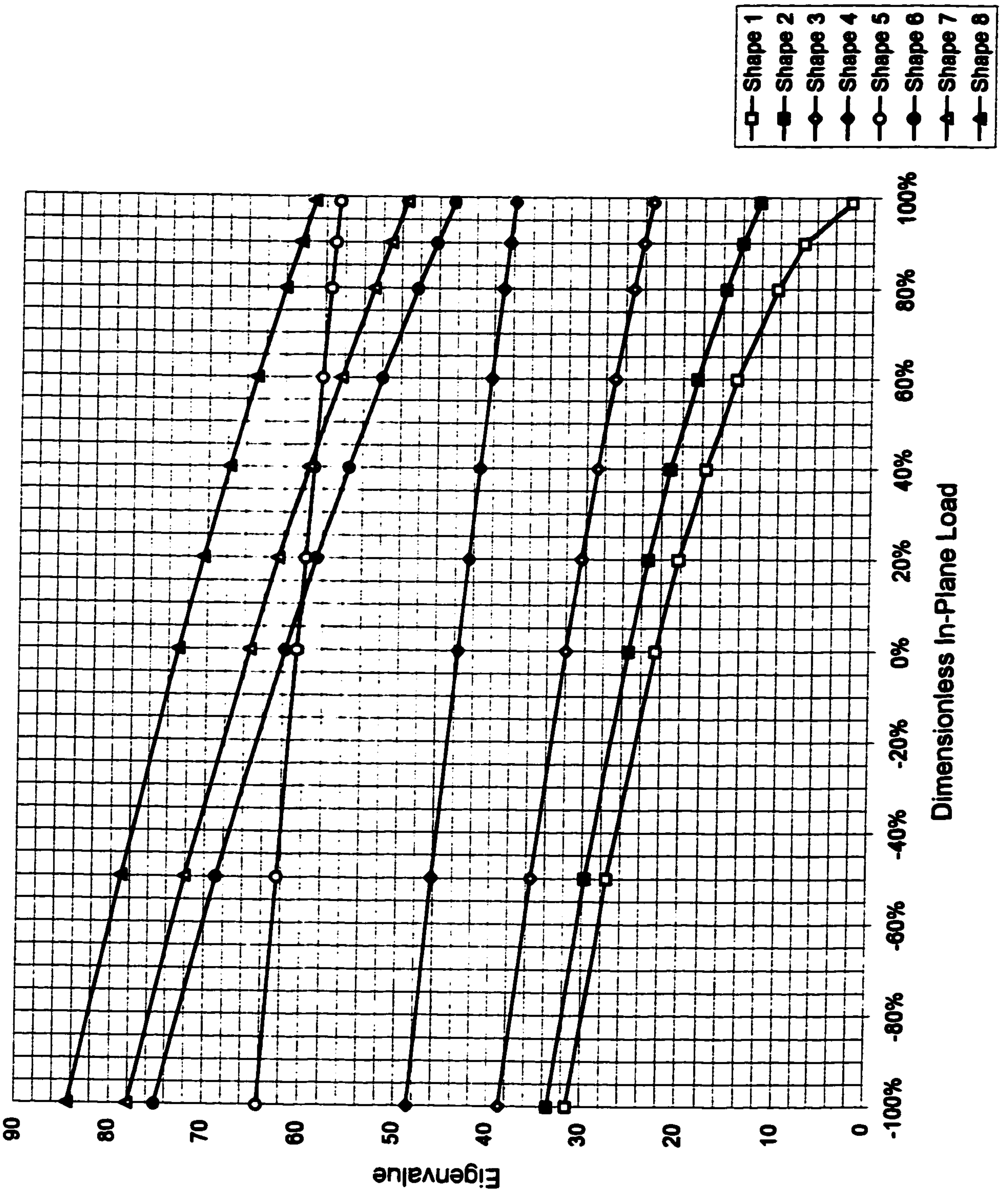

Figure 4.149 Mode shapes, CSCF plate, $\phi = 2 / 1$.

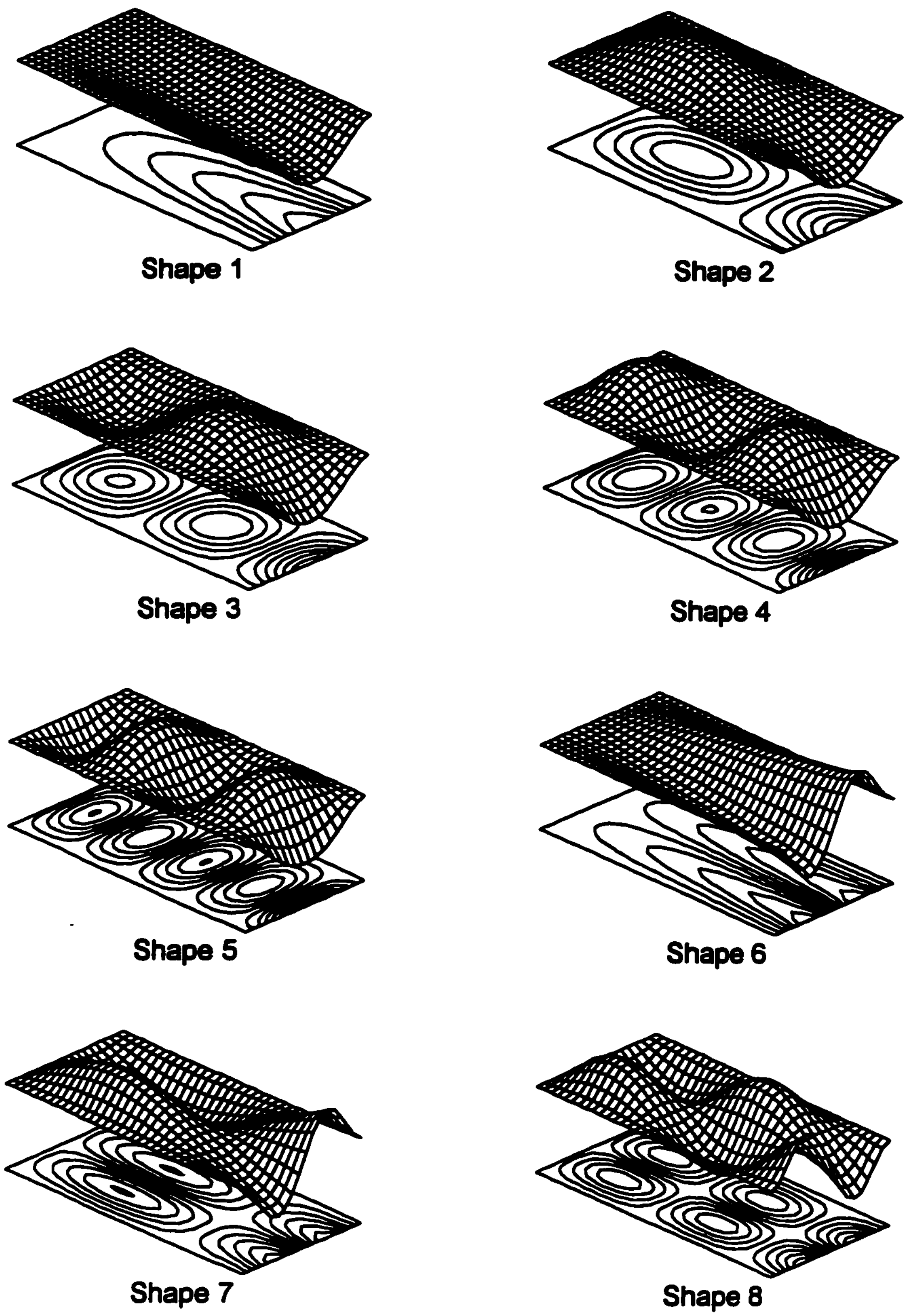

Table 4.81 Eigenvalues, CSCF plate, $\phi = 5 / 2$, $\lambda^2 = \omega a^2 (\rho / D)^{1/2}$.

Mode	In-plane load as a percentage of buckling load								
	-100%	-50%	0%	20%	40%	60%	80%	90%	99%
	Present solution								
1	31.34	27.30	22.44	20.14	17.50	14.34	10.18	7.22	2.29
2	32.59	28.75	24.22	22.12	19.77	17.06	13.79	11.80	9.65
3	35.63	32.18	28.26	26.50	24.60	22.53	20.22	18.94	17.71
4	41.31	38.41	35.23	33.86	32.43	30.92	29.31	28.47	27.69
5	50.34	48.02	45.56	44.53	43.47	42.38	41.25	40.67	40.14
6	63.06	61.24	59.36	58.59	55.36	51.92	48.21	46.24	44.39
7	74.92	68.63	61.63	58.59	57.80	54.75	51.26	49.42	47.70
8	76.86	70.75	64.01	61.09	58.01	57.00	56.18	55.54	54.02
	Finite element solution [18]								
1	31.32	27.28	22.43	20.13	17.49	14.33	10.18	7.21	2.29
2	32.56	28.72	24.19	22.09	19.74	17.04	13.77	11.78	9.62
3	35.58	32.14	28.21	26.46	24.56	22.49	20.17	18.90	17.66
4	41.22	38.32	35.15	33.78	32.34	30.83	29.22	28.38	27.60
5	50.21	47.89	45.42	44.39	43.33	42.23	41.10	40.52	39.99
6	62.87	61.06	59.17	58.40	55.25	51.81	48.11	46.14	44.28
7	74.80	68.51	61.53	58.48	57.61	54.59	51.10	49.25	47.53
8	76.70	70.59	63.85	60.93	57.85	56.81	55.99	55.32	53.80
	Percent difference								
1	-0.08%	-0.08%	-0.07%	-0.06%	-0.06%	-0.05%	-0.05%	-0.04%	-0.03%
2	-0.10%	-0.10%	-0.10%	-0.10%	-0.11%	-0.12%	-0.16%	-0.20%	-0.29%
3	-0.14%	-0.14%	-0.15%	-0.16%	-0.17%	-0.19%	-0.22%	-0.24%	-0.28%
4	-0.21%	-0.22%	-0.24%	-0.25%	-0.26%	-0.28%	-0.31%	-0.32%	-0.34%
5	-0.27%	-0.29%	-0.31%	-0.31%	-0.32%	-0.34%	-0.35%	-0.36%	-0.37%
6	-0.29%	-0.30%	-0.31%	-0.32%	-0.19%	-0.20%	-0.22%	-0.23%	-0.24%
7	-0.16%	-0.17%	-0.18%	-0.18%	-0.33%	-0.30%	-0.33%	-0.34%	-0.36%
8	-0.21%	-0.23%	-0.25%	-0.26%	-0.28%	-0.33%	-0.34%	-0.40%	-0.42%

Figure 4.150 Eigenvalue curves, CSCF plate, $\phi = 5 / 2$,

$P_\xi = - N_x b^2 / D$, $\lambda^2 = \omega a^2 (\rho / D)^{1/2}$.

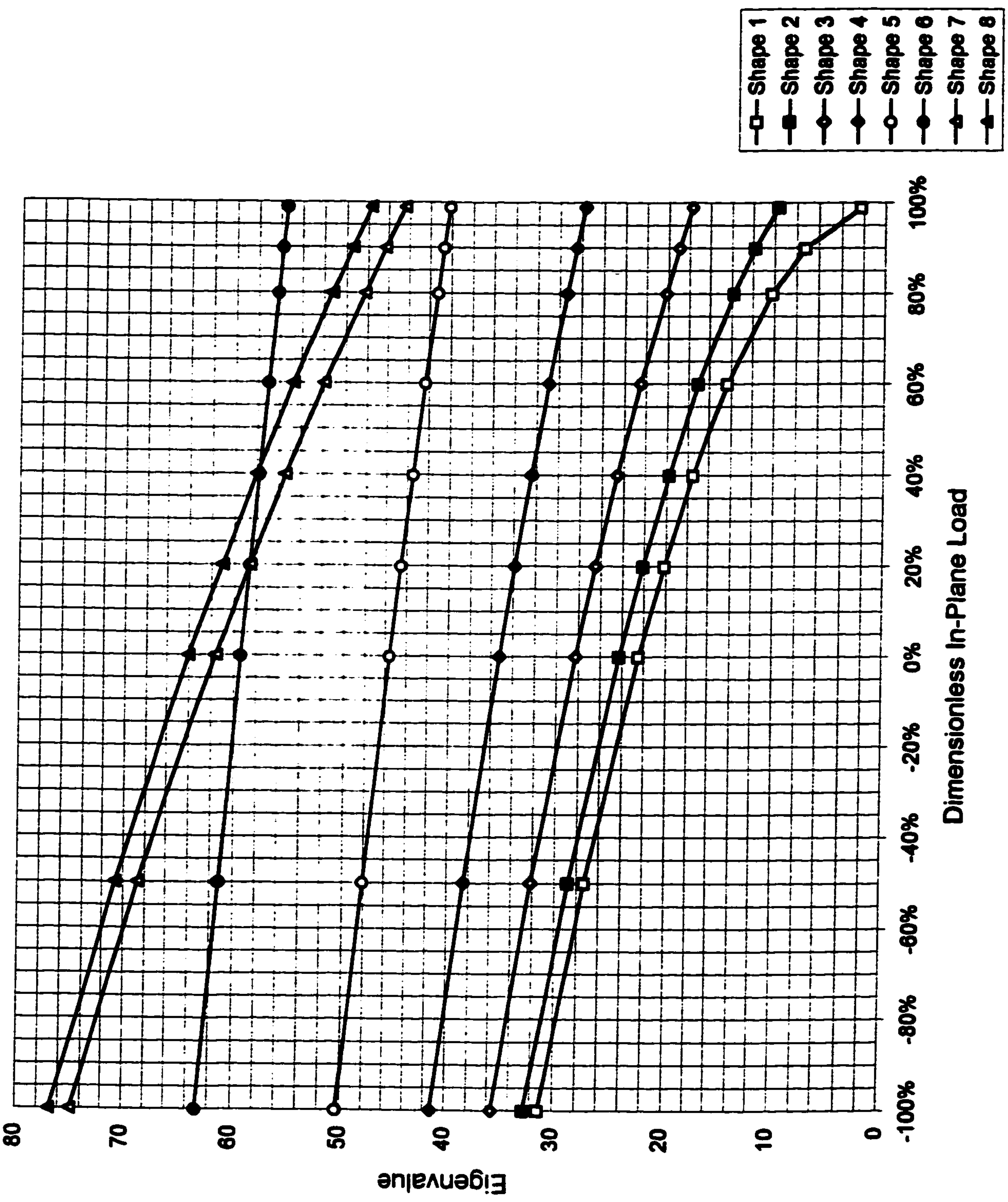

Figure 4.151 Mode shapes, CSCF plate, $\phi = 5 / 2$.

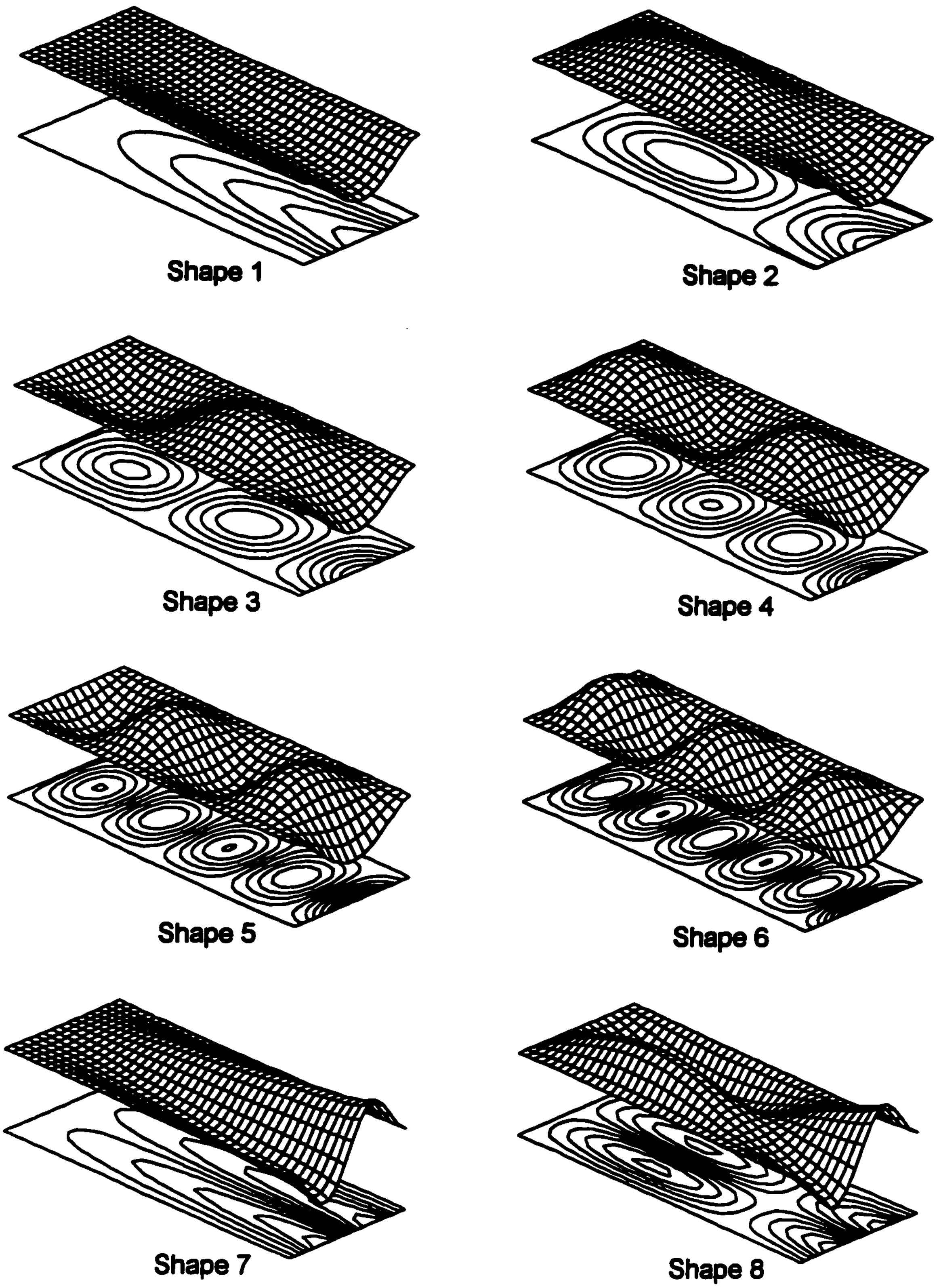

Table 4.82 Eigenvalues, CSCF plate, $\phi = 3 / 1$, $\lambda^2 = \omega a^2 (\rho / D)^{1/2}$.

Mode	In-plane load as a percentage of buckling load								
	-100%	-50%	0%	20%	40%	60%	80%	90%	99%
	Present solution								
1	31.28	27.25	22.40	20.10	17.47	14.31	10.16	7.20	2.28
2	32.14	28.25	23.63	21.47	19.04	16.22	12.75	10.56	8.08
3	34.13	30.51	26.33	24.43	22.35	20.04	17.38	15.87	14.37
4	37.72	34.52	30.92	29.35	27.67	25.86	23.90	22.85	21.86
5	43.43	40.70	37.75	36.48	35.17	33.79	32.34	31.59	30.90
6	51.58	49.33	46.95	45.96	44.94	43.89	42.80	42.25	41.74
7	62.31	60.48	58.58	57.79	55.33	51.90	48.21	46.25	44.41
8	74.84	68.56	61.59	58.55	57.00	53.90	50.37	48.50	46.75
	Finite element solution [18]								
1	31.26	27.23	22.39	20.09	17.45	14.30	10.16	7.20	2.28
2	32.11	28.21	23.60	21.44	19.02	16.20	12.72	10.53	8.04
3	34.07	30.46	26.28	24.38	22.31	19.99	17.33	15.82	14.31
4	37.64	34.43	30.84	29.26	27.58	25.77	23.80	22.75	21.75
5	43.29	40.56	37.60	36.33	35.01	33.63	32.18	31.43	30.73
6	51.37	49.12	46.74	45.74	44.71	43.66	42.57	42.02	41.51
7	62.04	60.21	58.31	57.52	55.22	51.79	48.10	46.14	44.29
8	74.71	68.43	61.47	58.43	56.72	53.72	50.18	48.31	46.55
	Percent difference								
1	-0.09%	-0.08%	-0.07%	-0.07%	-0.06%	-0.06%	-0.05%	-0.06%	-0.22%
2	-0.11%	-0.11%	-0.11%	-0.12%	-0.14%	-0.17%	-0.24%	-0.32%	-0.53%
3	-0.15%	-0.16%	-0.18%	-0.19%	-0.21%	-0.24%	-0.30%	-0.36%	-0.42%
4	-0.23%	-0.25%	-0.28%	-0.30%	-0.33%	-0.36%	-0.41%	-0.45%	-0.48%
5	-0.33%	-0.35%	-0.39%	-0.41%	-0.43%	-0.46%	-0.50%	-0.52%	-0.55%
6	-0.41%	-0.43%	-0.46%	-0.48%	-0.49%	-0.51%	-0.54%	-0.55%	-0.56%
7	-0.42%	-0.44%	-0.46%	-0.47%	-0.21%	-0.22%	-0.23%	-0.25%	-0.26%
8	-0.18%	-0.18%	-0.19%	-0.20%	-0.48%	-0.35%	-0.38%	-0.40%	-0.43%

Figure 4.152 Eigenvalue curves, CSCF plate, $\phi = 3 / 1$,

$P_\xi = - N_x b^2 / D$, $\lambda^2 = \omega a^2 (\rho / D)^{1/2}$.

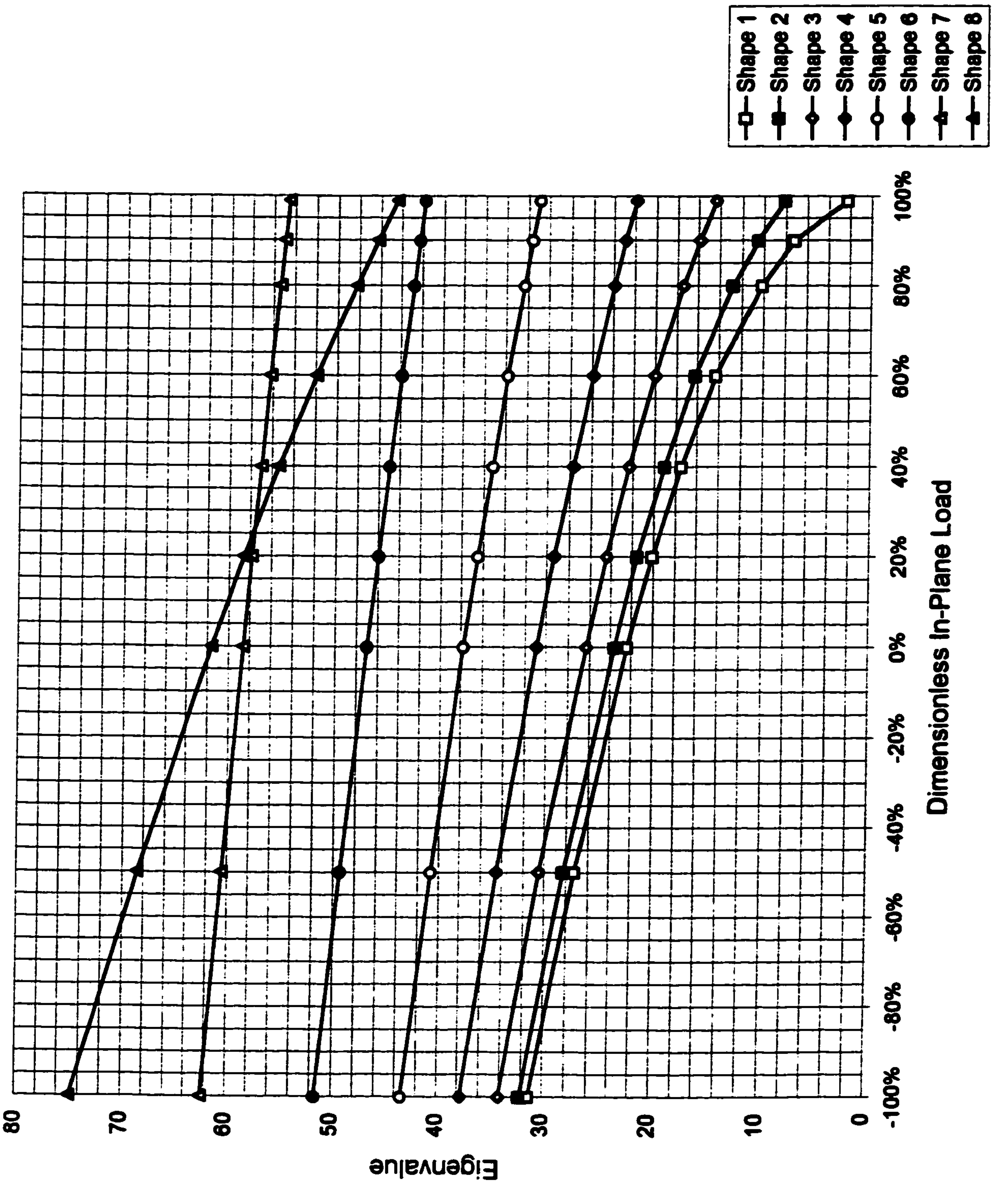

Figure 4.153 Mode shapes, CSCF plate, $\phi = 3 / 1$.

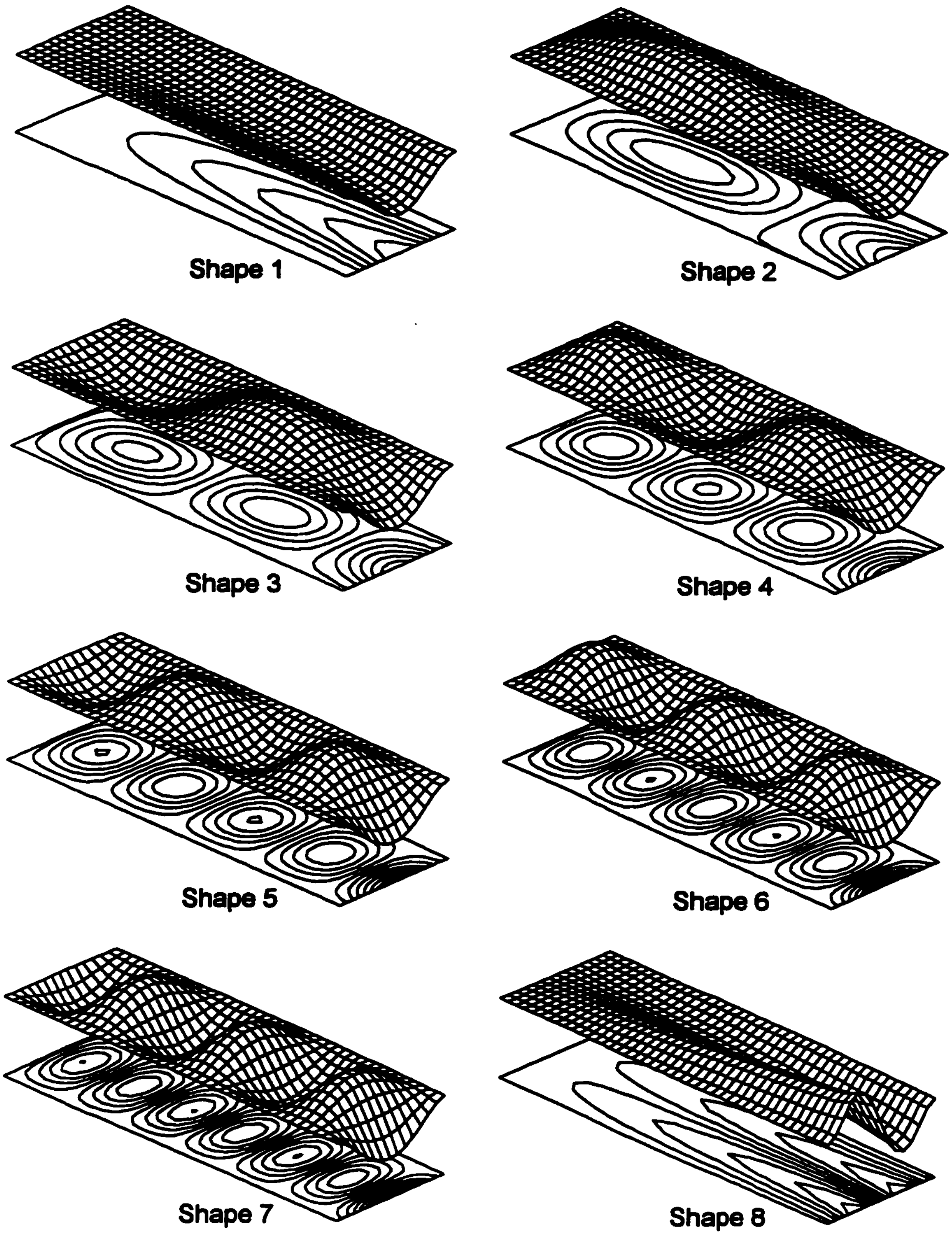

Table 4.83 Eigenvalues, CCCF plate, $\phi = 1 / 3$, $\lambda^2 = \omega a^2 (\rho / D)^{1/2}$.

Mode	In-plane load as a percentage of buckling load								
	-100%	-50%	0%	20%	40%	60%	80%	90%	99%
					Present solution				
1	61.27	54.14	45.65	41.65	37.07	31.57	24.24	18.99	8.54
2	115.81	100.89	83.02	74.54	64.85	53.24	37.89	26.90	11.53
3	184.79	164.34	140.76	130.08	118.40	105.41	90.61	82.28	74.09
4	215.88	214.06	212.21	206.54	193.98	180.54	166.01	158.26	150.94
5	263.76	245.38	218.37	211.47	210.72	209.96	209.20	208.82	208.47
6	269.72	257.87	251.72	249.21	246.67	244.10	241.50	240.18	238.99
7	334.48	323.89	312.77	303.19	290.21	276.57	262.21	254.72	247.80
8	371.92	345.04	315.95	308.52	303.88	299.20	294.45	292.04	289.85
					Finite element solution [18]				
1	61.29	54.15	45.65	41.63	37.05	31.54	24.19	18.93	8.54
2	115.91	100.96	83.07	74.59	64.88	53.26	37.90	26.90	11.45
3	185.08	164.62	141.03	130.36	118.68	105.70	90.92	82.61	74.45
4	215.57	213.75	211.89	207.35	194.82	181.41	166.93	159.21	151.93
5	263.21	246.15	219.16	211.15	210.39	209.63	208.87	208.49	208.14
6	270.45	257.28	251.10	248.58	246.04	243.44	240.83	239.51	238.31
7	333.46	322.82	311.72	304.91	292.08	278.50	264.22	256.78	249.89
8	373.57	346.74	317.65	307.45	302.69	297.98	293.19	290.77	288.57
					Percent difference				
1	0.04%	0.02%	-0.01%	-0.03%	-0.05%	-0.10%	-0.19%	-0.31%	-0.01%
2	0.08%	0.07%	0.07%	0.06%	0.06%	0.05%	0.04%	0.03%	-0.76%
3	0.16%	0.17%	0.19%	0.21%	0.23%	0.27%	0.34%	0.40%	0.48%
4	-0.14%	-0.14%	-0.15%	0.39%	0.44%	0.48%	0.55%	0.60%	0.65%
5	-0.21%	0.31%	0.36%	-0.15%	-0.16%	-0.16%	-0.16%	-0.16%	-0.16%
6	0.27%	-0.23%	-0.25%	-0.25%	-0.26%	-0.27%	-0.27%	-0.28%	-0.28%
7	-0.30%	-0.33%	-0.34%	0.57%	0.64%	0.70%	0.77%	0.81%	0.84%
8	0.44%	0.49%	0.54%	-0.35%	-0.39%	-0.41%	-0.43%	-0.43%	-0.44%

Figure 4.154 Eigenvalue curves, CCCF plate, $\phi = 1 / 3$, $P_\xi = - N_x b^2 / D$, $\lambda^2 = \omega a^2 (\rho / D)^{1/2}$.

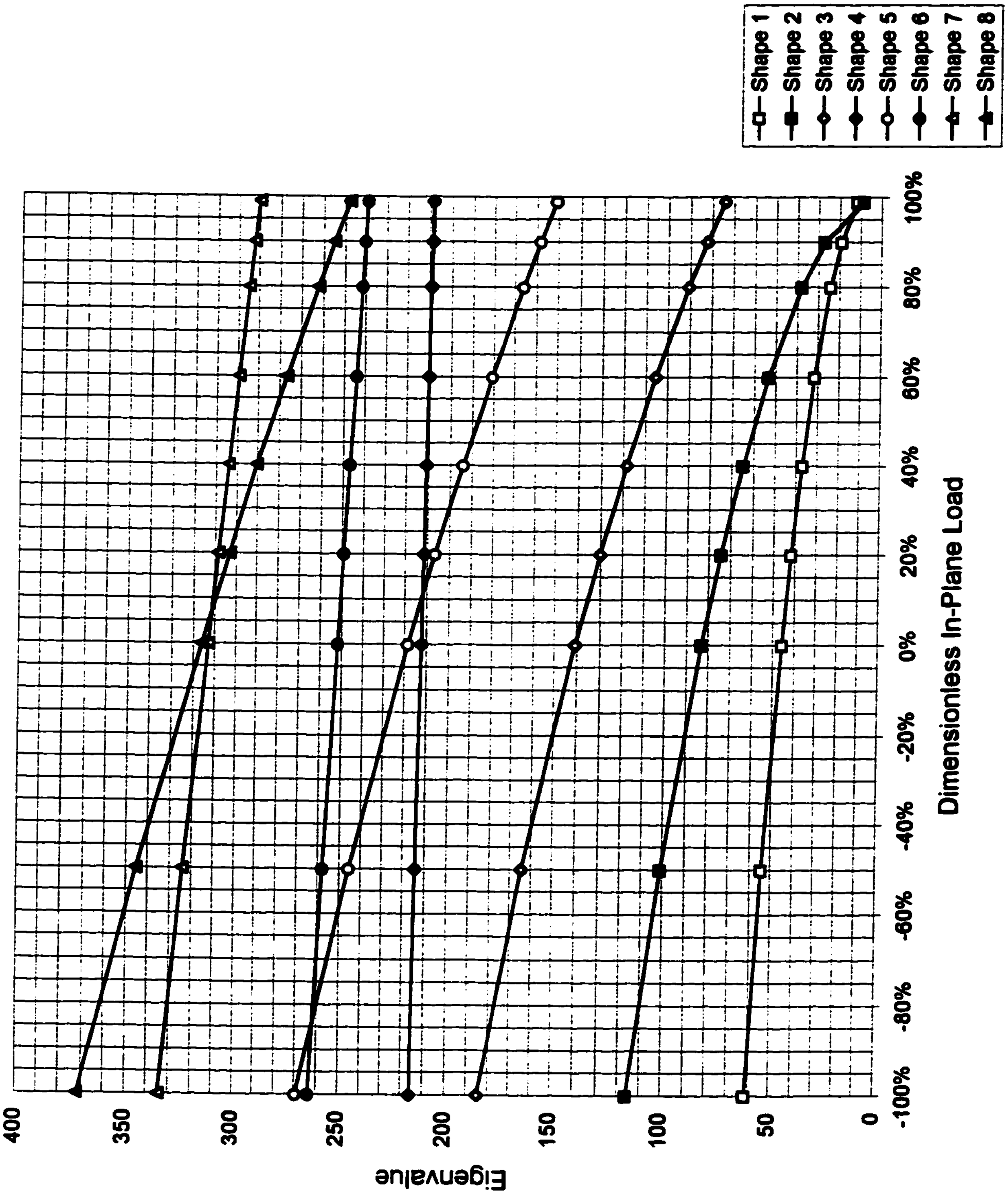

Figure 4.155 Mode shapes, CCCF plate, $\phi = 1 / 3$.

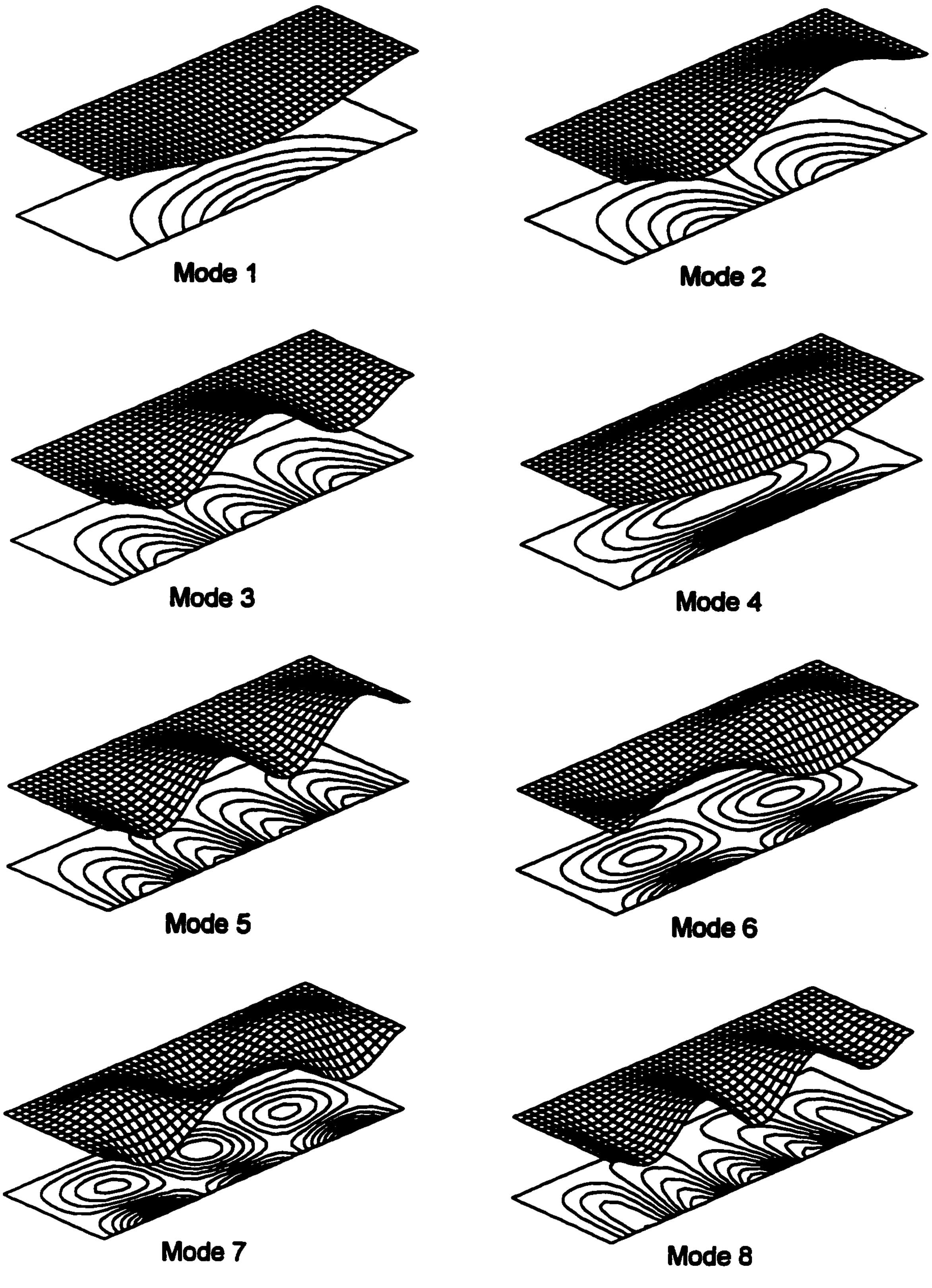

Table 4.84 Eigenvalues, CCCF plate, $\phi = 2 / 5$, $\lambda^2 = \omega a^2 (\rho / D)^{1/2}$.

Mode	In-plane load as a percentage of buckling load								
	-100%	-50%	0%	20%	40%	60%	80%	90%	99%
	Present solution								
1	51.16	44.82	37.21	33.57	29.40	24.34	17.53	12.54	4.01
2	102.35	90.00	75.44	68.67	61.08	52.31	41.57	34.91	27.50
3	155.81	151.95	133.65	125.52	116.81	107.37	97.03	91.42	86.09
4	168.34	154.05	152.08	151.31	150.53	149.75	148.96	148.56	148.20
5	203.56	197.85	191.93	189.50	186.99	183.38	173.52	168.18	163.22
6	251.07	232.22	211.65	202.83	193.63	185.03	182.10	180.80	179.62
7	272.31	262.76	252.81	248.71	244.53	240.27	235.93	233.73	231.72
8	351.85	331.28	309.32	300.08	290.55	280.69	270.46	265.21	260.39
	Finite element solution [18]								
1	51.17	44.83	37.21	33.58	29.40	24.33	17.52	12.53	4.02
2	102.43	90.08	75.52	68.74	61.16	52.39	41.67	35.03	27.65
3	155.61	152.22	133.95	125.83	117.13	107.72	97.39	91.81	86.49
4	168.62	153.86	151.87	151.10	150.32	149.54	148.75	148.35	147.99
5	203.19	197.46	191.53	189.09	186.59	183.67	174.44	169.13	164.20
6	251.81	232.98	212.46	203.65	194.47	185.21	181.67	180.35	179.17
7	271.66	262.07	252.08	247.96	243.76	239.49	235.12	232.91	230.89
8	353.47	332.96	311.08	301.88	292.39	282.57	272.41	267.18	262.39
	Percent difference								
1	0.03%	0.02%	0.01%	0.01%	0.00%	-0.01%	-0.03%	-0.03%	0.05%
2	0.08%	0.09%	0.10%	0.11%	0.13%	0.16%	0.24%	0.34%	0.54%
3	-0.13%	0.18%	0.22%	0.25%	0.27%	0.32%	0.38%	0.43%	0.47%
4	0.16%	-0.12%	-0.14%	-0.14%	-0.14%	-0.14%	-0.14%	-0.14%	-0.15%
5	-0.18%	-0.20%	-0.21%	-0.22%	-0.22%	0.15%	0.53%	0.57%	0.60%
6	0.29%	0.33%	0.38%	0.41%	0.43%	0.10%	-0.24%	-0.25%	-0.25%
7	-0.24%	-0.26%	-0.29%	-0.30%	-0.32%	-0.33%	-0.34%	-0.35%	-0.36%
8	0.46%	0.51%	0.57%	0.60%	0.63%	0.67%	0.72%	0.74%	0.77%

Figure 4.156 Eigenvalue curves, CCCF plate, $\phi = 2 / 5$,

$P_\xi = -N_x b^2 / D$, $\lambda^2 = \omega a^2 (\rho / D)^{1/2}$.

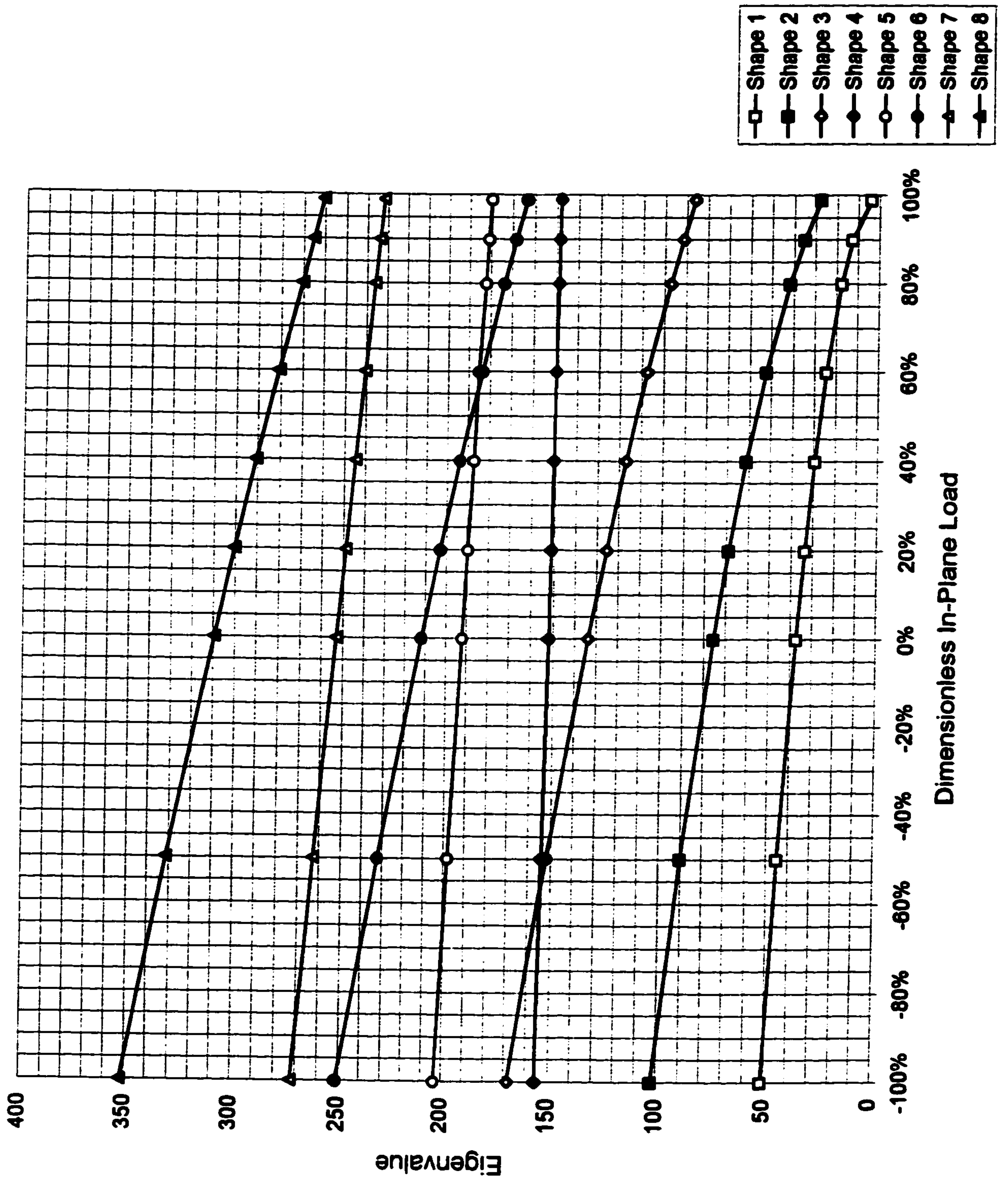

Figure 4.157 Mode shapes, CCCF plate, $\phi = 2 / 5$.

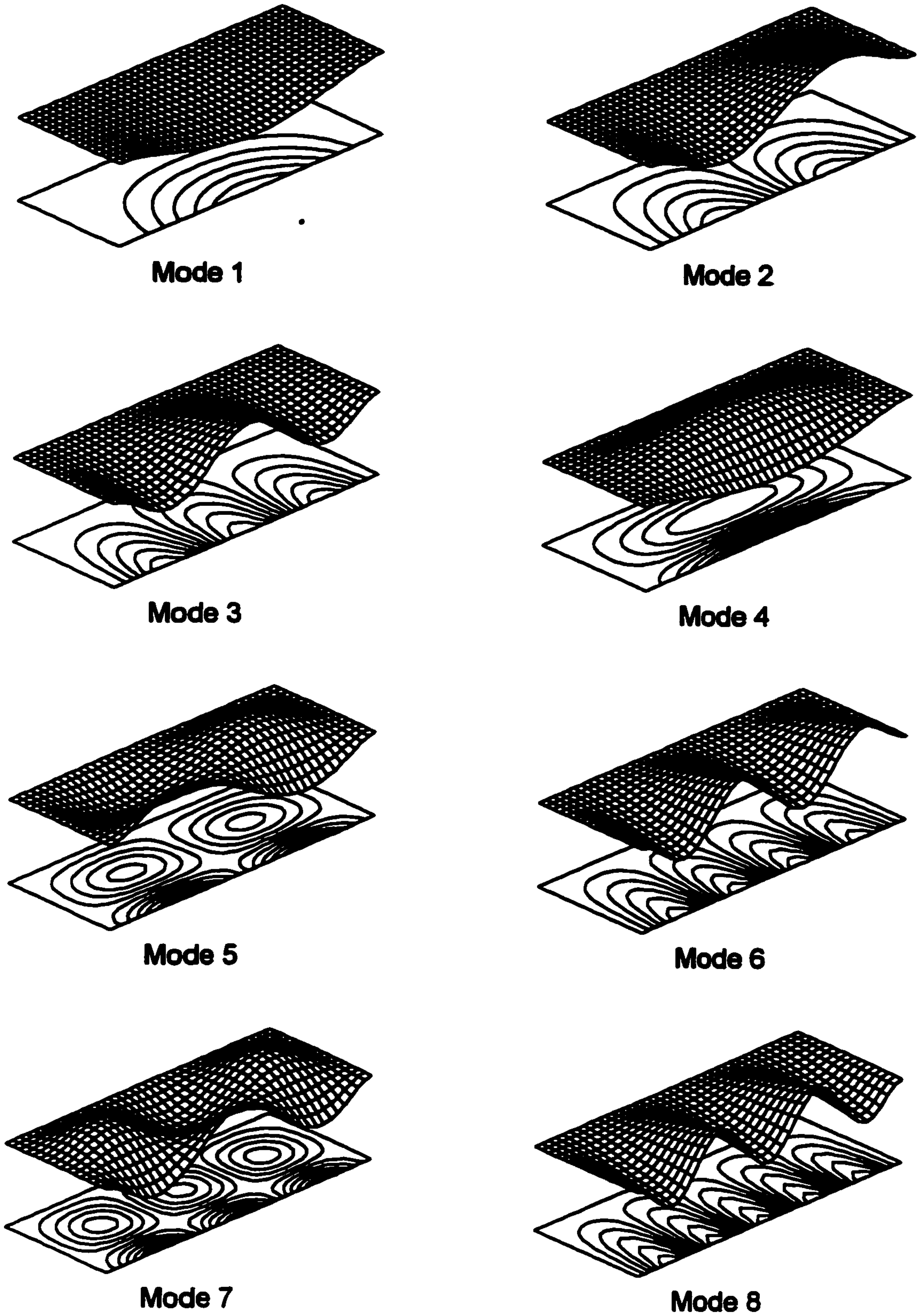

Table 4.85 Eigenvalues, CCCF plate, $\phi = 1 / 2$, $\lambda^2 = \omega a^2 (\rho / D)^{1/2}$.

Mode	In-plane load as a percentage of buckling load								
	-100%	-50%	0%	20%	40%	60%	80%	90%	99%
	Present solution								
1	42.72	37.32	30.82	27.72	24.17	19.89	14.20	10.09	3.21
2	90.69	80.93	69.68	64.58	59.01	52.80	45.70	41.67	37.65
3	107.06	105.13	103.14	102.33	101.50	100.66	99.73	98.54	95.44
4	154.23	141.86	128.25	122.36	116.18	109.65	102.77	99.87	99.16
5	154.34	148.99	143.41	141.11	138.76	136.36	133.92	132.68	131.55
6	220.81	212.49	203.80	200.17	193.67	186.94	179.96	176.37	173.07
7	235.38	221.40	206.47	200.21	196.55	192.82	189.01	187.07	185.31
8	261.03	260.26	259.50	259.19	258.88	258.57	258.26	258.10	257.96
	Finite element solution [18]								
1	42.74	37.33	30.83	27.73	24.18	19.89	14.20	10.10	3.21
2	90.78	81.01	69.76	64.66	59.09	52.89	45.80	41.77	37.76
3	106.96	105.02	103.02	102.21	101.39	100.54	99.63	98.70	95.78
4	154.15	142.14	128.54	122.66	116.48	109.96	103.08	99.92	99.05
5	154.50	148.78	143.18	140.87	138.52	136.11	133.66	132.42	131.29
6	220.49	212.14	203.43	199.83	194.45	187.74	180.78	177.20	173.91
7	236.08	222.13	207.22	200.94	196.15	192.40	188.58	186.63	184.86
8	260.46	259.69	258.92	258.61	258.30	257.99	257.68	257.52	257.38
	Percent difference								
1	0.05%	0.04%	0.04%	0.03%	0.03%	0.02%	0.02%	0.01%	0.02%
2	0.10%	0.11%	0.12%	0.13%	0.15%	0.17%	0.22%	0.25%	0.29%
3	-0.10%	-0.10%	-0.11%	-0.11%	-0.12%	-0.12%	-0.10%	0.16%	0.35%
4	-0.05%	0.20%	0.23%	0.24%	0.26%	0.29%	0.30%	0.05%	-0.11%
5	0.10%	-0.14%	-0.16%	-0.17%	-0.17%	-0.18%	-0.19%	-0.19%	-0.20%
6	-0.14%	-0.16%	-0.18%	-0.17%	0.40%	0.43%	0.46%	0.47%	0.49%
7	0.30%	0.33%	0.36%	0.36%	-0.20%	-0.22%	-0.23%	-0.23%	-0.24%
8	-0.22%	-0.22%	-0.22%	-0.22%	-0.22%	-0.22%	-0.22%	-0.23%	-0.23%

Figure 4.158 Eigenvalue curves, CCCF plate, $\phi = 1 / 2$,
$P_\xi = - N_x b^2 / D$, $\lambda^2 = \omega a^2 (\rho / D)^{1/2}$.

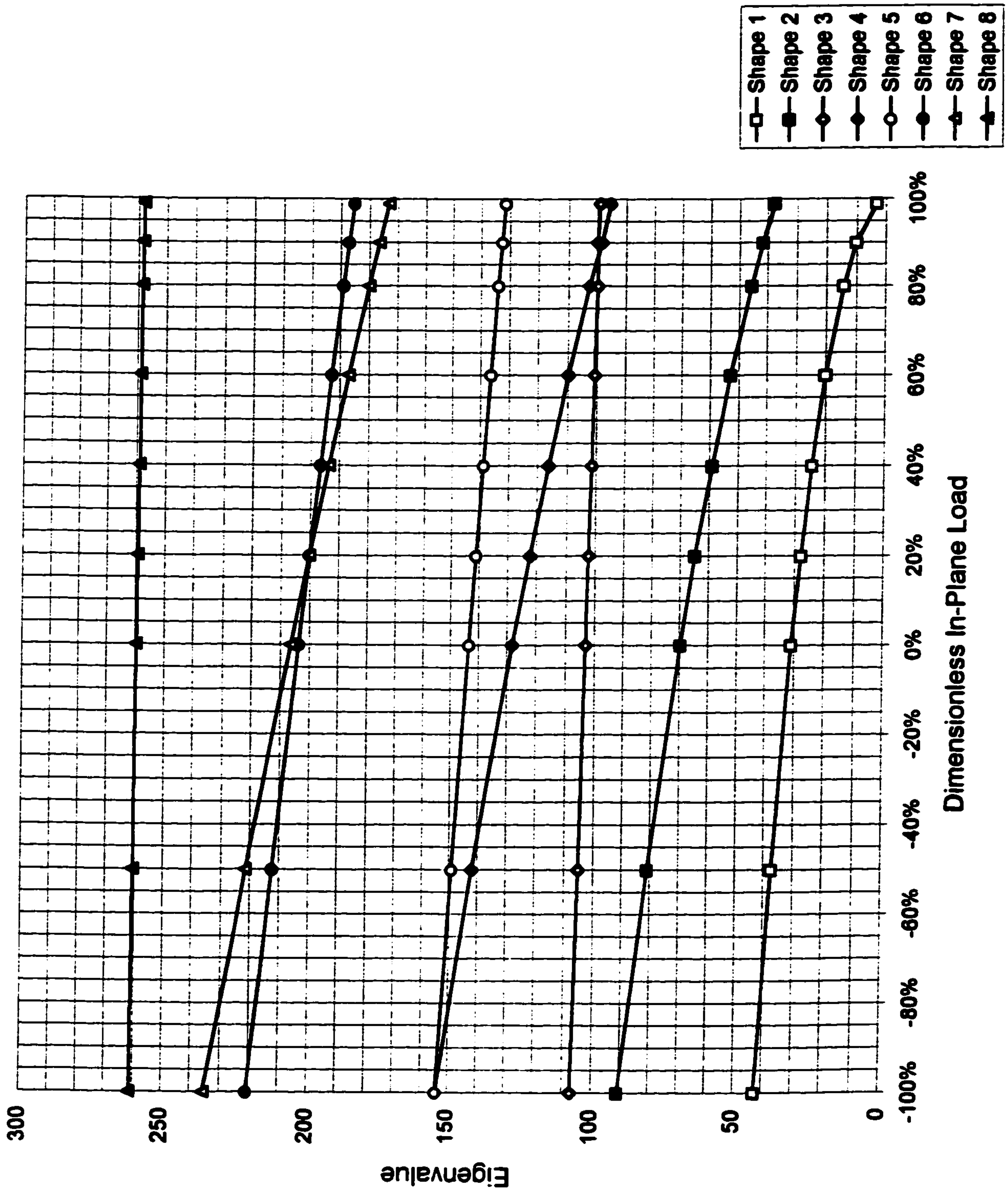

Figure 4.159 Mode shapes, CCCF plate, $\phi = 1 / 2$.

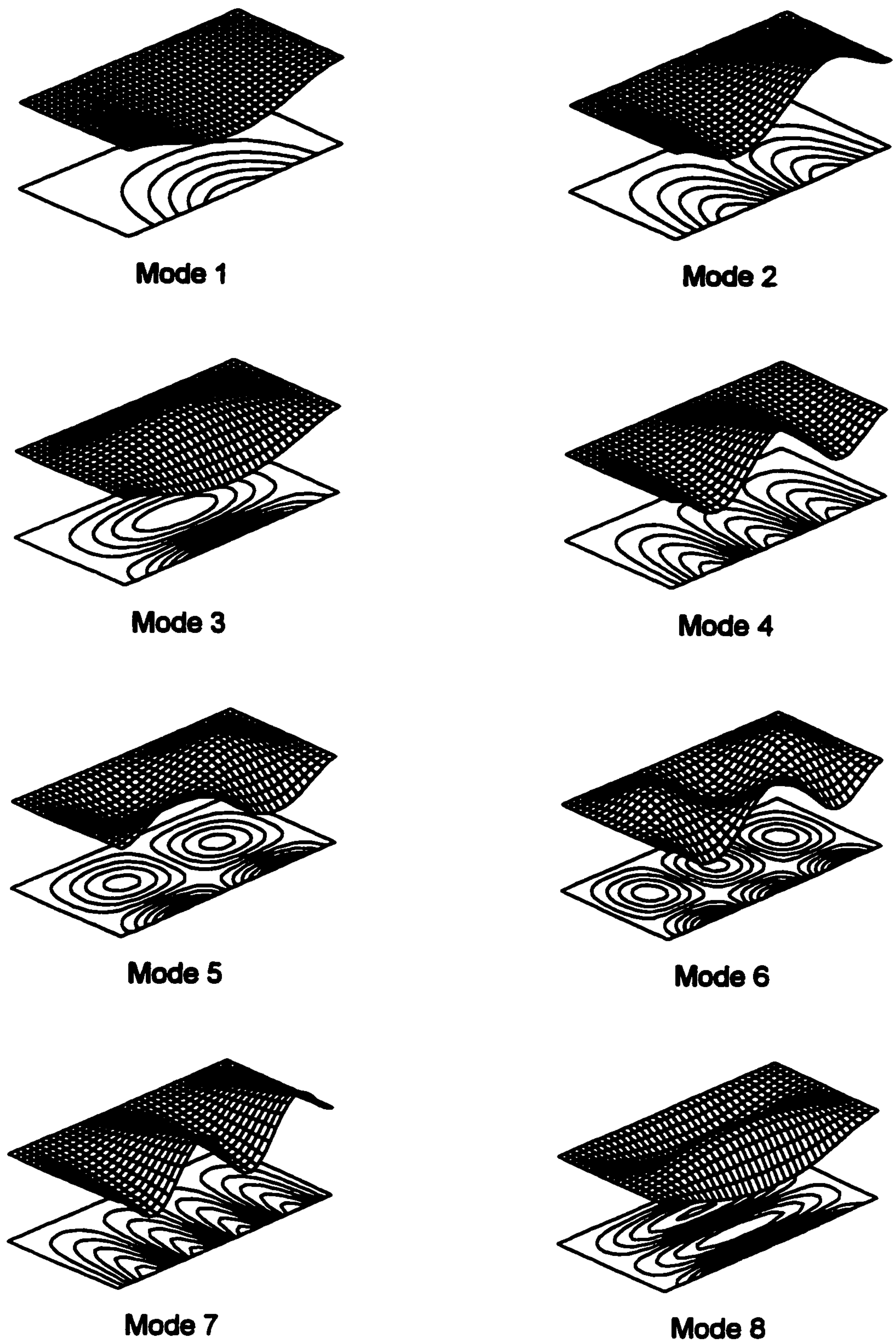

Table 4.86 Eigenvalues, CCCF plate, $\phi = 2/3$, $\lambda^2 = \omega a^2 (\rho / D)^{1/2}$.

Mode	In-plane load as a percentage of buckling load								
	-100%	-50%	0%	20%	40%	60%	80%	90%	99%
	Present solution								
1	36.79	32.09	26.43	23.74	20.66	16.96	12.06	8.56	2.72
2	70.22	67.97	65.60	61.61	57.32	52.66	47.51	44.70	42.01
3	82.51	74.57	65.63	64.66	63.67	62.66	61.63	61.11	60.63
4	117.10	111.77	106.15	103.81	101.40	98.94	96.39	95.10	93.91
5	144.59	134.87	124.37	119.91	115.27	110.43	105.36	102.73	100.31
6	154.20	153.22	152.22	151.81	151.39	150.95	150.39	149.83	148.72
7	181.59	174.03	166.12	162.84	159.51	156.11	152.75	151.33	150.63
8	196.73	193.68	190.57	189.31	188.03	186.73	183.15	180.56	178.19
	Finite element solution [18]								
1	36.81	32.11	26.45	23.75	20.67	16.96	12.07	8.56	2.72
2	70.18	67.93	65.58	61.68	57.39	52.73	47.59	44.78	42.08
3	82.59	74.65	65.67	64.61	63.62	62.61	61.57	61.05	60.57
4	117.03	111.70	106.06	103.71	101.31	98.83	96.28	94.98	93.79
5	144.81	135.10	124.60	120.14	115.50	110.66	105.60	102.98	100.56
6	153.97	152.98	151.98	151.57	151.16	150.72	150.17	149.63	148.55
7	181.50	173.93	166.00	162.71	159.37	155.96	152.58	151.13	150.39
8	196.33	193.27	190.15	188.88	187.61	186.31	183.71	181.14	178.78
	Percent difference								
1	0.06%	0.05%	0.05%	0.05%	0.05%	0.05%	0.04%	0.04%	-0.01%
2	-0.06%	-0.06%	-0.02%	0.11%	0.13%	0.14%	0.16%	0.17%	0.19%
3	0.10%	0.10%	0.06%	-0.08%	-0.08%	-0.08%	-0.09%	-0.09%	-0.10%
4	-0.06%	-0.07%	-0.08%	-0.09%	-0.10%	-0.11%	-0.12%	-0.12%	-0.13%
5	0.15%	0.17%	0.18%	0.19%	0.20%	0.21%	0.23%	0.24%	0.25%
6	-0.15%	-0.15%	-0.15%	-0.16%	-0.16%	-0.16%	-0.15%	-0.13%	-0.11%
7	-0.05%	-0.06%	-0.07%	-0.08%	-0.09%	-0.10%	-0.11%	-0.13%	-0.16%
8	-0.20%	-0.21%	-0.22%	-0.22%	-0.23%	-0.23%	0.31%	0.32%	0.33%

Figure 4.160 Eigenvalue curves, CCCF plate, $\phi = 2 / 3$,

$P_\xi = - N_x b^2 / D$, $\lambda^2 = \omega a^2 (\rho / D)^{1/2}$.

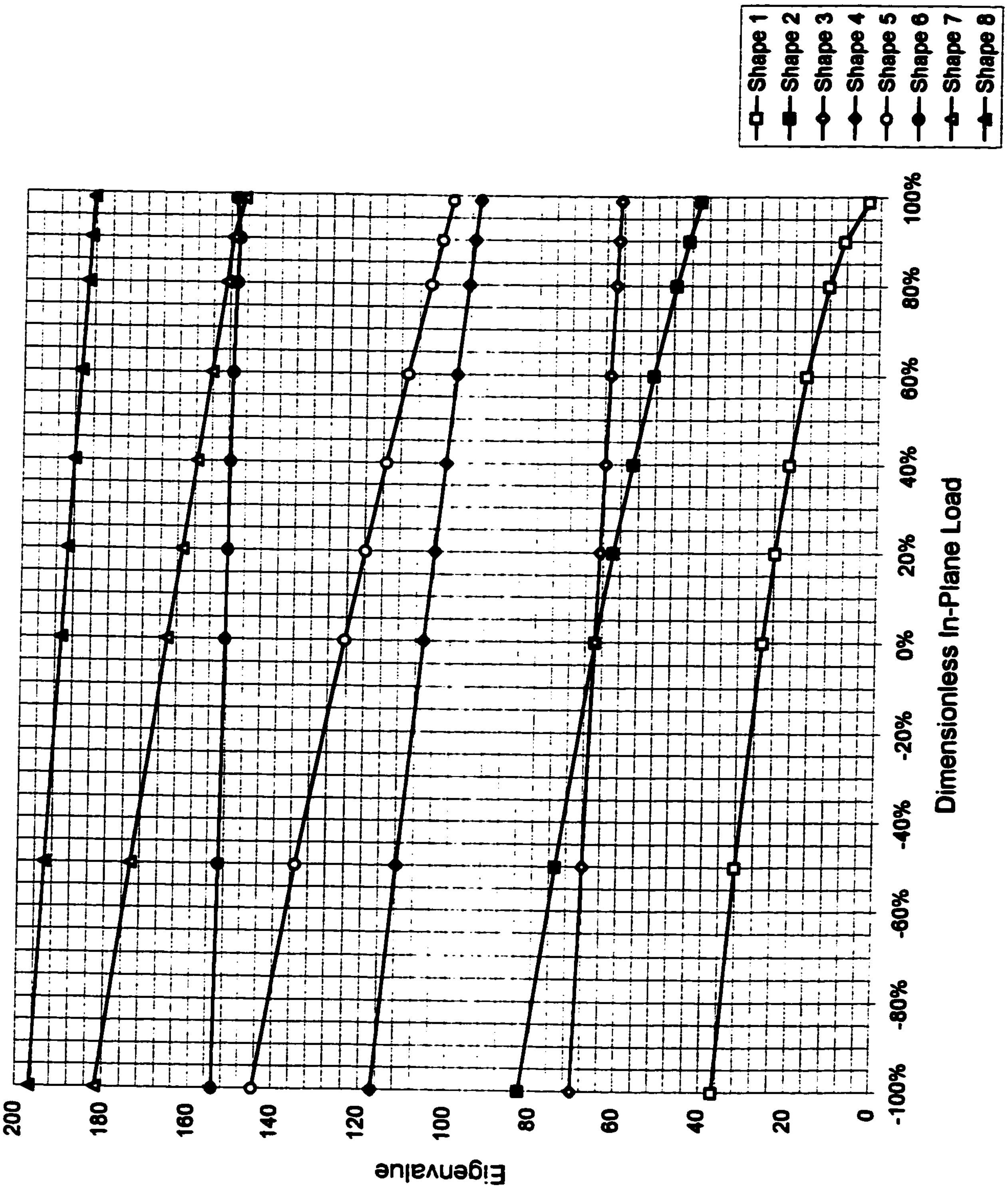

Figure 4.161 Mode shapes, CCCF plate, $\phi = 2 / 3$.

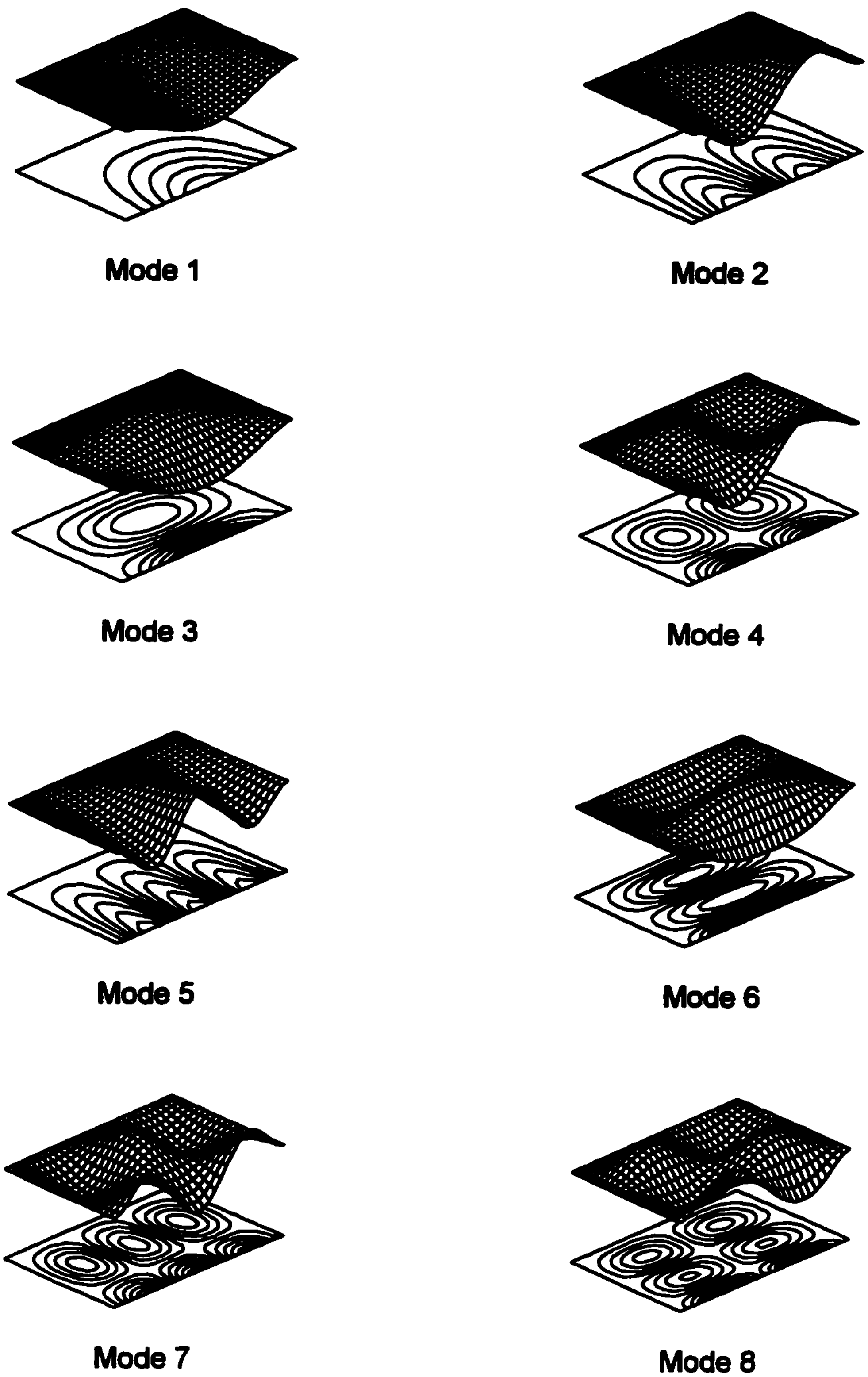

Table 4.87 Eigenvalues, CCCF plate, $\phi = 1 / 1$, $\lambda^2 = \omega a^2 (\rho / D)^{1/2}$.

Mode	In-plane load as a percentage of buckling load								
	-100%	-50%	0%	20%	40%	60%	80%	90%	99%
				Present solution					
1	33.22	28.95	23.81	21.37	18.58	15.23	10.82	7.67	2.43
2	45.90	42.99	39.83	38.48	37.07	35.59	34.03	33.22	32.47
3	77.54	70.69	63.02	59.66	56.08	52.24	48.08	45.84	43.73
4	79.79	78.20	76.56	75.90	75.06	72.29	69.39	67.90	66.52
5	91.98	86.35	80.29	77.72	75.22	74.54	73.84	73.49	73.18
6	124.52	120.49	116.31	114.59	112.84	110.50	106.41	104.31	102.38
7	136.13	130.69	121.94	118.25	114.44	111.06	109.24	108.32	107.49
8	138.87	135.23	134.31	133.94	133.42	130.09	126.65	124.89	123.29
				Finite element solution [18]					
1	33.23	28.96	23.82	21.38	18.59	15.24	10.83	7.68	2.43
2	45.89	42.98	39.82	38.46	37.05	35.57	34.02	33.20	32.45
3	77.57	70.71	63.05	59.68	56.11	52.26	48.10	45.86	43.75
4	79.73	78.13	76.50	75.83	75.02	72.24	69.35	67.85	66.47
5	91.96	86.32	80.26	77.69	75.15	74.47	73.78	73.43	73.11
6	124.37	120.34	116.15	114.42	112.68	110.55	106.46	104.36	102.43
7	135.97	130.73	121.99	118.30	114.49	110.88	109.07	108.15	107.31
8	138.92	135.06	134.16	133.78	133.29	129.99	126.55	124.79	123.18
				Percent difference					
1	0.03%	0.03%	0.04%	0.04%	0.04%	0.04%	0.04%	0.04%	0.06%
2	-0.01%	-0.02%	-0.03%	-0.03%	-0.04%	-0.05%	-0.05%	-0.06%	-0.06%
3	0.03%	0.04%	0.04%	0.04%	0.04%	0.04%	0.04%	0.05%	0.05%
4	-0.07%	-0.08%	-0.08%	-0.08%	-0.05%	-0.06%	-0.07%	-0.07%	-0.08%
5	-0.03%	-0.03%	-0.04%	-0.05%	-0.09%	-0.09%	-0.09%	-0.09%	-0.09%
6	-0.12%	-0.13%	-0.14%	-0.14%	-0.15%	0.05%	0.05%	0.05%	0.05%
7	-0.12%	0.04%	0.04%	0.04%	0.04%	-0.16%	-0.16%	-0.16%	-0.17%
8	0.03%	-0.12%	-0.12%	-0.12%	-0.09%	-0.08%	-0.08%	-0.08%	-0.08%

Figure 4.162 Eigenvalue curves, CCCF plate, $\phi = 1 / 1$,

$P_\xi = - N_x b^2 / D$, $\lambda^2 = \omega a^2 (\rho / D)^{1/2}$.

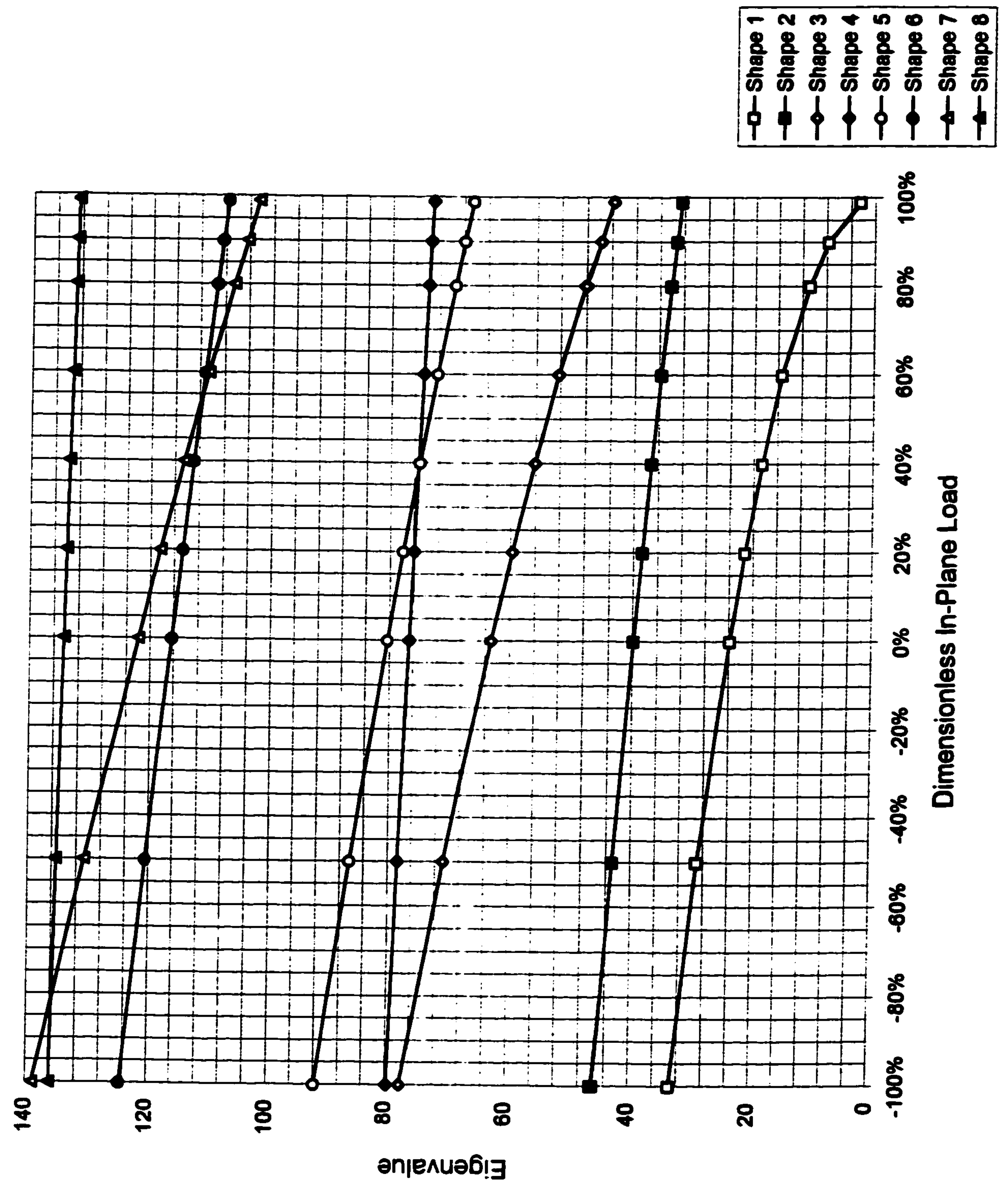

Figure 4.163 Mode shapes, CCCF plate, ϕ = 1 / 1.

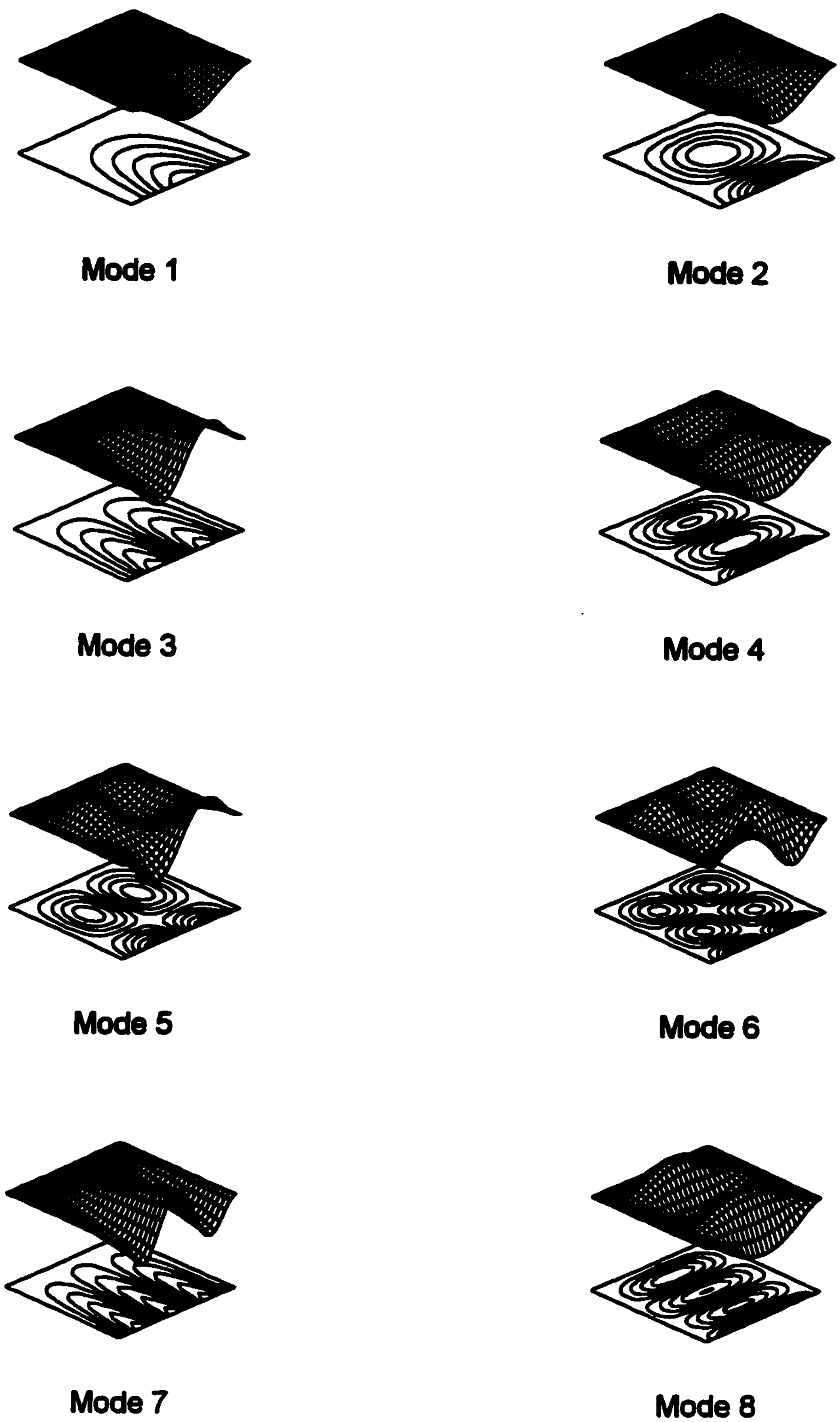

Table 4.88 Eigenvalues, CCCF plate, $\phi = 3 / 2$, $\lambda^2 = \omega a^2 (\rho / D)^{1/2}$.

Mode	In-plane load as a percentage of buckling load								
	-100%	-50%	0%	20%	40%	60%	80%	90%	99%
	Present solution								
1	31.92	27.81	22.86	20.52	17.83	14.62	10.38	7.36	2.33
2	36.68	33.22	29.28	27.53	25.64	23.58	21.29	20.04	18.83
3	49.32	46.85	44.21	43.10	41.96	40.77	39.55	38.91	38.33
4	72.03	69.25	62.05	58.91	55.57	52.01	48.16	46.12	44.19
5	75.72	70.39	68.71	66.63	63.73	60.67	57.44	55.75	54.19
6	81.78	75.87	69.41	68.02	67.32	66.61	65.89	65.53	65.20
7	94.92	89.93	84.62	82.39	80.09	77.71	75.26	73.99	72.84
8	104.85	103.76	102.64	102.19	101.74	101.28	100.82	100.50	99.67
	Finite element solution [18]								
1	31.91	27.80	22.86	20.52	17.83	14.61	10.38	7.36	2.33
2	36.67	33.21	29.27	27.52	25.63	23.56	21.28	20.02	18.82
3	49.28	46.81	44.18	43.07	41.92	40.74	39.51	38.88	38.30
4	71.96	69.20	62.01	58.86	55.53	51.96	48.12	46.07	44.14
5	75.67	70.33	68.64	66.55	63.65	60.59	57.36	55.67	54.10
6	81.70	75.79	69.33	67.95	67.26	66.55	65.83	65.46	65.13
7	94.78	89.79	84.47	82.23	79.93	77.56	75.10	73.83	72.68
8	104.77	103.68	102.56	102.11	101.66	101.21	100.74	100.20	99.36
	Percent difference								
1	-0.02%	-0.02%	-0.01%	-0.01%	-0.01%	0.00%	0.00%	0.00%	0.01%
2	-0.04%	-0.03%	-0.04%	-0.04%	-0.04%	-0.05%	-0.05%	-0.06%	-0.07%
3	-0.07%	-0.08%	-0.08%	-0.08%	-0.09%	-0.09%	-0.10%	-0.10%	-0.10%
4	-0.09%	-0.07%	-0.07%	-0.08%	-0.08%	-0.09%	-0.10%	-0.10%	-0.11%
5	-0.06%	-0.09%	-0.10%	-0.12%	-0.13%	-0.14%	-0.15%	-0.16%	-0.17%
6	-0.10%	-0.10%	-0.11%	-0.10%	-0.10%	-0.10%	-0.10%	-0.10%	-0.10%
7	-0.15%	-0.16%	-0.18%	-0.18%	-0.19%	-0.20%	-0.21%	-0.22%	-0.22%
8	-0.07%	-0.08%	-0.08%	-0.08%	-0.08%	-0.08%	-0.08%	-0.30%	-0.30%

Figure 4.164 Eigenvalue curves, CCCF plate, $\phi = 3 / 2$,
$P_\xi = - N_x b^2 / D$, $\lambda^2 = \omega a^2 (\rho / D)^{1/2}$.

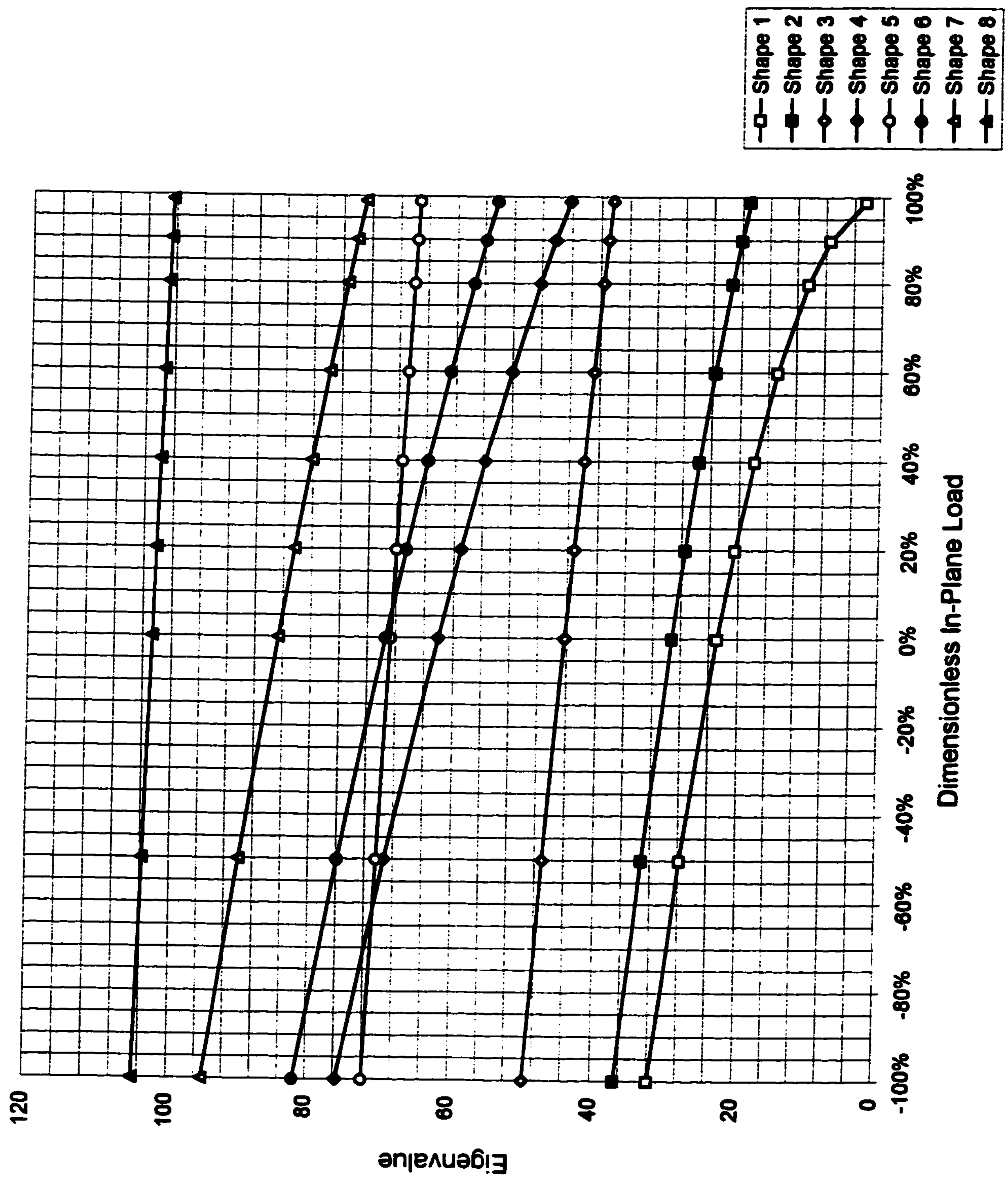

Figure 4.165 Mode shapes, CCCF plate, $\phi = 3 / 2$.

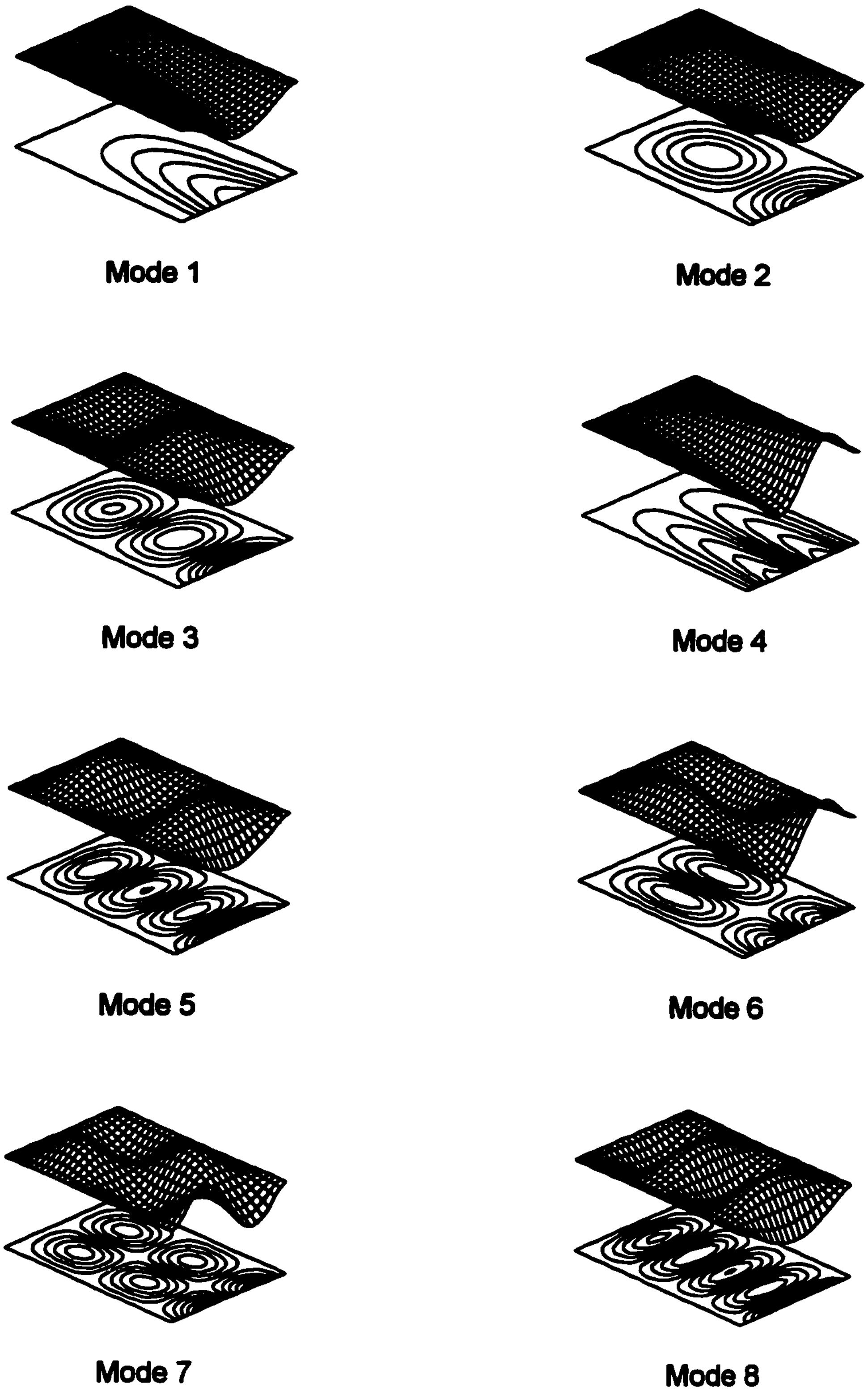

Table 4.89 Eigenvalues, CCCF plate, $\phi = 2 / 1$, $\lambda^2 = \omega a^2 (\rho / D)^{1/2}$.

Mode	In-plane load as a percentage of buckling load								
	-100%	-50%	0%	20%	40%	60%	80%	90%	99%
	Present solution								
1	31.54	27.47	22.59	20.27	17.61	14.43	10.25	7.26	2.30
2	33.97	30.26	25.96	23.99	21.83	19.40	16.58	14.96	13.32
3	40.08	37.04	33.67	32.21	30.67	29.04	27.29	26.36	25.50
4	51.36	49.06	46.62	45.60	44.55	43.47	42.35	41.78	41.26
5	68.42	66.74	61.76	58.68	55.42	51.93	48.18	46.19	44.31
6	75.18	68.83	65.00	62.95	59.93	56.74	53.35	51.56	49.90
7	78.50	72.46	65.82	64.29	63.56	62.83	62.08	61.70	60.50
8	85.46	79.98	74.07	71.55	68.93	66.20	63.35	61.87	61.36
	Finite element solution [18]								
1	31.52	27.46	22.58	20.26	17.60	14.43	10.25	7.26	2.30
2	33.94	30.24	25.94	23.97	21.81	19.38	16.57	14.94	13.30
3	40.04	37.00	33.63	32.17	30.63	29.00	27.24	26.32	25.45
4	51.28	48.98	46.54	45.52	44.47	43.39	42.27	41.70	41.18
5	68.32	66.64	61.68	58.60	55.33	51.85	48.10	46.10	44.22
6	75.08	68.73	64.90	62.82	59.80	56.61	53.21	51.43	49.76
7	78.37	72.33	65.69	64.18	63.46	62.72	61.98	61.60	60.30
8	85.28	79.80	73.88	71.36	68.74	66.01	63.15	61.66	61.25
	Percent difference								
1	-0.06%	-0.05%	-0.04%	-0.04%	-0.04%	-0.03%	-0.03%	-0.03%	-0.04%
2	-0.07%	-0.07%	-0.07%	-0.07%	-0.07%	-0.08%	-0.10%	-0.11%	-0.14%
3	-0.11%	-0.11%	-0.12%	-0.13%	-0.13%	-0.14%	-0.15%	-0.16%	-0.17%
4	-0.15%	-0.15%	-0.16%	-0.17%	-0.17%	-0.18%	-0.19%	-0.19%	-0.19%
5	-0.15%	-0.15%	-0.14%	-0.15%	-0.15%	-0.16%	-0.18%	-0.19%	-0.20%
6	-0.13%	-0.13%	-0.16%	-0.20%	-0.22%	-0.23%	-0.25%	-0.27%	-0.28%
7	-0.17%	-0.18%	-0.19%	-0.16%	-0.16%	-0.17%	-0.17%	-0.17%	-0.34%
8	-0.22%	-0.23%	-0.25%	-0.27%	-0.28%	-0.30%	-0.31%	-0.33%	-0.17%

Figure 4.166 Eigenvalue curves, CCCF plate, $\phi = 2 / 1$,
$P_{\xi} = - N_x b^2 / D$, $\lambda^2 = \omega a^2 (\rho / D)^{1/2}$.

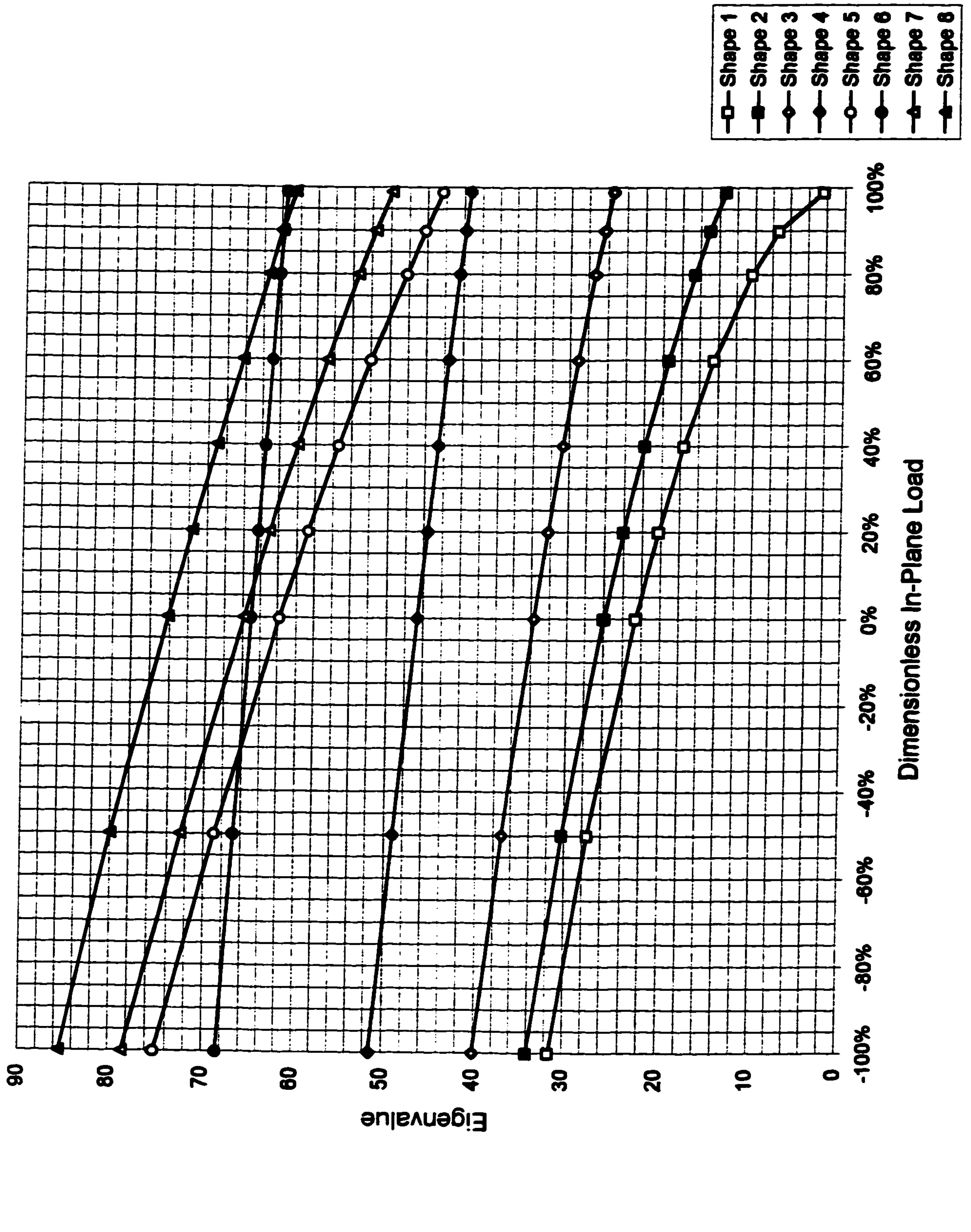

Figure 4.167 Mode shapes, CCCF plate, $\phi = 2 / 1$.

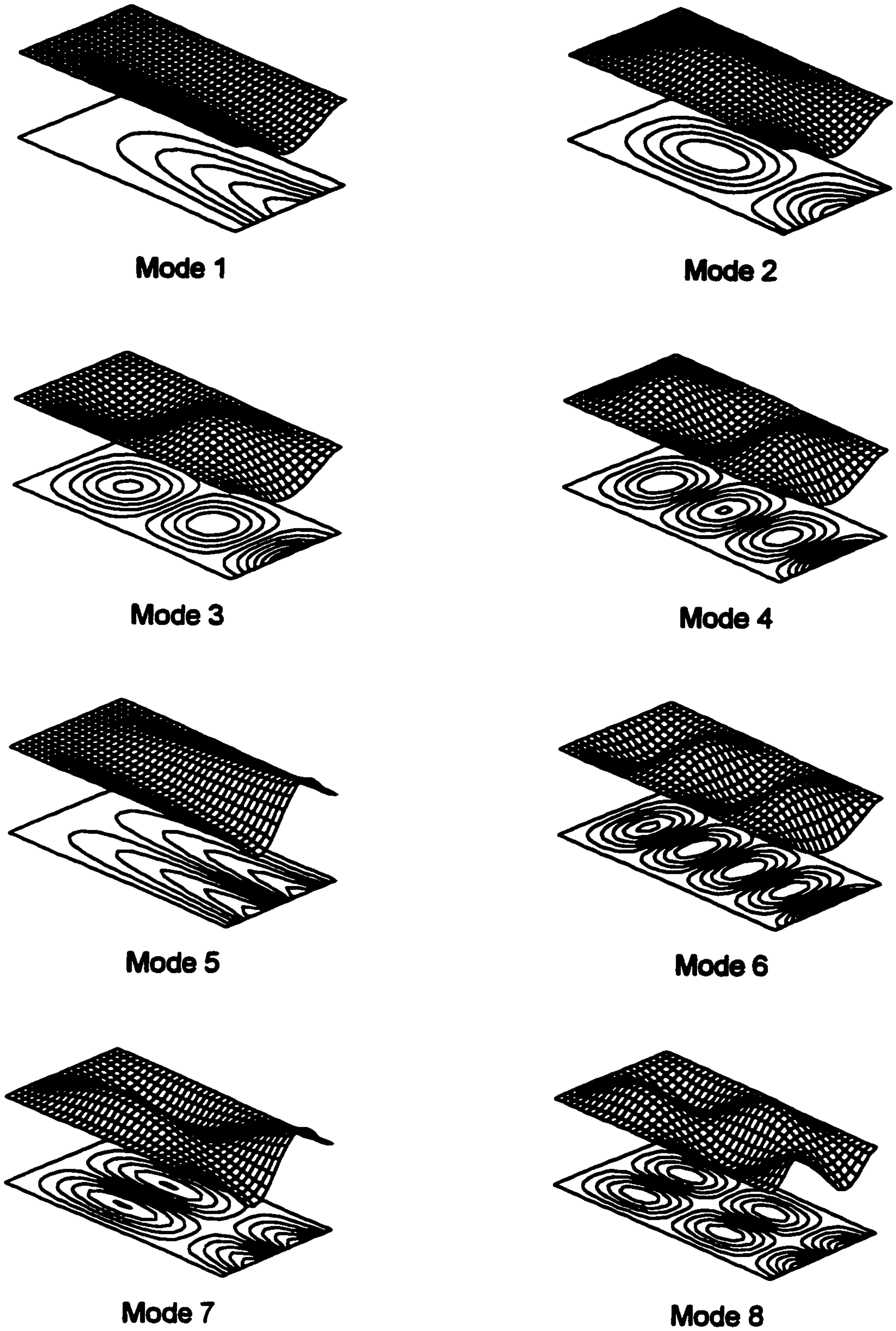

Table 4.90 Eigenvalues, CCCF plate, $\phi = 5 / 2$, $\lambda^2 = \omega a^2 (\rho / D)^{1/2}$.

Mode	In-plane load as a percentage of buckling load								
	-100%	-50%	0%	20%	40%	60%	80%	90%	99%
				Present solution					
1	31.38	27.33	22.47	20.16	17.52	14.36	10.20	7.22	2.29
2	32.85	29.03	24.54	22.46	20.14	17.50	14.32	12.41	10.38
3	36.35	32.97	29.15	27.45	25.62	23.63	21.44	20.24	19.09
4	42.76	39.96	36.91	35.61	34.25	32.82	31.31	30.52	29.79
5	52.69	50.47	48.13	47.16	46.16	45.13	44.07	43.53	43.03
6	66.35	64.62	61.65	58.59	55.36	51.91	48.19	46.22	44.36
7	74.96	68.66	62.84	61.31	58.23	54.97	51.49	49.66	47.94
8	77.07	70.96	64.22	62.11	61.37	60.61	57.86	56.25	54.75
				Finite element solution [18]					
1	31.36	27.31	22.46	20.15	17.51	14.35	10.19	7.22	2.29
2	32.81	29.00	24.51	22.44	20.12	17.47	14.30	12.39	10.35
3	36.30	32.93	29.10	27.40	25.57	23.58	21.39	20.19	19.04
4	42.67	39.87	36.83	35.52	34.16	32.73	31.22	30.43	29.70
5	52.55	50.34	48.00	47.02	46.02	44.99	43.93	43.38	42.89
6	66.19	64.46	61.54	58.49	55.25	51.80	48.09	46.11	44.26
7	74.84	68.54	62.68	61.15	58.07	54.81	51.32	49.48	47.76
8	76.90	70.80	64.06	61.95	61.20	60.45	57.63	56.01	54.51
				Percent difference					
1	-0.08%	-0.07%	-0.06%	-0.05%	-0.05%	-0.05%	-0.04%	-0.04%	-0.02%
2	-0.10%	-0.09%	-0.10%	-0.10%	-0.11%	-0.13%	-0.17%	-0.21%	-0.28%
3	-0.14%	-0.14%	-0.15%	-0.16%	-0.18%	-0.20%	-0.23%	-0.25%	-0.28%
4	-0.20%	-0.21%	-0.23%	-0.24%	-0.26%	-0.27%	-0.30%	-0.31%	-0.32%
5	-0.25%	-0.26%	-0.28%	-0.29%	-0.29%	-0.30%	-0.32%	-0.32%	-0.33%
6	-0.24%	-0.25%	-0.17%	-0.18%	-0.19%	-0.20%	-0.22%	-0.23%	-0.24%
7	-0.16%	-0.16%	-0.26%	-0.26%	-0.28%	-0.30%	-0.33%	-0.35%	-0.37%
8	-0.21%	-0.23%	-0.25%	-0.26%	-0.27%	-0.27%	-0.40%	-0.42%	-0.44%

Figure 4.168 Eigenvalue curves, CCCF plate, $\phi = 5 / 2$,

$P_\xi = - N_x b^2 / D$, $\lambda^2 = \omega a^2 (\rho / D)^{1/2}$.

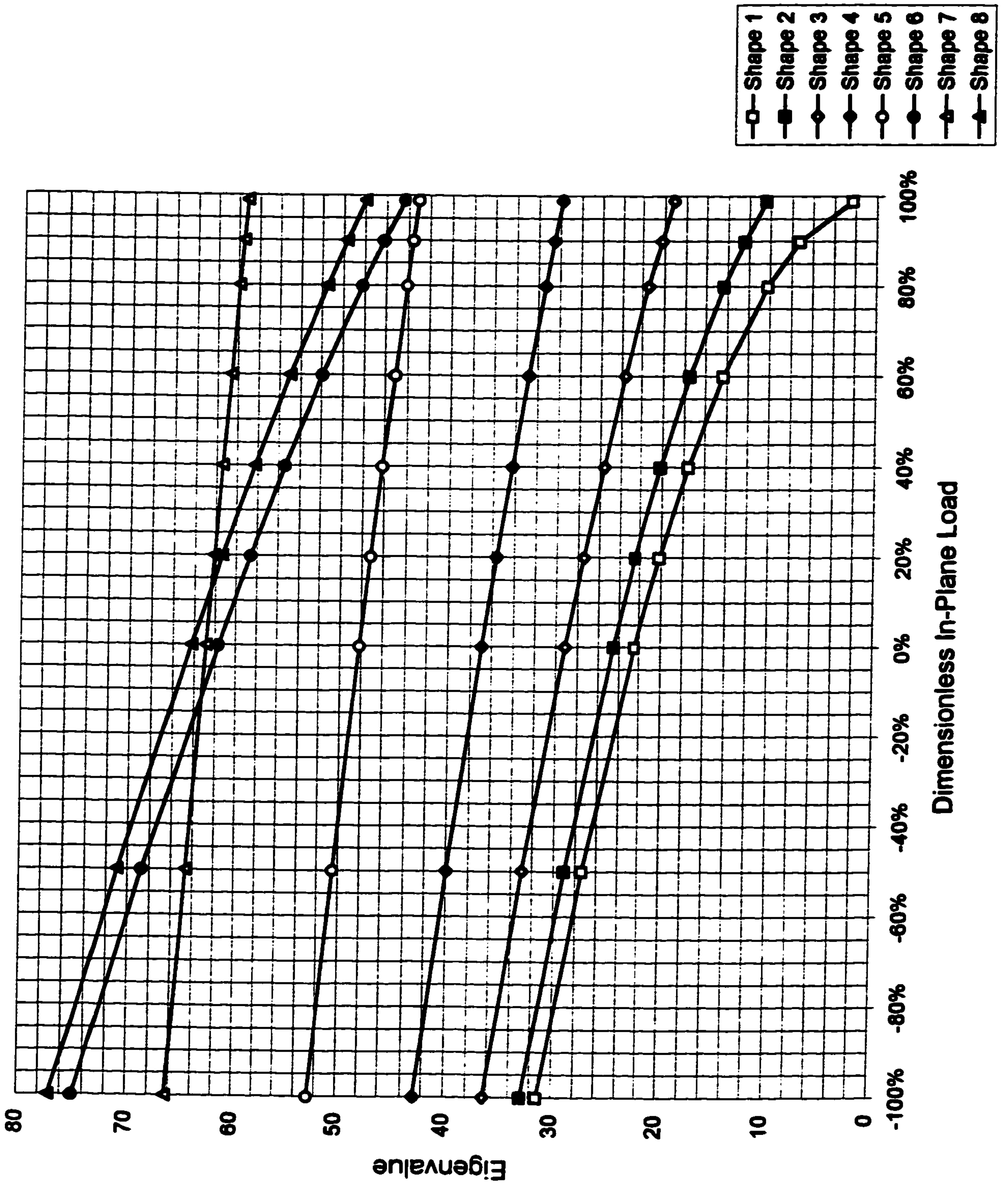

Figure 4.169 Mode shapes, CCCF plate, $\phi = 5 / 2$.

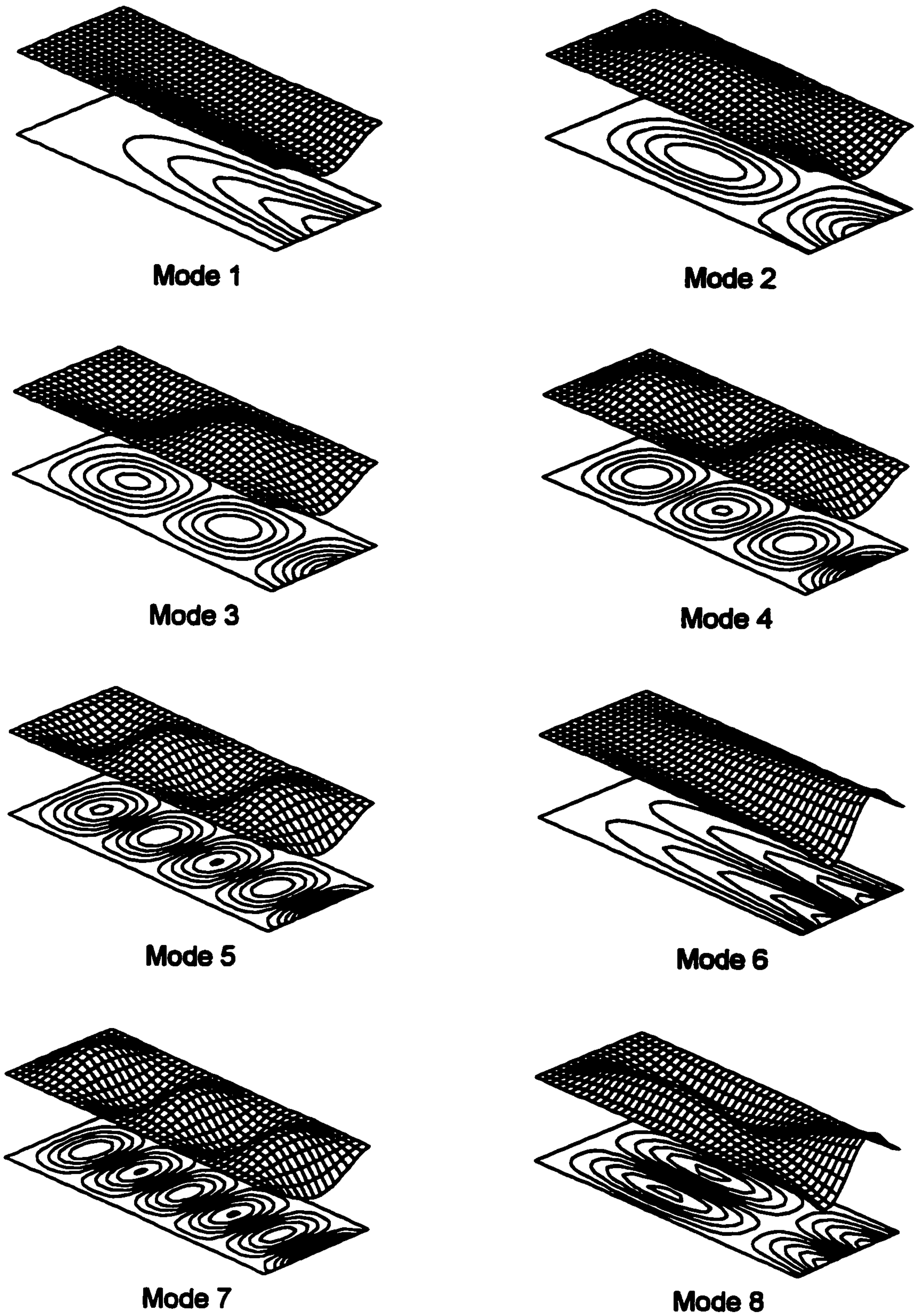

Table 4.91 Eigenvalues, CCCF plate, $\phi = 3 / 1$, $\lambda^2 = \omega a^2 (\rho / D)^{1/2}$.

Mode	In-plane load as a percentage of buckling load								
	-100%	-50%	0%	20%	40%	60%	80%	90%	99%
					Present solution				
1	31.30	27.27	22.42	20.11	17.48	14.32	10.17	7.21	2.28
2	32.28	28.40	23.81	21.67	19.27	16.48	13.07	10.94	8.58
3	34.53	30.96	26.85	24.99	22.96	20.71	18.16	16.72	15.30
4	38.56	35.42	31.93	30.41	28.79	27.06	25.20	24.20	23.26
5	44.82	42.19	39.34	38.13	36.87	35.56	34.19	33.48	32.82
6	53.61	51.45	49.17	48.22	47.25	46.25	45.23	44.70	44.22
7	65.00	63.25	61.43	58.55	55.33	51.90	48.20	46.24	44.39
8	74.86	68.57	61.60	60.44	57.33	54.03	50.51	48.64	46.89
					Finite element solution [18]				
1	31.28	27.25	22.40	20.10	17.47	14.31	10.16	7.20	2.28
2	32.25	28.37	23.78	21.64	19.24	16.45	13.04	10.91	8.53
3	34.48	30.91	26.80	24.94	22.91	20.66	18.10	16.66	15.24
4	38.47	35.34	31.84	30.32	28.70	26.96	25.09	24.09	23.15
5	44.68	42.04	39.19	37.98	36.72	35.40	34.03	33.31	32.66
6	53.41	51.25	48.97	48.02	47.04	46.04	45.01	44.48	44.00
7	64.77	63.01	61.19	58.44	55.22	51.78	48.09	46.12	44.28
8	74.73	68.45	61.48	60.26	57.15	53.85	50.31	48.44	46.69
					Percent difference				
1	-0.09%	-0.08%	-0.07%	-0.06%	-0.06%	-0.05%	-0.05%	-0.05%	-0.17%
2	-0.11%	-0.11%	-0.11%	-0.13%	-0.14%	-0.17%	-0.24%	-0.32%	-0.51%
3	-0.15%	-0.16%	-0.18%	-0.20%	-0.22%	-0.25%	-0.31%	-0.36%	-0.43%
4	-0.23%	-0.25%	-0.28%	-0.30%	-0.33%	-0.36%	-0.41%	-0.44%	-0.48%
5	-0.32%	-0.34%	-0.38%	-0.40%	-0.42%	-0.44%	-0.48%	-0.50%	-0.52%
6	-0.37%	-0.39%	-0.42%	-0.43%	-0.45%	-0.46%	-0.48%	-0.49%	-0.50%
7	-0.36%	-0.37%	-0.39%	-0.19%	-0.20%	-0.22%	-0.23%	-0.24%	-0.26%
8	-0.18%	-0.18%	-0.19%	-0.30%	-0.32%	-0.35%	-0.39%	-0.41%	-0.43%

Figure 4.170 Eigenvalue curves, CCCF plate, $\phi = 3 / 1$,
$P_\xi = - N_x b^2 / D$, $\lambda^2 = \omega a^2 (\rho / D)^{1/2}$.

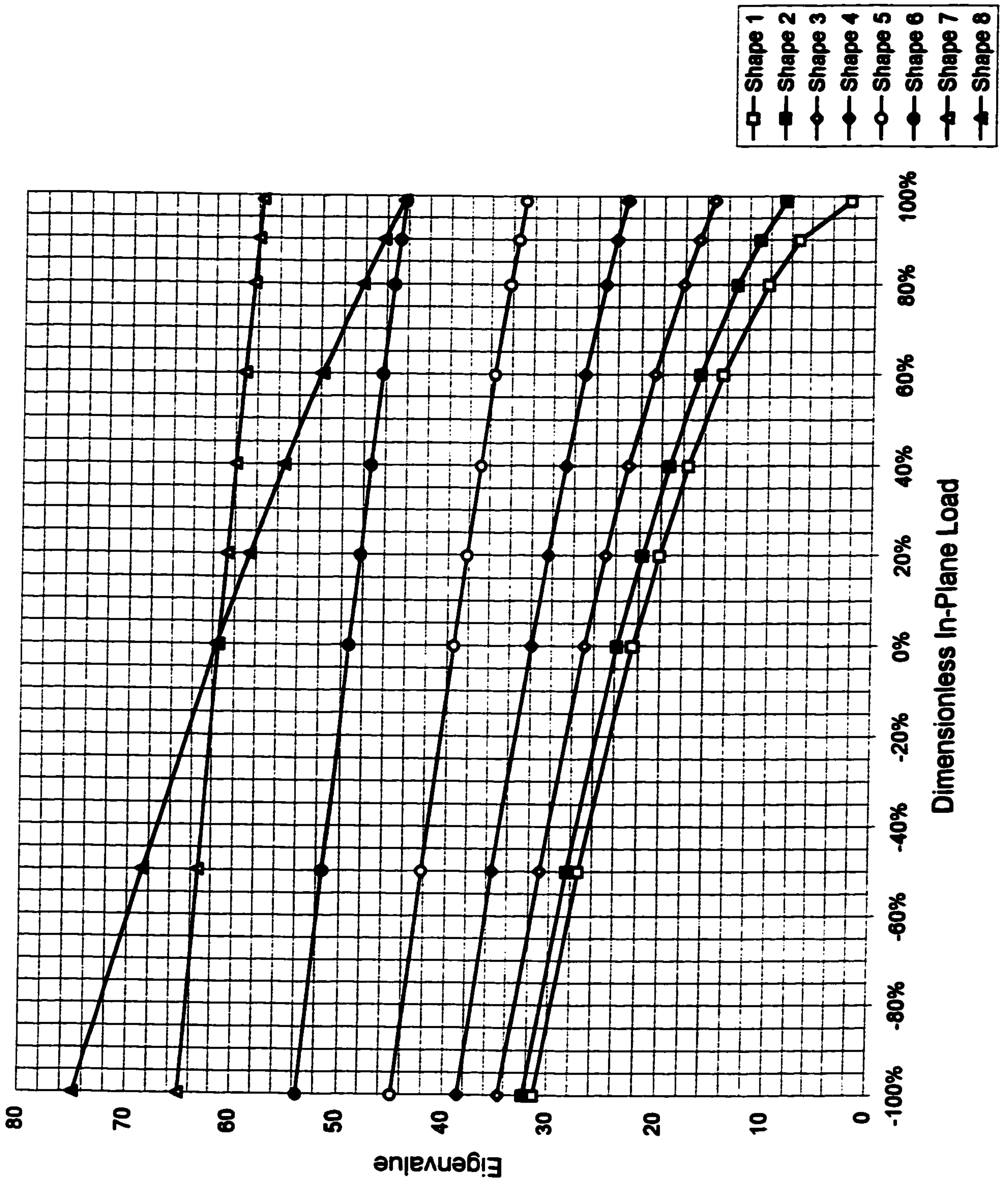

Figure 4.171 Mode shapes, CCCF plate, $\phi = 3 / 1$.

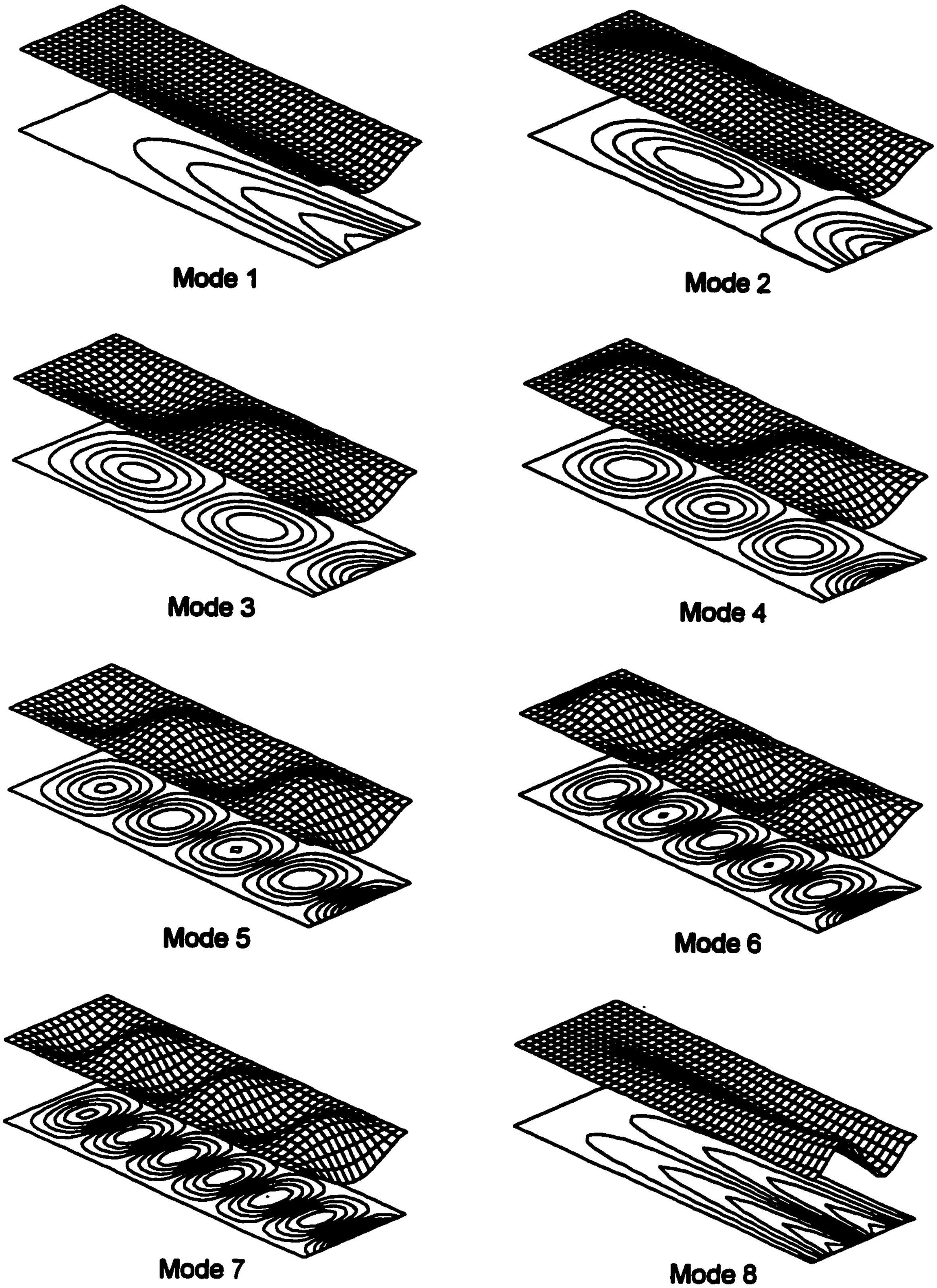

5 Discussion of Results

The free vibration and buckling analyses of nine plates subject to various in-plane loads have been presented by means of computed eigenvalues, eigenvalue curves, and associated mode shapes. These results confirm the validity of the mathematical solutions derived. Convergence of the numerical results are discussed.

5.1 Buckling Analysis Results

In Tables 4.1 and 4.2, excellent agreement was found between the present solution method and Timoshenko's [17] solution method. This was expected since both methods utilize Lévy-type solutions, which are analytical in nature.

Although the approximate buckling loads listed in Table 4.6 were comparable to the analytic buckling loads, relative differences of 5% were typical. Error of this order could be unacceptable for some applications. This is especially discouraging since values tended to be on the high side, meaning that the true buckling load for the plate had been exceeded. Characteristic beam functions in Rayleigh's method were used to derive the formula [11]. The use of different shape functions in the derivation could cause the solution to give more accurate results, as suggested by Bassily [10]. The weakness in Rayleigh-Ritz methods of solution is that the plate results are only as good as the initially assumed shape of deflection. Some qualitative judgement, based primarily on experience, enters the analysis.

Despite the drawbacks, the formula is powerful in its own sense because no plate or vibration theory need be known by the user. Buckling loads can be calculated by hand. Note that the buckling mode may not necessarily be the primary mode (or shape with no nodal lines). Modes with one nodal line must be examined before a critical buckling load can be confidently identified. Although these multiple calculations are relatively simple, the work put into evaluating loads can become tedious.

Results presented in Table 4.7 compared extremely well, proving that ANSYS [18] can adequately handle buckling problems by use of the finite element method. The only modelling concern which arose was to ensure that enough nodes were included in the model so that the proper buckling mode shape, and hence load, was obtained. Also note that ANSYS can be expensive in terms of computer hardware, software, and execution time. These comments also hold true for any developed finite element code.

The method of superposition is favoured over these other methods of solution due to its high convergency and analytic nature which does not require prior knowledge of the shape of deflection for accurate load calculations. This also applies to plate vibration. In short, the method determines coefficients of trigonometric series representing the shape function which will satisfy the governing differential equation and boundary conditions of the problem. In essence, the buckling mode shape is determined in the solution. The superimposed building block solutions themselves are analytically exact, and any desired degree of accuracy can be obtained in the total solution. A single FORTRAN program was developed for the present method of solution, which produced buckling and free vibration results for all nine plates examined. Convergence is discussed in the following section.

The buckling load curves indicate that a plate's critical load increases with aspect ratio. This is explained by the fact that as a plate's aspect ratio increases, the length of its free edges decreases, making the plate stiffer. Note that buckling loads for plates with more clamped edges and less free edges are comparatively larger. The elastic stability of the plate is solely dependent upon its strength or stiffness. Close examination of Figures 4.5, 4.7, and 4.9 for the SCSF, SCCF, and CCCF plates respectively reveals small bumps or regions of levelling for small aspect ratios. This is an indication that the critical buckling mode shape has changed. This is further explained in the next section.

5.2 Free Vibration Analysis Results

Once again, the approximate formula used by Dickinson [11] gave results higher than expected by a maximum of 5%. In general, however, the average error in eigenvalues decreased to about 2%. It is believed that the discrepancy in results is originating from the shape functions used in the Rayleigh method. Great effort is used in obtaining higher mode eigenvalues if the mode shape is unknown since several cases for nodal line combinations must be considered. For example, 5 eigenvalues must be calculated before the third mode of free vibration can confidently be chosen.

Eigenvalues listed in Tables 4.11 to 4.91 compared very well with an average difference of only 0.3%. However, the ANSYS [18] batch file used for the free vibration analysis (appendix C) took over 24 hours to fully execute on a relatively powerful computer system. The plate is carefully modelled with enough elements to accurately obtain 8 modes of free vibration. It was decided that a 30 × 30 mesh would adequately define mode shapes for any aspect ratio. Mesh refinement becomes very important in free vibration analysis due to the number of hills and valleys which could be present in a complex mode shape. For example, a minimum of five equally spaced points are needed to roughly define one sine wave, as shown in Figure 5.1.

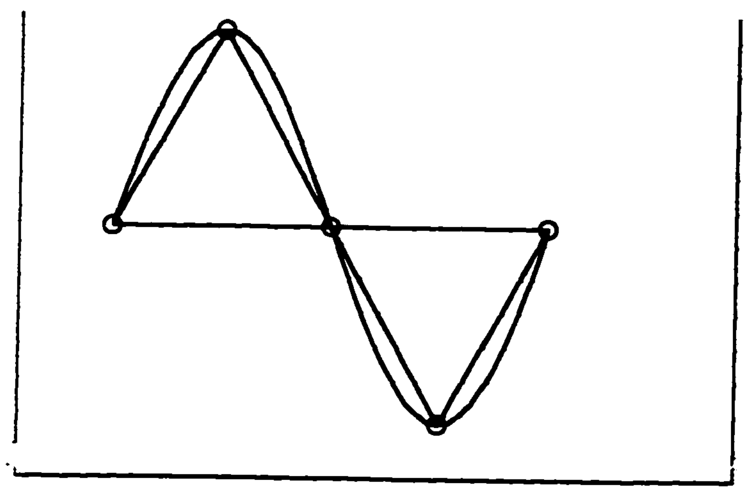

Figure 5.1 Representation of a sine wave with 3 and 5 nodes.

The numerical convergency of a plate eigenvalue determined by a superimposed solution is dependent upon the type of boundary conditions present, symmetry in the boundary conditions, and the complexity of the mode shape associated with the eigenvalue. A single term in a building block solution can give an exact eigenvalue in some instances. However, as many as 16 terms may be needed to obtain 4 digits of accuracy for other investigations. These characteristics arise from the nature of Fourier series and their ability to represent certain shapes.

A general Fourier series is composed of both sine and cosine functions. These are commonly referred to as odd and even functions respectively due to their form about an origin. An odd or sine function has a negative mirror image about an origin such that $f(x) = -f(-x)$. Conversely, an even or cosine function has a positive mirror image about an origin such that $f(x) = f(-x)$. These two sets of functions are orthogonal to each other. Now consider a plate which has the same boundary conditions along two opposing edges. Mode shapes will be either symmetrical or antisymmetrical about a point midway between the edges. This means that only one set of functions are contributing to the series solution even though all terms are considered. Coefficients for half of the terms will be calculated as zero. Gorman [16] avoids this inefficiency in solutions by separating symmetrical and antisymmetrical modes of vibration for each plate examined. For example, the CFCF plate would be investigated by using 4 superimposed solutions: one for fully symmetric modes, one for fully antisymmetric modes, and two for combined symmetric and antisymmetric modes. Although less terms are needed to obtain accurate eigenvalues, this method was not incorporated into the present solution due to the larger number of building block solutions required. Also, as with the approximate formula [11], modes need to be sorted out manually since multiple solutions are used for a single plate.

Another aspect of Fourier-type series solutions is that the number of terms used to adequately represent a shape increases as it becomes complex. This means that higher modes of vibration will require more terms than the fundamental mode in order to ensure a certain degree of accuracy. Typically, 8 terms give at least 3 digits of accuracy and 16 terms give at least 4 digits of accuracy in the presented solutions. Twenty terms were conservatively used to calculate results listed in section 4.

Note that plates with two opposing pinned edges will use only one specific term in each Lévy-type building block solution. Section 2.3 explains how the sine function itself satisfies the governing equation of motion and the boundary conditions for simple support. However, at least 8 terms should be used in a superimposed solution to ensure that the specific term needed for a mode is present.

The eigenvalue curves presented in section 4.2 show that compressive in-plane loads cause natural frequencies to lower until a state of buckling is achieved. Tensile loads cause natural frequencies to rise. As noted earlier, each line represents a specific mode shape as its stiffness is affected by in-plane load, and hence its natural frequency. Intersecting curves signify an eigenvalue where two mode shapes exist simultaneously. Beyond this point, the two mode shapes involved exchange order. This is an interesting phenomenon which illustrates not only that in-plane load effects stiffness, but also effects each particular mode shape differently. Difficulties are often encountered in determining eigenvalues and mode shapes in the vicinity of these double root regions. Creating eigenvalue versus in-plane load graphs aided in ensuring that no roots were missed in the free vibration analysis.

Special attention is given to Figures 4.82 and 4.84 for the SCSF plate and Figure 4.154 for the CCCF plate where the first and second mode shapes interchange. This enforces the results shown in Figures 4.5 and 4.9 where dips in the buckling curves signify a change in the buckling mode shape.

The associated mode shapes have been depicted using three-dimensional mesh and contour plots and show harmonic plate deflection for each mode. The displacement matrix for each shape is obtained by first determining the eigenvector (or building block amplitude coefficients) associated with each eigenvalue. Problems are sometimes encountered in accomplishing this task. At a double root, the separation of modes becomes impossible and suitable eigenvectors can not be calculated. For plates with pinned support on opposing edges, the specific term being used in the solution needs to be determined. In the past, an arbitrary term was set to unity and calculation of the eigenvector was attempted. Under special conditions, this works very well. However, with the current plate solutions, care must be taken not to assign unity to a coefficient which should actually equal zero. Theoretically, it should be possible to scale the now singular coefficient matrix and forward row reduce in order to find a zero along the diagonal. The location of this zero value represents the independent coefficient. The row with the zero is removed and the column is moved to the far right. The linear solution for the remaining coefficients is found and the independent coefficient is given a value of -1. However, in nearly all cases, the coefficient matrix is only near-singular due to numerical error. This causes inaccurate determination of the independent variable in some cases. In such situations, a term must be set to unity manually.

6 Conclusions

The free vibration analysis of rectangular plates with at least one free edge under unilateral in-plane loads have been solved by the method of superposition. The solution method consisted of first determining the analytically exact Lévy-type solutions of several building blocks. These building block solutions are then superimposed and boundary conditions for the total plate are enforced. Once the equations arising from the enforcement are established, it is a straight forward procedure to generate coefficient matrices and determinants so that eigenvalues and eigenvectors can be determined. The plate solutions presented can also be used to determine critical plate buckling loads, which are a limiting case of plate vibration.

Good agreement was obtained in comparing results with those generated by ANSYS [18], a general purpose finite element program. The eigenvalue and buckling load curves indicate that the analysis is accurate.

The present method of solution can easily be modified to include specially orthotropic plates. All derivative terms in the governing equation of motion are present, but coefficients change due to the presence of orthotropic plate material. This simply changes coefficients in the building block solutions. The current FORTRAN code could be appropriately altered under the proper supervision.

The superposition method of solution is attractive due to its analytic nature and high convergency. No mode shape assumptions are required prior to eigenvalue evaluation. The method has been used to solve the deflection, buckling, and free vibration of plates of various shape, edge conditions, and material properties. Although thin plate theory is usually used in derivations, some work has been done on Mindlin-type plates. Once building block solutions have been established, a variety of plate problems can be solved.

7 References

[1] A. W. LEISSA, Vibration of plates. National Aeronautical and Space Administration of America, SP-160 (1969).

[2] R. G. ANDERSON, B. M. IRONS, and O. C. ZIENKIEWICZ, Vibration and stability of plates using finite element methods. *International Journal of Solids and Structures* **4**, 1031-1055 (1968).

[3] H. C. CHAN and O. FOO, Vibration of rectangular plates subjected to in-plane forces by the finite strip method. *Journal of Sound and Vibration* **64**, 589- (1979).

[4] S. P. VIRK, Effects of static loads on dynamic response. *Proceedings of the 2nd Conference on Computing in Civil Engineering, Baltimore, Md, June 9-13, 1980* 133-139 (1980).

[5] B. TABARROK, R. G. FENTON, and A. M. ELSAIE, Lateral vibrations of square plates subject to in-plane loadings. *Journal of Sound and Vibration* **112**, 295-303 (1987).

[6] J. P. SINGH and S. S. DEY, Transverse vibration of rectangular plates subjected to in-plane forces by a difference based variational approach. *International Journal of Mechanical Science* **37**, 591-599 (1990).

[7] S. M. DICKINSON, Lateral vibration of rectangular plates subject to in-plane forces. *Journal of Sound and Vibration* **16**, 465-472 (1971).

[8] S. M. DICKINSON, The flexural vibration of rectangular orthotropic plates subject to in-plane forces. *Journal of Applied Mechanics* **38**, 699-700 (1971).

[9] S. F. BASSILY and S. M. DICKINSON, Buckling and lateral vibration of rectangular plates subject to in-plane loads - a Ritz approach. *Journal of Sound and Vibration* **24**, 219-239 (1972).

[10] S. F. BASSILY and S. M. DICKINSON, Buckling and vibration of in-plane loaded plates treated by a unified Ritz approach. *Journal of Sound and Vibration* **59**, 1-14 (1978).

[11] S. M. DICKINSON, The buckling and frequency of flexural vibration of rectangular isotropic and orthotropic plates using Rayleigh's method. *Journal of Sound and Vibration* **61**, 1-8 (1978).

[12] S. R. SONI and C. L. AMBA RAO, Vibrations of orthotropic rectangular plates under in-plane forces. *Computers and Structures* **4**, 1105-1115 (1974).

[13] S. D. YU and D. J. GORMAN, Free vibration of fully clamped rectangular plates subjected to constant in-plane loads. *Proceedings of the CSME Mechanical Engineering Forum*, 1990.

[14] W. L. CLEGHORN and S. D. YU, Analysis of buckling of rectangular plates using the method of superposition. *Transactions of the Canadian Society for Mechanical Engineering* **16**, 185-199 (1992).

[15] S. TIMOSHENKO and S. WOINOWSKY-KRIEGER, Theory of Plates and Shells. Toronto: McGraw-Hill (1959).

[16] D. J. GORMAN, Free Vibration Analysis of Rectangular Plates. New York: Elsevier North-Holland (1982).

[17] S. TIMOSHENKO and J. GERE, Theory of Elastic Stability. Toronto: McGraw-Hill (1961).

[18] ANSYS Inc., ANSYS version 5.2, 1996.

Appendix A
Building Block Contributions

This appendix lists the contributions given by each building block towards enforcing a particular boundary condition in the superimposed solution. Plates analyzed in sections 3.10 through 3.12 will use values from sections A.1 through A.4 while plates analyzed in sections 3.13 through 3.17 will use values from sections A.5 through A.8. Integrals used in the following equations are solved for in appendix B. It is important to note that amplitude factors should be excluded from the following coefficients since building block amplitudes are unknown. They are solved for in the superimposed solution by enforcing boundary conditions. Therefore, treat building block coefficients A, B, C, and D as A / E, B / E, C / E, and D / E in the following equations.

A.1 SRSV Building Block Contributions

A.1.1 Bending Moment at η = 1.

General Term

$$a_m = Y_m''(1) - \nu(m\pi\phi)^2 Y_m(1)$$

Case 1 Term

$$\begin{aligned} a_m = {} & \left[\left(\beta_m^2 - \gamma_m^2 - \nu(m\pi\phi)^2\right)A_m - 2\beta_m\gamma_m D_m\right]\sinh(\beta_m)\sin(\gamma_m) \\ & + \left[\left(\beta_m^2 - \gamma_m^2 - \nu(m\pi\phi)^2\right)D_m + 2\beta_m\gamma_m A_m\right]\cosh(\beta_m)\cos(\gamma_m) \end{aligned}$$

Case 2 Term

$$a_m = \left(\beta_m^2 - \nu(m\pi\phi)^2\right)B_m\cosh(\beta_m) - \left(\gamma_m^2 + \nu(m\pi\phi)^2\right)D_m\cos(\gamma_m)$$

Case 3 Term

$$a_m = \left(\beta_m^2 - \nu(m\pi\phi)^2\right)B_m\cosh(\beta_m) + \left(\gamma_m^2 - \nu(m\pi\phi)^2\right)D_m\cosh(\gamma_m)$$

A.1.2 Slope at $\xi = 1$.

General Term

$$e_{m0} = m\pi(-1)^m\int_0^1 Y_m(\eta)\,d\eta$$

$$e_{mn} = 2m\pi(-1)^m\int_0^1 Y_m(\eta)\cos(n\pi\eta)\,d\eta$$

Case 1 Term

$$e_{m0} = m\pi(-1)^m\left[A_m\int_0^1 \sinh(\beta_m\eta)\sin(\gamma_m\eta)\,d\eta + D_m\int_0^1 \cosh(\beta_m\eta)\cos(\gamma_m\eta)\,d\eta\right]$$

$$e_{mn} = 2m\pi(-1)^m\left[A_m\int_0^1 \sinh(\beta_m\eta)\sin(\gamma_m\eta)\cos(n\pi\eta)\,d\eta + D_m\int_0^1 \cosh(\beta_m\eta)\cos(\gamma_m\eta)\cos(n\pi\eta)\,d\eta\right]$$

Case 2 Term

$$e_{m0} = m\pi(-1)^m\left[B_m\int_0^1 \cosh(\beta_m\eta)\,d\eta + D_m\int_0^1 \cos(\gamma_m\eta)\,d\eta\right]$$

$$e_{mn} = 2m\pi(-1)^m\left[B_m\int_0^1 \cosh(\beta_m\eta)\cos(n\pi\eta)\,d\eta + D_m\int_0^1 \cos(\gamma_m\eta)\cos(n\pi\eta)\,d\eta\right]$$

Case 3 Term

$$e_{m0} = m\pi(-1)^m\left[B_m\int_0^1 \cosh(\beta_m\eta)\,d\eta + D_m\int_0^1 \cosh(\gamma_m\eta)\,d\eta\right]$$

$$e_{mn} = 2m\pi(-1)^m\left[B_m\int_0^1 \cosh(\beta_m\eta)\cos(n\pi\eta)\,d\eta + D_m\int_0^1 \cosh(\gamma_m\eta)\cos(n\pi\eta)\,d\eta\right]$$

A.1.3 Bending Moment at $\eta = 0$.

General Term

$$i_m = Y_m''(0) - \nu(m\pi\phi)^2 Y_m(0)$$

Case 1 Term

$$i_m = \left(\beta_m^2 - \gamma_m^2 - \nu(m\pi\phi)^2\right)D_m + 2\beta_m\gamma_m A_m$$

Case 2 Term

$$i_m = \left(\beta_m^2 - \nu(m\pi\phi)^2\right)B_m - \left(\gamma_m^2 + \nu(m\pi\phi)^2\right)D_m$$

Case 3 Term

$$i_m = \left(\beta_m^2 - \nu(m\pi\phi)^2\right)B_m + \left(\gamma_m^2 - \nu(m\pi\phi)^2\right)D_m$$

A.1.4 Slope at $\xi = 0$.

General Term

$$s_{m0} = m\pi\int_0^1 Y_m(\eta)\,d\eta$$

$$s_{mn} = 2m\pi\int_0^1 Y_m(\eta)\cos(n\pi\eta)\,d\eta$$

Case 1 Term

$$s_{m0} = m\pi\left[A_m\int_0^1 \sinh(\beta_m\eta)\sin(\gamma_m\eta)\,d\eta + D_m\int_0^1 \cosh(\beta_m\eta)\cos(\gamma_m\eta)\,d\eta\right]$$

$$s_{mn} = 2m\pi\left[A_m\int_0^1 \sinh(\beta_m\eta)\sin(\gamma_m\eta)\cos(n\pi\eta)\,d\eta + D_m\int_0^1 \cosh(\beta_m\eta)\cos(\gamma_m\eta)\cos(n\pi\eta)\,d\eta\right]$$

Case 2 Term

$$s_{m0} = m\pi\left[B_m\int_0^1 \cosh(\beta_m\eta)\,d\eta + D_m\int_0^1 \cos(\gamma_m\eta)\,d\eta\right]$$

$$s_{mn} = 2m\pi\left[B_m\int_0^1 \cosh(\beta_m\eta)\cos(n\pi\eta)\,d\eta + D_m\int_0^1 \cos(\gamma_m\eta)\cos(n\pi\eta)\,d\eta\right]$$

Case 3 Term

$$s_{m0} = m\pi\left[B_m\int_0^1 \cosh(\beta_m\eta)\,d\eta + D_m\int_0^1 \cosh(\gamma_m\eta)\,d\eta\right]$$

$$s_{mn} = 2m\pi\left[B_m\int_0^1 \cosh(\beta_m\eta)\cos(n\pi\eta)\,d\eta + D_m\int_0^1 \cosh(\gamma_m\eta)\cos(n\pi\eta)\,d\eta\right]$$

A.2 SRWR Building Block Contributions

A.2.1 Bending Moment at $\eta = 1$.

General Term

$$b_{mn} = 2\nu\phi^2(-1)^n\int_0^1 Y_n''(\xi)\sin(m\pi\xi)\,d\xi - 2(n\pi)^2(-1)^n\int_0^1 Y_n(\xi)\sin(m\pi\xi)\,d\xi$$

Case 1 Term

$$b_{mn} = 2(-1)^n\Big[\big(\nu\phi^2(\beta_n^2-\gamma_n^2)-(n\pi)^2\big)B_n + 2\nu\phi^2\beta_n\gamma_n C_n\Big]\int_0^1 \sinh(\beta_n\xi)\cos(\gamma_n\xi)\sin(m\pi\xi)\,d\xi$$

$$+ 2(-1)^n\Big[\big(\nu\phi^2(\beta_n^2-\gamma_n^2)-(n\pi)^2\big)C_n - 2\nu\phi^2\beta_n\gamma_n B_n\Big]\int_0^1 \cosh(\beta_n\xi)\sin(\gamma_n\xi)\sin(m\pi\xi)\,d\xi$$

Case 2 Term

$$b_{mn} = 2(-1)^n\big(\nu\phi^2\beta_n^2-(n\pi)^2\big)A_n\int_0^1 \sinh(\beta_n\xi)\sin(m\pi\xi)\,d\xi$$

$$- 2(-1)^n\big(\nu\phi^2\gamma_n^2+(n\pi)^2\big)C_n\int_0^1 \sin(\gamma_n\xi)\sin(m\pi\xi)\,d\xi$$

Case 3 Term

$$b_{mn} = 2(-1)^n\big(\nu\phi^2\beta_n^2-(n\pi)^2\big)A_n\int_0^1 \sinh(\beta_n\xi)\sin(m\pi\xi)\,d\xi$$

$$+ 2(-1)^n\big(\nu\phi^2\gamma_n^2-(n\pi)^2\big)C_n\int_0^1 \sinh(\gamma_n\xi)\sin(m\pi\xi)\,d\xi$$

Case 4 Term

$$b_{mn} = -\,2(-1)^n\big(\nu\phi^2\beta_n^2+(n\pi)^2\big)A_n\int_0^1 \sin(\beta_n\xi)\sin(m\pi\xi)\,d\xi$$

$$- 2(-1)^n\big(\nu\phi^2\gamma_n^2+(n\pi)^2\big)C_n\int_0^1 \sin(\gamma_n\xi)\sin(m\pi\xi)\,d\xi$$

A.2.2 Slope at $\xi = 1$.

General Term

$$f_n = Y_n'(1)$$

Case 1 Term

$$f_n = (C_n\beta_n - B_n\gamma_n)\sinh(\beta_n)\sin(\gamma_n) + (B_n\beta_n + C_n\gamma_n)\cosh(\beta_n)\cos(\gamma_n)$$

Case 2 Term

$$f_n = A_n\beta_n\cosh(\beta_n) + C_n\gamma_n\cos(\gamma_n)$$

Case 3 Term

$$f_n = A_n\beta_n\cosh(\beta_n) + C_n\gamma_n\cosh(\gamma_n)$$

Case 4 Term

$$f_n = A_n\beta_n\cos(\beta_n) + C_n\gamma_n\cos(\gamma_n)$$

A.2.3 Bending Moment at $\eta = 0$.

General Term

$$j_{mn} = 2\nu\phi^2\int_0^1 Y_n''(\xi)\sin(m\pi\xi)\,d\xi - 2(n\pi)^2\int_0^1 Y_n(\xi)\sin(m\pi\xi)\,d\xi$$

Case 1 Term

$$j_{mn} = 2\left[\left(\nu\phi^2\left(\beta_n^2-\gamma_n^2\right)-(n\pi)^2\right)B_n + 2\nu\phi^2\beta_n\gamma_n C_n\right]\int_0^1 \sinh(\beta_n\xi)\cos(\gamma_n\xi)\sin(m\pi\xi)\,d\xi$$

$$+ 2\left[\left(\nu\phi^2\left(\beta_n^2-\gamma_n^2\right)-(n\pi)^2\right)C_n - 2\nu\phi^2\beta_n\gamma_n B_n\right]\int_0^1 \cosh(\beta_n\xi)\sin(\gamma_n\xi)\sin(m\pi\xi)\,d\xi$$

Case 2 Term

$$j_{mn} = 2\left(\nu\phi^2\beta_n^2-(n\pi)^2\right)A_n\int_0^1 \sinh(\beta_n\xi)\sin(m\pi\xi)\,d\xi$$

$$-\ 2\left(\nu\phi^2\gamma_n^2+(n\pi)^2\right)C_n\int_0^1 \sin(\gamma_n\xi)\sin(m\pi\xi)\,d\xi$$

Case 3 Term

$$j_{mn} = 2\left(\nu\phi^2\beta_n^2-(n\pi)^2\right)A_n\int_0^1 \sinh(\beta_n\xi)\sin(m\pi\xi)\,d\xi$$

$$+\ 2\left(\nu\phi^2\gamma_n^2-(n\pi)^2\right)C_n\int_0^1 \sinh(\gamma_n\xi)\sin(m\pi\xi)\,d\xi$$

Case 4 Term

$$j_{mn} = -\ 2\left(\nu\phi^2\beta_n^2+(n\pi)^2\right)A_n\int_0^1 \sin(\beta_n\xi)\sin(m\pi\xi)\,d\xi$$

$$-\ 2\left(\nu\phi^2\gamma_n^2+(n\pi)^2\right)C_n\int_0^1 \sin(\gamma_n\xi)\sin(m\pi\xi)\,d\xi$$

A.2.4 Slope at $\xi = 0$.

General Term

$$t_n = Y_n'(0)$$

Case 1 Term

$$t_n = B_n\beta_n + C_n\gamma_n$$

Case 2 Term

$$t_n = A_n\beta_n + C_n\gamma_n$$

Case 3 Term

$$t_n = A_n\beta_n + C_n\gamma_n$$

Case 4 Term

$$t_n = A_n\beta_n + C_n\gamma_n$$

A.3 SVSR Building Block Contributions

A.3.1 Bending Moment at $\eta = 1$.

General Term

$$c_p = Y_p''(0) - \nu(p\pi\phi)^2 Y_p(0)$$

Case 1 Term

$$c_p = \left(\beta_p^2 - \gamma_p^2 - \nu(p\pi\phi)^2\right)D_p + 2\beta_p\gamma_p A_p$$

Case 2 Term

$$c_p = \left(\beta_p^2 - \nu(p\pi\phi)^2\right)B_p - \left(\gamma_p^2 + \nu(p\pi\phi)^2\right)D_p$$

Case 3 Term

$$c_p = \left(\beta_p^2 - \nu(p\pi\phi)^2\right)B_p + \left(\gamma_p^2 - \nu(p\pi\phi)^2\right)D_p$$

A.3.2 Slope at $\xi = 1$.

General Term

$$g_{p0} = p\pi(-1)^p \int_0^1 Y_p(1-\eta)\,d\eta$$

$$g_{pn} = 2p\pi(-1)^p \int_0^1 Y_p(1-\eta)\cos(n\pi\eta)\,d\eta$$

Case 1 Term

$$g_{p0} = p\pi(-1)^p\left[A_p\int_0^1 \sinh(\beta_p(1-\eta))\sin(\gamma_p(1-\eta))\,d\eta + D_p\int_0^1 \cosh(\beta_p(1-\eta))\cos(\gamma_p(1-\eta))\,d\eta\right]$$

$$g_{pn} = 2p\pi(-1)^p\left[A_p\int_0^1 \sinh(\beta_p(1-\eta))\sin(\gamma_p(1-\eta))\cos(n\pi\eta)\,d\eta\right.$$

$$\left. + D_p\int_0^1 \cosh(\beta_p(1-\eta))\cos(\gamma_p(1-\eta))\cos(n\pi\eta)\,d\eta\right]$$

Case 2 Term

$$g_{p0} = p\pi(-1)^p\left[B_p\int_0^1 \cosh(\beta_p(1-\eta))\,d\eta + D_p\int_0^1 \cos(\gamma_p(1-\eta))\,d\eta\right]$$

$$g_{pn} = 2p\pi(-1)^p\left[B_p\int_0^1 \cosh(\beta_p(1-\eta))\cos(n\pi\eta)\,d\eta + D_p\int_0^1 \cos(\gamma_p(1-\eta))\cos(n\pi\eta)\,d\eta\right]$$

Case 3 Term

$$g_{p0} = p\pi(-1)^p\left[B_p\int_0^1 \cosh(\beta_p(1-\eta))\,d\eta + D_p\int_0^1 \cosh(\gamma_p(1-\eta))\,d\eta\right]$$

$$g_{pn} = 2p\pi(-1)^p\left[B_p\int_0^1 \cosh(\beta_p(1-\eta))\cos(n\pi\eta)\,d\eta + D_p\int_0^1 \cosh(\gamma_p(1-\eta))\cos(n\pi\eta)\,d\eta\right]$$

A.3.3 Bending Moment at $\eta = 0$.

General Term

$$k_p = Y_p''(1) - \nu(p\pi\phi)^2 Y_p(1)$$

Case 1 Term

$$k_p = \left[\left(\beta_p^2-\gamma_p^2-\nu(p\pi\phi)^2\right)A_p - 2\beta_p\gamma_p D_p\right]\sinh(\beta_p)\sin(\gamma_p)$$
$$+\left[\left(\beta_p^2-\gamma_p^2-\nu(p\pi\phi)^2\right)D_p + 2\beta_p\gamma_p A_p\right]\cosh(\beta_p)\cos(\gamma_p)$$

Case 2 Term

$$k_p = \left(\beta_p^2-\nu(p\pi\phi)^2\right)B_p\cosh(\beta_p) - \left(\gamma_p^2+\nu(p\pi\phi)^2\right)D_p\cos(\gamma_p)$$

Case 3 Term

$$k_p = \left(\beta_p^2-\nu(p\pi\phi)^2\right)B_p\cosh(\beta_p) + \left(\gamma_p^2-\nu(p\pi\phi)^2\right)D_p\cosh(\gamma_p)$$

A.3.4 Slope at $\xi = 0$.

General Term

$$u_{p0} = p\pi\int_0^1 Y_p(1-\eta)\,d\eta$$

$$u_{pn} = 2p\pi\int_0^1 Y_p(1-\eta)\cos(n\pi\eta)\,d\eta$$

Case 1 Term

$$u_{p0} = p\pi\left[A_p\int_0^1 \sinh(\beta_p(1-\eta))\sin(\gamma_p(1-\eta))\,d\eta + D_p\int_0^1 \cosh(\beta_p(1-\eta))\cos(\gamma_p(1-\eta))\,d\eta\right]$$

$$u_{pn} = 2p\pi\left[A_p\int_0^1 \sinh(\beta_p(1-\eta))\sin(\gamma_p(1-\eta))\cos(n\pi\eta)\,d\eta\right.$$
$$\left.+ D_p\int_0^1 \cosh(\beta_p(1-\eta))\cos(\gamma_p(1-\eta))\cos(n\pi\eta)\,d\eta\right]$$

Case 2 Term

$$u_{p0} = p\pi\left[B_p\int_0^1 \cosh(\beta_p(1-\eta))d\eta + D_p\int_0^1 \cos(\gamma_p(1-\eta))d\eta\right]$$

$$u_{pn} = 2p\pi\left[B_p\int_0^1 \cosh(\beta_p(1-\eta))\cos(n\pi\eta)d\eta + D_p\int_0^1 \cos(\gamma_p(1-\eta))\cos(n\pi\eta)d\eta\right]$$

Case 3 Term

$$u_{p0} = p\pi\left[B_p\int_0^1 \cosh(\beta_p(1-\eta))d\eta + D_p\int_0^1 \cosh(\gamma_p(1-\eta))d\eta\right]$$

$$u_{pn} = 2p\pi\left[B_p\int_0^1 \cosh(\beta_p(1-\eta))\cos(n\pi\eta)d\eta + D_p\int_0^1 \cosh(\gamma_p(1-\eta))\cos(n\pi\eta)d\eta\right]$$

A.4 WRSR Building Block Contributions

A.4.1 Bending Moment at $\eta = 1$.

General Term

$$d_{mq} = 2\nu\phi^2(-1)^q\int_0^1 Y_q''(1-\xi)\sin(m\pi\xi)d\xi - 2(q\pi)^2(-1)^q\int_0^1 Y_q(1-\xi)\sin(m\pi\xi)d\xi$$

Case 1 Term

$$d_{mq} = 2(-1)^q\left[\left(\nu\phi^2\left(\beta_q^2-\gamma_q^2\right)-(q\pi)^2\right)B_q + 2\nu\phi^2\beta_q\gamma_q C_q\right]\int_0^1 \sinh(\beta_q(1-\xi))\cos(\gamma_q(1-\xi))\sin(m\pi\xi)d\xi$$

$$+ 2(-1)^q\left[\left(\nu\phi^2\left(\beta_q^2-\gamma_q^2\right)-(q\pi)^2\right)C_q - 2\nu\phi^2\beta_q\gamma_q B_q\right]\int_0^1 \cosh(\beta_q(1-\xi))\sin(\gamma_q(1-\xi))\sin(m\pi\xi)d\xi$$

Case 2 Term

$$d_{mq} = 2(-1)^q\left(\nu\phi^2\beta_q^2-(q\pi)^2\right)A_q\int_0^1 \sinh(\beta_q(1-\xi))\sin(m\pi\xi)d\xi$$

$$-\ 2(-1)^q\left(\nu\phi^2\gamma_q^2+(q\pi)^2\right)C_q\int_0^1 \sin(\gamma_q(1-\xi))\sin(m\pi\xi)d\xi$$

Case 3 Term

$$d_{mq} = 2(-1)^q\left(\nu\phi^2\beta_q^2-(q\pi)^2\right)A_q\int_0^1 \sinh(\beta_q(1-\xi))\sin(m\pi\xi)d\xi$$

$$+\ 2(-1)^q\left(\nu\phi^2\gamma_q^2-(q\pi)^2\right)C_q\int_0^1 \sinh(\gamma_q(1-\xi))\sin(m\pi\xi)d\xi$$

Case 4 Term

$$d_{mq} = -\ 2(-1)^q\left(\nu\phi^2\beta_q^2+(q\pi)^2\right)A_q\int_0^1 \sin(\beta_q(1-\xi))\sin(m\pi\xi)d\xi$$

$$-\ 2(-1)^q\left(\nu\phi^2\gamma_q^2+(q\pi)^2\right)C_q\int_0^1 \sin(\gamma_q(1-\xi))\sin(m\pi\xi)d\xi$$

A.4.2 Slope at $\xi = 1$.

General Term

$$h_q = -\ Y_q'(0)$$

Case 1 Term

$$h_q = -\ B_q\beta_q\ -\ C_q\gamma_q$$

Case 2 Term

$$h_q = -\ A_q\beta_q\ -\ C_q\gamma_q$$

Case 3 Term

$$h_q = -A_q\beta_q - C_q\gamma_q$$

Case 4 Term

$$h_q = -A_q\beta_q - C_q\gamma_q$$

A.4.3 Bending Moment at $\eta = 0$.

General Term

$$l_{mq} = 2\nu\phi^2\int_0^1 Y_q''(1-\xi)\sin(m\pi\xi)\,d\xi - 2(q\pi)^2\int_0^1 Y_q(1-\xi)\sin(m\pi\xi)\,d\xi$$

Case 1 Term

$$l_{mq} = 2\left[\left(\nu\phi^2\left(\beta_q^2-\gamma_q^2\right)-(q\pi)^2\right)B_q + 2\nu\phi^2\beta_q\gamma_q C_q\right]\int_0^1 \sinh(\beta_q(1-\xi))\cos(\gamma_q(1-\xi))\sin(m\pi\xi)\,d\xi$$

$$+ 2\left[\left(\nu\phi^2\left(\beta_q^2-\gamma_q^2\right)-(q\pi)^2\right)C_q - 2\nu\phi^2\beta_q\gamma_q B_q\right]\int_0^1 \cosh(\beta_q(1-\xi))\sin(\gamma_q(1-\xi))\sin(m\pi\xi)\,d\xi$$

Case 2 Term

$$l_{mq} = 2\left(\nu\phi^2\beta_q^2-(q\pi)^2\right)A_q\int_0^1 \sinh(\beta_q(1-\xi))\sin(m\pi\xi)\,d\xi$$

$$- 2\left(\nu\phi^2\gamma_q^2+(q\pi)^2\right)C_q\int_0^1 \sin(\gamma_q(1-\xi))\sin(m\pi\xi)\,d\xi$$

Case 3 Term

$$L_{mq} = 2\left(\nu\phi^2\beta_q^2-(q\pi)^2\right)A_q\int_0^1 \sinh(\beta_q(1-\xi))\sin(m\pi\xi)\,d\xi$$

$$+\ 2\left(\nu\phi^2\gamma_q^2-(q\pi)^2\right)C_q\int_0^1 \sinh(\gamma_q(1-\xi))\sin(m\pi\xi)\,d\xi$$

Case 4 Term

$$L_{mq} = -\ 2\left(\nu\phi^2\beta_q^2+(q\pi)^2\right)A_q\int_0^1 \sin(\beta_q(1-\xi))\sin(m\pi\xi)\,d\xi$$

$$-\ 2\left(\nu\phi^2\gamma_q^2+(q\pi)^2\right)C_q\int_0^1 \sin(\gamma_q(1-\xi))\sin(m\pi\xi)\,d\xi$$

A.4.4 Slope at $\xi = 0$.

General Term

$$v_q = -\ Y_q'(1)$$

Case 1 Term

$$v_q = -\ (C_q\beta_q - B_q\gamma_q)\sinh(\beta_q)\sin(\gamma_q) - (B_q\beta_q + C_q\gamma_q)\cosh(\beta_q)\cos(\gamma_q)$$

Case 2 Term

$$v_q = -\ A_q\beta_q\cosh(\beta_q) - C_q\gamma_q\cos(\gamma_q)$$

Case 3 Term

$$v_q = -\ A_q\beta_q\cosh(\beta_q) - C_q\gamma_q\cosh(\gamma_q)$$

Case 4 Term

$$v_q = -\ A_q\beta_q\cos(\beta_q) - C_q\gamma_q\cos(\gamma_q)$$

A.5 SSSV Building Block Contributions

A.5.1 Bending Moment at $\eta = 1$.

General Term

$$a_m = Y_m''(1) - \nu(m\pi\phi)^2 Y_m(1)$$

Case 1 Term

$$a_m = \left[\left(\beta_m^2 - \gamma_m^2 - \nu(m\pi\phi)^2\right)B_m + 2\beta_m\gamma_m C_m\right]\sinh(\beta_m)\cos(\gamma_m)$$
$$+ \left[\left(\beta_m^2 - \gamma_m^2 - \nu(m\pi\phi)^2\right)C_m - 2\beta_m\gamma_m B_m\right]\cosh(\beta_m)\sin(\gamma_m)$$

Case 2 Term

$$a_m = \left(\beta_m^2 - \nu(m\pi\phi)^2\right)A_m\sinh(\beta_m) - \left(\gamma_m^2 + \nu(m\pi\phi)^2\right)C_m\sin(\gamma_m)$$

Case 3 Term

$$a_m = \left(\beta_m^2 - \nu(m\pi\phi)^2\right)A_m\sinh(\beta_m) + \left(\gamma_m^2 - \nu(m\pi\phi)^2\right)C_m\sinh(\gamma_m)$$

A.5.2 Slope at $\xi = 1$.

General Term

$$e_{mn} = 2m\pi(-1)^m\int_0^1 Y_m(\eta)\sin\left(\frac{n\pi\eta}{2}\right)d\eta$$

Case 1 Term

$$e_{mn} = 2m\pi(-1)^m\left[B_m\int_0^1 \sinh(\beta_m\eta)\cos(\gamma_m\eta)\sin\left(\frac{n\pi\eta}{2}\right)d\eta + C_m\int_0^1 \cosh(\beta_m\eta)\sin(\gamma_m\eta)\sin\left(\frac{n\pi\eta}{2}\right)d\eta\right]$$

Case 2 Term

$$e_{mn} = 2m\pi(-1)^m\left[A_m\int_0^1 \sinh(\beta_m\eta)\sin\left(\frac{n\pi\eta}{2}\right)d\eta + C_m\int_0^1 \sin(\gamma_m\eta)\sin\left(\frac{n\pi\eta}{2}\right)d\eta\right]$$

Case 3 Term

$$e_{mn} = 2m\pi(-1)^m\left[A_m\int_0^1 \sinh(\beta_m\eta)\sin\left(\frac{n\pi\eta}{2}\right)d\eta + C_m\int_0^1 \sinh(\gamma_m\eta)\sin\left(\frac{n\pi\eta}{2}\right)d\eta\right]$$

A.5.3 Slope at $\eta = 0$.

General Term

$$i_m = Y_m'(0)$$

Case 1 Term

$$i_m = B_m\beta_m + C_m\gamma_m$$

Case 2 Term

$$i_m = A_m\beta_m + C_m\gamma_m$$

Case 3 Term

$$i_m = A_m\beta_m + C_m\gamma_m$$

A.5.4 Slope at $\xi = 0$.

General Term

$$s_{mn} = 2m\pi\int_0^1 Y_m(\eta)\sin\left(\frac{n\pi\eta}{2}\right)d\eta$$

Case 1 Term

$$s_{mn} = 2m\pi\left[B_m\int_0^1 \sinh(\beta_m\eta)\cos(\gamma_m\eta)\sin\left(\frac{n\pi\eta}{2}\right)d\eta + C_m\int_0^1 \cosh(\beta_m\eta)\sin(\gamma_m\eta)\sin\left(\frac{n\pi\eta}{2}\right)d\eta\right]$$

Case 2 Term

$$s_{mn} = 2m\pi\left[A_m\int_0^1 \sinh(\beta_m\eta)\sin\left(\frac{n\pi\eta}{2}\right)d\eta + C_m\int_0^1 \sin(\gamma_m\eta)\sin\left(\frac{n\pi\eta}{2}\right)d\eta\right]$$

Case 3 Term

$$s_{mn} = 2m\pi\left[A_m\int_0^1 \sinh(\beta_m\eta)\sin\left(\frac{n\pi\eta}{2}\right)d\eta + C_m\int_0^1 \sinh(\gamma_m\eta)\sin\left(\frac{n\pi\eta}{2}\right)d\eta\right]$$

A.6 SSWR Building Block Contributions

A.6.1 Bending Moment at $\eta = 1$.

General Term

$$b_{mn} = 2\nu\phi^2(-1)^{\left(\frac{n-1}{2}\right)}\int_0^1 Y_n''(\xi)\sin(m\pi\xi)d\xi - 2\left(\frac{n\pi}{2}\right)^2(-1)^{\left(\frac{n-1}{2}\right)}\int_0^1 Y_n(\xi)\sin(m\pi\xi)d\xi$$

Case 1 Term

$$b_{mn} = 2(-1)^{\left(\frac{n-1}{2}\right)}\left[\left(\nu\phi^2(\beta_n^2-\gamma_n^2)-\left(\frac{n\pi}{2}\right)^2\right)B_n + 2\nu\phi^2\beta_n\gamma_nC_n\right]\int_0^1 \sinh(\beta_n\xi)\cos(\gamma_n\xi)\sin(m\pi\xi)d\xi$$

$$+ 2(-1)^{\left(\frac{n-1}{2}\right)}\left[\left(\nu\phi^2(\beta_n^2-\gamma_n^2)-\left(\frac{n\pi}{2}\right)^2\right)C_n - 2\nu\phi^2\beta_n\gamma_nB_n\right]\int_0^1 \cosh(\beta_n\xi)\sin(\gamma_n\xi)\sin(m\pi\xi)d\xi$$

Case 2 Term

$$b_{mn} = 2(-1)^{\left(\frac{n-1}{2}\right)}\left(\nu\phi^2\beta_n^2-\left(\frac{n\pi}{2}\right)^2\right)A_n\int_0^1 \sinh(\beta_n\xi)\sin(m\pi\xi)d\xi$$

$$- 2(-1)^{\left(\frac{n-1}{2}\right)}\left(\nu\phi^2\gamma_n^2+\left(\frac{n\pi}{2}\right)^2\right)C_n\int_0^1 \sin(\gamma_n\xi)\sin(m\pi\xi)d\xi$$

Case 3 Term

$$b_{mn} = 2(-1)^{\left(\frac{n-1}{2}\right)}\left(\nu\phi^2\beta_n^2-\left(\frac{n\pi}{2}\right)^2\right)A_n\int_0^1 \sinh(\beta_n\xi)\sin(m\pi\xi)\,d\xi$$

$$+\ 2(-1)^{\left(\frac{n-1}{2}\right)}\left(\nu\phi^2\gamma_n^2-\left(\frac{n\pi}{2}\right)^2\right)C_n\int_0^1 \sinh(\gamma_n\xi)\sin(m\pi\xi)\,d\xi$$

Case 4 Term

$$b_{mn} = -\ 2(-1)^{\left(\frac{n-1}{2}\right)}\left(\nu\phi^2\beta_n^2+\left(\frac{n\pi}{2}\right)^2\right)A_n\int_0^1 \sin(\beta_n\xi)\sin(m\pi\xi)\,d\xi$$

$$-\ 2(-1)^{\left(\frac{n-1}{2}\right)}\left(\nu\phi^2\gamma_n^2+\left(\frac{n\pi}{2}\right)^2\right)C_n\int_0^1 \sin(\gamma_n\xi)\sin(m\pi\xi)\,d\xi$$

A.6.2 Slope at $\xi = 1$.

General Term

$$f_n = Y_n'(1)$$

Case 1 Term

$$f_n = (C_n\beta_n - B_n\gamma_n)\sinh(\beta_n)\sin(\gamma_n) + (B_n\beta_n + C_n\gamma_n)\cosh(\beta_n)\cos(\gamma_n)$$

Case 2 Term

$$f_n = A_n\beta_n\cosh(\beta_n) + C_n\gamma_n\cos(\gamma_n)$$

Case 3 Term

$$f_n = A_n\beta_n\cosh(\beta_n) + C_n\gamma_n\cosh(\gamma_n)$$

Case 4 Term

$$f_n = A_n\beta_n\cos(\beta_n) + C_n\gamma_n\cos(\gamma_n)$$

A.6.3 Slope at $\eta = 0$.

General Term

$$j_{mn} = n\pi \int_0^1 Y_n(\xi)\sin(m\pi\xi)\,d\xi$$

Case 1 Term

$$j_{mn} = n\pi\left[B_n\int_0^1 \sinh(\beta_n\xi)\cos(\gamma_n\xi)\sin(m\pi\xi)\,d\xi + C_n\int_0^1 \cosh(\beta_n\xi)\sin(\gamma_n\xi)\sin(m\pi\xi)\,d\xi\right]$$

Case 2 Term

$$j_{mn} = n\pi\left[A_n\int_0^1 \sinh(\beta_n\xi)\sin(m\pi\xi)\,d\xi + C_n\int_0^1 \sin(\gamma_n\xi)\sin(m\pi\xi)\,d\xi\right]$$

Case 3 Term

$$j_{mn} = n\pi\left[A_n\int_0^1 \sinh(\beta_n\xi)\sin(m\pi\xi)\,d\xi + C_n\int_0^1 \sinh(\gamma_n\xi)\sin(m\pi\xi)\,d\xi\right]$$

Case 4 Term

$$j_{mn} = n\pi\left[A_n\int_0^1 \sin(\beta_n\xi)\sin(m\pi\xi)\,d\xi + C_n\int_0^1 \sin(\gamma_n\xi)\sin(m\pi\xi)\,d\xi\right]$$

A.6.4 Slope at $\xi = 0$.

General Term

$$t_n = Y_n'(0)$$

Case 1 Term

$$t_n = B_n\beta_n + C_n\gamma_n$$

Case 2 Term

$$t_n = A_n\beta_n + C_n\gamma_n$$

Case 3 Term

$$t_n = A_n\beta_n + C_n\gamma_n$$

Case 4 Term

$$t_n = A_n\beta_n + C_n\gamma_n$$

A.7 SWSR Building Block Contributions

A.7.1 Bending Moment at $\eta = 1$.

General Term

$$c_p = Y_p''(0) - \nu(p\pi\phi)^2 Y_p(0)$$

Case 1 Term

$$c_p = \left(\beta_p^2 - \gamma_p^2 - \nu(p\pi\phi)^2\right)D_p + 2\beta_p\gamma_p A_p$$

Case 2 Term

$$c_p = \left(\beta_p^2 - \nu(p\pi\phi)^2\right)B_p - \left(\gamma_p^2 + \nu(p\pi\phi)^2\right)D_p$$

Case 3 Term

$$c_p = \left(\beta_p^2 - \nu(p\pi\phi)^2\right)B_p + \left(\gamma_p^2 - \nu(p\pi\phi)^2\right)D_p$$

A.7.2 Slope at $\xi = 1$.

General Term

$$g_{pn} = 2p\pi(-1)^p \int_0^1 Y_p(1-\eta)\sin\left(\frac{n\pi\eta}{2}\right)d\eta$$

Case 1 Term

$$g_{pn} = 2p\pi(-1)^p\left[A_p\int_0^1 \sinh(\beta_p(1-\eta))\sin(\gamma_p(1-\eta))\sin\left(\frac{n\pi\eta}{2}\right)d\eta\right.$$

$$\left.+ D_p\int_0^1 \cosh(\beta_p(1-\eta))\cos(\gamma_p(1-\eta))\sin\left(\frac{n\pi\eta}{2}\right)d\eta\right]$$

Case 2 Term

$$g_{pn} = 2p\pi(-1)^p\left[B_p\int_0^1 \cosh(\beta_p(1-\eta))\sin\left(\frac{n\pi\eta}{2}\right)d\eta + D_p\int_0^1 \cos(\gamma_p(1-\eta))\sin\left(\frac{n\pi\eta}{2}\right)d\eta\right]$$

Case 3 Term

$$g_{pn} = 2p\pi(-1)^p\left[B_p\int_0^1 \cosh(\beta_p(1-\eta))\sin\left(\frac{n\pi\eta}{2}\right)d\eta + D_p\int_0^1 \cosh(\gamma_p(1-\eta))\sin\left(\frac{n\pi\eta}{2}\right)d\eta\right]$$

A.7.3 Slope at $\eta = 0$.

General Term

$$k_p = -Y_p'(1)$$

Case 1 Term

$$k_p = -(D_p\beta_p + A_p\gamma_p)\sinh(\beta_p)\cos(\gamma_p) - (A_p\beta_p - D_p\gamma_p)\cosh(\beta_p)\sin(\gamma_p)$$

Case 2 Term

$$k_p = -B_p\beta_p\sinh(\beta_p) + D_p\gamma_p\sin(\gamma_p)$$

Case 3 Term

$$k_p = -B_p\beta_p\sinh(\beta_p) - D_p\gamma_p\sinh(\gamma_p)$$

A.7.4 Slope at $\xi = 0$.

General Term

$$u_{pn} = 2p\pi \int_0^1 Y_p(1-\eta)\sin\left(\frac{n\pi\eta}{2}\right)d\eta$$

Case 1 Term

$$u_{pn} = 2p\pi\left[A_p\int_0^1 \sinh(\beta_p(1-\eta))\sin(\gamma_p(1-\eta))\sin\left(\frac{n\pi\eta}{2}\right)d\eta\right.$$

$$\left. + D_p\int_0^1 \cosh(\beta_p(1-\eta))\cos(\gamma_p(1-\eta))\sin\left(\frac{n\pi\eta}{2}\right)d\eta\right]$$

Case 2 Term

$$u_{pn} = 2p\pi\left[B_p\int_0^1 \cosh(\beta_p(1-\eta))\sin\left(\frac{n\pi\eta}{2}\right)d\eta + D_p\int_0^1 \cos(\gamma_p(1-\eta))\sin\left(\frac{n\pi\eta}{2}\right)d\eta\right]$$

Case 3 Term

$$u_{pn} = 2p\pi\left[B_p\int_0^1 \cosh(\beta_p(1-\eta))\sin\left(\frac{n\pi\eta}{2}\right)d\eta + D_p\int_0^1 \cosh(\gamma_p(1-\eta))\sin\left(\frac{n\pi\eta}{2}\right)d\eta\right]$$

A.8 WSSR Building Block Contributions

A.8.1 Bending Moment at $\eta = 1$.

General Term

$$d_{mq} = 2\nu\phi^2(-1)^{\left(\frac{q-1}{2}\right)}\int_0^1 Y_q''(1-\xi)\sin(m\pi\xi)d\xi - 2\left(\frac{q\pi}{2}\right)^2(-1)^{\left(\frac{q-1}{2}\right)}\int_0^1 Y_q(1-\xi)\sin(m\pi\xi)d\xi$$

Case 1 Term

$$d_{mq} = 2(-1)^{\left(\frac{q-1}{2}\right)}\left[\left(\nu\phi^2\left(\beta_q^2-\gamma_q^2\right)-\left(\frac{q\pi}{2}\right)^2\right)B_q + 2\nu\phi^2\beta_q\gamma_q C_q\right]\int_0^1 \sinh(\beta_q(1-\xi))\cos(\gamma_q(1-\xi))\sin(m\pi\xi)\,d\xi$$

$$+ 2(-1)^{\left(\frac{q-1}{2}\right)}\left[\left(\nu\phi^2\left(\beta_q^2-\gamma_q^2\right)-\left(\frac{q\pi}{2}\right)^2\right)C_q - 2\nu\phi^2\beta_q\gamma_q B_q\right]\int_0^1 \cosh(\beta_q(1-\xi))\sin(\gamma_q(1-\xi))\sin(m\pi\xi)\,d\xi$$

Case 2 Term

$$d_{mq} = 2(-1)^{\left(\frac{q-1}{2}\right)}\left(\nu\phi^2\beta_q^2-\left(\frac{q\pi}{2}\right)^2\right)A_q\int_0^1 \sinh(\beta_q(1-\xi))\sin(m\pi\xi)\,d\xi$$

$$- 2(-1)^{\left(\frac{q-1}{2}\right)}\left(\nu\phi^2\gamma_q^2+\left(\frac{q\pi}{2}\right)^2\right)C_q\int_0^1 \sin(\gamma_q(1-\xi))\sin(m\pi\xi)\,d\xi$$

Case 3 Term

$$d_{mq} = 2(-1)^{\left(\frac{q-1}{2}\right)}\left(\nu\phi^2\beta_q^2-\left(\frac{q\pi}{2}\right)^2\right)A_q\int_0^1 \sinh(\beta_q(1-\xi))\sin(m\pi\xi)\,d\xi$$

$$+ 2(-1)^{\left(\frac{q-1}{2}\right)}\left(\nu\phi^2\gamma_q^2-\left(\frac{q\pi}{2}\right)^2\right)C_q\int_0^1 \sinh(\gamma_q(1-\xi))\sin(m\pi\xi)\,d\xi$$

Case 4 Term

$$d_{mq} = -2(-1)^{\left(\frac{q-1}{2}\right)}\left(\nu\phi^2\beta_q^2+\left(\frac{q\pi}{2}\right)^2\right)A_q\int_0^1 \sin(\beta_q(1-\xi))\sin(m\pi\xi)\,d\xi$$

$$- 2(-1)^{\left(\frac{q-1}{2}\right)}\left(\nu\phi^2\gamma_q^2+\left(\frac{q\pi}{2}\right)^2\right)C_q\int_0^1 \sin(\gamma_q(1-\xi))\sin(m\pi\xi)\,d\xi$$

A.8.2 Slope at $\xi = 1$.

General Term

$$h_q = -Y_q'(0)$$

Case 1 Term

$$h_q = -B_q\beta_q - C_q\gamma_q$$

Case 2 Term

$$h_q = -A_q\beta_q - C_q\gamma_q$$

Case 3 Term

$$h_q = -A_q\beta_q - C_q\gamma_q$$

Case 4 Term

$$h_q = -A_q\beta_q - C_q\gamma_q$$

A.8.3 Slope at $\eta = 0$.

General Term

$$l_{mq} = q\pi\int_0^1 Y_q(1-\xi)\sin(m\pi\xi)\,d\xi$$

Case 1 Term

$$l_{mq} = q\pi\left[B_q\int_0^1 \sinh(\beta_q(1-\xi))\cos(\gamma_q(1-\xi))\sin(m\pi\xi)\,d\xi\right.$$

$$\left.+\,C_q\int_0^1 \cosh(\beta_q(1-\xi))\sin(\gamma_q(1-\xi))\sin(m\pi\xi)\,d\xi\right]$$

Case 2 Term

$$I_{mq} = q\pi\left[A_q\int_0^1 \sinh(\beta_q(1-\xi))\sin(m\pi\xi)\,d\xi + C_q\int_0^1 \sin(\gamma_q(1-\xi))\sin(m\pi\xi)\,d\xi\right]$$

Case 3 Term

$$I_{mq} = q\pi\left[A_q\int_0^1 \sinh(\beta_q(1-\xi))\sin(m\pi\xi)\,d\xi + C_q\int_0^1 \sinh(\gamma_q(1-\xi))\sin(m\pi\xi)\,d\xi\right]$$

Case 4 Term

$$I_{mq} = q\pi\left[A_q\int_0^1 \sin(\beta_q(1-\xi))\sin(m\pi\xi)\,d\xi + C_q\int_0^1 \sin(\gamma_q(1-\xi))\sin(m\pi\xi)\,d\xi\right]$$

A.8.4 Slope at $\xi = 0$.

General Term

$$v_q = -Y_q'(1)$$

Case 1 Term

$$v_q = -(C_q\beta_q - B_q\gamma_q)\sinh(\beta_q)\sin(\gamma_q) - (B_q\beta_q + C_q\gamma_q)\cosh(\beta_q)\cos(\gamma_q)$$

Case 2 Term

$$v_q = -A_q\beta_q\cosh(\beta_q) - C_q\gamma_q\cos(\gamma_q)$$

Case 3 Term

$$v_q = -A_q\beta_q\cosh(\beta_q) - C_q\gamma_q\cosh(\gamma_q)$$

Case 4 Term

$$v_q = -A_q\beta_q\cos(\beta_q) - C_q\gamma_q\cos(\gamma_q)$$

Appendix B
List of Solved Integrals

The following integrals are used in the definitions of the building block contributions listed in appendix A. Integrals enter the superimposed solution when building block solutions must be expanded in Fourier series.

$$\int_0^1 \cos(Ax)\,dx = \frac{\sin(A)}{A}$$

$$\int_0^1 \cosh(Ax)\,dx = \frac{\sinh(A)}{A}$$

$$\int_0^1 \cos(A(1-x))\,dx = \int_0^1 \cos(Ax)\,dx$$

$$\int_0^1 \cosh(A(1-x))\,dx = \int_0^1 \cosh(Ax)\,dx$$

$$\int_0^1 \sin(Ax)\sin(Bx)\,dx = \frac{A\cos(A)\sin(B) - B\sin(A)\cos(B)}{B^2 - A^2}$$

$$\int_0^1 \sin(Ax)\cos(Bx)\,dx = \frac{A\cos(A)\cos(B) + B\sin(A)\sin(B) - A}{B^2 - A^2}$$

$$\int_0^1 \cos(Ax)\cos(Bx)\,dx = \frac{1}{2}\int_0^1 \cos((A+B)x)\,dx + \frac{1}{2}\int_0^1 \cos((A-B)x)\,dx$$

$$\int_0^1 \sinh(Ax)\sin(Bx)\,dx = \frac{A\cosh(A)\sin(B) - B\sinh(A)\cos(B)}{A^2 + B^2}$$

$$\int_0^1 \sinh(Ax)\cos(Bx)\,dx = \frac{A\cosh(A)\cos(B) + B\sinh(A)\sin(B) - A}{A^2 + B^2}$$

$$\int_0^1 \cosh(Ax)\sin(Bx)\,dx = \frac{A\sinh(A)\sin(B) - B\cosh(A)\cos(B) + B}{A^2 + B^2}$$

$$\int_0^1 \cosh(Ax)\cos(Bx)\,dx = \frac{A\sinh(A)\cos(B) + B\cosh(A)\sin(B)}{A^2 + B^2}$$

$$\int_0^1 \sinh(Ax)\sin(Bx)\sin(Cx)\,dx = \frac{1}{2}\int_0^1 \sinh(Ax)\cos((B-C)x)\,dx - \frac{1}{2}\int_0^1 \sinh(Ax)\cos((B+C)x)\,dx$$

$$\int_0^1 \sinh(Ax)\sin(Bx)\cos(Cx)\,dx = \frac{1}{2}\int_0^1 \sinh(Ax)\sin((B+C)x)\,dx + \frac{1}{2}\int_0^1 \sinh(Ax)\sin((B-C)x)\,dx$$

$$\int_0^1 \sinh(Ax)\cos(Bx)\cos(Cx)\,dx = \frac{1}{2}\int_0^1 \sinh(Ax)\cos((B+C)x)\,dx + \frac{1}{2}\int_0^1 \sinh(Ax)\cos((B-C)x)\,dx$$

$$\int_0^1 \cosh(Ax)\sin(Bx)\sin(Cx)\,dx = \frac{1}{2}\int_0^1 \cosh(Ax)\cos((B-C)x)\,dx - \frac{1}{2}\int_0^1 \cosh(Ax)\cos((B+C)x)\,dx$$

$$\int_0^1 \cosh(Ax)\sin(Bx)\cos(Cx)\,dx = \frac{1}{2}\int_0^1 \cosh(Ax)\sin((C+B)x)\,dx - \frac{1}{2}\int_0^1 \cosh(Ax)\sin((C-B)x)\,dx$$

$$\int_0^1 \cosh(Ax)\cos(Bx)\cos(Cx)\,dx = \frac{1}{2}\int_0^1 \cosh(Ax)\cos((B+C)x)\,dx + \frac{1}{2}\int_0^1 \cosh(Ax)\cos((B-C)x)\,dx$$

$$\int_0^1 \sin(A(1-x))\sin(Bx)\,dx = \sin(A)\int_0^1 \sin(Bx)\cos(Ax)\,dx - \cos(A)\int_0^1 \sin(Ax)\sin(Bx)\,dx$$

$$\int_0^1 \cos(A(1-x))\sin(Bx)\,dx = \cos(A)\int_0^1 \sin(Bx)\cos(Ax)\,dx + \sin(A)\int_0^1 \sin(Ax)\sin(Bx)\,dx$$

$$\int_0^1 \cos(A(1-x))\cos(Bx)\,dx = \cos(A)\int_0^1 \cos(Ax)\cos(Bx)\,dx + \sin(A)\int_0^1 \sin(Ax)\cos(Bx)\,dx$$

$$\int_0^1 \sinh(A(1-x))\sin(Bx)\,dx = \sin(B)\int_0^1 \sinh(Ax)\cos(Bx)\,dx - \cos(B)\int_0^1 \sinh(Ax)\sin(Bx)\,dx$$

$$\int_0^1 \cosh(A(1-x))\sin(Bx)\,dx = \sin(B)\int_0^1 \cosh(Ax)\cos(Bx)\,dx - \cos(B)\int_0^1 \cosh(Ax)\sin(Bx)\,dx$$

$$\int_0^1 \cosh(A(1-x))\cos(Bx)\,dx = \sin(B)\int_0^1 \cosh(Ax)\sin(Bx)\,dx + \cos(B)\int_0^1 \cosh(Ax)\cos(Bx)\,dx$$

$$\int_0^1 \sinh(A(1-x))\sin(B(1-x))\,dx = \int_0^1 \sinh(Ax)\sin(Bx)\,dx$$

$$\int_0^1 \cosh(A(1-x))\cos(B(1-x))\,dx = \int_0^1 \cosh(Ax)\cos(Bx)\,dx$$

$$\int_0^1 \sinh(A(1-x))\sin(B(1-x))\sin(Cx)\,dx =$$

$$\sin(C)\int_0^1 \sinh(Ax)\sin(Bx)\cos(Cx)\,dx - \cos(C)\int_0^1 \sinh(Ax)\sin(Bx)\sin(Cx)\,dx$$

$$\int_0^1 \sinh(A(1-x))\sin(B(1-x))\cos(Cx)\,dx =$$

$$\cos(C)\int_0^1 \sinh(Ax)\sin(Bx)\cos(Cx)\,dx + \sin(C)\int_0^1 \sinh(Ax)\sin(Bx)\sin(Cx)\,dx$$

$$\int_0^1 \sinh(A(1-x))\cos(B(1-x))\sin(Cx)\,dx =$$

$$\sin(C)\int_0^1 \sinh(Ax)\cos(Bx)\cos(Cx)\,dx - \cos(C)\int_0^1 \sinh(Ax)\cos(Bx)\sin(Cx)\,dx$$

$$\int_0^1 \cosh(A(1-x))\sin(B(1-x))\sin(Cx)\,dx =$$

$$\sin(C)\int_0^1 \cosh(Ax)\sin(Bx)\cos(Cx)\,dx - \cos(C)\int_0^1 \cosh(Ax)\sin(Bx)\sin(Cx)\,dx$$

$$\int_0^1 \cosh(A(1-x))\cos(B(1-x))\sin(Cx)\,dx =$$

$$\sin(C)\int_0^1 \cosh(Ax)\cos(Bx)\cos(Cx)\,dx - \cos(C)\int_0^1 \cosh(Ax)\cos(Bx)\sin(Cx)\,dx$$

$$\int_0^1 \cosh(A(1-x))\cos(B(1-x))\cos(Cx)\,dx =$$

$$\cos(C)\int_0^1 \cosh(Ax)\cos(Bx)\cos(Cx)\,dx + \sin(C)\int_0^1 \cosh(Ax)\cos(Bx)\sin(Cx)\,dx$$

Appendix C
FEM Analysis Details

Four node elastic quadrilateral shell elements are utilized in the FEM analyses. Shear deflection is not included in this thin-shell element which has 6 degrees of freedom per node: translations and rotations for the 3 global coordinate directions. The element features stress stiffening and large deflection capabilities. Normal and in-plane loadings are permitted. Note that pressure loads are converted into equivalent nodal forces and that both membrane and bending stiffnesses are used in the solution. All parameters are defined using the following system of units: ft, s, lb. Lateral plate dimensions are selected using aspect ratios and a minimum edge length of 1 ft. For example, a plate of aspect ratio 2/3 will be 1.5 ft long in the x-direction and 1 ft long in the y-direction. All plates are 1/8 in thick. Material properties are chosen so that the FEM results can be converted to a dimensionless format with a minimum amount of effort. For plate buckling,

$$P_\xi = b\, P_x\,,$$

where P_x is calculated by ANSYS [18]. For plate free vibration,

$$\lambda^2 = 2\,\pi\, f\, a^2\,,$$

where f is calculated by ANSYS [18].

The following files were used to obtain FEM results for plate buckling and vibration. All ANSYS [18] jobs were executed on the Babcock & Wilcox HP735 workstation platforms in accordance with quality assurance procedures. The parameters listed in Table C.1 are used in the FEM model and in calculations.

Table C.1 Parameters used in the FEM analyses.

Parameter	Description	Number	Unit (SI)
a	Plate length along x-axis	1, 1.5, 2, 2.5, 3	ft (m)
b	Plate length along y-axis	1, 1.5, 2, 2.5, 3	ft (m)
t	Plate thickness	$1 / (8 \times 12)$	ft (m)
E	Modulus of elasticity	9439542.1	lb / ft^2 (N / m^2)
ν	Poisson's ratio	0.333	-
ρ	Density	8×12	$lb\ s^2 / ft^4$ (kg / m^2)
D	Plate flexural rigidity	1	lb ft (N m)
P_x	Total load in x-direction	-	lb (N)
f	Frequency	-	Hz
P_ξ	Dimensionless in-plane load	$P_x\ b$	-
λ^2	Eigenvalue	$2 \pi f a^2$	-

```
! PB.INP - ANSYS 5.2 Input File
! Buckling analysis of thin rectangular plates.
! Warning - Boundary conditions must be saved
!           in bc.inp prior to execution.

/batch
phi=
*dim,phi,array,9       ! Plate aspect ratios.
phi(1)=1/3
phi(2)=2/5
phi(3)=1/2
phi(4)=2/3
phi(5)=1
phi(6)=3/2
phi(7)=2
phi(8)=5/2
phi(9)=3
t=1/8/12               ! Plate thickness (ft).
divx=30                ! Divisions along x-axis.
divy=30                ! Divisions along y-axis.
*do,i,1,9
/gopr
parsav,all
/clear,nostart
parres,new
*if,phi(i),ge,1,then
a=1                    ! Plate edge lengths (ft).
b=phi(i)               ! Shorter edge is 1 ft.
*else                  ! Remaining edge satisfies
a=1/phi(i)             ! plate aspect ratio.
b=1
*endif
/prep7
k,1                    ! Keypoints.
k,2,a
k,3,,b
k,4,a,b
l,1,2                  ! Lines.
l,3,4
l,1,3
l,2,4
lsel,s,line,,1,2       ! Line divisions for elements.
lesize,all,,,divx
lsel,inve
lesize,all,,,divy
lsel,all
a,1,2,4,3              ! Area.
et,1,shell63           ! 4 node shell element.
mp,ex,1,9439542.1      ! Modulus of elasticity (lb / ft2).
mp,nuxy,1,0.333        ! Poisson's ratio.
r,1,t                  ! Element real constants.
amesh,all              ! Mesh area into 900 elements.
bc=0
/inp,bc,inp            ! Plate boundary conditions.
*if,bc,ne,1,then
fini
/exit,nosave
*endif
nsel,s,loc,x,a
sf,all,pres,1/b        ! Unit in-plane load (lb / in).
nsel,all
/view,,1,1,-1          ! Model viewing options.
/psf,pres,2
```

```
/pbc,u,,1
/pbc,rot,,1
fini
/solu
sstif,on
antype,static          ! Static analysis.
solve
fini
/solu
antype,buckle          ! Buckling analysis.
pstres,on
bucopt,subsp,2         ! First 2 modes of buckling.
total
outpr
solve
fini
/solu
expass,on
mxpand
outpr
solve
fini
/post1
/out,pcrit,out,,append
set,list               ! Write load factors (lb)
/out                   ! to file pcrit.out.
fini
*enddo
! PB.INP - END
```

```
! PV.INP - ANSYS 5.2 Input File
! Free vibration analysis of thin rectangular plates.
! Warning - Boundary conditions must be saved in
!           bc.inp prior to execution and buckling
!           loads must be saved in pbl.inp.

/batch
pbl=
*dim,pbl,array,9
/inp,pbl,inp           ! Buckling loads (lb).
phi=
*dim,phi,array,9       ! Plate aspect ratios.
phi(1)=1/3
phi(2)=2/5
phi(3)=1/2
phi(4)=2/3
phi(5)=1
phi(6)=3/2
phi(7)=2
phi(8)=5/2
phi(9)=3
pc=
*dim,pc,array,9        ! In-plane load factors.
pc(1)=-1
pc(2)=-0.5
pc(3)=0
pc(4)=0.2
pc(5)=0.4
pc(6)=0.6
```

```
pc(7)=0.8
pc(8)=0.9
pc(9)=0.99
t=1/8/12                ! Plate thickness (ft).
divx=30                 ! Divisions along x-axis.
divy=30                 ! Divisions along y-axis.
*do,i,1,9
/gopr
parsav,all
/clear,nostart
parres,new
*if,phi(i),ge,1,then
a=1                     ! Plate edge lengths (ft).
b=phi(i)                ! Shorter edge is 1 ft.
*else                   ! Remaining edge satisfies
a=1/phi(i)              ! plate aspect ratio.
b=1
*endif
/prep7
k,1                     ! Keypoints.
k,2,a
k,3,,b
k,4,a,b
l,1,2                   ! Lines.
l,3,4
l,1,3
l,2,4
lsel,s,line,,1,2        ! Line divisions for elements.
lesize,all,,,divx
lsel,inve
lesize,all,,,divy
lsel,all
a,1,2,4,3               ! Area.
et,1,shell63            ! 4 node shell element.
mp,ex,1,9439542.1       ! Modulus of elasticity (lb / ft2).
mp,nuxy,1,0.333         ! Poisson's ratio.
mp,dens,1,1/t           ! Density (lb s2 / ft4).
r,1,t                   ! Element real constants.
amesh,all               ! Mesh area into 900 elements.
bc=0
/inp,bc,inp             ! Plate boundary conditions.
*if,bc,ne,1,then
fini
/exit,nosave
*endif
fini
save
*do,j,1,9
/gopr
parsav,all
/clear,nostart
resume
parres,new
px=pc(j)*pbl(i)         ! In-plane load.
*if,px,ne,0,then        ! Plate pre-stressing to
/solu                   ! account for in-plane load.
nsel,s,loc,x,a
*if,j,gt,1,then
sfdel,all,pres
*endif
sf,all,pres,px/b        ! In-plane load (lb / in).
nsel,all
sstif,on
```

```
pstres,on
antype,static,new
solve
fini
*endif
/solu
antype,modal,new    ! Modal analysis.
modopt,subsp,9,,,on ! Find 9 modes of vibration.
*if,px,ne,0,then
pstres,on
*else
pstres,off
*endif
total
mode
outpr
mxpand
solve
fini
/post1
/out,freq,out,,append
set,list            ! Write frequencies (Hz) to
/out                ! file freq.out.
fini
*enddo
*enddo
! PV.INP - END
```

```
! CCCFBC - ANSYS 5.2 Input File
! Boundary conditions for the CCCF plate.

bc=1
nsel,s,loc,x,0
d,all,ux
d,all,uz
d,all,roty
nsel,s,loc,y,0
d,all,uy
d,all,uz
d,all,rotx
nsel,s,loc,x,a
d,all,uz
d,all,roty
nsel,all
! CCCFBC - END
```

```
! CFCFBC - ANSYS 5.2 Input File
! Boundary conditions for the CFCF plate.

bc=1
nsel,s,loc,x,0
d,all,ux
d,all,uz
d,all,roty
nsel,r,loc,y,b/2
d,all,uy
nsel,s,loc,x,a
d,all,uz
d,all,roty
nsel,r,loc,y,b/2
d,all,uy
nsel,all
! CFCFBC - END
```

```
! CSCFBC - ANSYS 5.2 Input File
! Boundary conditions for the CSCF plate.

bc=1
nsel,s,loc,x,0
d,all,ux
d,all,uz
d,all,roty
nsel,s,loc,y,0
d,all,uy
d,all,uz
nsel,s,loc,x,a
d,all,uz
d,all,roty
nsel,all
! CSCFBC - END
```

```
! SCCFBC - ANSYS 5.2 Input File
! Boundary conditions for the SCCF plate.

bc=1
nsel,s,loc,x,0
d,all,ux
d,all,uz
nsel,s,loc,y,0
d,all,uy
d,all,uz
d,all,rotx
nsel,s,loc,x,a
d,all,uz
d,all,roty
nsel,all
! SCCFBC - END
```

```
! SCSFBC - ANSYS 5.2 Input File
! Boundary conditions for the SCSF plate.

bc=1
nsel,s,loc,x,0
d,all,ux
d,all,uz
nsel,s,loc,y,0
d,all,uy
d,all,uz
d,all,rotx
nsel,s,loc,x,a
d,all,uz
nsel,all
! SCSFBC - END
```

```
! SFCFBC - ANSYS 5.2 Input File
! Boundary conditions for the SFCF plate.

bc=1
nsel,s,loc,x,0
d,all,ux
d,all,uz
nsel,r,loc,y,b/2
d,all,uy
nsel,s,loc,x,a
d,all,uz
d,all,roty
nsel,r,loc,y,b/2
d,all,uy
nsel,all
! SFCFBC - END
```

```
! SFSFBC - ANSYS 5.2 Input File
! Boundary conditions for the SFSF plate.

bc=1
nsel,s,loc,x,0
d,all,ux
d,all,uz
nsel,r,loc,y,b/2
d,all,uy
nsel,s,loc,x,a
d,all,uz
nsel,r,loc,y,b/2
d,all,uy
nsel,all
! SFSFBC - END
```

```
! SSCFBC - ANSYS 5.2 Input File
! Boundary conditions for the SSCF plate.

bc=1
nsel,s,loc,x,0
d,all,ux
d,all,uz
nsel,s,loc,y,0
d,all,uy
d,all,uz
nsel,s,loc,x,a
d,all,uz
d,all,roty
nsel,all
! SSCFBC - END
```

```
! SSSFBC - ANSYS 5.2 Input File
! Boundary conditions for the SSSF plate.

bc=1
nsel,s,loc,x,0
d,all,ux
d,all,uz
nsel,s,loc,y,0
d,all,uy
d,all,uz
nsel,s,loc,x,a
d,all,uz
nsel,all
! SSSFBC - END
```

Appendix D

FORTRAN Program Listing

```
C23456789012345678901234567890123456789012345678901234567890123456789012

C     This program calculates eigenvalues, mode shapes, and
C     buckling loads for the following plates:  CCCF, CFCF, CSCF,
C     SCCF, SCSF, SFCF, SFSF, SSSF, and SSCF.  The method of
C     analysis involves the superposition of the following
C     building block solutions:  SSSV, SSWR, SWSR, WSSR,
C     SRSV, SRWR, SVSR, and WRSR.  The building block solutions
C     are of the Levy-type, and Fourier coefficients in the trigenometric
C     series are adjusted to satisfy the plate's boundary conditions.
C     Scans give three decimals of accuracy by use of the numerical
C     bisection method.  Poisson's ratio (v) is set to 0.333.  The in-plane
C     loads (Px) are dimensionless and compression is positive.
C     The number of terms in a series (k) is limited from 1 to 30.
C     Shape matrices are limited in size (div) from 4x4 to 30x30.

      double precision phi,v,Px,sta,fin,inc,L2,det
      double precision x1,x2,y1,y2,xm,ym,dr
      integer job,k,counter,div,plate,n

      v=0.333d0
      dr=0.2d0/2.0d0
      n=ifix(alog(20000.0*sngl(dr))/alog(2.0)+0.99999)
100   write(6,*) '1.  CCCF (clamped-clamped-clamped-free) plate.'
      write(6,*) '2.  CFCF (clamped-free-clamped-free) plate.'
      write(6,*) '3.  CSCF (clamped-simply-clamped-free) plate.'
      write(6,*) '4.  SCCF (simple-clamped-clamped-free) plate.'
      write(6,*) '5.  SCSF (simple-clamped-simple-free) plate.'
      write(6,*) '6.  SFCF (simple-free-clamped-free) plate.'
      write(6,*) '7.  SFSF (simple-free-simple-free) plate.'
      write(6,*) '8.  SSCF (simple-simple-clamped-free) plate.'
      write(6,*) '9.  SSSF (simple-simple-simple-free) plate.'
      write(6,*) ' '
      read(5,*) plate
      if ((plate.gt.9).or.(plate.lt.1)) goto 100

1     write(6,*) '1.  Eigenvalue vs. Determinant Value listing.'
      write(6,*) '2.  Exact eigenvalue scan given approximate value.'
      write(6,*) '3.  Generate shape given exact eigenvalue.'
      write(6,*) '4.  Buckling Load vs. Determinant Value listing.'
      write(6,*) '5.  Exact buckling load scan given approximate value.'
      write(6,*) '6.  Plate menu.'
      write(6,*) '7.  Quit program.'
      write(6,*) ' '
      read(5,*) job
      if ((job.gt.7).or.(job.lt.1)) goto 1
      if (job.eq.2) goto 20
      if (job.eq.3) goto 30
      if (job.eq.4) goto 40
      if (job.eq.5) goto 50
      if (job.eq.6) goto 100
      if (job.eq.7) goto 60

10    write(6,*) 'Enter phi, Px, and k.'
      write(6,*) ' '
      read(5,*) phi,Px,k
      if (k.gt.30) k=30
      if (k.lt.2) k=2
11    write(6,*) 'Enter sta, fin, and inc for the range of L2.'
      write(6,*) ' '
      read(5,*) sta,fin,inc
      write(6,*) '    L2     det(L2)'
      do 12 L2=sta,fin,inc
```

```
        write(6,13) L2,det(phi,v,Px,L2,k,plate)
 12     continue
 13     format(1x,f8.4,e12.4)
        write(6,*) ' '
 14     write(6,*) '1.  Look at another range of eigenvalues using the sam
     2e parameters.'
        write(6,*) '2.  Look at another range of eigenvalues using differe
     2nt parameters.'
        write(6,*) '3.  Scan for an exact eigenvalue.'
        write(6,*) '4.  Return to main menu.'
        write(6,*) ' '
        read(5,*) job
        if ((job.gt.4).or.(job.lt.1)) goto 14
        if (job.eq.1) goto 11
        if (job.eq.2) goto 10
        if (job.eq.3) goto 21
        goto 1

 20     write(6,*) 'Enter phi, Px, and k.'
        write(6,*) ' '
        read(5,*) phi,Px,k
        if (k.gt.30) k=30
        if (k.lt.2) k=2
 21     write(6,*) 'Enter L2.'
        write(6,*) '(Note that L2 must be within 0.1 of the exact value.)'
c       See value of dr above.
        write(6,*) ' '
        read(5,*) L2
        x1=L2-dr
        y1=det(phi,v,Px,x1,k,plate)
        x2=L2+dr
        y2=det(phi,v,Px,x2,k,plate)
        do 22 counter=1,n
          xm=(x1+x2)/2
          ym=det(phi,v,Px,xm,k,plate)
          if (y1*ym.lt.0) then
            y2=ym
            x2=xm
          else
            y1=ym
            x1=xm
          endif
 22     continue
        if (dabs(y1).lt.dabs(y2)) then
          xm=x1
        else
          xm=x2
        endif
        write(6,23) xm
 23     format(1x,'L2 = ',f8.4)
        write(6,*) ' '
 24     write(6,*) '1.  Find another eigenvalue using the same parameters.
     2'
        write(6,*) '2.  Find another eigenvalue using different parameters
     2.'
        write(6,*) '3.  Return to main menu.'
        write(6,*) ' '
        read(5,*) job
        if ((job.gt.3).or.(job.lt.1)) goto 24
        if (job.eq.1) goto 21
        if (job.eq.2) goto 20
        goto 1
```

```
30    write(6,*) 'Enter phi, Px, k, and div.'
      write(6,*) ' '
      read(5,*) phi,Px,k,div
      if (k.gt.30) k=30
      if (k.lt.2) k=2
      if (div.gt.30) div=30
      if (div.lt.4) div=4
31    write(6,*) 'Enter L2.'
      write(6,*) ' '
      read(5,*) L2
      call shape(phi,v,Px,L2,k,div,plate)
32    write(6,*) '1.  Find another shape using the same parameters.'
      write(6,*) '2.  Find another shape using different parameters.'
      write(6,*) '3.  Return to main menu.'
      write(6,*) ' '
      read(5,*) job
      if ((job.gt.3).or.(job.lt.1)) goto 32
      if (job.eq.1) goto 31
      if (job.eq.2) goto 30
      goto 1

40    write(6,*) 'Enter phi and k.'
      write(6,*) ' '
      read(5,*) phi,k
      if (k.gt.30) k=30
      if (k.lt.2) k=2
41    write(6,*) 'Enter sta, fin, and inc for the range of Px.'
      write(6,*) '(Note that L2 is set to zero.)'
      write(6,*) ' '
      read(5,*) sta,fin,inc
      L2=1.0d-6
      write(6,*) '    Px     det(Px)'
      do 42 Px=sta,fin,inc
        write(6,43) Px,det(phi,v,Px,L2,k,plate)
42    continue
43    format(1x,f8.4,e12.4)
      write(6,*) ' '
44    write(6,*) '1.  Look at another range of loads using the same para
     2meters.'
      write(6,*) '2.  Look at another range of loads using different par
     2ameters.'
      write(6,*) '3.  Scan for an exact buckling load.'
      write(6,*) '4.  Return to main menu.'
      write(6,*) ' '
      read(5,*) job
      if ((job.gt.4).or.(job.lt.1)) goto 44
      if (job.eq.1) goto 41
      if (job.eq.2) goto 40
      if (job.eq.3) goto 51
      goto 1

50    write(6,*) 'Enter phi and k.'
      write(6,*) ' '
      read(5,*) phi,k
      if (k.gt.30) k=30
      if (k.lt.2) k=2
51    write(6,*) 'Enter Px.'
      write(6,*) '(Note that Px must be within 0.1 of the exact value.)'
C     See value of dr above.
      write(6,*) ' '
      read(5,*) Px
      L2=1.0d-6
      x1=Px-dr
```

```
      y1=det(phi,v,x1,L2,k,plate)
      x2=Px+dr
      y2=det(phi,v,x2,L2,k,plate)
      do 52 counter=1,n
        xm=(x1+x2)/2
        ym=det(phi,v,xm,L2,k,plate)
        if (y1*ym.lt.0) then
          y2=ym
          x2=xm
        else
          y1=ym
          x1=xm
        endif
52    continue
      if (dabs(y1).lt.dabs(y2)) then
        xm=x1
      else
        xm=x2
      endif
      write(6,53) xm
53    format(1x,'Pcrit = ',f8.4)
      write(6,*) ' '
54    write(6,*) '1.  Find another buckling load using the same paramete
     2rs.'
      write(6,*) '2.  Find another buckling load using different paramet
     2ers.'
      write(6,*) '3.  Return to main menu.'
      write(6,*) ' '
      read(5,*) job
      if ((job.gt.3).or.(job.lt.1)) goto 54
      if (job.eq.1) goto 51
      if (job.eq.2) goto 50
      goto 1
60    end


      function det(phi,v,Px,L2,k,plate)
      double precision det,phi,v,Px,L2
      double precision A(120,120),temp,sign
      integer i,j,k,l,row,plate,nbb

      if (plate.eq.1) call CCCF(phi,v,Px,L2,k,A)
      if (plate.eq.2) call CFCF(phi,v,Px,L2,k,A)
      if (plate.eq.3) call CSCF(phi,v,Px,L2,k,A)
      if (plate.eq.4) call SCCF(phi,v,Px,L2,k,A)
      if (plate.eq.5) call SCSF(phi,v,Px,L2,k,A)
      if (plate.eq.6) call SFCF(phi,v,Px,L2,k,A)
      if (plate.eq.7) call SFSF(phi,v,Px,L2,k,A)
      if (plate.eq.8) call SSCF(phi,v,Px,L2,k,A)
      if (plate.eq.9) call SSSF(phi,v,Px,L2,k,A)
      if (plate.eq.1) nbb=4
      if (plate.eq.2) nbb=4
      if (plate.eq.3) nbb=3
      if (plate.eq.4) nbb=3
      if (plate.eq.5) nbb=2
      if (plate.eq.6) nbb=3
      if (plate.eq.7) nbb=2
      if (plate.eq.8) nbb=2
      if (plate.eq.9) nbb=1
      sign=1
      do 10 i=1,nbb*k-1
        temp=0
        do 20 j=i,nbb*k
```

```
          if (dabs(A(j,i)).gt.dabs(temp)) then
            temp=A(j,i)
            row=j
          endif
 20     continue
        if (temp.eq.0) goto 15
        if (i.ne.row) then
          sign=-sign
          do 30 j=1,nbb*k
            temp=A(i,j)
            A(i,j)=A(row,j)
            A(row,j)=temp
 30       continue
        endif
        do 35 j=i+1,nbb*k
          temp=A(j,i)/A(i,i)
          do 35 l=i,nbb*k
            A(j,l)=A(j,l)-temp*A(i,l)
 35     continue
 15    continue
 10   continue
      det=sign
      do 40 i=1,nbb*k
        det=det*A(i,i)
 40   continue
      return
      end


      subroutine CCCF(phi,v,Px,L2,k,A)
      double precision phi,v,Px,L2,A(120,120),coef
      integer i,j,k,m,n

      do 10 i=1,4*k
        do 10 j=1,4*k
          A(i,j)=0
 10   continue
      do 20 i=1,k
        m=i
        n=2*i-1
        call SSSV(phi,v,Px,L2,m,n,2,coef)
        A(i+k,i)=coef
        call SSSV(phi,v,Px,L2,m,n,4,coef)
        A(i+3*k,i)=coef
        call SSWR(phi,v,Px,L2,m,n,1,coef)
        A(i,i+k)=coef
        call SSWR(phi,v,Px,L2,m,n,3,coef)
        A(i+2*k,i+k)=coef
        call SWSR(phi,v,Px,L2,m,n,2,coef)
        A(i+k,i+2*k)=coef
        call SWSR(phi,v,Px,L2,m,n,4,coef)
        A(i+3*k,i+2*k)=coef
        call WSSR(phi,v,Px,L2,m,n,1,coef)
        A(i,i+3*k)=coef
        call WSSR(phi,v,Px,L2,m,n,3,coef)
        A(i+2*k,i+3*k)=coef
        do 20 j=1,k
          m=i
          n=2*j-1
          call SSWR(phi,v,Px,L2,m,n,2,coef)
          A(i+k,j+k)=coef
          call SSWR(phi,v,Px,L2,m,n,4,coef)
          A(i+3*k,j+k)=coef
```

```
         call WSSR(phi,v,Px,L2,m,n,2,coef)
         A(i+k,j+3*k)=coef
         call WSSR(phi,v,Px,L2,m,n,4,coef)
         A(i+3*k,j+3*k)=coef
         m=j
         n=2*i-1
         call SSSV(phi,v,Px,L2,m,n,1,coef)
         A(i,j)=coef
         call SSSV(phi,v,Px,L2,m,n,3,coef)
         A(i+2*k,j)=coef
         call SWSR(phi,v,Px,L2,m,n,1,coef)
         A(i,j+2*k)=coef
         call SWSR(phi,v,Px,L2,m,n,3,coef)
         A(i+2*k,j+2*k)=coef
20    continue
      return
      end


      subroutine CFCF(phi,v,Px,L2,k,A)
      double precision phi,v,Px,L2,A(120,120),coef
      integer i,j,k,m,n

      do 10 i=1,4*k
        do 10 j=1,4*k
          A(i,j)=0
10    continue
      do 20 i=1,k
        m=i
        n=i-1
        call SRSV(phi,v,Px,L2,m,n,2,coef)
        A(i+k,i)=coef
        call SRSV(phi,v,Px,L2,m,n,4,coef)
        A(i+3*k,i)=coef
        call SRWR(phi,v,Px,L2,m,n,1,coef)
        A(i,i+k)=coef
        call SRWR(phi,v,Px,L2,m,n,3,coef)
        A(i+2*k,i+k)=coef
        call SVSR(phi,v,Px,L2,m,n,2,coef)
        A(i+k,i+2*k)=coef
        call SVSR(phi,v,Px,L2,m,n,4,coef)
        A(i+3*k,i+2*k)=coef
        call WRSR(phi,v,Px,L2,m,n,1,coef)
        A(i,i+3*k)=coef
        call WRSR(phi,v,Px,L2,m,n,3,coef)
        A(i+2*k,i+3*k)=coef
        do 20 j=1,k
          m=i
          n=j-1
          call SRWR(phi,v,Px,L2,m,n,2,coef)
          A(i+k,j+k)=coef
          call SRWR(phi,v,Px,L2,m,n,4,coef)
          A(i+3*k,j+k)=coef
          call WRSR(phi,v,Px,L2,m,n,2,coef)
          A(i+k,j+3*k)=coef
          call WRSR(phi,v,Px,L2,m,n,4,coef)
          A(i+3*k,j+3*k)=coef
          m=j
          n=i-1
          call SRSV(phi,v,Px,L2,m,n,1,coef)
          A(i,j)=coef
          call SRSV(phi,v,Px,L2,m,n,3,coef)
          A(i+2*k,j)=coef
```

```
          call SVSR(phi,v,Px,L2,m,n,1,coef)
          A(i,j+2*k)=coef
          call SVSR(phi,v,Px,L2,m,n,3,coef)
          A(i+2*k,j+2*k)=coef
 20   continue
      return
      end


      subroutine CSCF(phi,v,Px,L2,k,A)
      double precision phi,v,Px,L2,A(120,120),coef
      integer i,j,k,m,n

      do 10 i=1,3*k
        do 10 j=1,3*k
          A(i,j)=0
 10   continue
      do 20 i=1,k
        m=i
        n=2*i-1
        call SSSV(phi,v,Px,L2,m,n,4,coef)
        A(i+2*k,i)=coef
        call SSWR(phi,v,Px,L2,m,n,1,coef)
        A(i,i+k)=coef
        call SSWR(phi,v,Px,L2,m,n,3,coef)
        A(i+k,i+k)=coef
        call WSSR(phi,v,Px,L2,m,n,1,coef)
        A(i,i+2*k)=coef
        call WSSR(phi,v,Px,L2,m,n,3,coef)
        A(i+k,i+2*k)=coef
        do 20 j=1,k
          m=i
          n=2*j-1
          call SSWR(phi,v,Px,L2,m,n,4,coef)
          A(i+2*k,j+k)=coef
          call WSSR(phi,v,Px,L2,m,n,4,coef)
          A(i+2*k,j+2*k)=coef
          m=j
          n=2*i-1
          call SSSV(phi,v,Px,L2,m,n,1,coef)
          A(i,j)=coef
          call SSSV(phi,v,Px,L2,m,n,3,coef)
          A(i+k,j)=coef
 20   continue
      return
      end


      subroutine SCCF(phi,v,Px,L2,k,A)
      double precision phi,v,Px,L2,A(120,120),coef
      integer i,j,k,m,n

      do 10 i=1,3*k
        do 10 j=1,3*k
          A(i,j)=0
 10   continue
      do 20 i=1,k
        m=i
        n=2*i-1
        call SSSV(phi,v,Px,L2,m,n,2,coef)
        A(i,i)=coef
        call SSSV(phi,v,Px,L2,m,n,4,coef)
        A(i+2*k,i)=coef
```

```
      call SSWR(phi,v,Px,L2,m,n,3,coef)
      A(i+k,i+k)=coef
      call SWSR(phi,v,Px,L2,m,n,2,coef)
      A(i,i+2*k)=coef
      call SWSR(phi,v,Px,L2,m,n,4,coef)
      A(i+2*k,i+2*k)=coef
      do 20 j=1,k
        m=i
        n=2*j-1
        call SSWR(phi,v,Px,L2,m,n,2,coef)
        A(i,j+k)=coef
        call SSWR(phi,v,Px,L2,m,n,4,coef)
        A(i+2*k,j+k)=coef
        m=j
        n=2*i-1
        call SSSV(phi,v,Px,L2,m,n,3,coef)
        A(i+k,j)=coef
        call SWSR(phi,v,Px,L2,m,n,3,coef)
        A(i+k,j+2*k)=coef
 20   continue
      return
      end


      subroutine SCSF(phi,v,Px,L2,k,A)
      double precision phi,v,Px,L2,A(120,120),coef
      integer i,j,k,m,n

      do 10 i=1,2*k
        do 10 j=1,2*k
          A(i,j)=0
 10   continue
      do 20 i=1,k
        m=i
        n=2*i-1
        call SSSV(phi,v,Px,L2,m,n,2,coef)
        A(i,i)=coef
        call SSSV(phi,v,Px,L2,m,n,4,coef)
        A(i+k,i)=coef
        call SWSR(phi,v,Px,L2,m,n,2,coef)
        A(i,i+k)=coef
        call SWSR(phi,v,Px,L2,m,n,4,coef)
        A(i+k,i+k)=coef
 20   continue
      return
      end


      subroutine SFCF(phi,v,Px,L2,k,A)
      double precision phi,v,Px,L2,A(120,120),coef
      integer i,j,k,m,n

      do 10 i=1,3*k
        do 10 j=1,3*k
          A(i,j)=0
 10   continue
      do 20 i=1,k
        m=i
        n=i-1
        call SRSV(phi,v,Px,L2,m,n,2,coef)
        A(i,i)=coef
        call SRSV(phi,v,Px,L2,m,n,4,coef)
        A(i+2*k,i)=coef
```

```
        call SRWR(phi,v,Px,L2,m,n,3,coef)
        A(i+k,i+k)=coef
        call SVSR(phi,v,Px,L2,m,n,2,coef)
        A(i,i+2*k)=coef
        call SVSR(phi,v,Px,L2,m,n,4,coef)
        A(i+2*k,i+2*k)=coef
        do 20 j=1,k
          m=i
          n=j-1
          call SRWR(phi,v,Px,L2,m,n,2,coef)
          A(i,j+k)=coef
          call SRWR(phi,v,Px,L2,m,n,4,coef)
          A(i+2*k,j+k)=coef
          m=j
          n=i-1
          call SRSV(phi,v,Px,L2,m,n,3,coef)
          A(i+k,j)=coef
          call SVSR(phi,v,Px,L2,m,n,3,coef)
          A(i+k,j+2*k)=coef
 20   continue
      return
      end


      subroutine SFSF(phi,v,Px,L2,k,A)
      double precision phi,v,Px,L2,A(120,120),coef
      integer i,j,k,m,n

      do 10 i=1,2*k
        do 10 j=1,2*k
          A(i,j)=0
 10   continue
      do 20 i=1,k
        m=i
        n=i-1
        call SRSV(phi,v,Px,L2,m,n,2,coef)
        A(i,i)=coef
        call SRSV(phi,v,Px,L2,m,n,4,coef)
        A(i+k,i)=coef
        call SVSR(phi,v,Px,L2,m,n,2,coef)
        A(i,i+k)=coef
        call SVSR(phi,v,Px,L2,m,n,4,coef)
        A(i+k,i+k)=coef
 20   continue
      return
      end


      subroutine SSCF(phi,v,Px,L2,k,A)
      double precision phi,v,Px,L2,A(120,120),coef
      integer i,j,k,m,n

      do 10 i=1,2*k
        do 10 j=1,2*k
          A(i,j)=0
 10   continue
      do 20 i=1,k
        m=i
        n=2*i-1
        call SSSV(phi,v,Px,L2,m,n,4,coef)
        A(i+k,i)=coef
        call SSWR(phi,v,Px,L2,m,n,3,coef)
        A(i,i+k)=coef
```

```
      do 20 j=1,k
        m=i
        n=2*j-1
        call SSWR(phi,v,Px,L2,m,n,4,coef)
        A(i+k,j+k)=coef
        m=j
        n=2*i-1
        call SSSV(phi,v,Px,L2,m,n,3,coef)
        A(i,j)=coef
20    continue
      return
      end


      subroutine SSSF(phi,v,Px,L2,k,A)
      double precision phi,v,Px,L2,A(120,120),coef
      integer i,j,k,m,n

      do 10 i=1,k
        do 10 j=1,k
          A(i,j)=0
10    continue
      do 20 i=1,k
        m=i
        n=2*i-1
        call SSSV(phi,v,Px,L2,m,n,4,coef)
        A(i,i)=coef
20    continue
      return
      end


      subroutine shape(phi,v,Px,L2,k,div,plate)
      double precision phi,v,Px,L2
      double precision A(120,120),C(120),S(31,31)
      integer k,div,x,y,xx,yy,plate,nbb,i,j
      character*12 name

      if (plate.eq.1) call CCCF(phi,v,Px,L2,k,A)
      if (plate.eq.2) call CFCF(phi,v,Px,L2,k,A)
      if (plate.eq.3) call CSCF(phi,v,Px,L2,k,A)
      if (plate.eq.4) call SCCF(phi,v,Px,L2,k,A)
      if (plate.eq.5) call SCSF(phi,v,Px,L2,k,A)
      if (plate.eq.6) call SFCF(phi,v,Px,L2,k,A)
      if (plate.eq.7) call SFSF(phi,v,Px,L2,k,A)
      if (plate.eq.8) call SSCF(phi,v,Px,L2,k,A)
      if (plate.eq.9) call SSSF(phi,v,Px,L2,k,A)
      if (plate.eq.1) nbb=4
      if (plate.eq.2) nbb=4
      if (plate.eq.3) nbb=3
      if (plate.eq.4) nbb=3
      if (plate.eq.5) nbb=2
      if (plate.eq.6) nbb=3
      if (plate.eq.7) nbb=2
      if (plate.eq.8) nbb=2
      if (plate.eq.9) nbb=1
      call solve(A,k*nbb,C)
      if (phi.ge.1) then
        yy=div
        xx=ifix(div/sngl(phi)+0.5)
      else
        xx=div
        yy=ifix(div*sngl(phi)+0.5)
```

```
      endif
      do 100 x=1,xx+1
       do 100 y=1,yy+1
        S(x,y)=0
 100  continue
      if (plate.eq.1) call CCCFS(phi,v,Px,L2,k,xx,yy,S,C)
      if (plate.eq.2) call CFCFS(phi,v,Px,L2,k,xx,yy,S,C)
      if (plate.eq.3) call CSCFS(phi,v,Px,L2,k,xx,yy,S,C)
      if (plate.eq.4) call SCCFS(phi,v,Px,L2,k,xx,yy,S,C)
      if (plate.eq.5) call SCSFS(phi,v,Px,L2,k,xx,yy,S,C)
      if (plate.eq.6) call SFCFS(phi,v,Px,L2,k,xx,yy,S,C)
      if (plate.eq.7) call SFSFS(phi,v,Px,L2,k,xx,yy,S,C)
      if (plate.eq.8) call SSCFS(phi,v,Px,L2,k,xx,yy,S,C)
      if (plate.eq.9) call SSSFS(phi,v,Px,L2,k,xx,yy,S,C)
      write(6,*) 'Enter the output data file name...  '
      read(5,700) name
 700  format(a12)
      open(unit=1,file=name)
      do 600 x=1,xx+1
        write(1,601) (S(x,y),y=1,yy+1)
 600  continue
 601  format(1x,31e11.3)
      close(unit=1)
      return
      end


      subroutine CCCFS(phi,v,Px,L2,k,xx,yy,S,C)
      double precision phi,v,Px,L2,S(31,31)
      double precision C(120),C1(30),C2(30),C3(30),C4(30)
      integer k,xx,yy,i
      do 10 i=1,k
        C1(i)=C(i)
        C2(i)=C(i+k)
        C3(i)=C(i+2*k)
        C4(i)=C(i+3*k)
 10   continue
      call SSSVS(phi,v,Px,L2,k,xx,yy,S,C1)
      call SSWRS(phi,v,Px,L2,k,xx,yy,S,C2)
      call SWSRS(phi,v,Px,L2,k,xx,yy,S,C3)
      call WSSRS(phi,v,Px,L2,k,xx,yy,S,C4)
      return
      end


      subroutine CFCFS(phi,v,Px,L2,k,xx,yy,S,C)
      double precision phi,v,Px,L2,S(31,31)
      double precision C(120),C1(30),C2(30),C3(30),C4(30)
      integer k,xx,yy,i
      do 10 i=1,k
        C1(i)=C(i)
        C2(i)=C(i+k)
        C3(i)=C(i+2*k)
        C4(i)=C(i+3*k)
 10   continue
      call SRSVS(phi,v,Px,L2,k,xx,yy,S,C1)
      call SRWRS(phi,v,Px,L2,k,xx,yy,S,C2)
      call SVSRS(phi,v,Px,L2,k,xx,yy,S,C3)
      call WRSRS(phi,v,Px,L2,k,xx,yy,S,C4)
      return
      end
```

```
      subroutine CSCFS(phi,v,Px,L2,k,xx,yy,S,C)
      double precision phi,v,Px,L2,S(31,31)
      double precision C(120),C1(30),C2(30),C3(30)
      integer k,xx,yy,i
      do 10 i=1,k
        C1(i)=C(i)
        C2(i)=C(i+k)
        C3(i)=C(i+2*k)
10    continue
      call SSSVS(phi,v,Px,L2,k,xx,yy,S,C1)
      call SSWRS(phi,v,Px,L2,k,xx,yy,S,C2)
      call WSSRS(phi,v,Px,L2,k,xx,yy,S,C3)
      return
      end


      subroutine SCCFS(phi,v,Px,L2,k,xx,yy,S,C)
      double precision phi,v,Px,L2,S(31,31)
      double precision C(120),C1(30),C2(30),C3(30)
      integer k,xx,yy,i
      do 10 i=1,k
        C1(i)=C(i)
        C2(i)=C(i+k)
        C3(i)=C(i+2*k)
10    continue
      call SSSVS(phi,v,Px,L2,k,xx,yy,S,C1)
      call SSWRS(phi,v,Px,L2,k,xx,yy,S,C2)
      call SWSRS(phi,v,Px,L2,k,xx,yy,S,C3)
      return
      end


      subroutine SCSFS(phi,v,Px,L2,k,xx,yy,S,C)
      double precision phi,v,Px,L2,S(31,31)
      double precision C(120),C1(30),C2(30)
      integer k,xx,yy,i
      do 10 i=1,k
        C1(i)=C(i)
        C2(i)=C(i+k)
10    continue
      call SSSVS(phi,v,Px,L2,k,xx,yy,S,C1)
      call SWSRS(phi,v,Px,L2,k,xx,yy,S,C2)
      return
      end


      subroutine SFCFS(phi,v,Px,L2,k,xx,yy,S,C)
      double precision phi,v,Px,L2,S(31,31)
      double precision C(120),C1(30),C2(30),C3(30)
      integer k,xx,yy,i
      do 10 i=1,k
        C1(i)=C(i)
        C2(i)=C(i+k)
        C3(i)=C(i+2*k)
10    continue
      call SRSVS(phi,v,Px,L2,k,xx,yy,S,C1)
      call SRWRS(phi,v,Px,L2,k,xx,yy,S,C2)
      call SVSRS(phi,v,Px,L2,k,xx,yy,S,C3)
      return
      end


      subroutine SFSFS(phi,v,Px,L2,k,xx,yy,S,C)
```

```
      double precision phi,v,Px,L2,S(31,31)
      double precision C(120),C1(30),C2(30)
      integer k,xx,yy,i
      do 10 i=1,k
        C1(i)=C(i)
        C2(i)=C(i+k)
 10   continue
      call SRSVS(phi,v,Px,L2,k,xx,yy,S,C1)
      call SVSRS(phi,v,Px,L2,k,xx,yy,S,C2)
      return
      end


      subroutine SSCFS(phi,v,Px,L2,k,xx,yy,S,C)
      double precision phi,v,Px,L2,S(31,31)
      double precision C(120),C1(30),C2(30)
      integer k,xx,yy,i
      do 10 i=1,k
        C1(i)=C(i)
        C2(i)=C(i+k)
 10   continue
      call SSSVS(phi,v,Px,L2,k,xx,yy,S,C1)
      call SSWRS(phi,v,Px,L2,k,xx,yy,S,C2)
      return
      end


      subroutine SSSFS(phi,v,Px,L2,k,xx,yy,S,C)
      double precision phi,v,Px,L2,S(31,31)
      double precision C(120),C1(30)
      integer k,xx,yy,i
      do 10 i=1,k
        C1(i)=C(i)
 10   continue
      call SSSVS(phi,v,Px,L2,k,xx,yy,S,C1)
      return
      end


      subroutine SSSVS(phi,v,Px,L2,k,xx,yy,S,C)
      double precision phi,v,Px,L2,pi,vp,di,del,B,G,Q1,Q2
      double precision C(30),S(31,31),eta,xi
      integer k,x,y,m,n,i,xx,yy
      pi=4*datan(1.0d0)
C-----------------------------------------------------------------
C     W(x,y) = Y(y) sin(m pi x), where m=1,2,3,...
C-----------------------------------------------------------------
      do 200 i=1,k
       m=i
       vp=(2-v)*(m*pi*phi)**2
       di=(m*pi)**2
       del=(m*pi)**4-L2**2-Px*(m*pi/phi)**2
C-----------------------------------------------------------------
C     Case 1 solution
C     Y(y) = Q1 sinh(B y) cos(G y) + Q2 cosh(B y) sin(G y)
C-----------------------------------------------------------------
      if (di**2.lt.del) then
        B=dsqrt((dsqrt(del)+di)/2)*phi
        G=dsqrt((dsqrt(del)-di)/2)*phi
        Q1=(B*(vp-B**2+3*G**2)*dsinh(B)*dsin(G)
     2    +G*(vp+G**2-3*B**2)*dcosh(B)*dcos(G))
     3    /(-2*B*G*(B**2+G**2)*(dsinh(B)**2+dcos(G)**2))
       Q2=(G*(vp+G**2-3*B**2)*dsinh(B)*dsin(G)
```

```
     2     -B*(vp-B**2+3*G**2)*dcosh(B)*dcos(G))
     3     /(-2*B*G*(B**2+G**2)*(dsinh(B)**2+dcos(G)**2))
          do 210 y=1,yy+1
           eta=float(y-1)/yy
           do 210 x=1,xx+1
            xi=float(x-1)/xx
            S(x,y)=S(x,y)+C(i)*(Q1*dsinh(B*eta)*dcos(G*eta)+
     2      Q2*dcosh(B*eta)*dsin(G*eta))*dsin(m*pi*xi)
210       continue
C---------------------------------------------------------------------
C      Case 2 solution
C      Y(y) = Q1 sinh(B y) + Q2 sin(G y)
C---------------------------------------------------------------------
         elseif (del.lt.0) then
          B=dsqrt(dsqrt(di**2-del)+di)*phi
          G=dsqrt(dsqrt(di**2-del)-di)*phi
          Q1=(G**2+vp)/(B*(B**2+G**2)*dcosh(B))
          Q2=(B**2-vp)/(G*(B**2+G**2)*dcos(G))
          do 220 y=1,yy+1
           eta=float(y-1)/yy
           do 220 x=1,xx+1
            xi=float(x-1)/xx
            S(x,y)=S(x,y)+C(i)*(Q1*dsinh(B*eta)
     2      +Q2*dsin(G*eta))*dsin(m*pi*xi)
220       continue
C---------------------------------------------------------------------
C      Case 3 solution
C      Y(y) = Q1 sinh(B y) + Q2 sinh(G y)
C---------------------------------------------------------------------
         else
          B=dsqrt(di+dsqrt(di**2-del))*phi
          G=dsqrt(di-dsqrt(di**2-del))*phi
          Q1=(vp-G**2)/(B*(B**2-G**2)*dcosh(B))
          Q2=(B**2-vp)/(G*(B**2-G**2)*dcosh(G))
          do 230 y=1,yy+1
           eta=float(y-1)/yy
           do 230 x=1,xx+1
            xi=float(x-1)/xx
            S(x,y)=S(x,y)+C(i)*(Q1*dsinh(B*eta)
     2      +Q2*dsinh(G*eta))*dsin(m*pi*xi)
230       continue
         endif
200     continue
        return
        end


        subroutine SSWRS(phi,v,Px,L2,k,xx,yy,S,C)
        double precision phi,v,Px,L2,pi,vp,di,del,B,G,Q1,Q2
        double precision C(30),S(31,31),eta,xi
        integer k,x,y,m,n,i,xx,yy
        pi=4*datan(1.0d0)
C---------------------------------------------------------------------
C       W(x,y) = Y(x) sin(n pi y / 2), where n=1,3,5,...
C---------------------------------------------------------------------
        do 300 i=1,k
         n=2*i-1
         di=(n*pi/2)**2-Px/2
         del=(n*pi/2)**4-L2**2*phi**4
C---------------------------------------------------------------------
C       Case 1 solution
C       Y(x) = Q1 sinh(B x) cos(G x) + Q2 cosh(B x) sin(G x)
C---------------------------------------------------------------------
```

```
          if (di**2.lt.del) then
           B=dsqrt((dsqrt(del)+di)/2)/phi
           G=dsqrt((dsqrt(del)-di)/2)/phi
           Q1=dcosh(B)*dsin(G)
     2      /(2*B*G*(dcos(G)**2-dcosh(B)**2))
           Q2=-dsinh(B)*dcos(G)
     2      /(2*B*G*(dcos(G)**2-dcosh(B)**2))
           do 310 y=1,yy+1
            eta=float(y-1)/yy
            do 310 x=1,xx+1
             xi=float(x-1)/xx
             S(x,y)=S(x,y)+C(i)*(Q1*dsinh(B*xi)*dcos(G*xi)
     2       +Q2*dcosh(B*xi)*dsin(G*xi))*dsin(n*pi*eta/2)
310       continue
C--------------------------------------------------------------------
C     Case 2 solution
C     Y(x) = Q1 sinh(B x) + Q2 sin(G x)
C--------------------------------------------------------------------
          elseif (del.lt.0) then
           B=dsqrt(dsqrt(di**2-del)+di)/phi
           G=dsqrt(dsqrt(di**2-del)-di)/phi
           Q1=((B**2+G**2)*dsinh(B))**(-1)
           Q2=-((B**2+G**2)*dsin(G))**(-1)
           do 320 y=1,yy+1
            eta=float(y-1)/yy
            do 320 x=1,xx+1
             xi=float(x-1)/xx
             S(x,y)=S(x,y)+C(i)*(Q1*dsinh(B*xi)
     2       +Q2*dsin(G*xi))*dsin(n*pi*eta/2)
320       continue
C--------------------------------------------------------------------
C     Case 3 solution
C     Y(x) = Q1 sinh(B x) + Q2 sinh(G x)
C--------------------------------------------------------------------
          elseif (di.gt.0) then
           B=dsqrt(di+dsqrt(di**2-del))/phi
           G=dsqrt(di-dsqrt(di**2-del))/phi
           Q1=((B**2-G**2)*dsinh(B))**(-1)
           Q2=-((B**2-G**2)*dsinh(G))**(-1)
           do 330 y=1,yy+1
            eta=float(y-1)/yy
            do 330 x=1,xx+1
             xi=float(x-1)/xx
             S(x,y)=S(x,y)+C(i)*(Q1*dsinh(B*xi)
     2       +Q2*dsinh(G*xi))*dsin(n*pi*eta/2)
330       continue
C--------------------------------------------------------------------
C     Case 4 solution
C     Y(x) = Q1 sin(B x) + Q2 sin(G x)
C--------------------------------------------------------------------
          else
           B=dsqrt(-di+dsqrt(di**2-del))/phi
           G=dsqrt(-di-dsqrt(di**2-del))/phi
           Q1=((G**2-B**2)*dsin(B))**(-1)
           Q2=-((G**2-B**2)*dsin(G))**(-1)
           do 340 y=1,yy+1
            eta=float(y-1)/yy
            do 340 x=1,xx+1
             xi=float(x-1)/xx
             S(x,y)=S(x,y)+C(i)*(Q1*dsin(B*xi)
     2       +Q2*dsin(G*xi))*dsin(n*pi*eta/2)
340       continue
         endif
```

```
 300   continue
       return
       end


       subroutine SWSRS(phi,v,Px,L2,k,xx,yy,S,C)
       double precision phi,v,Px,L2,pi,vp,di,del,B,G,Q1,Q2
       double precision C(30),S(31,31),eta,xi
       integer k,x,y,m,n,i,xx,yy
       pi=4*datan(1.0d0)
C-----------------------------------------------------------------------
C      W(x,y) = Y(1-y) sin(m pi x), where m=1,2,3,...
C-----------------------------------------------------------------------
       do 400 i=1,k
       m=i
       di=(m*pi)**2
       del=(m*pi)**4-L2**2-Px*(m*pi/phi)**2
C-----------------------------------------------------------------------
C      Case 1 solution
C      Y(1-y) = Q1 sinh(B (1-y)) sin(G (1-y)) + Q2 cosh(B (1-y)) cos(G (1-y))
C-----------------------------------------------------------------------
       if (di**2.lt.del) then
         B=dsqrt((dsqrt(del)+di)/2)*phi
         G=dsqrt((dsqrt(del)-di)/2)*phi
         Q1=dcosh(B)*dcos(G)
     2    /(2*B*G*(dsinh(B)**2+dcos(G)**2))
         Q2=-dsinh(B)*dsin(G)
     2    /(2*B*G*(dsinh(B)**2+dcos(G)**2))
         do 410 y=1,yy+1
          eta=float(y-1)/yy
          do 410 x=1,xx+1
           xi=float(x-1)/xx
           S(x,y)=S(x,y)+C(i)*(Q1*dsinh(B*(1-eta))*dsin(G*(1-eta))
     2     +Q2*dcosh(B*(1-eta))*dcos(G*(1-eta)))*dsin(m*pi*xi)
410     continue
C-----------------------------------------------------------------------
C      Case 2 solution
C      Y(1-y) = Q1 cosh(B (1-y)) + Q2 cos(G (1-y))
C-----------------------------------------------------------------------
       elseif (del.lt.0) then
         B=dsqrt(dsqrt(di**2-del)+di)*phi
         G=dsqrt(dsqrt(di**2-del)-di)*phi
         Q1=((B**2+G**2)*dcosh(B))**(-1)
         Q2=-((B**2+G**2)*dcos(G))**(-1)
         do 420 y=1,yy+1
          eta=float(y-1)/yy
          do 420 x=1,xx+1
           xi=float(x-1)/xx
           S(x,y)=S(x,y)+C(i)*(Q1*dcosh(B*(1-eta))
     2     +Q2*dcos(G*(1-eta)))*dsin(m*pi*xi)
420     continue
C-----------------------------------------------------------------------
C      Case 3 solution
C      Y(1-y) = Q1 cosh(B (1-y)) + Q2  cosh(G (1-y))
C-----------------------------------------------------------------------
       else
         B=dsqrt(di+dsqrt(di**2-del))*phi
         G=dsqrt(di-dsqrt(di**2-del))*phi
         Q1=((B**2-G**2)*dcosh(B))**(-1)
         Q2=-((B**2-G**2)*dcosh(G))**(-1)
         do 430 y=1,yy+1
          eta=float(y-1)/yy
          do 430 x=1,xx+1
```

```
          xi=float(x-1)/xx
          S(x,y)=S(x,y)+C(i)*(Q1*dcosh(B*(1-eta))
     2    +Q2*dcosh(G*(1-eta)))*dsin(m*pi*xi)
 430    continue
        endif
 400    continue
        return
        end


        subroutine WSSRS(phi,v,Px,L2,k,xx,yy,S,C)
        double precision phi,v,Px,L2,pi,vp,di,del,B,G,Q1,Q2
        double precision C(30),S(31,31),eta,xi
        integer k,x,y,m,n,i,xx,yy
        pi=4*datan(1.0d0)
C-----------------------------------------------------------------
C       W(x,y) = Y(1-x) sin(n pi y / 2), where n=1,3,5,...
C-----------------------------------------------------------------
        do 500 i=1,k
        n=2*i-1
        di=(n*pi/2)**2-Px/2
        del=(n*pi/2)**4-L2**2*phi**4
C-----------------------------------------------------------------------
C       Case 1 solution
C       Y(1-x) = Q1 sinh(B (1-x)) cos(G (1-x)) + Q2 cosh(B (1-x)) sin(G (1-x))
C-----------------------------------------------------------------------
        if (di**2.lt.del) then
          B=dsqrt((dsqrt(del)+di)/2)/phi
          G=dsqrt((dsqrt(del)-di)/2)/phi
          Q1=dcosh(B)*dsin(G)
     2     /(2*B*G*(dcos(G)**2-dcosh(B)**2))
          Q2=-dsinh(B)*dcos(G)
     2     /(2*B*G*(dcos(G)**2-dcosh(B)**2))
          do 510 y=1,yy+1
           eta=float(y-1)/yy
           do 510 x=1,xx+1
            xi=float(x-1)/xx
            S(x,y)=S(x,y)+C(i)*(Q1*dsinh(B*(1-xi))*dcos(G*(1-xi))
     2      +Q2*dcosh(B*(1-xi))*dsin(G*(1-xi)))*dsin(n*pi*eta/2)
 510    continue
C-----------------------------------------------------------------
C       Case 2 solution
C       Y(1-x) = Q1 sinh(B (1-x)) + Q2 sin(G (1-x))
C-----------------------------------------------------------------
        elseif (del.lt.0) then
          B=dsqrt(dsqrt(di**2-del)+di)/phi
          G=dsqrt(dsqrt(di**2-del)-di)/phi
          Q1=((B**2+G**2)*dsinh(B))**(-1)
          Q2=-((B**2+G**2)*dsin(G))**(-1)
          do 520 y=1,yy+1
           eta=float(y-1)/yy
           do 520 x=1,xx+1
            xi=float(x-1)/xx
            S(x,y)=S(x,y)+C(i)*(Q1*dsinh(B*(1-xi))
     2      +Q2*dsin(G*(1-xi)))*dsin(n*pi*eta/2)
 520    continue
C-----------------------------------------------------------------
C       Case 3 solution
C       Y(1-x) = Q1 sinh(B (1-x)) + Q2 sinh(G (1-x))
C-----------------------------------------------------------------
        elseif (di.gt.0) then
          B=dsqrt(di+dsqrt(di**2-del))/phi
          G=dsqrt(di-dsqrt(di**2-del))/phi
```

```
         Q1=((B**2-G**2)*dsinh(B))**(-1)
         Q2=-((B**2-G**2)*dsinh(G))**(-1)
         do 530 y=1,yy+1
          eta=float(y-1)/yy
          do 530 x=1,xx+1
           xi=float(x-1)/xx
           S(x,y)=S(x,y)+C(i)*(Q1*dsinh(B*(1-xi))
     2     +Q2*dsinh(G*(1-xi)))*dsin(n*pi*eta/2)
530     continue
C-----------------------------------------------------------------------
C      Case 4 solution
C      Y(1-x) = Q1 sin(B (1-x)) + Q2 sin(G (1-x))
C-----------------------------------------------------------------------
        else
         B=dsqrt(-di+dsqrt(di**2-del))/phi
         G=dsqrt(-di-dsqrt(di**2-del))/phi
         Q1=((G**2-B**2)*dsin(B))**(-1)
         Q2=-((G**2-B**2)*dsin(G))**(-1)
         do 540 y=1,yy+1
          eta=float(y-1)/yy
          do 540 x=1,xx+1
           xi=float(x-1)/xx
           S(x,y)=S(x,y)+C(i)*(Q1*dsin(B*(1-xi))
     2     +Q2*dsin(G*(1-xi)))*dsin(n*pi*eta/2)
540     continue
        endif
500   continue
      return
      end


      subroutine SRSVS(phi,v,Px,L2,k,xx,yy,S,C)
      double precision phi,v,Px,L2,pi,vp,di,del,B,G,Q1,Q2
      double precision C(30),S(31,31),eta,xi
      integer k,x,y,m,n,i,xx,yy
      pi=4*datan(1.0d0)
C-----------------------------------------------------------------------
C     W(x,y) = Y(y) sin(m pi x), where m=1,2,3,...
C-----------------------------------------------------------------------
      do 200 i=1,k
       m=i
       vp=(2-v)*(m*pi*phi)**2
       di=(m*pi)**2
       del=(m*pi)**4-L2**2-Px*(m*pi/phi)**2
C-----------------------------------------------------------------------
C     Case 1 solution
C     Y(y) = Q1 sinh(B y) sin(G y) + Q2 cosh(B y) cos(G y)
C-----------------------------------------------------------------------
       if (di**2.lt.del) then
        B=dsqrt((dsqrt(del)+di)/2)*phi
        G=dsqrt((dsqrt(del)-di)/2)*phi
        Q1=(B*(B**2-3*G**2-vp)*dsinh(B)*dcos(G)
     2    +G*(G**2-3*B**2+vp)*dcosh(B)*dsin(G))
     3    /(-2*B*G*(B**2+G**2)*(dsinh(B)**2+dsin(G)**2))
        Q2=(G*(G**2-3*B**2+vp)*dsinh(B)*dcos(G)
     2    -B*(B**2-3*G**2-vp)*dcosh(B)*dsin(G))
     3    /(-2*B*G*(B**2+G**2)*(dsinh(B)**2+dsin(G)**2))
        do 210 y=1,yy+1
         eta=float(y-1)/yy
         do 210 x=1,xx+1
          xi=float(x-1)/xx
          S(x,y)=S(x,y)+C(i)*(Q1*dsinh(B*eta)*dsin(G*eta)+
     2    Q2*dcosh(B*eta)*dcos(G*eta))*dsin(m*pi*xi)
```

```
210    continue
C-----------------------------------------------------------------------
C      Case 2 solution
C      Y(y) = Q1 cosh(B y) + Q2 cos(G y)
C-----------------------------------------------------------------------
        elseif (del.lt.0) then
         B=dsqrt(dsqrt(di**2-del)+di)*phi
         G=dsqrt(dsqrt(di**2-del)-di)*phi
         Q1=(G**2+vp)/(B*(B**2+G**2)*dsinh(B))
         Q2=-(B**2-vp)/(G*(B**2+G**2)*dsin(G))
         do 220 y=1,yy+1
          eta=float(y-1)/yy
          do 220 x=1,xx+1
           xi=float(x-1)/xx
           S(x,y)=S(x,y)+C(i)*(Q1*dcosh(B*eta)
     2     +Q2*dcos(G*eta))*dsin(m*pi*xi)
220    continue
C-----------------------------------------------------------------------
C      Case 3 solution
C      Y(y) = Q1 cosh(B y) + Q2 cosh(G y)
C-----------------------------------------------------------------------
        else
         B=dsqrt(di+dsqrt(di**2-del))*phi
         G=dsqrt(di-dsqrt(di**2-del))*phi
         Q1=-(G**2-vp)/(B*(B**2-G**2)*dsinh(B))
         Q2=(B**2-vp)/(G*(B**2-G**2)*dsinh(G))
         do 230 y=1,yy+1
          eta=float(y-1)/yy
          do 230 x=1,xx+1
           xi=float(x-1)/xx
           S(x,y)=S(x,y)+C(i)*(Q1*dcosh(B*eta)
     2     +Q2*dcosh(G*eta))*dsin(m*pi*xi)
230    continue
        endif
200   continue
      return
      end


      subroutine SRWRS(phi,v,Px,L2,k,xx,yy,S,C)
      double precision phi,v,Px,L2,pi,vp,di,del,B,G,Q1,Q2
      double precision C(30),S(31,31),eta,xi
      integer k,x,y,m,n,i,xx,yy
      pi=4*datan(1.0d0)
C-----------------------------------------------------------------------
C     W(x,y) = Y(x) cos(n pi y), where n=0,1,2,...
C-----------------------------------------------------------------------
      do 300 i=1,k
      n=i-1
      di=(n*pi)**2-Px/2
      del=(n*pi)**4-L2**2*phi**4
C-----------------------------------------------------------------------
C     Case 1 solution
C     Y(x) = Q1 sinh(B x) cos(G x) + Q2 cosh(B x) sin(G x)
C-----------------------------------------------------------------------
       if (di**2.lt.del) then
        B=dsqrt((dsqrt(del)+di)/2)/phi
        G=dsqrt((dsqrt(del)-di)/2)/phi
        Q1=dcosh(B)*dsin(G)
     2     /(2*B*G*(dcos(G)**2-dcosh(B)**2))
        Q2=-dsinh(B)*dcos(G)
     2     /(2*B*G*(dcos(G)**2-dcosh(B)**2))
        do 310 y=1,yy+1
```

```
        eta=float(y-1)/yy
        do 310 x=1,xx+1
         xi=float(x-1)/xx
         S(x,y)=S(x,y)+C(i)*(Q1*dsinh(B*xi)*dcos(G*xi)
     2   +Q2*dcosh(B*xi)*dsin(G*xi))*dcos(n*pi*eta)
310    continue
C-----------------------------------------------------------------------
C     Case 2 solution
C     Y(x) = Q1 sinh(B x) + Q2 sin(G x)
C-----------------------------------------------------------------------
       elseif (del.lt.0) then
        B=dsqrt(dsqrt(di**2-del)+di)/phi
        G=dsqrt(dsqrt(di**2-del)-di)/phi
        Q1=((B**2+G**2)*dsinh(B))**(-1)
        Q2=-((B**2+G**2)*dsin(G))**(-1)
        do 320 y=1,yy+1
         eta=float(y-1)/yy
         do 320 x=1,xx+1
          xi=float(x-1)/xx
          S(x,y)=S(x,y)+C(i)*(Q1*dsinh(B*xi)
     2    +Q2*dsin(G*xi))*dcos(n*pi*eta)
320    continue
C-----------------------------------------------------------------------
C     Case 3 solution
C     Y(x) = Q1 sinh(B x) + Q2 sinh(G x)
C-----------------------------------------------------------------------
       elseif (di.gt.0) then
        B=dsqrt(di+dsqrt(di**2-del))/phi
        G=dsqrt(di-dsqrt(di**2-del))/phi
        Q1=((B**2-G**2)*dsinh(B))**(-1)
        Q2=-((B**2-G**2)*dsinh(G))**(-1)
        do 330 y=1,yy+1
         eta=float(y-1)/yy
         do 330 x=1,xx+1
          xi=float(x-1)/xx
          S(x,y)=S(x,y)+C(i)*(Q1*dsinh(B*xi)
     2    +Q2*dsinh(G*xi))*dcos(n*pi*eta)
330    continue
C-----------------------------------------------------------------------
C     Case 4 solution
C     Y(x) = Q1 sin(B x) + Q2 sin(G x)
C-----------------------------------------------------------------------
       else
        B=dsqrt(-di+dsqrt(di**2-del))/phi
        G=dsqrt(-di-dsqrt(di**2-del))/phi
        Q1=((G**2-B**2)*dsin(B))**(-1)
        Q2=-((G**2-B**2)*dsin(G))**(-1)
        do 340 y=1,yy+1
         eta=float(y-1)/yy
         do 340 x=1,xx+1
          xi=float(x-1)/xx
          S(x,y)=S(x,y)+C(i)*(Q1*dsin(B*xi)
     2    +Q2*dsin(G*xi))*dcos(n*pi*eta)
340    continue
      endif
300   continue
      return
      end


      subroutine SVSRS(phi,v,Px,L2,k,xx,yy,S,C)
      double precision phi,v,Px,L2,pi,vp,di,del,B,G,Q1,Q2
      double precision C(30),S(31,31),eta,xi
```

```
      integer k,x,y,m,n,i,xx,yy
      pi=4*datan(1.0d0)
C-----------------------------------------------------------------
C     W(x,y) = Y(1-y) sin(m pi x), where m=1,2,3,...
C-----------------------------------------------------------------
      do 400 i=1,k
      m=i
      vp=(2-v)*(m*pi*phi)**2
      di=(m*pi)**2
      del=(m*pi)**4-L2**2-Px*(m*pi/phi)**2
C-----------------------------------------------------------------
C     Case 1 solution
C     Y(1-y) = Q1 sinh(B(1-y)) sin(G(1-y)) + Q2 cosh(B(1-y)) cos(G(1-y))
C-----------------------------------------------------------------
      if (di**2.lt.del) then
        B=dsqrt((dsqrt(del)+di)/2)*phi
        G=dsqrt((dsqrt(del)-di)/2)*phi
        Q1=(B*(B**2-3*G**2-vp)*dsinh(B)*dcos(G)
     2     +G*(G**2-3*B**2+vp)*dcosh(B)*dsin(G))
     3     /(-2*B*G*(B**2+G**2)*(dsinh(B)**2+dsin(G)**2))
        Q2=(G*(G**2-3*B**2+vp)*dsinh(B)*dcos(G)
     2     -B*(B**2-3*G**2-vp)*dcosh(B)*dsin(G))
     3     /(-2*B*G*(B**2+G**2)*(dsinh(B)**2+dsin(G)**2))
        do 410 y=1,yy+1
         eta=float(y-1)/yy
         do 410 x=1,xx+1
          xi=float(x-1)/xx
          S(x,y)=S(x,y)+C(i)*(Q1*dsinh(B*(1-eta))*dsin(G*(1-eta))
     2    +Q2*dcosh(B*(1-eta))*dcos(G*(1-eta)))*dsin(m*pi*xi)
410     continue
C-----------------------------------------------------------------
C     Case 2 solution
C     Y(1-y) = Q1 cosh(B(1-y)) + Q2 cos(G(1-y))
C-----------------------------------------------------------------
      elseif (del.lt.0) then
        B=dsqrt(dsqrt(di**2-del)+di)*phi
        G=dsqrt(dsqrt(di**2-del)-di)*phi
        Q1=(G**2+vp)/(B*(B**2+G**2)*dsinh(B))
        Q2=-(B**2-vp)/(G*(B**2+G**2)*dsin(G))
        do 420 y=1,yy+1
         eta=float(y-1)/yy
         do 420 x=1,xx+1
          xi=float(x-1)/xx
          S(x,y)=S(x,y)+C(i)*(Q1*dcosh(B*(1-eta))
     2    +Q2*dcos(G*(1-eta)))*dsin(m*pi*xi)
420     continue
C-----------------------------------------------------------------
C     Case 3 solution
C     Y(1-y) = Q1 cosh(B(1-y)) + Q2 cosh(G(1-y))
C-----------------------------------------------------------------
      else
        B=dsqrt(di+dsqrt(di**2-del))*phi
        G=dsqrt(di-dsqrt(di**2-del))*phi
        Q1=-(G**2-vp)/(B*(B**2-G**2)*dsinh(B))
        Q2=(B**2-vp)/(G*(B**2-G**2)*dsinh(G))
        do 430 y=1,yy+1
         eta=float(y-1)/yy
         do 430 x=1,xx+1
          xi=float(x-1)/xx
          S(x,y)=S(x,y)+C(i)*(Q1*dcosh(B*(1-eta))
     2    +Q2*dcosh(G*(1-eta)))*dsin(m*pi*xi)
430     continue
      endif
```

```
 400   continue
       return
       end


       subroutine WRSRS(phi,v,Px,L2,k,xx,yy,S,C)
       double precision phi,v,Px,L2,pi,vp,di,del,B,G,Q1,Q2
       double precision C(30),S(31,31),eta,xi
       integer k,x,y,m,n,i,xx,yy
       pi=4*datan(1.0d0)
C-----------------------------------------------------------------------
C      W(x,y) = Y(1-x) cos(n pi y), where n=0,1,2,...
C-----------------------------------------------------------------------
       do 500 i=1,k
       n=i-1
       di=(n*pi)**2-Px/2
       del=(n*pi)**4-L2**2*phi**4
C--------------------------------------------------------------------------
C      Case 1 solution
C      Y(1-x) = Q1 sinh(B (1-x)) cos(G (1-x)) + Q2 cosh(B (1-x)) sin(G (1-x))
C--------------------------------------------------------------------------
       if (di**2.lt.del) then
         B=dsqrt((dsqrt(del)+di)/2)/phi
         G=dsqrt((dsqrt(del)-di)/2)/phi
         Q1=dcosh(B)*dsin(G)
     2     /(2*B*G*(dcos(G)**2-dcosh(B)**2))
         Q2=-dsinh(B)*dcos(G)
     2     /(2*B*G*(dcos(G)**2-dcosh(B)**2))
         do 510 y=1,yy+1
          eta=float(y-1)/yy
          do 510 x=1,xx+1
           xi=float(x-1)/xx
           S(x,y)=S(x,y)+C(i)*(Q1*dsinh(B*(1-xi))*dcos(G*(1-xi))
     2     +Q2*dcosh(B*(1-xi))*dsin(G*(1-xi)))*dcos(n*pi*eta)
510     continue
C-----------------------------------------------------------------------
C      Case 2 solution
C      Y(1-x) = Q1 sinh(B (1-x)) + Q2 sin(G (1-x))
C-----------------------------------------------------------------------
       elseif (del.lt.0) then
         B=dsqrt(dsqrt(di**2-del)+di)/phi
         G=dsqrt(dsqrt(di**2-del)-di)/phi
         Q1=((B**2+G**2)*dsinh(B))**(-1)
         Q2=-((B**2+G**2)*dsin(G))**(-1)
         do 520 y=1,yy+1
          eta=float(y-1)/yy
          do 520 x=1,xx+1
           xi=float(x-1)/xx
           S(x,y)=S(x,y)+C(i)*(Q1*dsinh(B*(1-xi))
     2     +Q2*dsin(G*(1-xi)))*dcos(n*pi*eta)
520     continue
C-----------------------------------------------------------------------
C      Case 3 solution
C      Y(1-x) = Q1 sinh(B (1-x)) + Q2 sinh(G (1-x))
C-----------------------------------------------------------------------
       elseif (di.gt.0) then
         B=dsqrt(di+dsqrt(di**2-del))/phi
         G=dsqrt(di-dsqrt(di**2-del))/phi
         Q1=((B**2-G**2)*dsinh(B))**(-1)
         Q2=-((B**2-G**2)*dsinh(G))**(-1)
         do 530 y=1,yy+1
          eta=float(y-1)/yy
          do 530 x=1,xx+1
```

```
           xi=float(x-1)/xx
           S(x,y)=S(x,y)+C(i)*(Q1*dsinh(B*(1-xi))
     2     +Q2*dsinh(G*(1-xi)))*dcos(n*pi*eta)
 530    continue
C----------------------------------------------------------------------
C       Case 4 solution
C       Y(1-x) = Q1 sin(B (1-x)) + Q2 sin(G (1-x))
C----------------------------------------------------------------------
        else
         B=dsqrt(-di+dsqrt(di**2-del))/phi
         G=dsqrt(-di-dsqrt(di**2-del))/phi
         Q1=((G**2-B**2)*dsin(B))**(-1)
         Q2=-((G**2-B**2)*dsin(G))**(-1)
         do 540 y=1,yy+1
          eta=float(y-1)/yy
          do 540 x=1,xx+1
           xi=float(x-1)/xx
           S(x,y)=S(x,y)+C(i)*(Q1*dsin(B*(1-xi))
     2     +Q2*dsin(G*(1-xi)))*dcos(n*pi*eta)
 540    continue
        endif
 500    continue
        return
        end


        subroutine solve(A,r,X)
        double precision temp,X(120),A(120,120)
        integer i,j,k,l,r,row

        do 1 i=1,r
         temp=0
         do 3 j=1,r
          temp=temp+dabs(A(i,j))
 3       continue
         if (dabs(temp).lt.1.0d-12) goto 2
         temp=r/temp
         do 4 j=1,r
          A(i,j)=temp*A(i,j)
 4       continue
 2       continue
 1      continue
        do 10 i=1,r-1
         l=i-1
 15      l=l+1
         if (l.gt.r) goto 45
         temp=0
         do 20 j=i,r
          if (dabs(A(j,l)).gt.dabs(temp)) then
           temp=A(j,l)
           row=j
          endif
 20      continue
         if (dabs(temp).lt.1.0d-12) goto 15
         if (i.ne.row) then
          do 30 j=1,r
           temp=A(i,j)
           A(i,j)=A(row,j)
           A(row,j)=temp
 30       continue
         endif
         do 40 j=i+1,r
          temp=A(j,l)/A(i,l)
```

```
        do 40 k=1,r
         A(j,k)=A(j,k)-A(i,k)*temp
 40     continue
 10    continue
 45    continue
       temp=A(1,1)
       row=1
       do 60 i=2,r
        if (dabs(A(i,i)).lt.dabs(temp)) then
         temp=A(i,i)
         row=i
        endif
 60    continue
       A(row,row)=0
       do 50 i=r,2,-1
        l=i-1
 55     l=l+1
        if (l.gt.r) goto 85
        if (dabs(A(i,l)).lt.1.0d-12) goto 55
        do 80 j=i-1,1,-1
         temp=A(j,l)/A(i,l)
         do 80 k=1,r
          A(j,k)=A(j,k)-A(i,k)*temp
 80     continue
 85     continue
 50    continue
       do 70 i=1,r
        if (i.ne.row) then
         X(i)=A(i,row)/A(i,i)
         if (dabs(X(i)).lt.1.0d-12) X(i)=0
        else
         X(i)=-1.0d0
        endif
 70    continue
       return
       end

C----------------------------------------------------------------------
C      The following integrals are evaluated from 0 to 1.
C      The function name represents the integral calculated.
C      For example, chmcms(A,B,C) calculates the integral
C      of cosh(A(1-x))cos(B(1-x))sin(Cx) dx from 0 to 1.
C----------------------------------------------------------------------

       function c(G)
       double precision c,G
       c=dsin(G)/G
       return
       end

       function ch(B)
       double precision ch,B
       ch=dsinh(B)/B
       return
       end

       function cm(G)
       double precision cm,G,c
       cm=c(G)
       return
       end
```

```
function chm(B)
double precision chm,B,ch
chm=ch(B)
return
end

function ss(A,B)
double precision ss,A,B
ss=(A*dcos(A)*dsin(B)-B*dsin(A)*dcos(B))/(B**2-A**2)
return
end

function sc(A,B)
double precision sc,A,B
sc=(A*dcos(A)*dcos(B)+B*dsin(A)*dsin(B)-A)/(B**2-A**2)
return
end

function cc(G,NP)
double precision cc,G,NP,c
cc=(c(G+NP)+c(G-NP))/2.0d0
return
end

function shs(B,G)
double precision shs,B,G
shs=(B*dsin(G)*dcosh(B)-G*dcos(G)*dsinh(B))/(B**2+G**2)
return
end

function shc(A,B)
double precision shc,A,B
shc=(A*dcosh(A)*dcos(B)+B*dsinh(A)*dsin(B)-A)/(A**2+B**2)
return
end

function chs(A,B)
double precision chs,A,B
chs=(A*dsinh(A)*dsin(B)-B*dcosh(A)*dcos(B)+B)/(A**2+B**2)
return
end

function chc(B,G)
double precision chc,B,G
chc=(B*dcos(G)*dsinh(B)+G*dsin(G)*dcosh(B))/(B**2+G**2)
return
end

function shss(A,B,C)
double precision shss,A,B,C,shc
shss=(shc(A,B-C)-shc(A,B+C))/2.0d0
return
end

function shsc(B,G,NP)
double precision shsc,B,G,NP,shs
shsc=(shs(B,G+NP)+shs(B,G-NP))/2.0d0
return
end

function shcc(A,B,C)
double precision shcc,A,B,C,shc
shcc=(shc(A,B+C)+shc(A,B-C))/2.0d0
```

```
return
end

function chss(B,G,NP)
double precision chss,B,G,NP,chc
chss=(chc(B,G-NP)-chc(B,G+NP))/2.0d0
return
end

function chsc(A,B,C)
double precision chsc,A,B,C,chs
chsc=(chs(A,C+B)-chs(A,C-B))/2.0d0
return
end

function chcc(B,G,NP)
double precision chcc,B,G,NP,chc
chcc=(chc(B,G+NP)+chc(B,G-NP))/2.0d0
return
end

function sms(A,B)
double precision sms,A,B,sc,ss
sms=dsin(A)*sc(B,A)-dcos(A)*ss(A,B)
return
end

function cms(A,B)
double precision cms,A,B,sc,ss
cms=dcos(A)*sc(B,A)+dsin(A)*ss(A,B)
return
end

function cmc(A,B)
double precision cmc,A,B,cc,sc
cmc=dcos(A)*cc(A,B)+dsin(A)*sc(A,B)
return
end

function shms(A,B)
double precision shms,A,B,shc,shs
shms=dsin(B)*shc(A,B)-dcos(B)*shs(A,B)
return
end

function chms(A,B)
double precision chms,A,B,chc,chs
chms=dsin(B)*chc(A,B)-dcos(B)*chs(A,B)
return
end

function chmc(A,B)
double precision chmc,A,B,chc,chs
chmc=dcos(B)*chc(A,B)+dsin(B)*chs(A,B)
return
end

function shmsm(B,G)
double precision shmsm,B,G,shs
shmsm=shs(B,G)
return
end
```

```
      function chmcm(B,G)
      double precision chmcm,B,G,chc
      chmcm=chc(B,G)
      return
      end

      function shmsms(A,B,C)
      double precision shmsms,A,B,C,shsc,shss
      shmsms=dsin(C)*shsc(A,B,C)-dcos(C)*shss(A,B,C)
      return
      end

      function shmsmc(A,B,C)
      double precision shmsmc,A,B,C,shsc,shss
      shmsmc=dcos(C)*shsc(A,B,C)+dsin(C)*shss(A,B,C)
      return
      end

      function shmcms(A,B,C)
      double precision shmcms,A,B,C,shcc,shsc
      shmcms=dsin(C)*shcc(A,B,C)-dcos(C)*shsc(A,C,B)
      return
      end

      function chmsms(A,B,C)
      double precision chmsms,A,B,C,chsc,chss
      chmsms=dsin(C)*chsc(A,B,C)-dcos(C)*chss(A,B,C)
      return
      end

      function chmcms(A,B,C)
      double precision chmcms,A,B,C,chcc,chsc
      chmcms=dsin(C)*chcc(A,B,C)-dcos(C)*chsc(A,C,B)
      return
      end

      function chmcmc(A,B,C)
      double precision chmcmc,A,B,C,chcc,chsc
      chmcmc=dcos(C)*chcc(A,B,C)+dsin(C)*chsc(A,C,B)
      return
      end


      subroutine SSSV(phi,v,Px,L2,m,n,side,coef)
      double precision phi,v,Px,L2,pi,vp,di,del,B,G,Q1,Q2,coef
      implicit double precision (c,s)
      integer m,n,case,side
C-----------------------------------------------------------------------
C     General Solution
C     W = Y(y) sin(m pi x), where m=1,2,3,...
C-----------------------------------------------------------------------
      pi=4*datan(1.0d0)
      vp=(2-v)*(m*pi*phi)**2
      di=(m*pi)**2
      del=(m*pi)**4-L2**2-Px*(m*pi/phi)**2
      if (del.eq.0) then
        write(6,*) 'Parameter singularity:  del = 0 in SSSV.'
        stop
      endif
      if (di**2.eq.del) then
        write(6,*) 'Parameter singularity:  di**2 - del = 0 in SSSV.'
        stop
      endif
```

```
      if (di**2.lt.del) then
C-----------------------------------------------------------------------
C     Case 1 solution
C     Y = Q1 sinh(B y) cos(G y) + Q2 cosh(B y) sin(G y)
C-----------------------------------------------------------------------
        case=1
        B=dsqrt((dsqrt(del)+di)/2)*phi
        G=dsqrt((dsqrt(del)-di)/2)*phi
        Q1=(B*(vp-B**2+3*G**2)*dsinh(B)*dsin(G)
     2    +G*(vp+G**2-3*B**2)*dcosh(B)*dcos(G))
     3    /(-2*B*G*(B**2+G**2)*(dsinh(B)**2+dcos(G)**2))
        Q2=(G*(vp+G**2-3*B**2)*dsinh(B)*dsin(G)
     2    -B*(vp-B**2+3*G**2)*dcosh(B)*dcos(G))
     3    /(-2*B*G*(B**2+G**2)*(dsinh(B)**2+dcos(G)**2))
      elseif (del.lt.0) then
C-----------------------------------------------------------------------
C     Case 2 solution
C     Y = Q1 sinh(B y) + Q2 sin(G y)
C-----------------------------------------------------------------------
        case=2
        B=dsqrt(dsqrt(di**2-del)+di)*phi
        G=dsqrt(dsqrt(di**2-del)-di)*phi
        Q1=(G**2+vp)/(B*(B**2+G**2)*dcosh(B))
        Q2=(B**2-vp)/(G*(B**2+G**2)*dcos(G))
      else
C-----------------------------------------------------------------------
C     Case 3 solution
C     Y = Q1 sinh(B y) + Q2 sinh(G y)
C-----------------------------------------------------------------------
        case=3
        B=dsqrt(di+dsqrt(di**2-del))*phi
        G=dsqrt(di-dsqrt(di**2-del))*phi
        Q1=(vp-G**2)/(B*(B**2-G**2)*dcosh(B))
        Q2=(B**2-vp)/(G*(B**2-G**2)*dcosh(G))
      endif
C-----------------------------------------------------------------------
C     Index for side
C     x=0  a.k.a.  side=1
C     y=0  a.k.a.  side=2
C     x=1  a.k.a.  side=3
C     y=1  a.k.a.  side=4
C-----------------------------------------------------------------------
      if (side.eq.1) then
        if (case.eq.1) then
          coef=(Q1*shsc(B,n*pi/2,G)+Q2*chss(B,n*pi/2,G))
     2      *2*m*pi
        elseif (case.eq.2) then
          coef=(Q1*shs(B,n*pi/2)+Q2*ss(G,n*pi/2))
     2      *2*m*pi
        else
          coef=(Q1*shs(B,n*pi/2)+Q2*shs(G,n*pi/2))
     2      *2*m*pi
        endif
      elseif (side.eq.2) then
        coef=Q1*B+Q2*G
      elseif (side.eq.3) then
        if (case.eq.1) then
          coef=(Q1*shsc(B,n*pi/2,G)+Q2*chss(B,n*pi/2,G))
     2      *2*m*pi*(-1)**m
        elseif (case.eq.2) then
          coef=(Q1*shs(B,n*pi/2)+Q2*ss(G,n*pi/2))
     2      *2*m*pi*(-1)**m
        else
```

```
          coef=(Q1*shs(B,n*pi/2)+Q2*shs(G,n*pi/2))
     2       *2*m*pi*(-1)**m
        endif
      else
        if (case.eq.1) then
          coef=(Q1*(B**2-G**2-v*(m*pi*phi)**2)+2*Q2*B*G)
     2       *dsinh(B)*dcos(G)
     3       +(Q2*(B**2-G**2-v*(m*pi*phi)**2)-2*Q1*B*G)
     4       *dcosh(B)*dsin(G)
        elseif (case.eq.2) then
          coef=(B**2-v*(m*pi*phi)**2)*Q1*dsinh(B)
     2       -(G**2+v*(m*pi*phi)**2)*Q2*dsin(G)
        else
          coef=(B**2-v*(m*pi*phi)**2)*Q1*dsinh(B)
     2       +(G**2-v*(m*pi*phi)**2)*Q2*dsinh(G)
        endif
      endif
      return
      end


      subroutine SSWR(phi,v,Px,L2,m,n,side,coef)
      double precision phi,v,Px,L2,pi,di,del,B,G,Q1,Q2,coef
      implicit double precision (c,s)
      integer m,n,case,side
C-----------------------------------------------------------------------
C     General Solution
C     W = Y(x) sin(n pi y / 2), where n=1,3,5,...
C-----------------------------------------------------------------------
      pi=4*datan(1.0d0)
      di=(n*pi/2)**2-Px/2
      del=(n*pi/2)**4-L2**2*phi**4
      if (del.eq.0) then
        write(6,*) 'Parameter singularity:  del = 0 in SSWR.'
        stop
      endif
      if (di**2.eq.del) then
        write(6,*) 'Parameter singularity:  di**2 - del = 0 in SSWR.'
        stop
      endif
      if (di**2.lt.del) then
C-----------------------------------------------------------------------
C     Case 1 solution
C     Y = Q1 sinh(B x) cos(G x) + Q2 cosh(B x) sin(G x)
C-----------------------------------------------------------------------
        case=1
        B=dsqrt((dsqrt(del)+di)/2)/phi
        G=dsqrt((dsqrt(del)-di)/2)/phi
        Q1=dcosh(B)*dsin(G)
     2   /(2*B*G*(dcos(G)**2-dcosh(B)**2))
        Q2=-dsinh(B)*dcos(G)
     2   /(2*B*G*(dcos(G)**2-dcosh(B)**2))
      elseif (del.lt.0) then
C-----------------------------------------------------------------------
C     Case 2 solution
C     Y = Q1 sinh(B x) + Q2 sin(G x)
C-----------------------------------------------------------------------
        case=2
        B=dsqrt(dsqrt(di**2-del)+di)/phi
        G=dsqrt(dsqrt(di**2-del)-di)/phi
        Q1=((B**2+G**2)*dsinh(B))**(-1)
        Q2=-((B**2+G**2)*dsin(G))**(-1)
      elseif (di.gt.0) then
```

```
C-----------------------------------------------------------------------
C     Case 3 solution
C     Y = Q1 sinh(B x) + Q2 sinh(G x)
C-----------------------------------------------------------------------
          case=3
          B=dsqrt(di+dsqrt(di**2-del))/phi
          G=dsqrt(di-dsqrt(di**2-del))/phi
          Q1=((B**2-G**2)*dsinh(B))**(-1)
          Q2=-((B**2-G**2)*dsinh(G))**(-1)
      else
C-----------------------------------------------------------------------
C     Case 4 solution
C     Y = Q1 sin(B x) + Q2 sin(G x)
C-----------------------------------------------------------------------
          case=4
          B=dsqrt(-di+dsqrt(di**2-del))/phi
          G=dsqrt(-di-dsqrt(di**2-del))/phi
          Q1=((G**2-B**2)*dsin(B))**(-1)
          Q2=-((G**2-B**2)*dsin(G))**(-1)
      endif
C-----------------------------------------------------------------------
C     Index
C     xi = 0 a.k.a. side = 1
C     eta = 0 a.k.a. side = 2
C     xi = 1 a.k.a. side = 3
C     eta = 1 a.k.a. side = 4
C-----------------------------------------------------------------------
      if (side.eq.1) then
        coef=Q1*B+Q2*G
      elseif (side.eq.2) then
        if (case.eq.1) then
          coef=n*pi*(Q1*shsc(B,m*pi,G)+Q2*chss(B,m*pi,G))
        elseif (case.eq.2) then
          coef=n*pi*(Q1*shs(B,m*pi)+Q2*ss(G,m*pi))
        elseif (case.eq.3) then
          coef=n*pi*(Q1*shs(B,m*pi)+Q2*shs(G,m*pi))
        else
          coef=n*pi*(Q1*ss(B,m*pi)+Q2*ss(G,m*pi))
        endif
      elseif (side.eq.3) then
        if (case.eq.1) then
          coef=(Q2*B-Q1*G)*dsinh(B)*dsin(G)
     2          +(Q1*B+Q2*G)*dcosh(B)*dcos(G)
        elseif (case.eq.2) then
          coef=Q1*B*dcosh(B)+Q2*G*dcos(G)
        elseif (case.eq.3) then
          coef=Q1*B*dcosh(B)+Q2*G*dcosh(G)
        else
          coef=Q1*B*dcos(B)+Q2*G*dcos(G)
        endif
      else
        if (case.eq.1) then
        coef=((Q1*(v*phi**2*(B**2-G**2)-(n*pi/2)**2)+2*v*phi**2*Q2*B*G)
     2    *shsc(B,m*pi,G)
     3    +(Q2*(v*phi**2*(B**2-G**2)-(n*pi/2)**2)-2*v*phi**2*Q1*B*G)
     4    *chss(B,m*pi,G))*2*(-1)**((n-1)/2)
        elseif (case.eq.2) then
        coef=((v*(B*phi)**2-(n*pi/2)**2)*Q1*shs(B,m*pi)
     2    -(v*(G*phi)**2+(n*pi/2)**2)*Q2*ss(G,m*pi))*2*(-1)**((n-1)/2)
        elseif (case.eq.3) then
        coef=((v*(B*phi)**2-(n*pi/2)**2)*Q1*shs(B,m*pi)
     2    +(v*(G*phi)**2-(n*pi/2)**2)*Q2*shs(G,m*pi))*2*(-1)**((n-1)/2)
        else
```

```
        coef=((v*(B*phi)**2+(n*pi/2)**2)*Q1*ss(B,m*pi)
     2     +(v*(G*phi)**2+(n*pi/2)**2)*Q2*ss(G,m*pi))*2*(-1)**((n+1)/2)
        endif
      endif
      return
      end


      subroutine SWSR(phi,v,Px,L2,m,n,side,coef)
      double precision phi,v,Px,L2,pi,di,del,B,G,Q1,Q2,coef
      implicit double precision (c,s)
      integer m,n,case,side
C-----------------------------------------------------------------------
C     General Solution
C     W = Y(1-y) sin(m pi x), where m=1,2,3,...
C-----------------------------------------------------------------------
      pi=4*datan(1.0d0)
      di=(m*pi)**2
      del=(m*pi)**4-L2**2-Px*(m*pi/phi)**2
      if (del.eq.0) then
        write(6,*) 'Parameter singularity:  del = 0 in SWSR.'
        stop
      endif
      if (di**2.eq.del) then
        write(6,*) 'Parameter singularity:  di**2 - del = 0 in SWSR.'
        stop
      endif
      if (di**2.lt.del) then
C-----------------------------------------------------------------------
C     Case 1 solution
C     Y = Q1 sinh(B (1-y)) sin(G (1-y)) + Q2 cosh(B (1-y)) cos(G (1-y))
C-----------------------------------------------------------------------
        case=1
        B=dsqrt((dsqrt(del)+di)/2)*phi
        G=dsqrt((dsqrt(del)-di)/2)*phi
        Q1=dcosh(B)*dcos(G)
     2   /(2*B*G*(dsinh(B)**2+dcos(G)**2))
        Q2=-dsinh(B)*dsin(G)
     2   /(2*B*G*(dsinh(B)**2+dcos(G)**2))
      elseif (del.lt.0) then
C-----------------------------------------------------------------------
C     Case 2 solution
C     Y = Q1 cosh(B (1-y)) + Q2 cos(G (1-y))
C-----------------------------------------------------------------------
        case=2
        B=dsqrt(dsqrt(di**2-del)+di)*phi
        G=dsqrt(dsqrt(di**2-del)-di)*phi
        Q1=((B**2+G**2)*dcosh(B))**(-1)
        Q2=-((B**2+G**2)*dcos(G))**(-1)
      else
C-----------------------------------------------------------------------
C     Case 3 solution
C     Y = Q1 cosh(B (1-y)) + Q2  cosh(G (1-y))
C-----------------------------------------------------------------------
        case=3
        B=dsqrt(di+dsqrt(di**2-del))*phi
        G=dsqrt(di-dsqrt(di**2-del))*phi
        Q1=((B**2-G**2)*dcosh(B))**(-1)
        Q2=-((B**2-G**2)*dcosh(G))**(-1)
      endif
C-----------------------------------------------------------------------
C     Index for side
C     x=0  a.k.a.  side=1
```

```
C     y=0  a.k.a.  side=2
C     x=1  a.k.a.  side=3
C     y=1  a.k.a.  side=4
C-----------------------------------------------------------------------
      if (side.eq.1) then
        if (case.eq.1) then
          coef=2*m*pi*(Q1*shmsms(B,G,n*pi/2)+Q2*chmcms(B,G,n*pi/2))
        elseif (case.eq.2) then
          coef=2*m*pi*(Q1*chms(B,n*pi/2)+Q2*cms(G,n*pi/2))
        else
          coef=2*m*pi*(Q1*chms(B,n*pi/2)+Q2*chms(G,n*pi/2))
        endif
      elseif (side.eq.2) then
        if (case.eq.1) then
          coef=-(Q1*G+Q2*B)*dsinh(B)*dcos(G)
     2          -(Q1*B-Q2*G)*dcosh(B)*dsin(G)
        elseif (case.eq.2) then
          coef=-Q1*B*dsinh(B)+Q2*G*dsin(G)
        else
          coef=-Q1*B*dsinh(B)-Q2*G*dsinh(G)
        endif
      elseif (side.eq.3) then
        if (case.eq.1) then
          coef=(Q1*shmsms(B,G,n*pi/2)+Q2*chmcms(B,G,n*pi/2))
     2       *2*m*pi*(-1)**m
        elseif (case.eq.2) then
          coef=2*m*pi*(-1)**m*(Q1*chms(B,n*pi/2)+Q2*cms(G,n*pi/2))
        else
          coef=2*m*pi*(-1)**m*(Q1*chms(B,n*pi/2)+Q2*chms(G,n*pi/2))
        endif
      else
        if (case.eq.1) then
          coef=Q1*2*B*G+Q2*(B**2-G**2-v*(m*pi*phi)**2)
        elseif (case.eq.2) then
          coef=Q1*(B**2-v*(m*pi*phi)**2)-Q2*(G**2+v*(m*pi*phi)**2)
        else
          coef=Q1*(B**2-v*(m*pi*phi)**2)+Q2*(G**2-v*(m*pi*phi)**2)
        endif
      endif
      return
      end


      subroutine WSSR(phi,v,Px,L2,m,n,side,coef)
      double precision phi,v,Px,L2,pi,di,del,B,G,Q1,Q2,coef
      implicit double precision (c,s)
      integer m,n,case,side
C-----------------------------------------------------------------------
C     General Solution
C     W = Y(1-x) sin(n pi y / 2), where n=1,3,5,...
C-----------------------------------------------------------------------
      pi=4*datan(1.0d0)
      di=(n*pi/2)**2-Px/2
      del=(n*pi/2)**4-L2**2*phi**4
      if (del.eq.0) then
        write(6,*) 'Parameter singularity:  del = 0 in WSSR.'
        stop
      endif
      if (di**2.eq.del) then
        write(6,*) 'Parameter singularity:  di**2 - del = 0 in WSSR.'
        stop
      endif
      if (di**2.lt.del) then
```

```
C------------------------------------------------------------------------
C     Case 1 solution
C     Y = Q1 sinh(B (1-x)) cos(G (1-x)) + Q2 cosh(B (1-x)) sin(G (1-x))
C------------------------------------------------------------------------
        case=1
        B=dsqrt((dsqrt(del)+di)/2)/phi
        G=dsqrt((dsqrt(del)-di)/2)/phi
        Q1=dcosh(B)*dsin(G)
     2   /(2*B*G*(dcos(G)**2-dcosh(B)**2))
        Q2=-dsinh(B)*dcos(G)
     2   /(2*B*G*(dcos(G)**2-dcosh(B)**2))
      elseif (del.lt.0) then
C------------------------------------------------------------------------
C     Case 2 solution
C     Y = Q1 sinh(B (1-x)) + Q2 sin(G (1-x))
C------------------------------------------------------------------------
        case=2
        B=dsqrt(dsqrt(di**2-del)+di)/phi
        G=dsqrt(dsqrt(di**2-del)-di)/phi
        Q1=((B**2+G**2)*dsinh(B))**(-1)
        Q2=-((B**2+G**2)*dsin(G))**(-1)
      elseif (di.gt.0) then
C------------------------------------------------------------------------
C     Case 3 solution
C     Y = Q1 sinh(B (1-x)) + Q2 sinh(G (1-x))
C------------------------------------------------------------------------
        case=3
        B=dsqrt(di+dsqrt(di**2-del))/phi
        G=dsqrt(di-dsqrt(di**2-del))/phi
        Q1=((B**2-G**2)*dsinh(B))**(-1)
        Q2=-((B**2-G**2)*dsinh(G))**(-1)
      else
C------------------------------------------------------------------------
C     Case 4 solution
C     Y = Q1 sin(B (1-x)) + Q2 sin(G (1-x))
C------------------------------------------------------------------------
        case=4
        B=dsqrt(-di+dsqrt(di**2-del))/phi
        G=dsqrt(-di-dsqrt(di**2-del))/phi
        Q1=((G**2-B**2)*dsin(B))**(-1)
        Q2=-((G**2-B**2)*dsin(G))**(-1)
      endif
C------------------------------------------------------------------------
C     Index
C     xi = 0 a.k.a. side = 1
C     eta = 0 a.k.a. side = 2
C     xi = 1 a.k.a. side = 3
C     eta = 1 a.k.a. side = 4
C------------------------------------------------------------------------
      if (side.eq.1) then
        if (case.eq.1) then
          coef=-(Q2*B-Q1*G)*dsinh(B)*dsin(G)
     2         -(Q1*B+Q2*G)*dcosh(B)*dcos(G)
        elseif (case.eq.2) then
          coef=-Q1*B*dcosh(B)-Q2*G*dcos(G)
        elseif (case.eq.3) then
          coef=-Q1*B*dcosh(B)-Q2*G*dcosh(G)
        else
          coef=-Q1*B*dcos(B)-Q2*G*dcos(G)
        endif
      elseif (side.eq.2) then
        if (case.eq.1) then
          coef=n*pi*(Q1*shmcms(B,G,m*pi)+Q2*chmsms(B,G,m*pi))
```

```
        elseif (case.eq.2) then
          coef=n*pi*(Q1*shms(B,m*pi)+Q2*sms(G,m*pi))
        elseif (case.eq.3) then
          coef=n*pi*(Q1*shms(B,m*pi)+Q2*shms(G,m*pi))
        else
          coef=n*pi*(Q1*sms(B,m*pi)+Q2*sms(G,m*pi))
        endif
      elseif (side.eq.3) then
        coef=-Q1*B-Q2*G
      else
        if (case.eq.1) then
        coef=((Q1*(v*phi**2*(B**2-G**2)-(n*pi/2)**2)+2*v*phi**2*Q2*B*G)
     2    *shmcms(B,G,m*pi)
     3    +(Q2*(v*phi**2*(B**2-G**2)-(n*pi/2)**2)-2*v*phi**2*Q1*B*G)
     4    *chmsms(B,G,m*pi))*2*(-1)**((n-1)/2)
        elseif (case.eq.2) then
        coef=((v*(B*phi)**2-(n*pi/2)**2)*Q1*shms(B,m*pi)
     2    -(v*(G*phi)**2+(n*pi/2)**2)*Q2*sms(G,m*pi))*2*(-1)**((n-1)/2)
        elseif (case.eq.3) then
        coef=((v*(B*phi)**2-(n*pi/2)**2)*Q1*shms(B,m*pi)
     2    +(v*(G*phi)**2-(n*pi/2)**2)*Q2*shms(G,m*pi))*2*(-1)**((n-1)/2)
        else
        coef=((v*(B*phi)**2+(n*pi/2)**2)*Q1*sms(B,m*pi)
     2    +(v*(G*phi)**2+(n*pi/2)**2)*Q2*sms(G,m*pi))*2*(-1)**((n+1)/2)
        endif
      endif
      return
      end


      subroutine SRSV(phi,v,Px,L2,m,n,side,coef)
      double precision phi,v,Px,L2,pi,vp,di,del,B,G,Q1,Q2,coef
      implicit double precision (c,s)
      integer m,n,case,side
C-----------------------------------------------------------------------
C     General Solution
C     W = Y(y) sin(m pi x), where m=1,2,3,...
C-----------------------------------------------------------------------
      pi=4*datan(1.0d0)
      vp=(2-v)*(m*pi*phi)**2
      di=(m*pi)**2
      del=(m*pi)**4-L2**2-Px*(m*pi/phi)**2
      if (del.eq.0) then
        write(6,*) 'Parameter singularity:  del = 0 in SRSV.'
        stop
      endif
      if (di**2.eq.del) then
        write(6,*) 'Parameter singularity:  di**2 - del = 0 in SRSV.'
        stop
      endif
      if (di**2.lt.del) then
C-----------------------------------------------------------------------
C     Case 1 solution
C     Y = Q1 sinh(B y) sin(G y) + Q2 cosh(B y) cos(G y)
C-----------------------------------------------------------------------
        case=1
        B=dsqrt((dsqrt(del)+di)/2)*phi
        G=dsqrt((dsqrt(del)-di)/2)*phi
        Q1=(B*(B**2-3*G**2-vp)*dsinh(B)*dcos(G)
     2    +G*(G**2-3*B**2+vp)*dcosh(B)*dsin(G))
     3    /(-2*B*G*(B**2+G**2)*(dsinh(B)**2+dsin(G)**2))
        Q2=(G*(G**2-3*B**2+vp)*dsinh(B)*dcos(G)
     2    -B*(B**2-3*G**2-vp)*dcosh(B)*dsin(G))
```

```
     3    /(-2*B*G*(B**2+G**2)*(dsinh(B)**2+dsin(G)**2))
      elseif (del.lt.0) then
C-----------------------------------------------------------------------
C     Case 2 solution
C     Y = Q1 cosh(B y) + Q2 cos(G y)
C-----------------------------------------------------------------------
        case=2
        B=dsqrt(dsqrt(di**2-del)+di)*phi
        G=dsqrt(dsqrt(di**2-del)-di)*phi
        Q1=(G**2+vp)/(B*(B**2+G**2)*dsinh(B))
        Q2=-(B**2-vp)/(G*(B**2+G**2)*dsin(G))
      else
C-----------------------------------------------------------------------
C     Case 3 solution
C     Y = Q1 cosh(B y) + Q2 cosh(G y)
C-----------------------------------------------------------------------
        case=3
        B=dsqrt(di+dsqrt(di**2-del))*phi
        G=dsqrt(di-dsqrt(di**2-del))*phi
        Q1=-(G**2-vp)/(B*(B**2-G**2)*dsinh(B))
        Q2=(B**2-vp)/(G*(B**2-G**2)*dsinh(G))
      endif
C-----------------------------------------------------------------------
C     Index for side
C     x=0  a.k.a.  side=1
C     y=0  a.k.a.  side=2
C     x=1  a.k.a.  side=3
C     y=1  a.k.a.  side=4
C-----------------------------------------------------------------------
      if (side.eq.1) then
        if (case.eq.1) then
          if (n.eq.0) then
            coef=(Q1*shs(B,G)+Q2*chc(B,G))*m*pi
          else
            coef=(Q1*shsc(B,G,n*pi)+Q2*chcc(B,G,n*pi))*2*m*pi
          endif
        elseif (case.eq.2) then
          if (n.eq.0) then
            coef=(Q1*ch(B)+Q2*c(G))*m*pi
          else
            coef=(Q1*chc(B,n*pi)+Q2*cc(G,n*pi))*2*m*pi
          endif
        else
          if (n.eq.0) then
            coef=(Q1*ch(B)+Q2*ch(G))*m*pi
          else
            coef=(Q1*chc(B,n*pi)+Q2*chc(G,n*pi))*2*m*pi
          endif
        endif
      elseif (side.eq.2) then
        if (case.eq.1) then
          coef=Q1*2*B*G+Q2*(B**2-G**2-v*(m*pi*phi)**2)
        elseif (case.eq.2) then
          coef=Q1*(B**2-v*(m*pi*phi)**2)-Q2*(G**2+v*(m*pi*phi)**2)
        else
          coef=Q1*(B**2-v*(m*pi*phi)**2)+Q2*(G**2-v*(m*pi*phi)**2)
        endif
      elseif (side.eq.3) then
        if (case.eq.1) then
          if (n.eq.0) then
            coef=(Q1*shs(B,G)+Q2*chc(B,G))*m*pi*(-1)**m
          else
            coef=(Q1*shsc(B,G,n*pi)+Q2*chcc(B,G,n*pi))*2*m*pi*(-1)**m
```

```
          endif
        elseif (case.eq.2) then
          if (n.eq.0) then
            coef=(Q1*ch(B)+Q2*c(G))*m*pi*(-1)**m
          else
            coef=(Q1*chc(B,n*pi)+Q2*cc(G,n*pi))*2*m*pi*(-1)**m
          endif
        else
          if (n.eq.0) then
            coef=(Q1*ch(B)+Q2*ch(G))*m*pi*(-1)**m
          else
            coef=(Q1*chc(B,n*pi)+Q2*chc(G,n*pi))*2*m*pi*(-1)**m
          endif
        endif
      else
        if (case.eq.1) then
          coef=(Q1*(B**2-G**2-v*(m*pi*phi)**2)-Q2*2*B*G)*dsinh(B)*dsin(G)
     2        +(Q1*2*B*G+Q2*(B**2-G**2-v*(m*pi*phi)**2))*dcosh(B)*dcos(G)
        elseif (case.eq.2) then
          coef=Q1*(B**2-v*(m*pi*phi)**2)*dcosh(B)
     2        -Q2*(G**2+v*(m*pi*phi)**2)*dcos(G)
        else
          coef=Q1*(B**2-v*(m*pi*phi)**2)*dcosh(B)
     2        +Q2*(G**2-v*(m*pi*phi)**2)*dcosh(G)
        endif
      endif
      return
      end


      subroutine SRWR(phi,v,Px,L2,m,n,side,coef)
      double precision phi,v,Px,L2,pi,di,del,B,G,Q1,Q2,coef
      implicit double precision (c,s)
      integer m,n,case,side
C-----------------------------------------------------------------
C     General Solution
C     W = Y(x) cos(n pi y), where n=0,1,2,...
C-----------------------------------------------------------------
      pi=4*datan(1.0d0)
      di=(n*pi)**2-Px/2
      del=(n*pi)**4-L2**2*phi**4
      if (del.eq.0) then
        write(6,*) 'Parameter singularity:  del = 0 in SRWR.'
        stop
      endif
      if (di**2.eq.del) then
        write(6,*) 'Parameter singularity:  di**2 - del = 0 in SRWR.'
        stop
      endif
      if (di**2.lt.del) then
C-----------------------------------------------------------------
C     Case 1 solution
C     Y = Q1 sinh(B x) cos(G x) + Q2 cosh(B x) sin(G x)
C-----------------------------------------------------------------
        case=1
        B=dsqrt((dsqrt(del)+di)/2)/phi
        G=dsqrt((dsqrt(del)-di)/2)/phi
        Q1=dcosh(B)*dsin(G)
     2    /(2*B*G*(dcos(G)**2-dcosh(B)**2))
        Q2=-dsinh(B)*dcos(G)
     2    /(2*B*G*(dcos(G)**2-dcosh(B)**2))
      elseif (del.lt.0) then
C-----------------------------------------------------------------
```

```
c     Case 2 solution
c     Y = Q1 sinh(B x) + Q2 sin(G x)
c-----------------------------------------------------------------
         case=2
         B=dsqrt(dsqrt(di**2-del)+di)/phi
         G=dsqrt(dsqrt(di**2-del)-di)/phi
         Q1=((B**2+G**2)*dsinh(B))**(-1)
         Q2=-((B**2+G**2)*dsin(G))**(-1)
      elseif (di.gt.0) then
c-----------------------------------------------------------------
c     Case 3 solution
c     Y = Q1 sinh(B x) + Q2 sinh(G x)
c-----------------------------------------------------------------
         case=3
         B=dsqrt(di+dsqrt(di**2-del))/phi
         G=dsqrt(di-dsqrt(di**2-del))/phi
         Q1=((B**2-G**2)*dsinh(B))**(-1)
         Q2=-((B**2-G**2)*dsinh(G))**(-1)
      else
c-----------------------------------------------------------------
c     Case 4 solution
c     Y = Q1 sin(B x) + Q2 sin(G x)
c-----------------------------------------------------------------
         case=4
         B=dsqrt(-di+dsqrt(di**2-del))/phi
         G=dsqrt(-di-dsqrt(di**2-del))/phi
         Q1=((G**2-B**2)*dsin(B))**(-1)
         Q2=-((G**2-B**2)*dsin(G))**(-1)
      endif
c-----------------------------------------------------------------
c     Index
c     xi = 0 a.k.a. side = 1
c     eta = 0 a.k.a. side = 2
c     xi = 1 a.k.a. side = 3
c     eta = 1 a.k.a. side = 4
c-----------------------------------------------------------------
      if (side.eq.1) then
        coef=Q1*B+Q2*G
      elseif (side.eq.2) then
        if (case.eq.1) then
          coef=((Q1*(B**2-G**2-(n*pi/phi)**2/v)+2*Q2*B*G)*shsc(B,m*pi,G)
     2         +(Q2*(B**2-G**2-(n*pi/phi)**2/v)-2*Q1*B*G)*chss(B,m*pi,G))
     3         *2*v*phi**2
        elseif (case.eq.2) then
          coef=2*Q1*(v*(B*phi)**2-(n*pi)**2)*shs(B,m*pi)
     2         -2*Q2*(v*(G*phi)**2+(n*pi)**2)*ss(G,m*pi)
        elseif (case.eq.3) then
          coef=2*Q1*(v*(B*phi)**2-(n*pi)**2)*shs(B,m*pi)
     2         +2*Q2*(v*(G*phi)**2-(n*pi)**2)*shs(G,m*pi)
        else
          coef=-2*Q1*(v*(B*phi)**2+(n*pi)**2)*ss(B,m*pi)
     2          -2*Q2*(v*(G*phi)**2+(n*pi)**2)*ss(G,m*pi)
        endif
      elseif (side.eq.3) then
        if (case.eq.1) then
          coef=(Q2*B-Q1*G)*dsinh(B)*dsin(G)
     2         +(Q1*B+Q2*G)*dcosh(B)*dcos(G)
        elseif (case.eq.2) then
          coef=Q1*B*dcosh(B)+Q2*G*dcos(G)
        elseif (case.eq.3) then
          coef=Q1*B*dcosh(B)+Q2*G*dcosh(G)
        else
          coef=Q1*B*dcos(B)+Q2*G*dcos(G)
```

```
         endif
       else
         if (case.eq.1) then
           coef=((Q1*(B**2-G**2-(n*pi/phi)**2/v)+2*Q2*B*G)*shsc(B,m*pi,G)
     2         +(Q2*(B**2-G**2-(n*pi/phi)**2/v)-2*Q1*B*G)*chss(B,m*pi,G))
     3         *2*v*phi**2*(-1)**n
         elseif (case.eq.2) then
           coef=(2*Q1*(v*(B*phi)**2-(n*pi)**2)*shs(B,m*pi)
     2          -2*Q2*(v*(G*phi)**2+(n*pi)**2)*ss(G,m*pi))*(-1)**n
         elseif (case.eq.3) then
           coef=(2*Q1*(v*(B*phi)**2-(n*pi)**2)*shs(B,m*pi)
     2          +2*Q2*(v*(G*phi)**2-(n*pi)**2)*shs(G,m*pi))*(-1)**n
         else
           coef=(-2*Q1*(v*(B*phi)**2+(n*pi)**2)*ss(B,m*pi)
     2            -2*Q2*(v*(G*phi)**2+(n*pi)**2)*ss(G,m*pi))*(-1)**n
         endif
       endif
       return
       end


       subroutine SVSR(phi,v,Px,L2,m,n,side,coef)
       double precision phi,v,Px,L2,pi,vp,di,del,B,G,Q1,Q2,coef
       implicit double precision (c,s)
       integer m,n,case,side
C-----------------------------------------------------------------------
C      General Solution
C      W = Y(y) sin(m pi x), where m=1,2,3,...
C-----------------------------------------------------------------------
       pi=4*datan(1.0d0)
       vp=(2-v)*(m*pi*phi)**2
       di=(m*pi)**2
       del=(m*pi)**4-L2**2-Px*(m*pi/phi)**2
       if (del.eq.0) then
         write(6,*) 'Parameter singularity:  del = 0 in SVSR.'
         stop
       endif
       if (di**2.eq.del) then
         write(6,*) 'Parameter singularity:  di**2 - del = 0 in SVSR.'
         stop
       endif
       if (di**2.lt.del) then
C-----------------------------------------------------------------------
C      Case 1 solution
C      Y = Q1 sinh(B(1-y)) sin(G(1-y)) + Q2 cosh(B(1-y)) cos(G(1-y))
C-----------------------------------------------------------------------
         case=1
         B=dsqrt((dsqrt(del)+di)/2)*phi
         G=dsqrt((dsqrt(del)-di)/2)*phi
         Q1=(B*(B**2-3*G**2-vp)*dsinh(B)*dcos(G)
     2     +G*(G**2-3*B**2+vp)*dcosh(B)*dsin(G))
     3     /(-2*B*G*(B**2+G**2)*(dsinh(B)**2+dsin(G)**2))
         Q2=(G*(G**2-3*B**2+vp)*dsinh(B)*dcos(G)
     2     -B*(B**2-3*G**2-vp)*dcosh(B)*dsin(G))
     3     /(-2*B*G*(B**2+G**2)*(dsinh(B)**2+dsin(G)**2))
       elseif (del.lt.0) then
C-----------------------------------------------------------------------
C      Case 2 solution
C      Y = Q1 cosh(B(1-y)) + Q2 cos(G(1-y))
C-----------------------------------------------------------------------
         case=2
         B=dsqrt(dsqrt(di**2-del)+di)*phi
         G=dsqrt(dsqrt(di**2-del)-di)*phi
```

```
          Q1=(G**2+vp)/(B*(B**2+G**2)*dsinh(B))
          Q2=-(B**2-vp)/(G*(B**2+G**2)*dsin(G))
        else
C-----------------------------------------------------------------------
C       Case 3 solution
C       Y = Q1 cosh(B(1-y)) + Q2 cosh(G(1-y))
C-----------------------------------------------------------------------
          case=3
          B=dsqrt(di+dsqrt(di**2-del))*phi
          G=dsqrt(di-dsqrt(di**2-del))*phi
          Q1=-(G**2-vp)/(B*(B**2-G**2)*dsinh(B))
          Q2=(B**2-vp)/(G*(B**2-G**2)*dsinh(G))
        endif
C-----------------------------------------------------------------------
C       Index for side
C       x=0  a.k.a.  side=1
C       y=0  a.k.a.  side=2
C       x=1  a.k.a.  side=3
C       y=1  a.k.a.  side=4
C-----------------------------------------------------------------------
        if (side.eq.1) then
          if (case.eq.1) then
            if (n.eq.0) then
              coef=(Q1*shmsm(B,G)+Q2*chmcm(B,G))*m*pi
            else
              coef=(Q1*shmsmc(B,G,n*pi)+Q2*chmcmc(B,G,n*pi))*2*m*pi
            endif
          elseif (case.eq.2) then
            if (n.eq.0) then
              coef=(Q1*chm(B)+Q2*cm(G))*m*pi
            else
              coef=(Q1*chmc(B,n*pi)+Q2*cmc(G,n*pi))*2*m*pi
            endif
          else
            if (n.eq.0) then
              coef=(Q1*chm(B)+Q2*chm(G))*m*pi
            else
              coef=(Q1*chmc(B,n*pi)+Q2*chmc(G,n*pi))*2*m*pi
            endif
          endif
        elseif (side.eq.2) then
          if (case.eq.1) then
           coef=(Q1*(B**2-G**2-v*(m*pi*phi)**2)-Q2*2*B*G)*dsinh(B)*dsin(G)
     2       +(Q1*2*B*G+Q2*(B**2-G**2-v*(m*pi*phi)**2))*dcosh(B)*dcos(G)
          elseif (case.eq.2) then
           coef=Q1*(B**2-v*(m*pi*phi)**2)*dcosh(B)
     2       -Q2*(G**2+v*(m*pi*phi)**2)*dcos(G)
          else
           coef=Q1*(B**2-v*(m*pi*phi)**2)*dcosh(B)
     2       +Q2*(G**2-v*(m*pi*phi)**2)*dcosh(G)
          endif
        elseif (side.eq.3) then
          if (case.eq.1) then
            if (n.eq.0) then
             coef=(Q1*shmsm(B,G)+Q2*chmcm(B,G))*m*pi*(-1)**m
            else
             coef=(Q1*shmsmc(B,G,n*pi)+Q2*chmcmc(B,G,n*pi))*2*m*pi*(-1)**m
            endif
          elseif (case.eq.2) then
            if (n.eq.0) then
              coef=(Q1*chm(B)+Q2*cm(G))*m*pi*(-1)**m
            else
              coef=(Q1*chmc(B,n*pi)+Q2*cmc(G,n*pi))*2*m*pi*(-1)**m
```

```
          endif
        else
          if (n.eq.0) then
            coef=(Q1*chm(B)+Q2*chm(G))*m*pi*(-1)**m
          else
            coef=(Q1*chmc(B,n*pi)+Q2*chmc(G,n*pi))*2*m*pi*(-1)**m
          endif
        endif
      else
        if (case.eq.1) then
          coef=Q1*2*B*G+Q2*(B**2-G**2-v*(m*pi*phi)**2)
        elseif (case.eq.2) then
          coef=Q1*(B**2-v*(m*pi*phi)**2)-Q2*(G**2+v*(m*pi*phi)**2)
        else
          coef=Q1*(B**2-v*(m*pi*phi)**2)+Q2*(G**2-v*(m*pi*phi)**2)
        endif
      endif
      return
      end


      subroutine WRSR(phi,v,Px,L2,m,n,side,coef)
      double precision phi,v,Px,L2,pi,di,del,B,G,Q1,Q2,coef
      implicit double precision (c,s)
      integer m,n,case,side
C-----------------------------------------------------------------------
C     General Solution
C     W = Y(x) cos(n pi y), where n=0,1,2,...
C-----------------------------------------------------------------------
      pi=4*datan(1.0d0)
      di=(n*pi)**2-Px/2
      del=(n*pi)**4-L2**2*phi**4
      if (del.eq.0) then
        write(6,*) 'Parameter singularity:  del = 0 in WRSR.'
        stop
      endif
      if (di**2.eq.del) then
        write(6,*) 'Parameter singularity:  di**2 - del = 0 in WRSR.'
        stop
      endif
      if (di**2.lt.del) then
C-----------------------------------------------------------------------
C     Case 1 solution
C     Y = Q1 sinh(B (1-x)) cos(G (1-x)) + Q2 cosh(B (1-x)) sin(G (1-x))
C-----------------------------------------------------------------------
        case=1
        B=dsqrt((dsqrt(del)+di)/2)/phi
        G=dsqrt((dsqrt(del)-di)/2)/phi
        Q1=dcosh(B)*dsin(G)
     2     /(2*B*G*(dcos(G)**2-dcosh(B)**2))
        Q2=-dsinh(B)*dcos(G)
     2     /(2*B*G*(dcos(G)**2-dcosh(B)**2))
      elseif (del.lt.0) then
C-----------------------------------------------------------------------
C     Case 2 solution
C     Y = Q1 sinh(B (1-x)) + Q2 sin(G (1-x))
C-----------------------------------------------------------------------
        case=2
        B=dsqrt(dsqrt(di**2-del)+di)/phi
        G=dsqrt(dsqrt(di**2-del)-di)/phi
        Q1=((B**2+G**2)*dsinh(B))**(-1)
        Q2=-((B**2+G**2)*dsin(G))**(-1)
      elseif (di.gt.0) then
```

```
C-----------------------------------------------------------------------
C     Case 3 solution
C     Y = Q1 sinh(B (1-x)) + Q2 sinh(G (1-x))
C-----------------------------------------------------------------------
        case=3
        B=dsqrt(di+dsqrt(di**2-del))/phi
        G=dsqrt(di-dsqrt(di**2-del))/phi
        Q1=((B**2-G**2)*dsinh(B))**(-1)
        Q2=-((B**2-G**2)*dsinh(G))**(-1)
      else
C-----------------------------------------------------------------------
C     Case 4 solution
C     Y = Q1 sin(B (1-x)) + Q2 sin(G (1-x))
C-----------------------------------------------------------------------
        case=4
        B=dsqrt(-di+dsqrt(di**2-del))/phi
        G=dsqrt(-di-dsqrt(di**2-del))/phi
        Q1=((G**2-B**2)*dsin(B))**(-1)
        Q2=-((G**2-B**2)*dsin(G))**(-1)
      endif
C-----------------------------------------------------------------------
C     Index
C     xi = 0 a.k.a. side = 1
C     eta = 0 a.k.a. side = 2
C     xi = 1 a.k.a. side = 3
C     eta = 1 a.k.a. side = 4
C-----------------------------------------------------------------------
      if (side.eq.1) then
        if (case.eq.1) then
          coef=(Q2*B-Q1*G)*dsinh(B)*dsin(G)
     2        +(Q1*B+Q2*G)*dcosh(B)*dcos(G)
        elseif (case.eq.2) then
          coef=Q1*B*dcosh(B)+Q2*G*dcos(G)
        elseif (case.eq.3) then
          coef=Q1*B*dcosh(B)+Q2*G*dcosh(G)
        else
          coef=Q1*B*dcos(B)+Q2*G*dcos(G)
        endif
        coef=-coef
      elseif (side.eq.2) then
       if (case.eq.1) then
        coef=((Q1*(B**2-G**2-(n*pi/phi)**2/v)+2*Q2*B*G)*shmcms(B,G,m*pi)
     2       +(Q2*(B**2-G**2-(n*pi/phi)**2/v)-2*Q1*B*G)*chmsms(B,G,m*pi))
     3       *2*v*phi**2
        elseif (case.eq.2) then
          coef=2*Q1*(v*(B*phi)**2-(n*pi)**2)*shms(B,m*pi)
     2        -2*Q2*(v*(G*phi)**2+(n*pi)**2)*sms(G,m*pi)
        elseif (case.eq.3) then
          coef=2*Q1*(v*(B*phi)**2-(n*pi)**2)*shms(B,m*pi)
     2        +2*Q2*(v*(G*phi)**2-(n*pi)**2)*shms(G,m*pi)
        else
          coef=-2*Q1*(v*(B*phi)**2+(n*pi)**2)*sms(B,m*pi)
     2          -2*Q2*(v*(G*phi)**2+(n*pi)**2)*sms(G,m*pi)
        endif
      elseif (side.eq.3) then
        coef=Q1*B+Q2*G
        coef=-coef
      else
       if (case.eq.1) then
        coef=((Q1*(B**2-G**2-(n*pi/phi)**2/v)+2*Q2*B*G)*shmcms(B,G,m*pi)
     2       +(Q2*(B**2-G**2-(n*pi/phi)**2/v)-2*Q1*B*G)*chmsms(B,G,m*pi))
     3       *2*v*phi**2*(-1)**n
       elseif (case.eq.2) then
```

```
      coef=(2*Q1*(v*(B*phi)**2-(n*pi)**2)*shms(B,m*pi)
     2        -2*Q2*(v*(G*phi)**2+(n*pi)**2)*sms(G,m*pi))*(-1)**n
    elseif (case.eq.3) then
      coef=(2*Q1*(v*(B*phi)**2-(n*pi)**2)*shms(B,m*pi)
     2        +2*Q2*(v*(G*phi)**2-(n*pi)**2)*shms(G,m*pi))*(-1)**n
    else
      coef=(-2*Q1*(v*(B*phi)**2+(n*pi)**2)*sms(B,m*pi)
     2         -2*Q2*(v*(G*phi)**2+(n*pi)**2)*sms(G,m*pi))*(-1)**n
    endif
  endif
  return
  end
```